DESIGN AND SYNTHESIS OF DIARYL (NITROGENOUS HETEROCYCLES) ALKANES FOR THEIR STRUCTURAL AND BIOLOGICAL STUDIES

Thesis submitted to

Department of Chemistry, Faculty of Science,
Banaras Hindu University, Varanasi-221005, India

For the degree of

Doctor of Philosophy

in

Chemistry

by

Amar kUMAR
M. Sc. (Chemistry)

Medicinal and Process Chemistry Division,
Central Drug Research Institute, Lucknow-226001, India

Enrolment No. 342212 **2012**

Dedicated
to
My Family

COPYRIGHT CERTIFICATE

UNDERTAKING FROM THE CANDIDATE

I, Amar Kumar, certify that the work embodied in this Ph. D. thesis is my own work carried out by me at Central Drug Research Institute, Lucknow, India under the joint supervision of Dr. Ranjana S. Khanna, Reader, Department of Chemistry, BHU, Varanasi, India and Dr. Kamlakar Avasthi, Sc. F, Medicinal & Process Chemistry Division, Central Drug Research Institute, Lucknow, India.

I have presented this thesis taking an extra pain and effort to enlighten the topic *"Design and Synthesis of Diaryl (Nitrogenous Heterocycles) Alkanes for their Structural and Biological Studies"*. Proper care has been taken on my behalf to ensure that there is no mistake in this thesis.

Date:

Place: Varanasi **(Amar Kumar)**

CANDIDATE'S DECLARATION

I, Amar Kumar, hereby declare that the work embodied in this Ph. D. thesis is my own work carried out by me at Central Drug Research Institute, Lucknow, India under the joint supervision of Dr. Ranjana S. Khanna, Reader, Department of Chemistry, BHU, Varanasi, India and Dr. Kamlakar Avasthi, Chief Scientist, Medicinal & Process Chemistry Division, Central Drug Research Institute, Lucknow, India. The matter embodied in this Ph. D. thesis has not been submitted for the award of any other degree/diploma.

I declare that I have faithfully acknowledged, given credit to and referred to the research workers whenever their works have been cited in the text and the body of the thesis. I further certify that I have not willfully lifted up some other's work, para, text, data, results etc. reported in the journals, books, magazines, reports, dissertations, thesis etc., or available at web-sites and included them in this Ph.D. thesis and cited as my own work.

Date:

Place: Varanasi **Amar Kumar**

CERTIFICATE FROM THE SUPERVISORS

This is to certify that the above statement made by the candidate is correct to the best of our knowledge.

Dr. Kamlakar Avasthi
(External supervisor)
Chief Scientist,
Medicinal & Process Chemistry Division,
CDRI, Lucknow

Dr. Ranjana S. Khanna
(Supervisor)
Reader,
Department of Chemistry, Faculty of Science,
BHU, Varanasi

Prof. B. Singh
Head,
Department of Chemistry,
Faculty of Science,
BHU, Varanasi

PRE-SUBMISSION SEMINAR COMPLETION CERTIFICATE

This is to certify that Mr. Amar Kumar, a bonafide scholar of this department, has successfully completed the pre-submission seminar requirement, which is a part of his Ph. D. programme.

Date:

Prof. B. Singh
Head,
Department of Chemistry,
Faculty of Science,
BHU, Varanasi

Place: Varanasi

COPYRIGHT TRANSFER CERTIFICATE

Title of the Thesis: *“Design and Synthesis of Diaryl (Nitrogenous Heterocycles) Alkanes for their Structural and Biological Studies”*

Candidate’s Name: Amar Kumar

COPYRIGHT TRANSFER

The undersigned hereby assigns to the Banaras Hindu University all rights under copyright that may exist in and for the above thesis submitted for the award of the Ph. D. degree.

Amar Kumar

DEPARTMENT OF CHEMISTRY
FACULTY OF SCIENCES
BANARAS HINDU UNIVERSITY
VARANASI-221005

Date:

CERTIFICATE

This is to certify that *Mr. Amar Kumar,* M. Sc. (Chemistry) has completed the research work for the full period prescribed under the Ph. D. ordinances of the Banaras Hindu University and the thesis entitled *"Design and Synthesis of Diaryl (Nitrogenous Heterocycles) Alkanes for their Structural and biological Studies"* which is being presented by him embodies the result of his investigation conducted during the period he worked as Ph. D. research scholar of the Department of Chemistry under my supervision.

Dr. Ranjana S. Khanna
(Supervisor)
Reader,
Department of Chemistry,
Faculty of Science
BHU, Varanasi

Prof. B. Singh
Head,
Department of Chemistry,
Faculty of Science,
BHU, Varanasi

Dr. Kamlakar Avasthi,
Chief Scientist,
Medicinal & Process Chemistry,
Central Drug Research Institute,
Lucknow 226001,
India

Central Drug Research Institute, CSIR

Date:

CERTIFICATE

This is to certify that the work embodied in this thesis entitled ***“Design and Synthesis of Diaryl (Nitrogenous Heterocycles) Alkanes for their Structural and biological Studies”*** has been carried out by ***Mr. Amar Kumar*** under my supervision at Central Drug Research Institute, Lucknow. The work fulfills all requirements for the degree of philosophy. The work presented in this thesis is original and has not been submitted for any other degree/diploma.

Dr. Kamlakar Avasthi

ACKNOWLEDGEMENTS

All praises be to **ALMIGHTY** the most gracious, the most merciful, the cherisher and the sustainer of the worlds who guides us in darkness and helps in difficulties. This piece of work would have not been accomplished without His help.

I offer my profound gratitude to my supervisor ***Dr. Ranjana S. Khanna***, Reader, Department of Chemistry, Banaras Hindu University, Varanasi for her constant encouragement, moral support and timely advice throughout this period.

Words alone are insufficient to express my deep sense of gratitude and indebtedness towards my external supervisor ***Dr. Kamlakar Avasthi***, Chief Scientist, Medicinal & Process Chemistry Division, CDRI, Lucknow for creative suggestions, motivation and exemplary guidance throughout the course of my doctoral research.

I am extremely thankful to *Dr. T. K. Chakraborty*, Director, CDRI, Lucknow, *Dr. S. B. Katti*, Head of the Medicinal & Process Chemistry Division, CDRI, Lucknow, *Dr. C. M. Gupta*, former Director, CDRI, Lucknow, *Dr. A. K. Saxena* and *Dr. Chandan Singh*, Former Head of the Medicinal & Process Chemistry Division, Lucknow for providing the opportunity to carry out research work at this reputed institute.

I sincerely thank to *Prof. Lalji. Singh*, Vice-Chancellor of BHU, *Prof. B. Singh*, Head of the Department of Chemistry, Banaras Hindu University, *Prof. D. P. Singh*, former Vice-Chancellor of BHU, *Prof. T. R. Rao* and *Prof. N. K. Singh*, former Heads of the Department of Chemistry, Banaras Hindu University for providing the opportunity for Ph. D. registration.

I would like to acknowledge *Prof. R. M. Singh*, Department of Chemistry, Banaras Hindu University, *Prof. Om Prakash*, Department of Biochemistry, Banaras Hindu University and *Dr. Ashish K. Tewari*, Department of Chemistry, Banaras Hindu University for observing my progress throughout this period.

I would like to express my sincere thanks to my collaborators *Dr. P. R. Maulik*, *Mr. Ruchir Kant*, *Dr. Rishi Kumar* and *Dr. Reshmi Raghunandan*, Molecular & Structural Biology Division, CDRI, Lucknow for providing X-ray crystallographic data, *Dr. P. K. Shukla*, Fermentation Technology Division, CDRI, Lucknow and *Dr. Madhu Dikshit*, Pharmocology, Division, CDRI, Lucknow for providing biological activity data.

I am thankful to SAIF, CDRI, Lucknow for providing spectral and elemental analysis data and CSIR, New-Delhi for the financial support.

I would like to express my deep appreciation for the cooperation and support of my labmates *Dr. S. M. Farooq, Dr. S. Aswal, Dr. D. Bhagat, Dr. Amantullah, Mr. Pradeep Srivastava, Mithilesh Sharma, Tej Prakash, Lakshmi Shukla, Ashok K. Maurya, Ashu Gupta, Neelam Mishra, Sonal Rastogi, Deepika Parashar, Anjan Nayak, Reema Sharma, Deepak Kumar, Priyanka Patwal, Ankita Bajpai, Dr. Ramendra Pratap, Dr. Fateh Veer, Dr. Manish Dixit, Dr. Deepti Verma, Dr. Sumit Chaurasia, Dr. Amit Kumar, Vijay Kumar, Amrita Parihar, Gaurav Taneja, Salil Pratap, Pankaj Nag, Ashutosh Raghuvanshi, Shahida, Ajay Jha, Ashutosh Sharma.*

I shall always remain grateful to my dear friends *Maneesh Kumar Gupta, Chandra Saurabh Azad, Imran Khan, Deepti saxena, Mukesh Kumar, Sugandha Sharma, Ajay Arya, Satinath Sarkar, Shahnawaz Khan, Kuldeep, Anand, Manish Sinha, Shyam Raj Yadav, Ram Najar Kushwaha, Satinath Sarkar, Som, Amit, Dr. Balendu, Dr. Devesh Sawant, Dr. Vikash, Dr. Sunil Sharma, Dr. Ravi Shankar, Dr. Ravi Beniwal, Dr. Niraj Krishna Naikade, Dr. Ajit Shankar, Dr. Dinesh Yadav, Dr. Biswajit, Dr. Bisth, Dr. Sarad Porwal, Dr. Shailesh, Dr. Somnath Nag, Dr. Naresh Sunduru, Dr. Md. Saquib, Irfan Husain, Imran Ansari, Kamil Husain, Faheem Khan, Piyush Agarwal, Sahaj Gupta, Santosh, Neeraj, Vineet, Shashi, Himanshu, Dr. Amit Singh and Dr. Rashmi Dubey* for their direct and indirect support.

I am deeply indebted to *Dr.Ved Prakash Singh and Pravin Singh for their help and support.*

I am extraordinarily fortunate in having *Dr. Pranav Kumar, Maj. Ranvir Singh*, *Dinesh Pradhan*, *Himanshu Shekhar*, *Prakash*, *Rajiv*, *Raju*, *Nilesh*, *Dr. Pravin K. Singh*, *Pankaj Singh*, *Rupesh Singh*, *Neeraj Jha*, *Anand Kumar*, *Dhananjay Singh*, *Amrendra*, *Dr. Ishwar Vats*, *Dr. Snehlata*, *Dr. Sunil Singh*, *Dr. Sunil Arya*, *Hemant Garg*, *Dr. Lokeshwari*, *Dr. Darshan*, *Dr. Hema*, *Dr. Sunil Upadhayay*, *Dr. Anshuman Mangalum*, *Dr. Nihar Ranjan* and *Dr. Saurav Jyoti Sarma* as friends who helped me in my professional, as well as personal problems.

I also thank to my Motimahal friends like *Kiran, Abhishek, Pancham, Manuraj, Sumanto, Anil*, *Vivekanand*, *Swayam*, *Rajesh*, *Vivekanand*, *Arif*, *Asif*, *Bhatiya*, *Subhash*, *Ankit Makwan*, *Salil, Brajesh*, *Javed*, *Amit* and *Vineet Maurya* for making cheerful environment during my stay at hostel and I also thank to the Motimahal Society and staff for providing me neat and clean residential environment.

One cannot forget the strength and support that one gets from the family. With gratitude and reverence, I acknowledge and admire the unconditional love, support, encouragement and blessings bestowed on me by ***Maa***, ***Papa***, ***Bhaiya***, ***Bhabhi***, ***Didi*** and ***Jijaji*** without their affection and support the present effort would have remained an unrealized dream. Also My wife, ***Dr. Meenakshi*** deserves special heartfelt thanks for her unconditional love and care for me which has been a great support for me at times of distress.

Finally, I would like to thank everybody who was important to the successful realization of thesis, as well as expressing my apology that I could not mention personally one by one.

Amar Kumar

CONTENTS

Page No.

Synthesis, ^{1}H NMR and X-ray crystallographic studies of triazolo-[4,5-*d*]pyrimidine core based flexible symmetric polymethylene linker compounds

Synthesis, ^{1}H NMR and X-ray crystallographic studies of pyrazolo[3,4-*d*]pyrimidine and Phthalazinone/Quinazolinone/ Benzotriazinone based flexible dissymmetric polymethylene and butylidine linker compounds

LIST OF ABBREVIATIONS

Å	angstrom
AMP	adenosine monophosphate
ATP	adenosine triphosphate
br s	broad singlet
$CDCl_3$	deuterated chloroform
$CHCl_3$	chloroform
δ	chemical shift in ppm
dUMP	diuridine monophosphate
dTMP	dithymidine monophosphate
d	doublet
DMF	dimethylformamide
DNA	deoxyribonucleic acid
DMSO-d_6	deuterated dimethylsulfoxide
EtOAc	ethyl acetate
g	gram
cGMP	cyclic guanine monophosphate
h	hour
HRMS	high resolution mass spectrometry
Hz	hertz
IR	infrared
J	coupling constant (in NMR spectroscopy)
m	multiplet

mg	milligram
ml	mililiter
MeOH	methanol
mp	melting point
MS	mass spectrometry
m/z	mass to charge ratio
NMR	nuclear magnetic resonance
PP	pyrazolo[3,4-*d*]pyrimidine
PDE	phosphodiesterase
po	per oral
ppm	parts per million
quin	quintet
q	quartet
RNA	ribonucleic acid
r. t.	room temperature
s	singlet
sept	septet
t	triplet
THF	tetrahydrofuran
TLC	thin layer chromatography
UV	ultraviolet

PREFACE

Interactions can be broadly classified as covalent and noncovalent. Noncovalent interactions are those interactions which does not involve sharing of electrons. Noncovalent interactions form a very wide domain of weak interactions such as ion–ion, ion–dipole, dipole–dipole, classical and non-classical hydrogen bonds, arene–arene (π–π interaction), CH…π interaction, O…arene interaction, S…arene interaction, van der Waals interactions, hydrophobic interactions etc. Molecular organization and molecular interactions are based on noncovalent interactions. Noncovalent interactions are critical in maintaining the three-dimensional structure of large molecules, such as proteins and nucleic acids and are involved in many biological processes. Though noncovalent interactions are weak by nature, combined strength of several noncovalent interactions is sufficient to have a significant effect.

Among noncovalent interactions, arene–arene interactions play vital role in stabilizing DNA/RNA structures, protein folding, protein–protein interaction, drug–receptor interaction, asymmetric synthesis, molecular tweezers, supramolecular assemblies etc. Despite their importance, the nature of arene–arene interactions is not well understood because of their weakness and complex nature of mechanism. There are a large number of noncovalent interactions in biological recognition systems; therefore, it is very difficult to find out the contribution of an individual arene–arene interaction from the myriad of other noncovalent interactions. To overcome this difficulty, a number of small molecule model systems have been developed for studying arene–arene interactions in simpler and more controlled environments.

One of the strategies adopted for making models is to link two arene moieties with *trimethylene* linker as it provides suitable distance (3.4 Å) required for the arene–arene interaction. In order to study stacking interactions of nucleic acid bases Browne *et al.* (1968) synthesized nucleotide analogues in which the bases were connected by a *trimethylene* linker. The research group at CDRI, Lucknow, following Browne *et al.* strategy has been engaged since 1995 for studying the arene–arene interactions in pyrazolo[3,4-*d*]pyrimidine (**PP**) core (which is isomeric with the biologically important purine) based symmetric and dissymmetric *trimethylene* compounds. These studies have shown that **PP** core has strong arene–arene interaction propensity. In addition, proper positioning of the linker and substituent are also important for intramolecular π–π stacking interactions.

Present work involves the study of effect of increasing and decreasing the number of ring nitrogen in Pyrazolo[3,4-*d*]pyrimidine (**PP**) nucleus on intramolecular and intermolecular π–π interactions. Also investigation of role of arene interactions in controlling the conformation of 1,2 diaryl ethanes has been done. Finally, the interplay of weak hydrogen bonding such as C-H…N, C-H…O etc. and arene interactions in controlling the conformation of the molecule has been studied. The thesis consists of four chapters which are summarized below.

The first chapter of the present work deals with the synthesis of Triazolo[4,5-*d*]pyrimidine (**TP**) core based flexible symmetric polymethylene linker compounds for studying the effect of increasing the number of ring nitrogen in **PP** core on intramolecular and intermolecular π–π interactions.

The second chapter of the present work deals with the synthesis of Pyrrolo[2,3-*d*]pyrimidine (**PyP**) core based flexible symmetric polymethylene linker compounds for studying the effect of decreasing the number of ring nitrogen in **PP** core on intramolecular and intermolecular π–π interactions.

The third chapter of the present work deals with the synthesis of **PP** core based dissymmetrical *ethylene* linker compounds having Phthalazinone/Quinazolinone/ Benzotriazinone on the other end for studying the role of arene interactions in controlling the conformation of 1,2 diaryl ethanes.

The fourth chapter of the present work deals with the synthesis of **PP** core based dissymmetrical *polymethylene* and *butylidine* linker compounds having Phthalazinone/Quinazolinone/ Benzotriazinone on the other end for studying the conformation directing role of arene interactions in such molecules.

CHAPTER-1

Synthesis, ^{1}H NMR and X-ray crystallographic studies of triazolo[4,5-*d*]pyrimidine core based flexible symmetric polymethylene linker compounds

1.1 Introduction

Atoms and molecules can interact together leading to the formation of a molecule, by covalent interactions, or a molecular cluster, by noncovalent interactions. A covalent bond is formed when partially occupied orbitals of the interacting atoms overlap and a pair of electrons are shared by these atoms. Covalent bonds are shorter than 2 Å. In case of noncovalent interactions no such sharing of electrons takes place and these interactions act at distances of several angstroms. Non-covalent interactions were first recognized by J. D. van der Waals in the nineteenth century.[1] Since then it has now been recognized that non-covalent interactions are involved in a vast number of phenomena related to the whole realm of molecular and macromolecular science such as molecular recognition, drug receptor interactions, solvent effect in reactions and the ability of geckos to climb rapidly up smooth vertical surfaces, even flat glass.[2] Weak noncovalent interactions like stacking interactions (arene/π–π interactions), C-H….π, etc., unlike their stronger counterparts (for e.g. classical hydrogen bonding which are well characterized) are not well understood. Due to their weak nature they are difficult to observe in presence of stronger forces such as classical hydrogen bonding (involving two hetero atoms like O, N/S) and thus they are difficult to study both theoretically and experimentally.[2, 3] These forces often work together and their collective effect brings a change in molecular structure as well as in supramolecular structure. In nature where functions of biomacromolecules like proteins, enzymes, DNA, etc., which are directly related to their structure these weak forces play a very important role since easy formation as well as easy decomposition of molecular structures are required. These forces are sensitive to the environmental conditions and a slight change of conditions like temperature, pH etc., can bring about a significant change in conformation and hence function.

Interactions involving two or more aromatic groups are known as π–π interactions.[4] These are among the most important but least understood of the noncovalent interactions. Recent studies have provided new insight into the driving forces, stability and selectivity of these interactions. These interactions, though modest in energy, play a crucial role in such diverse areas as protein folding, base-to-base stacking in DNA/RNA, host-guest binding in supramolecular assemblies, crystal engineering, drug-receptor interactions and other molecular recognition processes.

1.1.1 The Nature and Geometry of Aromatic Interaction

The attraction between two aromatic residues present in the same or different molecules is known as arene–arene interaction or π–π interaction. The π–π interactions are weak in strength with the energy ranging from 0-50 kj/mol.[5] There are four types of π–π interaction geometries, face-to-face, edge-to-face, parallel displaced and Y-shaped (**Fig. 1a**).[6] Edge-to-face and parallel-displaced geometries are the most common geometries found in structural chemistry.[7]

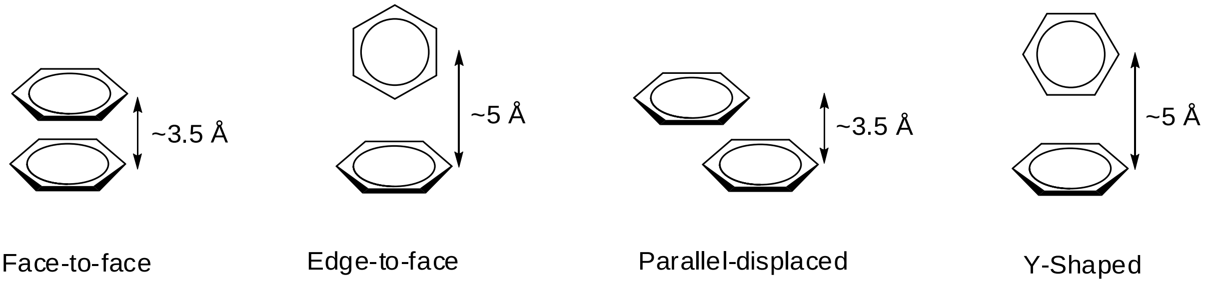

Figure 1a. Four types of π–π interaction geometries.

Computational studies on benzene dimer showed that the edge-to-face and parallel-displaced geometries are nearly iso-energetic with binding energy of about 2 kcal/mol.[8a,8b] Face-to-face stacked geometry is commonly observed with donor–acceptor pairs. The benzene-perfluorobenzene interaction is an excellent example of this type of aromatic interaction, and has been calculated to provide -15.5 kJ/mol stability.[8c] In addition, there are also continuums of intermediate geometries.[9a-9c] Different computational techniques used for studying non-covalent interactions, including π–π interactions have been reviewed recently.[10a]

There are four basic packing types for aromatic compounds reported in literature (**Fig. 1b**).[10b] In simple herringbone structure, the nearest neighbours are non parallel. In sandwich-herringbone packing, the herringbone motif is made up of sandwich-like diads. In the third type, called β, the main interactions are between parallel translated molecules. The fourth type, called γ is characterised by 'graphitic' planes.

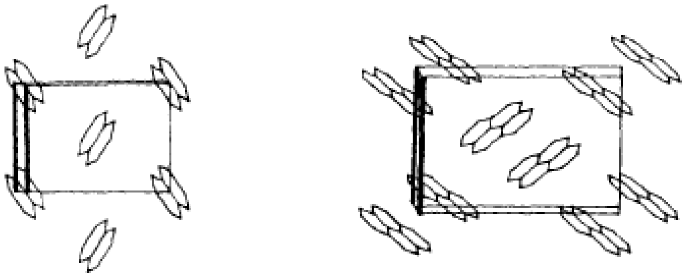

Simple-herringbone sandwich-herringbone

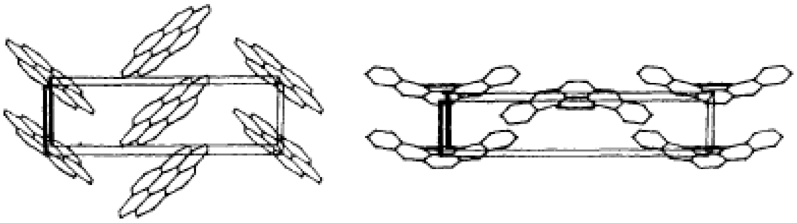

β-Type γ-Type

Figure 1b. Four basic packing types for aromatic compounds.

The nature of arene–arene interaction is still not well understood.[7, 11] Arene interactions have been proposed to consist of van der Waals, hydrophobic and electrostatic forces, however, and contribution and magnitude of each of these components may vary from case to case and is a matter of many investigations. Hunter and Sanders (1990) proposed an electrostatic model to explain the strong geometrical requirements for interactions between aromatic molecules.[12] They considered the σ-framework and the π-electrons separately and demonstrated that net favorable π–π interactions are actually the result of σ–π attractions that overcome π–repulsions. By using an idealized π–system, some general rules for predicting the geometry of favorable π–π interactions were derived. The electrostatic component has been proposed to arise from the interactions of the quadrupole moments of the aromatic rings. Though, benzene has no net dipole, it has an unequal distribution of charge, with greater electron-density on above and below the faces of the ring and reduced electron-density on the edge, which gives rise to the quadrupole moment. The edge-to-face and parallel-displaced geometries are stabilized due to electrostatic σ–π attraction while the face-to-face geometry is destabilized due to π–π repulsion (**Fig. 2**). Generally, electron withdrawing groups in aromatic rings reinforce while electron donating groups weaken π–π interactions. Presence of heteroatom in aromatic ring also reinforces the π–π interactions.

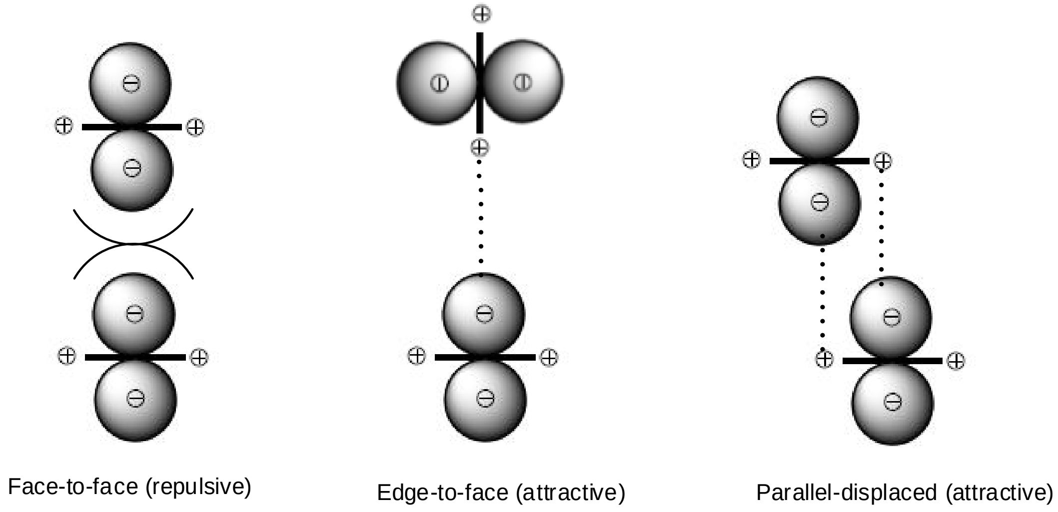

Figure 2. Electrostatic interaction between σ and π-systems of aromatic molecules.

For example, highly accurate quantum chemical computations revealed that benzene–pyridine and pyridine dimer bind more strongly than the benzene dimer in several configurations, and in contrast to the benzene dimer, parallel-displaced configurations can be significantly preferred over T-shaped configurations.[13]

Recently, it has been found from the survey of crystallographic data stored in Cambridge crystallographic database that the stacking interactions in crystals of simple aromatic hydrocarbons become important only for molecules with more than three rings. [14] Whereas for crystals of nitrogen substituted heterocyclic aromatic molecule, the stacking interactions become important for doubly substituted single ring molecules itself. Generally speaking, the stacking is reinforced with the increasing number of nitrogen in the ring.[14] Substitution of the hydrogen atom of an aromatic hydrocarbon by an electron withdrawing atom like F, Cl etc. or an electron withdrawing group like NO_2 reinforces the stacking interactions.[14]

1.1.2 Importance of Aromatic Interactions

1.1.2.1 Aromatic Interactions in Biological Systems

Aromatic interactions are ubiquitous in nature. They are believed to provide stability to duplex DNA,[15] they have been proposed to contribute to the unique properties of thermophilic proteins,[16] they may play a role in aggregation of amyloid β in Alzheimer's disease,[17] and they are common motifs in bio-molecular recognition.

In DNA, aromatic interactions occur between adjacent nucleotides and increases the stability of the molecular structure. The nitrogenous bases of the nucleotides are made from either purine or pyrimidine rings, consisting of aromatic rings. Within the DNA molecule, the aromatic rings are positioned nearly perpendicular to the length of the DNA strands. Thus, the faces of the aromatic rings are arranged parallel to each other, allowing the bases to participate in aromatic interaction.

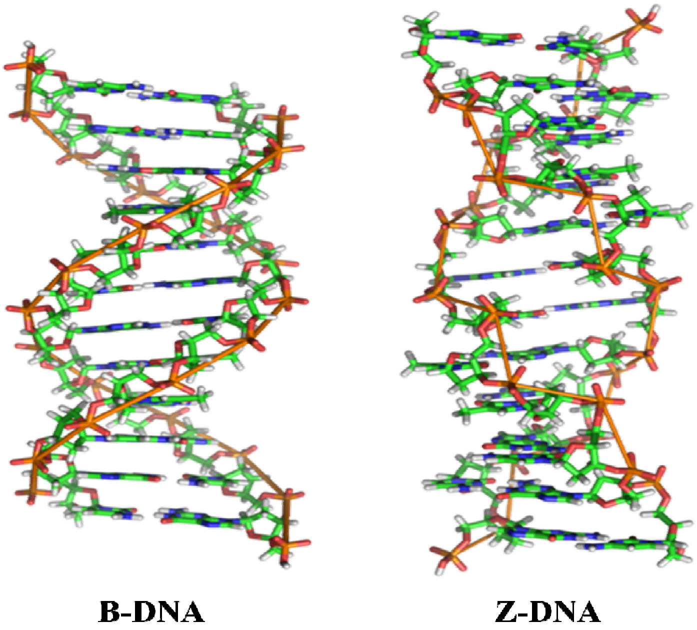

Figure 3. Base pair stacking in B and Z forms of DNA.

In their original X-ray crystallographic study involving 34 high-resolution protein structures, Burley and Petsko analyzed the frequency of aromatic pairs and their interaction geometry (distance and dihedral angle) and concluded that around 60 % of aromatic side chains of phenylalanine, tyrosine, and tryptophan were involved in arene interactions.[18] Aromatic rings separated by distances ranging from 4.5 to 7 Å and dihedral angles near 90° were found to be the most common. Pair-wise nonbonded potential energy calculations indicated that 54 % of the aromatic interactions are attractive by 1-2 kcal/mol. In a study of a larger database of 52 proteins, Hunter, *et al.* examined the orientational preferences of phenylalanine side chains in proteins using crytallographically derived atomic coordinates.[19] They observed that these interacting pairs are found in a wide range of T-shaped (edge-to-face) and parallel-displaced (offset-stacked) arrangements, but they are scattered over a wide variety of conformational space with no strongly preferred single orientation. McGaughey, *et al.* extended the analysis to a larger sample of proteins and suggested that the parallel-displaced geometry was a preferred orientation.[20] Remarkably, none of these two studies described the face-to-face geometry.

Aromatic-aromatic interactions between phenylalanine side chains in peptides have been probed by the structure determination in crystals of three peptides: Boc-Val-Ala-Phe-Aib- Val-Ala-Phe-Aib-OMe, I; Boc-Val-Ala-Phe-Aib-Val-Ala-Phe-Aib-Val-Ala-Phe-Aib-OMe, II; Boc-Aib-Ala-Phe-Aib-Phe-Ala-Val-Aib-OMe, III (Fig. 23).[21] X-ray diffraction studies reveal that all three peptides adopt helical conformations in the solid state with the Phe side chains projecting outward. Interhelix association in the crystals is promoted by Phe-Phe interactions. A total of 15 unique aromatic pairs have been characterized in the three independent crystal structures. The distances between the centroids of aromatic pair ranges from 5.11 to 6.86 Å, while the distance of closest approach of ring carbon atoms ranges from 3.27 to 4.59 Å. T-shaped and parallel-displaced arrangements of aromatic pairs were observed, in addition to several examples of inclined arrangements.

Aromatic π–π interactions not only determine biological structures but also modulate the physical properties of residues at enzyme active sites. In CuII-containing redox metalloproteins, the stacking of a CuII-coordinated His imidazole with a Phe side chain in the second coordination sphere affects the properties of the imidazole ring, such as its pKa value, the reduction potential E_m of the metal center, and the electron-transfer (ET) properties of the protein.[22] Intramolecular stacking between a phenyl ring and the pyridine ring of a nicotinamide derivative increases the basicity of the pyridine N atom by about 0.5 pKa units.[23]

1.1.2.2 Aromatic Interactions in Organic Synthesis

Arene–arene interactions can play a significant role in organic synthesis.[24] These interactions have been proposed to influence the yield and/or selectivity of different reaction types: intra- and intermolecular photochemical reactions, [25] allylic oxidations, [26] ruthenium-catalyzed transfer hydrogenations,[27] titanium-catalyzed oxidations of sulfides,[28] and others.[29]

Asymmetric di-hydroxylation of styrene (**1**) with optically active diamine (**2**) gave corresponding *R* diol (**3**) in 83% yield and 96% ee (**Fig. 4**).[30] The reason for enantioselectivity was favorable π–π interaction between the substrate and naphthyl group; exposing the *si* face to hydroxylation and shielding the *re* face for the attack.

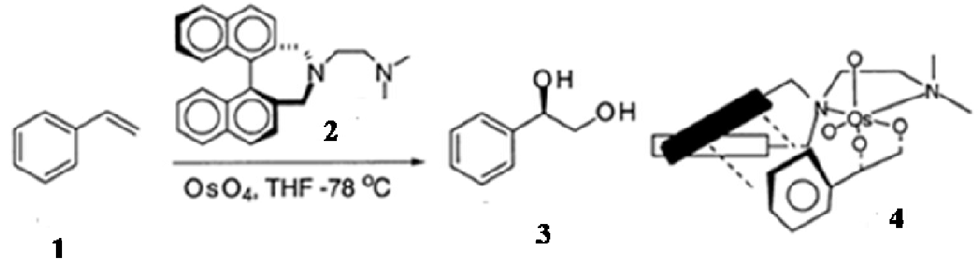

Figure 4. Enatioselective dihydroxylation of styrene.[30]

McIntosh *et al.* found that the benzylation of naphthyl cyclohexane (**8**) gave corresponding benzylated (**9**) product with >98% de. The de was attributed to the π–π interactions which in turn established an anti-gauche orientation for the enolate dianion (**Fig. 5**).[31]

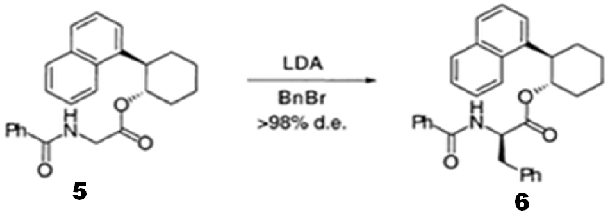

Figure 5. Diestereoselective benzylation.

Metal free Friedel-Crafts alkylation of substituted pyrrole (**7**) with cinnamaldehyde (**8**) in the presence of imidazolidinone catalyst (**9**) gave alkylated product **10 (Fig. 6**) in 97% ee. It was suggested that π–shielding of the cinnamaldehyde derived iminium ion (**11**) contributed to facial selectivity.[32]

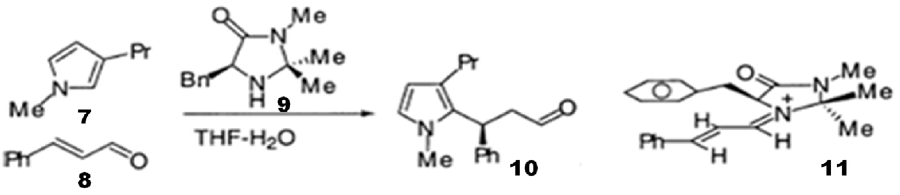

Figure 6. Enantioselective metal free Friedel-Crafts alkylation of substituted pyrrole.

The *exo*/*endo* ratio in epoxidation of compound **12** (**Fig. 7**) was significantly affected by the nature of the substituent present in phenyl ring. The proportion of *endo* product (**14**) increased with the increasing electron withdrawing tendency of the substituent. This result was rationalized by considering that the transition state (**15**) for *endo* product was stabilized by π–π interaction between phenyl ring of m-CPBA and substrate, and the stability of the transition state (**15**) was further enhanced by increasing electron withdrawing substituents.[33]

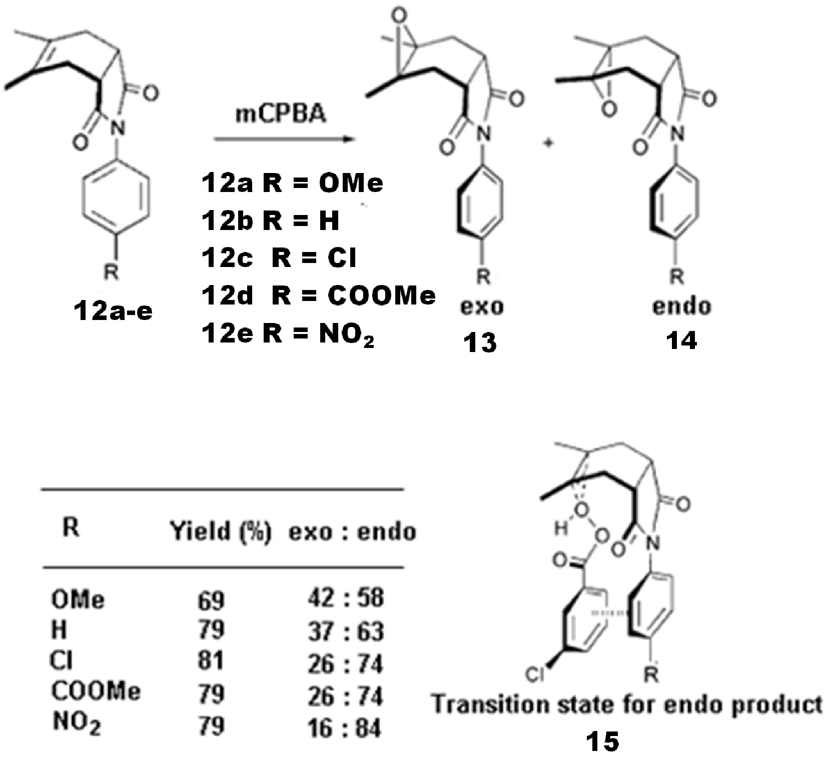

R	Yield (%)	exo : endo
OMe	69	42 : 58
H	79	37 : 63
Cl	81	26 : 74
COOMe	79	26 : 74
NO$_2$	79	16 : 84

Figure 7. Stereoselective epoxidation.

In asymmetric allylation of aromatic and heteroaromatic aldehydes (**16**) reaction rates were enhanced and enantioselectivity were observed for electron-deficient benzaldehydes, in comparison to phenyl or electron-donor-substituted aldehydes, when performing the reaction with a methoxynaphthalene bearing isoquinoline N-oxide catalyst (**18**).[34] This points to a role of arene-arene interactions between the reacting aldehyde and the catalyst. Additionally, the loss of selectivity when exchanging the solvent from dichloromethane to acetonitrile supports the role of aromatic interactions in the transformation. Enantioselectivity was further enhanced using an electron-rich trimethoxyphenyl N-oxide catalyst (**Fig. 8a**).

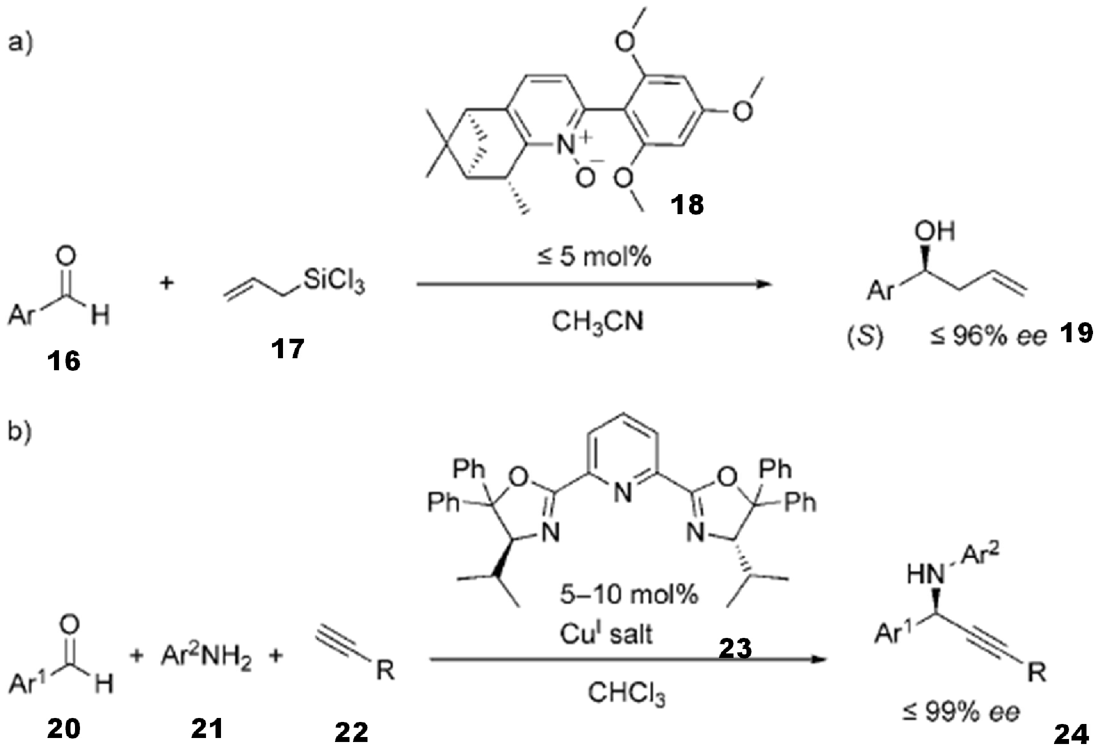

Figure 8. (a) Allylation of aromatic aldehydes with chiral pyridine- type N-oxides (b) For the three-component synthesis of propargylamines.

Aromatic interactions have also been proposed to influence the stereo chemical outcome in the synthesis of aromatic propargylamines (**24**, **Fig. 8b**).[35] A chiral CuI complex with a pyridine bis(oxazoline) ligand (**23**) was found to catalyze the reaction of aromatic aldehydes (**20**) with amines (**21**) and alkynes (**22**) to give propargylamines with high yield and enantioselectivity. In the postulated transition state, the ligand complexes the substrate in a manner which enables two edge-to-face and one aromatic stacking interaction, thus blocking one face from the attack of the copper acetylide.

1.1.2.3 Aromatic Interactions in Structure Based Drug Design

Aromatic interactions are one of the most important non-covalent interactions involved in binding of drug with receptor as majority of the drugs are aromatic and the concentration of aromatic amino acid residue is particularly high in the cavity of receptor. Thus, proper understanding of aromatic interaction is needed for structure based drug design. Aricept (E2020, **25**) is a drug developed to treat symptoms of Alzheimer's disease. The X-ray crystallographic analysis of the complex of Aricept (E2020) with the enzyme acetyl cholinesterase revealed π–π, OH…π, and cation–π interactions as major forces that stabilize the association (**Fig. 9**).[36]

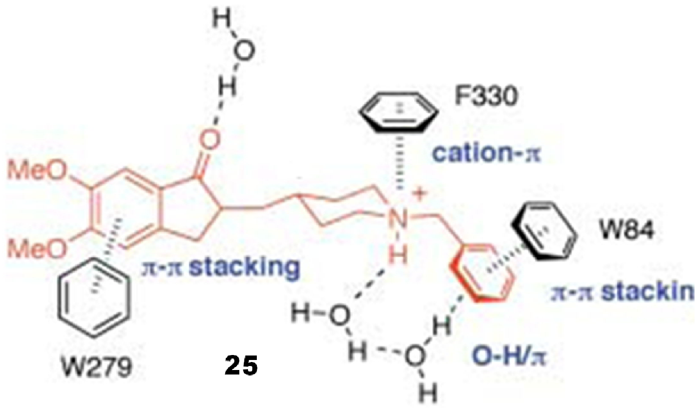

Figure 9. Binding mode of the anti-Alzheimer drug E2020 within the active site of acetyl cholinesterase from Torpedo californica.

Aromatic interaction plays a pivotal role in intercalation of drugs into DNA.[37] The intercalation prevents DNA replication by inhibiting topoisomerase enzyme. The DNA intercalators contain aromatic residue which intercalate between DNA base pairs and the intercalator-DNA complex is stabilized by π–π interaction between aromatic residue of intercalator and nitrogenous bases of DNA. For example, daunomycin (**26**, **Fig. 10**) is a chemotherapeutic of anthracycline family which has been used since 40 years for the treatment of specific type of leukemia (acute myeloid

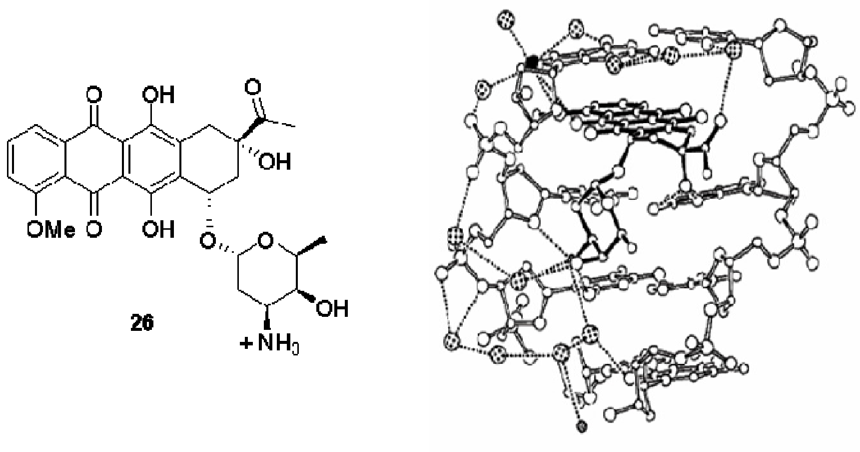

Figure 10. Daunomycin (26) and Daunomycin-DNA complex d (CGATGC).

leukemia and acute lymphocytic leukemia). Structural study showed that it bound to the DNA preferentially via intercalation between GC base pairs in triplet sequences composed of two adjacent GC and CG followed by AT base pairs (**Fig. 7**).[37a] DFT calculation showed that the complex gained 2/3 of its overall stability from π–π stacking interactions.[37b]

The anti cancer drug 1843U89 (**3**) binds the active site of thymidylatesynthase and inhibits the transformation of dUMP to dTMP which is essential for the production of DNA. X-Ray structure of ternary complex revealed that the drug interacted with active site and dUMP through aromatic interactions (**Fig. 11**).[38]

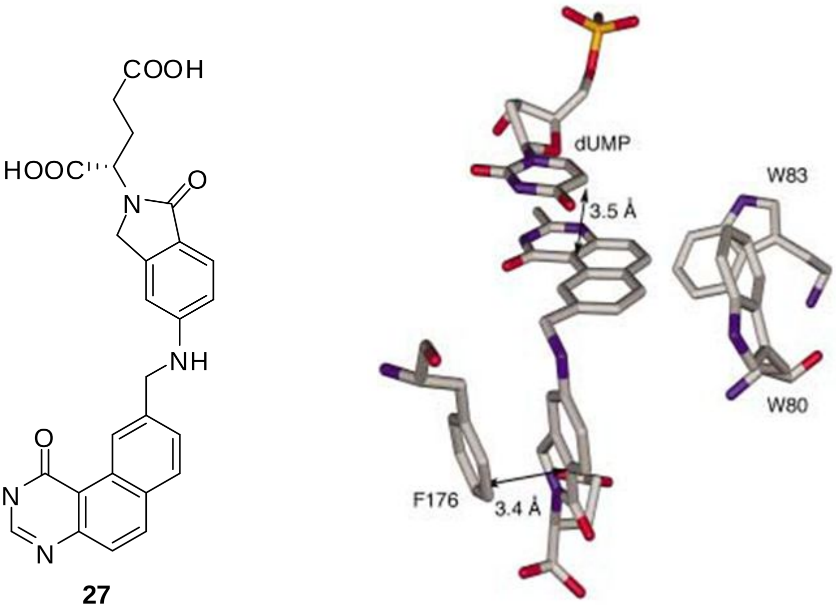

27

Figure 11. Aromatic Interaction between dUMP and the anticancer drug 1843U89 bound at the active site of thymidylate synthase.

1.1.3 Models used for studying aromatic interactions

Due to the weak nature of aromatic interactions it is very difficult to study these types of interactions both experimentally and theoretically. In biological systems where other stronger interactions like classical hydrogen bonding coexists with these weak interactions it is not possible to study the role played by these interactions. Thus, small molecule model systems have been developed to study arene–arene interactions in simpler and more controlled environments. This has been documented in several reviews.[4,39] The following section highlights some of the flexible models used in the literature for the study of aromatic interactions.

One of the major advantages using the flexible models is that flexible systems can relax into the optimum geometry for aromatic π–π interaction and therefore provide a better opportunity to characterize the geometrical preferences caused by these interactions. In this regard, Browne *et. al.* pioneered the use of *polymethylene* linker, especially a *trimethylene* linker for studying stacking interactions among nucleic acid bases. (**Fig. 12**).[40a]

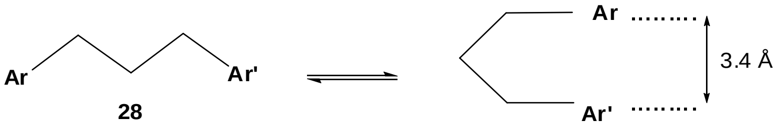

Open Conformation Closed conformation

Where Ar and Ar′ are 9-substituted adenine or guanine or
1-substituted cytosine, thymine or uracil residues

Figure 12. Browne *et al.* model.

Nucleic acid bases containing purines and pyrimidines are stacked one above the other in nucleic acids with a distance of 3.4 Å between adjacent bases. The use of *"trimethylene linker"* is based on the fact that it gives a desired distance of 3.4 Å if two aromatic systems are stacked when connected by it. This linker at the same time does not dictate stacking, as in the absence of stacking interactions the molecule may remain open. They synthesized a series of twelve di-nucleotide analogs in which the bases are connected by a *trimethylene* chain, $B\text{-}(CH_2)_3\text{-}B'$, where B and B′ are 9-substituted adenine or guanine or 1-substituted cytosine, thymine or uracil residues (**Fig. 13**). These compounds were studied optically at concentrations low enough to preclude formation of intermolecular complexes so that the perturbations associated with the 1:1 interaction of a pair of bases could be characterized, namely by UV spectra in aqueous solution at r.t. and by emission spectra in 1:1 ethylene-glycol-waterglass in the vicinity of 77ºK. In the series of $B\text{-}(CH_2)_3\text{-}B'$ the order of interaction in neutral aqueous solution is purine-purine > purine-pyrimidine > pyrimidine-pyrimidine as judged by hypochromism (decrease in integrated UV absorption intensity of $B\text{-}C_n\text{-}B'$ compared with equimolar $B\text{-}(CH_2)_2\text{-}CH_3$ and $B'\text{-}(CH_2)_2\text{-}CH_3$). The length of *polymethylene* chain was also changed to C_2 and C_6. In a series of 9,9′-polymethylene-bis(adenines) the order of interaction deduced from hypochromism and emission studies was n = 3 > 2 & 6. Reduced interaction at n = 2 reflected the impossibility of this molecule assuming folded, parallel-plane conformation which would allow maximal interaction as in Ad-C_3-Ad. An entropy effect was probably responsible for decreased interaction in the n = 6 compound relative to n = 3.

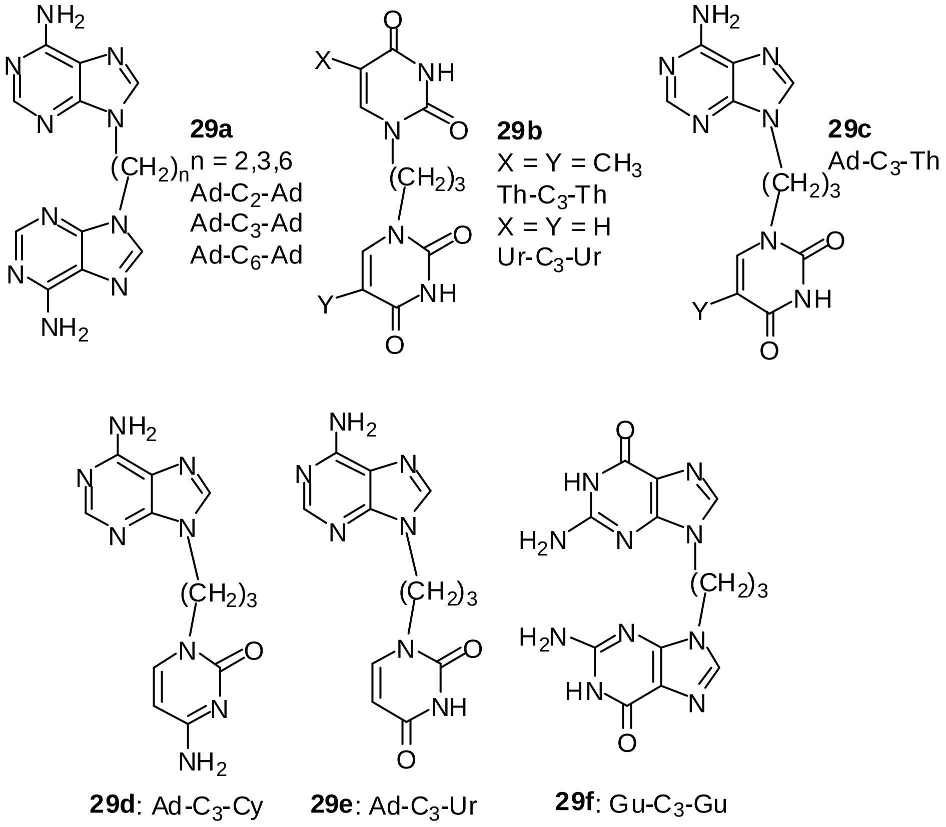
29a n = 2,3,6
Ad-C_2-Ad
Ad-C_3-Ad
Ad-C_6-Ad

29b X = Y = CH_3
Th-C_3-Th
X = Y = H
Ur-C_3-Ur

29c Ad-C_3-Th

29d: Ad-C_3-Cy

29e: Ad-C_3-Ur

29f: Gu-C_3-Gu

Figure 13. Dinucleotide analogs connected by polymeyhylene linker.

The orientation effect studies were done by Leonard and Ito by synthesizing six different trimethylene-bis(adenine) isomers having different positions of attachment to the terminal adenines and therefore having differently oriented ring-axis permissible in their stacked conformations, in order to determine stacking interactions between two parallel adenine rings oriented at different axis angles toward each other (**Fig. 14**).[40b] The percent hypochromism '*H*' for the long wavelength UV absorption band for each of these compounds has been determined by comparison of the UV spectrum of trimethylene-bis-adenine in aqueous solution with the composite spectrum of the two half molecules, the appropriate propyl-adenines. The '*% H*' follows a dependence upon the folded conformations available to the individual trimethylene-bis(adenines).

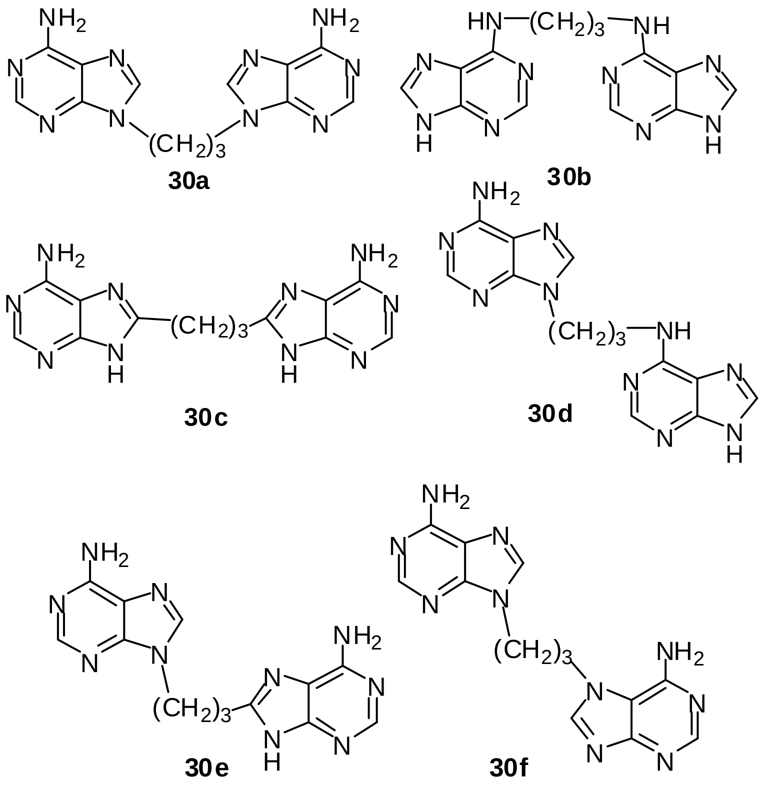

Figure 14. Dimers of adenine linked through different positions to study orientation effect on stacking.

Later on, Leonard (1979) reviewed *trimethylene* bridged flexible diaryl compounds showing stacking interactions in solution, however, no single X-ray structure of such compounds was reported in this review.[40c]

Since these initial reports, various studies have been directed towards modeling aromatic interactions using this methodology. In this context, compounds having *polymethylene* chains or other linkers between two adenine rings or between adenine and aromatic molecules such as other nucleic acid bases, indole, flavin, DNA intercalating molecules and naphthalene have been studied as model compounds for the stacking interactions. Bis(theophyllin-8-yl)propane (**32, Fig. 15**) is considered as the first *trimethylene* linker compound to show intramolecular APPI in solid state with extensive hydrogen bonding.[41] Here it is important to mention that this compound belongs to biologically important xanthine class which is well known for face-to-face intermolecular stacking by X-ray crystallography.[42]

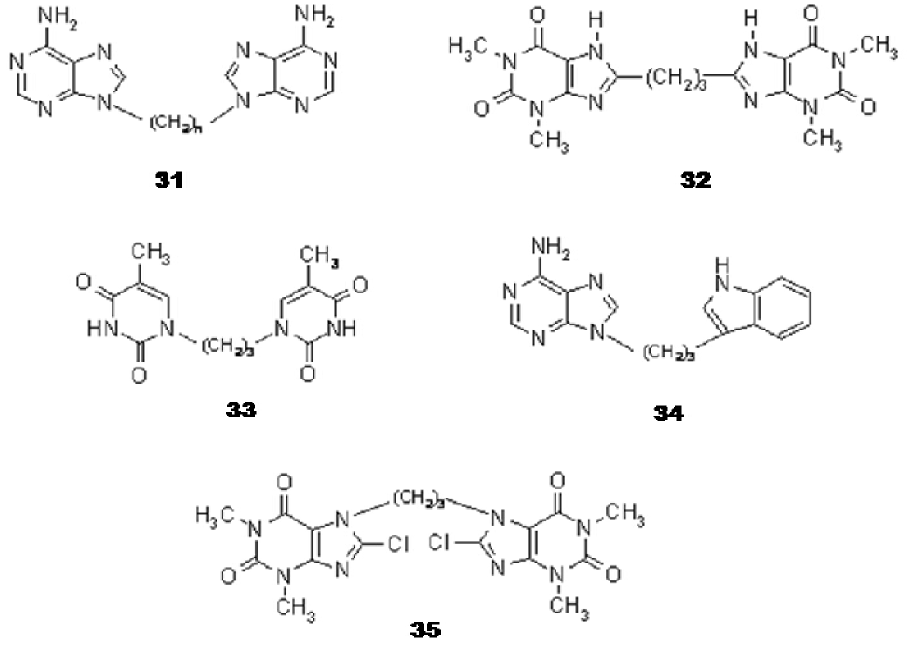

Figure 15. Different *trimethylene* linker compounds in the literature.

Bis-thymine (**33, Fig. 15**) is another related compound which shows intramolecular APPI in X-ray structure though with extensive H-bonding.[43] Compound **34 (Fig. 15)** shows intramolecular APPI by UV studies,[44] however, **34 (Fig. 15)** and its methyl iodide salt failed to show any intramolecular APPI when studied by X-ray crystallography.[45,46] Avasthi *et al.* have reported Xray crystal structure of 1,3-bis(8-chlorotheophyllin-7-yl)propane (**35, Fig. 15**) which is closely related to **32** but does not have ionizable protons like **32**, without any intramolecular

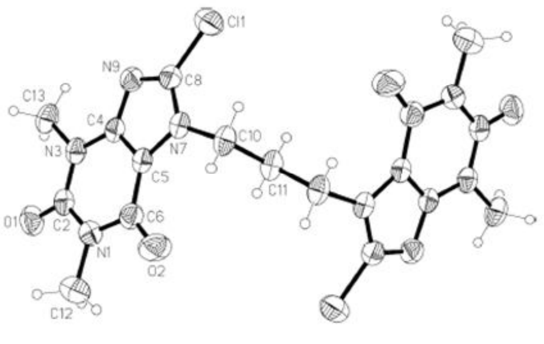

Figure 16. ORTEP diagram of **35** showing open conformation.

folding (**Fig. 16**).[47] It is important to mention that in compounds **31**, **33** and **35** the *propylene* linker is between two N atoms while in **32** it is positioned between two C atoms and finally in **34** it is between one N and one C atom.

Similar linear *polymethylene* linkers have been utilized by Itahara to investigate stacking interactions between various purine, pyrimidine and xanthine bases in solution by ^{1}H NMR. Some of the systems (**36**-**40**, **Fig. 17**) studied by Itahara are shown below.[48, 49,50] The N^6-methylation was found to increase the population of intermolecular aggregates in the buffer solution at pD 7.0 and had an additive effect on aggregation which was interpreted due to hydrophobic effect of the N^6-methyl groups. The aggregation of **36a** and **36b (Fig. 17**) was found to depend on the length of the *polymethylene* chains.[50] A relationship between the chemical shifts of adenine and xanthine ring protons of 7-[-(6-aminopurin-9-yl)alkyl]-1,3-dimethylxanthines (**39**) and the number of carbons (n = 2-10) in their *polymethylene* chains has been compared with that of 1-[-(6-aminopurin-9-yl)alkyl]-3,7-dimethylxanthines (**40**) in the buffer solutions at pD 7.0, 1.0 and 13.0 and in organic solvents. The relationship of **39** is clearly distinct from that of **40**. The concentration dependence and the effects of temperature on

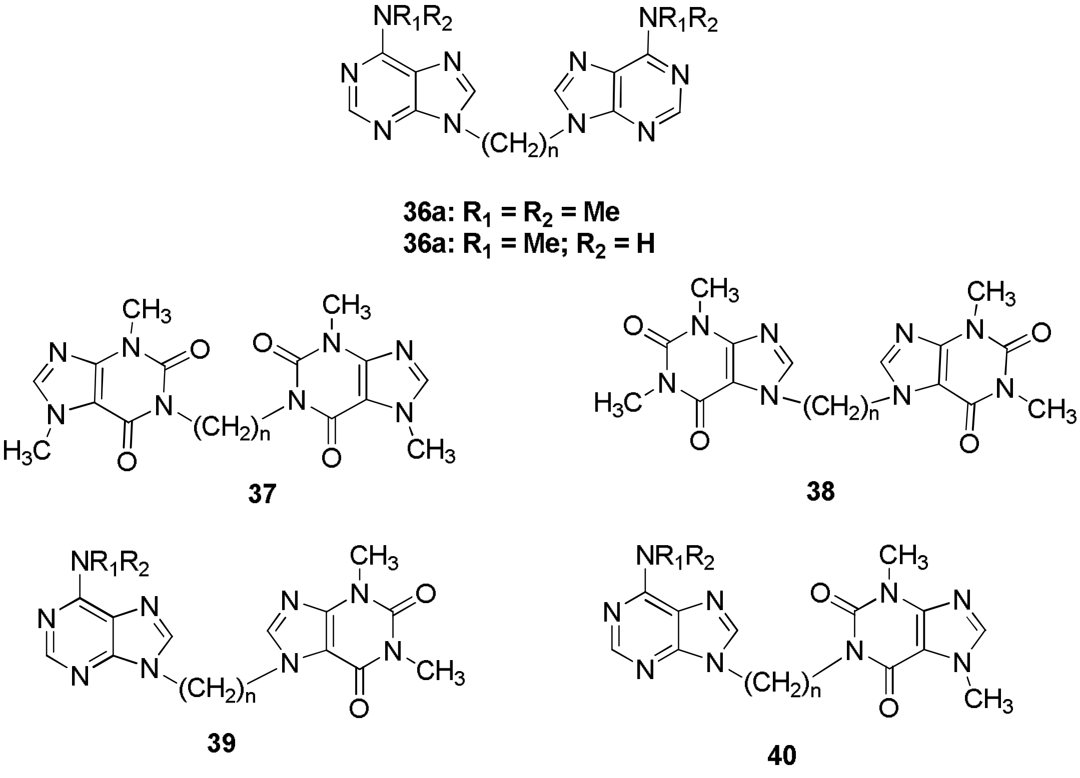
36a: $R_1 = R_2 = Me$
36a: $R_1 = Me; R_2 = H$

37

38

39

40

Figure 17. *Polymethylene* linker compounds of purine and xanthine bases used by Itahara.

the chemical shifts of **39** and **40** have also been investigated. While the upfield shifts of the ring protons of **39** and **40** in the buffer solutions at pD 7.0 and 13.0 are explained in terms of stacking interactions between adenine and xanthine rings, the results in the buffer solution at pD 1.0 may be due to cation–π interactions.

Zachariasse *et al*. reported synthesis of a large series of α,ω-bis(2-pyrenylcarboxy)alkanes (**41a-p, Fig. 18**).[51] Evidence for intramolecular pyrene dimers was obtained by ^{1}H NMR spectra showing shielding of all the aromatic protons with respect to model; 2-substituted pyrenes. The dimer (**41g-p, Fig. 18**) showed a symmetrical sandwich structure, whereas, the dimers (**41a-f, Fig. 17**) attributed geometry in which the pyrenyl moieties were shifted along their long axis. Intramolecular aromatic π–π stacking was also reported in closely related compound **42 (Fig. 17)**.[52]

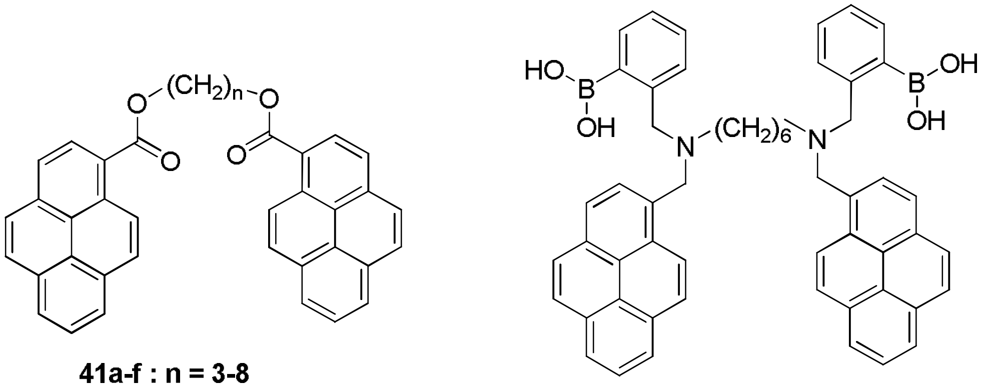

41a-f : n = 3-8
41g-p: n = 9-16, 22, 32

42

Figure 18. *Polymethylene* linked pyrenyl compounds.

A number of models containing quinolines (model for antimalarial drug chloroquine),[53] proflavin,[54] and acridine (model for quinacrine),[55] have been synthesized in which the aromatic part of the drug is linked to the base by *polymethylene* chains of varying length. The degree of stacking in water and geometries of intramolecular complexes were determined by using UV, ^{1}H NMR and fluorescence spectroscopy. Among all the synthesized models, strongest interactions were observed in acridine series. The model compound **43a (Fig. 19**) in which acridine ring of quinacrine is linked to adenine by a "*trimethylene bridge*" exists totally as a folded conformation in water.[55] Constant *et al.* synthesized related compounds (**43d-i**) and

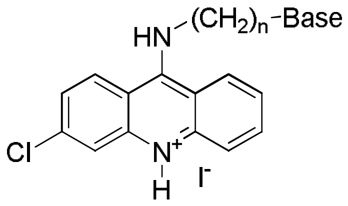

43a-c : n = 3,5,6; Base = 9-adenyl
43d-f: n = 3,5,6; Base = 9-thymyl
43g-i: n = 3,5,6; Base = 9-guanyl

Figure 19. *Polymethylene* linked quinacrine compounds.

found that all molecules exist mainly in folded conformations in water in the temperature range 0-90°C.[56]

PUVA therapy, a photochemotherapy employing psoralen and UVA, has been used for a long time in the treatment of a number of skin disorders, such as psoriases, vitiligo, mycosis fungicides, chronic leukemia, and so on. In this, formation of an intercalated complex between psoralens and DNA is an important step, which markedly affects the successive covalent photobinding to the macromolecule. In order to investigate these processes, some of synthetic models related to DNA-intercalating molecules were prepared. Decout *et al.* prepared a series of psoralen-O-$(CH_2)_3$-adenine **(44, Fig. 19**) and 8-methoxypsoralenadenine (**45, Fig. 19**) and showed that *polymethylene* bridges allow intermolecular ring-ring stacking between the two aromatic units.[57] The model **44** showed the highest value of hypochromism indicating most

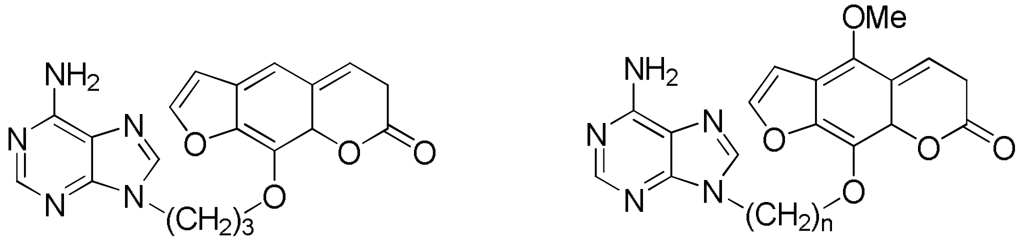

44

45a-d: n = 2,3,5,6

Figure 20. *Polymethylene* linked quinacrine compounds.

efficient ring-ring stacking between the two aromatic units linked by four atoms **45a** showed much stronger fluorescence than all other compounds **45b-d** indicating that the complexes adopt different preferred geometries according to chain length.

Hydrophobic effect has a significant influence on aromatic interactions since water molecules prefer to interact with itself rather than with aromatic surfaces. Newcomb and Gellman carried out a series of experiments to investigate this effect for two covalently tethered aromatic groups. A comparison of the stacking tendencies of hydrocarbon (phenyl and naphthyl) and heterocyclic (adenine) rings in aqueous solution was carried out using ^{1}H NMR spectroscopy to study the conformational properties of carboxylate derivatives **46-50** (**Fig**. **21**).[58] Large negative shifts of the adenine protons of **46** were observed compared with the control **49**. This is indicative of an intramolecular aromatic interaction in **46**. In contrast, **47** and **50** have similar spectra which indicate that there is no intramolecular interaction for the di-naphthyl derivative. An X-ray structure of a phenyl derivative **51** showed the phenyl rings splayed far apart. In **48**, negative shifts on both rings indicate significant stacking. DMSO destroyed the interaction. If the

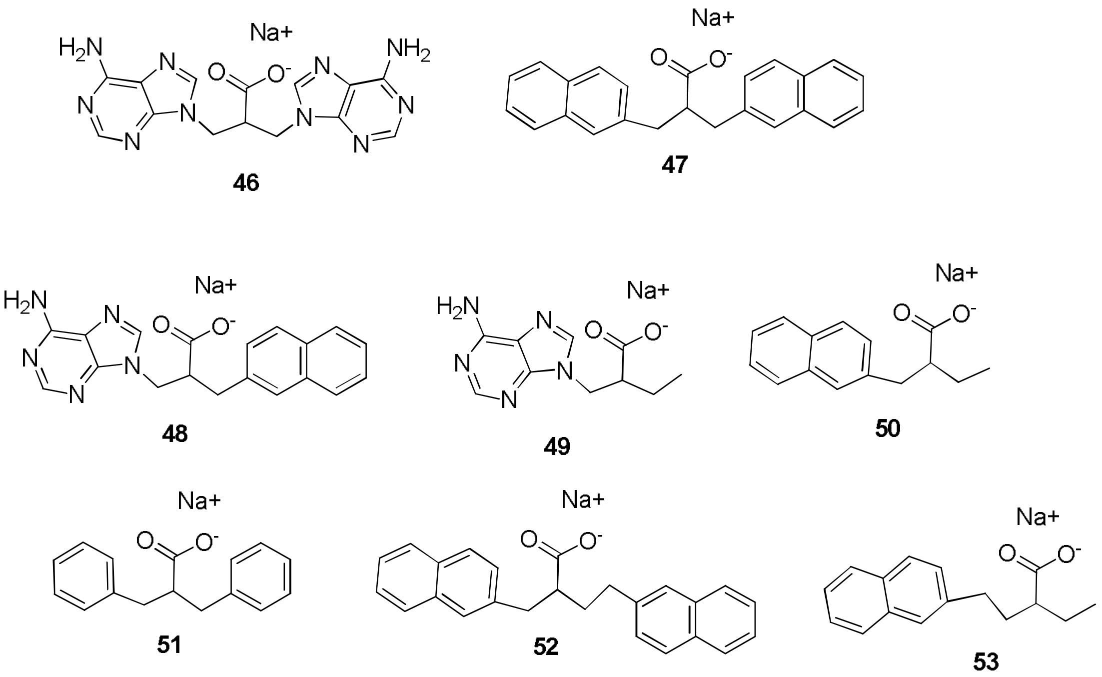

Figure 21. Compounds used to probe intramolecular aromatic interactions in water.

intramolecular stacking was due solely to the hydrophobic effect, then **47** would exhibit a stacking interaction. The results are most consistent with the alignment of partial positive and negative charges on neighbouring groups as the main force influencing the stacking interactions.

Naphthyl units connected by a flexible linker were prepared to further probe hydrophobic collapse.[59] The three atom linker previously used forced a near parallel arrangement, but the four atom linker in **52** allowed different approaches of the aromatic moieties. An X-ray crystal structure of **52** showed an edge-to-face arrangement of the naphthyl rings and ^{1}H NMR experiments showed that the naphthyl rings are in close proximity in aqueous solution. The chemical shift differences between **52** and **53** in benzene were very similar to those in water, which suggests that the hydrophobic effect have little influence on the folding of this molecule.

Herrandon *et al.* investigated intramolecular interactions between different aromatic groups in a series of di-esters consisting of two aromatic groups linked by a *2-methyl-1,3-propanedioxy* spacer by ^{1}H NMR study (**Fig. 22**).[60] This spacer permitted U-shaped conformations which placed the two terminal aromatic groups close together, parallel in a face-to-face arrangement. For the symmetrical di-esters **54** and **55** neither the chemical shifts of the aromatic group protons nor the vicinal coupling constants measured in the spacer provided any evidence for a high fraction of U-shaped conformers. In both the cases, the conformational distribution of the spacer was similar to that found for **59**, indicating that the planar aromatic groups in **54** and **55** experienced no significant mutual attractive interactions.

In contrast, substantial up-field shifts were observed in the resonance frequencies of all aromatic protons in the anthracenyl and 3,5-dinitrophenyl groups of the unsymmetrical di-ester **56** relative to those for the aromatic protons of the respective monoesters **57**, **58** and symmetrical di-esters **54** and **55**. Analysis of the temperature dependence of the vicinal coupling constants indicated highly populated gauche states of the two central C-C bonds of the spacer chain, consistent with a total fraction of U-shaped conformers of about 80% at ambient temperature. From the analysis of NOE experiments dinitrophenyl ring in **56** was found to be centered almost directly above the central ring of the anthracenyl group with a distance of 3.1 Å between the central point of the dinitrophenyl ring and the anthracenyl plane, and an angle of about 20° between the para axes of the two aromatic groups. The stabilization of the U-shaped conformers in **56** was rationalized in terms of quadrupole interactions between the two aromatic groups. The quadrupole moments associated with the two aromatic groups in **56** had opposite sign, resulting in a significant attractive interaction when the groups were oriented face-to-face. For the symmetrical diesters, **54** and **55**, the interacting aromatic groups had identical quadrupole moments and the interaction was repulsive in the face-to-face arrangement.

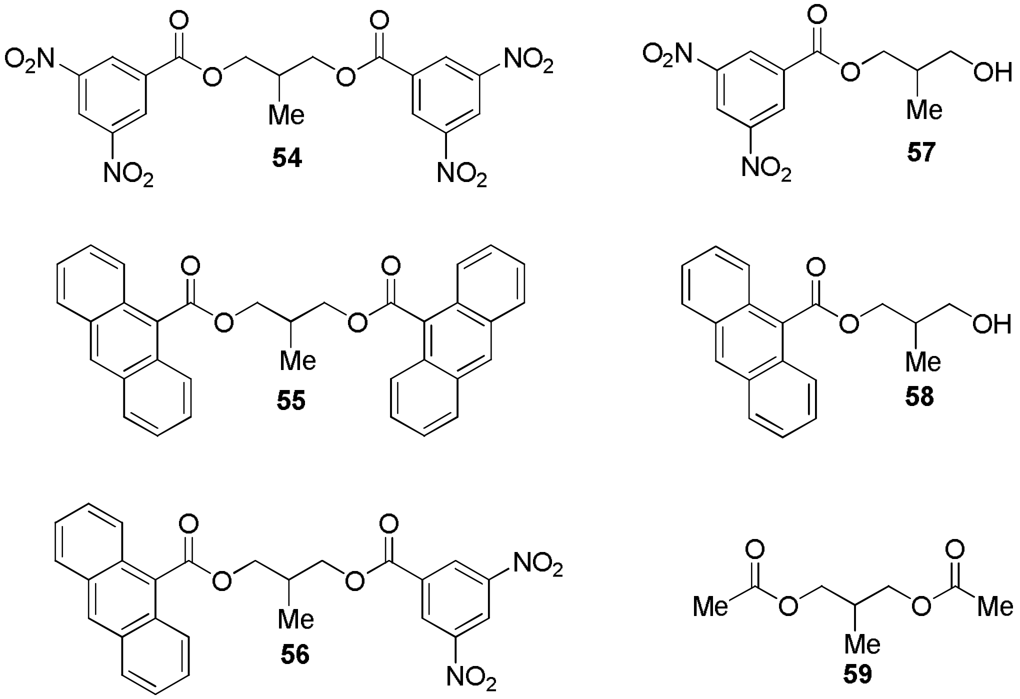

Figure 22. *2-Methyl-1,3-propanedioxy* spacer based diesters and monoesters.

To understand the driving forces of aromatic stacking interactions in water, Pang *et al.* (1999) performed conformational searches, molecular dynamics simulations, potential of mean force (PMF) and free energy perturbation (FEP) calculations, syntheses and ^{1}H NMR studies on sodium 2,2-bis(indol-1-yl-methyl)acetate (**60**).[61] The conformational searches on **60** revealed that the *isobutyric acid* linker allowed the molecule to adopt the tilted T-shaped stacked, off-center stacked, face-to-face stacked, and non-stacked conformations in a vacuum (**Fig. 18**). The PMF and FEP calculations suggested that the most thermodynamically stable conformers in water were the tilted T-shaped stacked and non-stacked conformers. The ^{1}H NMR result of **60** in D_2O and DMSO-d_6 at 22 °C revealed that both the tilted T-shaped stacked and nonstacked conformers were populated in D_2O and DMSO-d_6. Furthermore, population of the tilted T-shaped stacked conformation was greater in D_2O than in DMSO-d_6. These results, therefore, suggested that the hydrophobic effect played an important role in the stacking interaction of **60** in water. On the basis of the above study it was concluded that indole was not a good moiety for studying arene interaction.

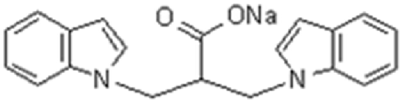

60

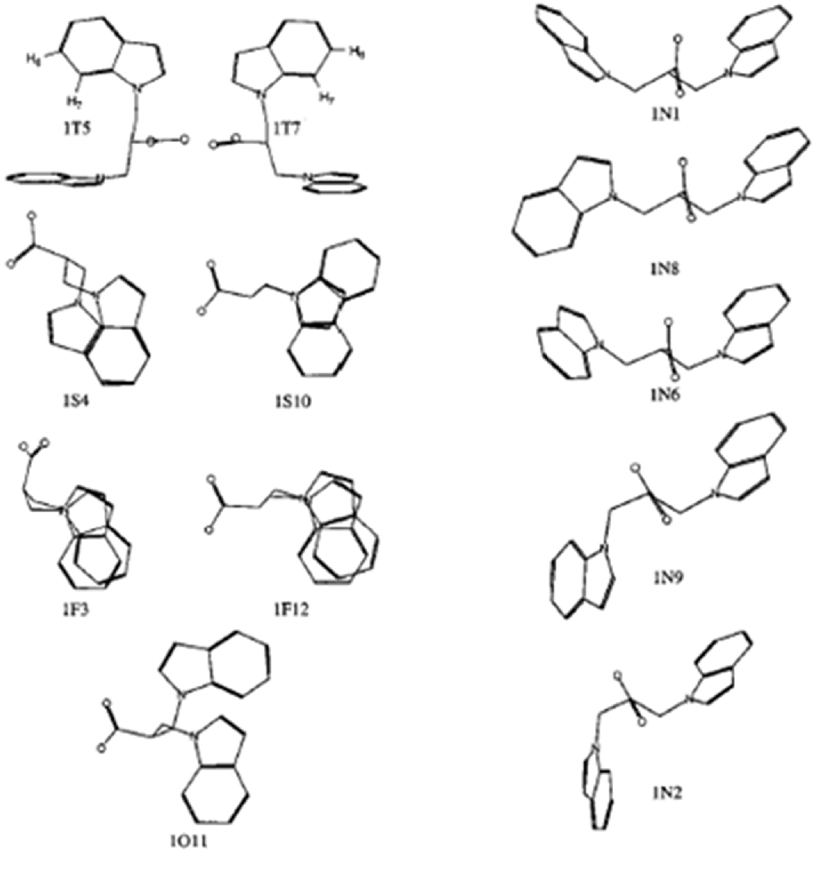

Figure 23. Conformations of **60** identified from the conformational search.

The research group at CSIR-CDRI, Lucknow has been working on pyrazolo[3,4-*d*]pyrimidine (PP) core based polymethylene, especially, *trimethylene* linker compounds for investigating the conformation directing roles of arene–arene interactions. In 1995, Avasthi *et al.* reported, for the first time, the use of PP ring system (**61**) which is isomeric with biologically significant purine (**62**) system for studying aromatic π–π interaction (**Fig. 24**).

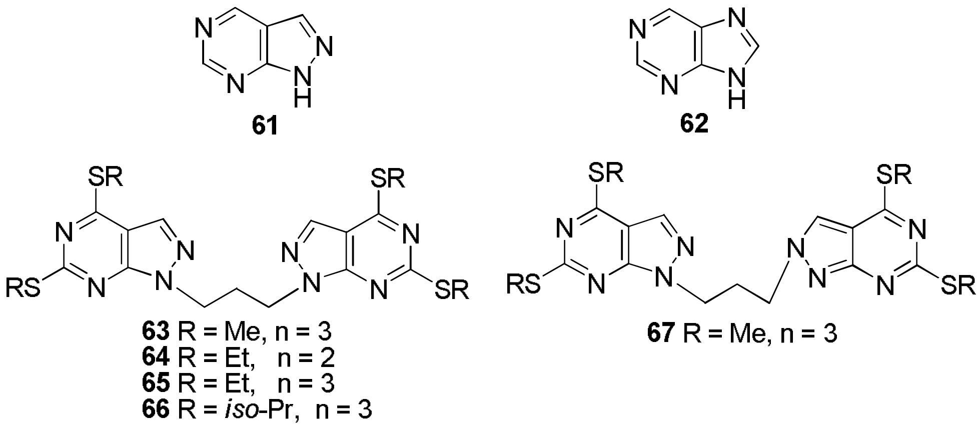

61

62

63 R = Me, n = 3
64 R = Et, n = 2
65 R = Et, n = 3
66 R = *iso*-Pr, n = 3

67 R = Me, n = 3

Figure 24. Pyrazolo[3,4-*d*]pyrimidine based *trimethylene* compounds.

The most important feature of these new fully flexible models is that they do not contain any strong ionizing groups such as OH, NH, NH_2, SH etc., capable of forming classical H-bonding. This strategy was devised so that contribution of weaker arene–arene interactions towards conformation control, if any, could be determined without interference of stronger conventional H-bonding. Synthesis of the 1,3-bis(4,6-dimethylsulfanyl-1*H*-pyrazolo[3,4-*d*]pyrimidin-1-yl)propane (**63**, **Fig. 24**) was reported as the first example based on PP core which showed unusual intramolecular arene–arene stacking interactions in solution by ^{1}H NMR data analysis.[62]

This unusual folding was due to intramolecular stacking as confirmed by X-ray crystallographic studies. The X-ray crystal structure revealed that **63** was folded at the centre of the *trimethylene* bridge to form an unusual *U-motif* and the two PP rings were nearly planar with an angle between the least-squares planes of 13.2° (ORTEP diagram shown in **Fig. 25**).[63] The centroids of these two interacting moieties are represented as X1A and X1B. The X1A to X1B distance is 3.71 Å which confirms that the two aromatic moieties are stacked due to intramolecular π–π interaction.

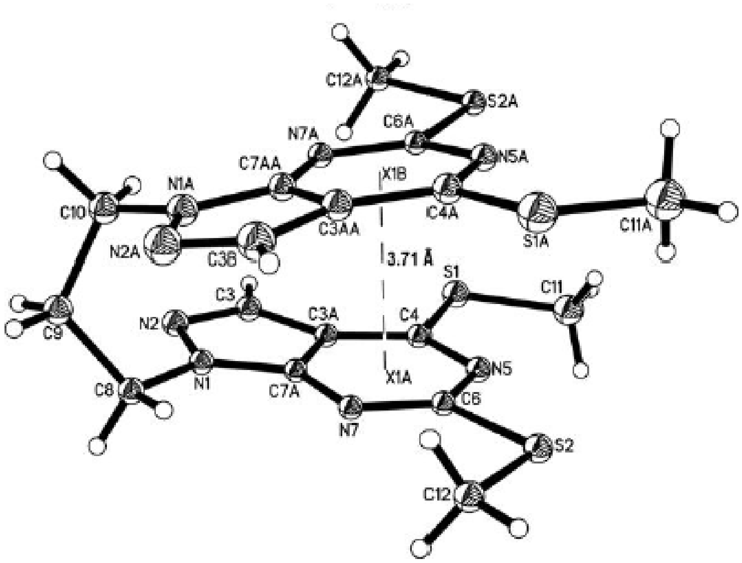

Figure 25. ORTEP diagram of **63** with atomic numbering scheme.

Robustness of the unusual *U-motif* formed due to intra-molecular stacking in **63** was further confirmed in ethyl- (**65**)[64] and *iso*-propyl analogs (**66**)[65] as shown in **Fig. 26** and **27** respectively. Interestingly, while all the three compounds showed unusual *U-motif*, only **63** and **65** showed comparable intermolecular stacking.

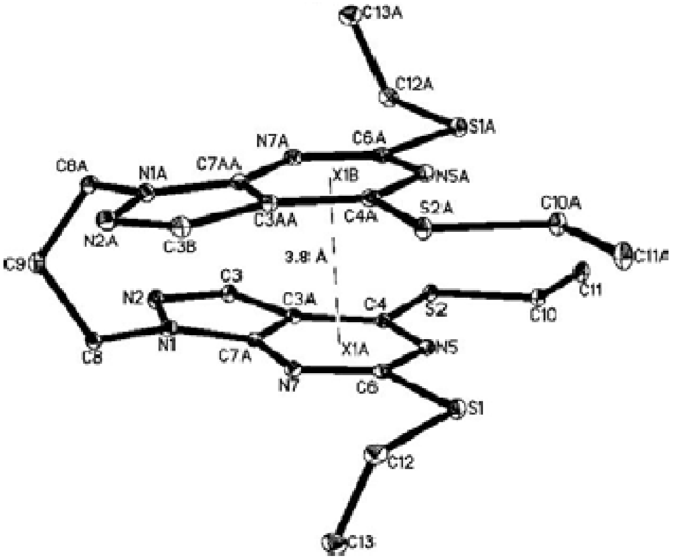

Figure 26. ORTEP diagram of **65** with atomic numbering scheme.

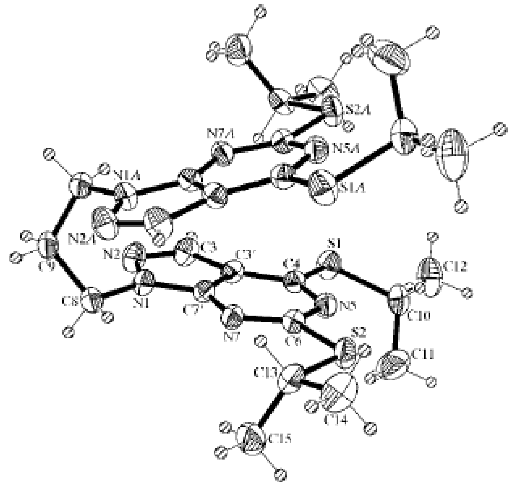

Figure 27. ORTEP diagram of **66** with the atomic labeling scheme.

The most striking effect of the bulky *iso*-Pr group in **66** was the disappearance of intermolecular π–π interaction and appearance of an intermolecular CH…π interaction between methyl of an *iso*-Pr group and the PP ring of the adjacent molecule (CH…π = 3.12 Å) (**Fig. 28**).

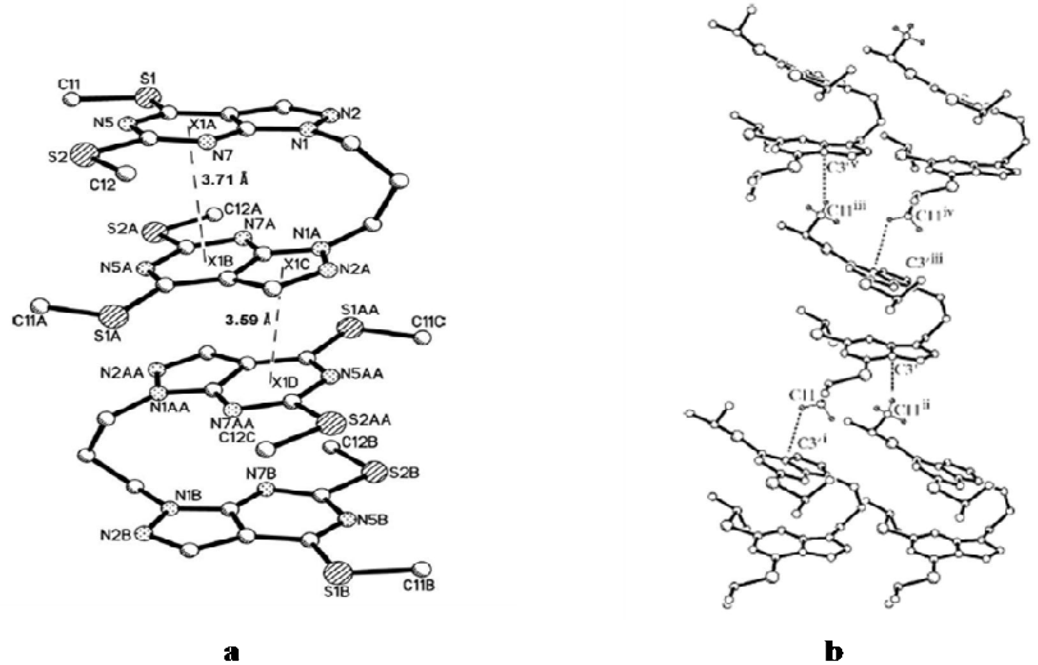

a

b

Figure 28. (a) Packing diagram of **63** showing intermolecular stacking between pyrazolo and pyrimidino rings. (b) Crystal-packing diagram of **66** showing the intermolecular CH…π stacking interactions (dashed lines).

Surprisingly, compound **67**, which was positional isomer of compound **63**, did not show intramolecular stacking by X-ray crystallography (**Fig. 29**).[66] Thus, indicating that proper positioning of the *trimethylene* linker to achieve proper orientation of two involved arenes was crucial and mere presence of a *trimethylene* linker was not enough to show intramolecular stacking in dissymmetrical arene system.

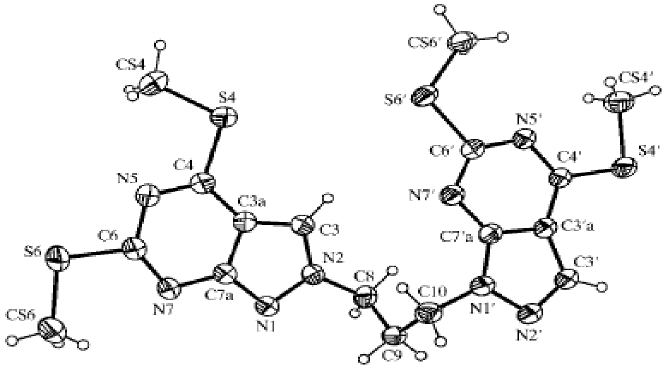

Figure 29. ORTEP diagram of **67** showing open conformation.[41]

Avasthi *et al.* later on reported synthesis[67] and X-ray structures of **69**[68] derived from **63** via intermediate **68** (**Fig. 30**). Proton NMR data analysis of this compound like earlier compounds (**63**, **64** and **65**) indicated intramolecular stacking.[66] Formation of the unusual *U-motif* due to intramolecular stacking was also confirmed by X-ray crystallography. Intramolecular folding and dimerization of the molecule due to CH…O interaction are shown in **Fig. 31**. Significance of *trimethylene* linker for facilitating intramolecular stacking, from crystal engineering point

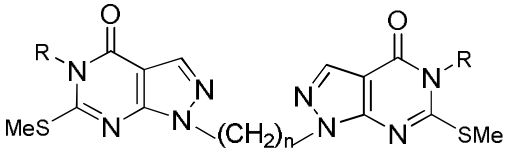

68: R = H, n = 3
69: R = Me, n = 3
70: R = Me, n = 4
71: R = CH_2Ph, n = 3

Figure 30. Homolog of **63** and compounds derived from **63**.

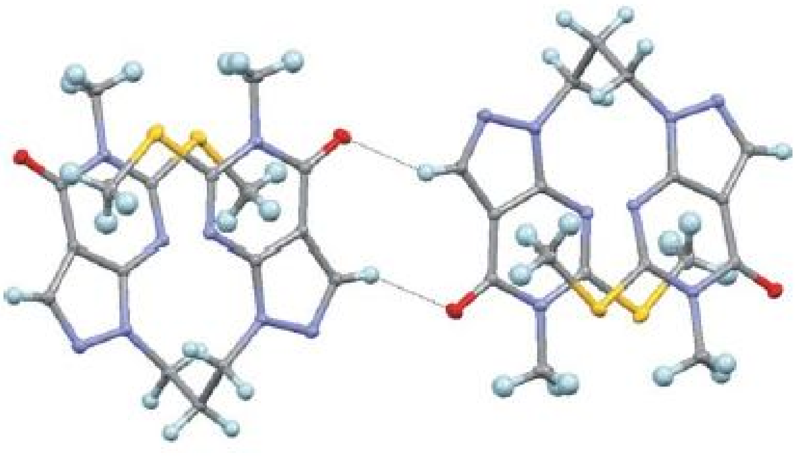

Figure 31. Dimerization of the molecule **69** due to CH…O interaction.

of view was further highlighted by the fact that **70**, a higher homolog of **64**, did not show any intramolecular stacking by ^{1}H NMR data analysis[67] and in fact a fully extended, normally expected, conformation was observed by X-ray crystallography[69] (**Fig. 32**).

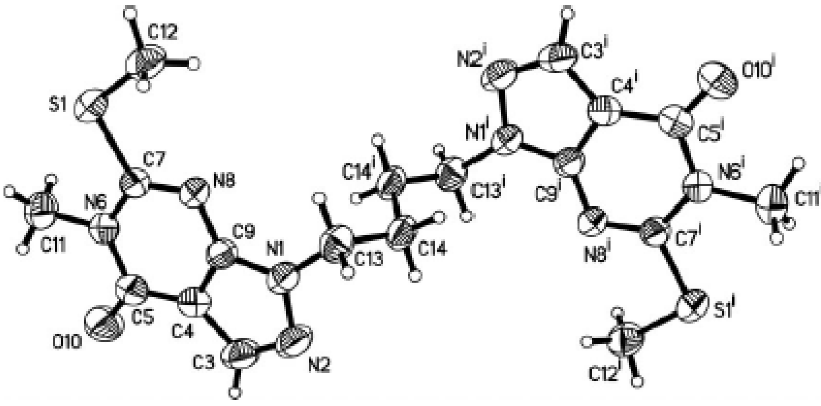

Figure 32. Displacement ellipsoid plot (50% probability), showing the molecular structure of **70** with the atomic labeling scheme.

Later on the first pair of two isomeric, dissymmetric *trimethylene* compounds **72** and **73** (**Fig. 33**) based on PP was reported by Avasthi *et al.* (2006).[70] Compound **72** showed folded conformation in solution as well as in solid state due to π–π interaction while **73** was open in solution. The same group synthesized dissymmetrical *trimethylene* compound **74** by replacing one PP core of the first compound **63** by triazolo[4,5-*d*]pyrimidine based residue for NMR and

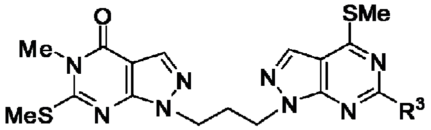

72

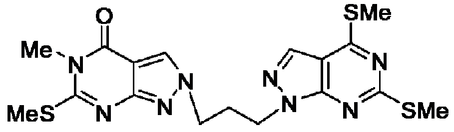

73

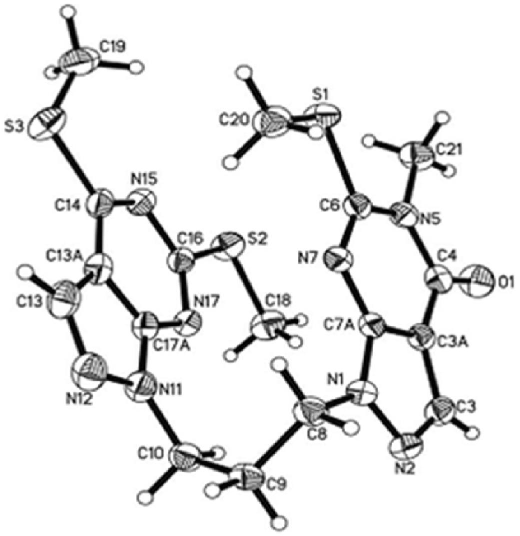

72

Figure 33. ORTEP Diagram of **72** (at 30% probability level) with atomic labeling scheme.

X-ray crystallographic study.[71] The compound was folded both in solution and solid state due to intramolecular π–π stacking interaction (**Fig. 34**).

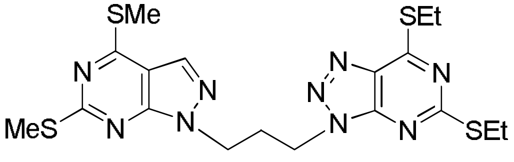

74

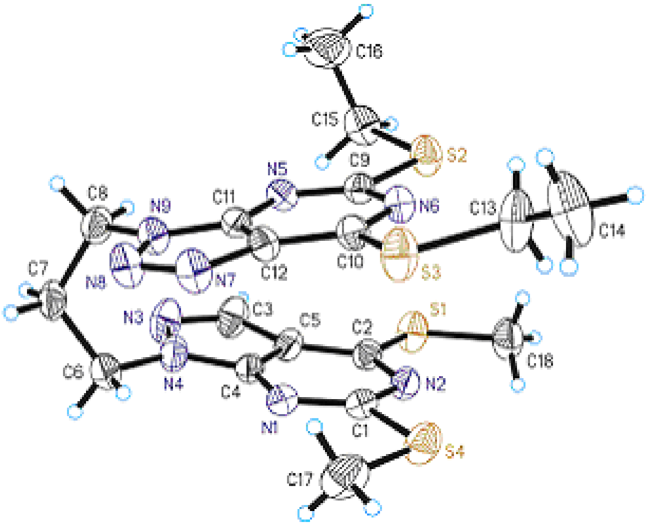

Figure 34. ORTEP diagram of **74** showing intramolecular arene–arene interaction.

To expand the generality and scope of the truly flexible models for studying arene interactions substituent effect were studied by the same group[72]

Recently, ^{1}H NMR, CD and X-ray crystallographic study on related PP core based *polymethylene* compounds (**75-76**, **Fig. 35**) have been reported by research group from BHU, India. These were folded in solution by ^{1}H NMR and CD studies, however, X-ray crystallography of **76a** showed an open conformation (**Fig. 35**).[73]

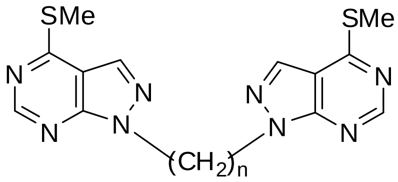

75a n = 2
76a n = 3

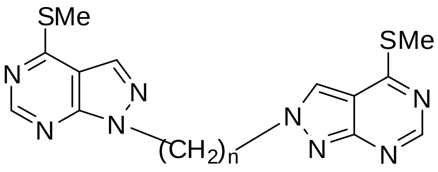

75b n = 2
76b n = 3

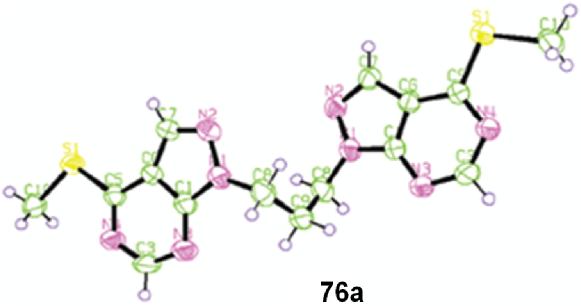

76a

Figure 35. 4-Methylsulfanylpyrazolo[3,4-*d*]pyrimidine based *ethylene* and *propylene* compounds.[73]

Brief review of the literature work on arene interaction shows that nature of such interaction is not well understood yet and more experimental and theoretical research needs to be done for their successful application to areas like stereochemistry,[24-33] supramolecular chemistry,[5,39] crystal engineering[76] and drug-development.[4]

In continuation of our work on PP core based *polymethylene* compounds for investigating the conformation directing roles of arene–arene interactions we wanted to see the effect of increasing the number of ring nitrogen in the pyrazole portion of pyrazolo[3,4-*d*]pyrimidine nucleus. In this chapter synthesis and characterization of triazolo[4,5-*d*]pyrimidine core based dissymmetric *polymethylene* compounds are reported. The results obtained by these studies can be applied for the purine related systems as this system can also be considered as 8-azaanalog of purine.

Due to its structural resemblance with the biological important purine nucleus triazolo[4,5-*d*]-pyrimidines (8-azapurines) are important molecules from biological point of view and are perceived to have useful properties as antimetabolites in purine biochemical reactions. In literature several triazolo[4,5-*d*]pyrimidine and triazolo[4,5-*d*]pyrimidine nucleosides have been synthesized and studied for its biological activities.[75] Thus these compounds have been studied as adenosine deaminase inhibitors.[75a] In vitro and in vivo studies of nickel complexes with triazolo[4,5-*d*]pyrimidine derivatives have been found active against *Trypanosoma cruzi* which causes Chagas' disease.[75b] Triazolo[4,5-*d*]pyrimidine derivatives have also been shown to inhibit phosphoinositide 3-kinases (PI3K) as well as mTOR (mammalian target of rapamycin).[75c] Studies have shown that these type of compounds can act as antagonists of the human A_{2A} adenosine receptor.[75d] In vivo studies in rats and dogs have shown affinity of triazolo[4,5-*d*]pyrimidine derivatives to bind to corticotropin-releasing factor receptor.[75e] Also nucleosides of triazolo[4,5-*d*]pyrimidine derivatives have been known to possess antiviral activity,[75f-g] and antitumor activity.[75g]

1.2 Objective

1. Synthesis, ^{1}H NMR and X-ray crystallographic study of triazolo[4,5-*d*]pyrimidines core based symmetric *polymethylene* compounds for studying arene interaction in solution and solid state.
2. To submit the compounds for biological activity.

1.3 Synthesis and characterization

[1,2,3]Triazolo[4,5-*d*]pyrimidines can in principle be synthesized by either a triazole-first approach (assembly of a suitably substituted triazole followed by cyclization) or the pyrimidine-first approach (assembly of a suitable substituted pyrimidine followed by cyclization). Both approaches have been described in the literature,[76] with the triazole-first approach particularly described in the published literature[77] and the pyrimidine-first approach described in the patent literature[78] (**Scheme 1**).

(i) Triazole-first approach:

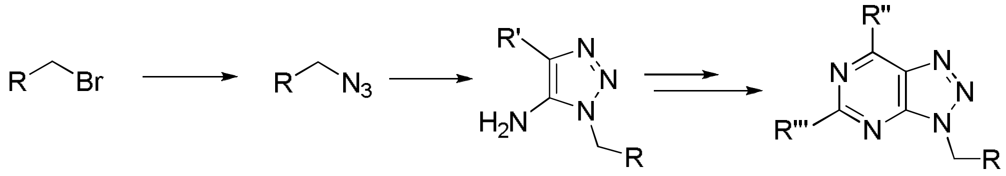

(ii) Pyrimidine-first approach:

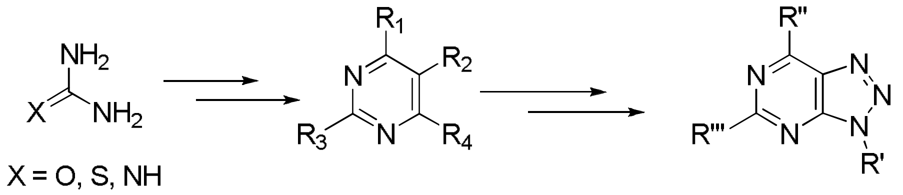

Scheme 1: Literature methods for the synthesis of triazolo[4,5-*d*]pyrimidine system.

1.3.1 Synthesis and characterization of 1,n-bis(5,7-bis(methylthio)-3*H*-[1,2,3]triazolo[4,5-*d*]pyrimidin-3-yl)alkane (82a-e, Scheme 2) and 3-butyl-5,7-bis(methylthio)-3*H*-[1,2,3]-triazolo[4,5-*d*]pyrimidine (87, Scheme 3).

For the preparation of dimers of triazolo[4,5-*d*]pyrimidines required for our study we first synthesized the triazolopyrimidine base using the procedures described in the literature.[79] The reaction of triazolo[4,5-*d*]pyrimidine with 1,3-dibromopropane gave very complex reaction mixture which was very difficult to separate through column chromatography. Moreover, the yield of the most important compound in our study 1,3-bis(5,7-bis(methylthio)-3*H*-[1,2,3]triazolo[4,5-*d*]pyrimidin-3-yl)propane **(82b)** which we were able to separate by repeated coloum chromatography and crystallization was very low (< 5%). So we decided to approach this problem through triazole first approach. This method has two advantage (i) only one isomer is obtained as product and that too the required compounds 1,n-bis(5,7-bis(methylthio)-3*H*-[1,2,3]triazolo[4,5-*d*]pyrimidin-3-yl)alkane **(82a-e)** in good yields (ii) purification of compounds, for synthetic purpose, column chromatography was not required**.** General Procedure for synthesis of 1,n-bis(5,7-bis(methylthio)-3H-[1,2,3]triazolo[4,5-*d*]pyrimidin-3-yl)alkane is shown in the following **Scheme 2** and described in experimental section.

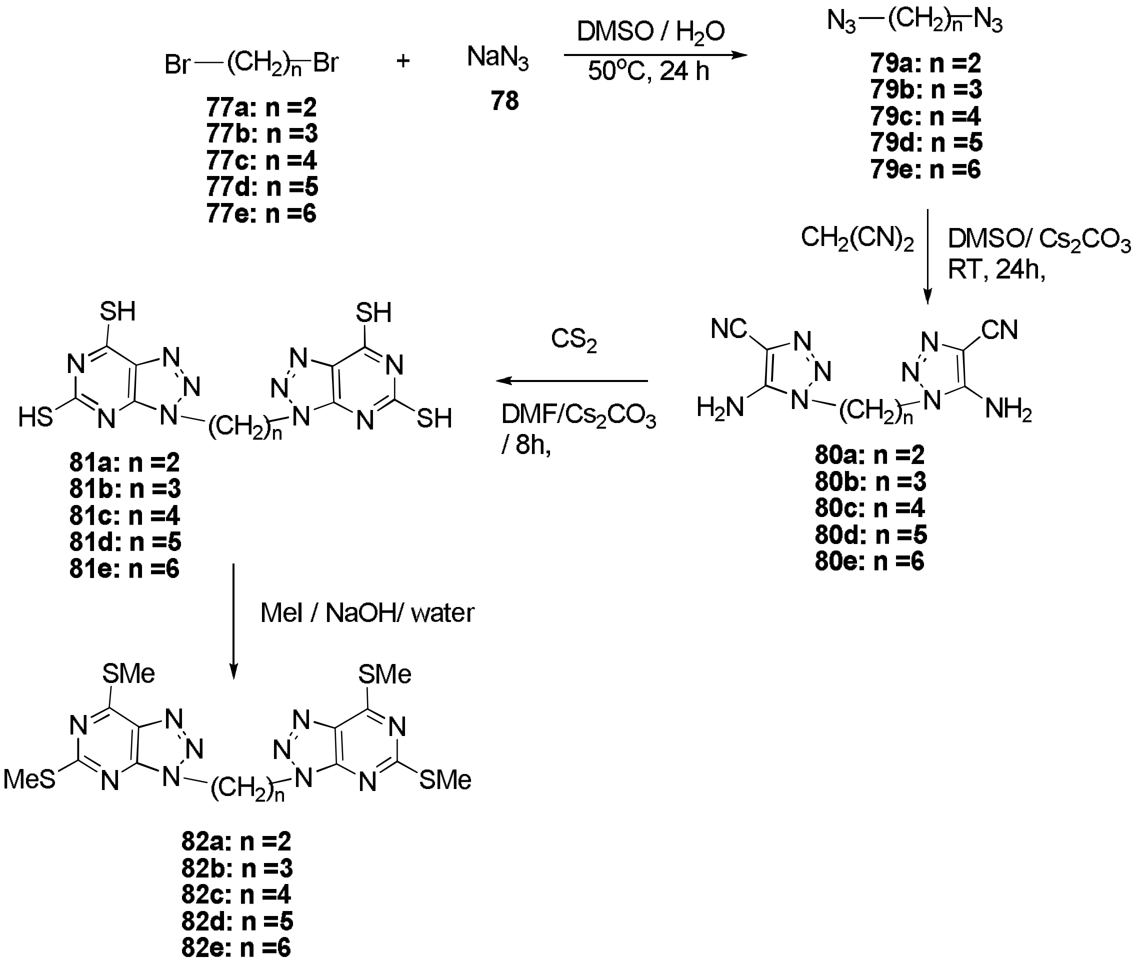

Scheme 2: General Procedure for synthesis of 1,n-bis(5,7-bis(methylthio)-3*H*-[1,2,3]triazolo[4,5-*d*]pyrimidin-3-yl)alkanes (**82a-e**)

The respective monomer 3-butyl-5,7-bis(methylthio)-3*H*-[1,2,3]triazolo[4,5-*d*]pyrimidine (**87)**, required as reference compound in the ^{1}H NMR study was synthesized using the same approach as in **Scheme 2** and is shown in **Scheme 3.**

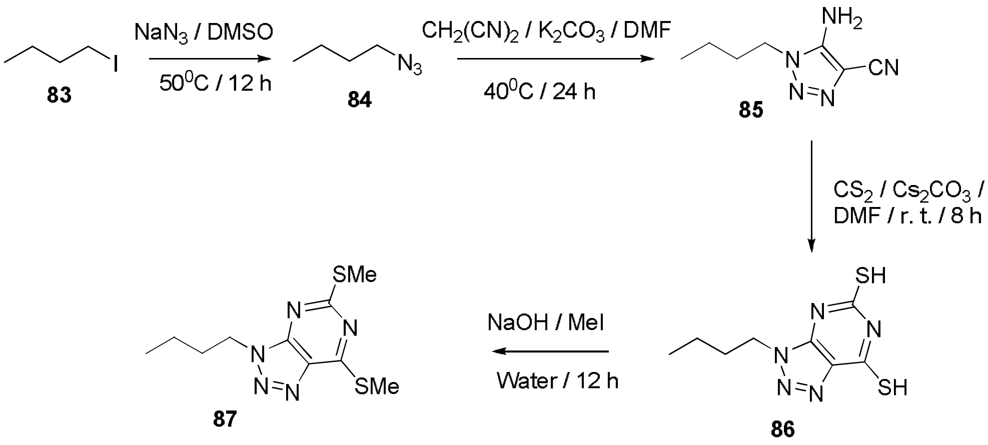

Scheme 3: General Procedure for synthesis of 3-butyl-5,7-bis(methylthio)-3*H*-[1,2,3]triazolo[4,5-*d*]pyrimidine (**87**).

The first step in this synthetic **Scheme 2** and **3** is preparation of azide from halides and is well reported in literature.[80] Since azides are potentially explosive compounds so they were not stored and were used as soon as they were prepared for next step.

The next step consists of condensation reaction of these azides with malononitrile to obtain the aminocyano triazole ring which was characterized by the help of mass and ^{1}H NMR data. The reaction of azides with active methylene compounds such as malononitrile, ethylacetoacetate, etc. are well reported in literature.[81a]

Aminocyano triazole ring thus formed is condensed with carbon disulfide to generate the pyrimidine ring. This type of reaction is also well reported in literature for the preparation of pyrazolo[3,4-*d*]pyrimidine ring.[81b] in which pyridine is used as a base and as a solvent. However a variation in the reaction condition had to be made in case of triazolo pyrimidine case. The above reaction is dependent both upon basicity of the amino group and upon the ability of the o-situated nitrile group to act as a site for nucleophillic addition. In case of reaction of aminobenzonitriles with carbon disulfide in pyridine it has been reported that 2-amino-5-methoxybenzonitrile reacts rapidly with carbon disulfide in pyridine to give the corresponding quinazoline-2,4(1*H*,3*H*)-dithione in quantitative yield while on the other hand, 2-amino-5-nitrobenzonitrile failed to react even after prolonged heating with carbon disulfide in pyridine.[80b]

Since triazolo ring (**80** and **85**) is more electron deficient than the corresponding pyrazole ring the basicity of the amino group attached to the ring is less and hence the lone pair of the amino group is not readily available for reacting with carbon disulfide and reaction does not proceed smoothly. However the reaction proceeds smoothly and at r.t. when cesium carbonate is used as a base and DMF as a solvent. The use of a stronger base like cesium carbonate in DMF is that it abstracts the proton of the amino group and thus the attack on the carbon of carbon disulfide takes place and the reaction proceeds smoothly as before. This reaction also proceeds with ease in case of NaH/ DMF condition at low temperature (5^o C - 10^o C) and in K_2CO_3/ DMF condition at 40^o C. Therefore a base which is strong enough to abstract the proton from the amino group is required to initiate the reaction and hence cesium carbonate as a base and DMF as a solvent is used for the reaction of compounds **80** and **85** with CS_2. These compounds were characterized mainly by analyzing the mass spectra.

Finally, methylation of the thiol groups yielded the required compound (**82** sand **87**). The characterization of these compounds was done by analyzing the Mass and ^{1}HNMR data and is described in the experimental section. In the ^{1}HNMR spectra of compound **87** the two SMe protons appears at 2.75 and 2.64 ppm.

Proton NMR of compound **82a** shows two singlets at δ 2.40 and 2.72 for two SMe groups and a singlet at δ 5.12 for NCH_2. Mass spectrum shows base peak corresponding to $[M+H]^+$ at *m/z* 453.

Proton NMR of compound **82b** shows two singlets at δ 2.50 and 2.75 for two SMe groups, a quintet at δ 2.89 for CH_2 protons and a triplet at δ 4.60 for NCH_2. Mass spectrum shows base peak corresponding to $[M+H]^+$ at *m/z* 467.

Proton NMR of compound **82c** shows a broad singlet at δ 2.05 for CH_2 protons, two singlets at δ 2.60 and 2.75 for SMe, a broad singlet at δ 4.64 for NCH_2 protons. Mass spectrum shows base peak corresponding to $[M+H]^+$ at *m/z* 481.

Proton NMR of compound **82d** shows two multiplets between δ 1.36-1.44 and 2.02-2.15 for CH_2 protons, two singlets at δ 2.61 and 2.75 for SMe, a broad singlet at δ 4.56 for NCH_2 protons. Mass spectrum shows base peak corresponding to $[M+H]^+$ at *m/z* 495.

Proton NMR of compound **82e** shows two broad singlets at δ 1.40 and 2.00 for CH_2 protons, two singlets at δ 2.63 and 2.75 for SMe, a broad singlet at δ 4.56 for NCH_2 protons. Mass spectrum shows base peak corresponding to $[M+H]^+$ at *m/z* 509.

Proton NMR of compound **87** shows multiplets between δ 0.92-1.00 for CH_3, between δ 1.30-1.40 and 1.94-2.04 for CH_2, between δ 4.54-4.60 for NCH_2 and two singlets at δ 2.64 and 2.75 for SMe,. Mass spectrum shows base peak corresponding to $[M+H]^+$ at *m/z* 270.

To study the effects of substitution on arene interactions 5- SMe and 7-SMe group were substituted by various electron withdrawing and electron donating groups as described in following sections.

1.3.2 Nucleophilic substitution reactions at 5 and 7 positions

The SMe group at 7-position of compounds (**82a-e**) can be easily substituted by various nucleophiles like pyrrolidine, methoxide ion, hydroxide ion etc. to give 7-substituted pyrrolidino, methoxy and hydroxyl substituted products. The SMe group at 5-positions has to be first converted to SO_2Me, a better leaving group, for substitution reaction by a nucleophile like methoxide ion.

1.3.2.1 Nucleophilic substitution of 7-methylsulfanyl group by pyrrolidino group.

1.3.2.1.1 Synthesis and characterization of 1,2-bis(5-methylthio-7-pyrrolidin-1-yl-3*H*-[1,2,3]triazolo[4,5-*d*]pyrimidin-3-yl)ethane (88a, Scheme 4), 1,3-bis(5-methylthio-7-pyrrolidin-1-yl-3*H*-[1,2,3]triazolo[4,5-*d*]pyrimidin-3-yl)propane (88b, Scheme 4), Synthesis of 1,4-bis(5-methylthio-7-pyrrolidin-1-yl-3*H*-[1,2,3]triazolo[4,5-*d*]pyrimidin-3-yl)butane (88c, Scheme 4) and 3-butyl-5-methylthio-7-pyrrolidin-1-yl-3*H*-[1,2,3]triazolo[4,5-*d*]pyri-midine (89, Scheme 4).

The reaction of compound **82a-c** and **87** with pyrrolidine under refluxing conditions yielded compound **88a-c** and **97** respectively in which 7 SMe group is replaced by pyrrolidino group (**Scheme 4**) and was purified by column chromatography. The corresponding monomer (**89**) was synthesized from compound **87** under similar conditions (**Scheme 4**). Compound was characterized by NMR and mass spectrometric techniques.

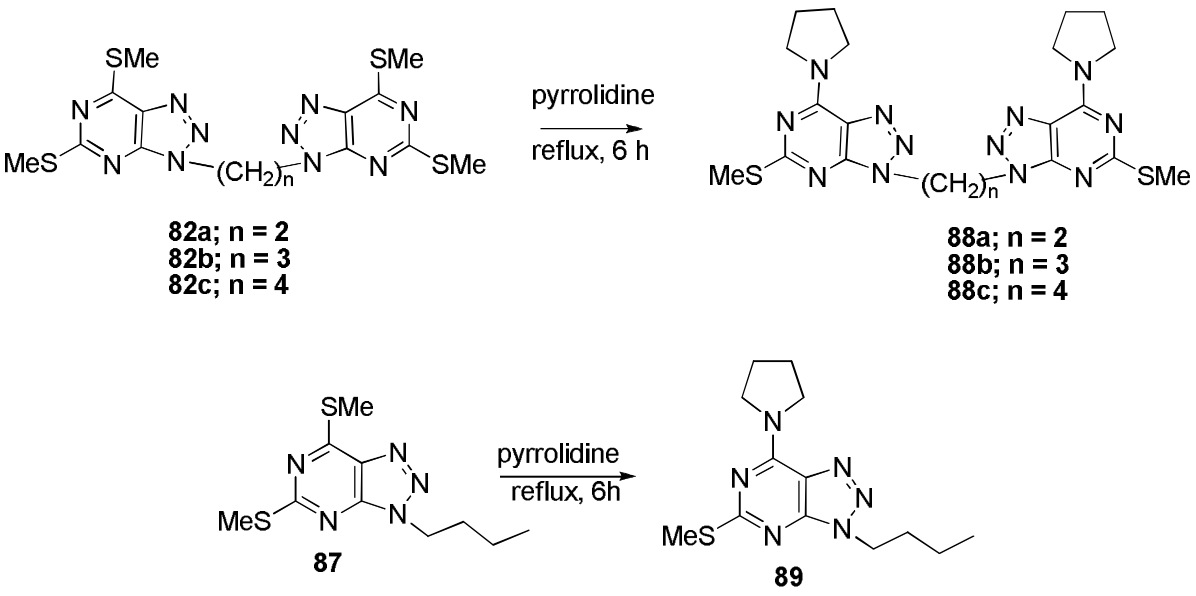

Scheme 4: General Procedure for synthesis of pyrrolidine derivatives.

Proton NMR of compound **88a** shows a multiplet between δ 1.94-2.16 for pyrrodinyl CH_2, a singlet at δ 2.41 for SMe, two multiplets between δ 3.70-3.80 and 4.10-4.20 for pyrrodinyl NCH_2, and δ 5.01 for NCH_2. Mass spectrum shows base peak corresponding to $[M+H]^+$ at *m/z* 499.

Proton NMR of compound **88b** shows a multiplet between δ 1.94-2.20 for pyrrodinyl CH_2, a singlet at δ 2.49 for SMe, a quintet at δ 2.75 for CH_2, two triplets at δ 3.79 and 4.21 for pyrrodinyl NCH_2, and a triplet at δ 4.57 for NCH_2. Mass spectrum shows base peak corresponding to $[M+H]^+$ at *m/z* 513.

Proton NMR of compound **88c** shows a multiplet between δ 1.94-2.10 for pyrrodinyl CH_2, a multiplet between δ 2.11-2.18 for CH_2, a singlet at δ 2.54 for SMe, two multiplets between δ 3.77-3.83 and 4.17-4.23 for pyrrodinyl NCH_2, and a multiplet between δ 4.55-4.58 for NCH_2. Mass spectrum shows base peak corresponding to $[M+H]^+$ at *m/z* 527.

Proton NMR of compound **89** shows a multiplet between δ 0.90-0.99 for CH_3, a multiplet between δ 1.30-1.44 for CH_2, a multiplet between δ 1.90-2.20 for pyrrodinyl and linker CH_2 a singlet at δ 2.58 for SMe, , two triplets at δ 3.80 and 4.22 for pyrrodinyl NCH_2, and a triplet at δ 4.49 for NCH_2. Mass spectrum shows base peak corresponding to $[M+H]^+$ at *m/z* 293.

1.3.2.2 Nucleophilic substitution of 7-methylsulfanyl group by methoxy group

1.3.2.2.1 Synthesis and characterization of 1,2-bis(7-methoxy-5-(methylthio)-3*H*-[1,2,3]triazolo[4,5-*d*]pyrimidin-3-yl)ethane (90a, Scheme 5), 1,3-bis(7-methoxy-5-(methylthio)-3*H*-[1,2,3]triazolo[4,5-*d*]pyrimidin-3-yl)propane (90b, Scheme 5), 1,4-bis(7-methoxy-5-methylthio-3*H*-[1,2,3]triazolo[4,5-*d*]pyrimidin-3-yl)butane (90c, Scheme 5) and 3-butyl-7-methoxy-5-methylthio-3*H*-[1,2,3]triazolo[4,5-*d*]pyrimidine (91, Scheme 5).

Reaction of compound **82a-c** with NaOMe in methanol under refluxing conditions yielded **90a-c** respectively in which 7-SMe is replaced by 7-OMe group (**Scheme 5**) and was purified by column chromatography. The corresponding monomer (**91**) was synthesized from compound **87** under similar conditions (**Scheme 5**). Compounds were characterized by NMR and mass spectrometric techniques.

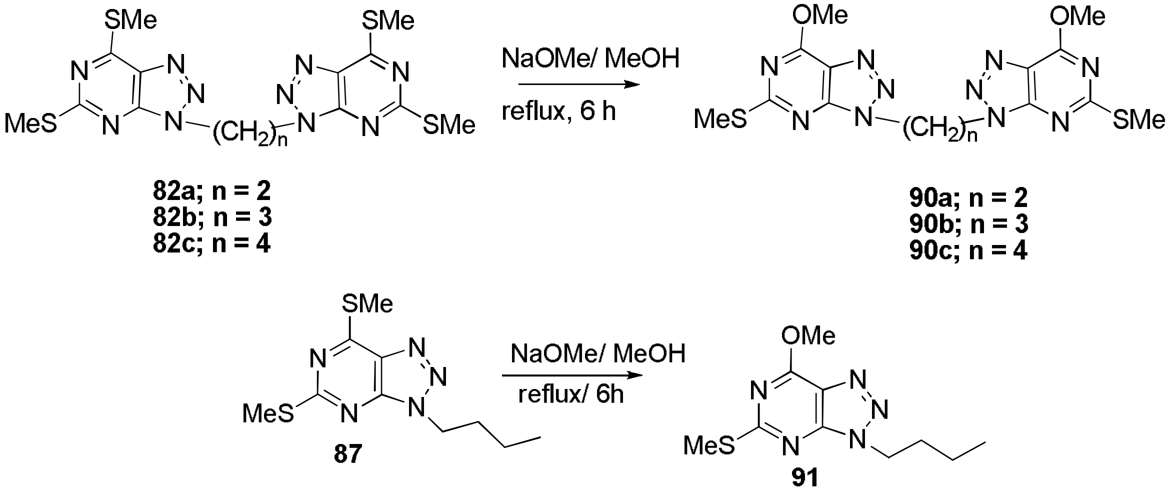

Scheme 5: General Procedure for synthesis of methoxy derivatives.

Proton NMR of compound **90a** shows , a singlet at δ 2.40 for SMe,, a singlet at δ 4.20 for OMe, and δ 5.13 for NCH$_2$. Mass spectrum shows base peak corresponding to $[M+H]^+$ at *m/z* 421.

Proton NMR of compound **90b** shows a singlet at δ 2.49 for SMe, a quintet at δ 2.90 for CH$_2$, a singlet at δ 4.24 for OMe and a triplet at δ 4.60 for NCH$_2$. Mass spectrum shows base peak corresponding to $[M+H]^+$ at *m/z* 435.

Proton NMR of compound **90c** shows a broad singlet at δ 2.05 for CH$_2$, a singlet at δ 2.60 for SMe, a singlet at δ 4.24 for OMe and a broad singlet at δ 4.65 for NCH$_2$. Mass spectrum shows base peak corresponding to $[M+H]^+$ at *m/z* 449.

Proton NMR of compound **91** shows a multiplet between δ 0.90-1.00 for CH_3, two multiplet between δ 1.31-1.40 and 1.94-2.02 for CH_2, a singlet at δ 2.64 for SMe, a singlet at δ 4.24 for OMe and a multiplet between δ 4.52-4.60 for NCH_2. Mass spectrum shows base peak corresponding to $[M+H]^+$ at *m/z* 254.

1.3.2.3 Nucleophilic substitution of 7-methylsulfanyl group by hydroxy group

1.3.2.3.1 Synthesis and characterization of 3,3'-(ethane-1,2-diyl)bis(5-methylthio-3*H*-[1,2,3]triazolo[4,5-*d*]pyrimidin-7(6*H*)-one) (92a, Scheme 6), 3,3'-(propane-1,3-diyl)bis(5-(methylthio)-3*H*-[1,2,3]triazolo[4,5-*d*]pyrimidin-7(6*H*)-one) (92b, Scheme 6), 3,3'-(butane-1,4-diyl)bis(5-(methylthio)-3*H*-[1,2,3]triazolo[4,5-*d*]pyrimidin-7(6*H*)-one) (92c, Scheme 6) and 3-butyl-5-methylthio-3*H*-[1,2,3]triazolo[4,5-*d*]pyrimidin-7(6*H*)-one (93, Scheme 6).

Reaction of Compound **82a-c** with aq. NaOH in methanol under refluxing conditions yielded compound **92a-c** respectively (**Scheme 6**) and was purified using the procedure described in the experimental section. The corresponding monomer (**93**) was synthesized from compound **87** under similar conditions (**Scheme 6**). Compound was characterized by NMR and mass spectrometric techniques.

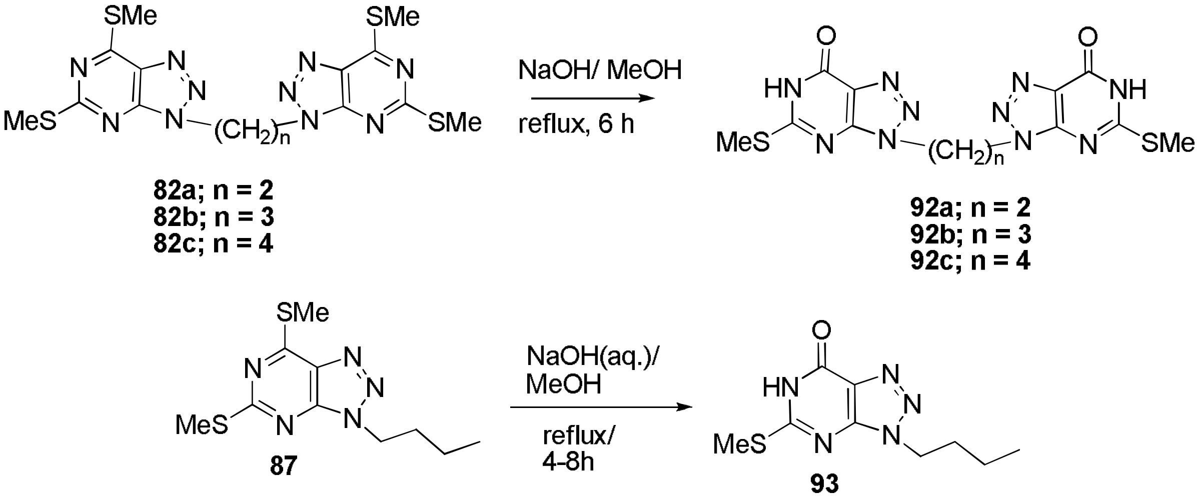

Scheme 6: General Procedure for synthesis of hydroxy derivatives.

Proton NMR in DMSO-d_6 of compound **92a** shows, a singlet at δ 2.28 for SMe, a singlet at δ 4.97 for NCH_2, and a broad singlet at δ 14.10 for NH. Mass spectrum shows base peak corresponding to $[M+H]^+$ at *m/z* 393.

Proton NMR in DMSO-d_6 of compound **92b** shows, a singlet at δ 2.40 for SMe,, a broad singlet at singlet δ 2.72, a singlet at at δ 4.43 for NCH_2, and a broad singlet at δ 12.81 for NH. Mass spectrum shows base peak corresponding to $[M+H]^+$ at *m/z* 393.

Proton NMR in DMSO-d_6 of compound **92c** shows a broad singlet at δ 1.90 for CH_2, a singlet at δ 2.52 for SMe, a singlet at δ 4.53 for NCH_2 and a broad singlet at δ 12.81 for NH. Mass spectrum shows base peak corresponding to $[M+H]^+$ at *m/z* 421.

Proton NMR in DMSO-d_6 of compound **93** shows a multiplet between δ 0.85-0.95 for CH_3, two multiplet between δ 1.22-1.29 and 1.82-1.94 for CH_2, a singlet at δ 2.59 for SMe, and a multiplet between δ 4.46-4.50 for NCH_2. Mass spectrum shows base peak corresponding to $[M+H]^+$ at *m/z* 240.

1.3.2.4 Conversion of 7-hydroxy group to 7-chloro group[81c]

1.3.2.4.1 Synthesis and characterization of 1,2-bis(7-chloro-5-methylthio-3*H*-[1,2,3]triazolo[4,5-*d*]pyrimidin-3-yl)ethane (94a, Scheme 7), 1,3-bis(7-chloro-5-methylthio-3*H*-[1,2,3]triazolo[4,5-*d*]pyrimidin-3-yl)propane (94b, Scheme 7), 1,4-bis(7-chloro-5-methylthio-3*H*-[1,2,3]triazolo[4,5-*d*]pyrimidin-3-yl)butane (94c, Scheme 7) and 3-butyl-7-chloro-5-methylthio-3*H*-[1,2,3]triazolo[4,5-*d*]pyrimidine (95, Scheme 7).

Reaction of compound **92a-c** with a mixture of $SOCl_2$ and DMF in boiling $CHCl_3$ yielded **94a-c** respectively which has a chloro group at 7 position (**Scheme 7**). Reaction of compound **92a-c** with $POCl_3$ under refluxing conditions or at heating condition (70° C) gave a resin like product which could not identified. The chloro group at 7-position is very reactive and chances of polymerization under $POCl_3$ condition are high. Therefore a milder condition of $SOCl_2$ + DMF is required to convert the hydroxyl group to chloro group.[81c] The corresponding monomer (**95**) was synthesized from compound **93** under similar conditions (**Scheme 7**). The compound was purified using column chromatography and was characterized by NMR and mass spectrometric techniques.

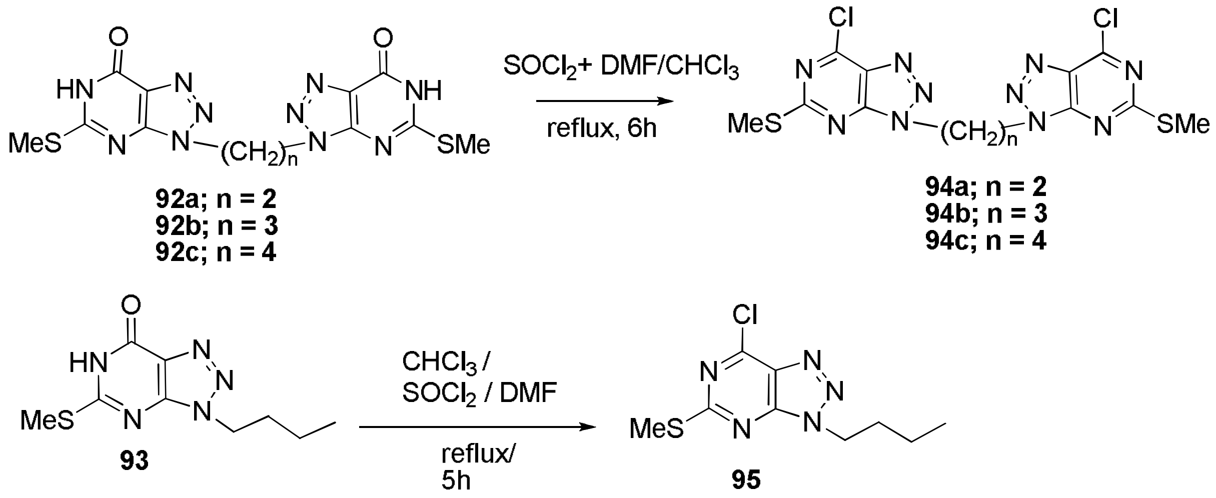

Scheme 7: General Procedure for synthesis of chloro derivatives.

Proton NMR of compound **94a** shows, a singlet at δ 2.46 for SMe, and δ 5.21 for NCH_2. Mass spectrum shows base peak corresponding to $[M+H]^+$ at *m/z* 429.

Proton NMR of compound **94b** shows a singlet at δ 2.55 for SMe, a quintet at δ 2.95 for CH_2 and a triplet at δ 4.69 for NCH_2. Mass spectrum shows base peak corresponding to $[M+H]^+$ at *m/z* 444.

Proton NMR of compound **94c** shows a broad singlet at δ 2.12 for CH_2, a singlet at δ 2.62 for SMe, and a a broad singlet at δ 4.70 for NCH_2. Mass spectrum shows base peak corresponding to $[M+H]^+$ at *m/z* 458.

Proton NMR of compound **95** shows a triplet at δ 0.99 for CH_3, two multiplet between δ 1.30-1.44 and 2.00-2.10 for CH_2, a singlet at δ 2.66 for SMe, and a triplet at δ 4.64 for NCH_2. Mass spectrum shows base peak corresponding to $[M+H]^+$ at *m/z* 258.

1.3.2.5 Methylation of 3,3'-(alkane-1,n-diyl)bis(5-(methylthio)-3*H*-[1,2,3]triazolo[4,5-*d*]pyrimidin-7(6*H*)-one).

1.3.2.5.1 Synthesis and characterization of 3,3'-(ethane-1,2-diyl)bis(6-methyl-5-methylthio-3*H*-[1,2,3]triazolo[4,5-*d*]pyrimidin-7(6*H*)-one) (96a, Scheme 8), 3,3'-(propane-1,3-diyl)bis(6-methyl-5-methylthio-3*H*-[1,2,3]triazolo[4,5-*d*]pyrimidin-7(6*H*)-one) (96b, Scheme 8), 3,3'-(butane-1,4-diyl)bis(6-methyl-5-methylthio-3*H*-[1,2,3]triazolo[4,5-*d*]pyrimidin-7(6*H*)-one) (96c, Scheme 8), and 3-butyl-6-methyl-5-methylthio-3*H*-[1,2,3]triazolo[4,5-*d*]pyrimidin-7(6*H*)-one (97, Scheme 8).

Reaction of compound **92a-c** with methyl iodide using sodium hydroxide in water at r.t. yielded **96a-c** as a major product (> 95% of total product) and compound **90a-c** as a minor product (< 5% of total product) respectively (**Scheme 8**). The corresponding monomer (**97**) was synthesized from compound **93** under similar conditions (**Scheme 8**). The compounds were separated by column chromatography and were characterized by NMR and mass spectrometric techniques.

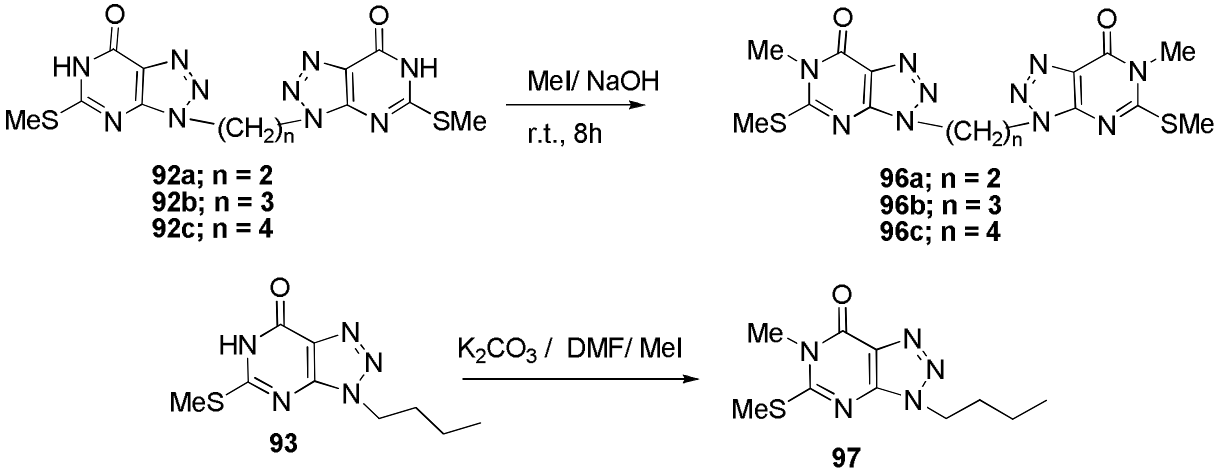

Scheme 8: General Procedure for synthesis of 6-N-methyl derivatives.

Proton NMR of compound **96a** shows, a singlet at δ 2.33 for SMe, a singlet at δ 2.65 for NMe, and δ 5.02 for NCH_2. Mass spectrum shows base peak corresponding to $[M+H]^+$ at *m/z* 421.

Proton NMR of compound **96b** shows a singlet at δ 2.44 for SMe, a quintet at δ 2.97 for CH_2, a singlet at δ 3.58 for NMe and a triplet at δ 4.40 for NCH_2. Mass spectrum shows base peak corresponding to $[M+H]^+$ at *m/z* 435.

Proton NMR of compound **96c** shows a broad singlet at δ 2.06 for CH_2, a singlet at δ 2.59 for SMe, , a singlet at δ 3.60 for NMe and a broad singlet at δ 4.52 for NCH_2 . Mass spectrum shows base peak corresponding to $[M+H]^+$ at *m/z* 449.

Proton NMR of compound **97** shows a triplet at δ 0.97 for CH_3, a multiplet between δ 1.28-1.44, a quintet at δ 1.99 for CH_2, a singlet at δ 2.67 for SMe, a singlet at δ 3.62 for NMe and a triplet at δ 4.50 for NCH_2. Mass spectrum shows base peak corresponding to $[M+H]^+$ at *m/z* 254.

1.3.2.6 Nucleophilic substitution of 7-chloro group by dimethylamino group.

1.3.2.6.1 Synthesis and characterization of 3,3'-(propane-1,3-diyl)bis(*N*,*N*-dimethyl-5-methylthio-3*H*-[1,2,3]triazolo[4,5-*d*]pyrimidin-7-amine) (98, Scheme 9), 3-butyl-*N*,*N*-dimethyl-5-methylthio-3*H*-[1,2,3]triazolo[4,5-*d*]pyrimidin-7-amine (99, Scheme 9).

Reaction of compound **94b** with 50% aqueous dimethylamine solution at 80°C in a steel bomb yielded compound **98** and was purified by column chromatography (**Scheme 9**). The corresponding monomer (**99**) was synthesized from compound **95** under similar conditions (**Scheme 9**). Compounds were characterized by NMR and mass spectrometric techniques.

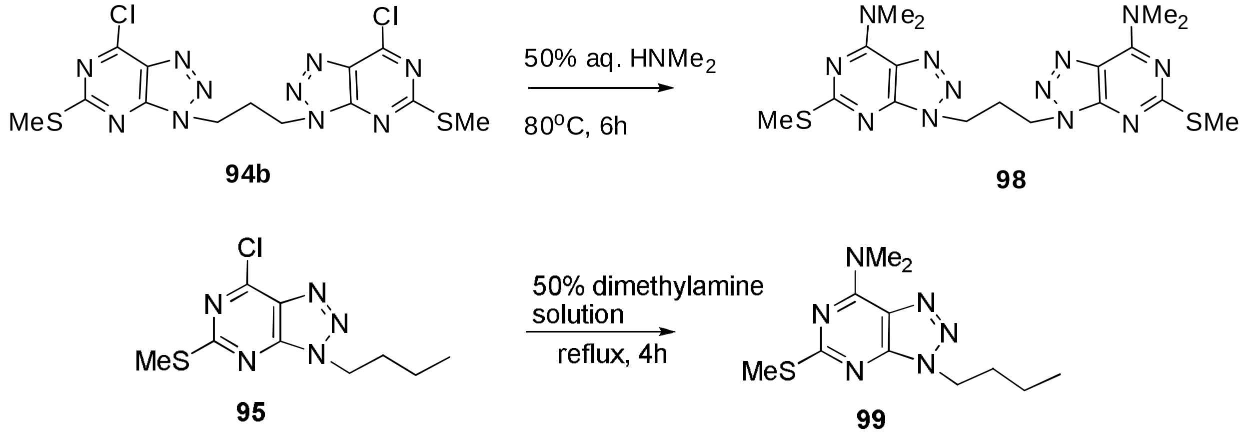

Scheme 9: General Procedure for synthesis of dimethylamino derivatives

Proton NMR of compound **98** shows a singlet at δ 2.49 for SMe, a quintet at δ 2.75 for CH_2, two singlets at δ 3.33 and 3.83 for NMe and a triplet at δ 4.57 for NCH_2. Mass spectrum shows base peak corresponding to $[M+H]^+$ at *m/z* 461.

Proton NMR of compound **99** shows a multiplet between δ 0.92-0.99 for CH_3, two multiplet between δ 1.30-1.40, a quintet at δ 1.96 for CH_2, a singlet at δ 2.58 for SMe, two singlets at δ 3.34 and 3.83 for NMe and a triplet at δ 4.49 for NCH_2. Mass spectrum shows base peak corresponding to $[M+H]^+$ at *m/z* 267.

1.3.2.7 Oxidation of 5-methylsulfanyl group to 5-methylsulfonyl group.

1.3.2.7.1 Synthesis and characterization of 1,3-bis(5-methylsulfonyl-7-pyrrolidin-1-yl-3*H*-[1,2,3]triazolo[4,5-*d*]pyrimidin-3-yl)propane (100, Scheme 10), 1,2-bis(7-methoxy-5-methylsulfonyl-3*H*-[1,2,3]triazolo[4,5-*d*]pyrimidin-3-yl)ethane (101a, Scheme 10), 1,3-bis(7-methoxy-5-methylsulfonyl-3*H*-[1,2,3]triazolo[4,5-*d*]pyrimidin-3-yl)propane (101b, Scheme 10), 3-butyl-5-methylsulfonyl-7-pyrrolidin-1-yl-3*H*-[1,2,3]triazolo[4,5-*d*]pyri-

midine (102, Scheme 10) and 3-butyl-7-methoxy-5-methylsulfonyl-3*H*-[1,2,3]triazolo[4,5-*d*]pyrimidine (103, Scheme 10).

Reaction of compound **88b** in acetone with oxone dissolved in minimum amount of water at 0° C yielded compound **100** respectively in which 5-SMe is oxidized to 5-SO_2Me group (**Scheme 10**). Similarly reaction of compound **90a-b** with oxone yielded compound **101a-b** (**Scheme 10**). The compounds were purified by column chromatography and were characterized by NMR and mass spectrometric techniques.

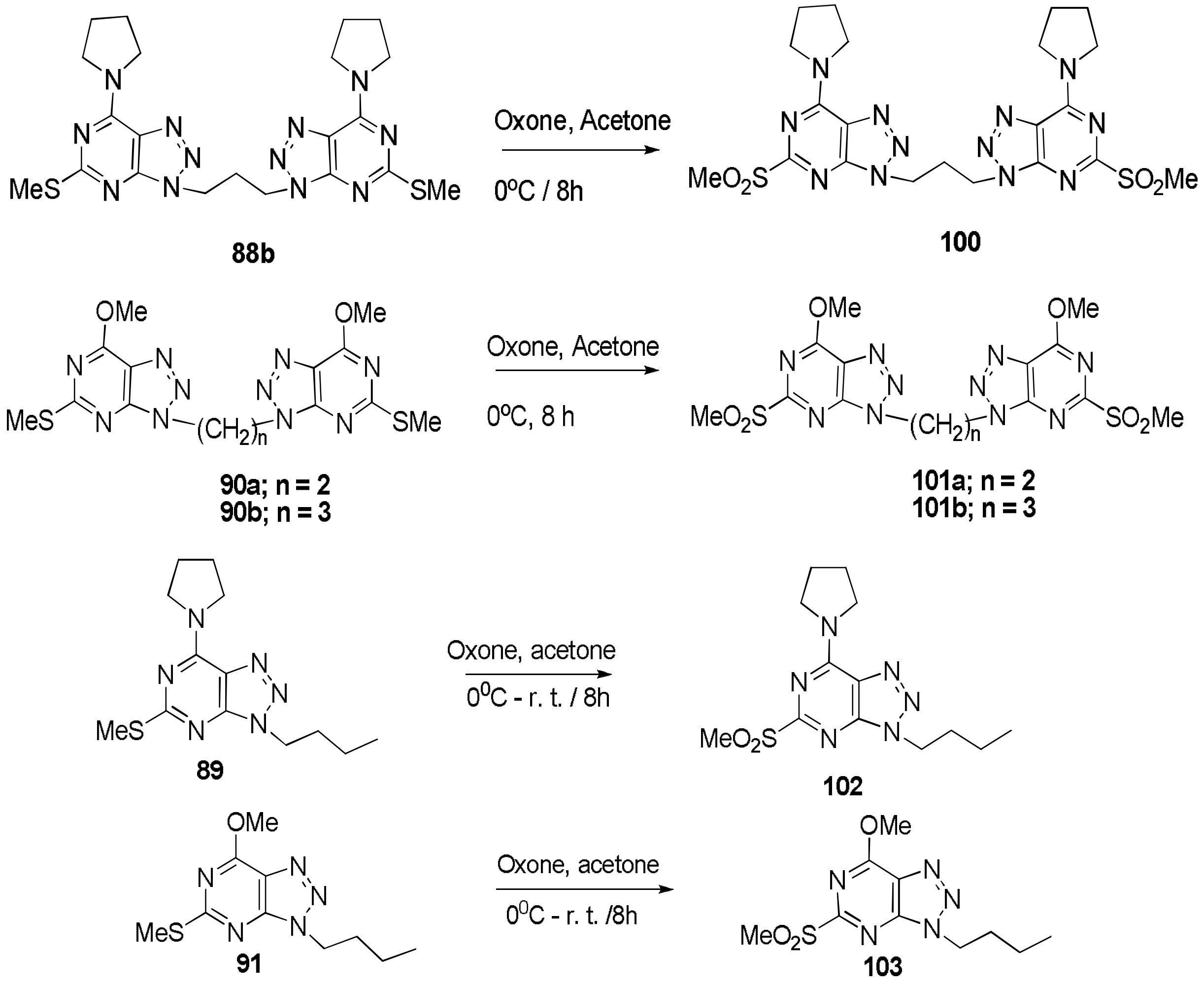

Scheme 10: General Procedure for synthesis of methylsulfonyl derivatives.

Proton NMR of compound **100** shows a multiplet between δ 2.00-2.30 for pyrrodinyl CH_2, a quintet at δ 2.90 for CH_2, a singlet at δ 3.28 for SO_2Me, two triplets at δ 3.88 and 4.29 for pyrrodinyl NCH_2, and a triplet at δ 4.64 for NCH_2. Mass spectrum shows base peak corresponding to $[M+H]^+$ at *m/z* 577.

Proton NMR of compound **101a** shows, a singlet at δ 3.27 for SO_2Me, a singlet at δ 4.37 for OMe, and δ 5.36 for NCH_2. Mass spectrum shows base peak corresponding to $[M+H]^+$ at *m/z* 484.

Proton NMR of compound **101b** shows a quintet at δ 3.02 for CH_2, a singlet at δ 3.38 for SO_2Me, a singlet at δ 4.41 for OMe and a triplet at δ 4.80 for NCH_2. Mass spectrum shows base peak corresponding to $[M+H]^+$ at *m/z* 499.

Proton NMR of compound **102** shows a triplet at δ 0.97 for CH_3, a multiplet between δ 1.28-1.42 for CH_2, a multiplet between δ 1.90-2.20 for pyrrodinyl and linker CH_2 a singlet at δ 3.35for SO_2Me, two triplets at δ 3.90 and 4.30 for pyrrodinyl NCH_2, and a triplet at δ 4.61 for NCH_2. Mass spectrum shows base peak corresponding to $[M+H]^+$ at *m/z* 325.

Proton NMR of compound **103** shows a multiplet between δ 0.94-1.04 for CH_3, two multiplet between δ 1.36-1.44 and 1.98-2.06 for CH_2, a singlet at δ 3.42 for SO_2Me, a singlet at δ 4.26 for OMe and a multiplet between δ 4.58-4.64 for NCH_2. Mass spectrum shows base peak corresponding to $[M+H]^+$ at *m/z* 286.

1.3.2.8 Nucleophilic substitution of 5-methylsulfonyl group by methoxy group.

1.3.2.8.1 Synthesis and characterization of 1,3-bis(5,7-dimethoxy-3*H*-[1,2,3]triazolo[4,5-*d*]pyrimidin-3-yl)propane (104, Scheme 11) and 3-butyl-5, 7-dimethoxy-3*H*-[1,2,3]triazolo[4,5-*d*]pyrimidine (105, Scheme 11).

Reaction of compounds **101b** with sodium methoxide under refluxing conditions yielded compound **104** (**Scheme 11**). The corresponding monomer (**105**) was synthesized from compound **103** under similar conditions (**Scheme 11**). The compounds were purified by column chromatography and were characterized by NMR and mass spectrometric techniques.

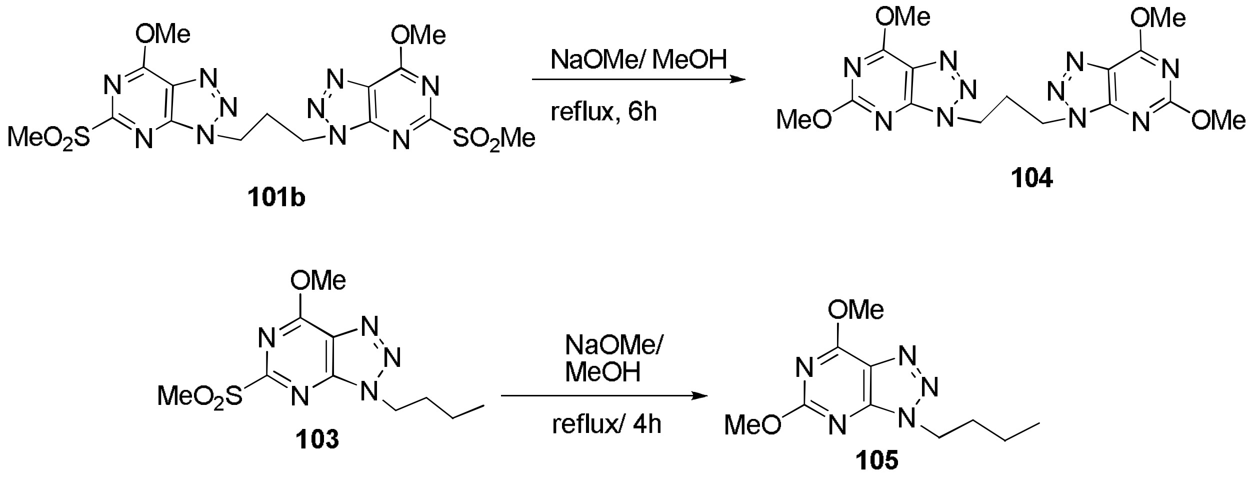

Scheme 11: General procedure for synthesis of 5, 7-dimethoxy derivatives.

Proton NMR of compound **96** shows a quintet at δ 2.84 for CH$_2$ protons, two singlets at δ 4.01 and 4.24 for OMe, and a triplet at δ 4.63 for NCH$_2$. Mass spectrum shows base peak corresponding to $[M+H]^+$ at *m/z* 403.

Proton NMR of compound **105** shows multiplets between δ 0.88-0.94 for CH$_3$, between δ 1.28-1.38 and 1.92-2.01 for CH$_2$, two singlets at δ 4.20 and 4.24for OMe and a multiplet between δ 4.54-4.60 for NCH$_2$. Mass spectrum shows base peak corresponding to $[M+H]^+$ at *m/z* 238.

1.4 Result and discussion

The present study was undertaken to determine the effect of increasing number of ring nitrogen on the robustness of the *U-motif* seen in 4,6-disubstituted-1*H*-pyrazolo[3,4-*d*]pyrimidine compounds from molecular recognition and crystal engineering point of view. Generally, electronic effects are considered to play significant role in stacking interactions. Earlier studies on pyrazolo[3,4-*d*]pyrimidine based symmetrical and dissymmetrical *polymethylene* especially *trimethylene* compounds revealed that 4,6-dialkylsulfanyl-1*H*-pyrazolo[3,4-*d*]pyrimidine had strong stacking tendency.[62-72] Thus, we decided to synthesize symmetrical *polymethylene* 5,7-disubstituted-triazolo[4,5-*d*]pyrimidine compounds in which CH of the pyrazolo part of pyrazolo[3,4-*d*]pyrimidine nucleus is replaced by nitrogen. This introduction of nitrogen in ring was expected to bring a profound change in the electronic distribution of the nucleus and thus might have significant change in the solution and solid state conformation of the molecule and thus on the stacking behavior of the molecule. Moreover 3,5,7-trisubstituted[1,2,3]triazolo[4,5-

d]pyrimidines can be considered as 8-aza analogues of more important biologically relevant purine molecules. Thus the information obtained through such studies can also be useful in the better understanding of the functioning of such molecules in various processes like molecular recognition and drug receptor interactions.

1.4.1 ^{1}H NMR study.

Magnetic anisotropy induced by the aromatic π–electrons which is manifested as an upfield shift in δ values of the affected protons has been used to probe the intramolecular proximity by ^{1}H NMR spectroscopy. One of the most useful strategies employed to study arene interactions include connecting two aromatic moieties with *polymethylene* linker so that arene interactions could be studied by ^{1}H NMR spectroscopy at molecular level. [40,48-50] This is because ^{1}H NMR is normally done in solution phase at very low concentration so no intermolecular interactions can be seen as the molecules are away from each other and surrounded by excess solvent molecules. Therefore, to convert intermolecular (supramolecular) problem into intramolecular one, flexible models consisting of two arene residues and a *polymethylene* linker, are used. This way a properly placed linker, especially a *trimethylene* linker, between two arene residues helps detection of the **APPI** (aromatic π–π interaction) by ^{1}H NMR in solution.

This present study was carried out to investigate the effect of varying the separation between the rings on the magnitude of stacking interaction in the series Ar-$(CH_2)_n$-Ar where Ar = 5,7-bis(methylthio)-3*H*-[1,2,3]triazolo[4,5-*d*]pyrimidine and n = 2-6. The effect of substituents on **APPI** of triazolo[4,5-*d*]pyrimidine compounds was also investigated.

As in case of 4,6-dimethylsulfanyl-1*H*-pyrazolo[3,4-*d*]pyrimidine where the 6-SMe protons shows considerable upfield shift in the ^{1}H NMR study,[62] the corresponding 5-SMe protons in dimers of 5,7-bis(methylthio)-3*H*-[1,2,3]triazolo[4,5-*d*]pyrimidine **(82a-e)** show upfield shift in the ^{1}H NMR study as compared to the monomer compound 3-butyl-5,7-bis(methylthio)-3*H*-[1,2,3]triazolo[4,5-*d*]pyrimidine (**87**). Also the upfield shifts decreases gradually as we move from n = 2 to n = 6. (**Table1**). This shows that the aromatic moieties spend less time near to each other as the length of the linker increases i.e. longer linker leads to greater time-average separation of the two rings connected by the longer chain. For n = 2 the difference in the chemical shifts of the methylsulfanyl protons as compared to the monomer methylsulfanyl proton is 0.24 ppm; for n = 3 it is 0.14 ppm; for n = 4 it is 0.04; for n = 5 it is 0.03 ppm; and for n = 6 it is 0.01 ppm. Thus, significant upfield shift for the methylsulfanyl protons takes place only when n = 2/3. This trend is quite similar to the trend seen in corresponding PP compounds.

Table 1: Important ^{1}H NMR shifts

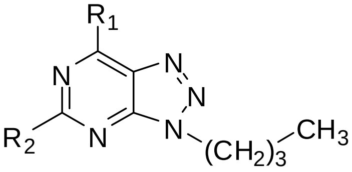

87, 89, 91, 95, 99, 102, 103, 105

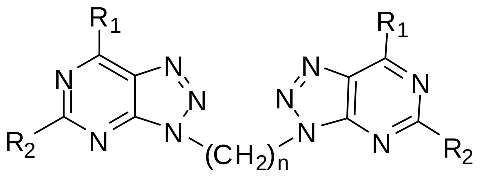

82, 88, 90, 94, 98, 100, 104

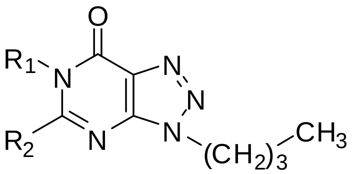

93, 97

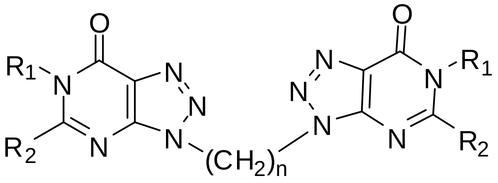

92,96

S. No.	**Comp. no.**	**n**	**R_1**	**R_2**	**δ 5-SMe/ SO_2Me/ OMe**	**Δδ = δ 5- SCH_3/SO_2Me/OMe (monomer) – δ5- SCH_3/SO_2Me/OMe (dimeric comp.)**
1	**87**	-	SMe	SMe	2.64	-
2	**89**	-	Pyrrolidine	SMe	2.58	-
3	**91**	-	OMe	SMe	2.64	-
4	**93**	-	H	SMe	2.59	-
5	**95**	-	Cl	SMe	2.66	-
6	**97**	-	Me	SMe	2.67	-
7	**99**	-	NMe_2	SMe	2.58	-
8	**102**	-	pyrrolidine	SO_2Me	3.35	-
9	**103**	-	OMe	SO_2Me	3.42	-
10	**105**	-	OMe	OMe	4.20	
11	**82a**	2	SMe	SMe	2.40	0.24
12	**82b**	3	SMe	SMe	2.50	0.16
13	**82c**	4	SMe	SMe	2.60	0.04
14	**82d**	5	SMe	SMe	2.61	0.03
15	**82e**	6	SMe	SMe	2.63	0.01
16	**88a**	2	Pyrrolidine	SMe	2.41	0.17
17	**88b**	3	Pyrrolidine	SMe	2.49	0.09
18	**88c**	4	Pyrrolidine	SMe	2.54	0.04
19	**90a**	2	OMe	SMe	2.40	0.24
20	**90b**	3	OMe	SMe	2.49	0.15

21	**90c**	4	OMe	SMe	2.60	0.04
22	**92a**	2	H	SMe	2.28	0.31
23	**92b**	3	H	SMe	2.40	0.18
24	**92c**	4	H	SMe	2.52	0.07
25	**94a**	2	Cl	SMe	2.46	0.20
26	**94b**	3	Cl	SMe	2.55	0.11
27	**94c**	4	Cl	SMe	2.62	0.04
28	**96a**	2	Me	SMe	2.33	0.34
29	**96b**	3	Me	SMe	2.44	0.24
30	**96c**	4	Me	SMe	2.59	0.08
31	**98**	3	NMe_2	SMe	2.49	0.09
32	**100**	3	pyrrolidine	SO_2Me	3.28	0.07
33	**101a**	2	OMe	SO_2Me	3.27	0.13
34	**101b**	3	OMe	SO_2Me	3.35	0.07
35	**104**	3	OMe	OMe	4.01	0.19

Thus, for n = 4-6 upfield shift for the methylsulfanyl protons is not significant indicating products stay most of the time in open/extended conformation. However, in case of *ethylene* linker i.e., n = 2 the aromatic moieties cannot attain parallel plane conformation mainly due to steric reasons. In this case there are two extreme possibilities; (i) the aromatic moieties can be near to each other attaining *syn* or *gauche* conformation in which case we get an upfield shift in the protons or (ii) the aromatic moieties can be far away from each other attaining *anti* conformation in which case we do not get any upfield shift in the protons (**Fig. 36**). In between these two extreme conformations infinite number of other conformations are also possible. Similar results were seen in the dimers of 5-methylthio-3*H*-[1,2,3]triazolo[4,5-*d*]pyrimidin-7(6*H*)-one **(92a)** and 6- methyl-5-methylthio-3*H*-[1,2,3]triazolo[4,5-*d*]pyrimidin-7(6*H*)-one (**96a**) which can be considered as aza analogs of important guanine moieties.

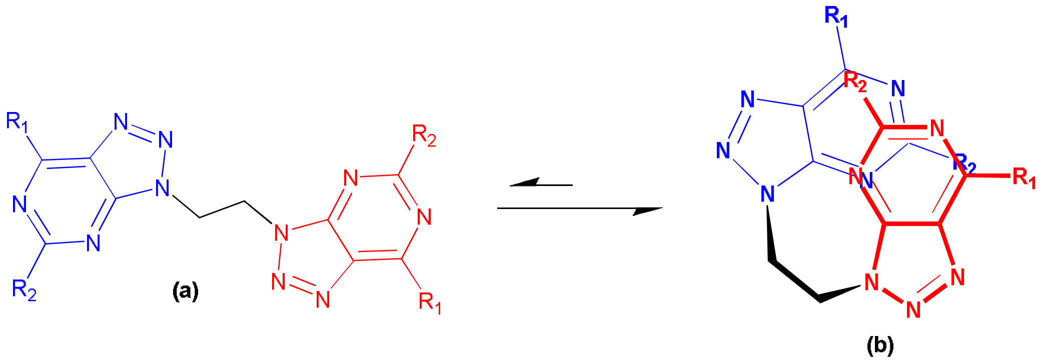

Figure 36. (a) *Anti* conformation (b) *syn* conformation

To study the effect of substituents on **APPI** we substituted the methylsulfanyl groups at 5 and 7 positions with various electron donating substituents like methoxy, dimethylamino etc. and various electron withdrawing substituents like chloro and sulfonyl groups. In case of *ethylene* and *trimethylene* linker compounds on moving from weakly electron withdrawing methylsulfanyl group (**82a-b, Table 1**) to weakly electron donating group methoxy group (**90a-b, Table 1**) did not have any significant effect on the chemical shift of the 5-SMe protons but on moving to the pyrrolidine group (**88a-b**, **Table 1**) which is strong electron donating in nature, the change in the upfield shifts is reduced (from 0.24 ppm to 0.17 ppm for n =2 and from 0.16 ppm to 0.09 ppm for n =3) which indicates to the less interaction between the aromatic moieties. This holds for the *trimethylene* linker compound **98** (**Table 1**) which has dimethylamino group as substituent. This decrease in interaction on increasing the electron density follows rule of Hunter and Sanders suggested for stacking.[12] In case of chloro substituent (**94**) again we see a slight decrease in the difference of chemical shift (0.20 ppm, **Table 1**). Chloro group is well known for having electron withdrawing effect as well as mesomeric effect. These two effects acts in opposite direction and if mesomeric effect outweighs the electron withdrawing effect of the chloro group the electron density of the triazolo pyrimidine nucleus will increase and thus the stacking tendency of the triazolo pyrimidine nucleus may decrease as suggested by the Hunters and Sanders rule.[12] However when 5-SMe of the triazolo ring is oxidized to SO_2Me, there is a significant decrease in the difference of the chemical shift (0.15 ppm in **95a,** n=2; 0.07 ppm in **95b**, n =3 and 0.07 ppm in **94b**, n =3, **Table 1**). In case of SO_2Me group, the methyl protons are relatively far from the nucleus as compared to the methyl protons in the SMe group. Therefore the chances of methyl protons of sulfonyl group coming in the anisotropic region of the second ring are less and hence the lower difference in the upfield shifts. Analogous results were seen in the case of pyrazolo[3,4-*d*]pyrimidine compounds.[83] Again when SO_2Me group at 5 position in compound **101** is replaced by OMe group in compound **104** the difference in the upfield shift between compound **104** and the reference compound **105** is 0.19 (**Table 1**). The methyl protons in 5 OMe group is more close to the ring as compared to the methyl of the 5-SO_2Me and therefore has more chance to come in the anisotropic region of the other triazolo pyrimidine ring and hence the increased difference (**Table 1**). The compounds **92a-c** and **96a-c** contain a pyrimidone ring instead of pyrimidine ring and can be considered as analogues of biologically important guanine nucleus. The pyrimidone ring is more electron deficient than the pyrimidine ring and thus it was expected to show more stacking propensity. The difference in the chemical shifts between the compounds **92a-c** and the reference compound **93** is 0.31, 0.18 and 0.07 respectively, which is more than the corresponding pyrimidine ring compounds (**Table 1**). Also, the solvent used in recording the spectra of compounds **92a-c** and **93** is DMSO-d_6 which is more polar than $CDCl_3$. It is reported in literature that polar solvents increases stacking propensity between aromatic moieties[82] and this may also be one of the reason for greater difference in the upfield shifts in the ^{1}H NMR analysis of triazolo pyrimidone moieties **92a-c** as compared to the triazolo pyrimidine moieties (**Table 1**). In case of compounds **96a-c** the difference in the upfield shifts as compared to the reference compound **97** is 0.29, 0.24 and 0.08 respectively (**Table 1**). The ^{1}H NMR spectra of **96a-c** and **97** were recorded in $CDCl_3$ and the upfield shifts are greater than the triazolo pyrimidine ring compounds connected with the same linker (**Table1**).

This ^{1}H NMR study of the effect of changing the substituents at 5- and 7-positions of the triazolo[4,5-*d*]pyrimidine and triazolo[4,5-*d*]pyrimidone nucleus clearly shows that the there is little effect of changing the substituent at these positions on the conformation of the molecule in the solution state. These results are analogous to the results earlier obtained from the study on pyrazolo[3,4-*d*]pyrimidine nucleus where also we see little effect on changing the substituent (from strong electron withdrawing cyano[72] and sulfonyl[83] group to electron donating methoxy[72]) on the overall conformation of the molecule. Similarly, as in case of pyrazolo[3,4-*d*]pyrimidine nucleus the effect of changing the length of linker has a profound effect on the stacking interaction. The above study shows that the stacking behavior of the triazolo[4,5-*d*]-pyrimidine nucleus is quite similar to the pyrazolo[3,4-*d*]pyrimidine nucleus in the solution state thus enhancing the scope of *trimethylene* linker for studying intramolecular interaction.

1.4.2 X-Ray crystallographic study

In this present study we were able to prepare and study crystals of 1,3-bis(7-methoxy-5-methylthio-3*H*-[1,2,3]triazolo[4,5-*d*]pyrimidin-3-yl)propane (**90b**) and 3,3′-(propane-1,3-diyl)bis(6-methyl-5-methylthio-3*H*-[1,2,3]triazolo[4,5-d]pyrimidin-7(6*H*)-one) (**96b**). Crystal structure of compound **90b** shows folded conformation and two molecules of quite similar conformation were present in the asymmetric unit (**Fig. 37**). Different intramolecular distances and angle between the least squares planes are in the following **Table 2**.

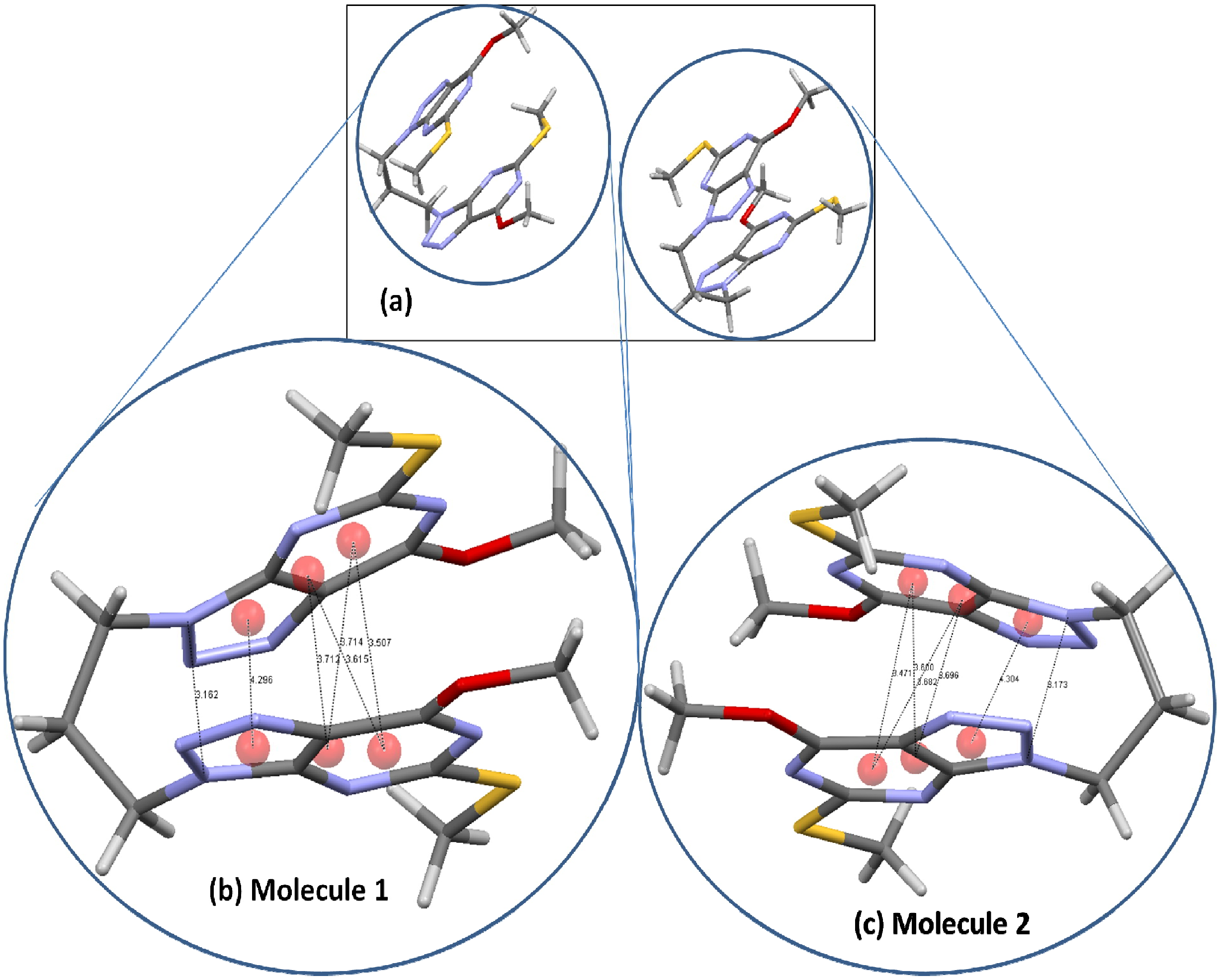

Figure 37: Crystal structure of compound **90b** showing folded conformation. (a) asymmetric unit showing two molecules (b) and (c) enlarged view of the two molecules showing different intramolecular distances

Table 2: Different intramolecular distances and angle between the least squares planes of crystal structure of **90b.**

S.No.	**Type of intramolecular property**	**Molecule 1 Distance in (A^0) and angle in (^{0})**	**Molecule 2 Distance in (A^0) and angle in (^{0})**
1.	Distance between two N atoms in the two molecules connecting the *trimethylene* linker	3.162	3.173
2.	The distance between centroids of two six-member pyrimidine ring	3.507	3.471
3.	The distance between centroids of two five-member triazol ring	4.296	4.304
4.	The distance between centroids of two nine-member triazolo[4,5-*d*]pyrimidine ring	3.712	3.696
5.	The distance between centroids of one nine-member triazolo[4,5-*d*]pyrimidine ring and one six-member pyrimidine ring	3.615 and 3.714	3.600 and 3.682
6.	The distance between centroids of one five-member triazolo ring and one six-member pyrimidine ring	4.077 and 4.275	4.090 and 4.252
7.	The distance between centroids of one five-member triazolo ring and nine-member triazolo[4,5-*d*]pyrimidine ring	4.039 and 4.152	4.049 and 4.141
8.	Angle between the least squares planes	13.37	11.46

The above distance between the two six- member pyrimidine ring is very close to the sum of the van der waals radii of the rings which is approximately equal to 3.5 A^0. This shows that there is a strong $\pi - \pi$ interaction between these two pyrimidine rings. The triazolo rings are far apart from each other which show that there is no intramolecular $\pi - \pi$ interaction between them. The angle between the least squares planes of these triazolo[4,5-*d*]pyrimidine rings shows near parallel orientation of these molecules. These results are very similar to results obtained in the studies of similar pyrazolo[3,4-*d*]pyrimidine rings.[72] In fact the intramolecular distance between the two six membered pyrimidine ring is better than the similar pyrazolo[3,4-*d*]pyrimidine compounds.

Crystal structure of compound **96b** (**Fig. 38**) shows folded conformation. Various crystallographic parameters of this molecule are shown in the table below (**Table 3**). This table also shows the various crystallographic parameters for the corresponding pyrazolo[3,4-*d*]pyrimidone compound **69** (**Fig. 30**). From this table it is clear the distances in compound **96b** is shorter than the corresponding pyrazolo[3,4-*d*]pyrimidone compound **69** which clearly indicates stronger π–π interaction between the two triazolo pyrimidone rings.

Table 3: Comparision of various crystallographic parameters of compound 96b and corresponding pyrazolo[3,4-*d*]pyrimidinone compound 69 (Fig. 30).

S.No.	Type of intramolecular property	**96b** Distance in (A^0) and angle in (^{0})	**69** Distance in (A^0) and angle in (^{0})
1.	Distance between two N atoms in the two molecules connecting the *trimethylene* linker	3.264	3.350
2.	The distance between centroids of two six-member pyrimidone ring	3.584	3.771
3.	The distance between centroids of two five-member triazole and pyrazole ring	4.473	4.621
4.	The distance between centroids of two nine-member triazolo[4,5-*d*]pyrimidone and pyrazolo[3,4-*d*] pyrimidone ring	3.871	4.034
5.	The distance between centroids of one nine-member respective triazolo[4,5-*d*]pyrimidone and pyrazolo[3,4-*d*] pyrimidone ring and one six-member pyrimidone ring	3.750 and 3.833	3.989 and 3.948
6.	The distance between centroids of one five-member respective triazole and pyrazole ring and one six-member pyrimidone ring	4.258 and 4.426	4.557 and 4.469
7.	The distance between centroids of one five-member respective triazole and pyrazole ring and nine-member respective triazolo[4,5-*d*]pyrimidone and pyrazolo[3,4-*d*] pyrimidone ring	4.226 and 4.322	4.456 and 4.404
8.	Angle between the least squares planes	10.71	12.48

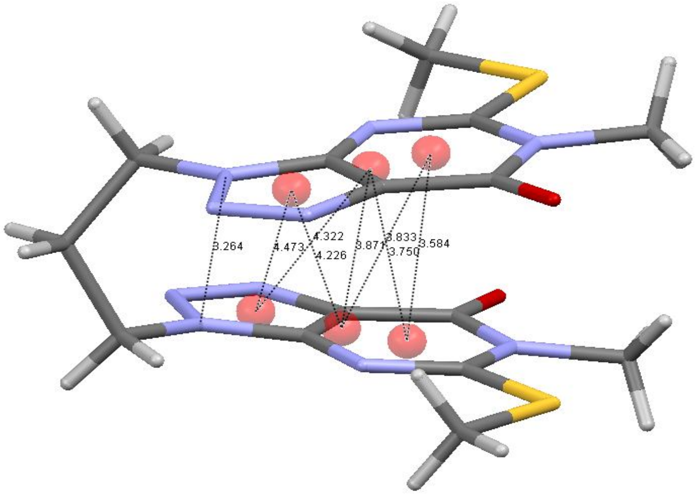

Figure 38. Crystal structure of compound **96b** showing folded conformation

1.4.3 Biological activity

Compounds **82b-e**, **88b**, **90b**, **92b**, **96b**, and **101b** were screened for antithrombotic activity in collaboration with Dr. Madhu Dixit, Fermentation Technology Division, CDRI, Lucknow. None of the compounds showed significant activity.

1.5 Conclusion

In conclusion present work shows that the stacking propensity of triazolo[4,5-*d*]pyrimidine moiety is comparable to the pyrazolo[3,4-*d*]pyrimidine moiety both in solution and solid state and important results are summarized below.

(i) In the solution state studies (^{1}H NMR analysis) of triazolo[4,5-*d*]pyrimidine and triazolo[4,5-*d*]pyrimidone moieties the groups at the 5-position clearly shows an upfield shift in case of *ethylene* and *propylene* linker compounds and this upfield shift decreases with the increase of the length of the linker. Similar results are seen in the pyrazolo[3,4-*d*]pyrimidine and pyrazolo[3,4-*d*]pyrimidone based *polymethylene* linker compounds where the groups substituted at 6-position (corresponding to the 5-position of triazolo[4,5-*d*]pyrimidine ring) shows an upfield shift in case of *ethylene* and *propylene* linker compounds and this upfield shift decreases with the increase of the length of the linker.

(ii) The effect of change of substituents does not significantly affect the stacking propensity of the triazolo[4,5-*d*]pyrimidine nucleus in the solution state as seen in case of pyrazolo[3,4-*d*]pyrimidine based *polymethylene* linker compounds.

(iii) In the solid state studies, in case of the *propylene* linker compounds (**89b** and **96b**) the intramolecular orientation of the two rings with respect to each other is similar to the results obtained earlier with corresponding *propylene* linker compounds of pyrazolo[3,4-*d*]pyrimidine nucleus. The six member pyrimidine part of the triazolo[4,5-*d*]pyrimidine rings partially overlap each other while the five member triazolo part of the triazolo[4,5-*d*]pyrimidine rings are far away which is again quite similar to the corresponding pyrazolo[3,4-*d*]pyrimidine compounds.

1.6 Experimental Section

1.6.1 Synthesis of 3-butyl-5,7-bis(methylthio)-3*H*-[1,2,3]triazolo[4,5-*d*]pyrimidine (87).

1.6.1.1 Synthesis of 1-azidobutane (84).

To a 500 ml round bottom flask containing 250 ml DMSO (250 ml) added NaN_3 (9.75g, 0.15 mol) and the mixture was stirred for 12-24 h at r.t. until no solid was observed. 1-iodobutane (**83**) (18.4 g, 0.10 mol) was added and the reaction mixture stirred at 50^0 C for another 12 -24 h. water was added in portions (5 x 20ml) while allowing the reaction mixture to cool to r.t. between portions. The mixture was extracted with ether (4 x 50 ml). The extracts were combined and washed with water (2 x100 ml) and dried over sodium sulphate. The solvent was removed under vacuum to yield 1-azidobutane **(84)** as clear oil. The yield of this reaction is reported to be nearly 100% in literature.[79]

Caution 1: Azides are **explosive** in nature. Hence further purification and storage of azides was avoided and the synthesized compound was immediately consumed in the next step assuming a yield of about 95%.

Caution 2: Azides are known to form explosive mixtures with halogenated solvents like dichloromethane, chloroform etc., hence as a precaution **halogenated solvents** should not be used for extraction.

1.6.1.2 Synthesis of 5-amino-1-butyl-1*H*-1,2,3-triazole-4-carbonitrile (85).

To a suspension of potassium carbonate (1.65g. 0.012mol) in dimethyl sulfoxide (50 mL) was added 1g (0.01 mol) of 1-azidobutane **(84)** and 0.72g of malononitrile (0.011 mol) at r.t., the mixture was stirred at same temperature for 36 hours. After dilution of the mixture with water (100 ml) the reaction mixture was kept overnight so that complete precipitation could take place which was filtered and air dried. This compound (**85**) had sufficient purity and was used as such in the next step. A small amount of this compound was further purified by column chromatography (ethyl acetate + hexane) for analytical purpose. The characterization of the compound was done on the basis of ^{1}H NMR and MS.

85: Yield: 50- 65%; mp: 154–156 °C; MS (ESI) m/z 166 $[M+H]^+$; ^1H NMR (300 MHz, $CDCl_3$) δ (ppm): 0.94-0.98 (m, 3H, CH_3), 1.32-1.46 (m, 3H, CH_2), 1.82-190 (m, 2H, CH_2), 4.10-4.18 (m, 2H, NCH_2), 4.67 (s, 4H, NH_2).

1.6.1.3 Synthesis of 3-butyl-3*H*-[1,2,3]triazolo[4,5-*d*]pyrimidine-5,7-dithiol (86).

To a round bottom flask containing 50 ml DMF added **85** (1.66g, 0.010 mol) and cesium carbonate (3.91g, 0.012 mol) and stirred for about 15 minutes. Then CS_2 (0.81g, 0.012 mol) was added and the reaction mixture was further stirred at r.t. for about 8 h. DMF was removed under reduced pressure and ice-cold water was added to the reaction mixture and the solution acidified with aq. solution of HCl till the pH of the solution becomes ≈ 2. To this aq. solution of NaOH was added till the pH becomes around 9. This solution is passed through a G3 sintered funnel to remove un-dissolved material. The filtrate is again acidified with aq. HCl to make the pH of the solution just acidic (≈ 6.5 to 7). This was kept overnight so that complete precipitation takes place. The precipitate is filtered and air dried to yield compound **86**. The characterization of the compound was done on the basis of ^1H NMR and MS.

86: Yield: 50- 65%; mp: > 250 °C; MS (ESI) m/z 242 $[M+H]^+$; ^1H NMR (300 MHz, DMSO-*d_6*) δ (ppm): 0.92-0.98 (m, 3H, CH_3), 1.30-1.35 (m, 2H, CH_2), 1.74-1.82 (m, 2H, CH_2), 4.42-4.48 (m, 2H, NCH_2), 8.36 (s, 4H, SH).

1.6.1.4 Synthesis of 3-butyl-5,7-bis(methylthio)-3*H*-[1,2,3]triazolo[4,5-*d*]pyrimidine (87).

To a round bottom flask containing 50 ml water added NaOH pellets (0.8 g, 0.020 mol), **86** (2.41g, 0.010 mol) and methyl iodide (2.84g, 0.02 mol). The reaction was stirred for about 12h and the precipitate is filtered and air dried. This precipitate is further purified by column chromatography using a mixture of ethyl acetate and hexane in increasing polarity yielding compound **87**. The characterization of the compound was done on the basis of ^1H NMR and MS.

87: Yield: 50- 60%; mp: 110–112 °C; MS (ESI) m/z 270 $[M+H]^+$; ^1H NMR (300 MHz, $CDCl_3$) δ (ppm): 0.92-1.00 (m, 3H, CH_3), 1.30-1.40 (m, 2H, CH_2), 1.94-2.04 (m, 2H, CH_2), 2.64 (s, 6H, SCH_3), 2.75 (s, 6H, SCH_3), 4.54-4.6 (m, 2H, NCH_2).

1.6.2 General Procedure for synthesis of 1,n-bis(5,7-bis(methylthio)-3*H*-[1,2,3]triazolo-[4,5- *d*]pyrimidin-3-yl)alkane.

The compounds in **Scheme 2** were synthesized using the procedures used in the synthesis of analogous compounds in **Scheme 3** described in **Section 1.6.1** with adjustment in the molar quantities of reactants.

1.6.2.1 Synthesis of 1,n-diazidoalkane (79a-e).

Synthesis of azides (**79a-e**) was done according to the literature procedure [79] and azides were consumed as soon as prepared.

1.6.2.2 Synthesis of 1,1′-(alkane-1,n-diyl)bis(5-amino-1*H*-1,2,3-triazole-4-carbonitrile) (80a-e).

Compounds **80a-e** were synthesized using the procedure described in section 1.6.1.2 with adjustments in the molar quantities.

1.6.2.2.1 Synthesis of 1,1′-(ethane-1,2-diyl)bis(5-amino-1*H*-1,2,3-triazole-4-carbonitrile) (80a).

80a: Yield: 30%; mp: > 250 °C; MS (ESI) m/z 245 $[M+H]^+$.

1.6.2.2.2 Synthesis of 1,1′-(propane-1,3-diyl)bis(5-amino-1*H*-1,2,3-triazole-4-carbonitrile) (80b).

80b: Yield: 45%; mp: > 250 °C; MS (ESI) m/z 245 $[M+H]^+$; ^1H NMR (300 MHz, DMSO-d_6) δ (ppm): 2.16 (quintet, J = 7.0 Hz, 2H, CH_2), 4.16 (t, J = 7.0 Hz, 4H, NCH_2), 7.08 (s, 4H, NH_2).

1.6.2.2.3 Synthesis of 1,1′-(butane-1,4-diyl)bis(5-amino-1*H*-1,2,3-triazole-4-carbonitrile) (80c).

80c: Yield: 45%; mp: 210-212 °C; MS (ESI) m/z 245 $[M+H]^+$; ^1H NMR (300 MHz, DMSO-d_6) δ (ppm): 1.69 (bs, 4H, CH_2), 4.15 (bs, 4H, NCH_2), 7.02 (s, 4H, NH_2).

1.6.2.2.4 Synthesis of 1,1′-(pentane-1,5-diyl)bis(5-amino-1*H*-1,2,3-triazole-4-carbonitrile) (80d).

80d: Yield: 45%; mp: 194-196 °C; MS (ESI) m/z 245 $[M+H]^+$; ^1H NMR (300 MHz, DMSO-d_6) δ (ppm): 1.69 (bs, 4H, CH_2), 4.15 (bs, 4H, NCH_2), 7.02 (s, 4H, NH_2).

1.6.2.2.5 Synthesis of 1,1′-(hexane-1,6-diyl)bis(5-amino-1*H*-1,2,3-triazole-4-carbonitrile) (80e).

80e: Yield: 45%; mp: 200-202 °C; MS (ESI) m/z 245 $[M+H]^+$; ^1H NMR (300 MHz, DMSO-d_6) δ (ppm): 1.22-1.28 (m, 2H, CH_2), 1.68-1.76 (m, 4H, CH_2), 4.10 (t, J = 6.8 Hz, 4H, NCH_2), 7.0 (s, 4H, NCH_2),

1.6.2.3 Synthesis of 3,3′-(alkane-1,n-diyl)bis(3*H*-[1,2,3]triazolo[4,5-*d*]pyrimidine-5,7-dithiol) (81a-e).

Compounds **80a-e** was synthesized using the procedure described in **Section 1.6.1.3** with adjustments in the molar quantities of the reactants.

1.6.2.3.1 Synthesis of 3,3′-(ethane-1,2-diyl)bis(3*H*-[1,2,3]triazolo[4,5-*d*]pyrimidine-5,7-dithiol) (81a).

81a: Yield: 40-45%; mp: > 250 °C; MS (ESI) m/z 397 $[M+H]^+$.

1.6.2.3.2 Synthesis of 3,3′-(propane-1,3-diyl)bis(3*H*-[1,2,3]triazolo[4,5-*d*]pyrimidine-5,7-dithiol) (81b).

81b: Yield: 45-50%; mp: > 250 °C; MS (ESI) m/z 411 $[M+H]^+$.

1.6.2.3.3 Synthesis of 3,3′-(butane-1,4-diyl)bis(3*H*-[1,2,3]triazolo[4,5-*d*]pyrimidine-5,7-dithiol) (81c).

81c: Yield: 45-50%; mp: > 250 °C; MS (ESI) m/z 425 $[M+H]^+$; ^{1}H NMR (300 MHz, DMSO-d_6) δ (ppm): 1.81 (bs, 4H, CH_2), 4.30 (bs, 4H, NCH_2), 11.38 (bs, 4H, SH).

1.6.2.3.4 Synthesis of 3,3′-(pentane-1,5-diyl)bis(3*H*-[1,2,3]triazolo[4,5-*d*]pyrimidine-5,7-dithiol) (81d).

81d: Yield: 45-50%; mp:> 250 °C; MS (ESI) m/z 439 $[M+H]^+$.

1.6.2.3.5 Synthesis of 3,3′-(hexane-1,6-diyl)bis(3*H*-[1,2,3]triazolo[4,5-*d*]pyrimidine-5,7-dithiol) (81e).

81e: Yield: 45%; mp: > 250 °C; MS (ESI) m/z 453 $[M+H]^+$.

1.6.2.4 Synthesis of 1,n-bis(5,7-bis(methylthio)-3*H*-[1,2,3]triazolo[4,5-*d*]pyrimidin-3-yl)alkane (82a-e).

Compounds **82a-e** was synthesized using the procedure described in **Section 1.6.1.4** with adjustments in the molar quantities of the reactants.

1.6.2.4.1 Synthesis of 1,2-bis(5,7-bis(methylthio)-3*H*-[1,2,3]triazolo[4,5-*d*]pyrimidin-3-yl)ethane (82a).

82a: Yield: 75%; mp: 190-192 °C; MS (ESI) m/z 453 $[M+H]^+$; ^{1}H NMR (300 MHz, $CDCl_3$) δ (ppm): 2.40 (s, 6H, SCH_3), 2.72 (s, 6H, SCH_3), 5.12 (s, 4H, NCH_2); ^{13}C NMR (75 MHz, $CDCl_3$) δ (ppm): 12.30, 14.70, 46.30, 131.90, 148.14, 164.94, 170.06; Anal. Calcd. for $C_{14}H_{16}N_{10}S_4$: C, 37.15; H, 3.56; N, 30.95; Found: C, 37.55; H, 3.75; N, 31.09.

1.6.2.4.2 Synthesis of 1,3-bis(5,7-bis(methylthio)-3*H*-[1,2,3]triazolo[4,5-*d*]pyrimidin-3-yl)propane (82b).

82b: Yield: 70%; mp: 140-142 °C; MS (ESI) m/z 467 $[M+H]^+$; ^1H NMR (300 MHz, $CDCl_3$) δ (ppm): 2.50 (s, 6H, SCH_3), 2.75 (s, 6H, SCH_3), 2.89 (q, 2H, *J* = 6.6 Hz, CH_2), 4.60 (t, 4H, *J* = 6.6 Hz, NCH_2); ^{13}C NMR (75 MHz, $CDCl_3$) δ (ppm): 12.10, 14.61, 28.03, 43.30, 131.95, 148.04, 164.90, 170.00; Anal. Calcd. for $C_{15}H_{18}N_{10}S_4$: C, 38.61; H, 3.89; N, 30.02; Found: C, 38.59; H, 4.05; N, 38.79.

1.6.2.4.3 Synthesis of 1,4-bis(5,7-bis(methylthio)-3*H*-[1,2,3]triazolo[4,5-*d*]pyrimidin-3-yl)butane (82c).

82c: Yield: 72%; mp: 164-166 °C; MS (ESI) m/z 467 $[M+H]^+$; ^1H NMR (300 MHz, $CDCl_3$) δ (ppm): 2.05 (bs, 4H, CH_2), 2.60 (s, 6H, SCH_3), 2.75 (s, 6H, SCH_3), 4.64 (bs, 4H, NCH_2); ^{13}C NMR (75 MHz, $CDCl_3$) δ (ppm): 12.10, 14.67, 26.03, 45.81, 131.93, 148.06, 164.88, 170.02; Anal. Calcd. for $C_{16}H_{20}N_{10}S_4$: C, 39.98; H, 4.19; N, 29.14; Found: C, 39.95; H, 4.21; N, 29.29.

1.6.2.4.4 Synthesis of 1,5-bis(5,7-bis(methylthio)-3*H*-[1,2,3]triazolo[4,5-*d*]pyrimidin-3-yl)pentane (82d).

82d: Yield: 72%; mp: 136-138 °C; MS (ESI) m/z 495 $[M+H]^+$; ^1H NMR (300 MHz, $CDCl_3$) δ (ppm): 1.36-1.44(m, 2H, CH_2), 2.02-2.15 (m, 4H, CH_2), 2.61 (s, 6H, SCH_3), 2.75 (s, 6H, SCH_3), 4.56 (bs, 4H, NCH_2); ^{13}C NMR (75 MHz, $CDCl_3$) δ (ppm): 12.10, 14.67, 26.03, 28.90, 45.81, 132.01, 148.04, 164.80, 170.05; Anal. Calcd. for $C_{17}H_{22}N_{10}S_4$: C, 41.28; H, 4.48; N, 28.31; Found: C, 41.38; H, 4.71; N, 28.29.

1.6.2.4.5 Synthesis of 1,6-bis(5,7-bis(methylthio)-3*H*-[1,2,3]triazolo[4,5-*d*]pyrimidin-3-yl)hexane (82e).

82e: Yield: 72%; mp: 124-126 °C; MS (ESI) m/z 509 $[M+H]^+$; ^1H NMR (300 MHz, $CDCl_3$) δ (ppm): 1.40 (bs, 4H, CH_2), 2.00 (bs, 4H, CH_2), 2.63 (s, 6H, SCH_3), 2.75 (s, 6H, SCH_3), 4.56 (bs, 4H, NCH_2); ^{13}C NMR (75 MHz, $CDCl_3$) δ (ppm): 11.97, 14.63, 25.85, 29.03, 46.52, 132.11, 148.01, 164.83, 170.09; Anal. Calcd. for $C_{18}H_{24}N_{10}S_4$: C, 41.28; H, 4.48; N, 28.31; Found: C, 41.38; H, 4.71; N, 28.29.

1.6.3 Synthesis of various 3-butyl-5,7-disubstituted-3*H*-[1,2,3]triazolo[4,5-*d*]pyrimidine and 1,n-disubstituted-3*H*-[1,2,3]triazolo[4,5-*d*]pyrimidin-3-yl)alkane.

The dimeric compounds **88a-c**, **90a-c**, **92a-c**, **94a-c**, **96a-c**, **98**, **100**, **101a-b**, **104** were synthesized using the procedure described for the synthesis of corresponding monomeric compounds **89**, **91**, **93**, **95**, **97**, **99**, **102**, **103** and **105** respectively with adjustments in the molar quantities of the reactants.

1.6.3.1 Synthesis of 3-butyl-5-methylthio-7-pyrrolidin-1-yl-3*H*-[1,2,3]triazolo[4,5-*d*]pyrimidine (89).

The compound **87** (0.53g, 0.002 mole) and pyrrolidine (5ml) was refluxed for 6h. Excess of pyrrolidine was removed under reduced pressure. Ice cold water (50 ml) was added to the reaction mixture and neutralized it with a dilute solution of acetic acid. The reaction mixture extracted with 150 ml of chloroform (50 ml x 3) and was dried over sodium sulfate. The residue obtained by the removal of chloroform under reduced pressure was purified by column chromatography on silica gel using mixture of ethyl acetate-hexane in increasing polarity to give pure compound **89**.

89: Yield: 50- 65%; mp: 78–80 °C; MS (ESI) m/z 240 $[M+H]^+$; ^1H NMR (300 MHz, $CDCl_3$) δ (ppm): 0.90-0.99 (m, 3H, CH_3), 1.30-1.44 (m, 2H, CH_2), 1.90-2.20 (m, 6H, CH_2), 2.58 (s, 3H, SCH_3), 3.80 (t, 2H, J = 6 Hz, NCH_2), 4.22 (t, 2H, J = 6 Hz, NCH_2), 4.49 (t, 2H, J = 6 Hz, NCH_2).

1.6.3.2.1 Synthesis of 1,2-bis(5-methylthio-7-pyrrolidin-1-yl-3*H*-[1,2,3]triazolo[4,5-*d*]pyrimidin-3-yl)ethane (88a).

88a:Yield: 90%; mp: 210-212 °C; MS (ESI) m/z 499 $[M+H]^+$; ^1H NMR (300 MHz, $CDCl_3$) δ (ppm): 1.94-2.16 (m, 8H, pyrrolidine-H), 2.41(s, 6H, SCH_3), 3.70-3.80 (m, 4H, pyrrolidine-H), 4.10-4.20 (m, 4H, pyrrolidine-H), 5.01 (s, 4H, NCH_2); ^{13}C NMR (75 MHz, $CDCl_3$) δ (ppm): 14.26, 24.24, 26.04, 45.76, 47.42, 49.27, 124.11, 150.44, 151.56, 170.20; Anal. Calcd. for $C_{20}H_{26}N_{12}S_2$: C, 48.17; H, 5.26; N, 33.71; Found: C, 48.20; H, 5.35; N, 33.81.

1.6.3.2.2 Synthesis of 1,3-bis(5-methylthio-7-pyrrolidin-1-yl-3*H*-[1,2,3]triazolo[4,5-*d*]pyrimidin-3-yl)propane (88b).

88b:Yield: 90%; mp: 182-184 °C; MS (ESI) m/z 513 $[M+H]^+$; ^1H NMR (300 MHz, $CDCl_3$) δ (ppm): 1.94-2.20 (m, 8H, pyrrolidine-H), 2.49(s, 6H, SCH_3), 2.75 (q, 2H, J = 10.2 Hz, CH_2), 3.79 (t, 4H, J = 10 Hz, pyrrolidine-H), 4.21 (t, 4H, J = 10 Hz, pyrrolidine-H), 4.57 (t, 2H, J = 10.2 Hz, NCH_2); ^{13}C NMR (75 MHz, $CDCl_3$) δ (ppm): 14.40, 24.24, 26.04, 28.47, 43.46, 47.42, 49.27, 124.09, 150.46, 151.54, 170.21. Anal. Calcd. for $C_{21}H_{28}N_{12}S_2$: C, 49.20; H, 5.51; N, 32.79; Found: C, 49.10; H, 5.45; N, 32.89.

1.6.3.2.3 Synthesis of 1,4-bis(5-methylthio-7-pyrrolidin-1-yl-3*H*-[1,2,3]triazolo[4,5-*d*]-pyrimidin-3-yl)butane (88c).

88c: Yield: 90%; mp: 160-162 °C; MS (ESI) m/z 527 $[M+H]^+$; ^1H NMR (300 MHz, $CDCl_3$) δ (ppm): 1.94-2.10 (m, 8H, pyrrolidine-H), 2.11-2.18 (m, 4H, CH_2), 2.54 (s, 6H, SCH_3), 3.77-3.83 (m, 4H, pyrrolidine-H), 4.17-4.23 (m, 4H, pyrrolidine-H), 4.55-4.58 (m, 2H, NCH_2); ^{13}C NMR (75 MHz, $CDCl_3$) δ (ppm): 14.46, 24.23, 25.93, 45.38, 47.43, 49.27, 124.09, 150.41, 151.57, 170.12; Anal. Calcd. for $C_{22}H_{30}N_{12}S_2$: C, 50.17; H, 5.74; N, 31.91; Found: C, 50.27; H, 5.85; N, 31.90.

1.6.3.3 Synthesis of 3-butyl-7-methoxy-5-methylthio-3*H*-[1,2,3]triazolo[4,5-*d*]pyrimidine (91).

To a 250 ml round bottom flask containing 100 ml of anhydrous methanol added the compound **87** (0.53 g, 0.002 mole) and kept on refluxing with stirring for 30 minutes. Sodium methoxide (0.28 g, 0.0052 moles) was added and the mixture was further refluxed for 6h. Methanol was removed under reduced pressure and ice cold water was added to round bottom flask and the solution was neutralized with dilute acidic acid. The solution was kept for 8-10h so that complete precipitation occurred. The solid precipitate was filtered, washed with water and air dried at 80 °C. This was purified by column chromatography on silica gel using mixture of ethyl acetate-hexane in increasing polarity to give pure compound **91**.

91: Yield: 70- 75%; mp: 108-110 °C; MS (ESI) m/z 254 $[M+H]^+$; ^1H NMR (300 MHz, $CDCl_3$) δ (ppm): 0.90-1.00 (m, 3H, CH_3), 1.31-1.40 (m, 2H, CH_2), 1.94-2.02 (m, 2H, CH_2), 2.64 (s, 3H, SCH_3), 4.24 (s, 3H, OCH_3), 4.52-4.6 (m, 2H, NCH_2).

1.6.3.4.1 Synthesis of 1,2-bis(7-methoxy-5-(methylthio)-3*H*-[1,2,3]triazolo[4,5-*d*]pyrimidin-3-yl)ethane (90a).

90a:Yield: 85%; mp: 152-154 °C; MS (ESI) m/z 421 $[M+H]^+$; ^1H NMR (300 MHz, $CDCl_3$) δ (ppm): 2.40 (s, 6H, SCH_3), 4.20 (s, 6H, OCH_3), 5.13 (s, 4H, NCH_2); ^{13}C NMR (75 MHz, $CDCl_3$) δ (ppm): 14.22, 46.24, 55.08, 123.76, 152.00, 160.37, 171.63; Anal. Calcd. for $C_{14}H_{16}N_{10}O_2S_2$: C, 39.99; H, 3.84; N, 33.31; Found: C, 40.09; H, 3.95; N, 33.29.

1.6.3.4.2 Synthesis of 1,3-bis(7-methoxy-5-(methylthio)-3*H*-[1,2,3]triazolo[4,5-*d*]-pyrimidin-3-yl)propane (90b).

90b:Yield: 80%; mp: 128-130 °C; MS (ESI) m/z 435 $[M+H]^+$; ^1H NMR (300 MHz, $CDCl_3$) δ (ppm): 2.49 (s, 6H, SCH_3), 2.90 (q, 2H, *J* = 6.6 Hz, CH_2), 4.24 (s, 6H, OCH_3), 4.60 (t, 4H, *J* = 6.6 Hz, NCH_2); ^{13}C NMR (75 MHz, $CDCl_3$) δ (ppm): 14.39, 27.95, 43.22, 55.04, 123.76, 151.63, 160.40, 171.76; Anal. Calcd. for $C_{15}H_{18}N_{10}$ O_2S_2: C, 41.46; H, 4.18; N, 32.24; Found: C, 41.60; H, 4.25; N, 32.79.

1.6.3.4.3 Synthesis of 1,4-bis(7-methoxy-5-methylthio-3*H*-[1,2,3]triazolo[4,5-*d*]pyrimidin-3-yl)butane (90c).

90c:Yield: 80%; mp: 142-144 °C; MS (ESI) m/z 449 $[M+H]^+$; ^1H NMR (300 MHz, $CDCl_3$) δ (ppm): 2.05 (bs, 4H, CH_2), 2.60 (s, 6H, SCH_3), 4.24 (s, 6H, OCH_3), 4.65 (bs, 4H, NCH_2); ^{13}C NMR (75 MHz, $CDCl_3$) δ (ppm): 14.43, 26.15, 45.32, 55.06, 123.74, 151.65, 160.42, 171.74; Anal. Calcd. for $C_{16}H_{20}N_{10}O_2S_2$: C, 42.85; H, 4.49; N, 31.23; Found: C, 42.89; H, 4.55; N, 31.39.

1.6.3.5 Synthesis of 3-butyl-5-methylthio-3*H*-[1,2,3]triazolo[4,5-*d*]pyrimidin-7(6*H*)-one (93).

The compound **87** (2.69g, 0.010 mole) was added to a round bottom flask containing 200 ml of methanol and kept on refluxing with stirring for about 30 minutes, Aqueous NaOH (1.6g dissolved in 20ml of water, 0.040 mol) was added drop wise to it over 30 minutes. The reaction mixture was further refluxed for 4h and then it was cooled in ice bath and acidified with acetic acid till the pH of the solution is around 6 and kept for another 8-10h so that complete precipitation has occurred. The solid precipitate is filtered, washed with water and air dried at 80 $^{\circ}$C. The resulting product was heated with a mixture of chloroform and hexane (40:60) and filtered hot. The compound **93** was obtained as solid precipitate.

93: Yield: 50- 65%; mp: 144–146 °C; MS (ESI) m/z 240 $[M+H]^+$; ^1H NMR (300 MHz, DMSO-d_6) δ (ppm): 0.85-0.95 (m, 3H, CH_3), 1.22-1.29 (m, 2H, $CH_{2)}$, 1.82-1.94 (m, 2H, CH_2), 2.59 (s, 3H, SCH_3), 4.46-4.50 (m, 2H, NCH_2), 12.88 (bs, 1H, NH).

1.6.3.6.1 Synthesis of 3,3′-(ethane-1,2-diyl)bis(5-methylthio-3*H*-[1,2,3]triazolo[4,5-*d*]pyrimidin-7(6*H*)-one) (92a).

92a: Yield: 82%; mp: > 250 °C; MS (ESI) m/z 393 $[M+H]^+$; ^1H NMR (300 MHz, DMSO-d_6) δ (ppm): 2.28(s, 6H, SCH_3), 4.97 (s, 4H, NCH_2); 14.10 (bs,2H, NH) ^{13}C NMR (75 MHz, DMSO-d_6) δ (ppm): 12.95, 43.96, 127.07, 148.68, 155.46, 162.41; Anal. Calcd. for $C_{12}H_{12}N_{10}O_2S_2$: C, 36.73; H, 3.08; N, 35.69; Found: C, 36.88; H, 3.18; N, 35.79.

1.6.3.6.2 Synthesis of 3,3′-(propane-1,3-diyl)bis(5-(methylthio)-3*H*-[1,2,3]triazolo[4,5-*d*]pyrimidin-7(6*H*)-one) (92b).

92b:Yield: 80%; mp: 220-222 °C; MS (ESI) m/z 407 $[M+H]^+$; ^1H NMR (300 MHz, DMSO-d_6) δ (ppm): 2.40(s, 6H, SCH_3), 2.72 (bs, 2H, CH_2), 4.43 (s, 4H, NCH_2); 12.81 (bs,2H, NH) ^{13}C NMR (75 MHz, DMSO-d_6) δ (ppm): 12.90, 27.16, 42.96, 126.97, 148.49, 155.29, 162.51; Anal. Calcd. for $C_{13}H_{14}N_{10}O_2S_2$: C, 38.42; H, 3.47; N, 34.46; Found: C, 38.52; H, 3.68; N, 35.01.

1.6.3.6.3 Synthesis of 3,3′-(butane-1,4-diyl)bis(5-(methylthio)-3*H*-[1,2,3]triazolo[4,5-*d*]pyrimidin-7(6*H*)-one) (92c).

92c: Yield: 80%; mp: 194-196 °C; MS (ESI) m/z 421 $[M+H]^+$; ^1H NMR (300 MHz, DMSO-d_6) δ (ppm): 1.90 (bs, 4H, CH_2), 2.52(s, 6H, SCH_3), 4.53 (s, 4H, NCH_2); 12.91 (bs,2H, NH) ^{13}C NMR (75 MHz, DMSO-d_6) δ (ppm): 13.13, 25.32, 45.60, 127.10, 148.50, 155.37, 162.52; Anal. Calcd. for $C_{14}H_{16}N_{10}O_2S_2$: C, 39.99; H, 3.84; N, 33.31; Found: C, 40.05; H, 3.98; N, 33.51.

1.6.3.7 Synthesis of 3-butyl-7-chloro-5-(methylthio)-3*H*-[1,2,3]triazolo[4,5-*d*]pyrimidine (95).

To a 250 ml round bottom flask containing 100 ml of chloroform added compound **93** (0.47g, 0.002 mole) and kept on stirring at around 60^0C for 10 minutes. A mixture of $SOCl_2$ (4.5 ml) and DMF (0.8 ml) was added drop wise for about 30 minutes. This reaction mixture was further refluxed for 5 h. Excess chloroform was removed under reduced pressure and crushed ice was added. This was neutralized with a dilute solution of $NaHCO_3$ under ice cold condition and extracted with chloroform. The residue obtained by the removal of chloroform under reduced pressure was purified by column chromatography on silica gel using mixture of ethyl acetate-hexane in increasing polarity to give pure compound **95**.

95: Yield: 50- 65%; mp: 94–96 °C; MS (ESI) m/z 258 $[M+H]^+$; ^1H NMR (300 MHz, $CDCl_3$) δ (ppm): 0.99 (t, 3H, J = 6 Hz, CH_3), 1.30-1.44 (m, 2H, CH_2), 2.00-2.10 (m, 2H, CH_2), 2.66 (s, 3H, SCH_3), 4.64 (t, 2H, J = 6 Hz, NCH_2).

1.6.3.8.1 Synthesis of 1,2-bis(7-chloro-5-methylthio-3*H*-[1,2,3]triazolo[4,5-*d*]pyrimidin-3-yl)ethane (94a).

94a: Yield: 85%; mp 184–186 °C; MS (ESI) m/z 429 $[M+H]^+$; ^1H NMR (300 MHz, $CDCl_3$) δ (ppm): 2.46(s, 6H, SCH_3), 5.21 (s, NCH_2); ^{13}C NMR (75 MHz, $CDCl_3$) δ (ppm): 14.55, 46.44, 131.60, 150.96, 153.20, 172.60; Anal. Calcd. for $C_{12}H_{10}Cl_2N_{10}S_2$: C, 33.57; H, 2.35; N, 32.63; Found: C, 33.67; H, 2.42; N, 32.79.

1.6.3.8.2 Synthesis of 1,3-bis(7-chloro-5-methylthio-3*H*-[1,2,3]triazolo[4,5-*d*]pyrimidin-3-yl)propane (94b).

94b:Yield: 95%; mp: 162–164 °C; MS (ESI) m/z 444 $[M+H]^+$; ^1H NMR (300 MHz, $CDCl_3$) δ (ppm): 2.55(s, 6H, SCH_3), 2.95 (q, 2H, J = 6.6 Hz, CH_2), 4.69 (t, 4H, J = 6.6 Hz, NCH_2); ^{13}C NMR (75 MHz, $CDCl_3$): δ (ppm): 14.75, 27.91, 43.77, 131.60, 150.62, 153.14, 172.26; Anal. Calcd. for $C_{13}H_{12}Cl_2N_{10}S_2$: C, 35.22; H, 2.73; N, 31.59; Found: C, 35.20; H, 2.92; N, 31.49.

1.6.3.8.3 Synthesis of 1,4-bis(7-chloro-5-methylthio-3*H*-[1,2,3]triazolo[4,5-*d*]pyrimidin-3-yl)butane (94c).

94c: Yield: 92%; mp: 168–170 °C; MS (ESI) m/z 458 $[M+H]^+$; ^1H NMR (300 MHz, $CDCl_3$) δ (ppm): 2.12 (bs, 4H, CH_2), 2.62 (s, 6H, SCH_3), 4.70 (bs, 4H, NCH_2); ^{13}C NMR (75 MHz, $CDCl_3$) δ (ppm): 14.84, 25.98, 46.27, 131.60, 150.72, 153.11, 172.16; Anal. Calcd. for $C_{14}H_{14}Cl_2N_{10}S_2$: C, 36.76; H, 3.09; N, 30.62; Found: C, 36.86; H, 3.11; N, 30.69.

1.6.3.9 Synthesis of 3-butyl-6-methyl-5-methylthio-3*H*-[1,2,3]triazolo[4,5-*d*]pyrimidin-7(6*H*)-one (97).

Compound **93** (0.24g, 0.001 mol) was added to a flask containing 5 ml of DMF and K_2CO_3(0.15g, 0.0011 mol) and stirred for 15 min. Methyl iodide (0.15g, 0.0011 mol) was added to the reaction mixture and stirring was continued for another 6 h. Excess DMF was removed under reduced pressure. The reaction mixure extracted with 60 ml of chloroform (20 ml x 3) and was dried over sodium sulfate. The residue obtained by the removal of chloroform under reduced pressure was purified by column chromatography on silica gel using mixture of ethyl acetate-hexane in increasing polarity to give pure compound **97**.

97: Yield: 50- 65%; mp: 134–136 °C; MS (ESI) m/z 254 $[M+H]^+$; ^1H NMR (300 MHz, $CDCl_3$) δ (ppm): 0.97 (t, 3H, J = 6 Hz, CH_3), 1.28-1.44 (m, 2H, CH_2), 1.99 (quintet, 2H, J = 6 Hz, CH_2), 2.67 (s, 3H, SCH_3), 3.62 (s, 3H, NCH_3), 3.83 (s, 3H, CH_3), 4.50 (t, 2H, J = 6 Hz, NCH_2).

1.6.3.10.1 Synthesis of 3,3′-(ethane-1,2-diyl)bis(6-methyl-5-methylthio-3*H*-[1,2,3]triazolo-[4,5-*d*]pyrimidin-7(6*H*)-one) (96a).

96a: Yield: 70%; mp: > 250 °C; MS (ESI) m/z 421 $[M+H]^+$; ^1H NMR (300 MHz, $CDCl_3$) δ (ppm): 2.38 (s, 6H, SCH_3), 2.65 (s, 6H, NCH_3), 5.02 (s, 4H, NCH_2). ^{13}C NMR (75 MHz, $CDCl_3$ + DMSO-*d*$_6$) δ (ppm): 14.13, 39.32, 44.30, 126.10, 149.50, 154.37, 170.52; Anal. Calcd. for $C_{14}H_{16}N_{10}O_6S_2$: C, 39.99; H, 3.84; N, 33.31; Found: C, 40.36; H, 4.16; N, 33.50.

1.6.3.10.2 Synthesis of 3,3′-(propane-1,3-diyl)bis(6-methyl-5-methylthio-3*H*-[1,2,3]-triazolo[4,5-*d*]pyrimidin-7(6*H*)-one) (96b).

96b: Yield: 80%; mp: > 250 °C; MS (ESI) m/z 435 $[M+H]^+$; ^1H NMR (300 MHz, $CDCl_3$) δ (ppm): 2.44 (s, 6H, SCH_3), 2.97 (q, 2H, J = 6.39 Hz, CH_2), 3.58 (s, 6H, NCH_3), 4.40 (t, 4H, *J* = 6.39 Hz, NCH_2). ^{13}C NMR (75 MHz, $CDCl_3$) δ (ppm): 14.40, 28.41, 37.38, 43.45, 124.05, 150.80, 153.56, 169.95 Anal. Calcd. for $C_{15}H_{18}N_{10}O_2S_2$: C, 41.46.14; H, 4.18; N, 32.24; Found: C, 41.36; H, 4.20; N, 32.30.

1.6.3.10.3 Synthesis of 3,3′-(butane-1,4-diyl)bis(6-methyl-5-methylthio-3*H*-[1,2,3]triazolo-[4,5-*d*]pyrimidin-7(6*H*)-one) (96c).

96c: Yield: 78%; mp: > 250 °C; MS (ESI) m/z 449 $[M+H]^+$; ^1H NMR (300 MHz, $CDCl_3$) δ (ppm): 2.06 (bs, 4H, CH_2), 2.59 (s, 6H, SCH_3), 3.60(s, 6H, NCH_3), 4.52 (bs, 4H, NCH_2). ^{13}C NMR (75 MHz, $CDCl_3$): δ (ppm): 14.36, 28.01, 37.32, 43.47, 123.95, 150.70, 153.60, 169.90; Anal. Calcd. for $C_{16}H_{20}N_{10}O_2S_2$: C, 42.85; H, 4.49; N, 31.23; Found: C, 42.90; H, 4.60; N, 31.28.

1.6.3.11 Synthesis of 3-butyl-N,N-dimethyl-5-methylthio-3*H*-[1,2,3]triazolo[4,5-*d*]pyrimidin-7-amine (99).

Compound **95** (0.25g, 0.001 mole) and dimethyl amine (50% water solution, 10ml) was refluxed for 4h. Excess of dimethyl amine solution was removed under reduced pressure. Ice cold water (50 ml) was added to the reaction mixture and neutralized it with a dilute solution of acetic acid. The reaction mixture was extracted with 60 ml of chloroform (20 ml x 3) and dried over sodium sulfate. The residue obtained by the removal of chloroform under reduced pressure was purified by column chromatography on silica gel using mixture of ethyl acetate-hexane in increasing polarity to give pure compound **99**.

99: Yield: 80-85%; mp: 80–82 °C; MS (ESI) m/z 267 $[M+H]^+$; ^1H NMR (300 MHz, $CDCl_3)$ δ (ppm): 0.92-0.99 (m, 3H, CH_3), 1.30-1.40 (m, 2H, $CH_2)$, 1.96 (t, 2H, *J* = 6 Hz, $CH_2)$, 2.58 (s, 3H, SCH_3), 3.34 (s, 3H, CH_3), 3.83 (s, 3H, CH_3), 4.49 (t, 2H, *J* = 6 Hz, $NCH_2)$.

1.6.3.12 Synthesis of 3,3′-(propane-1,3-diyl)bis(*N*,*N*-dimethyl-5-methylthio-3*H*-[1,2,3]triazolo[4,5-*d*]pyrimidin-7-amine) (98).

98: Yield: 90%; 146-148 °C; MS (ESI) m/z 461 $[M+H]^+$; ^1H NMR (300 MHz, $CDCl_3$) δ (ppm): 2.49 (s, 6H, SCH_3), 2.75 (q , 2H, *J* = 6.0 Hz, CH_2), 3.33 (s, 6H, NCH_3), 3.83 (s, 6H, NCH_3), 4.57 (t, 4H, *J* = 6.0 Hz, NCH_2); ^{13}C NMR (75 MHz, $CDCl_3$) δ (ppm): 14.39, 28.41, 37.37, 39.77, 43.44, 14.04, 150.79, 153.55, 169.94; Anal. Calcd. for $C_{17}H_{24}N_{12}S_2$: C, 44.33; H, 5.25; N, 36.49; Found: C, 44.53; H, 5.35; N, 36.52.

1.6.3.13 Synthesis of 3-butyl-5-methylsulfonyl-7-pyrrolidin-1-yl-3*H*-[1,2,3]triazolo[4,5-*d*]pyrimidine (102).

To a stirred solution of Compound **89** (0.29g, 0.001 mol) in acetone (50 ml) placed in ice bath added oxone (2.5g, 0.004mol , 2.5g dissolved in 5 ml of water) dropwise for 15 minutes and stirred for 8h. Excess acetone was removed under reduced pressure and 50 ml of water was added. The reaction mixure extracted with 60 ml of chloroform (20 ml x 3) and was dried over sodium sulfate. The residue obtained by the removal of chloroform under reduced pressure was purified by column chromatography on silica gel using mixture of ethyl acetate-hexane in increasing polarity to give pure **3-** Compound **102**.

102: Yield: 78- 80%; mp 128–130 °C; MS (ESI) m/z 325 $[M+H]^+$; ^1H NMR (300 MHz, $CDCl_3)$ δ (ppm): 0.94-1.04 (m, 3H, CH_3), 1.32-1.46 (m, 2H, CH_2), 1.90-2.30 (m, 6H, CH_2), 3.35 (s, 3H, SO_2CH_3), 3.90 (t, 2H, *J* = 6 Hz, NCH_2), 4.32 (t, 2H, *J* = 6 Hz, NCH_2), 4.59 (t, 2H, *J* = 6 Hz, NCH_2).

1.6.3.14 Synthesis of 1,3-bis(5-methylsulfonyl-7-pyrrolidin-1-yl-3*H*-[1,2,3]triazolo[4,5-*d*]pyrimidin-3-yl)propane (100).

100: Yield: 90%; mp: > 220 °C; MS (ESI) m/z 577 $[M+H]^+$; ^1H NMR (300 MHz, $CDCl_3$) δ (ppm): 2.00-2.30 (m , 8H, CH_2), 2.90 (t, 2H, *J* = 6.0 Hz, CH_2), 3.28 (s, 6H, SCH_3), 3.88 (t, 4H, *J* = 6.0 Hz, NCH_2), 4.29 (t, 4H, *J* = 6.0 Hz, NCH_2), 4.64 (t, 4H, *J* = 6.0 Hz, NCH_2); ^{13}C NMR (75 MHz, $CDCl_3$) δ (ppm): 28.30, 43.63, 55.03, 55.56, 123.25, 152.55, 162.88, 164.40; Anal. Calcd. for $C_{15}H_{18}N_{10}O_4$: C, 43.74; H, 4.89; N, 29.15; Found: C, 43.88; H, 4.92; N, 29.25.

1.6.3.15 Synthesis of 3-butyl-7-methoxy-5-methylsulfonyl-3*H*-[1,2,3]triazolo[4,5-*d*]pyrimidine (103).

To a stirred solution of Compound **91** (0.25g, 0.001 mol) in acetone (50 ml) placed in ice bath added oxone (2.5g, 0.004 mol , 2.5g dissolved in 5 ml of water) dropwise for 15 minutes and stirred for 8h. Excess acetone was removed under reduced pressure and 50 ml of water was added. The reaction mixure extracted with 60 ml of chloroform (20 ml x 3) and was dried over sodium sulfate. The residue obtained by the removal of chloroform under reduced pressure was purified by column chromatography on silica gel using mixture of ethyl acetate-hexane in increasing polarity to give pure Compound **103**.

103: Yield: 50- 65%; mp: 134–136 °C; MS (ESI) m/z 286 $[M+H]^+$; ^{1}H NMR (300 MHz, $CDCl_3$) δ (ppm): 0.94-1.04 (m, 3H, CH_3), 1.36-1.44 (m, 2H, CH_2), 1.98-2.06 (m, 2H, CH_2), 3.42 (s, 3H, SO_2CH_3), 4.26 (s, 3H, OCH_3), 4.58-4.64 (m, 2H, NCH_2).

1.6.3.16.1 Synthesis of 1,2-bis(7-methoxy-5-methylsulfonyl-3*H*-[1,2,3]triazolo[4,5-*d*]-pyrimidin-3-yl)ethane (101a).

101a: Yield: 90%; mp: 190-192 °C; MS (ESI) m/z 484 $[M+H]^+$; ^{1}H NMR (300 MHz, $CDCl_3$) δ (ppm): 3.27(s, 6H, SO_2CH_3), 4.37 (s, 6H, OCH_3), 5.36 (s, 4H, NCH_2); ^{13}C NMR (75 MHz, $CDCl_3$) δ (ppm): 39.19, 46.67, 56.45, 126.19, 150.70, 162.81, 163.15; Anal. Calcd. for $C_{14}H_{16}N_{10}O_6S_2$: C, 34.71; H, 3.33; N, 28.91; Found: C, 34.80; H, 3.41; N, 28.99.

1.6.3.16.2 Synthesis of 1,3-bis(7-methoxy-5-methylsulfonyl-3*H*-[1,2,3]triazolo[4,5-*d*]-pyrimidin-3-yl)propane (101b).

101b: Yield: 90%; mp: 182-184 °C; MS (ESI) m/z 499 $[M+H]^+$; ^{1}H NMR (300 MHz, $CDCl_3$) δ (ppm): 3.02 (q , 2H, $J = 6.0$ Hz, CH_2), 3.38 (s, 6H, SO_2CH_3), 4.41 (s, 6H, OCH_3), 4.80 (t, 4H, $J = 6.0$ Hz, NCH_2); ^{13}C NMR (75 MHz, $CDCl_3$) δ (ppm): 28.02, 39.39, 44.30, 56.50, 126.14, 150.74, 162.80, 163.14; Anal. Calcd. for $C_{15}H_{18}N_{10}O_6S_2$: C, 36.14; H, 3.64; N, 28.10; Found: C, 36.18; H, 3.66; N, 28.19.

1.6.3.17 Synthesis of 3-butyl-5, 7-dimethoxy-3*H*-[1,2,3]triazolo[4,5-*d*]pyrimidine (105).

To a 100 ml round bottom flask containing 20 ml of anhydrous methanol added compound **103** (0.28 g, 0.001 mole) and kept on refluxing with stirring for 10 minutes. Sodium methoxide (0.10 g, 0.002 moles) was added and the mixture was further refluxed for 4h. Methanol was removed under reduced pressure and ice cold water was added to round bottom flask and the solution was neutralized with dilute acidic acid. The solution was kept for 8-10h so that complete precipitation occurred. The solid precipitate was filtered, washed with water and air dried at 80 °C. This was purified by column chromatography on silica gel using mixture of ethyl acetate-hexane in increasing polarity to give pure compound **105**.

105: Yield: 60- 65%; mp: 102–104 °C; MS (ESI) m/z: 238 $[M+H]^+$; ^1H NMR (300 MHz, $CDCl_3$): δ (ppm): 0.88-0.94 (m, 3H, CH_3), 1.28-1.38 (m, 2H, CH_2), 1.92-2.01 (m, 2H, CH_2), 4.20 (s, 3H, SCH_3), 4.24 (s, 3H, OCH_3), 4.52-4.60 (m, 2H, NCH_2).

1.6.3.18 Synthesis of 1,3-bis(5,7-dimethoxy-3*H*-[1,2,3]triazolo[4,5-*d*]pyrimidin-3-yl)-propane (104).

104: Yield: 90%; mp: 128-130 °C; MS (ESI) m/z 403 $[M+H]^+$; ^1H NMR (300 MHz, $CDCl_3$) δ (ppm): 2.84 (q , 2H, J = 6.0 Hz, CH_2), 4.01 (s, 6H, OCH_3), 4.24 (s, 6H, OCH_3), 4.63 (t, 4H, J = 6.0 Hz, NCH_2); ^{13}C NMR (75 MHz, $CDCl_3$) δ (ppm): 28.30, 43.63, 55.03, 55.56, 123.25, 152.55, 162.88, 164.40; Anal. Calcd. for $C_{15}H_{18}N_{10}O_4$: C, 44.78; H, 4.51; N, 34.81; Found: C, 44.88; H, 4.52; N, 34.80.

1.7 References

1. Muller-Dethlefs, K.; Hobza, P. *Chem. Rev.* **2000**, *100*, 143.
2. (a) Hobza, P.; Zahradník, R.; Muller-Dethlefs, K. *Collect. Czech. Chem. Commun.* **2006**, *71*, 443.
3. Hobza, P.; Muller-Dethlefs, K. *Non-Covalent Interactions: Theory and Experiment* RSC Publishing, **2009**.
4. Salonen, L. S.; Ellermann, M.; Diederich F. *Angew. Chem. Int. Ed.* **2011**, *50*, 4808.
5. Steed, J.W.; Atwood, J.L. *Supramolecular Chemistry*; Wiley: Chichester, **2000**.
6. (a) Waters, M. L. *Curr. Opin. Chem. Biol.* **2002**, *6*, 736. (b) Headen, T.F.; Howard, C.A.; Skipper, N.T.; Wilkinson, M.A.; Bowron, D. T.; Soper, A.K. *J. Am. Chem. Soc.* **2010**, *132*, 5735. (c) Wheeler, S.E.; McNeil, A.J.; Muller, P.; Swager, T.M.; Houk, K.N. *J. Am. Chem. Soc.* **2010**, *132*, 3304.
7. Grimme, S.; Zhikol, O.A.; Shishkin, O.V.; Lyssenko, K.A.; Leszczynski, J. *Angew. Chem. Int. Ed.* **2008**, *47*, 3430.
8. (a) Hobza, P.; Selzle, H.L.; Schlag, E.W. *J. Phys. Chem.* **1996**, *100*, 18790. (b) Tsuzuki, S.; Uchimaru, T.; Matsumura, K.; Mikami, M.; Tanabe, K. *Chem. Phys. Lett.* **2000**, *319*, 547. (c) West, J.; Mecozzi, S.; Dougherty, D.A. *J. Phys. Org. Chem.* **1997**, *10*, 347.

9. (a) Blundell, T.; Singh, J.; Thornton, J.; Burley, S.K.; Petsko, G.A. *Science* **1986**, *234*, 1005. (b) Tsuzuki, S.; Honda, K.; Uchimaru, T.; Mikami, M.; Tanabe, K. *J. Am. Chem. Soc.* **2002**, *124*, 104.
10. (a) Riley, K.E.; Pitonak, M.; Jurecka, P.; Hobza, P. *Chem. Rev.* **2010**, *110,* 5023. (b) Desiraju, G.R.; Gavezzotti, A. *J. Chem. Soc. Chem. Commun.* **1989**, 621.
11. Hunter, C.A.; Lawson, K.R.; Perkins, J.; Urch, C.J. *J. Chem. Soc. Perkin Trans* **2001**, 651.
12. Hunter, C. A.; Sanders, J.K.M. *J. Am. Chem. Soc.* **1990**, *112,* 5525.
13. Hohenstein, E. G.; Sherrill, C.D. *J. Phys. Chem. A* **2009**, *113*, 878.
14. Choudhury, R.R.; Chitra, R. *CrystEngComm.* **2010**, *12,* 2113.
15. (a) Kool, E. T. *Annu. Rev. Biophys. Biomol. Struct.* **2001**, *30,* 1. (b) Sponer, J.; Riley, K. E.; Hobza, P. *Phys. Chem. Chem. Phys.* **2008**, *10*, 2595.
16. Kannan, N.; Vishveshwara, S. *Protein Eng.* **2000**, *13*, 753.
17. Gazit, E. *FASEB J.* **2002**, *16*, 77.
18. Burley, S. K.; Petsko, G. A. *Science* **1985**, *229*, 23.
19. Hunter, C. A.; Singh, J.; Thornton, J. M. *J. Mol. Biol.* **1991**, *218*, 837.
20. McGaughey, G. B.; Gagnu, M.; Rappe, A. K. *J. Biol. Chem.* **1998**, *273*, 15458.
21. Aravinda, S.; Shamala, N.; Das, C.; Sriranjini, A.; Karle, I. L.; Balaram, P. *J. Am. Chem. Soc.* **2003**, *125*, 5308.
22. Yanagisawa, S.; Crowley, P. B.; Firbank, S. J.; Lawler, A. T.; Hunter, D. M.; McFarlane, W.; Li, C.; Kohzuma, T.; Banfield, M. J.; Dennison, C. *J. Am. Chem. Soc.* **2008**, *130*, 15420.
23. Acharya, P.; Chattopadhyaya, J. *Pure Appl. Chem.* **2005**, *77*, 291.
24. a) Jones, G. B.; Chapman, B. J. *Synthesis* **1995**, 475. (b) Jones, G. B. *Tetrahedron* **2001**, *57*, 7999. (c) Nishio, M. *Tetrahedron* **2005**, *61*, 6923.
25. (a) Skoric, I.; Basaric, N.; Marinic, Z.; Visnjevac, A.; Kojic- Prodic, B.; Sindler-Kulyk, M. *Chem. Eur. J.* **2005**, *11*, 543. (b) Grimme, S.; Diedrich, C.; Korth, M. *Angew. Chem. Int. Ed.* **2006**, *45,* 625. (c) Karthikeyan, S.; Ramamurthy, V. *J. Org. Chem.* **2006**, *71*, 6409. (d) Karthikeyan, S.; Ramamurthy, V. *J. Org. Chem.* **2007**, *72*, 452. (e) Skoric, I.; Smehil, M.; Marinic, Z.; Molcanov, K.; Kojic-Prodic, B.; Sindler-Kulyk, M. *J. Photochem. Photobiol. A* **2009**, *207*, 190.
26. (a) Ginotra, S. K.; Singh, V. K. *Org. Biomol. Chem.* **2006**, *4,* 4370. (b) Ginotra, S. K.; Singh, V. K. *Tetrahedron* **2006**, *62*, 3573.
27. Brandt, P; Roth, P.; Andersson, P. G. *J. Org. Che*m. **2004**, *69*, 4885.

28. (a) Naso, F.; Capozzi, M. A. M.; Bottoni, A.; Calvaresi, M.; Bertolasi, V.; Capitelli, F.; Cardellicchio, C. *Chem. Eur. J.* **2009**, *15*, 13417. (b) Santoni, G.; Mba, M.; Bonchio, M.; Nugent, W. A.; Zonta, C.; Licini, G. *Chem. Eur. J.* **2010**, *16*, 645.

29. (a) Carb, J. J.; Lleds, A.; Vogt, D.; Bo, C. *Chem. Eur. J.* **2006,** *12*,1457. (b) Yamanaka, M.; Itoh, J.; Fuchibe, K.; Akiyama, T. *J. Am. Chem. Soc.* **2007**, *129*, 6756. (c) Bodkin, J. A. G.; Bacskay, B.; McLeod, M. D. *Org. Biomol. Chem.* **2008**, *6*, 2544. (d) Katagiri, K.; Tohaya, T.; Masu, H.; Tominaga, M.; Azumaya, I. *J. Org. Chem.* **2009**, *74*, 2804.

30. Rosini, C.; Tanturli, R.; Pertici, P.; Salvadori, P. *Tetrahedron: Asymmetry* **1996**, *7*, 2971.

31. McIntosh, J.M.; Kiser, E.J.; Tian, Z. *Can. J. Chem.* **1998**, *76*, 147.

32. Paras, N.A.; McMillan, D.W.C. *J. Am. Chem. Soc.* **2001**, *123*, 4370.

33. Kishikawa, K.; Naruse, M.; Kohmoto, S.; Yamamoto, M.; Yamaguchi, K. *J. Chem. Soc. Perkin Trans.* **2001**, *1*, 462.

34. (a) Malkov, A. V.; Dufkov, L.; Farrugia, L.; Kocovsky, P. *Angew. Chem. Int. Ed.* **2003**, *42*, 3674. (b) Malkov, A. V.; Bell, M.; Castelluzzo, F.; Kocovsky, P. *Org. Lett.* **2005**, *7*, 3219.

35. Bisai, A.; Singh, V. K. *Org. Lett.* **2006**, *8*, 2405.

36. (a) Kryger, G.; Silman, I.; Sussman, J.L. *J. Physiol.* **1998**, *92*, 191. (b) Kryger, G.; Silman, I.; Sussman, J.L. *Structure* **1999**, *7*, 297.

37. (a) Frederick, C. A.; Williams, L.D.; Ughetto, G.; van der Marel, G. A.; van Boom, J. H.; Rich, A.; Wang, A. H. J. *Biochemistry* **1990**, *29*, 2538. (b) Barone, G.; Guerra, C. F.; Noemi, A.; Lauria, S. A.; Almerico, A.M.; Bickelhaupt, F.M. *J. Biomol. Struct. Dyn.* **2008**, *26*, 115.

38. (a) Weichsel, A.; Montfort, W.R. *Nat. Struct. Biol.* **1995**, *2*, 1095. (b) Meyer, E.A.; Castellano, R.K.; Diederich, F. *Angew. Chem. Int. Ed.* **2003**, *42*, 1210.

39. (a) Hunter, C. A. *Chem. Soc. Rev.* **1994**, *23*, 101. (b) Hunter, C. A.; Lawson, K. R.,; Perkins, J.; Urch, C. J. *J. Chem. Soc. Perkin Trans.* **2001**, 651.

40. (a) Browne, D.T.; Eisinger, J.; Leonard, N.J. *J. Am. Chem.* Soc. **1968**, *90*, 7302. (b) Leonard, N. J.; Ito, K. *J. Am. Chem. Soc.* **1973**, *95*, 4010. (c) Leonard, N.J. *Acc. Chem. Res.* **1979**, *12*, 423.

41. Rosen, L. S.; Hybl, A. *Acta Crystallogr.* **1971**, *B27*, 952.

42. Falk, M.; Chew, W.; Walter, J. A.; Kwiatkowski, W.; Barclay, K. D.; Klassen, G. A. *Can. J. Chem.* **1998**, *76*, 48.

43. Frank, J. K.; Paul, I. C. *J. Am. Chem. Soc.* **1973**, *95*, 2324.

44. Mutai, K.; Gruber, B. A.; Leonard, N. J. *J. Am. Chem. Soc.* **1979**, *97*, 4095.

45. Bunick, G.; Voet, D. *Acta Crystallogr.* **1982**, *B38*, 575.

46. Ishida, T.; Shibata, M.; Fujii, K.; Inove, M. *Biochemistry* **1983**, *22*, 3571.

47. Maulik, P. R.; Avasthi, K.; Sarkhel, S.; Sharon, A.; Rawat, D. S.; Bal, C. *Acta Crystallogr*. **2001**, *E57*, o1163.

48. Itahara, T.; Imamura, K. *Bull. Chem. Soc. Jpn.* **1994**, *67*, 203.

49. Itahara, T. *J. Chem. Soc. Perkin Trans. 2* **1998**, 1455.

50. Itahara, T. *Bull. Chem. Soc. Jpn*. **2000**, *73*, 1621.

51. Reynders, P.; Kuhnle, W.; Zachariasse, K. A. *J. Am. Chem. Soc.* **1990**, *112*, 3929.

52. Arimori, S.; Bell, M. L.; Oh, C. S.; Frimat, K. A.; James, T. D. *J. Chem. Soc. Perkin Trans. 1* **2002**, 803.

53. Demunck, C.; Lhomme, J. *Bull. Soc. Chim. Fr.* **1980**, *5*, 316.

54. Constant, J. F.; Fahy, J.; Lhomme, J. *Tetrahedron Lett.* **1987**, *28*, 1777.

55. Bolte, J.; Demunck, C.; Lhomme, M. F.; Lhomme, J.; Barbet, J.; Roques, B. P. *J. Am. Chem. Soc.* **1982**, *104*, 760.

56. Constant, J. F.; Laugaa, P.; Roques, B. P.; Lhomme, J. *Biochemistry* **1988**, *27*, 3997.

57. Decout, J. L.; Lhomme, J. *Photochem. Photobiol.* **1983**, *37*, 155.

58. Newcomb, L. F.; Gellman, S. H. *J. Am. Chem. Soc.* **1994**, *116*, 4993.

59. Newcomb, L. F.; Haque, T. S.; Gellman, S. H. *J. Am. Chem. Soc.* **1995**, *117*, 6509.

60. Heaton, N. J.; Bello, P.; Herrandon, B.; del Campo, A.; Jimenez-Barbero, J. *J. Am. Chem. Soc*. **1998**, *120*, 12371.

61. Pang, Y.; Miller, J.L.; Kollman, P.A. *J. Am. Chem. Soc.* **1999**, *121*, 1717.

62. Avasthi, K.; Chandra, T.; Bhakuni, D.S. *Indian J. Chem.* **1995**, *34B*, 944.

63. Biswas, G.; Chandra, T.; Avasthi, K.; Maulik, P.R. *Acta Crystallogr.* **1995**, *C51*, 2453.

64. Avasthi, K.; Rawat, D.S.; Maulik, P.R.; Sarkhel, S.; Broder, C.; Howard, J. A. K. *Tetrahedron Lett.* **2001**, *42*, 7115.

65. Avasthi, K.; Farooq, S.M.; Rawat, D.S.; Sharon, A.; Maulik, P.R. *Acta Crystallogr*. **2003**, *C59*, o523.

66. Maulik, P.R.; Avasthi, K.; Sarkhel, S.; Chandra, T.; Rawat, D.S.; Logsdon, B.; Jacobson, R. A. *Acta Crystallogr*. **2000**, *C56*, 1361.

67. Avasthi, K.; Rawat, D.S.; Chandra, T.; Bhakuni, D.S. *Indian J. Chem.* **1998**, *37B*, 754.

68. Maulik, P.R.; Avasthi, K.; Biswas, G.; Rawat, D.S.; Sarkhel, S.; Chandra, T.; Bhakuni, D. S.; *Acta Crystallogr*. **1998**, *C54*, 275.

69. Avasthi, K.; Farooq, S.M.; Sharon, A.; Maulik, P.R.; *Acta Crystallogr*. **2002**, *E58*, o940.

70. Avasthi, K.; Farooq, S. M.; Raghunandan, R.; Maulik, P.R. *J. Mol. Struct.* **2006**, *785*, 106.

71. Avasthi, K.; Farooq, S. M.; Bal, C.; Kumar, R.; Tewari, A.K.; Maulik, P.R. *J. Mol. Struct.* **2007**, *842*, 100.

72. Avasthi, K.; Farooq, S. M.; Raghunandan, R.; Maulik, P.R. *J. Mol. Struct.* **2009**, *927*, 27.

73. Dubey, R.; Tewari, A.K.; Ravikumar, K.; Sridhar, B. *Bull. Korean Chem. Soc.* **2010**, *31*, 1326.

74. (a) Tanaka, T.; Tasaki, T.; Aoyama, Y. *J. Am. Chem. Soc.* **2002**, *124*, 12453. (b) Desiraju, G.R. *Angew. Chem. Int. Ed. Engl*. **1995**, *34*, 2311. (c) Desiraju, G.R. Crystal Engineering: *The Design of Organic Solids*, Elsevier, New York, 1989.

75. (a) Gillerman, I.; Fischer, B. *J. Med. Chem.* **2011**, *54*, 107. (b) Maldonado, C. R.; Marin, C.; Olmo, F.; Huertas, O.; Quiros, M.; Sanchez-Moreno, M.; Rosales, M. J.; Salas J. M. *J. Med. Chem.* **2010**, *53*, 6964. (c) Dehnhardt , C. M.; Venkatesan, A. M.; Santos, E. D.; Chen, Z.; Santos, O.; Ayral-Kaloustian, S.; Brooijmans, N.; Mallon, R.; Hollander, I.; Feldberg, L.; Lucas, J.; Chaudhary, I.; Yu, K.; Gibbons, J.; Abraham, R.; Mansour, T. S. *J. Med. Chem.* **2010**, *53*, 798. (d) Gillespie, R. J.; Bamford, S. J.; Botting, R.; Comer, M.; Denny, S.; Gaur, S.; Griffin, M.; Jordan, A. M.; Knight, A. R.; Lerpiniere, J.; Leonardi, S.; Lightowler, S.; McAteer, S.; Merrett, A.; Misra, A.; Padfield, A.; Reece, M.; Saadi, M.; Selwood, D. L.; Stratton, G. C.; Surry, D.; Todd, R.; Tong, X.; Ruston, V.; Upton, R.; Weiss, S. M. *J. Med. Chem.* **2009**, *52*, 33. (e) Chorvat, R. J.; Bakthavatchalam, R.; Beck, J. P.; Gilligan, P. J.; Wilde, R. G.; Cocuzza, A. J.; Hobbs, F. W.; Cheeseman, R. S.; Curry, M.; Rescinito, J. P.; Krenitsky, P.; Chidester, D.; Yarem, J. A.; Klaczkiewicz, J. D.; Hodge, C. N.; Aldrich, P. E.; Wasserman, Z. R.; Fernandez, C. H.; Zaczek, R.; Fitzgerald, L. W.; Huang, S. M.; Shen, H. L.; Wong, Y. N.; Chien, B. M.; Quon, C. Y.; Arvanitis A. *J. Med. Chem.* **1999,** *42*, 833. (f) Shealy, Y. F.; O'Dell, C. A.; Shannon, W. M.; Arnett G. *J. Med. Chem.* **1984**, *27*, 1416. (g) Hutzenlaub, W.; Tolman, R. L.; Robins R. K. *J. Med. Chem.* **1972**, *15*, 879. (h) Smith, C. W.; Sidwell, R. W.; Robins, R. K.; Tolman, R. L. *J. Med. Chem.* **1972**, *15*, 883.

76. Baindur, N.; Chadha, N.; Player, M. R. *J. Comb. Chem.* **2003,** *5*, 653.

77. (a) Betti, L.; Biagi, G.; Giannaccini, G.; Giorgi, I.; Livi, O.; Lucacchini, A.; Manera, C.; Scartoni, V. *Eur. J. Med. Chem.* **1999**, *34*, 867. (b) Betti, L.; Biagi, G.; Giannaccini, G.; Giorgi, I.; Livi, O.; Lucacchini, A.; Manera, C.; Scartoni, V. *J. Med. Chem.* **1998**, *41*, 668. (c) Biagi, G.; Franchi, M.; Giorgi, I.; Livi, O.; Scartoni, V. *J. Heterocycl. Chem.* **1989**, *26*, 39. (d) Barili, P. L.; Biagi, G.; Mucci, L.; Scartoni, V. *J. Heterocycl. Chem.* **1987**, *24*, 997. (e) Barili, P. L.; Biagi, G.; Livi, O.; Scartoni, V. *J. Heterocycl. Chem.* **1985**, *22*, 1607. (f) Higashino, T.; Katori, T.; Kawaraya, H.; Hayashi, E. *Chem. Pharm. Bull.* **1980**, *28*, 337.

78. (a) Guile, S.; Martin, B. *Preparation and Use of 1,2,3-triazolo[4, 5-d]pyrimidines as P2T Receptor Ligands.* PCT Int. Appl. WO 0238571 A1 20020516; **2002**. (b) Brown, R.;

Guile, S.; Pairaudeau, G.; Springthorpe, B. *Preparation and Use of 1,2,3-triazolo[4, 5-d]pyrimidines as P2T Receptor Ligands*. PCT Int. Appl. WO 0238570, A1 20020516; **2002**. (c) *Preparation of 7-Amino-3-benzyl-3H-1,2,3-triazolo[4,5-d]pyrimidines as anti-convulsants.* Eur. Pat. Appl. EP 288431, A1 19881026; **1988**.

79. Montgomery, J. A.; Shortnacy, A. T.; Arnett, G.; Shannon W. M. *J. Med. Chem.* **1977**, *20*, 401.

80. LoCoco, M. D.; Zhang, X.; Jordan, R. F. *J. Am. Chem. Soc.* **2004**, *126*, 15231.

81. (a) Cottrell, I. F.; Hands, D.; Houghton, P. G.; Humphrey, G. R.; Wright, S. H. B. *J. Heterocycl. Chem.* **1991,** *28*, 301. (b) Taylor, E.C.; McKillop, A.; Warrener R.N. *Tetrahedron* **1967**, *23*, 891. (c) Betti, L.; Biagi, G.; Giannaccini, G.; Giorgi, I.; Livi, O.; Lucacchini, A.; Manera, C.; Scartoni,; V. *Eur. J. Med. Chem.* **1999,** *34*, 867.

82. Denti, T. Z. M.; Gunsteren, W. F. V.; Diederich, F. *J. Am. Chem. Soc.* **1996,** *118*, 6044.

83. Avasthi, K.; Farooq, S.M.; Aswal, S.; Raghunandan, R.; Maulik, P.R. *J. Mol. Struct.* **2007**, *827*, 88.

CHAPTER-2

Synthesis, ^{1}H NMR and X-ray crystallographic studies of pyrrolo[2,3-*d*]pyrimidine core based flexible symmetric polymethylene linker compounds

2.1 Introduction

Purine (**1**) is one of the most important heterocycle present in nature consisting of a pyrimidine ring fused to an imidazole ring.[1] Two of the four bases in nucleic acids, adenine (**2**) and guanine (**3**), are purines. Other notable purines are hypoxanthine (**4**), xanthine (**5**), theobromine (**6**), caffeine (**7**), uric acid (**8**) and isoguanine (**9**) (**1-9**, **Fig. 1**).

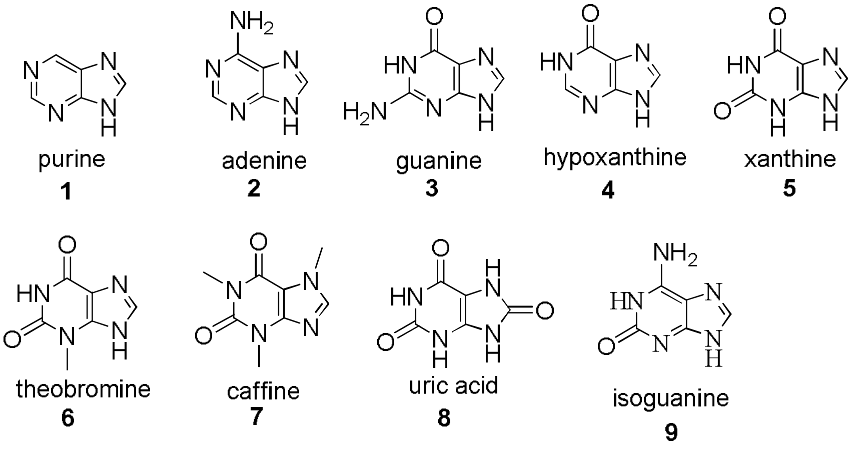

Figure 1. Important purines, including substituted purines and related compounds found in nature

Interest in purines has been considerably reinforced by analysis of the human genome. It is estimated that approximately 4–7% of all proteins encoded by the genome, including in particular, GPCRs (G-protein-coupled receptors), depend on purine nucleotides (ATP, GTP, cAMP, cGMP, NAD, FAD, PAPS. . .) as co-factors or co-substrates for their function, making these proteins a large family of potential therapeutic targets (**Fig. 2**).[2]

The screening of purine libraries against a wide variety of biological targets has contributed to opening new horizons for the development of purines as chemical-biology tools and hopefully as new therapeutic agents. A number of major purine-based drugs exist (**Fig. 3**) which find current application for the treatment of cancer (6-mercaptopurine,**10**, thioguanine, **11**),[3,4] systemic mastocytosis (2- chloro-20-deoxy adenosine **12**),[3,5–7] viral infections such as Herpes and AIDS (acyclovir, **13a**),[8] ganciclovir (**13b**),[9] carbovir (**14**),[10] abacavir (**15**),[3] ddA(**16**),[4] ddI (**17**)[5]),[11,12] and organ rejection (**18**, azathioprine).[13–16]

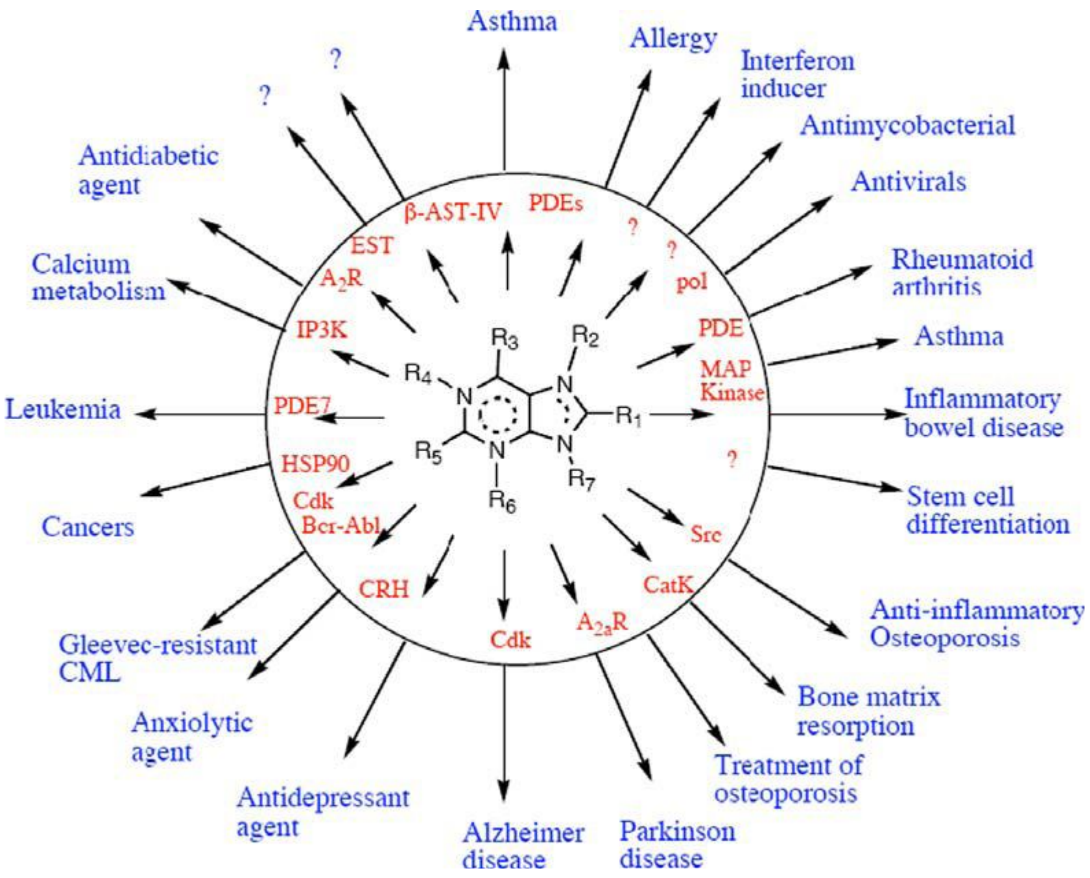

Figure 2.

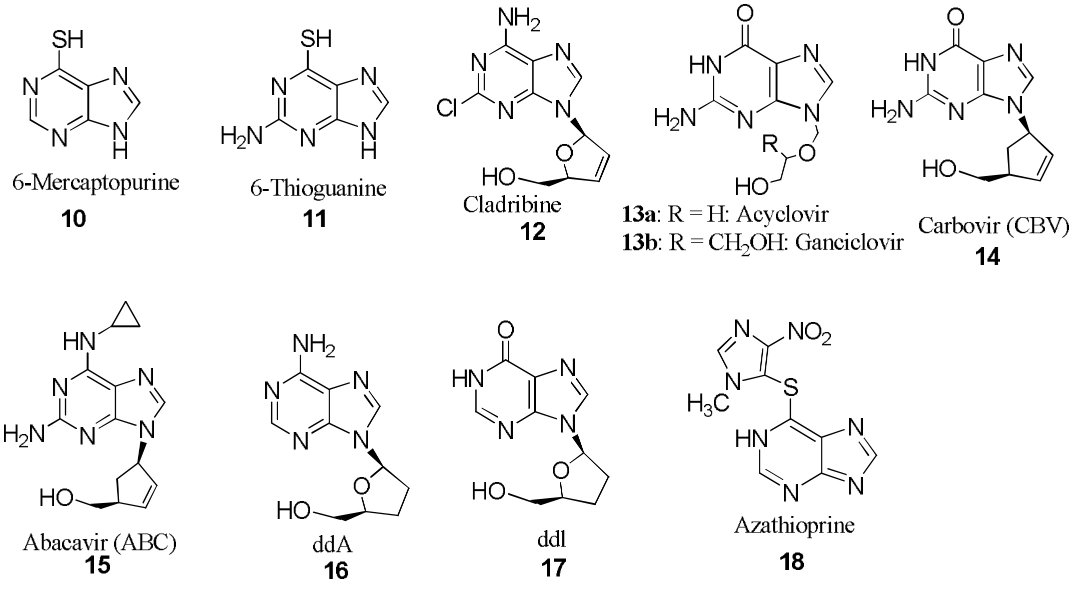

6-Mercaptopurine
10

6-Thioguanine
11

Cladribine
12

13a: R = H: Acyclovir
13b: R = CH_2OH: Ganciclovir

Carbovir (CBV)
14

Abacavir (ABC)
15

ddA
16

ddI
17

Azathioprine
18

Figure 3. Major purine-based drugs

These and other developments based on the purine scaffold have largely inspired parallel developments in the chemistry and biology of related heterocyclic systems, including pyrrolo-pyrimidines (**19**)[17–21] and (**20**),[22] pyrazolopyrimidines (**21**),[23–25] (**22**),[26] and (**23**),[27,28] imidazo-pyridines (**24**),[29,30] (**25**),[31] and (**26**),[32] triazolopyrimidines (**27**),[33] triazolotriazines (**28**),[34,35] triazolopyrazines (**29**),[36] pyrazolopyrazine (**30**),[37] imidazopyrazine (**31**),[38–41] (**19-31**, **Fig. 4**).

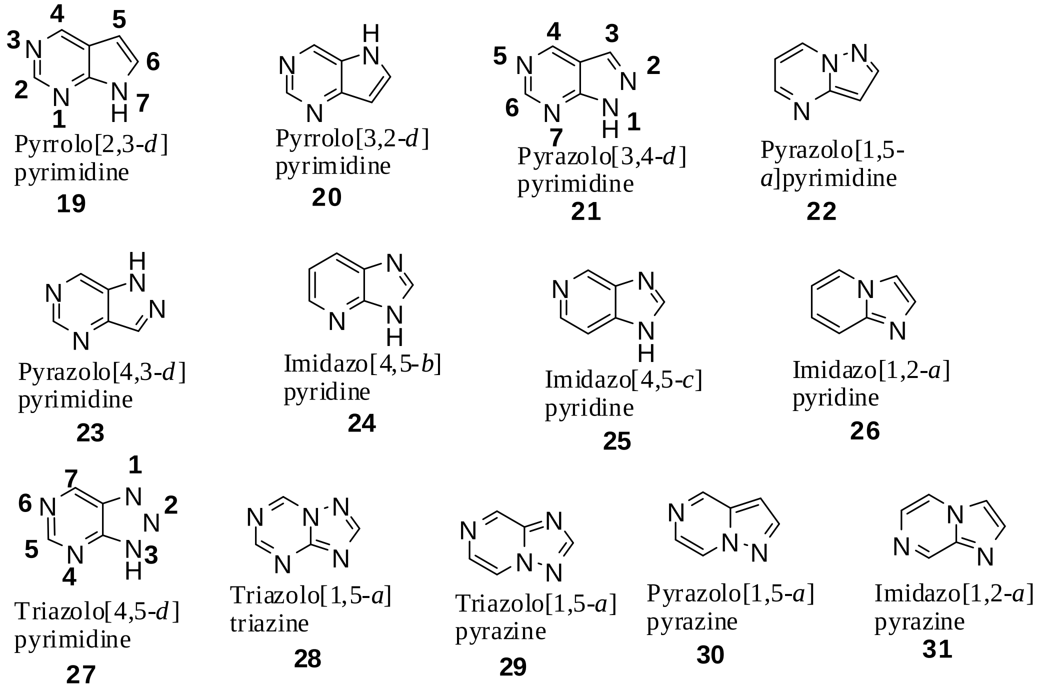

Figure 4. Various bicyclic heterocyclic systems related to purine

As mentioned earlier two of the four bases in nucleic acids, adenine (**2**) and guanine (**3**), are purines. The DNA double helix owes the intricate features of its structure to a collection of non covalent forces, the most notable being the hydrogen bonds between paired bases and stacking forces between neighboring pairs.[42] The factors contributing to the thermodynamic stability of the DNA double helix have been the source of scientific inquiry since the original discovery of this structure.[43] The understanding of contributing factors in DNA base pairing is important from at least two standpoints. First, it is such a basic part of biological function that its importance is almost implicit. Second, such knowledge can aid in the design of new biologically functional structures, which may be useful in biochemical study and potentially as therapeutic agents as well.[44] In order to generate new data to test the relative importance of H-bonding and base stacking in the structure, stability and functions of DNA, non-polar isosteric analogs of the natural DNA nucleosides have been designed.[45] The substituted benzenes were chosen as close steric analogs of pyrimidines and indoles as purine analogs and incorporated in to the synthetic oligonucleotides to measure their base pairing properties when placed opposite the natural DNA bases as well as each other. A study of the thermodynamic stacking affinities of the natural DNA bases and simple aromatic hydrocarbons (like benzene, naphthalene, anthracene and pyrene, (**32-40**) showed that hydrophobicity in addition to surface area is an important factor for enhancement in stacking.[46]

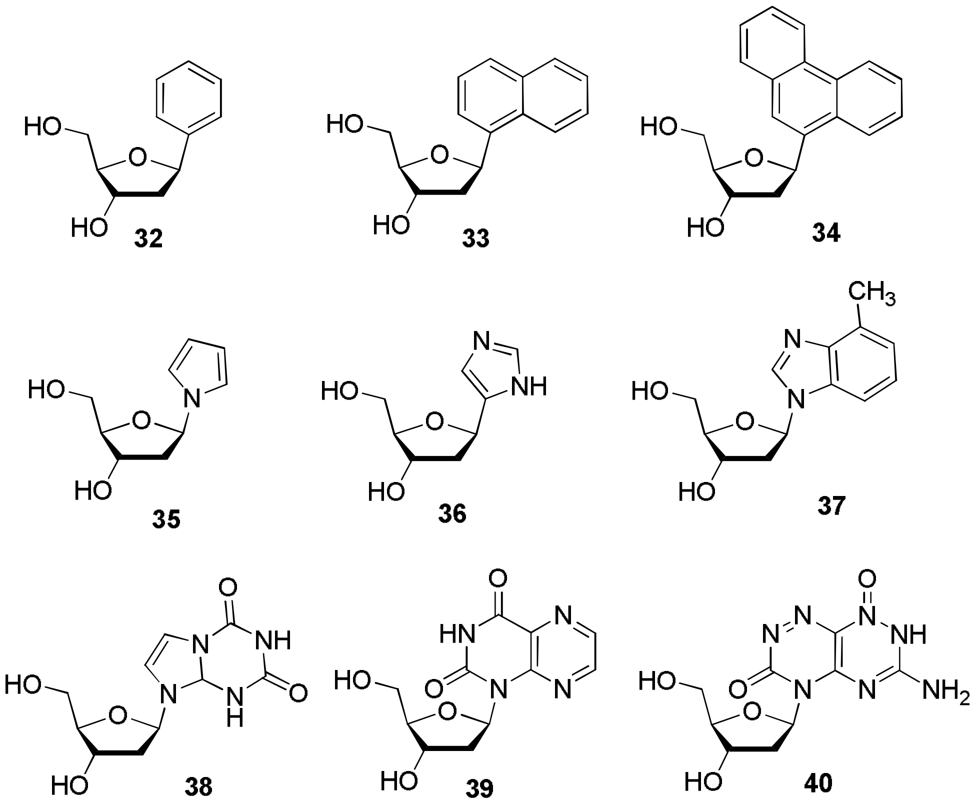

Figure 5. DNA base replacement studies by simple heterocycle/hydrocarbons

Nucleic acid bases are heteroaromatic with varied structures and electronic properties; hence it is likely that the electronic properties of the aromatic ring as well as its structural context play a significant role in directing the preferred geometries of intermolecular interactions. In this context various studies have been undertaken where within a series of base-modified nucleotides, a number of heterocyclic systems have been synthesized and incorporated in DNA and RNA.[46,47] Pyrazolo[3,4-*d*]pyrimidines,[48,49] indazoles,[50] benzimidazoles,[51] benzofurans,[52] benzothiophenes[52] etc. have been used for such studies. Increasing the surface area of DNA bases (by introducing aromatic heterocycles like pyridine, imidazole, thiazole, phenothiazine, phenoxazine etc. at 5-position or addition of extra rings fused to pyrimidines) has been found to stabilize significantly the helices, again possibly by enhancing stacking.[53,54] Recently, it has been shown that helices can be stabilized significantly by the addition of strongly stacking bases at the end of the helix, even when the bases in question do not undergo pairing. [55]

Variations in the orientation of base dipoles, sensitive to functional groups and to the distribution of charges on the neighbors, result in variation in stacking energies for the neighboring pairs. Variations in stacking energies are also reflected in a sequence dependence of the local structure. This relationship between sequence structure and stacking energy has important biological consequences e.g. for sequence specific interactions with proteins, drugs and water. Of further importance is the effect of local sequence environment on the efficiency of mismatch repair and mutation frequencies that bias the evolution of DNA sequences.[56] An evaluation of precise stacking is therefore needed to provide a more thorough explanation of many properties and functional interaction of DNA.

Browne *et al.* synthesized a series of 12 di-nucleotide analogs in which the bases were connected by a *trimethylene* linker (**41**-**52**, **Fig. 6**). These compounds were studied optically at concentrations low enough to preclude formation of intermolecular complexes so that the

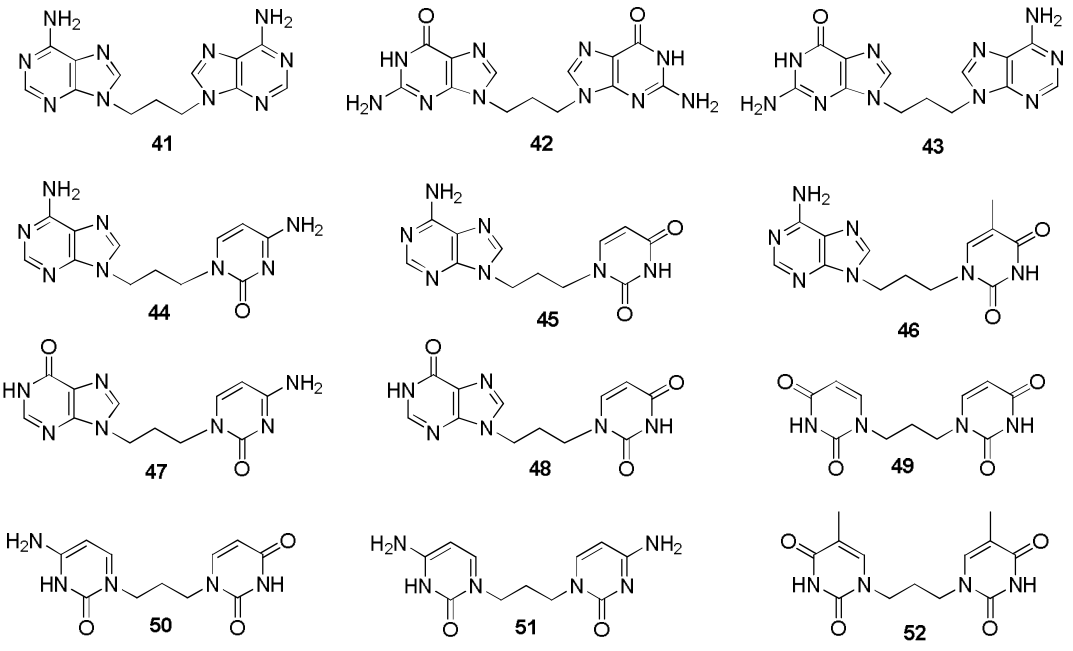

Figure 1. Nucleic acid bases based flexible *trimethylene* linker compounds

perturbations associated with the 1:1 interaction of a pair of bases could be characterized, namely, by ultraviolet spectra in aqueous solution at r.t. and by emission spectra in 1:1 ethylene glycol-water glass at 77 K. In the series of B-C3-B′, the order of interaction inneutral aqueous solution was purine-purine > purine-pyrimidine > pyrimidine-pyrimidine, as judged by hypochromism.[57]

Gellman *et al.* used *isobutyric* acid linker for studying stacking interaction in adenine in aqueous solution. The UV spectroscopic study showed nearly the same extent of stacking as observed for **41**, which indicated that the carboxylate substituent did not disrupt stacking. Stacking was also detectable via up-field shifts of the adenine ring from ^{1}H NMR study of **53** (**Fig. 7**).[58]

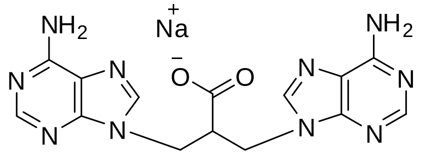

53

Figure 2. Sodium 3-(6-amino-9*H*-purin-9-yl)-2-((6-amino-9*H*-purin-9-yl)methyl)propanoate

Garcia-Raso *et al.* reported, for the first time, in 1999 the crystal structure **41** and its HCl salt **54.** The compound **41** adopted folded conformation in solid state as shown in **Fig 8a**. The conformation of **54** was quite different from **41** probably due to repulsive interaction between two protonated nitrogens (**Fig. 8b**).[59]

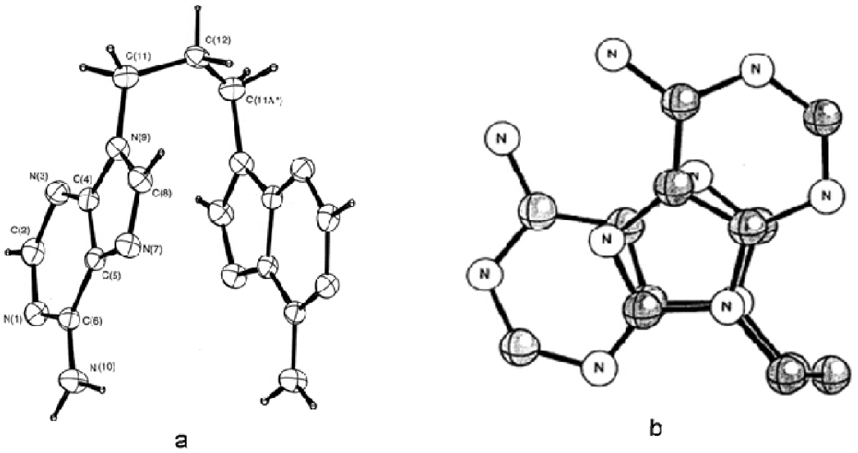

Figure 3. (**a**) ORTEP diagram of **41**[59]; (**b**) ORTEP diagram of **54**[59]

Since 1995 research group at CSIR-CDRI has been engaged in studying conformation directing role of arene–arene interactions on pyrazolo[3,4-*d*]pyrimidine (**PP**, **21**, **Fig. 4**) core, based flexible *propylene* linker models.[60,61] PP core is isomeric with purine and its derivatives show a wide range of biological activity.[62-66]

In continuation of this work on purine related molecules we wanted to study the effect of increasing and decreasing the number of ring nitrogen atoms with reference to PP core on stacking interactions. Thus, we synthesized triazolo[4,5-*d*]pyrimidine (TP, **27**, **Fig. 4**) core based *polymethylene* linker compounds and both solution and solid state studies were done and discussed in the previous chapter. In present chapter, we report the synthesis and characterization of pyrrolo[2,3-*d*]pyrimidine core (**19**, **Fig. 4**) based *polymethylene* linker compounds for studying their conformation directing role, if any, due to arene–arene interactions. The results obtained by these studies together with our earlier studies on PP core and TP core studies (described in previous chapter) may be helpful for better understanding of arene interactions in purine and related systems.

Pyrrolo[2,3-*d*]pyrimidine may be regarded as an analog of purine in which its N^7 has been replaced by a CH group. They have received much attention from chemical and biological view points since they show useful properties as antimetabolite in purine biochemical reactions. They act as antifolate inhibitors of dihydrofolate reductases,[67,68] tyrosine Kinase c-Src or Lck inhibitors,[69,70] cyclin dependent kinase (CDK) inhibitors[71,72] or adenosine receptor antagonists.[73,74] Also, these molecules show antitumor and radioprotective activity.[75] Pyrrolo[2,3-*d*]pyrimidine nucleus also occurs in nature as antibiotics (**Fig. 9a**) like tubercidin (**55**), toyocomycin (**56**) and sangivamycin (**57**).[76-79] These molecules exhibits antitumor properties.[78-82]

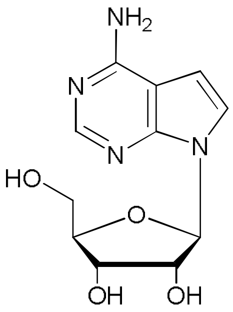

55. R = H, Tubercidin
56. R = CN, Toyocamycin
57. R = CONH2, Sangivamycin

Figure 9a. Pyrrolo[2,3-*d*]pyrimidine core based some important molecules found in nature

Cadeguomycin (**58**, **Fig. 9b**)[83-84] was isolated as a minor component together with tubercidin (**55**) and shows macrophage activity.[85-86] Rigidins (**59-62**, **Fig. 9b**) are pyrrolo pyrimidine core based alkaloids isolated from marine tunicates.[87] These molecules are reported to inhibit calmodulin-activated brain phosphodiesterase.[87]

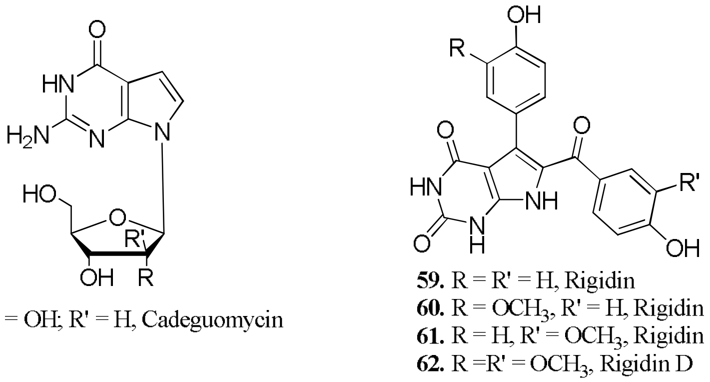

58. R = OH; R' = H, Cadeguomycin

59. R = R' = H, Rigidin
60. R = OCH_3, R' = H, Rigidin B
61. R = H, R' = OCH_3, Rigidin C
62. R =R' = OCH_3, Rigidin D

Figure 9b. Pyrrolo[2,3-*d*]pyrimidine core based some important molecules

Nucleoside Q, or queuosine, [88] (**63**, **Fig. 9c**) and its galactosylated, (**64**, **Fig. 9c**) mannosylated, (**65**, **Fig. 9c**) or amino acid modified derivatives (**66**, **Fig. 9c**)[89] are important hypermodified RNA bases present in the anticodon stem loop of various tRNAs.[90] Studies have shown that nucleoside Q is widely distributed in tRNA's of both plants and animals.[91] Nucleoside Q and its biosynthetic precursors have potential as biologically active compounds since deficiency of nucleoside Q is related to tumor growth.[91c] The aglycone of nucleoside Q and is known as queuine. Interestingly, the tRNA isolated from various tumors was found to be deficient in queuine.[92-94]

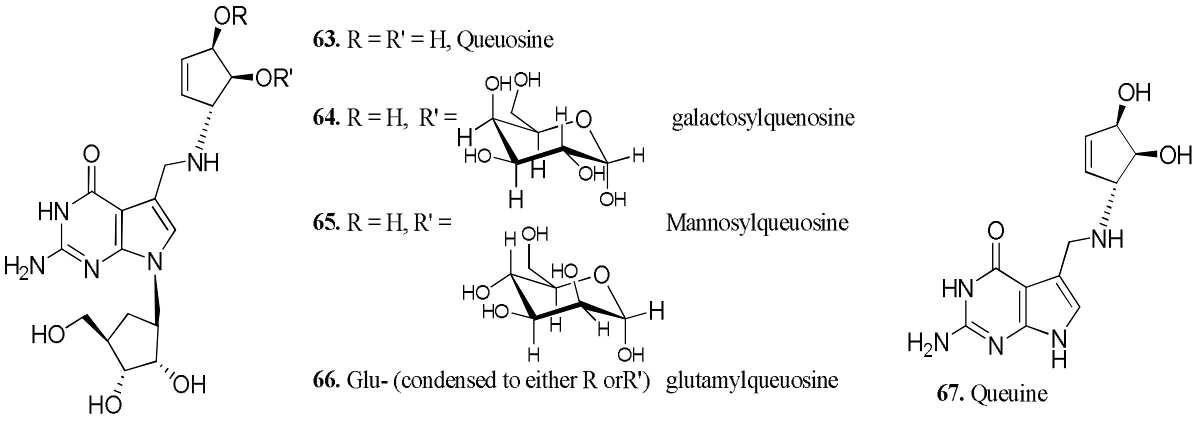

63. R = R' = H, Queuosine
64. R = H, R' = galactosylquenosine
65. R = H, R' = Mannosylqueuosine
66. Glu- (condensed to either R orR') glutamylqueuosine
67. Queuine

Figure 9c. Pyrrolo[2,3-*d*]pyrimidine core based some important molecules

Due to their close structural resemblance to the important purine molecule and also as an important structural unit of several natural products, pyrrolo[2,3-*d*]pyrimidine nucleus have been studied extensively and many such molecules have been synthesized as inhibitors of folate metabolism and biosynthesis,[95] as protein kinase inhibitors,[96] as antivirals,[97] in combating multidrug resistance,[98] in controlling gastric secretion[99] and as receptor antagonists.[100]

Premetrexed (**68**, **Fig. 10a**) inhibits enzymes that are required for purine and pyrimidine synthesis.[101] SLV320, **(69**, **Fig. 10a)** is a selective adenosine A1 receptor antagonist.[102] **PNU**-101033E (**70**, **Fig. 10a**) [103] and PNU-104067F (**71**, **Fig. 10a**) [104] are two brain-penetrating lipid-peroxidation-inhibiting pyrrolo pyrimidines and are found to possess neuroprotective activity in brain injury and Ischemia. PKI 166 (**72**, **Fig. 10a**) [105] and AEE-788 (**77**, **Fig. 10b**)[106] are tyrosine kinase inhibitors and are under clinical development. Antalarmin (**73**, **Fig. 10a**)[107] is a non-peptide drug that blocks the CRF-1 (corticotropin releasing factor-1) receptor, and, as a consequence, reduces the release of corticotropin in response to chronic stress.

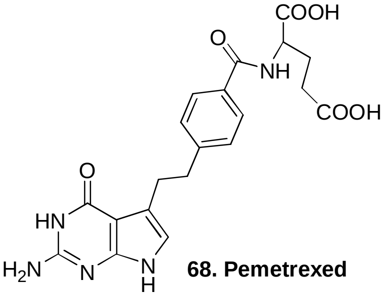

68. Pemetrexed

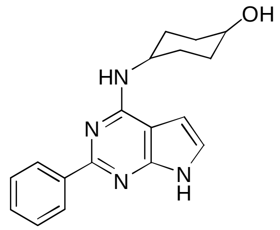

69. SLV 320

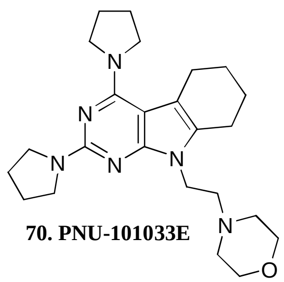

70. PNU-101033E

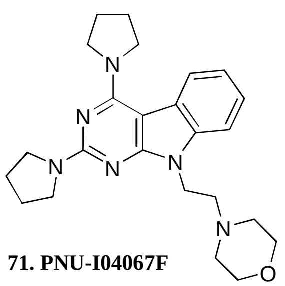

71. PNU-I04067F

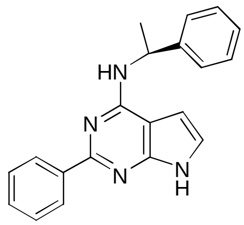

72. PKI 166

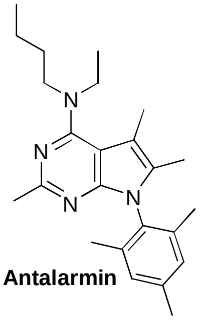

73. Antalarmin

Figure 10a. Pyrrolo[2,3-*d*]pyrimidine core based some important drugs and drug candidate molecules

Another molecule CP-154526, (**74, Fig. 10b**) [108] is a potent and selective nonpeptide antagonist of CRF receptors. NVP-ADW742 (**75, Fig. 10b**) [109] is an ATP-competitive inhibitor that inhibits IGF-IR autophosphorylation with a cellular IC50 of 0.1 to 0.2 μmol/L, which is approximately

16-fold lower than that of the insulin receptor. NVP-AEW541 (**76, Fig. 10b**)[110] is another molecule in this class and was found to inhibit the in vitro kinase activity of the recombinant IGF-IR kinase domain with an IC50 value of 0.15 µmol/L.

Tofacitinib (**78**, **Fig. 10b**)[111] (formerly tasocitinib, CP-690550) is a drug being investigated by Pfizer for the treatment of rheumatoid arthritis (RA), psoriasis, inflammatory bowel disease, and other immunological diseases, as well as for the prevention of organ transplant rejection. Ruxolitinib (**79, Fig. 10b**) [112] is being investigated for the treatment of myeloproliferative diseases, plaque psoriasis, and various types of cancer.

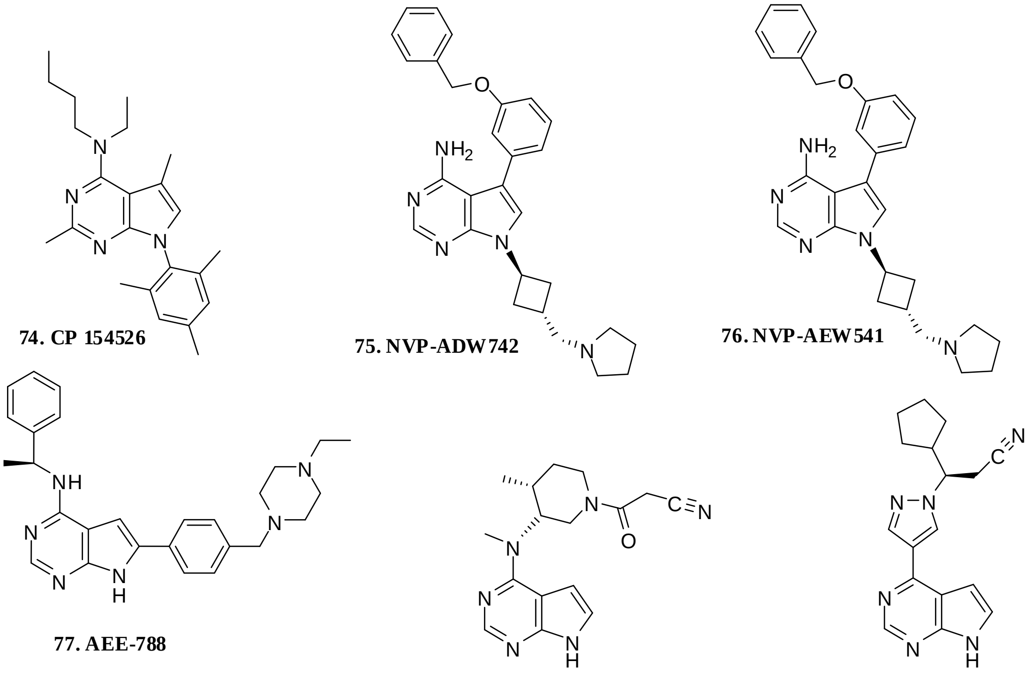

74. CP 154526

75. NVP-ADW742

76. NVP-AEW541

77. AEE-788

78. Tofacitinib

79. Ruxolitinib

Figure 10. Pyrrolo[2,3-*d*]pyrimidine core based some important drugs molecules and drug candidate molecules

The affinity of a drug depends on how tightly it can bind to its receptor through a set of non-covalent interactions. Arene–arene interactions are one of the important non-covalent interactions involved in binding of a drug to its receptor. Thus, proper understanding of arene-arene interaction is essential for rational drug-design. A brief review on nature and geometry of arene interactions has been presented in chapter one.

In the context of above discussion it is very important to study the role of arene interactions in purines and related systems. In this regard the use of flexible linkers to connect two aromatic moiety has been very helpful in the study of arene interactions and a brief discussion of such flexible linkers has been described in the previous chapter.

2.2 Objective

1. Synthesis, solution and solid state conformational studies of pyrrolo[2,3-*d*]pyrimidine (**19, Fig. 4**) core based *polymethylene* linker compounds for the study of conformation directing roles of arene–arene interactions of this nucleus.
2. To study the effect of decreasing the number of ring nitrogen on the stacking behavior as compared to the analogous pyrazolo[3,4-*d*]pyrimidine (PP) and triazolo[4,5-*d*]pyrimidine (TP) core based flexible molecules.
3. To study the effect of substituents on intramolecular and intermolecular stacking behavior of the molecule.

2.3 Synthesis and characterization

2.3.1 Synthesis and characterization of various monomeric pyrrolo[2,3-*d*]pyrimidine compounds (Scheme 1, 2 and 3).

The compound **82, 83, 87** and **88 (Scheme 1)** are important intermediates in the synthesis of various pyrrolo[2,3-*d*]pyrimidine as well as purine nucleus and were synthesized according to the literature procedures.[113] The NMR spectra of compounds were recorded in $CDCl_3$ unless otherwise stated.

2.3.1.1 Synthesis and characterization of 2-methylthio-3*H*-pyrrolo[2,3-*d*]pyrimidin-4(7*H*)-one (82, Scheme 1),[113] 4-chloro-2-methylthio-7*H*-pyrrolo[2,3-*d*]pyri-midine (83, Scheme 1),[114] 2-methylthio-7*H*-pyrrolo[2,3-*d*]pyrimidine-4-thiol (84, Scheme 1)[115] and 2,4-bis(methylthio)-7*H*-pyrrolo[2,3-*d*]pyrimidine (85, Scheme 1).

The compound **82**,[113] **83**,[114] and **84**[115] (**Scheme 1**) were synthesized following the procedures described in the literature. The required **85** (**Scheme 1**) was synthesized by reaction of compound **84** with methyl iodide and is described in the experimental section.

Proton NMR (DMSO-d_6) of the compound **82** shows a singlet at δ 2.50 for SMe, two multiplets for two aromatic protons at δ 6.34-6.36 and δ 6.89-6.91 and two NH protons at δ 11.74 and δ 12.03. Mass spectrum shows base peak corresponding to $[M+H]^+$ at *m/z* 182.

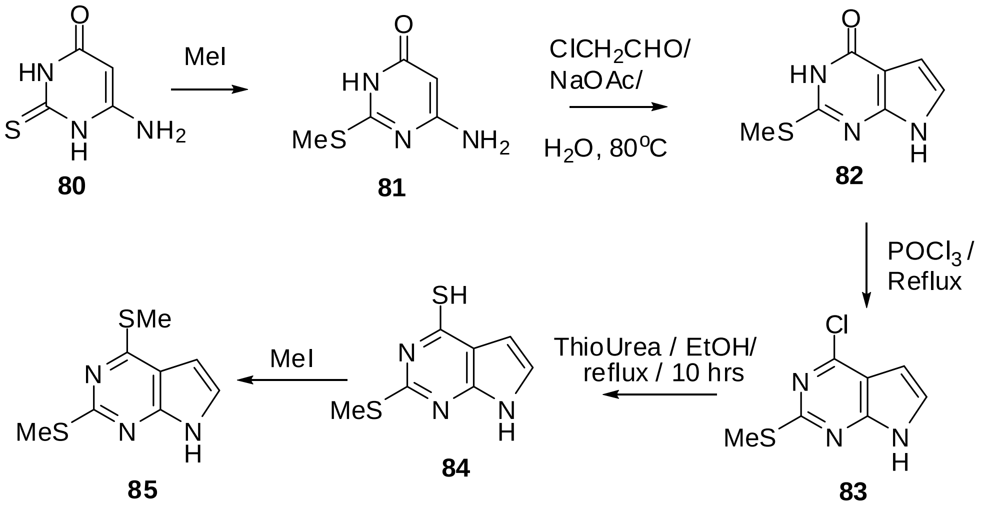

Scheme 1: Synthesis of various pyrrolo[2,3-*d*]pyrimidine compounds

Proton NMR of the compound **83** shows a singlet at δ 2.65 for SMe, two multiplets for two aromatic protons at δ 6.54-6.56 and δ 7.21-7.24 and one NH protons at δ 9.93. Mass spectrum shows base peak corresponding to $[M+H]^+$ at *m/z* 200.

Proton NMR ($CDCl_3$ + DMSO-d_6) of the compound **84** shows a singlet at δ 2.48 for SMe, two singlets for two aromatic protons at δ 6.59 and δ 6.88 and one NH or SH proton at δ 11.35. Mass spectrum shows base peak corresponding to $[M+H]^+$ at *m/z* 198.

Proton NMR of the compound **85** shows two singlet at δ 2.70 and δ 2.72 for two SMe, two multiplets for two aromatic protons at δ 6.46-6.48 and δ 7.13-7.15 and one NH proton at δ 10.76. Mass spectrum shows base peak corresponding to $[M+H]^+$ at *m/z* 212.

2.3.1.2 Synthesis and characterization of 3-methyl-2-methylthio-3*H*-pyrrolo[2,3-*d*]-pyrimidin-4(7*H*)-one (87, Scheme 2).[116]

The compound **87** (**Scheme 2**) was synthesized following the procedures described in the literature.[116]

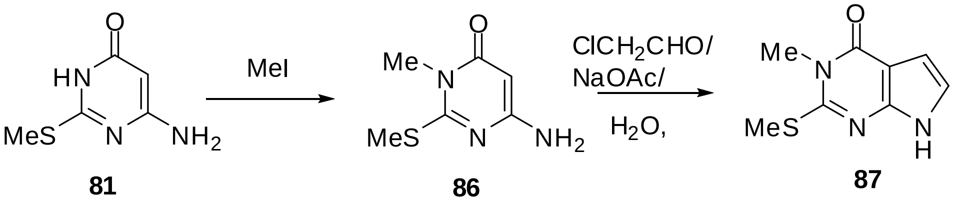

Scheme 2: Synthesis of compound **87**

Proton NMR of compound **87** shows a singlet at δ 2.59 for SMe, a singlet at δ 3.60 for NMe, two multiplets for two aromatic protons at δ 6.64-6.66 and δ 6.79-6.81 and one NH proton at δ 8.35. Mass spectrum shows base peak corresponding to [M+H]$^+$ at *m/z* 196.

2.3.1.3 Synthesis of various reference monomeric pyrrolo[2,3-*d*]pyrimidine compounds.

2.3.1.3.1 Synthesis and characterization of 4-chloro-7-methyl-2-methylthio-7*H*-pyrrolo[2,3-*d*]pyri-midine (88, Scheme 3), 4-methoxy-7-methyl-2-methylthio-7*H*-pyrrolo[2,3-*d*]pyrimidine (89, Scheme 3), 7-methyl-2,4-bis(methylthio)-7*H*-pyrrolo[2,3-*d*]pyrimidine (90, Scheme 3), 7-methyl-2-methylthio-4-pyrrolidin-1-yl-7*H*-pyrrolo[2,3-*d*]- pyrimidine (91, Scheme 1a) and 3,7-dimethyl-2-methylthio-3*H*-pyrrolo[2,3-*d*]pyrimidin-4(7*H*)-one (92, Scheme 3).

Methylation of compounds **83**, **85** and **87** with methyl iodide in DMF using cesium carbonate as a base gave compounds **88**, **90** and **92** respectively. Reaction of compound **88** with NaOMe in methanol under refluxing conditions yielded compound **89** and reaction of compound **90** with pyrrolidine under refluxing conditions gave compound **91**.

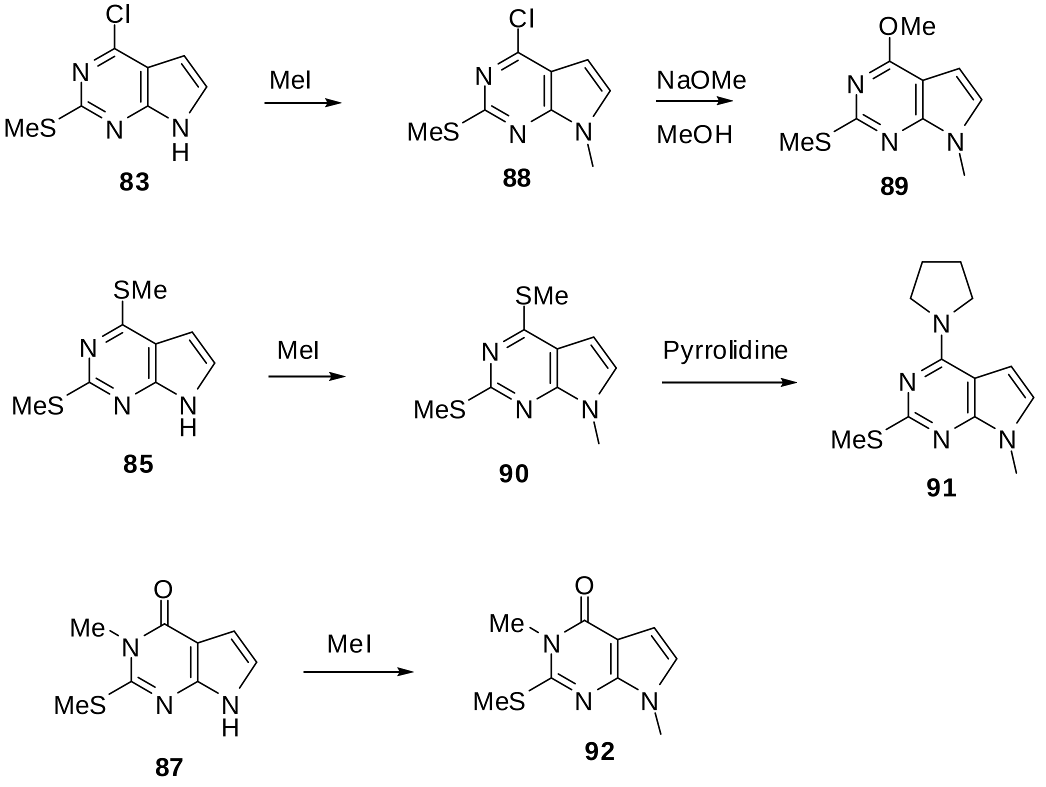

Scheme 3: Synthesis of various reference compounds with pyrrolo[2,3-*d*]pyrimidine core

Proton NMR of the compound **88** shows a singlet at δ 2.64 for SMe, two doublets for two aromatic protons at δ 6.48 and δ 7.02 and one NMe proton at δ 3.81. Mass spectrum shows base peak corresponding to $[M+H]^+$ at *m/z* 214.

Proton NMR of the compound **89** shows three singlets at δ 2.64, δ 3.79 and δ 4.10 for SMe, NMe and OMe protons respectively and two singlet for two aromatic protons at δ 6.42 and δ 6.84. Mass spectrum shows base peak corresponding to $[M+H]^+$ at *m/z* 210.

Proton NMR of the compound **90** shows two singlet at δ 2.65 and δ 2.68 for two SMe, two doublets for two aromatic protons at δ 6.38 and δ 6.88 and one NMe proton at δ 3.76. Mass spectrum shows base peak corresponding to $[M+H]^+$ at *m/z* 226.

Proton NMR of the compound **91** shows a singlet at δ 2.59, two doublets for two aromatic protons at δ 6.44 and δ 6.70, one singlet for NMe proton at δ3.73 and two broad singlets, one at δ 3.81 for pyrrolidinyl NCH_2 protons and other at δ 2.02 for pyrrolidinyl CH_2 protons. Mass spectrum shows base peak corresponding to $[M+H]^+$ at *m/z* 249.

Proton NMR of compound **92** shows a singlet at δ 2.63 for SMe, a singlet at δ 3.59 for NMe, a singlet at δ 3.72 and two doublets for two aromatic protons at δ 6.59 and δ 6.69. Mass spectrum shows base peak corresponding to $[M+H]^+$ at *m/z* 210.

2.3.1.4 Synthesis and characterization of 5,6-dimethyl-2,4-disubstituted-7*H*-pyrrolo[2,3-*d*]-pyrimidine (Scheme 4).

2.3.1.4.1 Synthesis and characterization of 2-amino-4,5-dimethyl-1*H*-pyrrole-3-carbonitrile (95,[117a] Scheme 4), 5,6-dimethyl-7*H*-pyrrolo[2,3-*d*]pyrimidine-2,4-dithiol (96, Scheme 4), 5,6-dimethyl-2,4-bis(methylthio)-7*H*-pyrrolo[2,3-*d*]pyrimidine (97, Scheme 4) and 5,6,7-trimethyl-2,4-bis(methylthio)-7*H*-pyrrolo[2,3-*d*]pyrimidine (98, Scheme 4).

The compound **95** was prepared following the literature procedure using alanine (**93**) as a starting material.[117a] The compound **96** was synthesized by the reaction of carbon disulfide in pyridine using the literature procedure[117b] (**Scheme 4**). The compound **97** was synthesized by the reaction of compound **96** with methyl iodide in water using sodium hydroxide as a base (**Scheme 4**). The compound **98** was synthesized by the reaction of compound **97** with methyl iodide in DMF using sodium hydride as a base (**Scheme 4**). These compounds were characterized by analysis of mass and NMR spectra.

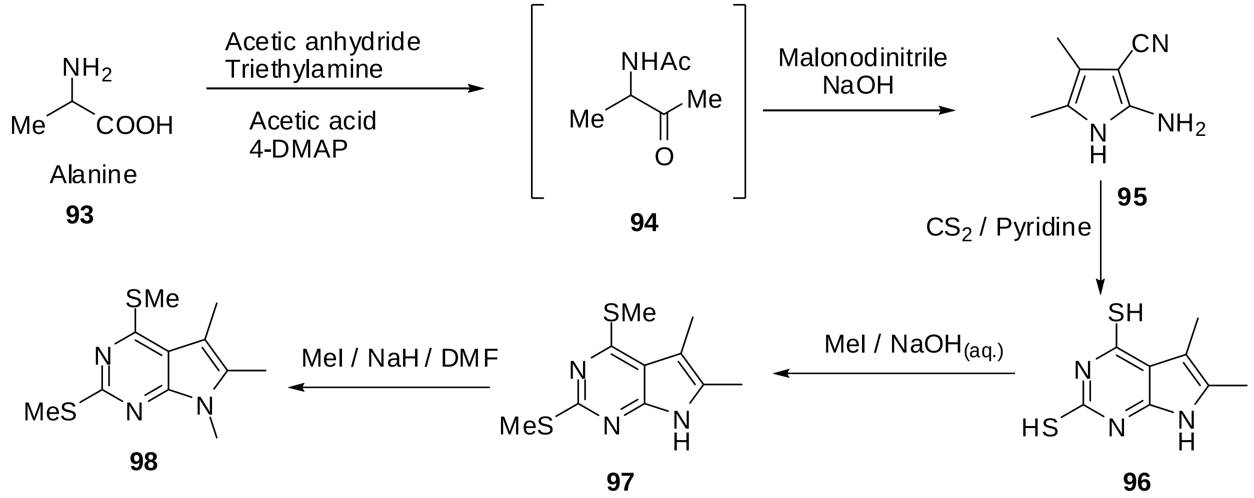

Scheme 4: Synthesis of monomeric 5, 6-dimethyl-pyrrolo[2,3-*d*]pyrimidine compounds

Proton NMR (DMSO-d_6) of the compound **95** shows peaks at δ 9.83 for NH, at δ 5.36 for NH_2, and at δ 1.92 and δ 1.83 for two methyl protons. Mass spectrum shows base peak corresponding to $[M+H]^+$ at *m/z* 136.

Proton NMR (DMSO-d_6) of the compound **96** shows four singlets at δ 2.11, δ 2.27 for two Me, and at δ 11.25 and δ 12.41 for SH and NH protons. Mass spectrum shows base peak corresponding to $[M+H]^+$ at *m/z* 212.

Proton NMR in $CDCl_3$ of compound **97** shows two singlet at δ 2.33 and δ 2.34 for two Me, two singlet at δ 2.63 and δ 2.66 for two SMe and one singlet for one NH proton at δ 9.13. Mass spectrum shows base peak corresponding to $[M+H]^+$ at *m/z* 240.

Proton NMR in $CDCl_3$ of compound **98** shows two singlet at δ 2.07 and δ 2.09 for two Me, one singlet at δ 2.56 SMe protons and one singlet for one NCH_3 proton at δ 3.26. Mass spectrum shows base peak corresponding to $[M+H]^+$ at *m/z* 254.

2.3.1.5 Synthesis and characterization of 5-methyl-2,4-bis(methylthio)-7*H*-pyrrolo[2,3-*d*]-pyrimidine (100, Scheme 5)[117] and 5,7-dimethyl-2,4-bis(methylthio)-7*H*-pyrrolo[2,3-*d*]-pyrimidine (101, Scheme 5).

The compound **100** was synthesized by following the literature procedure using glycine (**104**) as the starting material[118] (**Scheme 5**). Compound **101** was synthesized by the reaction of compound **105** with methyl iodide in DMF using sodium hydride as a base (**Scheme 5**). These compounds were characterized by analysis of mass and NMR spectra.

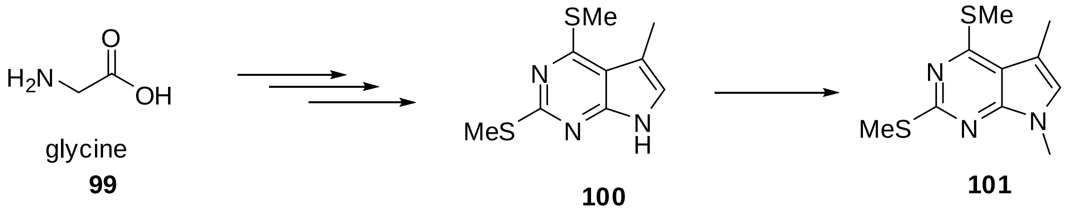

Scheme 5: Synthesis of 5-methyl-pyrrolo[2,3-*d*]pyrimidine compounds

Proton NMR of the compound **100** shows one singlet at δ 2.43 for 5-Me protons, two singlets at δ 2.66 and δ 2.68 for two SMe, one singlet at δ 6.78 for aromatic proton and one singlet at δ 9.44 for one NH proton. Mass spectrum shows base peak corresponding to $[M+H]^+$ at *m/z* 226.

Proton NMR of the compound **101** shows a singlet at δ 2.42 for 5-Me protons, two singlets at δ 2.64 and δ 2.67 for two SMe and one singlet δ 3.69 for NCH_2 protons and a singlet at δ 6.61 for aromatic proton. Mass spectrum shows base peak corresponding to $[M+H]^+$ at *m/z* 240.

2.3.2 Synthesis and characterization of various dimeric pyrrolo[2,3-*d*]pyrimidine compounds.

2.3.2.1 Synthesis and characterization of 1,n-bis(4-chloro-2-(methylthio)-1*H*-pyrrolo[2,3-*d*]-pyrimidin-1-yl)alkane (105-107, Scheme 6).

The compound **83** on reaction with 1,n-dibromopropane (**102-104**) in acetone using cesium carbonate as base gives compounds (**105-107**) as shown in **Scheme 6**. These compounds were characterized by analysis of mass and NMR spectra**.**

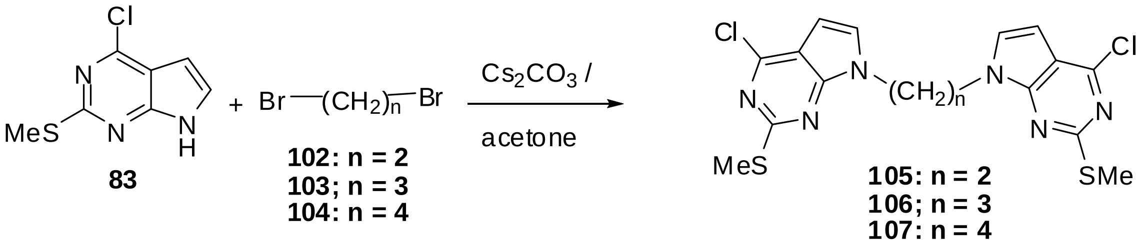

Scheme 6: Synthesis of compounds **105-107**

Proton NMR of the compound **105** shows a singlet at δ 2.51 for SMe, a singlet at δ 4.61 for NCH_2 and two doublets at δ 6.35 and δ 6.55 for two aromatic protons. Mass spectrum shows base peak corresponding to $[M+H]^+$ at *m/z* 426.

Proton NMR of the compound **106** shows a quintet at δ 2.49 for CH_2, a singlet at δ 2.58 for SMe, one triplet at δ 4.22 for NCH_2 and two doublets at δ 6.52 and δ 7.07 for two aromatic protons. Mass spectrum shows base peak corresponding to $[M+H]^+$ at *m/z* 440.

Proton NMR of the compound **107** shows a broad singlet at δ 1.84 for CH_2 protons, a singlet at δ 2.62 for SMe, a broad singlet at δ 4.26 for NCH_2 and two doublets at δ 6.51 and δ 7.01 for two aromatic protons. Mass spectrum shows base peak corresponding to $[M+H]^+$ at *m/z* 453.

2.3.2.2 Synthesis and characterization 1,n-bis(2,4-bis(methylthio)-7*H*-pyrrolo[2,3-*d*]-pyrimidin-7-yl)alkane (108-110, Scheme 7).

The compound **90** on reaction with 1,n-dibromopropane (**107-109**) in DMF using cesium carbonate as base gives compound (**108-110**) as shown in **Scheme 7**. These compounds were characterized by analysis of mass and NMR spectra**.**

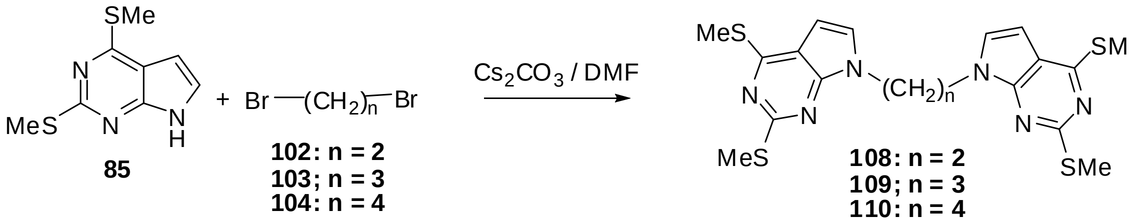

Scheme 7: Synthesis of compounds **108-110**

Proton NMR of the compound **108** shows two singlet at δ 2.58 and at δ 2.68 for SMe, one triplet at δ 4.57 for NCH_2 and two doublets at δ 6.24 and δ 6.36 for two aromatic protons. spectrum shows base peak corresponding to $[M+H]^+$ at *m/z* 449.

Proton NMR of the compound **109** shows a quintet at δ 2.41 for CH_2 protons, two singlets at δ 2.59 and at δ 2.69 for SMe, one triplet at δ 4.10 for NCH_2 and two doublets at δ 6.41 and δ 6.95 for two aromatic protons. Mass spectrum shows base peak corresponding to $[M+H]^+$ at *m/z* 463.

Proton NMR of the compound **110** shows a broad singlet at δ 1.77 for CH_2 protons, two singlets at δ 2.62 and at δ 2.68 for SMe, a broad singlet at δ 4.19 for NCH_2 and two doublets at δ 6.38 and δ 6.85 for two aromatic protons. Mass spectrum shows base peak corresponding to $[M+H]^+$ at *m/z* 477.

2.3.2.3 Synthesis and characterization of 7,7′-(alkane-1,n-diyl)bis(3-methyl-2-methylthio)-3*H*-pyrrolo[2,3-*d*]pyrimidin-4(7*H*)-one) (111-113, Scheme 8).

The compound **87** on reaction with 1,n-dibromopropane (**102-104**) in DMF using cesium carbonate as base gives compound (**111-113**) as shown in **Scheme 8**. These compounds were characterized by analysis of mass and NMR spectra.

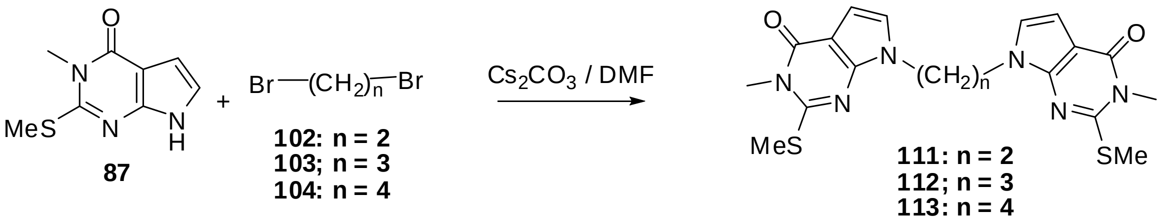

Scheme 8: Synthesis of compounds **111-113**

Proton NMR of the compound **111** shows, two singlets at δ 2.48 and at δ 3.56 for SMe and NMe protons respectively, a singlet at δ 4.46 for NCH_2 and two doublets at δ 6.35 and δ 6.49 for two aromatic protons. Mass spectrum shows base peak corresponding to $[M+H]^+$ at *m/z* 417.

Proton NMR of the compound **112** shows a singlet at δ 2.32 for SMe proton, a quintet at δ 2.39 for CH_2 protons, a singlet at δ 2.32 for NMe proton, a triplet at δ 4.03 for NCH_2 and two doublets at δ 6.64 and δ 6.74 for two aromatic protons. Mass spectrum shows base peak corresponding to $[M+H]^+$ at *m/z* 431.

Proton NMR of the compound **113** shows a broad singlet at δ 1.79 for CH_2 protons, two singlets at δ 2.51 and at δ 3.57 for SMe and NMe protons respectively, a broad singlet at δ 4.09 for NCH_2 and two doublets at δ 6.56 and δ 6.62 for two aromatic protons. Mass spectrum shows base peak corresponding to $[M+H]^+$ at *m/z* 445.

2.3.2.4 Synthesis and characterization of 1,3-bis(2-methylthio-4-pyrrolidin-1-yl-7*H*-pyrrolo[2,3-*d*]pyrimidin-7-yl)propane (114, Scheme 9) and 1,3-bis(4-methoxy-2-methylthio-7*H*-pyrrolo[2,3-*d*]pyrimidin-7-yl)propane (115, Scheme 9).

The compound **114** was synthesized by refluxing compound **106** with pyrrolidine and compound **115** was synthesized by refluxing compound **106** with sodium methoxide in methanol (**Scheme 9**). These compounds were characterized by analysis of Massand NMR spectra**.**

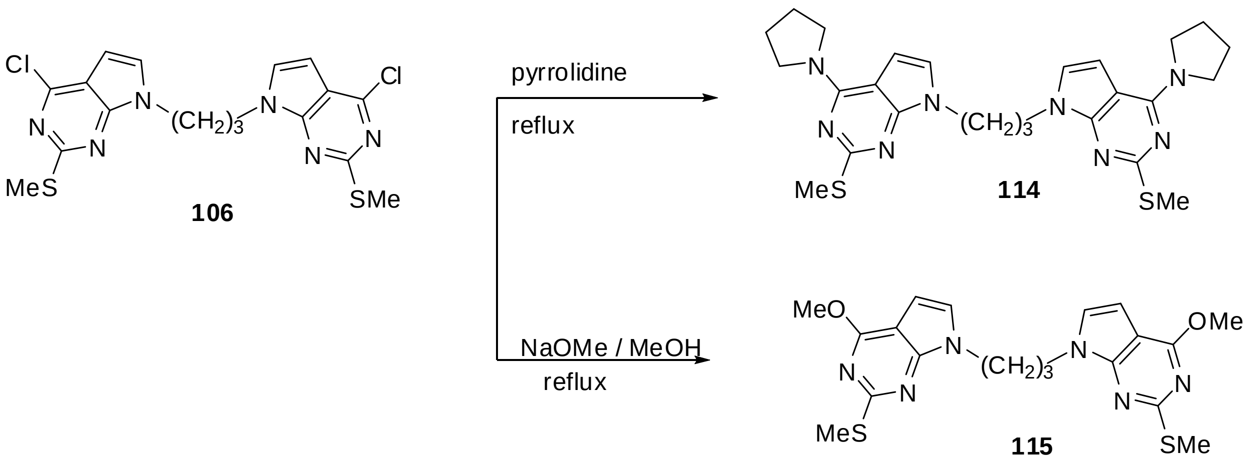

Scheme 9: Synthesis of compounds **114-115**

Proton NMR of the compound **114** shows a broad singlet at δ 2.01 for pyrrodinyl CH_2, a quintet δ 2.36 for CH_2, one singlet at δ 2.55 for SMe, a broad singlet at δ 3.80 for pyrrodinyl NCH_2, one triplet at δ 4.12 for NCH_2 and two doublets at δ 6.43 and δ 6.81 for two aromatic protons. Mass spectrum shows base peak corresponding to $[M+H]^+$ at *m/z* 509.

Proton NMR of the compound **115** , a quintet δ 2.44 for CH_2, one singlet at δ 2.56 for SMe,, one singlet at δ 4.09 for OMe, one triplet at δ 4.17 for NCH_2 and two doublets at δ 6.43 and δ 6.88 for two aromatic protons. Mass spectrum shows base peak corresponding to $[M+H]^+$ at *m/z* 432.

2.3.2.5 Synthesis and characterization of 1,n-bis(5,6-dimethyl-2,4-bis(methylthio)-7*H*-pyrrolo[2,3-*d*]pyrimidin-7-yl)alkane (116-118, Scheme 10).

The compound **102** on reaction with 1,n-dibromopropane (**107-109**) in DMF using sodium hydride as base gives compound (**116-118**) as shown in **Scheme 10**. These compounds were characterized by analysis of mass and NMR spectra**.**

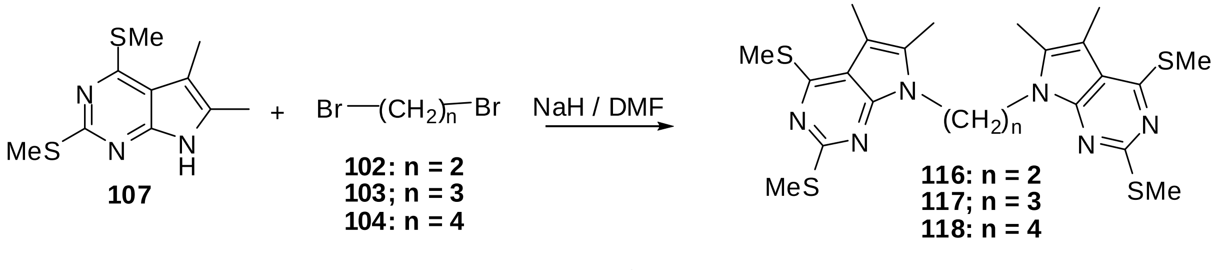

Scheme 10: Synthesis of compounds **116-118**

Proton NMR spectra of the compound **116** shows two singlet at δ 1.92 and δ 2.30 for CH_3 protons, two singlet at δ 2.58 and δ 2.64 for SMe protons and one singlet for NCH_2 protons at δ 4.37. Mass spectrum shows base peak corresponding to $[M+H]^+$ at *m/z* 505.

Proton NMR of the compound **117** , a multiplet in the range of δ 2.09-2.18 for CH_2 protons, two singlet at δ 2.18 and δ 2.33 for CH_3 protons, two singlet at δ 2.55 and δ 2.64 for SMe protons and one triplet at δ 4.17 for NCH_2 protons. Mass spectrum shows base peak corresponding to $[M+H]^+$ at *m/z* 519.

Proton NMR spectra of compound **118** shows a broad singlet at δ 1.58 for CH_2 protons, two singlets at δ 2.07 and δ 2.11 for CH_3 protons, two singlets at δ 2.57 for SMe protons and one triplet for NCH_2 protons at δ 3.71. Mass spectrum shows base peak corresponding to $[M+H]^+$ at *m/z* 533.

2.3.2.6 Synthesis and characterization of 1,n-bis(5-methyl-2,4-bis(methylthio)-7*H*-pyrrolo[2,3-*d*]pyrimidin-7-yl)propane (119-121, Scheme 11).

The compound **105** on reaction with 1,n-dibromopropane (**102-104**) in DMF using sodium hydride as base gives compound (**119-121**) as shown in **Scheme 7**. These compounds were characterized by analysis of mass and NMR spectra**.**

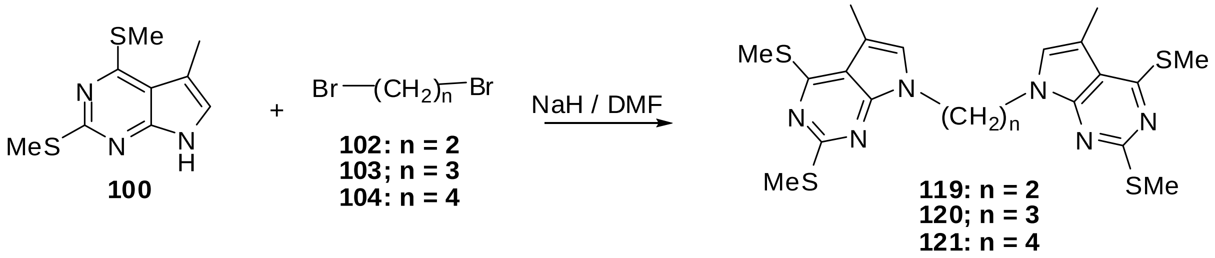

Scheme 11: Synthesis of compounds **119-121**

Proton NMR spectra of compound **119** shows one singlet at δ 2.29 for CH_3 protons, two singlet at δ 2.55 and δ 2.65 for SMe protons, one singlet for NCH_2 protons at δ 4.42 and one singlet at δ 6.18 for aromatic proton. Mass spectrum shows base peak corresponding to $[M+H]^+$ at *m/z* 477.

Proton NMR of the compound **120**, a multiplet in the range of δ 2.30-2.39 for CH_2 protons, one singlet at δ 2.39 for CH_3 protons, two singlet at δ 2.59 and δ 2.66 for SMe protons, one triplet at δ 4.06 for NCH_2 protons and one singlet at δ 6.62 for aromatic proton. Mass spectrum shows base peak corresponding to $[M+H]^+$ at *m/z* 491.

Proton NMR of the compound **121**, shows a broad singlet at δ 1.76 for CH_2 protons, a singlet at δ 2.40 for CH_3 protons, two singlets at δ 2.62 and δ 2.68 for SMe protons, one broad singlet for NCH_2 protons at δ 4.16 and a singlet at δ 6.60 for aromatic proton. Mass spectrum shows base peak corresponding to $[M+H]^+$ at *m/z* 505.

2.4 Result and discussion

The present study was undertaken to determine the effect of decreasing number of ring nitrogen on the robustness of the *U-motif* seen in 4,6-disubstituted-1*H*-pyrazolo[3,4-*d*]pyrimidine compounds from molecular recognition and crystal engineering point of view. Generally, electronic effects are considered to play significant role in stacking interactions. Thus we decided to synthesize symmetrical *polymethylene* especially *trimethylene* linked 2,4-disubstituted-7*H*-pyrrolo[2,3-*d*]pyrimidine compounds in which one N atom of the pyrazolo part of pyrazolo[3,4-*d*]pyrimidine nucleus is replaced by CH. This introduction of CH in ring was expected to bring a profound change in the electronic distribution of the nucleus and thus would have significant change in the solution and solid state conformation of the molecule and thus on the stacking behavior of the molecule. The information obtained through such studies can also be used in the studies of more important purine nucleus since pyrrolo[2,3-*d*]pyrimidine can be considered as an analogue of purine. These studies may also help in better understanding of the processes in which these molecules take part.

2.4.1 ^{1}H NMR study

In earlier studies on *polymethylene* linked, especially in case of *ethylene* and *trimethylene* linked, 4,6-disubstituted-1*H*-pyrazolo[3,4-*d*]pyrimidine compounds (**126-128**, **132-134**, **Fig. 11** and **Table 1**) we observed an upfield shift of protons of groups attached at 6-position as compared to the respective reference compounds.[118] Analogous results were obtained in case of *polymethylene* linked 5,7-disubstituted-triazolo[4,5-*d*]pyrimidine compounds (**129-131**, **135-137**, **Fig. 11** and **Table 1**) and has been discussed in the **Chapter 1**. Perusal of data in **Table 1** shows that while trend is same in both series magnitude of upfield shift is more for triazolo[4,5-*d*]-pyrimidine series. Proton NMR data of **Table 1** will be used with corresponding data on similar pyrrolo[2,3-*d*]pyrimidine compounds (**Fig. 12** and **Table 2 and 3**) for conformational analysis.

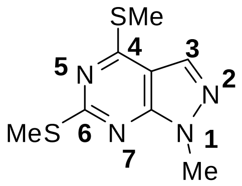

122

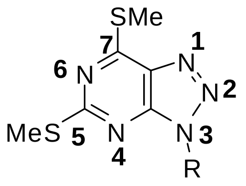

123: R = C_4H_9

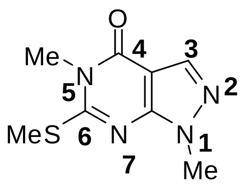

124

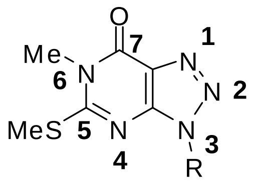

125: R = C_4H_9

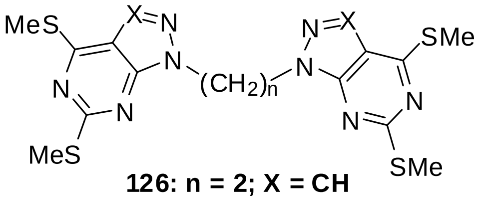

126: n = 2; X = CH
127: n = 3; X = CH
128: n = 4; X = CH
129: n = 2; X = N
130: n = 3; X = N
131: n = 4; X = N

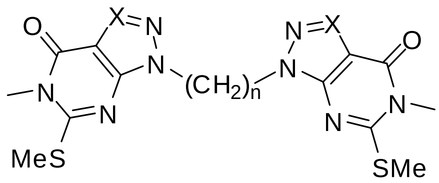

132: n = 2; X = CH
133: n = 3; X = CH
134: n = 4; X = CH
135: n = 2; X = N
136: n = 3; X = N
137: n = 4; X = N

Figure 11. Pyrazolo[3,4-*d*]pyrimidine (**PP**) and triazolo[4,5-*d*]pyrimidine compounds (**TP**)

Table 1: ^{1}H NMR shifts of various monomeric and dimeric pyrazolo[3,4-*d*]pyrimidine (**PP**) and Triazolo[4,5-*d*]pyrimidines (**TP**).
(Color code: Blue = *ethylene* linker; Red = *trimethylene* linker and Green = *butylene* linker).

S.No.	**Comp. No.**	**n**	**δ 6-SMe of PP/ 5-SMe of TP**	**δ 4-SMe of PP/ 7-SMe of TP/ 5-Me(PP)/6-Me(TP)**	**Δδ = δ 6-SMe/5-SMe (monomer) – δ 6-SMe/5-SMe (dimer)**
1.	**122** (PP)	-	2.66	2.62	-
2.	**123 (TP)**	-	**2.75**	**2.64**	-
3.	**124** (PP)	-	2.65	3.57	-
4.	**125 (TP)**	-	**2.67**	**3.62**	-
5.	**126 (PP)**	**2**	**2.44**	**2.66**	**0.22**
6.	**127 (PP)**	**3**	**2.45**	**2.67**	**0.21**
7.	**128 (PP)**	**4**	**2.53**	**2.62**	**0.13**
8.	**129 (TP)**	**2**	**2.40**	**2.72**	**0.35**
9.	130 (TP)	3	**2.50**	**2.75**	**0.25**
10.	**131 (TP)**	**4**	**2.60**	**2.75**	**0.15**
11.	**132 (PP)**	**2**	**2.48**	**3.48**	**0.17**
12.	**133 (PP)**	**3**	**2.29**	**3.51**	**0.36**
13.	**134 (PP)**	**4**	**2.58**	**3.55**	**0.07**
14.	**135 (TP)**	**2**	**2.38**	**3.60**	**0.29**
15.	**136 (TP)**	**3**	**2.44**	**3.58**	**0.23**
16.	**137 (TP)**	**4**	**2.59**	**3.60**	**0.08**

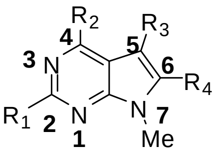

88, 89-91, 98, 101

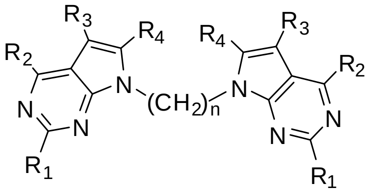

105-110, 114-121

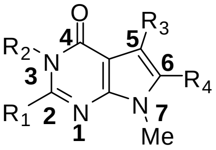

92

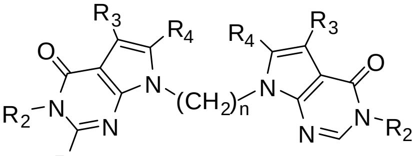

111-113

Figure 12: General structure of pyrrolo[2,3-*d*]pyrimidine and pyrrolo[2,3-*d*]pyrimidone compounds synthesized in the present study

Table 2: ^{1}H NMR shifts of various monomeric and dimeric pyrrolo[2,3-*d*]pyrimidines. (Color code: Blue = *ethylene* linker; Red = *trimethylene* linker and Green = *butylene* linker).

S. No.	Comp. No.	n	R_1	R_2	R_3	R_4	δ 2-SMe	δ 3-NMe/ 4-SMe/ OMe/pyrr.	δ 5-H/CH_3	δ 6-H/CH_3
1.	**88**	-	SMe	Cl	H	H	2.64	-	6.48	7.02
2.	**92**	-	SMe	Me	H	H	2.63	3.59	6.59	6.69
3.	**90**	-	SMe	SMe	H	H	2.68	2.65	6.38	6.88
4.	**91**	-	SMe	Pyrr.	H	H	2.59	3.81	6.44	6.70
5.	**89**	-	SMe	OMe	H	H	2.64	4.10	6.42	6.84
6.	**98**	-	SMe	SMe	CH_3	CH_3	2.56	2.56	2.07	2.09
7.	**101**	-	SMe	SMe	CH_3	H	2.67	2.64	2.41	6.61
8.	105	2	SMe	Cl	H	H	2.52	-	6.36	6.54
9.	106	3	SMe	Cl	H	H	2.56	-	6.50	7.05
10.	107	4	SMe	Cl	H	H	2.62		6.51	7.01
11.	108	2	SMe	SMe	H	H	2.58	2.68	6.24	6.36
12.	109	3	SMe	SMe	H	H	2.59	2.68	6.42	6.96
13.	110	4	SMe	SMe	H	H	2.62	2.68	6.38	6.85
14.	111	2	SMe	Me	H	H	2.47	3.56	6.34	6.49
15.	112	3	SMe	Me	H	H	2.31	3.53	6.63	6.73
16.	113	4	SMe	Me	H	H	2.50	3.56	6.55	6.61
17.	114	3	SMe	Pyrr.	H	H	2.55	3.80	6.43	6.80
18.	115	3	SMe	OMe	H	H	2.57	4.09	6.43	6.88
19.	116	2	SMe	SMe	CH_3	CH_3	2.58	2.64	1.92	2.30
20.	117	3	SMe	SMe	CH_3	CH_3	2.64	2.55	2.19	2.33
21.	118	4	SMe	SMe	CH_3	CH_3	2.57	2.57	2.07	2.11
22.	119	2	SMe	SMe	CH_3	H	2.65	2.55	2.29	6.18
23.	120	3	SMe	SMe	CH_3	H	2.66	2.58	2.38	6.62
24.	121	4	SMe	SMe	CH_3	H	2.68	2.62	2.40	6.60

In case of *polymethylene* linked 2,4-disubstituted-7*H*-pyrrolo[2,3-*d*]pyrimidine compounds the upfield shift of protons observed in groups attached to the 2-position as compared to the respective monomeric compounds is very less (**Fig. 12** and **Table 2 and 3**) as compared to the shifts observed in case of corresponding 4,6-disubstituted-1*H*-pyrazolo[3,4-*d*]pyrimidine compounds or 5,7-disubstituted-triazolo[4,5-*d*]pyrimidine compounds (**Fig. 11** and **Table 1**). This shows that the conformational arrangement of dimeric pyrrolo[2,3-*d*]pyrimidine compounds (**105-110** and **114-115**, **Fig. 12**) is different from the corresponding pyrazolo[3,4-*d*]pyrimidine or triazolo[4,5-*d*]pyrimidine compounds (**126-131**, **Fig. 11**).

Table 3: Difference in ^{1}H NMR shifts of protons in dimeric pyrrolo[2,3-*d*]pyrimidines compared to their respective monomeric compounds.
(Color code: Blue = *ethylene* linker; Red = *trimethylene* linker and Green = *butylene* linker).

S.No.	Comp. No.	n	Δδ = δ 2-SMe (monomer) – δ 2-SMe (compound)	Δδ = δ 5-H/CH_3 (monomer) – δ 5-H/CH_3 (compound)	Δδ = δ 6-H/CH_3 (monomer) – δ 6-H/CH_3 (compound)
1.	105	2	0.12	0.12	0.48
2.	106	3	0.08	-0.02	-0.03
3.	107	4	0.02	-0.03	0.01
4.	108	2	0.10	0.14	0.52
5.	109	3	0.09	-0.04	-0.08
6.	110	4	0.06	0.00	0.03
7.	111	2	0.16	0.25	0.20
8.	112	3	0.32	-0.04	-0.04
9.	113	4	0.13	0.04	0.08
10.	114	3	0.04	0.01	-0.10
11.	115	3	0.07	-0.01	-0.04
12.	116	2	-0.08	-0.23	0.17
13.	117	3	0.01	-0.12	-0.24
14.	118	4	-0.01	-0.04	0.02
15.	119	2	0.02	-0.14	0.43
16.	120	3	0.01	-0.17	-0.01
17.	121	4	-0.01	0.01	0.01

However, a comparison can be drawn in case of pyrrolo[2,3-*d*]pyrimidone compounds (**111-113, Fig. 12 and Table 2 and 3**) with the corresponding pyrazolo[3,4-*d*]pyrimidone or triazolo[4,5-*d*]pyrimidone compounds (**132-137**) (**Table 1**, **Fig. 11**). In this case the upfield shifts of 2-SMe pyrrolo[2,3-*d*]pyrimidone protons are comparable to 6-SMe protons of pyrazolo[3,4-*d*]pyrimidone as seen from the analysis of **Table 1** and **3**.

One more possible reason for this smaller upfield shits seen in the case of pyrrolo[2,3-*d*]pyrimidine is that the molecules may have a different conformational arrangement in which the groups attached at the 2-position may be far from the anisotropic region of the other ring and some other region may be close to the anisotropic region. To confirm this we synthesized compounds **115-121** (**Fig. 12**) and checked for the upfield shifts in the protons of 5-methyl and 6-methyl groups as well as in 2-methylsulfanyl and 4-methylsulfanyl protons (**Table 2** and **3**).

In case of *ethylene* linker compounds **105**, **108**, **111**, **116** and **119** (**Fig. 12 and Table 2 and 3**) we observe a significant downfield shift in the 6-H/CH_3 proton shift in the ^{1}HNMR spectra as compared to their respective monomeric compounds **88**, **90**, **92**, **98** and **101** (**Fig. 12 and Table 2 and 3**). The 5-H proton in case of **105**, **108** and **111** shows an upfield shift while the 5-Me protons in case of **116** and **119** shows a downfield shift as compared to their respective monomeric compounds (**Fig. 12 and Table 2 and 3**). The 2-SMe protons in case of compounds of **105**, **108** and **111** shows an upfield shift while there is no significant change in the shifts in SMe protons in case of compounds **116** and **119** as compared to their respective monomeric compounds (**Fig. 12 and Table 2 and 3**). These values indicates that the five membered pyrrole rings are more close to each other than the six membered pyrimidine/pyrimidone rings and the two pyrrolo pyrimidine rings are not in anti conformation. The probable solution state conformation in case of compounds **116** and **119** is shown in **Fig. 13**.

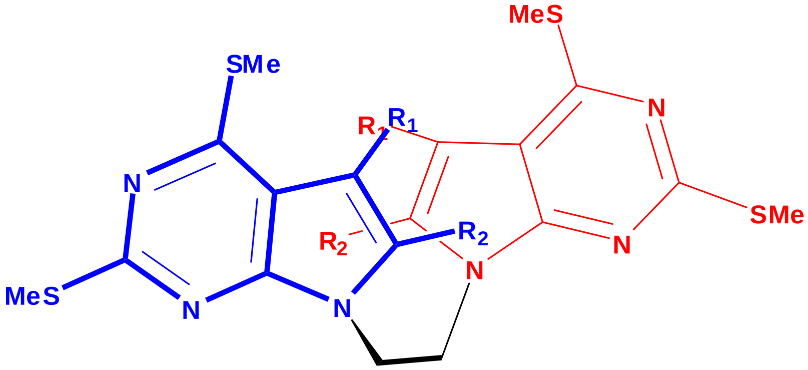

116: $R_1 = CH_3$; $R_2 = CH_3$
119: $R_1 = CH_3$; $R_2 = H$

Figure 13: Probable solution state conformation of compounds **116** and **119**

The corresponding upfield shift of 6-SMe in case of *ethylene* linked pyrazolo[3,4-*d*]pyrimidine compound **126, 132** (**Fig. 11 and Table 1**) and 5-SMe in case of *ethylene* linked triazolo[4,5-

d]pyrimidine **129**, **135** (**Fig. 11 and Table 1**) is larger as compared to their respective monomeric compounds **122**, **124** and **123**, **125** (**Fig. 11 and Table 1**). In these cases the NMR shifts indicate towards a conformation where the six-member pyrimidine rings are close to each other (**Fig. 11** and **Table 1**).

In case of *trimethylene* linker compounds **117** and **120** (**Fig. 12** and **Table 2** and **3**) there is no significant change in the proton NMR shift values of 2-SMe protons as compared with the respective monomeric compounds **98** and **101** (**Fig. 12** and **Table 2** and **3**). However we observe a downfield shift in the proton NMR shift values of 5-Me and 6-Me protons as compared with respective monomeric compounds. This indicates that the methyl protons are near to the periphery of the rings and are desheilded. This also indicates that the rings are not fully stretched but are close to each other, though not in a stacked conformation as seen in case of pyrazolo[3,4-*d*]pyrimidine compound **127**[60a] (**Fig. 14**). A similar but not so significant downfield shift is observed in case of compounds **106**, **109**, **114** and **115** (**Fig. 12** and **Table 2** and **3**).

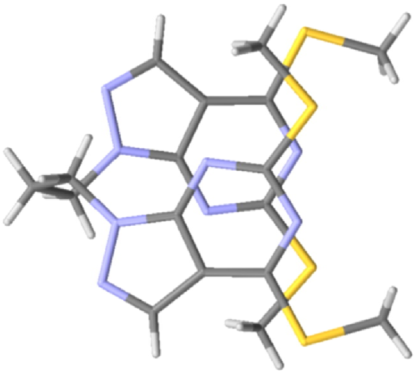

Figure 14: Crystal Structure of compound **127** showing stacked conformation

However, the pyrrolo pyrimidone compound **112** shows a significant upfield shift in the 2-SMe protons as compared to the monomeric compound **92** (**Fig. 12** and **Table 2** and **3**) and comparable to the corresponding upfield shifts in 6-SMe protons in pyrazolo pyrimidone compound **133** and 5-SMe protons in triazolo pyrimidone compound **136** (**Fig. 11** and **Table 1**). This indicates towards a similar conformational arrangement of these three molecules.

In case of *butylene* linked pyrrolo pyrimidine compounds **107**, **110**, **118** and **121** (**Fig. 12** and **Table 2** and **3**), there is no significant shifts in any of the protons as compared to the respective monomeric compounds **88**, **90**, **98** and **101** (**Fig. 12** and **Table 2** and **3**) indicating that there is no intramolecular interaction between the two rings. The corresponding pyrazolo[3,4-*d*]-pyrimidine compound **128** and triazolo[4,5-*d*]pyrimidine compound **131** show upfield shift in the 6-SMe and 5-SMe protons indicating that there is some interaction between the two rings (**Fig. 11** and **Table 1**).

In case of compound **113** there is an upfield shift in the 2-SMe protons as compared with the monomeric compound **92** which is indicative of some interaction between the two pyrrolo pyrimidone rings (**Fig. 12** and **Table 2** and **3**). Moreover the corresponding pyrazolo pyrimidone compound **134** and triazolo pyrimidone compound **137** shows comparable shift in 6-SMe and 5-SMe protons respectively as compared to their respective monomeric compounds **124** and **125** (**Fig. 11** and **Table 1**).

To summarize, the above ^{1}H NMR study indicates that the pyrrolo[2,3-*d*]pyrimidine compounds have a different conformational arrangement than the pyrazolo[3,4-*d*]pyrimidine or triazolo[4,5-*d*]pyrimidine compounds while the conformational arrangement of pyrrolo[2,3-*d*]pyrimidone compounds is similar to that of pyrazolo[3,4-*d*]pyrimidone or triazolo[4,5-*d*]pyrimidone compounds.

2.4.2 X-Ray crystallographic study

In this present study we were able to prepare and study the crystal structure of 1,3-bis(4-chloro-2-(methylthio)-7*H*-pyrrolo[2,3-*d*]pyrimidin-7-yl)propane (**106**) and 7,7'-(propane-1,3-diyl)bis(3-methyl-2-(methylthio)-3*H*-pyrrolo[2,3-*d*]pyrimidin-4(7H)-one) **(112).**

The crystal structure of **106** shows open conformation (**Fig. 15**). There is no intramolecular π- π interaction between the rings as shown from the intramolecular distances between the centroids of rings (**Table 4a**). However the distance between the two N atoms connecting the linker is 3.45 Å which shows that the rings are not fully stretched as in case of truly open structure. On careful analysis of the crystal structure we observe that the structure is stabilized by intramolecular C-H…N interactions (**Table 4b**) as shown in the **Fig. 15**.

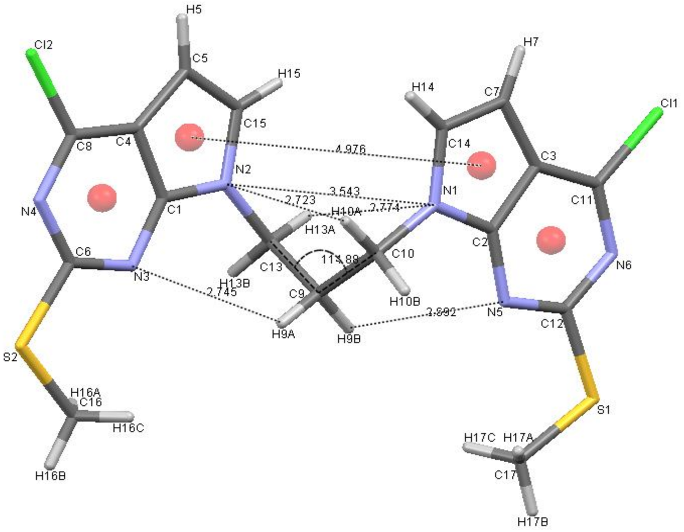

Figure 15: Crystal structure of **106** showing various intramolecular distances

Table 4a: Different intramolecular distances and angle between the least squares planes of **111** and **138**.

S. No.	**Type of intramolecular property**	Compound No.	
		106	**138**
1.	The distance between two N atoms in the two molecules connecting the *trimethylene* linker.	3.54 Å	3.80 Å
2.	The distance between centroids of two six-member pyrimidine ring.	8.13 Å	5.26 Å
3.	The distance between centroids of two five-member pyrrole ring.	4.98 Å	5.26 Å
4.	The distance between centroids of two nine-member pyrrolo[2,3-*d*]pyrimidine ring.	6.72 Å	5.35 Å
5.	Angle between the least squares planes.	1.31°	18.03°

Table 4b: Hydrogen bonding distances and angles:

S. No.	**Comp. No.**	**Distance of hydrogen and nitrogen (̊)**	**Distance of carbon and nitrogen (̊)**	**C-H…N ∟ (°)**
1.	**106**	C9-H9A….N3 = 2.745	C9….N3 = 3.309	117.71
		C9-H9B….N5 = 2.692	C9….N5 = 3.273	118.93
		C13-H13A….N1 = 2.774	C13….N1 = 3.038	96.30
		C10-H10A….N2 = 2.723	C10….N2 = 3.006	97.43
2.	**138**	C9-H9A….N2A = 2.783	C9….N2A = 3.086	98.90
		C9-H9B….N2 = 2.606	C9….N2 = 2.935	100.03
		C8A-H8AA….N1 = 2.752	C8A….N1 = 3.083	100.71
		C8-H8A….N1A = 2.717	C8….N1A = 3.059	101.35

The crystal structure of corresponding pyrazolo[3,4-*d*]pyrimidine compound i.e., **138** (**Fig. 16**) also has no intramolecular π–π interactions but is folded due to weak intramolecular S…S interaction.[60f] (**Fig 16**, **Table 4a)** Also, the distance between the two N atoms connecting the linker is 3.80 Å. On careful analysis of the crystal structure we observe that the structure is stabilized by intramolecular C-H…N interactions (**Table 4b**) as shown in the figure in addition to the intramolecular S…S interaction and similar to the hydrogen bonding seen in the crystal structure of compound **106**.

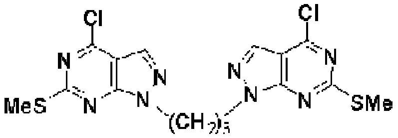

138

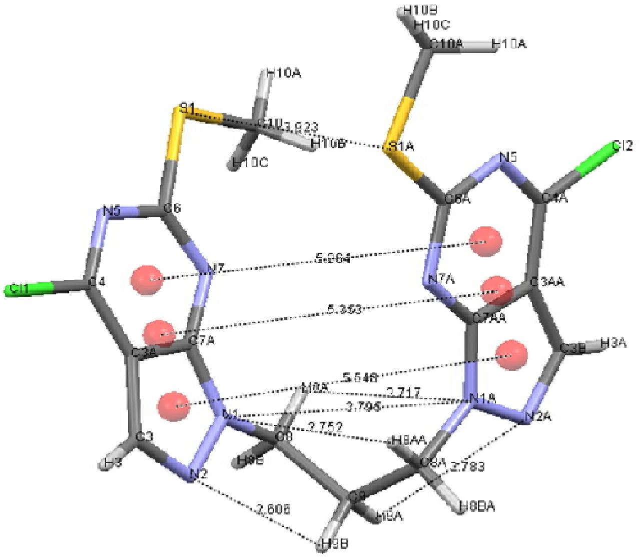

Figure 16: Crystal structure of 1,3-bis(4-chloro-6-(methylthio)-1*H*-pyrazolo[3,4-*d*]pyrimidin-1-yl)propane (**138**) showing various intramolecular distances.

The unit cell of **106** consists of two molecules having similar conformation without any intermolecular interactions between the two molecules. In order to find the intermolecular π–π interactions between the two rings, the extension of this unit cell arrangement of molecules showed that there is considerable amount of intermolecular stacking propensity as shown in the **Fig. 17** and **Table 5**. The values in the table are compared with the corresponding values of intermolecular distances of **138** reported in the literature.[60f]

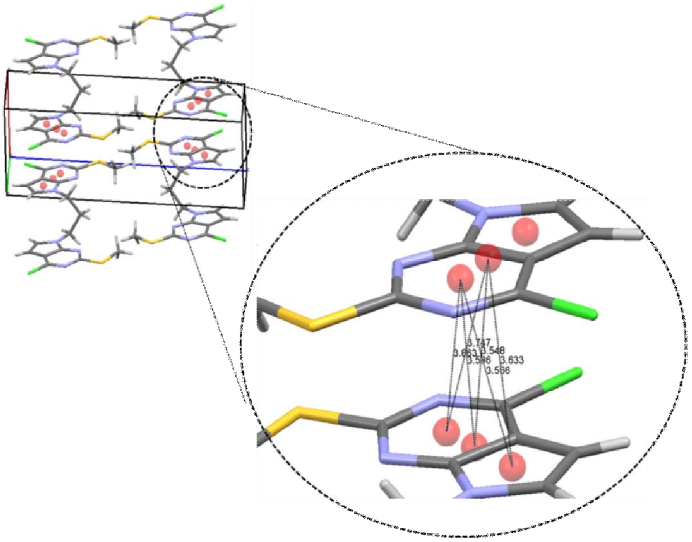

Figure 17: Extended unit cell arrangement of molecules of Compound **106** showing intermolecular π–π interactions.

Table 5: Intermolecular π -π interactions in **106** and **138**[60f]

S.No.	**Type of intermolecular property**	**106**	**138**
1.	The distance between centroids of two six-member pyrimidine ring	3.86	3.56
2.	The distance between centroids of two five-member pyrrole ring	4.04	4.67
3.	The distance between centroids of two nine-member pyrrolo[2,3-*d*]-pyrimidine ring	3.55	3.50
4.	The distance between centroid of one nine member pyrrolo[2,3-*d*]-pyrimidine ring and one six-member pyrimidine ring	3.75, 3.59	3.41
5.	The distance between centroid of one nine member pyrrolo[2,3-*d*]-pyrimidine ring and one five-member pyrrole ring	3.63, 3.85	3.95
6.	The distance between centroid of one six-member pyrimidine ring and one five-member pyrrole ring	3.94, 3.57	3.58

The above values in the **Table 4** and **Table 5** show that there is no intramolecular stacking between the rings in both compound **106** and **138**. However in case of intermolecular stacking interactions the stacking propensity in compound **106** seems to be less than that of compound **138** as shown from the distances between the rings.

The crystal structure of 7,7'-(propane-1,3-diyl)bis(3-methyl-2-(methylthio)-3*H*-pyrrolo[2,3-*d*]pyrimidin-4(7*H*)-one) **(112)** shows folded conformation (**Fig. 19**) . The distance between the two centroids of six member pyrimidone rings is 4.07 Ǻ. This distance is well within values seen in case of stacked pyrazolo[3,4-*d*]compounds **139** (4.14 Ǻ), **140** (4.13 Ǻ), and **141** (4.23 Ǻ) (**Fig. 18**).[60f] The distance between the two N atoms connecting the linker is 3.46 Ǻ which is less than the distance between the two N atoms connecting the linker in compound **141** (3.50 Ǻ).

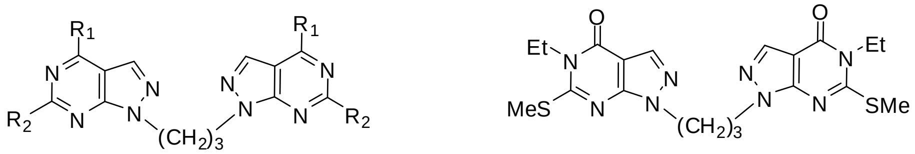

139: R_1 = O-iPr; R_2 = SO_2Me
140: R_1 = O-iPr; R_2 = SO_2Et

141

Figure 18

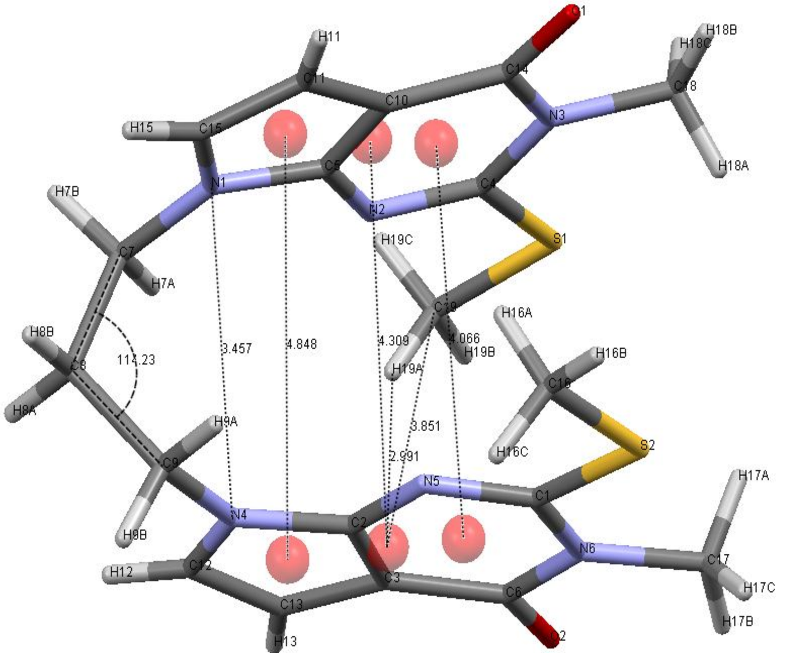

Figure 19. Crystal structure of **112** showing various intramolecular distances

Various crystallographic parameters of compound **112** are shown in the table below. This table also shows the various crystallographic parameters for the corresponding pyrazolo[3,4-*d*]pyrimidone compound **133**[60f, 60i] (**Fig. 11**) and triazolo[4,5-*d*]pyrimidone **136** (**Fig. 11** and previous chapter).

Table 6: Various crystallographic parameters for compounds **117**, **133** and **136**.

S.No.	**Type of intramolecular property**	**117** **Distance in (˚) and angle in (^{0})**	**133** **Distance in (˚) and angle in (^{0})**	**136** **Distance in (˚) and angle in (^{0})**
1.	The distance between two N atoms in the two molecules connecting the *trimethylene* linker	3.457	3.350	3.264
2.	The distance between centroids of two six-member pyrimidone ring	4.066	3.771	3.584
3.	The distance between centroids of two	4.848	4.621	4.473

	five-member triazole and pyrazole ring			
4.	The distance between centroids of two nine-member triazolo[4,5-*d*]pyrimidone and pyrazolo[3,4-*d*] pyrimidone ring	4.309	4.034	3.871
5.	The distance between centroids of one nine-member respective triazolo[4,5-*d*]pyrimidone and pyrazolo[3,4-*d*] pyrimidone ring and one six-member pyrimidone ring	4.205 and 4.295	3.989 and 3.948	3.750 and 3.833
6.	The distance between centroids of one five-member respective triazole and pyrazole ring and one six-member pyrimidone ring	4.667 and 4.853	4.557 and 4.469	4.258 and 4.426
7.	The distance between centroids of one five-member respective triazole and pyrazole ring and nine-member respective triazolo[4,5-*d*]pyrimidone and pyrazolo[3,4-*d*] pyrimidone ring	4.623 and 4.730	4.456 and 4.404	4.226 and 4.322
8.	Angle between the least squares planes	16.27	12.48	10.71

Analysis of the various distances between the two rings attached with the *trimethylene* linker in **Table 6** shows that the intramolecular stacking propensity increases as the number of ring nitrogen increases. Moreover the angle between the two least square planes of the rings decreases with the increase of ring nitrogen indicating that the two rings tends to take a more parallel orientation which may further facilitate the intramolecular stacking interaction.

2.5 Conclusions

In conclusion present work shows that the stacking propensity of *polymethylene* linked pyrrolo[2,3-*d*]pyrimidine compounds is less than the corresponding pyrazolo[3,4-*d*]pyrimidine compounds both in solution and solid state while the stacking propensity of *polymethylene* linked pyrrolo[2,3-*d*]pyrimidone compounds is comparable to the corresponding pyrazolo[3,4-*d*]pyrimidone compounds in solution **and solid state**. Important results are summarized below.

(i) In the solution state studies (^{1}H NMR analysis) of *ethylene* linked pyrrolo pyrimidine and pyrrolo pyrimidone compounds there is significant upfield shift in 6-H/CH_3 protons indicating that the two pyrrole rings are close to each other while the shift in case of SMe protons of pyrimidine rings is not significant. This shows that the pyrimidine rings are not close to each other especially in case of compounds **116** and **119** (**Fig 12** and **Table 2 and 3**). This result is in contrast to the conformations suggested by the *ethylene* linked pyrazolo pyrimidine or triazolo pyrimidine compounds in which pyrimidine rings appears to be close to each other (**Fig. 11** and **Table 1**).

(ii) In the solution state studies (^{1}H NMR analysis) of *propylene* linked pyrrolo pyrimidine compounds the upfield shifts in the 2-SMe protons is very less (**Table 2** and **3**) compared to the corresponding 6-SMe shifts in pyrazolo pyrimidine compounds (**Table 1**). Also a small downfield shift is observed in the 5-H/CH_3 and 6-H/CH_3 protons (**Table 2** and **3**). These values suggest an open conformation in which the two rings are not fully stretched as in case of truly open structure. The downfield shifts in the 5-H/CH_3 and 6-H/CH_3 suggest that these protons are near to the periphery of the other ring and thus experience a deshielding effect.

The X-ray structure of compound **106** also shows similar type of conformation. In this case the structure is open but not fully stretched and is stabilized by intramolecular C-H…N interactions.

In case of *propylene* linked pyrrolo pyrimidone compound **112** there is a significant upfield shift in the 2-SMe protons (**Fig. 12** and **Table 2** and **3**) comparable to the corresponding upfield shift observed in case of 6-SMe protons of pyrazolo pyrimidone compound (**133**) and 5-SMe protons of triazolo pyrimidone (**136**) compound suggesting folded conformation (**Fig. 11** and **Table 1**). The solid state structutre of this compound also shows a folded conformation similar to the corresponding pyrazolopyrimidone and triazolopyrimidone compound. Analysis of the various distances between the two rings shows that the intramolecular stacking propensity increases as the number of ring nitrogen increases. Thus distances are maximum in **112** (No. of ring nitrogen = 3), decreases in case of **133** (No. of ring nitrogen = 4) and is least in **136** (No. of ring nitrogen = 5).

(iii) In the solution state studies (^{1}H NMR analysis) of *butylene* linked pyrrolo pyrimidine compounds the upfield shifts in the SMe protons or 5-H/CH_3 and 6-H/CH_3 is very less suggesting that there is almost no interactions between the rings (**Fig. 12** and **Table 2** and **3**). In case of pyrrolo pyrimidone compound **113** there is a detectable upfield shift in the 2-SMe protons but is significantly less than the corresponding *propylene* linker compound **112** indicating decrease in the stacking interaction on increasing the length of the linker (**Fig. 12** and **Table 2** and **3**). These results were also observed in case of pyrazolo pyrimidone compounds and triazolo pyrimidone compounds (**Fig. 11** and **Table 1**).

2.6 Experimental Section

2.6.1 Synthesis of 2-methylthio-3*H*-pyrrolo[2,3-*d*]pyrimidin-4(7*H*)-one (82).

To a 500 ml round bottom flask containing 250 ml water added the compound **81** (15.7g, 0.1 mol) and anhydrous sodium acetate (8.2g, 0.01 mole) and the mixture was stirred for 1h at 80-85 °C. To this stirred mixture 50% aqueous chloroacetaldehyde solution (14ml, 0.11mole) was added at once. The reaction mixture was carefully observed for a change of color from light yellow to light brown. After that the reaction mixture was continuously monitored by TLC analysis every 5 minutes for almost 20-30 minutes. The solid from the reaction mixture is filtered hot and washed rapidly with water, methanol and then with chloroform. The product **82** obtained (light brown to grey in color) (7-8g) is very sparingly soluble in cold methanol or cold chloroform and is sufficiently pure to be used in the next step as such. A small amount of the product was further purified by column chromatography for analytical purpose.

82: Yield: 40- 45%; mp: > 250 °C; MS (ESI) m/z 183 $[M+H]^+$; ^1H NMR (300 MHz, DMSO-d_6) δ (ppm): 2.51(s, 3H, SCH_3), 6.34-6.36 (m, 1H, Ar-H), 6.90-6.92 (m, 1H, Ar-H), 11.74 (s, 1H, NH), 12.03 (s, 1H, NH).

2.6.2 Synthesis of 4-chloro-2-methylthio-7*H*-pyrrolo[2,3-*d*]pyrimidine (83).

To a 100 ml round bottom flask containing the compound **82** (9.1g, 0.05 mol) added $POCl_3$ (18.6ml, 0.20 mol) and refluxed the reaction mixture for 6 hr. $POCl_3$ was removed under reduced pressure and crushed ice was added to the reaction mixture to quench the the remaining $POCl_3$. The reaction mixture was extracted with Chloroform, washed with a dilute solution of sodium bicarbonate and dried over sodium sulphate The residue obtained by the removal of chloroform under reduced pressure was purified by column chromatography on silica gel using mixture of ethyl acetate-hexane in increasing polarity to give pure compound **83**.

83: Yield: 65- 75%; mp: 204-206 °C; MS (ESI) m/z 200$[M+H]^+$; ^1H NMR (300 MHz, $CDCl_3$) δ (ppm): 2.58(s, 3H, SCH_3), 6.48-6.50 (m, 1H, Ar-H), 7.14-7.16 (m, 1H, Ar-H), 9.50 (s, 1H, NH).

2.6.3 Synthesis of 2-methylthio-7*H*-pyrrolo[2,3-*d*]pyrimidine-4-thiol (84).

To a 100 ml round bottom flask containing 95% ethanol (50ml) added the compound **83** (1.9g, 0.01 mol) and thiourea (0.83g, 0.011mol) and refluxed the reaction mixture for 12 hr. The light yellow precipitate which appeared were collected by filtration and washed with water and dried in vacuum. This residue obtained was sufficiently pure to be used in the next step.

84: Yield: 55- 65%; mp: > 250 °C; MS (ESI) m/z 198 $[M+H]^+$; ^1H NMR (300 MHz, $CDCl_3$ + DMSO-d_6) δ (ppm): 2.48(s, 3H, SCH_3), 6.59 (s, 1H, Ar-H), 6.88 (s, 1H, Ar-H), 11.35 (s, 1H, NH or SH).

2.6.4 Synthesis of 6-amino-3-methyl-2-methylthio-pyrimidin-4(3*H*)-one (86)

To a 500 ml round bottom flask containing 200 ml water added the compound **81** (15.7g, 0.1 mol) and KOH (5.6g, 0.1mol) and stirred for 10 minutes. Dimethyl sulfate (13.8g, 0.11 mol) is then added to the mixture and the reaction mixture was stirred for 2 hr. The precipitate obtained was collected by filtration and dried to give compound **86**.

86: Yield: 90%; mp: > 250 °C; MS (ESI) m/z 172.

2.6.5 Synthesis of 2,4-bis(methylthio)-7*H*-pyrrolo[2,3-*d*]pyrimidine (85).

To a 100 ml round bottom flask containing 20 ml water added the compound **84** (0.19g, 0.001 mol) and NaOH (0.04g, 0.001mol) and then methyl iodide (142mg, 0.001 mol) .The reaction mixture was stirred for 12 hr and was monitored by TLC. The precipitate obtained was collected by filtration and purified by column chromatography on silica gel using mixture of ethyl acetate-hexane in increasing polarity to give pure compound **85**.

85: Yield: 75- 85%; mp: 210–212 °C; MS (ESI) m/z 212 $[M+H]^+$; ^1H NMR (300 MHz, $CDCl_3$) δ (ppm): 2.70 (s, 3H, SCH_3), 2.73 (s, 3H, SCH_3), 6.46-6.48 (m, 1H, Ar-H), 7.13-7.15 (m, 1H, Ar-H), 10.765 (s, 1H, NH).

2.6.6 Synthesis of 3-methyl-2-methylthio-3*H*-pyrrolo[2,3-*d*]pyrimidin-4(7*H*)-one (87).

To a 100 ml round bottom flask containing 20 ml water added compound **86** (0.85g, 5 mmol) and anhydrous sodium acetate (0.4g, 5 mmol) and the mixture was refluxed for 1h. To this refluxing mixture 50% aqueous chloroacetaldehyde solution (1.4ml, 10 mmol) was added at once. The reaction mixture was further refluxed for 1 hr and then allowed to attain r.t. The solid from the reaction mixture is filtered and washed rapidly with water and dried. The product compound **87** obtained sufficiently pure to be used in the next step as such. A small amount of the product was further purified by column chromatography on silica gel using mixture of ethyl acetate-chloroform in increasing polarity.

87: Yield: 75%; mp: > 250 °C; MS (ESI) m/z 196 $[M+H]^+$; ^1H NMR (300 MHz, $CDCl_3$) δ (ppm): 2.59 (s, 3H, SCH_3), 3.60 (s, 3H, NCH_3), 6.64-6.66 (m, 1H, Ar-H), 6.79-6.81 (m, 1H, Ar-H), 8.35 (s, 1H, NH).

2.6.7 Synthesis of 4-chloro-7-methyl-2-methylthio-7*H*-pyrrolo[2,3-*d*]pyrimidine (88).

To a 100 ml round bottom flask containing acetone (10 ml) and DMF (0.5 ml) added compound **83** (0.19g, 1mmol) and Cesium carbonate (0.39g, 1.2 mmol) and then methyl iodide (142 mg, 1 mmol) .The reaction mixture was stirred for 8 hr. The reaction was monitored by TLC and after the completition of reaction water (15ml) was added to the reaction mixture and stirred for 10 minutes. The residue obtained was collected by filtration and purified by column chromatography on silica gel using mixture of ethyl acetate-hexane in increasing polarity to give pure compound **88**.

88: Yield: 75- 85%; mp: 134–136 °C; MS (ESI) m/z 214 $[M+H]^+$; ^1H NMR (300 MHz, $CDCl_3$) δ (ppm): 2.57 (s, 3H, SCH_3), 3.74 (s, 3H, NCH_3), 6.41 (d, J = 3Hz, 1H, Ar-H), 6.95 (d, J = 3Hz, 1H, Ar-H).

2.6.8 Synthesis of 3,7-dimethyl-2-methylthio-3*H*-pyrrolo[2,3-*d*]pyrimidin-4(7*H*)-one (92).

To a 100 ml round bottom flask containing DMF (5 ml) added compound **87** (0.19g, 1mmol) and Cesium carbonate (0.39g, 1.2 mmol) and then methyl iodide (142 mg, 1 mmol) .The reaction mixture was stirred for 8 hr. The reaction was monitored by TLC and after the competition of reaction water (15ml) was added to the reaction mixture and stirred for 10 minutes. The residue obtained was collected by filtration and purified by column chromatography on silica gel using mixture of ethyl acetate-hexane in increasing polarity to give pure compound **92**.

92: Yield: 75%; mp: 148–150 °C; MS (ESI) m/z 210 $[M+H]^+$; ^1H NMR (300 MHz, $CDCl_3$) δ (ppm): 2.63 (s, 3H, SCH_3), 3.59 (s, 3H, NCH_3), 3.72 (s, 3H, NCH_3), 6.59 (d, J = 3Hz, 1H, Ar-H), 6.69 (d, J = 3Hz, 1H, Ar-H).

2.6.9 Synthesis of 7-methyl-2,4-bis(methylthio)-7*H*-pyrrolo[2,3-*d*]pyrimidine (90).

To a 100 ml round bottom flask containing DMF (5 ml) added compound **85** (0.21g, 1mmol) and Cesium carbonate (0.39g, 1.2 mmol) and then methyl iodide (142 mg, 1 mmol) .The reaction mixture was stirred for 8 hr. The reaction was monitored by TLC and after the completition of reaction water (15ml) was added to the reaction mixture and stirred for 10 minutes. The residue obtained was collected by filtration and purified by column chromatography on silica gel using mixture of ethyl acetate-hexane in increasing polarity to give pure compound **90.**

90: Yield: 75- 85%; mp: 102–104 °C; MS (ESI) m/z 227 $[M+H]^+$; ^1H NMR (300 MHz, $CDCl_3$) δ (ppm): 2.65 (s, 3H, SCH_3), 2.68 (s, 3H, SCH_3), 3.76 (s, 3H, NCH_3), 6.39 (d, *J* = 3.52Hz, 1H, Ar-H), 6.89 (d, *J* = 3.52Hz, 1H, Ar-H). ^{13}C NMR (75 MHz, $CDCl_3$) *δ* (ppm): 11.74, 14.35, 30.98, 98.63, 112.81, 126.41, 149.53, 161.14, 163.26.

2.6.10 Synthesis of 7-methyl-2-methylthio-4-pyrrolidin-1-yl-7*H*-pyrrolo[2,3-*d*]pyrimidine (91).

To a 100 ml round bottom flask containing compound **90** (110mg, 0.5 mmol) added pyrrolidine (1ml) and refluxed the reaction mixture for 36 hr. Excess pyrrolidine was removed under reduced pressure and ice cold water was added to the reaction mixture and neutralized with a dilute solution of acetic acid. The reaction mixture was extracted with Chloroform and dried over sodium sulphate The residue obtained by the removal of chloroform under reduced pressure was purified by column chromatography on silica gel using mixture of ethyl acetate-hexane in increasing polarity to give pure compound **91**.

91: Yield: 85%; mp: 114–116 °C; MS (ESI) m/z 249 $[M+H]^+$; ^1H NMR (300 MHz, $CDCl_3$) δ (ppm): 2.02 (bs, 4H, CH_2 pyrrolidinyl), 2.59 (s, 3H, SCH_3), 3.73 (s, 3H, NCH_3), 3.81(bs, 4H, NCH_2 pyrrolidinyl), 6.44 (d, *J* = 3.5Hz, 1H, Ar-H), 6.70 (d, *J* = 3.5Hz, 1H, Ar-H).

2.6.11 Synthesis of 4-methoxy-7-methyl-2-methylthio-7*H*-pyrrolo[2,3-*d*]pyrimidine (89).

To a 100 ml round bottom flask containing anhydrous methanol added compound **88** (110mg, 0.5 mmol) and sodium methoxide (540mg, 10mmol) and refluxed the reaction mixture for 36 hr. Methanol was removed under reduced pressure and ice cold water was added to the reaction mixture and neutralized with a dilute solution of acetic acid.. The reaction mixture was extracted with chloroform and dried over sodium sulphate The residue obtained by the removal of chloroform under reduced pressure was purified by column chromatography on silica gel using mixture of ethyl acetate-hexane in increasing polarity to give pure compound **89**.

89: Yield: 75%; mp: 104–106 °C; MS (ESI) m/z 210 $[M+H]^+$; ^1H NMR (300 MHz, $CDCl_3$) δ (ppm): 2.64 (s, 3H, SCH_3), 3.79 (s, 3H, NCH_3), 4.10 (s, 3H, SCH_3), 6.42 (s. 1H, Ar-H), 6.84 (s, 1H, Ar-H).

2.6.12 Synthesis of 2-amino-4,5-dimethyl-1*H*-pyrrole-3-carbonitrile (95).

Acetic anhydride (33.8.5 g, 0.33 mol), acetic acid (4.5 g, 0.075 mol), triethylamine (37.95 g, 0.375 mol) and 4-(dimethylamino)pyridine (0.18 g, 0.0015 mol) were charged into a reaction vessel and heated to 50 °C. Racemic alanine (13.5 g, .15 mol) was added as a solid over 2 h thereby maintaining reaction temperature at 45 to 55 °C. After completion of alanine addition, the reaction mixture was stirred at 50 °C for an additional 8 h. Acetic anhydride, triethylamine, and acetic acid were distilled off by vacuum distillation (10-15 mbar), gradually raising the jacket temperature to a maximum of 100 °C. The residue was cooled to r.t. and diluted with water (100 ml). Malonodinitrile (9.45 g, 0.14mol) was added, and this mixture was slowly added to 50 g of aqueous sodium hydroxide solution (30%). The speed of addition was adjusted so that the reaction temperature did not exceed 60 °C. The resulting suspension was cooled to 0 °C, filtered, washed with water, and dried in vacuum at 55 °C to yield 16.8 g (83% calculated from alanine) of compound **95**.

95: Yield: 85%; mp: 170–172 °C; MS (ESI) m/z 136 $[M+H]^+$; ^1H NMR (300 MHz, DMSO-d_6) δ (ppm): 1.83 (s, 3H, CH_3), 1.92 (s, 3H, CH_3), 5.36 (s, 3H, NH_2), 9.83 (s, 1H, NH).

2.6.13 Synthesis of 5,6-dimethyl-7*H*-pyrrolo[2,3-*d*]pyrimidine-2,4-dithiol (96).

To a 500 ml round bottom flask added pyridine (100 ml), compound **95** (13.5g, 0.1 mol) and carbon disulfide (11.4g, 0.15 mol) and stirred at 40^{o}C for 2 h. The reaction mixture was transferred to a 2 lit. conical flask and kept on ice bath. Added 50% HCl solution slowly to get pH around 2-3 and then added sodium hydroxide solution to obtain pH around 7. The precipitate thus obtained is filtered, washed with water and dried to yield compound **96**.

96: Yield: 74%; mp: > 220 °C; MS (ESI) m/z 212 $[M+H]^+$; ^1H NMR (300 MHz, DMSO-d_6) δ (ppm): 2.11 (s, 3H, CH_3), 2.27 (s, 3H, CH_3), 11.25(s, 1H, SH or NH), 12.41 (s, 1H, SH or NH).

2.6.14 Synthesis of 5,6-dimethyl-2,4-bis(methylthio)-7*H*-pyrrolo[2,3-*d*]pyrimidine (97).

To a 100 ml round bottom flask containing 20 ml water added compound **96** (0.21g, 0.001 mol) and NaOH (0.08g, 0.002mol) and then methyl iodide (284mg, 0.002 mol) .The reaction mixture was stirred for 12 hr and was monitored by TLC. The precipitate obtained was collected by filtration and purified by column chromatography on silica gel using mixture of ethyl acetate-hexane in increasing polarity to give pure compound **97**.

97: Yield: 84%; mp: 180–182 °C; MS (ESI) m/z 240 $[M+H]^+$; ^1H NMR (300 MHz, $CDCl_3$) δ (ppm): 2.33 (s, 3H, CH_3), 2.34 (s, 3H, CH_3), 2.63 (s, 3H, SCH_3), 2.66 (s, 3H, SCH_3), 9.13 (s, 1H, NH).

2.6.15 Synthesis of 5,6,7-trimethyl-2,4-bis(methylthio)-7*H*-pyrrolo[2,3-*d*]pyrimidine (98).

To a 100 ml round bottom flask containing 10 ml anhydrous DMF added compound **97** (0.24g, 0.001 mol) and NaH (3mg, 0.0012 mol) and then methyl iodide (142 mg, 0.001 mol) .The reaction mixture was stirred for 8 hr and was monitored by TLC. DMF was removed under reduced pressure and ice cold water was added to the reaction mixture. The reaction mixture was extracted with Chloroform and dried over sodium sulphate. The residue obtained by the removal of chloroform under reduced pressure was purified by column chromatography on silica gel using mixture of ethyl acetate-hexane in increasing polarity to give pure compound **98**.

98: Yield: 80%; mp: 70–72 °C; MS (ESI) m/z 254 $[M+H]^+$; ^1H NMR (300 MHz, $CDCl_3$) δ (ppm): 2.07 (s, 3H, CH_3), 2.09 (s, 3H, CH_3), 2.56 (s, 6H, SCH_3), 3.26 (s, 3H, NCH_3).

2.6.16 Synthesis of 5,7-dimethyl-2,4-bis(methylthio)-7*H*-pyrrolo[2,3-*d*]pyrimidine (101).

Compound **101** was synthesized from compound **105** following the procedure used in the synthesis of compound **98**.

101: Yield: 80%; mp: 66–68 °C; MS (ESI) m/z 240 $[M+H]^+$; ^1H NMR (300 MHz, $CDCl_3$) δ (ppm): 2.41 (s, 3H, CH_3), 2.64 (s, 3H, SCH_3), 2.67 (s, 6H, SCH_3), 3.69 (s, 3H, NCH_3), 6.61 (s, 1H, Ar-H).

2.6.17 Synthesis of 1,2-bis(4-chloro-2-methylthio-7*H*-pyrrolo[2,3-*d*]pyrimidin-7-yl)ethane (105).

To a 100 ml round bottom flask containing 10 ml acetone added compound **83** (0.20g, 0.001 mol) and Cs_2CO_3 (390 mg, 0.0012 mol) and then 1, 2-dibromoethane (94 mg, 0.001 mol). The reaction mixture was stirred for 12 hr and was monitored by TLC. Acetone was removed under reduced pressure and ice cold water was added to the reaction mixture. The reaction mixture was extracted with chloroform and dried over sodium sulphate. The residue obtained by the removal of chloroform under reduced pressure was purified by column chromatography on silica gel using mixture of ethyl acetate-hexane in increasing polarity to give pure compound **105**.

105: Yield: 80%; mp: 170–172 °C; MS (ESI) m/z 426 $[M+H]^+$; ^1H NMR (300 MHz, $CDCl_3$) δ (ppm): 2.51 (s, 6H, SCH_3), 4.61 (s, 4H, NCH_2), 6.35 (d, J = 3 Hz, 2H, Ar-H), 6.55 (d, J = 3 Hz, 2H, Ar-H). Anal. Calcd. for $C_{16}H_{14}Cl_2N_6S_2$: C, 45.18; H, 3.32; N, 19.76; Found: C, 45.28; H, 3.36; N, 19.82.

2.6.18 Synthesis of 1,3-bis(4-chloro-2-methylthio-7*H*-pyrrolo[2,3-*d*]pyrimidin-7-yl)propane (106).

Compound **106** was synthesized from compound **83** following the procedure used in the synthesis of compound **105**.

106: Yield: 82%; mp: 140–142 °C; MS (ESI) m/z 440 $[M+H]^+$; ^1H NMR (300 MHz, $CDCl_3$) δ (ppm): 2.49 (quint, 2H, CH_2), 2.58 (s, 6H, SCH_3), 4.22 (s, 4H, NCH_2), 6.52 (d, J = 3 Hz, 2H, Ar-H), 7.07 (d, J = 3Hz, 2H, Ar-H). ^{13}C NMR (75 MHz, $CDCl_3$) δ (ppm): 14.39, 30.04, 42.04, 100.10, 114.05, 127.21, 151.96, 152.14,164.48 Anal. Calcd. for $C_{17}H_{16}Cl_2N_6S_2$: C, 46.47; H, 3.67; N, 19.13; Found: C, 46.53; H, 3.75; N, 19.22.

2.6.19 Synthesis of 1,4-bis(4-chloro-2-methylthio-7*H*-pyrrolo[2,3-*d*]pyrimidin-7-yl)propane (107).

Compound **107** was synthesized from compound **83** following the procedure used in the synthesis of compound **105**.

107: Yield: 80%; mp: 134–136 °C; MS (ESI) m/z 454 $[M+H]^+$; ^1H NMR (300 MHz, $CDCl_3$) δ (ppm): 1.84 (bs, 4H, CH_2), 2.62 (s, 6H, SCH_3), 4.26 (s, 4H, NCH_2), 6.51 (d, J = 3 Hz, 2H, Ar-H), 7.01 (d, J = 3 Hz, 2H, Ar-H). ^{13}C NMR (75 MHz, $CDCl_3$) δ (ppm): 14.49, 26.95, 43.98, 99.94, 113.95, 127.26, 151.98, 152.24,164.30 Anal. Calcd. for $C_{18}H_{18}Cl_2N_6S_2$: C, 47.68; H, 4.00; N, 18.54; Found: C, 47.73; H, 4.05; N, 18.62.

2.6.20 Synthesis of 1,2-bis(2,4-bis(methylthio)-7*H*-pyrrolo[2,3-*d*]pyrimidin-7-yl)ethane (108).

To a 100 ml round bottom flask containing 10 ml anhydrous DMF added compound **85** (0.21g, 0.001 mol) and Cs_2CO_3 (390 mg, 0.0012 mol) and then 1, 2-dibromoethane (94 mg, 0.001 mol). The reaction mixture was stirred for 12 hr and was monitored by TLC. DMF was removed under reduced pressure and ice cold water was added to the reaction mixture. The reaction mixture was extracted with chloroform and dried over sodium sulphate. The residue obtained by the removal of chloroform under reduced pressure was purified by column chromatography on silica gel using mixture of ethyl acetate-hexane in increasing polarity to give pure compound **108**.

108: Yield: 81%; mp: 182–184 °C; MS (ESI) m/z 449 $[M+H]^+$; ^1H NMR (300 MHz, $CDCl_3$) δ (ppm): 2.58 (s, 6H, SCH_3), 2.68 (s, 6H, SCH_3), 4.57 (s, 4H, NCH_2), 6.24 (s, 2H, Ar-H), 6.36 (s, 2H, Ar-H). ^{13}C NMR (75 MHz, $CDCl_3$) δ (ppm): 11.81, 14.30, 44.56, 99.10, 125.58, 144.85, 149.19, 161.61, 181.54. Anal. Calcd. for $C_{18}H_{20}N_6S_4$: C, 48.19; H, 4.49; N, 18.73; Found: C, 48.23; H, 4.55; N, 18.82.

2.6.21 Synthesis of 1,3-bis(2,4-bis(methylthio)-7*H*-pyrrolo[2,3-*d*]pyrimidin-7-yl)propane (109).

Compound **109** was synthesized from compound **83** following the procedure used in the synthesis of compound **108**.

109: Yield: 80%; mp: 110–112 °C; MS (ESI) m/z 463 $[M+H]^+$; ^1H NMR (300 MHz, $CDCl_3$) δ (ppm): 2.41 (quint, 4H, CH_2), 2.59 (s, 6H, SCH_3), 2.69 (s, 6H, SCH_3), 4.10 (s, 4H, NCH_2), 6.41 (d, *J* = 3 Hz, 2H, Ar-H), 6.95 (d, *J* = 3 Hz, 2H, Ar-H). ^{13}C NMR (75 MHz, $CDCl_3$) δ (ppm): 11.77, 14.28, 29.62, 30.36, 41.65, 99.03, 112.86, 125.30, 149.18, 161.40, 163.30. Anal. Calcd. for $C_{19}H_{22}N_6S_4$: C, 49.32; H, 4.79; N, 18.16; Found: C, 49.43; H, 4.81; N, 18.22.

2.6.22 Synthesis of 1,4-bis(2,4-bis(methylthio)-7*H*-pyrrolo[2,3-*d*]pyrimidin-7-yl)butane (110).

Compound **110** was synthesized from compound **83** following the procedure used in the synthesis of compound **108**.

110: Yield: 80%; mp: 106–108 °C; MS (ESI) m/z 477$[M+H]^+$; ^1H NMR (300 MHz, $CDCl_3$) δ (ppm): 1.77 (bs, 6H, CH_2), 2.62 (s, 6H, SCH_3), 2.68 (s, 6H, SCH_3), 4.19 (s, 4H, NCH_2), 6.38 (d, *J* = 3 Hz, 2H, Ar-H), 6.95 (d, *J* = 3 Hz, 2H, Ar-H). ^{13}C NMR (75 MHz, $CDCl_3$) δ (ppm): 11.80, 14.36, 27.50, 42.25, 99.05, 112.05, 125.40, 149.28, 161.52, 163.55; Anal. Calcd. for $C_{17}H_{24}N_{12}S_2$: C, 44.33; H, 5.25; N, 36.49; Found: C, 44.53; H, 5.35; N, 36.52.

2.6.23 Synthesis of 7,7′-(ethane-1,2-diyl)bis(3-methyl-2-methylthio-3*H*-pyrrolo[2,3-*d*]-pyrimidin-4(7*H*)-one) (111).

To a 100 ml round bottom flask containing 10 ml anhydrous DMF added compound **87** (195mg, 0.001 mol) and Cs_2CO_3 (390 mg, 0.0012 mol) and then 1, 2-dibromoethane (94 mg, 0.001 mol). The reaction mixture was stirred for 12 hr and was monitored by TLC. DMF was removed under reduced pressure and ice cold water was added to the reaction mixture. The reaction mixture was extracted with chloroform and dried over sodium sulphate. The residue obtained by the removal of chloroform under reduced pressure was purified by column chromatography on silica gel using mixture of ethyl acetate-hexane in increasing polarity to give pure compound **111**.

111: Yield: 80%; mp: 190–192 °C; MS (ESI) m/z 417 $[M+H]^+$; ^1H NMR (300 MHz, $CDCl_3$) δ (ppm): 2.48 (s, 6H, SCH_3), 3.56 (s, 4H, NCH_3), 4.46 (s, 4H, NCH_2), 6.35 (d, *J* = 3 Hz, 2H, Ar-H), 6.49 (d, *J* = 3 Hz, 2H, Ar-H). ^{13}C NMR (75 MHz, $CDCl_3$) δ (ppm): 14.93, 29.82, 45.01, 102.93, 104.07, 121.74, 146.63, 156.73, 159.07. Anal. Calcd. for $C_{18}H_{20}N_6O_2S_2$: C, 51.90; H, 4.84; N, 20.18; Found: C, 51.98; H, 4.90; N, 20.32.

2.6.24 Synthesis of 7,7′-(propane-1,3-diyl)bis(3-methyl-2-methylthio-3*H*-pyrrolo[2,3-*d*]-pyrimidin-4(7*H*)-one) (112).

Compound **112** was synthesized from compound **83** following the procedure used in the synthesis of compound **111**.

112: Yield: 80%; mp: 142–144 °C; MS (ESI) m/z 431 $[M+H]^+$; ^1H NMR (300 MHz, $CDCl_3$) δ (ppm): 2.32 (s, 6H, SCH_3), 2.41(quint, *J* = 6Hz, 2H, CH_2), 3.54 (s, 4H, NCH_3), 4.03 (t, *J* = 6Hz, 4H, NCH_2), 6.64 (d, *J* = 3 Hz, 2H, Ar-H), 6.74 (d, *J* = 3 Hz, 2H, Ar-H). ^{13}C NMR (75 MHz, $CDCl_3$) δ (ppm): 14.74, 29.80, 40.06, 103.06, 103.77, 120.57, 146.75, 156.34, 159.07 Anal. Calcd. for $C_{19}H_{22}N_6O_2S_2$: C, 53.00; H, 5.15; N, 19.52; Found: C, 53.08; H, 5.19; N, 19.62.

2.6.25 Synthesis of 7,7′-(butane-1,4-diyl)bis(3-methyl-2-methylthio-3*H*-pyrrolo[2,3-*d*]-pyrimidin-4(7*H*)-one) (113).

Compound **118** was synthesized from compound **81** following the procedure used in the synthesis of compound **111**.

113: Yield: 80%; mp: 132–134 °C; MS (ESI) m/z 445 $[M+H]^+$; ^{1}H NMR (300 MHz, $CDCl_3$) δ (ppm): 1.79(bs, 4H, CH_2), 2.51 (s, 6H, SCH_3), 3.57 (s, 4H, NCH_3), 4.09 (bs, 4H, NCH_2), 6.56 (d, *J* = 3 Hz, 2H, Ar-H), 6.62 (d, *J* = 3 Hz, 2H, Ar-H). ^{13}C NMR (75 MHz, $CDCl_3$) δ (ppm): 14.70, 28.80, 41.06, 102.90, 103.97, 120.47, 146.25, 155.84, 158.90 Anal. Calcd. for $C_{20}H_{24}N_6O_2S_2$: C, 54.03; H, 5.44; N, 18.90; Found: C, 54.08; H, 5.59; N, 19.02.

2.6.26 Synthesis of 1,3-bis(2-methylthio-4-pyrrolidin-1-yl-7*H*-pyrrolo[2,3-*d*]pyrimidin-7-yl)-propane (114).

To a 50 ml round bottom flask containing compound **106** (100mg, 0.23 mmol) added pyrrolidine (1ml) and refluxed the reaction mixture for 10 hr. Excess pyrrolidine was removed under reduced pressure and ice cold water was added to the reaction mixture and neutralized with a dilute solution of acetic acid.. The reaction mixture was extracted with Chloroform and dried over sodium sulphate The residue obtained by the removal of chloroform under reduced pressure was purified by column chromatography on silica gel using mixture of ethyl acetate-hexane in increasing polarity to give pure compound **114**.

114: Yield: 80%; mp: 122–124 °C; MS (ESI) m/z 509 $[M+H]^+$; ^{1}H NMR (300 MHz, $CDCl_3$) δ (ppm): 2.01 (bs, 8H, pyrrolidinyl CH_2), 2.36 (quint, *J* = 6 Hz, 2H, CH_2), 2.55 (s, 6H, SCH_3), 3.80(bs, 8H, pyrrolidinyl CH_2), 4.12 (t, *J* = 6 Hz, 4H, NCH_2), 6.43 (d, *J* = 3 Hz, 2H, Ar-H), 6.81 (d, *J* = 3 Hz, 2H, Ar-H). ^{13}C NMR (75 MHz, $CDCl_3$) δ (ppm): 14.16, 29.66, 30.60, 41.72, 47.73, 100.48, 100.96, 121.73, 151.07, 154.72, 163.18. Anal. Calcd. for $C_{25}H_{32}N_8S_2$: C, 59.03; H, 6.34; N, 22.03; Found: C, 59.09; H, 6.38; N, 22.05.

2.6.27 Synthesis of 1,3-bis(4-methoxy-2-methylthio-7*H*-pyrrolo[2,3-*d*]pyrimidin-7-yl)-propane (115).

To a 100 ml round bottom flask containing anhydrous methanol was added compound **106** (100mg, 0.23 mmol) and sodium methoxide (270mg, 5mmol) and the reaction mixture refluxed for 10 hr. Methanol was removed under reduced pressure and ice cold water was added to the reaction mixture and neutralized with a dilute solution of acetic acid. The reaction mixture was extracted with chloroform and dried over sodium sulphate The residue obtained by the removal of chloroform under reduced pressure was purified by column chromatography on silica gel using mixture of ethyl acetate-hexane in increasing polarity to give pure compound **115**.

115: Yield: 80%; mp: 110–112 °C; MS (ESI) m/z 431 $[M+H]^+$; ^1H NMR (300 MHz, $CDCl_3$) δ (ppm): 2.44 (quint, *J* = 6 Hz, 2H, CH_2), 2.56 (s, 6H, SCH_3), 4.09 (s, 6H, OCH_3), 4.17 (t, *J* = 6 Hz, 4H, NCH_2), 6.43 (d, *J* = 3 Hz, 2H, Ar-H), 6.88 (d, *J* = 3 Hz, 2H, Ar-H). ^{13}C NMR (75 MHz, $CDCl_3$) δ (ppm): 14.22, 30.56, 41.89, 53.64, 98.68, 102.22, 124.15, 152.84, 162.46, 163.41. Anal. Calcd. for $C_{19}H_{22}N_6O_2S_4$: C, 53.00; H, 5.15; N, 19.52; Found: C, 53.05; H, 5.19; N, 19.62.

2.6.28 Synthesis of 1,2-bis(5,6-dimethyl-2,4-bis(methylthio)-7*H*-pyrrolo[2,3-*d*]pyrimidin-7-yl)ethane (116).

To a 100 ml round bottom flask containing 10 ml anhydrous DMF was added compound **97** (100mg, 0.42 mmol) and NaH (12 mg, 0.5 mmol) and then 1, 2-dibromoethane (40 mg, 0.21 mmol). The reaction mixture was stirred for 12 hr and was monitored by TLC. DMF was removed under reduced pressure and ice cold water was added to the reaction mixture. The reaction mixture was extracted with chloroform and dried over sodium sulphate. The residue obtained by the removal of chloroform under reduced pressure was purified by column chromatography on silica gel using mixture of ethyl acetate-hexane in increasing polarity to give pure compound **116**.

116: Yield: 80%; mp: 130–132 °C; MS (ESI) m/z 505 $[M+H]^+$; ^1H NMR (300 MHz, $CDCl_3$) δ (ppm): 1.92 (s, 6H, CH_3), 2.30 (s, 6H, CH_3), 2.58 (s, 6H, SCH_3), 2.64 (s, 6H, SCH_3), 4.37 (s, 4H, NCH_2). Anal. Calcd. for $C_{22}H_{28}N_6S_4$: C, 52.35; H, 5.59; N, 16.65; Found: C, 52.45; H, 5.61; N, 16.68.

2.6.29 Synthesis of 1,3-bis(5,6-dimethyl-2,4-bis(methylthio)-7*H*-pyrrolo[2,3-*d*]pyrimidin-7-yl)propane (117).

Compound **117** was synthesized from compound **97** following the procedure used in the synthesis of compound **111**.

117: Yield: 80%; mp: 98–100 °C; MS (ESI) m/z 519 $[M+H]^+$; ^1H NMR (300 MHz, $CDCl_3$) δ (ppm): 2.09-2.18 (m, 2H, CH_2), 2.18 (s, 6H, CH_3), 2.33 (s, 6H, CH_3), 2.55 (s, 6H, SCH_3), 2.64 (s, 6H, SCH_3), 4.17 (s, 4H, NCH_2). ^{13}C NMR (75 MHz, $CDCl_3$) δ (ppm): 9.56, 9.91, 15.28, 31.20, 40.32, 81.14, 116.09, 116.86, 121.67, 141.30, 170.42; Anal. Calcd. for $C_{23}H_{30}N_6S_4$: C, 53.25; H, 5.83; N, 16.20; Found: C, 53.28; H, 5.81; N, 16.24.

2.6.30 Synthesis of 1,4-bis(5,6-dimethyl-2,4-bis(methylthio)-7*H*-pyrrolo[2,3-*d*]pyrimidin-7-yl)butane (118).

Compound **118** was synthesized from compound **97** following the procedure used in the synthesis of compound **116**.

118: Yield: 80%; mp: 90–92 °C; MS (ESI) m/z 533 $[M+H]^+$; ^1H NMR (300 MHz, $CDCl_3$) δ (ppm): 1.58 (m, 2H, CH_2), 2.07 (s, 6H, CH_3), 2.11 (s, 6H, CH_3), 2.57 (s, 12H, SCH_3), 3.71 (t, *J* = 6 Hz, 4H, NCH_2). Anal. Calcd. for $C_{24}H_{32}N_6S_4$: C, 54.10; H, 6.05; N, 15.77; Found: C, 54.15; H, 6.10; N, 15.80.

2.6.31 Synthesis of 1,2-bis(5-methyl-2,4-bis(methylthio)-7*H*-pyrrolo[2,3-*d*]pyrimidin-7-yl)ethane (119).

To a 100 ml round bottom flask containing 10 ml anhydrous DMF added compound **100** (100mg, 0.44 mmol) and NaH (12 mg, 0.5 mmol) and then 1, 2-dibromoethane (42 mg, 0.22 mmol). The reaction mixture was stirred for 12 hr and was monitored by TLC. DMF was removed under reduced pressure and ice cold water was added to the reaction mixture. The reaction mixture was extracted with chloroform and dried over sodium sulphate. The residue obtained by the removal of chloroform under reduced pressure was purified by column chromatography on silica gel using mixture of ethyl acetate-hexane in increasing polarity to give pure compound **119**.

119: Yield: 80%; mp: 142–144 °C; MS (ESI) m/z 477 $[M+H]^+$; ^1H NMR (300 MHz, $CDCl_3$) δ (ppm): 2.29 (s, 6H, CH_3), 2.55 (s, 6H, SCH_3), 2.65 (s, 6H, SCH_3), 4.42 (s, 4H, NCH_2), 6.18 (s, 2H, Ar-H). Anal. Calcd. for $C_{20}H_{24}N_6S_4$: C, 50.39; H, 5.07; N, 17.63; Found: C, 50.42; H, 5.05; N, 17.70.

2.6.32 Synthesis of 1,3-bis(5-methyl-2,4-bis(methylthio)-7*H*-pyrrolo[2,3-*d*]pyrimidin-7-yl)propane (120).

Compound **120** was synthesized from compound **100** following the procedure used in the synthesis of compound **119**.

120: Yield: 80%; mp: 102–104 °C; MS (ESI) m/z 491 $[M+H]^+$; ^1H NMR (300 MHz, $CDCl_3$) δ (ppm): 2.30-2.39 (s, 2H, CH_2), 2.39 (s, 6H, CH_3), 2.59 (s, 6H, SCH_3), 2.66 (s, 6H, SCH_3), 4.06

(s, 4H, NCH_2), 6.62 (s, 2H, Ar-H). ^{13}C NMR (75 MHz, $CDCl_3$) δ (ppm): 11.98, 12.32, 14.46, 29.20, 43.22, 110.65, 113.20, 122.28, 149.82, 162.05, 163.08; Anal. Calcd. for $C_{21}H_{26}N_6S_4$: C, 51.40; H, 5.34; N, 17.13; Found: C, 51.43; H, 5.38; N, 17.16.

2.6.33 Synthesis of 1,4-bis(5-methyl-2,4-bis(methylthio)-7*H*-pyrrolo[2,3-*d*]pyrimidin-7-yl)butane (121).

Compound **121** was synthesized from compound **100** following the procedure used in the synthesis of compound **119**.

121: Yield: 80%; mp: 110–112 °C; MS (ESI) m/z 505 $[M+H]^+$; ^{1}H NMR (300 MHz, $CDCl_3$) δ (ppm): 1.76 (s, 4H, CH_2), 2.40 (s, 6H, CH_3), 2.62 (s, 6H, SCH_3), 2.68 (s, 6H, SCH_3), 4.16 (s, 4H, NCH_2), 6.60 (s, 2H, Ar-H). ^{13}C NMR (75 MHz, $CDCl_3$) δ (ppm): 11.88,12.28, 14.36, 27.04, 43.11, 110.60, 113.05, 122.77, 149.61, 161.79, 162.74; Anal. Calcd. for $C_{17}H_{24}N_{12}S_2$: C, 52.35; H, 5.59; N, 16.65; Found: C, 52.38; H, 5.64; N, 16.68.

2.7 References

1. Rosemeyer, H. *Chem. Biodivers.* **2004**, *1*, 361.
2. (a) Legraverend, M.; Grierson, D. S. *Bioorg. Med. Chem.* **2006**, *14*, 3987. (b) Legraverend, M. *Tetrahedron* **2008**, *64*, 8585.
3. Johnson, S. A.; Thomas, W. *Hematol. Oncol.* **2000**, *18*,141.
4. Hoffmann, M.; Chrzanowska, M.; Hermann, T.; Rychlewski, J. *J. Med. Chem*. **2005**, 48, 4482.
5. Mey, U.; Strehl, J.; Gorschluter, M.; Ziske, C.; Glasmacher, A.; Pralle, H.; Schmidt-Wolf, I. *Lancet Oncol.* **2003**, *4*, 86.
6. Kluin-Nelemans, H. C.; Oldhoff, J. M.; van Doormaal, J. J.; van't Wout, J. W.; Verhoef, G.; Gerrits, W. B. J.; van Dobbenburgh, O. A.; Pasmans, S. G.; Fijnheer, R. *Blood* **2003**, *102*, 4270.
7. Lamanna, N.; Weiss, M. *Adv. Pharmacol*. **2004**, *51*, 107.
8. Imbach, P.; Capraro, H. G.; Furet, P.; Mett, H.; Meyer, T.; Zimmermann, J. *Bioorg. Med. Chem. Lett.* **1999**, *9*, 91.
9. Toyota, A.; Katagiri, N.; Kaneko, C. *Heterocycles* **1993**, *36*, 1625.
10. Dorff, P. H.; Garigipati, R. S. *Tetrahedron Lett*. **2001**, *42*, 2771.
11. Balzarini, J.; Aquarob, S.; Hassan-Abdallah, A.; Daluged, S. M.; Pernob, C. F.; McGuiganc, C. *FEBS Lett*. **2004**, *573*, 38.
12. De Clercq, E. *Clin. Microb. Rev*. **1997**, *10*, 674.

13. Sinico, R. A.; Sabadini, E.; Borlandelli, S.; Cosci, P.; Di Toma, L.; Imbasciati, E. *J. Nephrol.* **2003**, *16*, 272.

14. Drognitz, O.; Benz, S.; Pfeffer, F.; Fischer, C.; Makowiec, F.; Schareck, W.; Hopt, U. T. *Transplantation* **2004**, *78*, 1802.

15. Maltzman, J. S.; Koretzky, G. A. *J. Clin. Invest*. **2003**, *111*, 1122.

16. Rumbo, C.; Shneider, B.; Emre, S. *Pediatr. Transplant.* **2004**, *8*, 571.

17. Altmann, E.; Missbach, M.; Green, J.; Susa, M.; Wagenknecht, H.-A.; Widler, L. *Bioorg. Med. Chem. Lett.* **2001**, *11*, 853.

18. Arnold, L. D.; Calderwood, D. J.; Dixon, R. W.; Johnston, D. N.; Kamens, J. S.; Munschauer, R.; Rafferty, P.; Ratnofsky, S. E. *Bioorg. Med. Chem. Lett.* **2000**, *10*, 2167.

19. Calderwood, D. J.; Johnston, D. N.; Munschauer, R.; Rafferty, P. *Bioorg. Med. Chem. Lett.* **2002**, *12*, 1683.

20. Chien, T. C.; Meade, E. A.; Hinkley, J. M.; Townsend, L. B. *Org. Lett*. **2004**, *6*, 2857.

21. Gangjee, A.; Jain, H. D.; Kisliuk, R. L. *Bioorg. Med. Chem. Lett.* **2005**, *15*, 2225.

22. Norman, M. H.; Chen, N.; Chen, Z.; Fotsch, C.; Hale, C.; Han, N.; Hurt, R.; Jenkins, T.; Kincaid, J.; Liu, L.; Lu, Y.; Moreno, O.; Santora, V. J.; Sonnenberg, J. D.; Karbon, W. *J. Med. Chem.* **2000**, *43*, 4288.

23. Ali, A.; Taylor, G. E.; Ellsworth, K.; Harris, G.; Painter, R.; Silver, L. L.; Young, K. *J. Med. Chem.* **2003**, *46*, 1824.

24. Burchat, A. F.; Calderwood, D. J.; Friedman, M. M.; Hirst, G. C.; Li, B.; Rafferty, P.; Ritter, K.; Skinner, B. S. *Bioorg. Med. Chem. Lett.* **2002**, *12*, 1687.

25. Kim, D. C.; Lee, Y. R.; Yang, B.S.; Shin, K. J.; Kim, D. J.; Chung, B. Y.; Yoo, K. H. *Eur. J. Med. Chem.* **2003**, *38*, 525.

26. Williamson, D. S.; Parratt, M. J.; Bower, J. F.; Moore, J. D.; Richardson, C. M.; Dokurno, P.; Cansfield, A. D.; Francis, G. L.; Hebdon, R. J.; Howes, R.; Jackson, P. S.; Lockie, A. M.; Murray, J. B.; Nunns, C. L.; Powles, J.; Robertson, A.; Surgenor, A. E.; Torrance, C. J. *Bioorg. Med. Chem. Lett.* **2005**, *15*, 863.

27. Moravcova, D.; Krystof, V.; Havlicek, L.; Moravec, J.; Lenobel, R.; Strnad, M. *Bioorg. Med. Chem. Lett.* **2003**, *13*, 2989.

28. Yuan, J.; Gulianello, M.; De Lombaert, S.; Brodbeck, R.; Kieltyka, A.; Hodgetts, K. J. *Bioorg. Med. Chem. Lett.* **2002**, *12*, 2133.

29. Arvanitis, A. G.; Rescinito, J. T.; Arnold, C. R.; Wilde, R. G.; Cain, G. A.; Sun, J. H.; Yan, J. S.; Teleha, C. A.; Fitzgerald, L. W.; McElroy, J. *Bioorg. Med. Chem. Lett.* **2003**, *13*, 125.

30. Kuethe, J. T.; Wong, A.; Davies, I. W. *J. Org. Chem.* **2004**, *69*, 7752.

31. Ramasamy, K.; Imamura, N.; Hanna, N. B.; Finch, R. A.; Avery, T. L.; Robins, R. K.; Revankar, G. R. *J. Med. Chem.* **1990**, *33*, 1220.

32. Abe, Y.; Kayakiri, H.; Satoh, S.; Inoue, T.; Sawada, Y.; Inamura, N.; Asano, M.; Aramori, I.; Hatori, C.; Sawai, H.; Oku, T.; Tanaka, H. *J. Med. Chem.* **1998**, *41*, 4062.

33. Baindur, N.; Chadha, N.; Player, M. R. *J. Comb. Chem.* **2003**, *5*, 653.

34. Vu, C. B.; Shields, P.; Peng, B.; Kumaravel, G.; Jin, X.; Phadke, D.; Wang, J.; Engber, T.; Ayyub, E.; Petter, R. C. *Bioorg. Med. Chem. Lett.* **2004**, *14*, 4835.

35. Vu, C. B.; Pan, D.; Peng, B.; Kumaravel, G.; Smits, G.; Jin, X.; Phadke, D.; Engber, T.; Huang, C.; Reilly, J.; Tam, S.; Grant, D.; Hetu, G.; Petter, R. C. *J. Med. Chem.* **2005**, *48*, 2009.

36. Yao, G.; Haque, S.; Sha, L.; Kumaravel, G.; Wang, J.; Engber, T. M.; Whalley, E. T.; Conlon, P. R.; Chang, H.; Kiesman, W. F.; Petter, R. C. *Bioorg. Med. Chem. Lett.* **2005**, *15*, 511.

37. Tamura, Y.; Miki, Y.; Ikeda, M. *J. Heterocycl. Chem.* **1975**, *12,* 119.

38. Ilyn, A. P.; Trifilenkov, A. S.; Tsirulnikov, S. A.; Kurashvily, I. D.; Ivachtchenko, A. V. *J. Comb. Chem.* **2005**, *7,* 806.

39. MacCoss, M.; Meurer, L. C.; Hoogsteen, K.; Springer, J. P.; Koo, G.; Peterson, L. B.; Tolman, R. L.; Emini, E. *J. Heterocycl. Chem.* **1993**, *30*, 1213.

40. Parra, S.; Vitse, O.; Benezech, V.; Deleuze-Masquefa, C.; Subra, G.; Bompart, J.; Escale, R.; Chapat, J. P.; Bonnet, P. A. *J. Heterocycl. Chem.* **2001**, *38*, 41.

41. Demirayak, S.; Kayagil, I. *J. Heterocycl. Chem.* **2005**, *42*, 319.

42. Kool, E. T. *Acc. Chem. Res.* **2002**, *35*, 936.

43. Watson, J. D.; Crick, F. H. C. *Nature* **1953**, *171*, 737.

44. McLaughlin, L. W.; Wilson, M.; Ha, S. B. *Comprehensive Natural Products Chemistry* Vol. VII, Elsevier Press: Oxford, UK, **1999**.

45. Schweitzer, B. A.; Kool, E. T. *J. Org. Chem.***1994**, *59*, 7238.

46. Guckian, K.; Schweitzer, B. A.; Ren, X. F.; Sheils, C. J.; Paris, P. L.; Tahmassebi, D. C.; Kool, E. T. *J. Am. Chem. Soc.* **1996**, *118*, 8182.

47. Seela, F.; Jawalekar, A. M.; Munster, I. *Helv. Chim. Acta* **2005**, *88*, 751.

48. Seela, F.; Jawalekar, A. M. *Helv. Chim. Acta* **2002**, *85*, 1857.

49. Becher, G.; He, J.; Seela, F. *Helv. Chim. Acta* **2001**, *84*, 1048.

50. Van, A. A.; Rozenski, J.; Loakes, D.; Pillet, N.; Scheppers, G.; Herdewijn, P. *Nucleic Acids Res.* **1995**, *23*, 4363.

51. Seela, F.; Bourgeois, W.; Rosemeyer, H.; Wenzel, T. *Helv. Chim. Acta* **1996**, *79*, 488.

52. Matsuda, S.; Henry; A. A.; Schultz, P. G.; Romesberg, F. E. *J. Am. Chem. Soc.* **2003**, *125*, 6134.

53. Gutierrez, A. J.; Terhorst, T. J.; Matteucci, M. D.; Froehler, B. C. *J. Am. Chem. Soc.* **1994**, *116*, 5540.

54. Lin, K. Y.; Jones, R. J.; Matteucci, M. *J. Am. Chem. Soc.* **1995**, *117*, 3873.

55. Ren, X. F.; Schweitzer, B. A.; Sheils, C. J.; Kool, E. T. *Angew. Chem. Int. Ed. Engl.* **1996**, *35*, 743.

56. Saenger, W.; *In Principles of Nucleic Acid Structure*, Ed.; Springer-Verlag: New York, **1984.**

57. Browne, D.T.; Eisinger, J.; Leonard, N.J. **1968**, *90*, 7302.

58. Newcomb, L.F.; Gellman, S.H. *J. Am. Chem. Soc.* **1994**, *116*, 4993.

59. Garcia-Raso, A.; Fiol, J. J.; Badenas, F.; Solans, X.; Font-Bardia, M. *Polyhedron* **1999**, *18*, 765.

60. (a) Biswas G.; Chandra T.; Avasthi, K.; Maulik, P. R. *Acta Crystallogr. Sect. C.* **1995**, *51*, 2453. (b) Avasthi, K.; Farooq, S. M.; Rawat, D. S.; Sharon, A.; Maulik, P. R. *Acta Crystallogr. Sect. C.* **2003**, *59*, o523. (c) Avasthi, K.; Aswal, S.; Kumar R.; Yadav, U.; Rawat, D.S.; Maulik, P. R. *J. Mol. Struct.* **2005**, *750*, 179. (d) Avasthi, K.; Farooq,S. M.; Aswal,S.; Raghunandan, R.; Maulik, P. R. *J. Mol. Struct.* **2007**, *827*, 88. (e) Avasthi, K.; Aswal, S.; Farooq, S. M.; R. Raghunandan, Maulik, P. R. *J. Mol. Struct.* **2008**, *888*, 327.
(f) Avasthi, K.; Farooq, S. M.; Raghunandan, R.; Maulik, P. R. *J. Mol. Struct.* **2009**, *927*, 27. (g) Avasthi, K.; Farooq, S. M.; Raghunandan, R.; Maulik, P. R. *J. Mol. Struct.* **2006**, *785*, 106. (h) Avasthi, K.; Farooq, S. M.; Bal, C.; Kumar R.; Tewari, A. K.; Maulik, P. R. *J. Mol. Struct.* **2007**, *842*, 100. (i) Maulik, P. R.; Avasthi, K.; Biswas, G.; Biswas, S.; Rawat, D. S.; Sarkhel, S.; Chandra, T.; Bhakuni, D. S. *Acta Crystallogr. Sect. C.* **1998**, *54*, 275. (j) Avasthi, K.; Aswal, S.; Maulik, P. R.; *Acta Crystallogr. Sect. C.* **2001**, *57*, 1324. (k) Avasthi, K.; Tewari, A. K.; Rawat, D.S.; Sharon, A.; Maulik, P. R. *Acta Crystallogr. Sect.C.* **2002**, *58*, o494.

61. Avasthi, K.; Ansari, A.; Kant, R.; Maulik, P. R.; Ravikumar, K.; Chattopadhyay, P.; Adhikary, N. D. *CrystEngComm.* **2011**, *13*, 2039.

62. Pacher, P.; Nivorozhkin, A. *Pharmacol. Rev.* **2006**, 87.

63. Davies, L.P; Chow, S.C.; Skerritt, J.H.; Brown, D.J.; Johnsten, G.A.R. *Life Sci.* **1984**, *34*, 2117.

64. Chebib, M.; McKeveney, D.; Quinn, R.J. *Bioorg. Med. Chem.* **2008**, *8*, 2581.

65. Fabio, C.; Antonella, N.; Annalisa, P.; Giada, A.L.; Giovanni, M.; Silvia, S.; Olga, B.; Angelo, R.; Francesco, B.; Chiara, B.; Paola, F.; Giulia, M.; Luisa, M.; Michele, M.; Cristina,T.; Fabrizio, M.; Maurizio B. *J. Med. Chem.* **2006,** *49*, 1549.

66. Hildick, B. G.; Shaw, G. *J. Chem. Soc.* **1971**, 1610.

67. Grem, J. L.; Chabner, B. A.; Collins, J. M. *Cancer Chemotherapy Principles and Practice*; *Lippincott: Philadelphia,* **1990**, 180.

68. Schilsky, R. L.; Perry, M. C. *The Chemotherapy Source Book. Baltimore* **1990**, 301.

69. Calderwood, D. J.; Johnson, D. N.; Munschauer, R.; Rafferty, P. *Bioorg. Med. Chem. Lett.* **2002**, *12*, 1683.

70. Almann, E.; Widler, L.; Missbach, M. *Mini Rev. Med. Chem.* **2002**, *2*, 208.

71. Morgan, D. O. *Cancer J. Sci. Am.* **1998**, *4*, 1081.

72. Kitagawa, M. *Oncogene* **1993**, *8*, 2425.

73. Esteve, C.; Nueda, A.; Diaz, J. L.; Beleta, J.; Cardenas, A.; Lozoya, E.; Cadavid, M. I.; Loza, M. I.; Ryder, H.; Vidal, B. *Bioorg. Med. Chem.* **2006**, *16*, 3642.

74. Merighi, S.; Miramdola, P.; Varanik, K.; Gessi, S.; Leung, E.; Baraldi, P. G.; Tabrizi, M. A.; Borea, P. A. *Pharmacol. Ther.* **2003**, *100*, 31.

75. Lauderback, C. M.; Breier, A. M.; Hackett, J.; Varadarajan, S.; Goodlett, M. J.; Butterfield, D. A. *Biochemica et Biophysica Acta* **2000**, *1501*, 149.

76. (a) Bhattacharya, B. K.; Rao, T. S.; Revankar G. R. *J. Chem. Soc. Perkin Trans I*, **1995**, 1543. (b) Nishimura, H.; Katagiri, K.; Sato, K.; Mayama M.; Shimaoka N. *J. Antibiot. Ser. A* **1956**, *9*, 60.

77. Anzai, K.; Nakamura G.; Suzuki, **S.** *J. Antiobiot. Ser. A* **1957**, *10*, 201.

78. Rao K. V.; Renn, D. W. *Antimicroh. Agents Chemother.* **1963**, 77.

79. Tolman, R. L.; Robins, R. K.; Townsend, L**.** B. *J. Am. Chem. Soc.* **1969,** *91*, 2102.

80. Rao, K. V. *J. Med, Chem.* **1968**, *11***,** 939.

81. Robins, R. K.; Revankar, G. R. in *Advances in Antiviral Drug Design*, ed. E. De Clerck, JAI Press, Greenwich, Conn. **1993**, 161.

82. Cavins, J. A. *Proc. Am. Assoc Cancer Res.* **1966**, *7*, 12.

83. Ramasamy, K.; Joshi, R.V.; Robins, R. K.; Revankar G. R. *J. Chem. Soc. Perkin Trans I* **1989,** 2375.

84. Tanaka, N.; Wu, R. T.; Okabe, T.; Yamashita, H.; Shimazu, A.; Nishimura, T. *J. Antibiot.* **1982**, *35*, 272.

85. Wu, R. T.; Okabe, T.; Namikoshi, M.; Okuda, **S.;** Nishimura, T.; Tanaka, N. *J. Antibiot.* **1982**, *35*, 279.

86. Yuan, B. D.; Wu, R. T.; Sato, I.; Okabe, T.; Suzuki, H.; Nishimura, T.; Tanaka, N. *J. Antibiot.* **1985**, *38*, 642.

87. (a) Kobayashi, J.; Cheng, J.; Kikuchi, Y.; Ishibashi, M.; Yamamura, S.; Ohizumi, Y.; Ohta T.; Nozoe, S. *Tetrahedron Lett.* **1990**, *31*, 4617. (b) Tsuda, M.; Nozawa, K.; Shimbo, K.; Kobayashi, J. *J. Nat. Prod.* **2003**, *66*, 292.

88. (a) Yokoyama, S.; Miyazawa, T.; Iitaka, Y.; Yamaizumi, Z.; Kasai, H.; Nishimura, S. *Nature* **1979**, *282*, 107. (b) Kasai, H.; Nakanishi, H.; Macfarlane, R. D.; Torgerson, D. F.; Ohashi, Z.; McCloskey, J. A.; Gross, H. J.; Nishimura, S. *J. Am. Chem. Soc.* **1976**, *98*, 5044. (c) Okada, M.; Nishimura, S. *Nucleic Acids Res.* **1977**, *4*, 2931.

89. (a) Blaise, M.; Becker, H. D.; Keith, G.; Cambillau, C.; Lapointe, J.; Giege, R.; Kern, D. *Nucleic Acids Res.* **2004**, *32*, 2768. (b) Salazar, J.; Ambrogelly, A.; Crain, P. F.; McCloskey, J. A.; Soll, D. *Proc. Natl. Acad. Sci. USA* **2004**, *101*, 7536. (c) Blaise, M.; Becker, H. D.; Lapointe, J.; Cambillau, C.; Giege, R.; Kern, D. *Biochimie* **2005**, *87*, 847.

90. (a) Goodman, H. M.; Abelson, J.; Landy, A.; Brenner, S.; Smith, J. D. *Nature* **1968**, *217*, 1019. (b) Doctor, B. P.; Loebel, J. E.; Sodd, M. A.; Winter, D. B. *Science* **1969**, *163*, 693.

91. (a) Kasai, H.; Kuchino, Y.; Nihei, K.; Nishimura, S. *Nucleic Acids Res*. **1975**, *2*, 1931. (b) Nishimura, S. *Progress in Nucleic Acid Research and Molecular Biology*; Cohen,W. E., Ed.; Academic: New York, **1983**; *28*, 49. (c) Farkas, W. R. *J. Biol. Chem*. **1980**, *225*, 6832.

92. Hoops, G. C.; Townsend, L. B.; Garcia, G. A. *Biochemistry* **1995**, *34*, 15381.

93. Okada, N.; Shindo-Okada, N.; Sato, S.; Itoh, Y. H.; Oda, K.; Nishimura, S. *Proc. Natl. Acad. Sci. USA* **1978**, *75*, 4247.

94. (a) Kinzie, S. D.;Thern, B.; Iwata-Reuyl, D. *Org. Lett*. **2000**, *2*, 1307. (b) Wersten, H. *Biofactors* **1988**, *1*, 27.

95. (a) Taylor, E. C.; Liu, B. *J. Org. Chem.* **2003**, *68*, 9938. (b) Gangjee, A.; Yang, J.; McGuire J. J.; Kisliuk, R. L. *Bioorg. Med. Chem.* **2006**, *14*, 8590. (c) Gangjee, A.; Li, W.; Yang J.; Kisliuk, R. L. *J. Med. Chem.* **2008**, *51*, 68.

96. (a) Moriarty, K. J.; Koblish, H. K.; Garrabrant, T.; Maisuria, J.; Khalil, E.; Ali, F.; Petrounia, I. P.; Crysler, C. S.; Maroney, A. C.; Johnson, D. L.; Galemno, Jr. R. A. *Bioorg.Med. Chem. Lett.* **2006**, *16*, 5778. (b) Clark, M. P.; George, K. M.; Bookland, R. G.; Chen, J.; Laughlin, S. K.; Thakur, K. D.; Lee, W.; Davis, J. R.; Cabrera, E. J.; Brugel, T. A.; VanRens, J. C.; Laufersweiler, M. J.; Maier, J. A.; M. P. Sabat, Golebiowski, A.; Easwaran, V.; Webster, M. E.; De B.; Zhang, G. *Bioorg. Med. Chem. Lett.* **2007**, *17*, 1250. (c) Olgen, S.; Isgor Y. G.; Coban, T. *Archiv der Pharmazie* **2008**, *341*, 113. (d) Vanotti, E.; Amici, R.; Bargioti, A.; Berthelesen, J.; Bosotti, R.; Cialovella, A.; Cirla, A.; Cristiani, C.; D Alessio, R.; Forte, B.; Isacchi, A.;.Martina, K.; Meninchincheri, M.; Molinari, A.; Montagnoli, A.; Orsini, P.; Pillan, A.; Roletto, F.; Scolaro, A.; Tibolla, M.; Valsasina, B.; Varasi, M.; Volpi D.; Santocanale, C. *J. Med. Chem.* **2008**, *51*, 487. (e) Gangjee, A.; Namjoshi, O. A.; Yu, J.M.; Ihnat, M. H.; Thorpe J. E.; Warnke, L. A. *Bioorg. Med. Chem.* **2008**, *16*, 5514. (f) Cai, Z.W.; Wei, D.; Schroeder, G. M.; Cornelius, L. A. M.; Kim, K.; Chen, X. T.; Schmidt, R. J.; Williams, D.K.; Tokarsi, J. S.; An, Y.M.; Sack, J. S.; Manne, V.; Kamath, A.; Zhang, Y. P.; Marathe, P.; Hunt, J. T.; Lombardo, L. J.; Fargnoli J.; Borzilleri, R. M. *Bioorg. Med. Chem. Lett.* **2008**, *18*, 3224.

97. (a) Townsend, L. B.; Drach, J. C. **2002** US patent 6342501. (b) Varaprasad, C. V.; Ramasamy, K. S.; Girardet, J. L.; Gunic, E.; Lai, V.; Zhong, W.; An H.; Hong, Z. *Bioorg. Chem.* **2007**, *35*, 25. (c) Koh, Y.-H.; Shim, J. H.; Girardet J. L.; Hong, Z. *Bioorg. Med. Chem. Lett.* **2007**, *17*, 5261.

98. Wang, S.; Folkes, A.; Chuckowree, I.; Cockcroft, X.; Sohal, S.; Miller, W.; Milton, J.; Wren, S. P.; Vicker, N.; Depledge, P.; Scott, J.; Smith, L.; Jones, H.; Mistry, P.; Faint, R.; Thompson D.; Cocks, S. *J. Med. Chem.* **2004**, *47*, 1329.

99. Palmer, A. M.; Munch, G.; Brehm, C.; Zimmerman, P. J.; Buhr, W.; Feth M. P.; Simon, W. A. *Bioorg. Med. Chem.* **2008**, *16*, 1511.

100. (a) Esteve, C.; Nueda, A.; Diaz, J. L.; Beleta, J.; Cardenas, A.; Lozoya, E.; Cadavid, M. I.; Loza, M. I.; Ryder H.; Vidal, B. *Bioorg. Med. Chem. Lett.* **2006**, *16*, 3642. (b) Gillespie, R. J.; Cliffe, I. A.; Dawson, C. E.; Dourish, C. T.; Gaur, S.; Jourdan, A. M.; Knight, A. R.; Lerpiniere, J.; Misra, A.; Pratt, R. M.; Roffey, J.; Stratton, G. C.; Upton, R.; Weiss S. M.;

Williamson, D. S. *Bioorg. Med. Chem. Lett.* **2008**, *18*, 2924.

101. McLeod, H. L.; Cassidy, J.; Powrie, R. H.; Priest, D. G.; Zorbas, M. A.; Synold, T. W.; Shibata, S.; Spicer, D.; Bissett, D.; Pithavala, Y. K.; Collier, M. A.; Paradiso, L. J.; Roberts, J. D. *Clin. Cancer Res.* **2000**, *6*, 2677.

102. Kalk, P.; Eggert, B.; Relle, K.; Godes, M.; Heiden, S.; Sharkovska, Y.; Fischer, Y.; Ziegler, D.; Bielenberg, G-W.; Hocher, B. *Br. J. Pharmacol.* **2007**, *151*, 1025.

103. Mattsson, P.; Aldskogius, H.; Svensson, M. *J Neurotrauma.* **1999**, *16*, 793.

104. Rauscher, F. M.; Sanders, R. A.; Watkins, J. B. *J. Biochem. Mol. Toxicol.* **2000**, *14*, 189.

105. Takada, T.; Weiss, H. M.; Kretz, O.; Gross, G.; Sugiyama, Y. *Drug Metab. Dispos.* **2004**, *32*, 1272.

106. Traxler, P.; Allegrini, P. R.; Brandt, R.; Brueggen, J.; Cozens, R.; Fabbro, D.; Grosios, K.; Lane, H. A.; McSheehy, P.; Mestan, J.; Meyer, T.; Tang, C.; Wartmann, M.; Wood, J.; Caravatti, G. *Cancer Res.* **2004**, *64*, 4931.

107. (a) Zoumakis, E.; Rice, K. C.; Gold, P.W.; Chrousos, G. P. *Annals of the New York Academy of Sciences* **2006**, *1083*, 239. (b) Webster, E. L.; Lewis, D. B.; Torpy, D. J.; Zachman, E. K.; Rice, K. C.; Chrousos, G. P. *Endocrinology* **1996**, *137*, 5747.

108. Schulz, D. W.; Mansbach, R. S.; Sprouse, J.; Braselton, J. P.; Collins, J.; Corman, M.; Dunaiskis, A.; Faraci, S.; Schmidt, A. W.; Seeger, T.; Seymour, P.; Tingley, F. D. 3rd; Winston, E. N.; Chen, Y. L.; Heym, J. *Proc. Natl. Acad. Sci. U.S.A.* **1996**, *93*, 10477.

109. Warshamana-Greene, G. S.; Litz, J.; Buchdunger, E.; Garcia-Echeverria, C.; Hofmann, F.; Krystal, G. W. *Clin Cancer Res.* **2005**, *15*, 1563.

110. Garcia-Echeverria, C.; Pearson, M. A.; Marti, A.; Meyer, T.; Mestan, J.; Zimmermann, J.; Gao, J.; Brueggen, J.; Capraro, H. G.; Cozens, R.; Evans, D. B.; Fabbro, D.; Furet, P.; Porta, D. G.; Liebetanz, J.; Martiny-Baron, G.; Ruetz, S.; Hofmann, F. *Cancer Cell* **2004**, *5*, 231.

111. Flanagan, M. E.; Blumenkopf, T. A.; Brissette, W. H.; Brown, M. F.; Casavant, J. M.; Shang-Poa, C.; Doty J. L.; Elliott E. A.; Fisher M. B.; Hines, M.; Kent C.; Kudlacz, E. M.; Lillie, B. M.; Magnuson, K. S.; McCurdy, S. P.; Munchhof, M. J.; Perry, B. D.; Sawyer, P. S.;. Strelevitz, T. J.; Subramanyam, C.; Sun, J.; Whipple, D. A.; Changelian, P. S. *J. Med. Chem.* **2010**, *53*, 8468.

112. Ostojic, A.; Vrhovac, R.; Verstovsek, S. *Future Oncol.* **2011**, *7*, 1035.

113. Noell, C. W.; Robins, R. K. *J. Heterocycl. Chem.* **1964**, *1*, 34.

114. Johns, C. O.; Hendrix, B. M. *J. Biol. Chem.* **1915**, *20*, 153.

115 Davoll, J. *J. Chem. Soc.* **1960**, 131.

116. Tolman, R. L.; Tolman, G. L.; Robins, R. K.; Townsend L. B. *J. Heterocycl. Chem.* **1970**, *7*, 799.

117. (a) Fischer, R. W.; Misun, M. *Org. Proc. Res. Dev.* **2001**, *5*, 581. (b) Taylor, E. C.; McKillop, A.; Warrener, R.N. *Tetrahedron* **1967**, *23*, 891.

118. Deo, K.; Avasthi, K.; Pratap, R.; Bhakuni, D. S.; Joshi, M. N. *Indian J. Chem. B Org.* **1990**, *29*, 459.

119. Avasthi, K.; Chandra, T.; Bhakuni, D.S. *Indian J. Chem.* **1995**, *34B*, 944.

CHAPTER-3

Synthesis, ^{1}H NMR and X-ray crystallographic studies of pyrazolo[3,4-*d*]pyrimidine and Phthalazinone/Quinazolinone/ Benzotriazinone based flexible dissymmetric ethylene linker compounds

3.1 INTRODUCTION

In nature structure and functions are intimately related. Biopolymers adopt distinct conformations in order to express functions that are important for the existence of life. Some examples are the sheet, helix, and turn motifs of proteins (**Fig. 1**), the double and triple helix, quadruplex, or hairpin motifs of nucleic acids, or the helical structures of carbohydrates such as starch. Without these preferred structures, important processes like expression and translation, recognition, catalysis, and transport in living systems could not be achieved. This conformational control is achieved largely through a complex and subtle interplay of noncovalent forces.

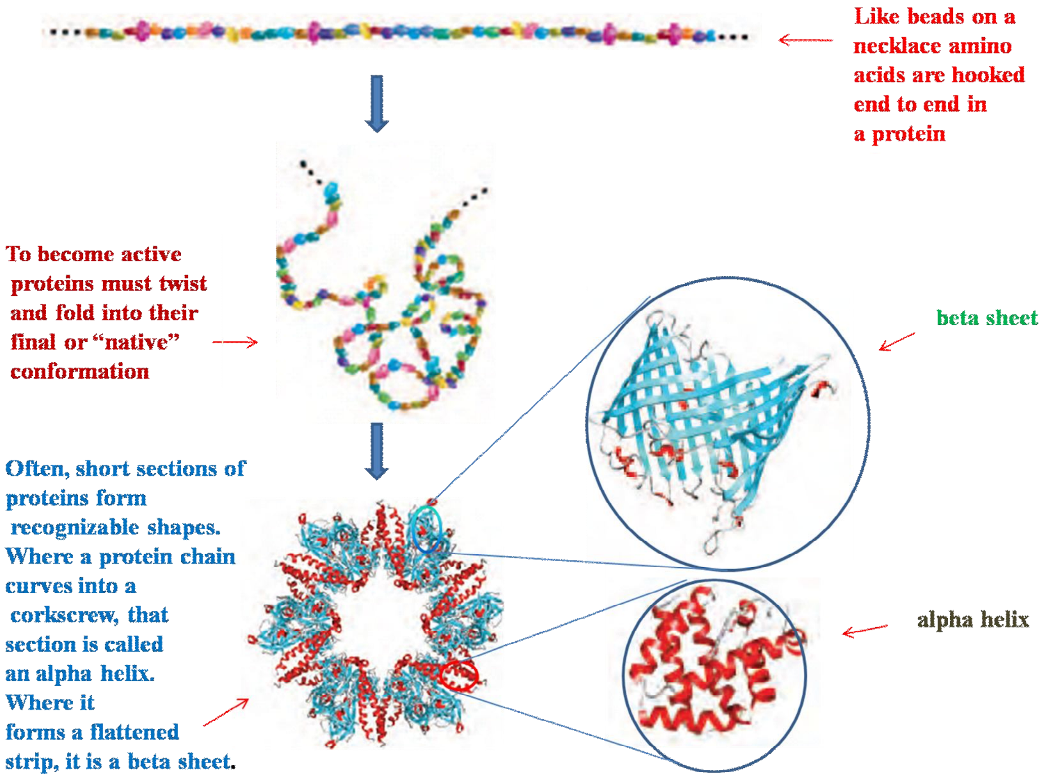
Like beads on a necklace amino acids are hooked end to end in a protein

To become active proteins must twist and fold into their final or "native" conformation

Often, short sections of proteins form recognizable shapes. Where a protein chain curves into a corkscrew, that section is called an alpha helix. Where it forms a flattened strip, it is a beta sheet.

Figure 1. Protein folding

Knowledge of noncovalent forces that control conformation in flexible compounds is thus, of fundamental importance. However, these forces, especially the weak ones, remain poorly understood and still remain a challenge to the scientific community.[1] The simplest of structure that one can envisage of such molecules is the ethane like molecules in which two groups are attached to its termini. In absence of any strong forces of attraction such as classical hydrogen bonding or metal ligand interaction, the intuitively satisfying explanation of steric interactions largely dominates the mindset of organic chemists when conformation of compounds are considered.[1] Steric effects arise from the fact that each atom within a molecule occupies a certain amount of space. If atoms are brought too close together compared with the sum of van der Waals distances, they repel each other as a result of exchange repulsion and this affects the molecule's preferred shape (conformation) and reactivity. Explanation of conformation of such structures are largely been dominated by the bulk of the groups attached to the termini which is known as "steric hindrance". However if they are at an appropriate distance, they attract each other by the London Dispersion force as illustrated in **Fig. 2.**[2]

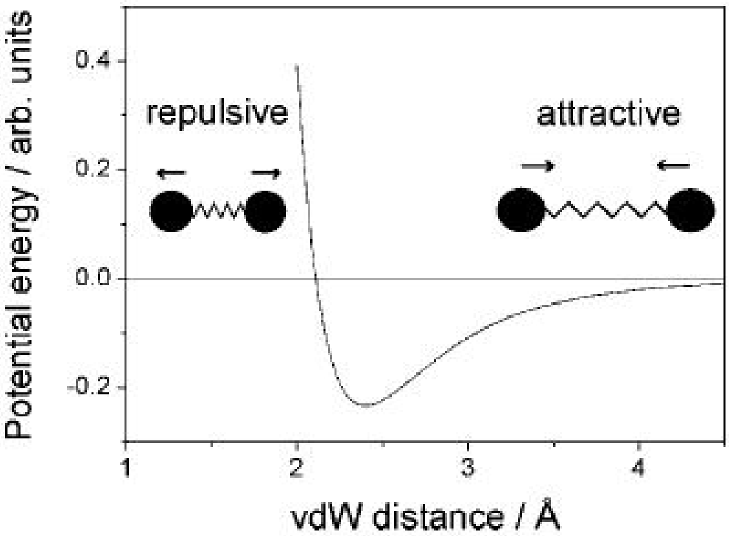

Figure 2. Van der Waals energy plot for the H/H interaction [2]

Examples for attractive steric effect has been shown by Carter,[3] Streitwieser,[4] and their co-workers in the conformational equilibrium of 1,3,5-trineopentylbenzene (**1**) and di-*t*-butylcyclooctatetraene (**2**) (**Fig. 3**)[2] In these cases, the attractive dispersion force outweighs the repulsive van der Waals force.[2]

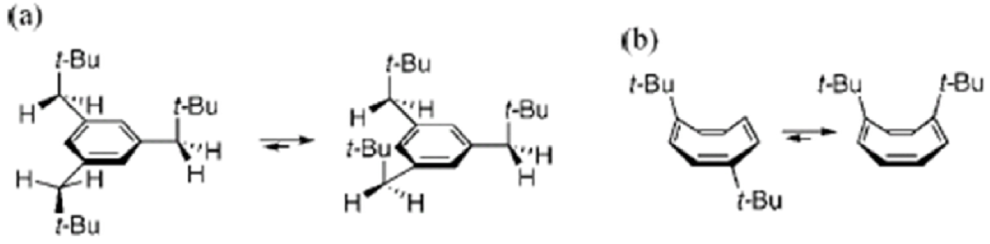

Figure 3. Attractive steric effect as exemplified by the conformational equilibrium of (a) 1,3,5-trineopentylbenzene (**1**) and (b) di-*t* butyl- cyclooctatetraene[2] (**2**)

Despite of these examples available in the literature steric effects are usually considered as “repulsive” forces. The success of the Cram rule[5] (**Fig. 4**)[2] and the Prelog rule,[6] according to which the allegedly bulkier groups are presumed to be in the anti relationship might have contributed to this trend of thinking.

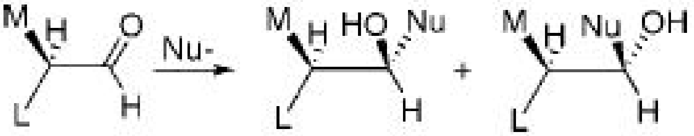

Figure 4. Cram open-chain model (L, largest; M, medium; Nu-, nucleophile)

Furthermore, success of this bulk repulsive approach in the steroid chemistry by Barton might have intensified this trend. In 1950, Barton explained the thermodynamic and reaction selectivity data of many steroidal compounds, which had remained unexplained to that date and thus founded the firm basis of conformational analysis in organic chemistry.[7] The anti conformation is favored in many cases, where “bulky” groups are in the vicinal relationship or in the axial position in a cyclohexane system. This is illustrated for n-butane (**3**) and methylcyclohexane (**4**) in **Fig. 5**.[2]

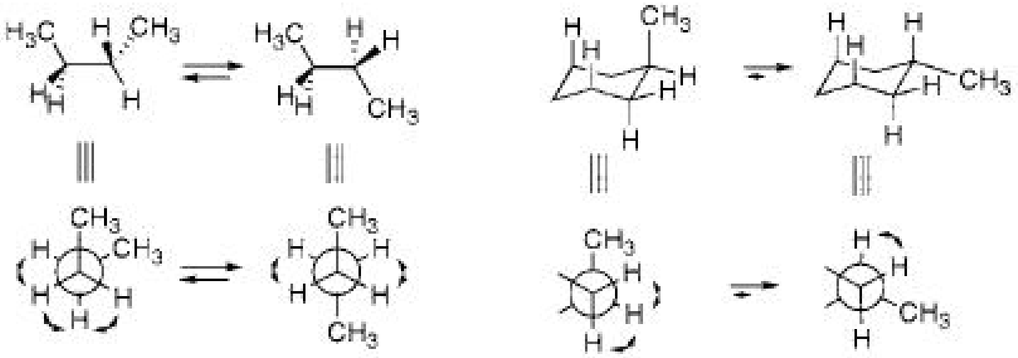

gauche (**a**) anti axial (**b**) equitorial

Figure 5. The *anti* conformation is favored in (a) *n*-butane (**3**) and (b) methylcyclohexane (**4**). Curved arrows indicate unfavorable vicinal H/H interactions

The complexity of this problem can be understood by the fact that the exact reason for the staggered nature of ethane (**Fig. 6**), the simplest of these structures, remains debatable.[8]

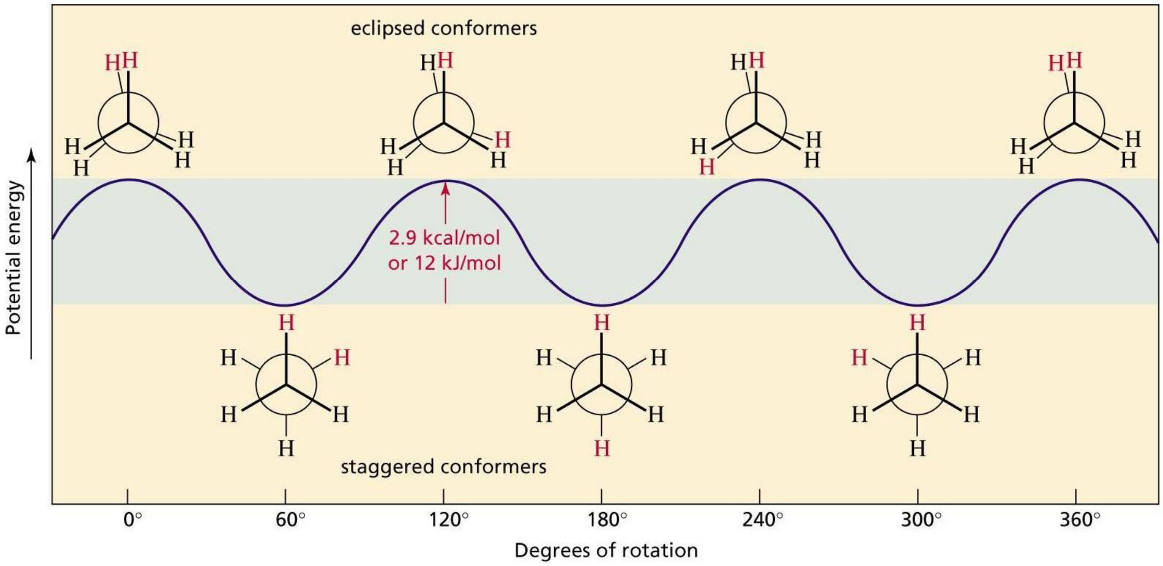

Figure 6. Spectroscopy shows that the preferred conformations of ethane (H_3C-CH_3) conformations are staggered and eclipsed conformations are simply transient states of the molecule (or energy barriers) between the staggered conformations; height of the rotational barrier is ≈ 3 kcal/mol

This picture becomes more complex as we move higher in the series i.e. in the case of 1, 2- di-substituted ethane. The barrier of rotation around the C-C single bond increases as the size of the substitution increases, for example, if H is replaced by halogens; steric interactions are expected to dominate with the result that anti conformation should be expected to be the preferred conformation of the molecule. But it is a well known fact that 1,2-difluoro ethane (**5**) adopts preferentially a gauche conformation.[9,10,11] This preference of 1,2-difluoroethane (DFE) for the gauche conformation (**Fig. 7a**)[10] over the eclipsed or trans structures (**Fig. 7b-d**)[10] is usually identified as the *gauche effect*. This preference extends to 2, 3-difluorobutane (**6**).[11]

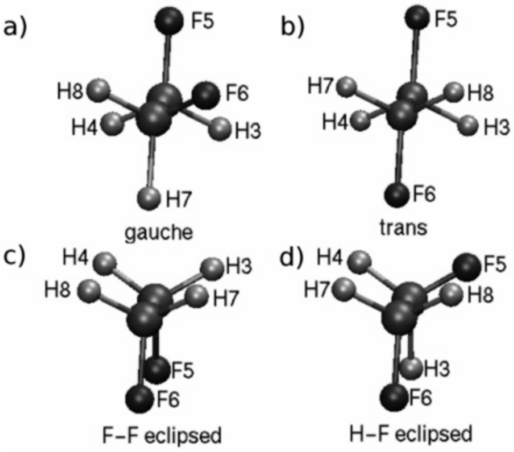

Figure 7. Conformers of Difluoroethane (**5**)

Electron diffraction, infrared and microwave experiments,[12-15] dipole moment analyses,[16] and diverse theoretical calculations[17] have securely established a ∠ FCCF dihedral angle near 71-72° (taking the F-F eclipsed position as 0°) for the stable equilibrium conformer.[10] Examples of the gauche effect are found in many molecules (e.g., the hydrogen positions in hydrazine[18] and in hydrogen peroxide[19]).

Moreover this gauche effect of fluorine has been utilized as a tool for influencing peptide conformation.[20] Also in *threo*- 1,2-diphenyl-1,2-difluoroethane (**7**) the steric repulsion of the phenyl rings has been overwhelmed by the fluorine gauche effect and as a result the phenyl groups are gauche to each other.[21] (**Fig. 8**).[21]

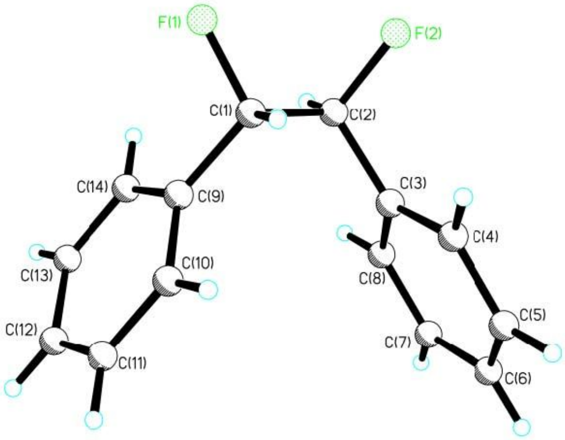

Figure 8. X-ray structure of *threo*- 1,2-diphenyl-1,2-difluoroethane (**7**)

Evidence has also accumulated for the preferred gauche conformation of 1-propyl chloride[22] (**8**) and 1- propyl fluoride[23] (**9**) (**Fig. 9)**[2].

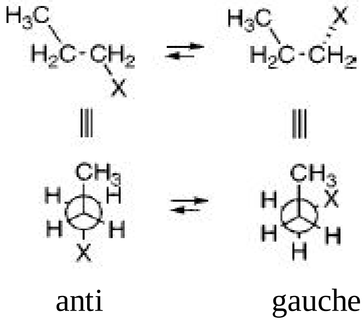

Figure 9. Preference of CH_3/X-*gauche* conformation in $CH_3CH_2CH_2$-X [2]

Preference of gauche conformation was also found for 1-butanol[24] (**10**), 1, 2-dimethoxyethane[25] (**11**) and 1-methoxy-2-(dimethylamino)-ethane[26] (**12**) in the studies done by Yoshida *et. al.* They found that the CH/O- interacted geometry is favored leading to the preference of the gauche conformation (**Fig. 10**).

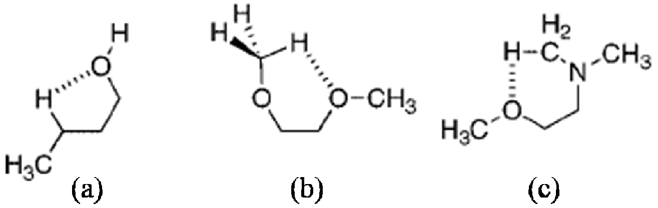

Figure 10. CH/O-interacted geometry of (a) 1-butanol (**10**), (b) 1,2-dimethoxyethane(**11**) and (c) 1-methoxy-2-(dimethylamino)-ethane (**12**) leading to the preferred gauche conformation[2]

Coexistence of gauche and anti conformation in the conformation equilibrium of n–butyl cyanide (**13**) was found by Bohn et al.[27] Similar conclusion was obtained for 1-hexyne[28] (**14**). The gauche structures were due to the weak CH/π interaction as shown in **Fig. 11**.[2]

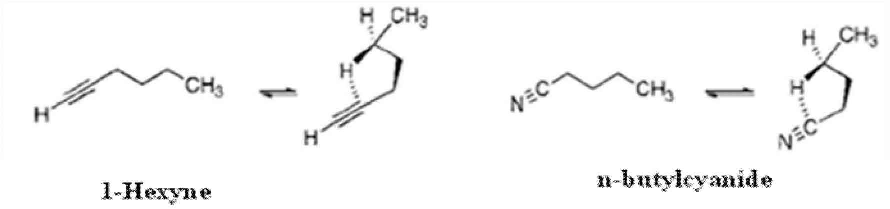

Figure 11. Coexistence of gauche and anti conformation of 1- hexyne (**14**) and n –butyl cyanide[2] (**13**)

In the case of alkyl benzenes, Hopkins, Powers and Smalley suggested that both anti and syn conformers coexist when the alkyl group is n-propyl or n-butyl.[29] Breen et al. demonstrated that, in 3-propyltoluene (**15**), the syn conformer is at least equally stable, compared to the anti conformer[30] (**Fig. 12**).[2]

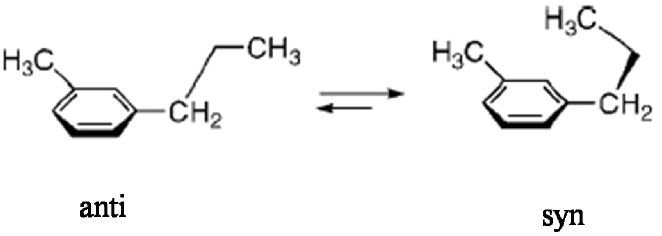

Figure 12. Conformers of 3-propyltoluene[2] (**15**)

The above examples in the literature clearly shows that the concept of steric interactions is not understood properly and are rather used loosely while dealing with conformation analysis. One of the main reasons of this is the lack of proper knowledge of weak noncovalent interactions which in many cases has energy range close to the barrier of rotation of ethane like molecules.

Arene interactions constitute one of such forces, and in spite of its established importance in chemistry,[31] biology[32] and drug development[33] its application as a tool in molecular recognition or crystal engineering remains a problem. For example, to answer which arene residue at the termini of *polymethylene* (e.g. *ethylene*, *propylene* etc.) linker will show intramolecular folding due to arene (especially off-stack face-to-face mode) interaction in solution is not easy even today. Furthermore when present in solution determining in which case it is strong enough to survive in solid state is even more difficult.

In the literature, various models based on different scaffolds to facilitate arene interactions have been proposed for their understanding.[34] These studies can be divided into two main types, first intermolecular[35] which is important from drug–receptor, protein–DNA, protein–protein interaction etc. and second intramolecular[36] which is important especially from DNA/RNA structures, where in single strand it is intramolecular while in double it is both inter- and intramolecular. Intramolecular arene interaction is also important at the molecular level for developing models for a better understanding of arene interactions in general and exploration of the newly emerging concept of conformational control in flexible compounds having at least two arene moieties connected by *polymethylene* linker (e.g. *propylene*,[36d–36g, 36q,37] and *ethylene*[36d, 36h–36j]) Electronic effects of the substituents are also widely believed to have a significant effect on arene interaction,[31,34–36] however, currently there is a lot of debate going on over this and new developments are emerging while older concepts are being challenged.[31b]

1,2-Diarylethanes are the simplest unbiased flexible model to understand how two arene moieties (similar/different) interact with each other intramolecularly for controlling observed folded conformation of the molecule both in solution and more importantly in the crystal state. Interestingly, 1,2-diphenylethane, 1,3-di-phenylpropane and 1,4-diphenylbutane are open in the solid state indicating that the phenyl moiety is not a good system for studying intramolecular arene interactions in such unbiased flexible models. In the absence of arene interactions, conformations of such 1,2-diphenylethanes due to the steric effect of the bulky arene residues, are normally expected to be anti and this is supported by the crystal structures of many 1,2-

diphenylethanes having a wide variety of electron donating and withdrawing substituents in the literature.[38] Even when the *ethylene* linker is between two N atoms the conformation remains anti, clearly indicating that a smaller van der Waals radii of the N atom in comparison to the C atom alone is not enough reason to show syn conformation in crystals.[38f–38h]

On the other hand, a few studies have shown that such structures are capable of existing in folded conformation in solution. A study, as early as 1968, by Leonard et al. on nucleic acid bases connected by *ethylene* and *propylene* linkers clearly showed, that intramolecular interactions between arene residues were responsible for observed folding in solution.[36d] A relatively large hypochromism (11.3%) was observed for 9,9'- dimethylenebisadenine **(**Ad-$(CH_2)_2$-Ad) (**17a**, **Fig. 13**). Maximum hypochromism value (16.5%) was observed for the 9,9 '-trimethylenebisadenine **(**Ad-$(CH_2)_3$-Ad) (**17b**, **Fig. 13**) which suggested that maximal interaction may be associated with parallel plane conformation. For the n = 2 case, however, the dihedral angle formed by the planes of the heterocycles can be about 39^0 at the lower limit. [36d] The authors have also reported that substantial hypochromisms were also observed at n = 2 level in model systems related to flavin-adenine dinucleotide and nicotinamide-adenine dinucleotide.[36d]

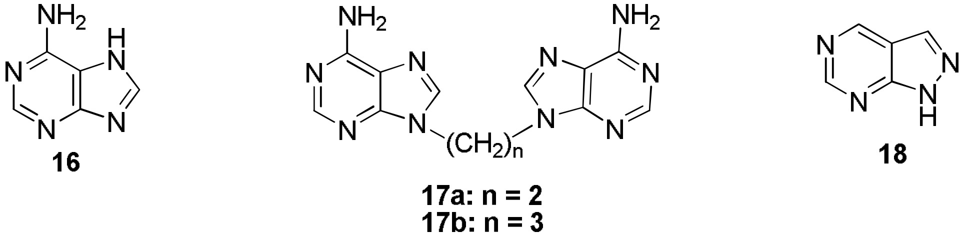

16

17a: n = 2
17b: n = 3

18

Figure 13

Later Itahara studied 9,9′-Diethylenebisadenine (**17a**, **Fig. 13)** by NMR. In his studies he also found that there is significant interaction between the adenine rings as shown by the upfield shifts of the protons of the adenine (**16**, **Fig. 13**) nucleus.[36h–36j] The shifts in the H2 proton (pyrimidine part of the adenine) is more than the H8 proton (imidazole part of the adenine) suggesting close proximity of the six membered pyrimidine rings. Significant interaction between adenine and xanthine nucleus joined by *ethylene* linker (1-[2-(6-aminopurin-9-yl)ethyl]-3,7-dimethylxanthine (**18**, **Fig. 14)** has also been shown by the same author in another study using the results obtained by the NMR shift values of the aromatic protons. Based on the results obtained, author has proposed the structure shown in **Fig.14**. The H-8 proton of the adenine comes into close proximity of the six membered ring of the xanthine (**19**, **Fig. 15**) nucleus as a result of which the shift of the H-8 proton moves upfield.

Figure 14. Proposed Solution state structure of 1-[2-(6-Aminopurin-9-yl)ethyl]-3,7-dimethylxanthine (**18**)

Studies in our lab on PP core based *ethylene* linker compounds (by ^{1}H NMR) showed similar results.[39] Here also, the upfeild shifts in 6-SMe protons of **20a** and **20b** indicate the close proximity of the pyrimidine ring. However the solid state structure of **20b** shows an open conformation.

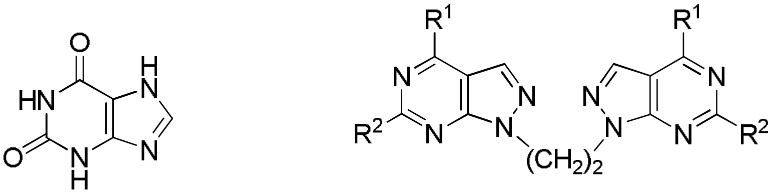

xanthine (**19**)

20a: $R^1 = R^2 =$ SMe
20b: $R^1 = R^2 =$ SEt

Figure 15

Recently, Dubey et al. described that *ethylene* linker compounds with PP cores at their termini show folded conformation in solution both by circular dichroism (CD) and variable temperature ^{1}H NMR studies, however, no solid state evidence for syn conformation due to arene interactions was provided.[40] One case, 1,2-bis[5-oxo-3-(n-propyl)-4,5-dihydro-3*H*- 1,2,4-triazol-4-yl]ethane (**21**) is known to have a syn conformation in the solid state[41] but it is not mentioned whether the extensive hydrogen bonding due to the water present in the molecule or the arene/O/ arene interactions is actually responsible for the observed syn conformation (**Fig.16a** and **16b**).

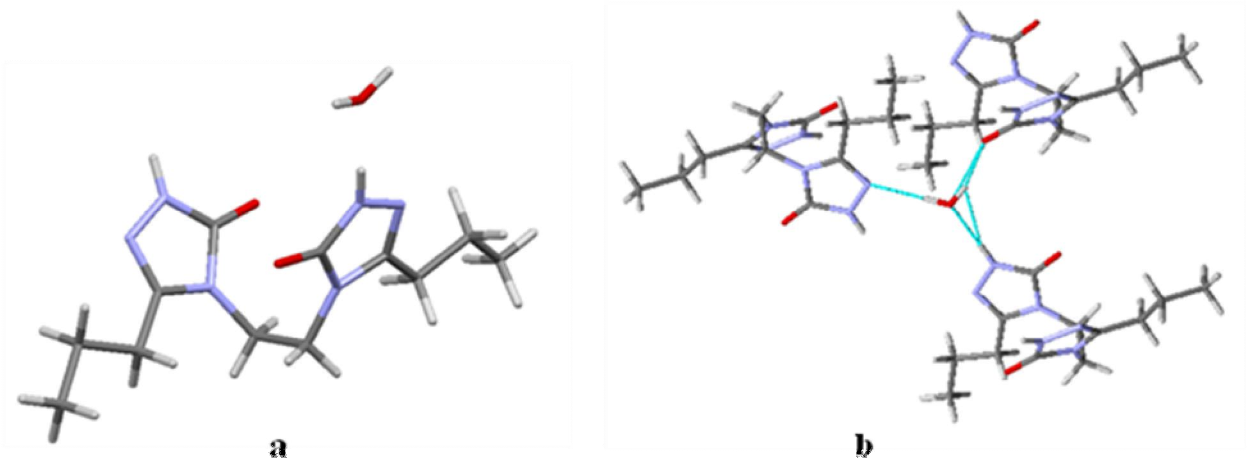

Figure 16. (a) Crystal structure of 1,2-Bis[5-oxo-3-(n-propyl)-4,5-dihydro-3H-1,2,4-triazol-4-yl]ethane (**21)** with water molecule.
(**b**) Extensive hydrogen bonded network with the water molecule

Since 1995, our work on PP core based flexible *propylene*/*Leonard* linker compounds has shown that intramolecular folding is possible due to arene interactions both in solution and more importantly in the solid state, from crystal engineering angle, as shown by more than a dozen truly flexible symmetrical (**22a-k** and **23a-c Fig. 17**) and two related dissymmetrical compounds (**24 and 25**, **Fig. 17**)[37,39] The main difference between **22** and **23** is that the pyrimidine of **22** is replaced by pyrimidone system in **23**. Very recently, the scope of the PP core for studying arene interaction in flexible symmetrical and dissymmetrical compounds has been considerably increased by replacing a truly flexible *propylene*/*Leonard* linker with a less mobile *butylidene* linker (**26**, **Fig. 17**)[42] Interestingly, Vogtle refers to singly linked molecules that adopt p-stacked conformations as ‘‘protophanes’’.[43]

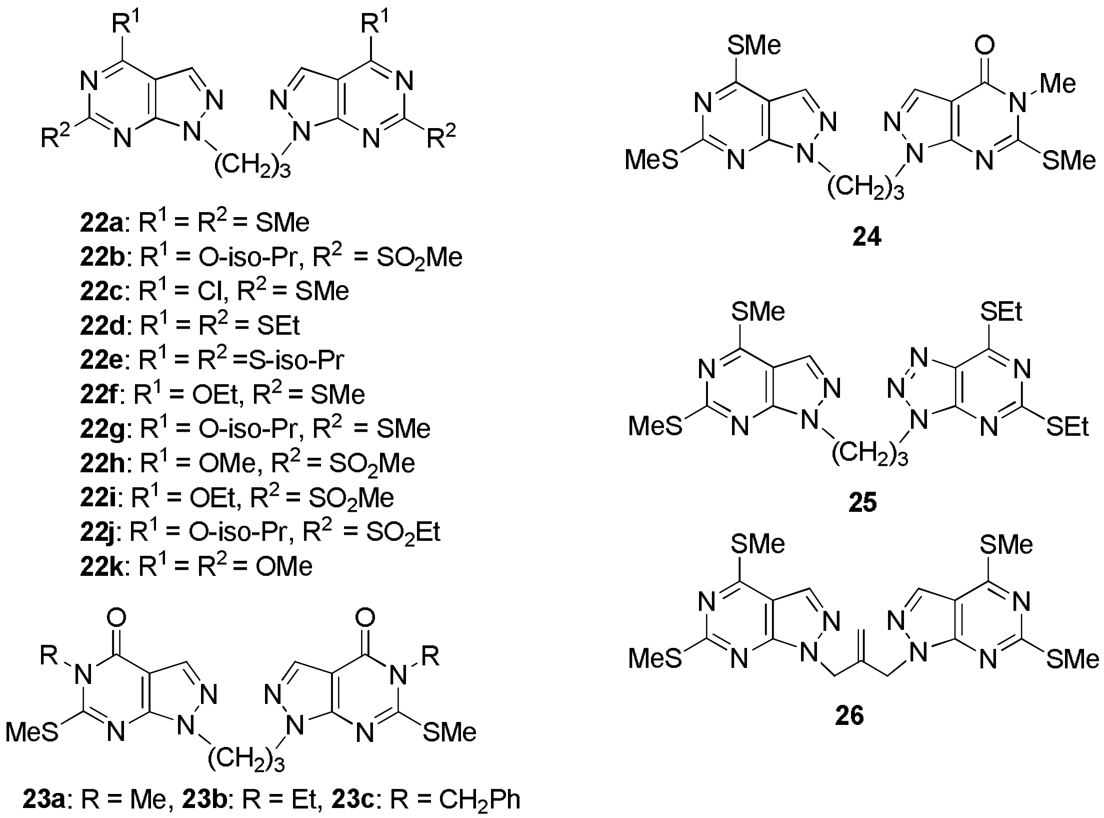

22a: $R^1 = R^2 = SMe$
22b: R^1 = O-iso-Pr, $R^2 = SO_2Me$
22c: $R^1 = Cl$, $R^2 = SMe$
22d: $R^1 = R^2 = SEt$
22e: $R^1 = R^2$ =S-iso-Pr
22f: $R^1 = OEt$, $R^2 = SMe$
22g: R^1 = O-iso-Pr, $R^2 = SMe$
22h: $R^1 = OMe$, $R^2 = SO_2Me$
22i: $R^1 = OEt$, $R^2 = SO_2Me$
22j: R^1 = O-iso-Pr, $R^2 = SO_2Et$
22k: $R^1 = R^2 = OMe$

23a: R = Me, **23b**: R = Et, **23c**: R = CH_2Ph

24

25

26

Figure 17: Pyrazolo[3,4-*d*]pyrimidine core based *flexible* linker compounds

These results have prompted us to apply PP core to common 1,2-n diarylethanes. Our initial efforts in getting syn conformation in the solid state due to intramolecular π–π interactions in the *ethylene* linker symmetrical compound based on PP core were not successful.[39c] A careful analysis of the crystal structures (**22a-k**; n = 3, **23a–c**, **Fig. 17**) revealed that except for **22b** (**Fig. 17**) having bulky groups at both 4- and 6-positions, five membered pyrazolo moieties are at a maximum distance from each other (e.g. 4.48 and 4.62 Å between centroids in **22a** and **23a**

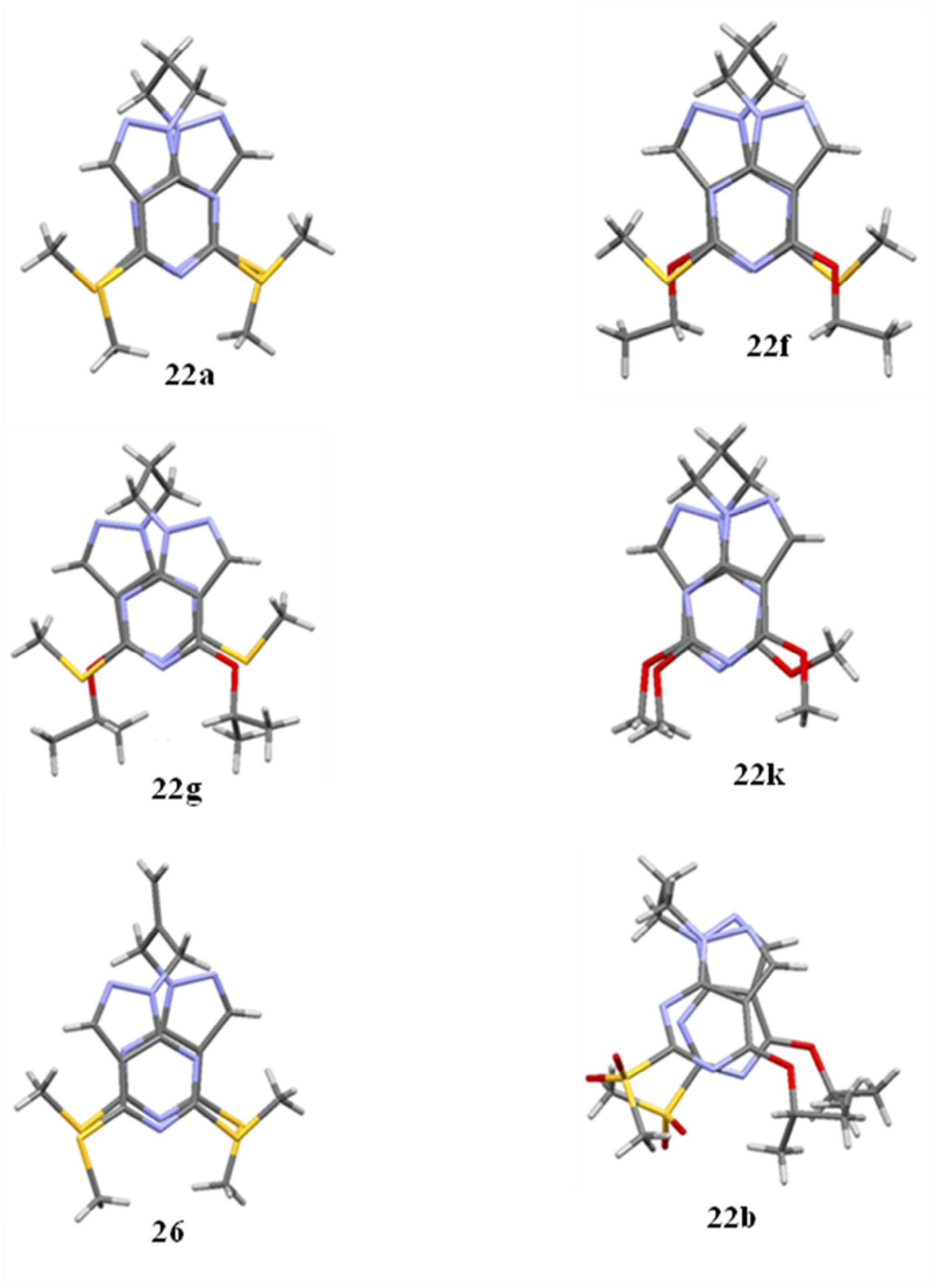

22a

22f

22g

22k

26

22b

Figure 18. Crystal Structure* of **22a**,[10a] **22f**, **22g**,[10c] **22k** and **26**,[11] showing that five member pyrazolo moieties are at maximum distance from each other while six member pyrimidine/pyrimidone residues are partially overlapped. In case of **22b**,[10e] however, pyrazolo moieties are partially overlapped

Table 1. Important geometrical data obtained from X-ray crystallographic studies

Compound No.	Distance between two N atoms connecting linker (Å)	Intramolecular π–π stacking[a] distance (Å)	Intermolecular π–π stacking[a-d] distance (Å)	Angle between the least-squares planes (°)	Ref. No.
22a	3.28	3.71[a]	3.67[a], 3.59[b], 3.54[c]	13.2(1)	37a
22b	3.09(4)	4.145[a], 3.775[b], 3.605[c]	4.10[a], 3.96[b] 4.30[a], 4.36[b]	21.54(1) 21.3(1)	37e
22c	3.80	No (5.26)	3.56[a], 3.58[b] 3.50[c], 3.87[c]	18.03	37f
22d	3.33(2)	3.8[a]	3.7[a]	13.2(1)	39c
22e	3.26(2)	4.0[a]	not observed	21.96(4)	37f
22f	3.35(2)	3.82[a], 4.05[c]	3.72[b], 3.81[c]	13.13(7)	37f
22g	3.24(3)	3.69[a], 3.84[c]	3.54[a],4.19[c]	14.99(2)	37f
22h	3.15	3.993[a]	3.99[a], 3.66[b]	26.11	37f
22i	3.20	3.969[a]	3.97[a], 3.94[b]	23.49	37f
22j	3.26(3)	4.136[a]	3.96[b], 3.42[c]	21.3(1)	37f
22k	3.41	3.76[a]	3.66[a], 3.76[b] 3.93c	6.72	37f
25	3.25(4)	3.77[a]	3.80[a], 3.72	15.5(1)	37f
23a	3.35	3.77[a]	3.65[a], 3.61[b]	12.48(5)	37f
23b	3.54	4.23[a]	3.765[a]	10.90	37f
23c	3.33	3.86[a]	3.63[b]	14.51	37f

[a] Distance between centroids of six membered rings.

[b] Distance between centroids of five and six membered rings.

[c] Distance between centroids of nine membered rings.

[d] Distance between centroids of five membered rings.

respectively) while six membered pyrimidine/pyrimidone residues are partially overlapped (e.g. 3.71 and 3.77 Å between centroids in **22a** and **23a** respectively).

Since for the *ethylene* linker homolog **20a** (**Fig. 15)** of the symmetrical *propylene* linker compound **22a** (**Fig. 17)** both **PP** moieties have to come close to each other in order to achieve a syn conformation and this situation may not be sterically/electronically favorable especially in the solid state where competing intermolecular interactions are present to give a more favorable anti conformation.

Therefore, it was decided to replace one pyrazolo[3,4-*d*]pyrimidinyl moiety in **20a** with another heteroaromatic nucleus which should satisfy two criteria. Firstly, it should be bicyclic and secondly it should have a pyrimidine ring. The simplest such structure is quinazoline which incidentally also has a structural isomer phthalazine. Thus 4(3*H*)-quinazolinone (**27, Fig. 19**), 1(*2H*)-phthalazinone (**28, Fig. 19**) and 4(3*H*)-benzotriazinone (**29, Fig. 19**) were chosen to replace one pyrazolo[3,4-*d*]pyrimidinyl moiety in **20a.** Another reason for choosing the quinazoline and phthalazine ring system was that it is the aza analog of quinoline nucleus which is known to show stacking interactions.[44a-d]

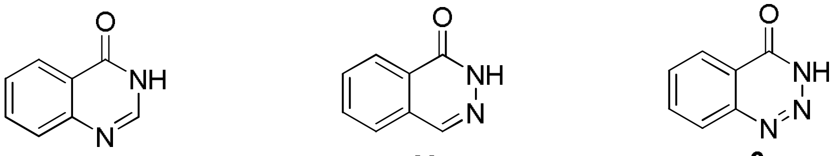

27 **28** **2**

4(3H)-quinazolinone 1(2H)-phthalazinone 4(3H)-benzotriazinone

Figure 19

Survey of literature revealed that stacking interaction between the aminoquinoline ring of the antimalarial chloroquine and the purine bases has been extensively studied by preparing and examining models in which the quinoline is linked to the base by a trimethylene chain. Bolte *et al.* synthesized compounds **30a** and **30b** (**Fig. 20**) and showed that % hypochromism value rose to a maximum of about 25% with decreasing temperature and both models were practically entirely in stacked conformation at 25° C.[44a]

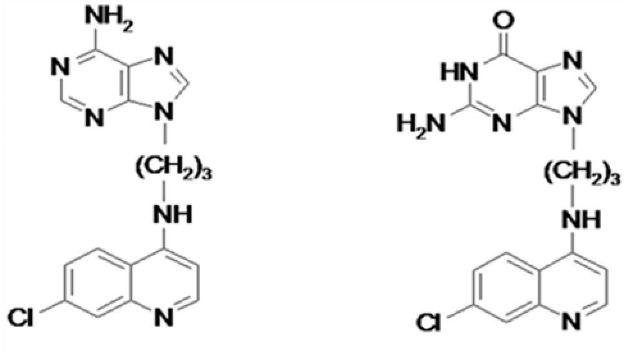

30a **30b**

Figure 20

The pyrimidine nucleus is embedded in a large number of alkaloids, drugs, antibiotics, agrochemicals, and antimicrobial agents.[45] Many fused pyrimidines, such as purines, pteridines, or quinazolines, belong to the most important and bioactive heterocyclic systems. Isolation of an antimalarial alkaloid from the Chinese plant Chang Shan in1946[46] gave a great impetus to the synthesis and investigation of biological activity of quinazolone derivatives, when it was found that ‘febrifugine’ **31** (**Fig. 21**), the antimalarial alkaloid isolated from these plants was a 4-quinazolone derivative substituted at the N-atom in the 3-position of the 4-quinazolone moiety.[46.47] Quinazolones have since been found to be biologically versatile compounds having antituberculars,[48] thromboxane A2 synthetase inhibitors,[49] antifungal,[50] antiviral,[51] anticonvulsant,[52] and blood platelet anti-aggregating activity.[53] Though extensive work has been done on synthesis and investigation of biological activity of these compounds, only two of them have till now found a firm place in the therapeutic practice namely methaqualone **32** (**Fig. 20**), which was introduced as an anxiolytic (Quaalude, Sopor) in 1965 as safe barbiturate substitutes and quinethazone **33** (**Fig. 21**) which is a diuretic.[54]

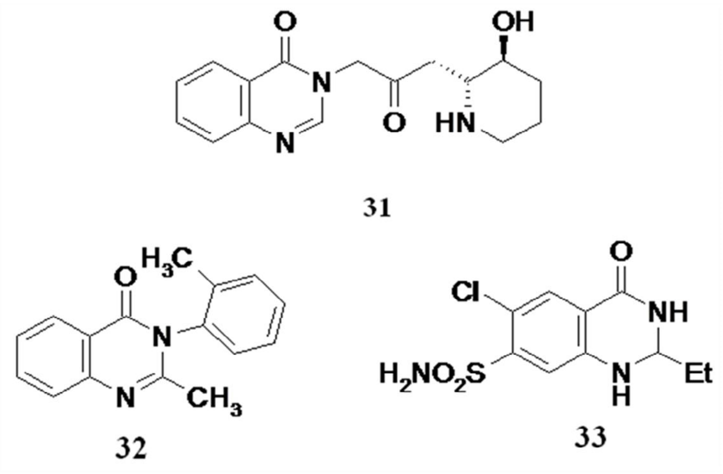

31

32

33

Figure 21. Important molecules containing quinazolinone nucleus

Phthalazin-1(2*H*)-ones bearing a substituent at C-4 represent key intermediates in the synthesis of various compounds with highly interesting pharmacological properties, such as the blood platelet aggregation inhibitor MY-54452 [1-(3-chloroanilino)-4-phenylphthalazine] (**34**, **Fig. 22**) which has been found to be also a selective phosphodiesterase VA inhibitor[55] or the thromboxane A2 synthetase inhibitor and bronchodilator, 2-[2-(1-imidazolyl)ethyl]-4-(3-pyridyl)phthalazin-1(2*H*)-one (**34**).**[56]** Moreover, a number of established drug molecules like *Hydralazine* (**35**),[57] *Budralazine* (**36**),[58] *Azelastine* (**37**),[59] *Ponalrestat* (**38**),[60] or *Zopolrestat* (**39**)[61] (**Fig. 22**) are accessible starting from the corresponding phthalazinones. Benzotriazinone derivatives have been demonstrated as potent positive allosteric AMPA receptor modulators.[62] Benzotriazinone derivatives have also been evaluated for local anaesthetic activity.[63]

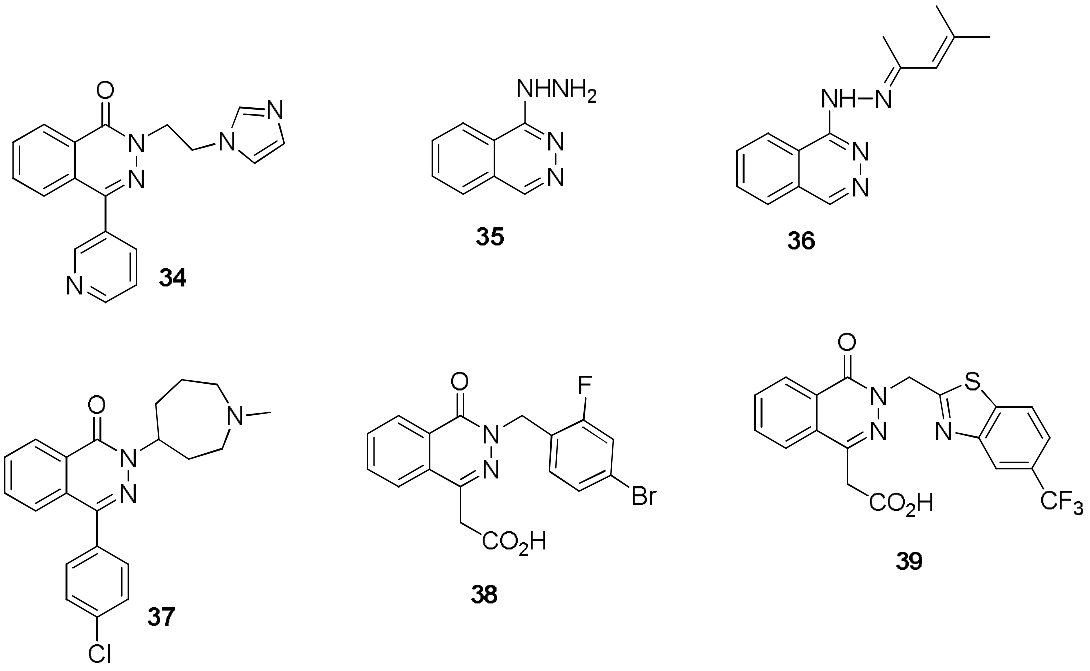

34 **35** **36** **37** **38** **39**

Figure 22. Important molecules containing phthalazinone nucleus

Therefore, in order to extend **pyrazolo[3,4-*d*]pyrimidine** work to other aromatic/heteroaromatic systems we decided to employ three related nucleus 4(3*H*)-quinazolinone, 1(2*H*)-phthalazinone and 4(3*H*)-benzotriazinone all of which retain a pyrimidine/pyrimidone framework and are also commercially available.

3.2 Objective

To study the effect of replacing one pyrazolo[3,4-*d*]pyrimidinyl moiety in **20a** with heteroaromatics like 4(3*H*)-quinazolinone, 1(2*H*)-phthalazinone and 4(3*H*)-benzotriazinone on inter/intramolecular stacking in context of change in position and number of heteroatom i.e. nitrogen in the heterodimers.

1) Nucleophilic substitution in a nucleus affects the electronic and steric properties of the molecule which can alter inter/intramolecular interaction pattern of the resulting molecule. Therefore, it was considered to replace methylsulfanyl group in 4,6-bis methylsulfanyl-1*H*-pyrazolo[3,4-*d*]pyrimidinyl moiety of the heterodimers by substituents like amines, hydroxyl, alkoxy etc. to study its overall effect on the conformation of the molecule.

Synthesis and characterization

3.3.1 Synthesis and characterization of 2-(2-(4,6-bis(methylthio)-1*H*-pyrazolo[3,4-*d*]pyrimidin-1-yl)ethyl)phthalazin-1(2*H*)-one (41), 3-(2-(4,6-bis(methylthio)-1*H*-pyrazolo[3,4-*d*]pyrimidin-1-yl)ethyl)quinazolin-4(3*H*)-one (42), 3-(2-(4,6-bis(methylthio)-1*H*-pyrazolo[3,4-*d*]pyrimidin-1-yl)ethyl)benzo[*d*][1,2,3]triazin-4(3*H*)-one (43) and 2-(2-(4,6-bis(methylthio)-2*H*-pyrazolo[3,4-*d*]pyrimidin-2-yl)ethyl)phthalazin-1(2*H*)-one (45).

Synthesis of compounds **41-45** was carried out following the procedures described in the literature[64] and is shown in **Scheme 1**. These compounds were characterized by NMR and Mass spectrometric techniques and were compared with the values reported in the thesis.

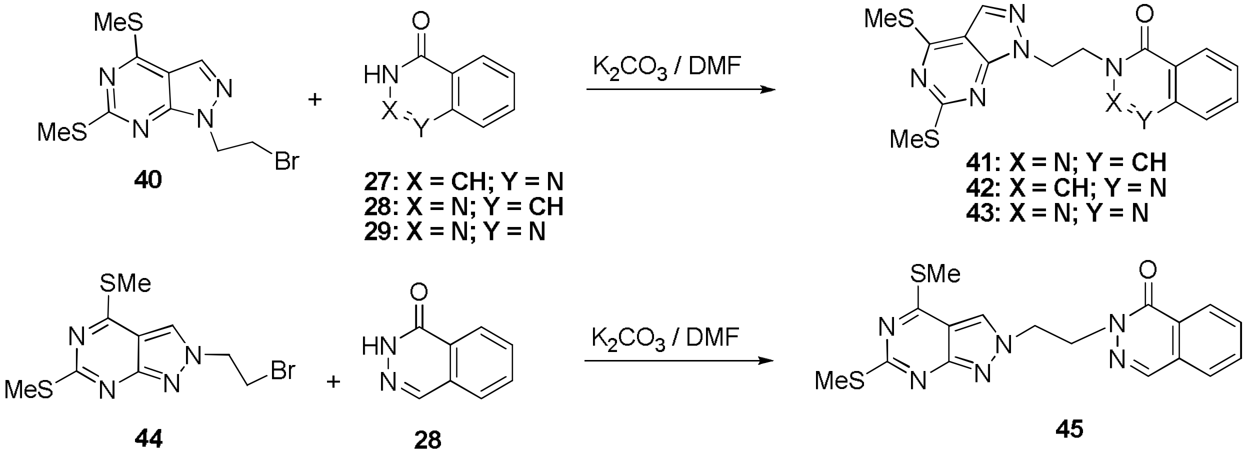

Scheme 1. Synthesis of compounds **41-43** and **45**

3.3.2 Regioselective nucleophilic substitution of 4-SMe group of different compounds.

3.3.2.1 Synthesis and characterization of 2-(2-(6-(methylthio)-4-(pyrrolidin-1-yl)-1*H*-pyrazolo[3,4-*d*]pyrimidin-1-yl)ethyl)phthalazin-1(2*H*)-one (46), 3-(2-(6-(methylthio)-4-(pyrrolidin-1-yl)-1*H*-pyrazolo[3,4-*d*]pyrimidin-1-yl)ethyl)quinazolin-4(3*H*)-one (47), 3-(2-(6-(methylthio)-4-(pyrrolidin-1-yl)-1*H*-pyrazolo[3,4-*d*]pyrimidin-1-yl)ethyl)benzo[*d*][1,2,3] triazin-4(3*H*)-one (48), 2-(2-(6-(methylthio)-4-(piperidin-1-yl)-1*H*-pyrazolo[3,4-*d*]-pyrimidin-1-yl)ethyl)phthalazin-1(2*H*)-one (49) and 2-(2-(6-(methylthio)-4-morpholino-1*H*-pyrazolo[3,4-*d*]pyrimidin-1-yl)ethyl)phthalazin-1(2*H*)-one (50).

Synthesis of starting materials (**46-47**) was carried out following general methodology described earlier.[64] Synthesis of new compounds **48-50** is described below.

Reaction of compound **41** with piperidine and morpholine under reflux conditions gave compound **49** and compound **50** respectively. Reaction of **43** with pyrrolidine**,** under reflux conditions gave compound **48** (**Scheme 2**). These compounds were characterized by NMR and Mass spectrometric techniques.

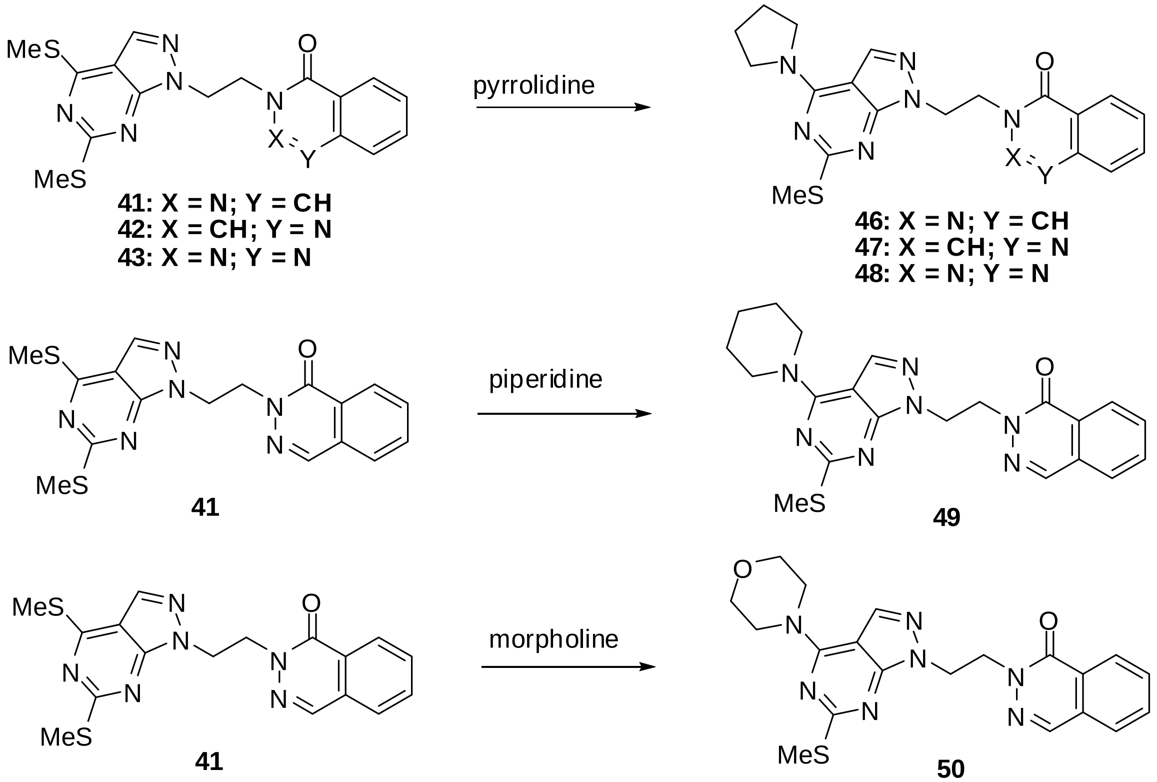

Scheme 2. Synthesis of compounds **46-50**

Proton NMR of **48** showed multiplets between δ 1.91 -1.96 and between δ 2.07 -2.12 for two pyrrolidinyl CH_2, one singlet at δ 2.20 for SMe protons, a multiplet between δ 3.65–3.73 for two pyrrolidinyl NCH_2, one singlet at δ 4.86 for two NCH_2, four multiplets between δ 7.73–7.78, between δ 7.86 -7.91, between δ 8.00–8.03 and between δ 8.30 -8.33, a singlet at δ 7.74 for five aromatic protons. Mass spectrum showed base peak corresponding to $[M+H]^+$ at *m/z* 409.

Proton NMR of **49** showed a multiplet between δ 1.64 -1.72 for three piperidinyl CH_2, one singlet at δ 2.21 for SMe protons, a multiplet between δ 3.82–3.87 for two piperidinyl CH_2, two multiplets between δ 4.65-4.68 and between δ 4.80 -4.84 for two NCH_2, three multiplets between δ 7.59–7.63, between δ 7.71 -7.80 and between δ 8.38 -8.41 two singlets at δ 7.81 and δ 7.87 for six aromatic protons. Mass spectrum showed base peak corresponding to $[M+H]^+$ at *m/z* 422.

Proton NMR of **50** showed one singlet at δ 2.21 for SMe protons, two multiplets between δ 3.80-3.83 for two morpholinyl NCH2 and between δ 3.88-3.91 for two morpholinyl OCH_2, two multiplets between δ 4.65-4.69 and between δ 4.82-4.86 for two NCH_2, three multiplets between δ 7.60–7.63, between δ 7.71 -7.79 and between δ 8.37 -8.40 two singlets at δ 7.80 and δ 7.87 for six aromatic protons. Mass spectrum showed base peak corresponding to $[M+H]^+$ at *m/z* 424.

3.3.2.2 Synthesis and characterization of 2-(2-(6-(methylthio)-4-oxo-4,5-dihydro-1*H*-pyrazolo[3,4-*d*]pyrimidin-1-yl)ethyl)phthalazin-1(2*H*)-one (51) and 3-(2-(6-(methylthio)-4-oxo-4,5-dihydro-1*H*-pyrazolo[3,4-*d*]pyrimidin-1-yl)ethyl)quinazolin-4(3*H*)-one (52).

Reaction of compound **41** with aq. NaOH in methanol under reflux conditions gave compound **51** and reaction of compound **42** under similar conditions gave compound **52**. These compounds were characterized by NMR and Mass spectrometric techniques.

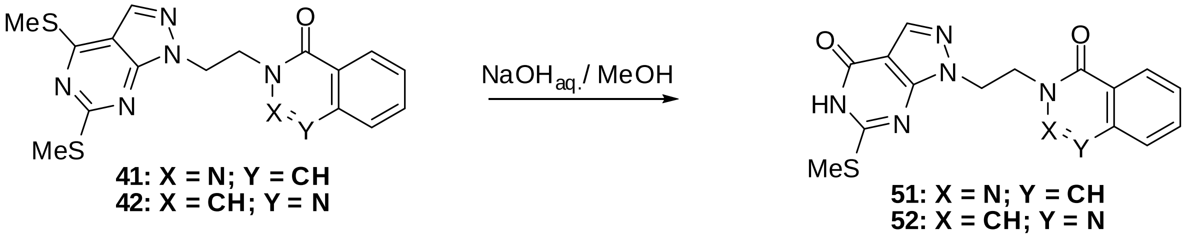

Scheme 3. Synthesis of compounds **51-52**

Proton NMR of **51** showed a singlet at δ 2.26 for SMe protons, two multiplets between δ 4.66-4.69 and between δ 4.80-4.83 for two NCH_2, three multiplets between δ 7.61 –7.64, between δ 7.74 -7.84 and between δ 8.39 -8.42 two singlets at δ 7.87 and δ 7.99 for six aromatic protons. Mass spectrum showed base peak corresponding to $[M+H]^+$ at *m/z* 355.

Proton NMR of **52** in DMSO-d_6 showed a singlet at δ 2.16 for SMe protons, two multiplets between δ 4.32-4.41 and between δ 4.61-4.71 for two NCH_2, three multiplets between δ 7.46 – 7.58, between δ 7.76 -7.84 and between δ 8.11 -8.15 two singlets at δ 7.58 and δ 8.00 for six aromatic protons. Mass spectrum showed base peak corresponding to $[M+H]^+$ at *m/z* 355.

3.3.2.3 Synthesis and characterization of 2-(2-(4-methoxy-6-(methylthio)-1*H*-pyrazolo-[3,4-*d*]pyrimidin-1-yl)ethyl)phthalazin-1(2*H*)-one (53), 3-(2-(4-methoxy-6-(methylthio)-1*H*-pyrazolo[3,4-*d*]pyrimidin-1-yl)ethyl)quinazolin-4(3*H*)-one (54), 2-(2-(4-methoxy-6-

(methylthio)2*H*-pyrazolo[3,4-*d*]pyrimidin-2-yl)ethyl)phthalazin-1(2*H*)-one (55), 3-(2-bromoethyl)benzo[*d*][1,2,3]triazin-4(3*H*)-one (57) 3-(2-(4-methoxy-6-(methylthio)-1*H*-pyrazolo[3,4-*d*]pyrimidin-1-yl)ethyl)benzo[*d*][1,2,3]triazin-4(3*H*)-one (59) and 3-(2-(4-methoxy-6-(methylthio)-2*H*-pyrazolo[3,4-*d*]pyrimidin-2-yl)ethyl)benzo[*d*][1,2,3]triazin-4(3*H*)-one(60).

Reaction of compound **41** with NaOMe in methanol under reflux conditions compound **53**, reaction of compound **42** under similar conditions gave compound **54** and reaction of compound **45** under similar conditions gave compound **55**.

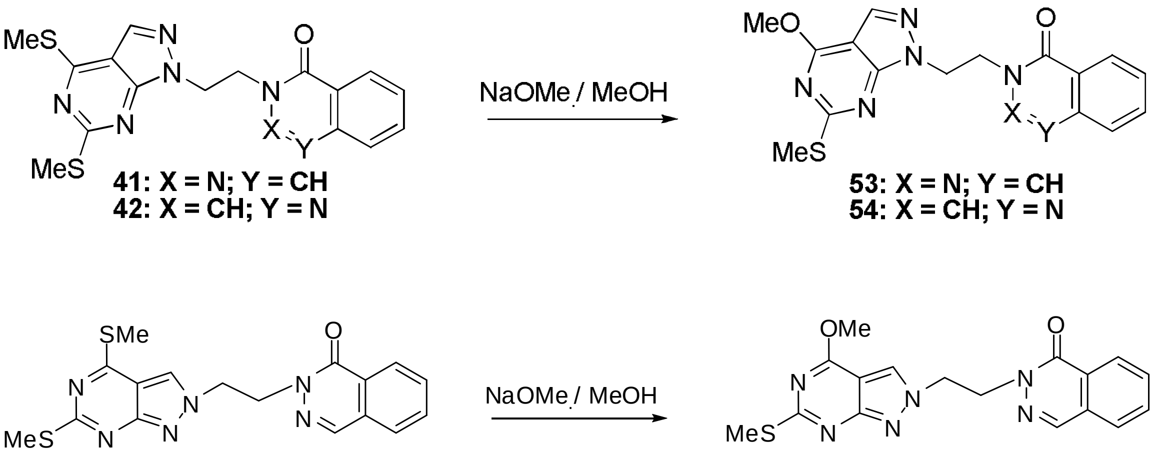

41: X = N; Y = CH
42: X = CH; Y = N

53: X = N; Y = CH
54: X = CH; Y = N

45

55

Scheme 4a. Synthesis of compounds **53-55**

Synthesis of compound **59** cannot be carried out under similar conditions since benzotriazinone ring is unstable under strong basic conditions, therefore this compound was synthesized by first synthesizing compound **57** by reacting compound **29** (**Scheme 1**) with 1,2 dibromoethane (**56**) in DMF using K_2CO_3 as base. Reaction of compound **57** with 4-methoxy-6-methylthio-1*H*-pyrazolo[3,4-*d*]pyrimidine (**58**) in DMF using K_2CO_3 as base gave a mixture of compound **59** and compound **60** which was separated by column chromatography. These compounds were characterized by NMR and Mass spectrometric techniques.

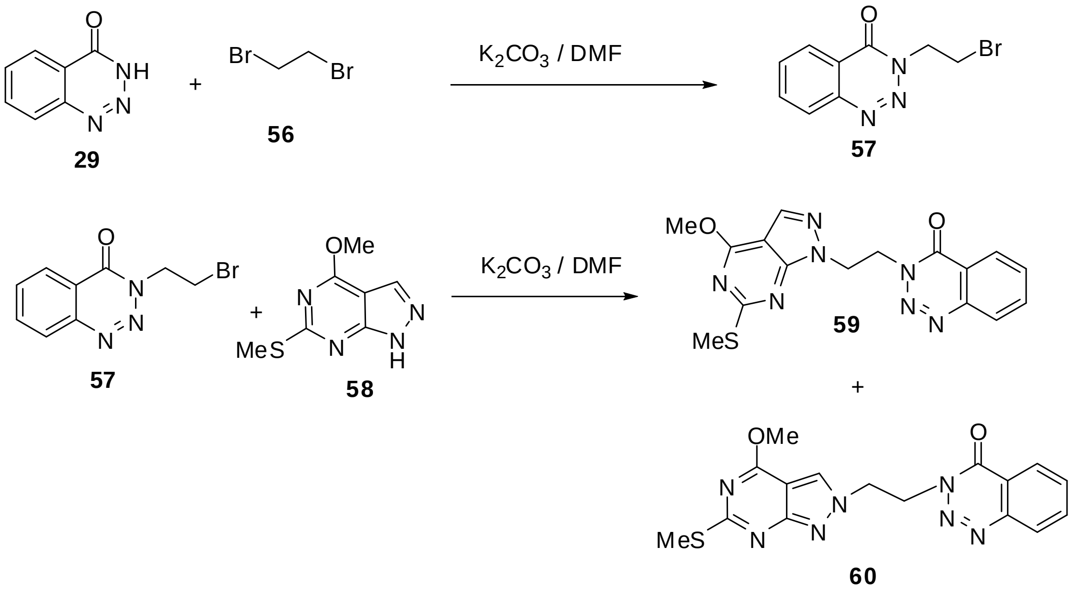

Scheme 4b. Synthesis of compounds **59-60**

Proton NMR of **53** showed two singlets at δ 2.25 for SMe and δ 4.06 for OMe group, two multiplets between δ 4.66–4.70 and between δ 4.85-4.89 for two NCH_2, three multiplets between δ 7.59–7.62, between δ 7.71 -7.81 and between δ 8.37 -8.40 two singlets at δ 7.82 and δ 7.86 for six aromatic protons. Mass spectrum showed base peak corresponding to $[M+H]^+$ at *m/z* 369.

Proton NMR of **54** showed two singlets δ 2.24 for SMe and δ 4.06 for OMe group, two multiplets between δ 4.46–4.48 and between δ 4.80-4.82 for two NCH_2, three multiplets between δ 7.57–7.60, between δ 7.71 -7.76 and between δ 8.30 -8.33 two singlets at δ 7.26 and δ 7.92 for six aromatic protons. Mass spectrum showed base peak corresponding to $[M+H]^+$ at *m/z* 369.

Proton NMR of **55** showed two singlets at δ 2.59 for SMe and δ 4.02 for OMe group, a singlet at δ 4.80 for two NCH_2, three multiplets between δ 7.63–7.66, between δ 7.73 -7.79 and between δ 8.37 -8.40 two singlets at δ 7.79 and δ 8.02 for six aromatic protons. Mass spectrum showed base peak corresponding to $[M+H]^+$ at *m/z* 369.

Proton NMR of **57** showed two triplets at δ 3.82 for CH_2Br and δ 4.87 for one NCH_2, two multiplets between δ 7.80-7.86 and between δ 7.95-8.00, two doublets at δ 8.18 and 8.37 for four aromatic protons. Mass spectrum showed base peak corresponding to $[M+H]^+$ at *m/z* 252.

Proton NMR of **59** showed two singlets at δ 2.26 for SMe and δ 4.04 for OMe group, a singlet at δ 4.91 for two NCH_2, two multiplets between δ 7.75–7.80, between δ 7.89 -7.94, two doublets at δ 8.04 and 8.31, a singlet at δ 7.84 for five aromatic protons. Mass spectrum showed base peak corresponding to $[M+H]^+$ at *m/z* 370.

Proton NMR of **60** showed two singlets at δ 2.61 for SMe and δ 4.05 for OMe group, two multiplets between δ 4.85–4.89 and between δ 5.04-5.08 for two NCH_2, two multiplets between δ 7.80–7.84, between δ 7.94 -7.99, two doublets at δ 8.12 and 8.34, a singlet at δ 7.83 for five aromatic protons. Mass spectrum showed base peak corresponding to $[M+H]^+$ at *m/z* 370.

3.3.3 Synthesis of chloro analogs.

3.3.3.1 Synthesis and characterization of 2-(2-(4-chloro-6-(methylthio)-1*H*-pyrazolo[3,4-*d*]-pyrimidin-1-yl)ethyl)phthalazin-1(2*H*)-one (61) and 3-(2-(4-chloro-6-(methylthio)-1*H*-pyrazolo[3,4-*d*]pyrimidin-1-yl)ethyl)quinazolin-4(3*H*)-one (62).

Reaction of **51** with $POCl_3$ under reflux conditions gave compound **61**, reaction of **52** under similar conditions gave compound **62**.

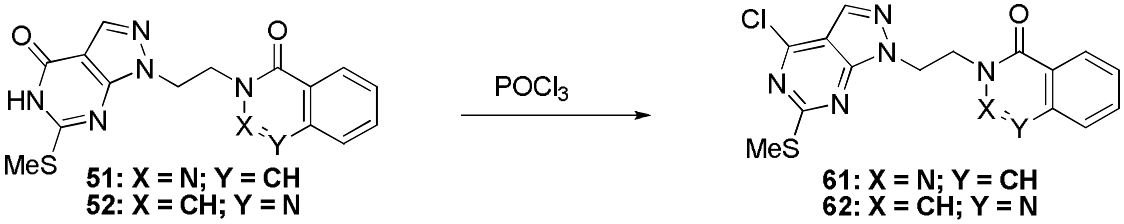

Scheme 5. Synthesis of compounds **61-62**

Proton NMR of **61** showed a singlet at δ 2.23 for SMe, two multiplets between δ 4.67–4.70 and between δ 4.91-4.93 for two NCH_2, three multiplets between δ 7.59–7.62, between δ 7.73 -7.82 and between δ 8.36 -8.39, two singlets at δ 7.79 and δ 7.98 for six aromatic protons. Mass spectrum showed base peak corresponding to $[M+H]^+$ at *m/z* 373.

Proton NMR of **62** showed a singlet at δ 2.25 for SMe, two multiplets between δ 4.46–4.50 and between δ 4.82-4.86 for two NCH_2, three multiplets between δ 7.46–7.57, between δ 7.69-7.74 and between δ 8.26-8.29, two singlets at δ 7.31 and δ 8.01 for six aromatic protons. Mass spectrum showed base peak corresponding to $[M+H]^+$ at *m/z* 373.

3.3.4 Oxidation of 6- SMe group of compounds 53, 54, 55, 59 and 61 to SO_2Me group.

3.1.4.1 Synthesis and characterization of 2-(2-(4-methoxy-6-methylsulfonyl-1*H*-pyrazolo [3,4-*d*]pyrimidin-1-yl)ethyl)phthalazin-1(2*H*)-one (63), 2-(2-(4-chloro-6-methylsulfonyl-1*H*-pyrazolo[3,4-*d*]pyrimidin-1-yl)ethyl)phthalazin-1(2*H*)-one (64), 3-(2-(4-methoxy-6-methylsulfonyl-1*H*-pyrazolo[3,4-*d*]pyrimidin-1-yl)ethyl)quinazolin-4(3*H*)-one (65), 3-(2-(4-methoxy-6-methylsulfonyl-1*H*-pyrazolo[3,4-*d*]pyrimidin-1-yl)ethyl)benzo[d][1,2,3]triazin-4(3*H*)-one (66) and 2-(2-(4-methoxy-6-(methylsulfonyl)-2*H*-pyrazolo[3,4-*d*]pyrimidin-2-yl)ethyl)phthalazin-1(2H)-one (67).

Reaction of **53** with oxone in acetone at $0^{o}C$ gave compound **63**. Similar reactions with **61, 54, 59** and **55** gave compound **64**, compound **65**, compound **66** and compound **67** respectively.

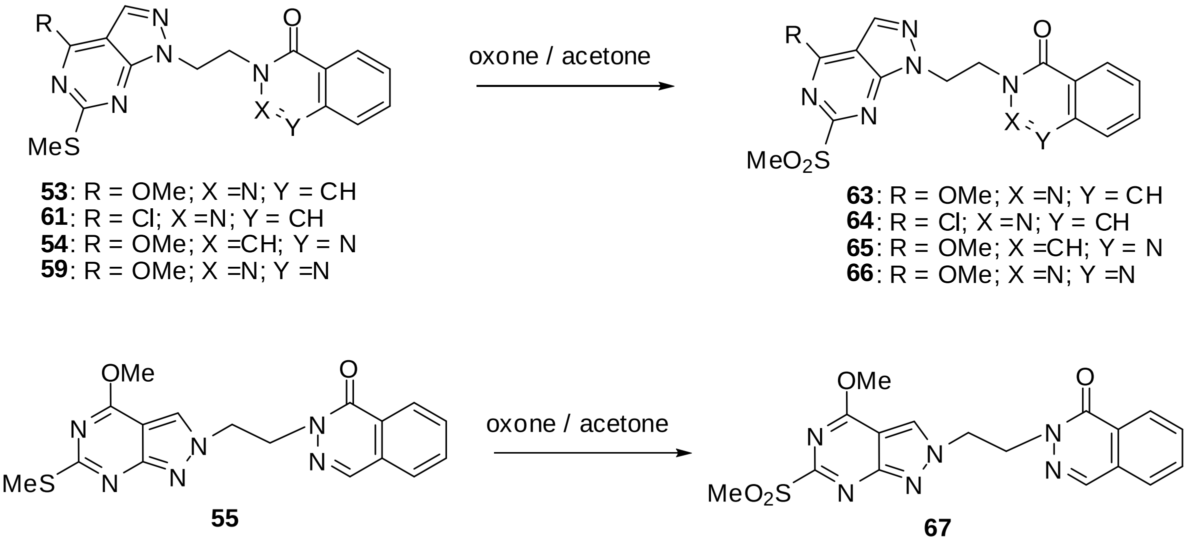

53: R = OMe; X =N; Y = CH
61: R = Cl; X =N; Y = CH
54: R = OMe; X =CH; Y = N
59: R = OMe; X =N; Y =N

63: R = OMe; X =N; Y = CH
64: R = Cl; X =N; Y = CH
65: R = OMe; X =CH; Y = N
66: R = OMe; X =N; Y =N

55

67

Scheme 6. Synthesis of compounds **63-67**

These compounds were characterized by NMR and Mass spectrometric techniques.

Proton NMR of **63** showed two singlets at δ 3.04 for SO_2Me and δ 4.23 for OMe, two multiplets between δ 4.70–4.73 and between δ 4.98–5.02 for two NCH_2, three multiplets between δ 7.63–7.66, between δ 7.73–7.86 and between 8.33–8.36, two singlets at δ 7.87 and δ 8.09 for six aromatic protons. Mass spectrum showed base peak corresponding to $[M+H]^+$ at *m/z* 401.

Proton NMR of **64** showed a singlet at δ 3.11 for SO_2Me, two multiplets between δ 4.72–4.75 and between δ 5.06–5.09 for two NCH_2, three multiplets between δ 7.64–7.66, between δ 7.73–7.84 and between 8.30–8.32, two singlets at δ 7.90 and δ 8.24 for six aromatic protons. Mass spectrum showed base peak corresponding to $[M+H]^+$ at *m/z* 405.

Proton NMR of **65** showed two singlets at δ 3.04 for SO_2Me and δ 4.24 for OMe, two multiplets between δ 4.52–4.55 and between δ 4.94–4.97 for two NCH_2, three multiplets between δ 7.49–7.60, between δ 7.72–7.77 and between 8.29–8.31, two singlets at δ 7.35 and δ 8.15 for six aromatic protons. Mass spectrum showed base peak corresponding to $[M+H]^+$ at *m/z* 401.

Proton NMR of **66** showed two singlets at δ 3.12 for SO_2Me and δ 4.22 for OMe, two multiplets between δ 4.93–4.96 and between δ 5.04–5.07 for two NCH_2, four multiplets between δ 7.77–7.84, between δ 7.91–7.97 between δ 8.04–8.08 and between δ 8.28–8.33, a singlet at δ 8.06 for five aromatic protons. Mass spectrum showed base peak corresponding to $[M+H]^+$ at *m/z* 402.

Proton NMR of **67** showed two singlets at δ 3.43 for SO_2Me and δ 4.21 for OMe, two multiplets between δ 4.82–4.86 and between δ 4.93–4.97 for two NCH_2, three multiplets between δ 7.66–7.69, between δ 7.77–7.86 and between 8.38–8.40, two singlets at δ 8.01 and δ 8.04 for six aromatic protons. Mass spectrum showed base peak corresponding to $[M+H]^+$ at *m/z* 401.

3.3.5 Synthesis and characterization of 2-(2-(4,6-dimethoxy-1*H*-pyrazolo[3,4-*d*]pyrimidin-1-yl)ethyl)phthalazin-1(2*H*)-one (68).

Reaction of **63** with sodium methoxide in methanol under reflux conditions gave compound **68**. This compound was characterized by NMR and Mass spectrometric techniques.

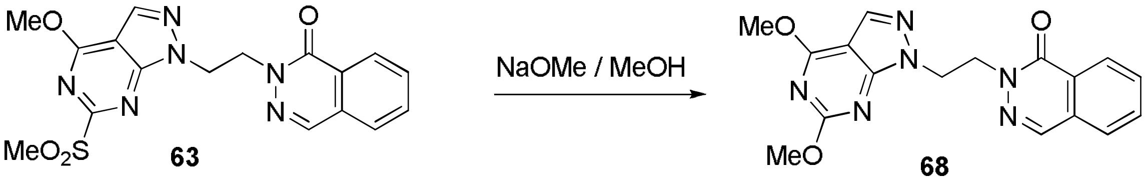

63

68

Scheme 7. Synthesis of compounds **68**

Proton NMR of **68** showed two singlets at δ 3.60 and δ 4.05 for two OMe groups, two multiplets between δ 4.66–4.70 and between δ 4.81 -4.84 for two NCH_2, three multiplets between δ 7.57–7.60, between δ 7.71 -7.79 and between δ 8.37 -8.39 two singlets at δ 7.83 and δ 7.85 for six aromatic protons. Mass spectrum showed base peak corresponding to $[M+H]^+$ at *m/z* 353.

3.3.6 Synthesis and characterization of 2-(2-(4-(dimethylamino)-6-(methylthio)-1*H*-pyrazolo[3,4-*d*]pyrimidin-1-yl)ethyl)phthalazin-1(2*H*)-one (69).

Reaction of 61 with 50% aq. dimethylamine solution under reflux conditions gave compound **69**. This compound was characterized by NMR and Mass spectrometric techniques.

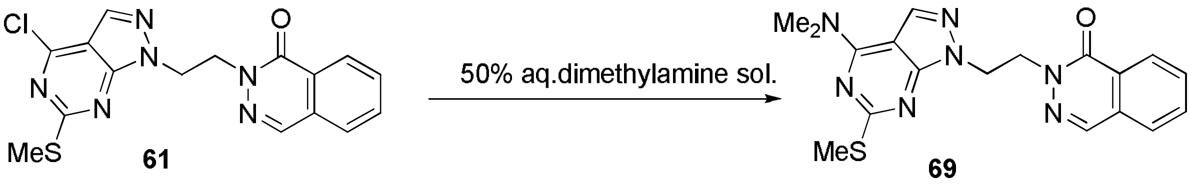

Scheme 8. Synthesis of compounds **69**

Proton NMR of **69** showed two singlets at δ 2.22 for SMe, and δ 3.31 for NMe_2 two multiplets between δ 4.64–4.68 and between δ 4.79 -4.83 for two NCH_2, three multiplets between δ 7.58–7.62, between δ 7.70 -7.79 and between δ 8.37 -8.40 two singlets at δ 7.81 and δ 7.86 for six aromatic protons. Mass spectrum showed base peak corresponding to $[M+H]^+$ at *m/z* 382.

3.3.7 Synthesis and characterization of 2-(2-(4,6-bis(methylthio)-1*H*-pyrazolo[3,4-*d*]-pyrimidin-1-yl)ethyl)phthalazine-1(2*H*)-thione (70).

Reaction of **41** with P_2S_5 in pyridine under reflux conditions gave compound **70**. This compound was characterized by NMR and Mass spectrometric techniques.

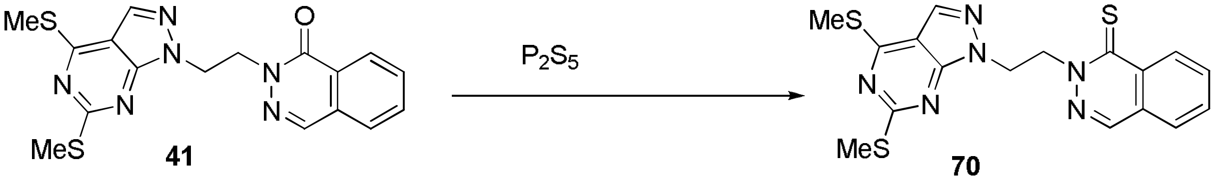

Scheme 9. Synthesis of compounds **70**

Proton NMR of **70 s**howed two singlets at δ 2.24 and δ 2.64 for two SMe groups, two multiplets between δ 5.04–5.07 and between δ 5.26 -5.29 for two NCH_2, three multiplets between δ 7.59–7.62, between δ 7.79 -7.84 and between δ 8.96 -8.99 two singlets at δ 7.90 and δ 8.01 for six aromatic protons. Mass spectrum showed base peak corresponding to $[M+H]^+$ at *m/z* 401.

3.3.8 Synthesis and characterization of 2-(2-(5-methyl-6-(methylthio)-4-oxo-4,5-dihydro-1*H*-pyrazolo[3,4-*d*]pyrimidin-1-yl)ethyl)phthalazin-1(2*H*)-one (71).

Reaction of **51** with methyl iodide in DMF using K_2CO_3 as base gave of compound **71**. This compound was characterized by NMR and Mass spectrometric techniques.

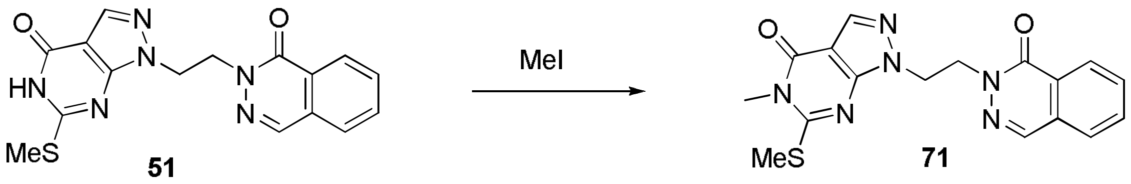

Scheme 10. Synthesis of compounds **71**

Proton NMR of **71** showed two singlets at δ 2.33 for SMe, and δ 3.42 for NMe, two multiplets between δ 4.64–4.68 and between δ 4.76 -4.79 for two NCH_2, three multiplets between δ 7.58–7.61, between δ 7.71 -7.80 and between δ 8.36 -8.39 two singlets at δ 7.86 and δ 7.95 for six aromatic protons. Mass spectrum showed base peak corresponding to $[M+H]^+$ at *m/z* 369.

3.3.9 Synthesis and characterization of 2-(2-(5-methyl-6-(methylsulfonyl)-4-oxo-4,5-dihydro-1*H*-pyrazolo[3,4-*d*]pyrimidin-1-yl)ethyl)phthalazin-1(2*H*)-one (72).

Reaction of **71** with oxone in acetone gave compound **72**. This compound was characterized by NMR and Mass spectrometric techniques.

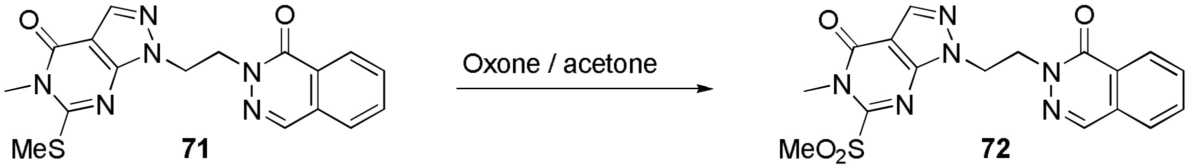

Scheme 11. Synthesis of compounds **72**

Proton NMR of **72** showed two singlets at δ 3.22 for SO_2Me and δ 3.77 for NMe, two multiplets between δ 4.69–4.71 and between δ 4.83 -4.87 for two NCH_2, three multiplets between δ 7.63–7.66, between δ 7.79 -7.84 and between δ 8.38 -8.41 two singlets at δ 7.88 and δ 8.13 for six aromatic protons. Mass spectrum showed base peak corresponding to $[M+H]^+$ at *m/z* 401.

3.3.10 Synthesis and characterization of reference compounds

Compound **73**, **77**, **78**, **79**, **81**, **82**, **83**, **84**, **85** and **89** were synthesized by literature procedures. Other reference compounds **74**, **75**, **76**, **80**, **86**, **87**, **88, 90 and 91** were synthesized by using the same procedures utilized in the synthesis of their respective dimeric compounds. These compounds were characterized by NMR and Mass spectrometric techniques.

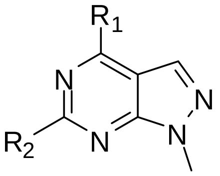

73: R_1 = SMe; R_2 = SMe;
74: R_1 = Pyrrolidine; R_2 = SMe
75: R_1 = piperidine; R_2 = SMe
76: R_1 = morpholine; R_2 = SMe
77: R_1 = OMe; R_2 = SMe
78: R_1 = Cl; R_2 = SMe
79: R_1 = OMe; R_2 = SO_2Me
80: R_1 = Cl; R_2 = SO_2Me
81: R_1 = OMe; R_2 = OMe
82: R_1 = NMe_2; R_2 = SMe

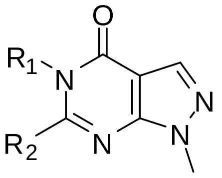

83: R_1 = H; R_2 = SMe;
84: R_1 = Me; R_2 = SMe
85: R_1 = Me; R_2 = SO_2Me

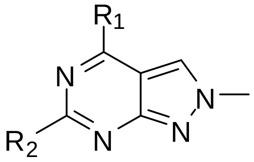

86: R_1 = SMe; R_2 = SMe;
87: R_1 = OMe; R_2 = SMe
88: R_1 = OMe; R_2 = SO_2Me

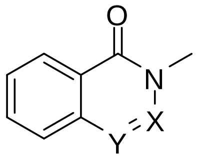

89:X = N; Y = CH
90:X =CH; Y = N
91:X = N; Y = N

Figure 22. Reference compounds

3.4 Result and discussion

In our earlier studies on *ethylene linker* based symmetrical pyrazolo[3,4-*d*]pyrimidine (**PP**) compounds we found that there was a large upfield shift in protons of groups attached at 6-position indicating folded or syn conformation due to intramolecular π–π interactions but our attempts in getting syn conformation in the solid state due to intramolecular π–π interactions in the *ethylene* linker symmetrical compound based on **PP** core were not successful.[39] The present study was undertaken to study the effect of replacing one side of *ethylene* linker based symmetrical pyrazolo[3,4-*d*]pyrimidine compound by quinazilinone, phthalazinone and benzotriazinone nucleus on conformation of the molecule both in solution and more importantly on solid state.

3.4.1 ^{1}H NMR study

In the present study of *ethylene* linker based dissymmetrical pyrazolo[3,4-*d*]pyrimidine compounds we observed an upfield shift in the protons of groups attached to the 6-position compared to their respective monomeric compounds and similar to the *ethylene* linker based symmetrical pyrazolo[3,4-*d*]pyrimidine compounds when the linker was attached to the *N*^{1} position of the pyrazolo[3,4-*d*]pyrimidine ring indicating the presence of folded conformation.[39] Upfield shift in the proton at 4-position in case of phthalazinone (**Pht.)** and proton at 2-position in case of quinazolinone (**Q**) is also observed (**Fig. 23** and **Table 2**)

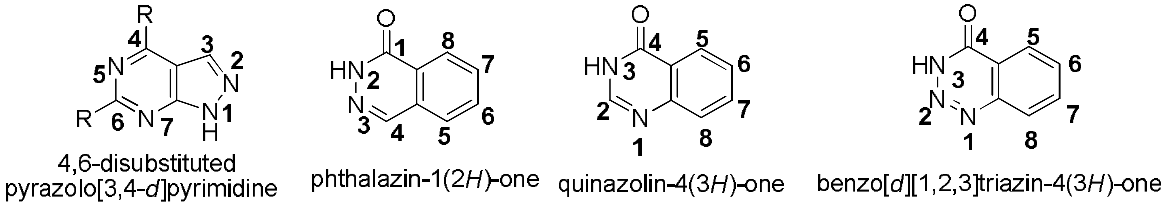

4,6-disubstituted pyrazolo[3,4-*d*]pyrimidine phthalazin-1(2*H*)-one quinazolin-4(3*H*)-one benzo[*d*][1,2,3]triazin-4(3*H*)-one

Figure 23. Numbering scheme for the heterocyclic nuclei used in the present study

However the *N*^{2} isomer (compound **45, 55, 67** and **60**, **Table 2**) did not show any significant upfield shift in any proton indicating open or anti conformation. This shows that there is a profound effect of attachment of linker on intramolecular π–π interactions and it is important that the linker is attached at the right position to show intramolecular stacking interactions. These results are similar to the results obtained in case of symmetrical *trimethylene* linker based symmetrical pyrazolo[3,4-*d*]pyrimidine compounds where the *N*^{1} isomer (compound **22a)** showed intramolecular stacking both in solution and solid state while the *N*^{2} isomer (compound **92**, **Fig. 24**) was devoid of intramolecular stacking both in solution and solid state.[65]

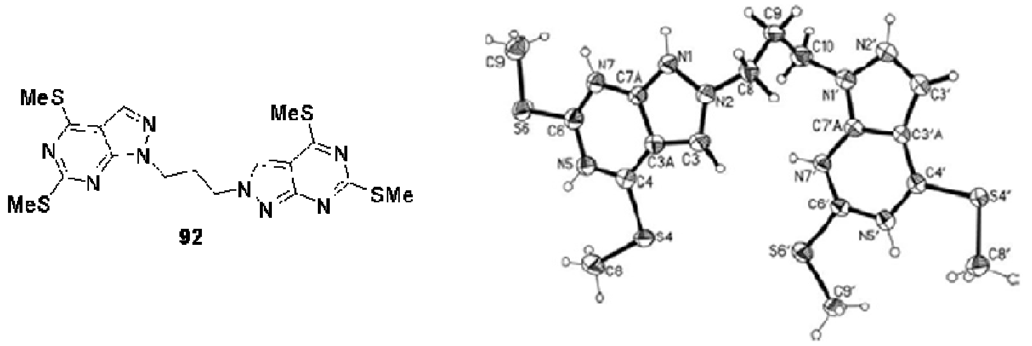

Figure 24. Crystal structure of compound **92** showing open conformation

Also there is no significant change in upfield shifts on changing the substituents from SMe group to pyrrolidine, methoxy, chloro etc. at 4-position or 6-position on intramolecular π–π interactions. This shows that the change of substituents does not change the intramolecular stacking behavior of the pyrazolo[3,4-*d*]pyrimidine nucleus. These results are also similar to the studies on *ethylene* and *trimethylene* linker based symmetrical pyrazolo[3,4-*d*]pyrimidine compounds (**20a-b**, **22a-k** and **23a-c**) where no significant change in the upfield shifts were observed[37,39] on changing the substituents at 4/6-position.

Also the change in the number of nitrogen atom or changing the position of nitrogen atom in the heteroaromatic nucleus (quinazolinone, phthalazinone and benzotriazinone) does not have significant effect on intramolecular π–π interactions as evident from the similar upfield shift of compounds **41**, **42** and **43** (**Scheme 1** and **Table 2**). This shows that these three nucleus have similar intramolecular stacking behavior with pyrazolo[3,4-*d*]pyrimidine nucleus. The change of oxygen atom in compound **41** to sulfur atom in compound **70** is also well tolerated (**Table 2**). Compounds **51**, **52**, **71** and **72** which have pyrazolo[3,4-*d*]pyrimidone nucleus show similar intramolecular π–π interactions as seen in the compounds having pyrazolo[3,4-*d*]pyrimidine nucleus. This result is again similar to the results obtained in the study of *trimethylene* linker based symmetrical pyrazolo[3,4-*d*]pyrimidine/pyrimidone compounds (**22a** and **23a**, **Fig. 17** and **18**). The above results are summarized in **Table 2** and illustrated in the following stack plots in **Fig. 25** for compounds **41**, **61**, **69**, **53**, and **63** which shows the upfield shifts of affected protons due to the intramolecular stacking interactions as compared to their respective monomeric compounds **73**, **78**, **82**, **77** and **79** for pyrazolo[3,4-*d*]pyrimidine protons along with the compound **89** for comparison of proton shifts of phthalazinone protons

Table 2: ^{1}H NMR shifts of compounds used in the present study

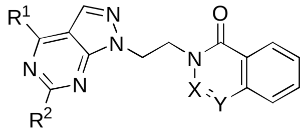

41, 46, 49, 50, 53, 61, 63, 64, 68, 69: X=N; Y=CH.
42, 47, 54, 62, 65: X=CH; Y=N.
43, 48, 59, 66: X=N; Y=N.

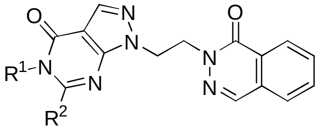

51, 71, 72: X=N; Y=CH.
52: X=CH; Y=N.

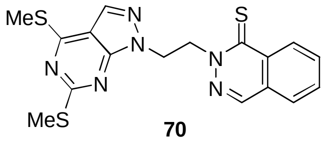

70

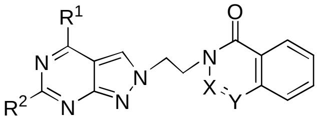

45,55,67: X=N; Y=CH.
60:X=N; Y=N.

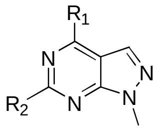

73-82

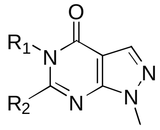

83-85

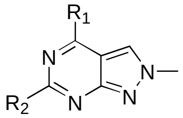

86-88

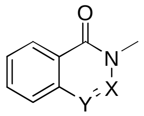

89-91

Comp. No.	**R_1**	**R_2**	**Δ 6-SMe/ SO_2Me/ OMe (PP)**	**δ 2-H/4-H (Q/Pht.)**	**Δδ = 6-SMe/ SO_2Me/ OMe (PP, mono)- 6-SMe/ SO_2Me/ OMe (PP, dimer)**	**Δδ = 2-H/4-H(Q/Pht., monomer) - 2-H/4-H (Q/Pht., dimer)**
73	SMe	SMe	2.68	-	-	-
86	SMe	SMe	2.67	-	-	-
74	pyrrolidine	SMe	2.58	-	-	-
75	piperidine	SMe	2.58	-	-	-
76	morpholine	SMe	2.58			
77	OMe	SMe	2.63			
78	Cl	SMe	2.64			
82	NMe_2	SMe	2.58			
79	OMe	SO_2Me	3.42			
80	Cl	SO_2Me	3.45			
81	OMe	OMe	4.07			
83	H	SMe	2.54^*			
84	Me	SMe	2.64			
85	Me	SO_2Me	3.57			
87	OMe	SMe	2.64			
88	OMe	SO_2Me	3.45			
89	-	-	-	8.14		
90	-	-	-	8.10		
41	SMe	SMe	2.25	7.82	0.43	0.32
42	SMe	SMe	2.28	7.26	0.40	0.84
43	SMe	SMe	2.29	-	0.39	
45	SMe	SMe	2.63	8.03	0.04	0.11
46	pyrrolidine	SMe	2.22	7.87	0.36	0.27
47	pyrrolidine	SMe	2.25	7.25	0.33	0.85
48	pyrrolidine	SMe	2.20	-	0.38	
49	piperidine	SMe	2.21	7.87	0.37	0.27
50	morpholine	SMe	2.21	7.87	0.37	0.27

51	H	SMe	2.26	7.87	-	0.27
52	H	SMe	2.16*	7.58*	0.38	-
53	OMe	SMe	2.25	7.82	0.38	0.32
54	OMe	SMe	2.24	7.26	0.39	0.84
55	OMe	SMe	2.59	8.02	0.05	0.12
59	OMe	SMe	2.26	-	0.37	
60	OMe	SMe	2.61	-	0.03	-
61	Cl	SMe	2.23	7.79	0.41	0.31
62	Cl	SMe	2.25	7.31	0.39	0.79
63	OMe	SO$_2$Me	3.04	7.87	0.38	0.27
64	Cl	SO$_2$Me	3.11	7.90	0.34	0.24
65	OMe	SO$_2$Me	3.04	7.35	0.38	0.75
66	OMe	SO$_2$Me	3.12	-	0.30	-
67	OMe	SO$_2$Me	3.43	8.04	0.02	0.10
68	OMe	OMe	3.60	7.83	0.47	0.31
69	NMe$_2$	SMe	2.23	7.87	0.35	0.27
70	SMe	SMe	2.24	7.90	0.44	-
71	Me	SMe	2.33	7.86	0.31	0.28
72	Me	SO$_2$Me	3.22	7.88	0.35	0.26

* data collected in DMSO-d_6

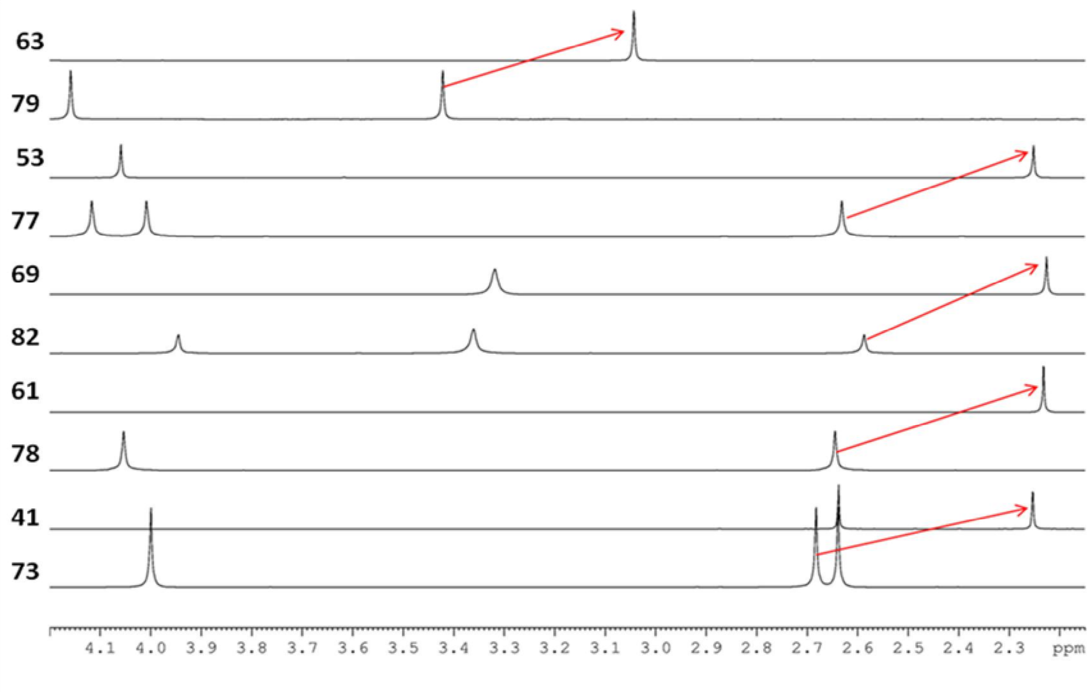

(**a**)

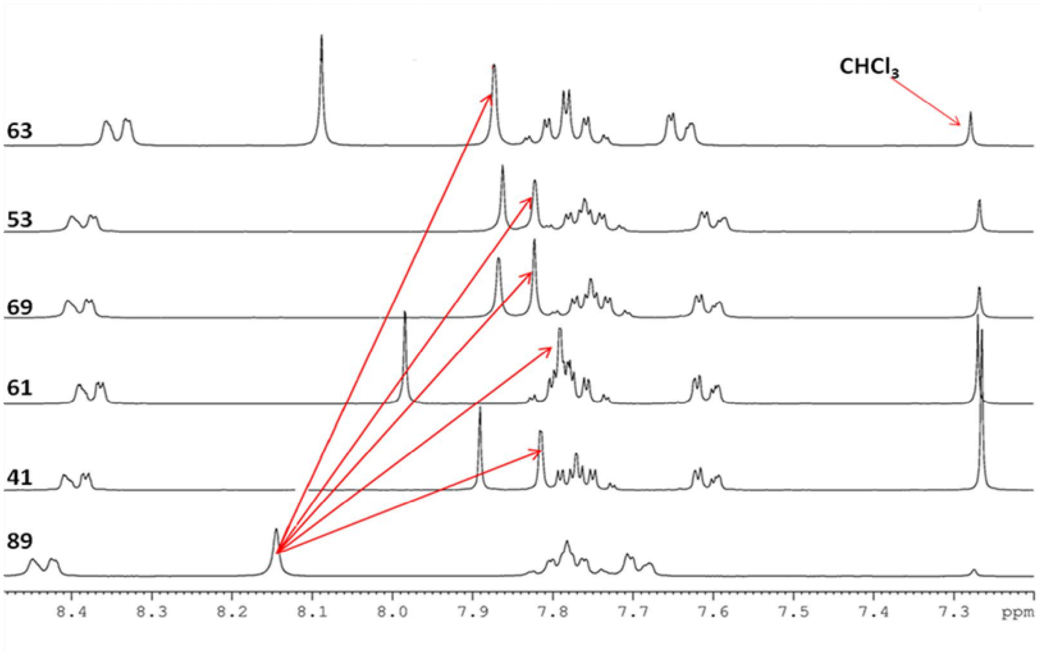

(**b**)

Figure 25. Stack plots showing upfield shifts in (**a**) pyrazolo[3,4-*d*]pyrimidine protons (b) upfield shifts in phthalazinone protons for compounds 41, 61, 69, 53 and 63 compared with their respective reference compounds

On the basis of above ^{1}H NMR study the conformation of compounds in which *ethylene* linker is attached at the N^1 position of pyrazolo[3,4-*d*]pyrimidine appears to be folded or syn. The probable conformation of compounds **41** and **42** are shown in **Fig. 26**.

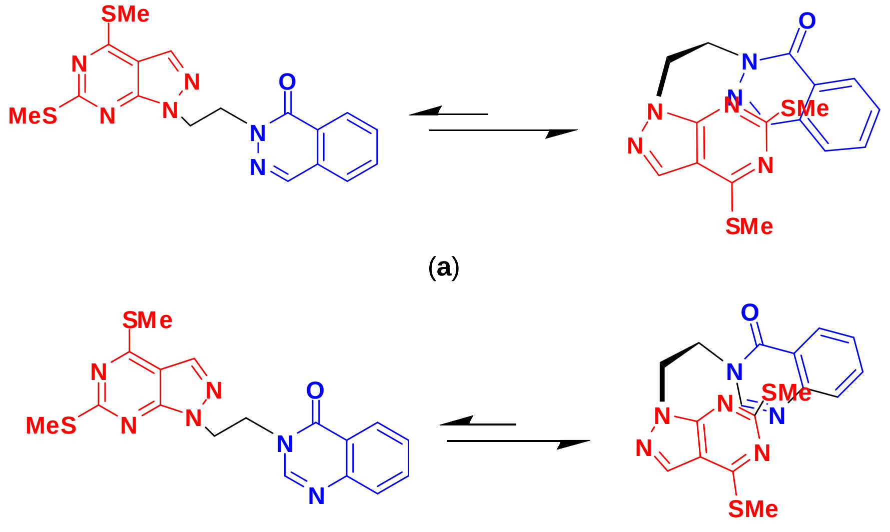

(**a**)

(**b**)

Figure 26. Proposed conformation of (a) compound **41** (b) compound **42** on the basis of ^{1}H NMR study

3.4.2 X-Ray crystallographic study

In this present study we were able to prepare and study crystals of 2-(2-(4,6-bis(methylthio)-1*H*-pyrazolo[3,4-*d*]pyrimidin-1-yl)ethyl)phthalazin-1(2*H*)-one(**41**),[64b] 2-(2-(4-methoxy-6-methylthio--1*H*-pyrazolo[3,4-*d*]pyrimidin-1-yl)ethyl)phthalazin-1(2*H*)-one (**53**), 2-(2-(4-chloro-6-methylthio -1*H*-pyrazolo[3,4-*d*]pyrimidin-1-yl)ethyl)phthalazin-1(2*H*)-one (**61**),[64b] 2-(2-(4-(dimethylamino)-6-(methylthio)-1*H*-pyrazolo[3,4-*d*]pyrimidin-1-yl)ethyl)phthalazin-1(2*H*)-one(**69**), 2-(2-(4-methoxy-6-(methylsulfonyl)-1*H*-pyrazolo[3,4-*d*]pyrimidin-1-yl)ethyl)phthalazin-1(2*H*)one (**63**),[64b] 2-(2-(4-chloro-6-(methylsulfonyl)-1*H*-pyrazolo[3,4-*d*]pyrimidin-1-yl)ethyl)-phthalazin-1(2*H*)-one(**64**)[64b] and 3-(2-(4-methoxy-6-(methylsulfonyl)-1*H*-pyrazolo[3,4-*d*]pyrimidin-1-yl)ethyl)quinazolin-4(3*H*)-one (**65**).[64b]

The solid state structure of **41** shows a *syn* conformation[64b] (**Fig. 27**). The torsion angle formed by NCCN atoms involving *ethylene* linker and two N atoms connecting it is 60.58^o, confirming *syn* conformation. The distance between two N atoms linking two arene moieties is 2.95 Å which is less than sum of van der Waals radii of two N atoms (3.10 Å i.e. 2x1.55 Å for N) and less than 3.09 seen in **22b** with extra C in its linker. The distance between centroids of five member pyrazole ring of **PP** core and six member pyrimidone ring of phthalazinone system is 4.28 Å which is similar to distance of 4.28 Å between centroids of six member pyrimidine and six member heterocyclic ring of phthalazinone system (**Fig.27**). It is important to mention that 4.23 Å is the maximum distance seen in folded compounds (**22a**, **22b**, **22d-22g** and **23a-23c**, **Fig. 17**, **Table 1**) that show such distance in the range of 3.69-4.23 Å. The distance between centroids of nine member **PP** core and six membered pyrimidone ring of phthalazinone system is 4.15 Å. Some close distances between two six member pyrimidine and pyrimidone ring of phthalazinone are C7A…N11= 3.42, N7…N10 = 3.42 and N7…C17 = 3.50 Å confirming intramolecular stacking. Finally, there is no intra-molecular S…arene (4.96 and 5.07 Å)[33a] or significant CH–π interactions[65] confirming that *syn* conformation is due to intramolecular π–π interactions.

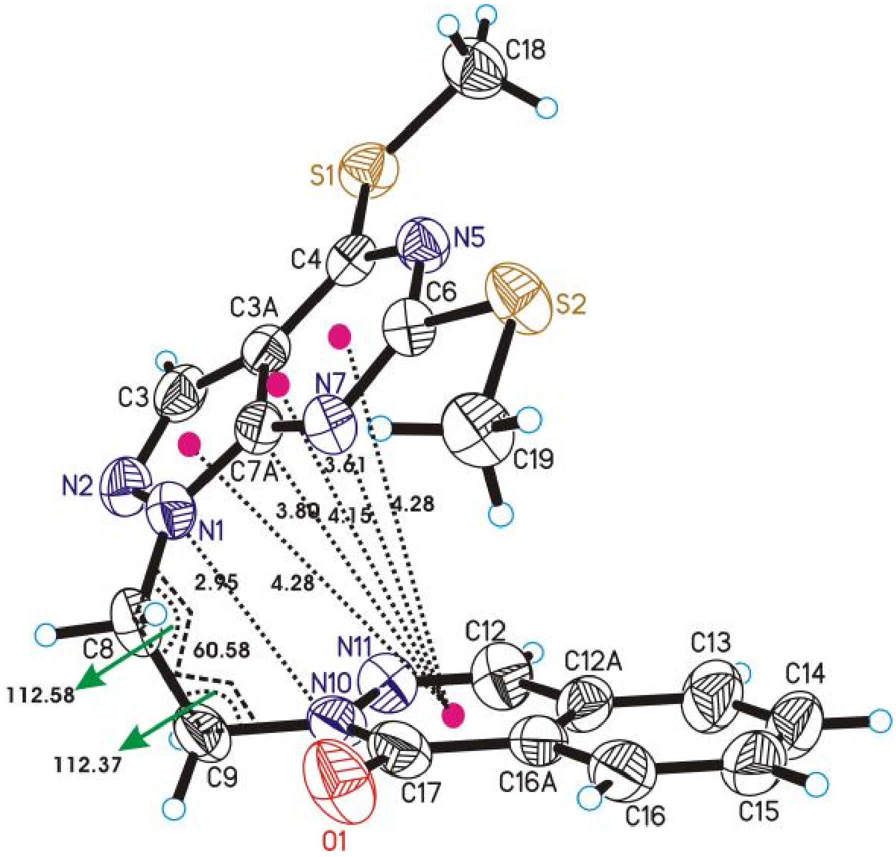

Figure 27. Crystal structure of **41** showing syn conformation with intramolecular π–π interactions[64b]

To test the robustness of *syn* conformation in **41** formed due to intramolecular arene interaction substituents effects were studied**.** The crystal structure of 2-(2-(4-methoxy-6-(methylthio)-1*H*-pyrazolo[3,4-*d*]pyrimidin-1-yl)ethyl)phthalazin-1(2*H*)-one (**53**) shows an *anti* conformation (**Fig. 28**). The torsion angle formed by NCCN atoms involving *ethylene* linker and two N atoms connecting it is 179.15º, confirming *anti* conformation. The distance between two N atoms linking two arene moieties is 3.75 Å which is more than sum of van der Waals radii of two N atoms (3.10 Å i.e. 2x1.55 Å for N). A comparable distance of 3.70 Å was also shown our earlier symmetrical *ethylene* compound **20b** (**Fig. 15**) with anti conformation.[39c]

This change of conformation from syn to anti on changing the substituent from weak electron withdrawing SMe group to weak electron donating OMe group was a bit surprising since this type of change was well tolerated in compounds **22f** (ethoxy) and **22g** (isopropoxy).

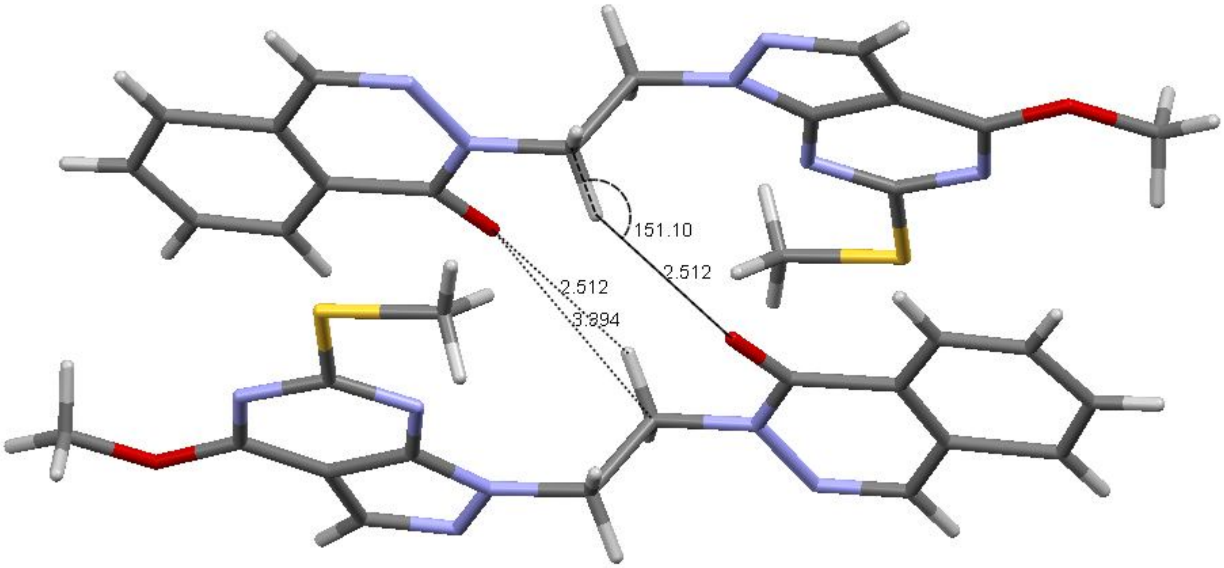

Figure 28. Crystal structure of **53** showing anti conformation with no intramolecular π–π interactions and strong C-H…O interactions between two molecules

One reason for this change of conformation may be that intermolecular interactions between the molecules in the solid state have overcome the intramolecular interactions. On careful analysis we observe that the structure is stabilized by strong C-H…O interactions[66] between two molecules as shown in the figure 26. The C-H…O distance being 2.51 Å which is shorter than the sum of van der Waals radii of hydrogen atom (1.2 Å) and oxygen atom (1.5 Å). The distance between carbon and oxygen is 3.39 Å and the C-H...O angle is 151.10^o. Also in the packing structure we observe intermolecular π–π interactions (**Fig. 29**). The distance between centroids of the six membered pyrimidine and six membered heterocyclic ring of the phthalazinone system 3.67 Å, the distance between centroids of nine membered pyrazolopyrimidine ring and ten membered phthalazinone ring is 3.64 Å, the distance between centroids of the five membered pyrazolo ring and six membered benzene ring if phthalazinone is 3.69 Å, the distance between centroids of the six membered pyrimidine and ten membered phthalazinone ring is 3.57 Å and the distance between centroids of six membered benzene and nine membered pyrazolopyrimidine is 3.63 Å. These distances are well within the limits of distances observed for intramolecular/ intermolecular π–π interactions (**Table 1**). In addition to these interactions we also observe a C-H…S interaction[67] (**Fig. 29**) The C-H…S distance being 2.80 Å which is shorter than the sum of van der Waals radii of hydrogen atom (1.2 Å) and sulphur atom (1.8 Å).

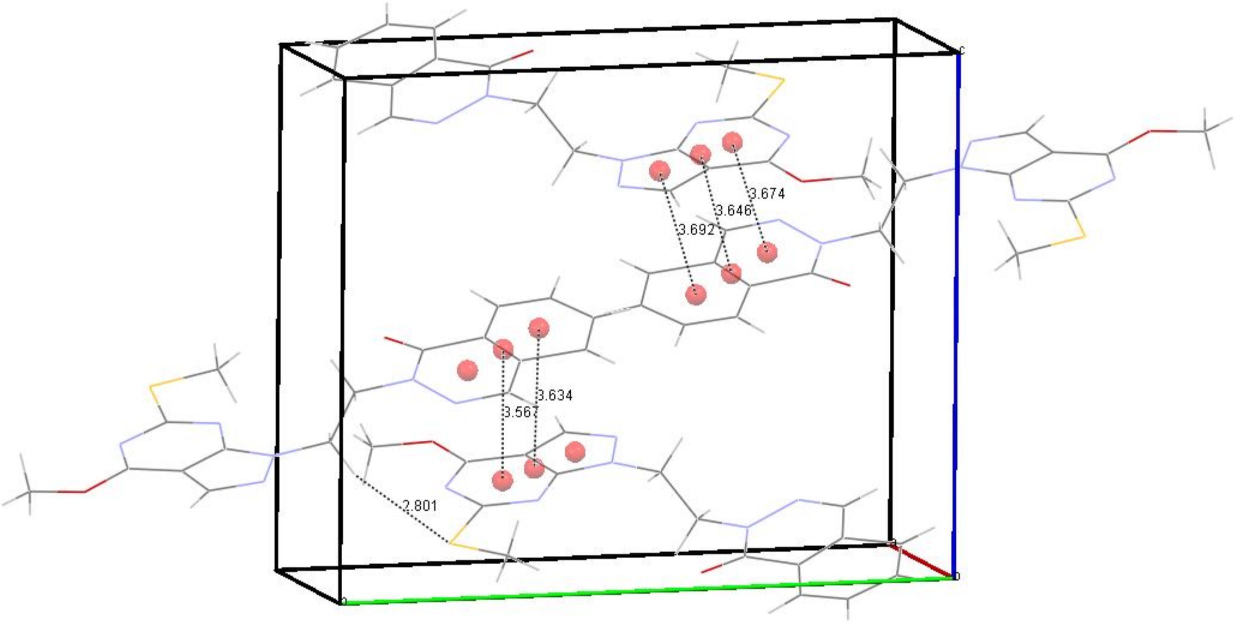

Figure 29. Packing structure of **53** showing intermolecular π–π interactions and C-H…S interactions

The C-H...S angle is 158.32^0 and the distance between carbon and sulphur (H-C…S) is 3.72 Å.

The crystal structure of 2-(2-(4-chloro-6-(methylthio)-1*H*-pyrazolo[3,4-*d*]pyrimidin-1-yl)ethyl)phthalazin-1(2*H*)-one (**61**) in which 4-SMe group of compound **41** is replaced by Cl group shows an *anti* conformation[64b] (**Fig. 30**). The torsion angle formed by NCCN atoms involving *ethylene* linker and two N atoms connecting it is 172.38°, confirming *anti* conformation. The distance between two N atoms linking two arene moieties is 3.72 Å which is more than sum of van der Waals radii of two N atoms (3.10 Å i.e. 2x1.55 Å for N). Here also we observe strong intermolecular interactions which might be one of the reasons for the anti conformation. A careful analysis of the crystal structure of compound **61** shows strong O…arene[67] dimerization (distance of oxygen atom and centroid of nine membered pyrazolopyrimidine ring = 3.25 Å) with the closest distance between O…C of 3.19 Å which is less than the van der Waals radii of O and C atoms. Additional C–H…O (C-H..O = 2.83 Å , H-C…O = 3.61 Å and ∠ C-H..O =138.1°) Cl…arene[68] (distance of chlorine atom and centroid of six membered benzene ring = 3.83 Å) and π–π interactions (distance of centroids of six membered pyrimidine and centroid of six membered benzene ring = 3.83 Å) are also present in this dimer.

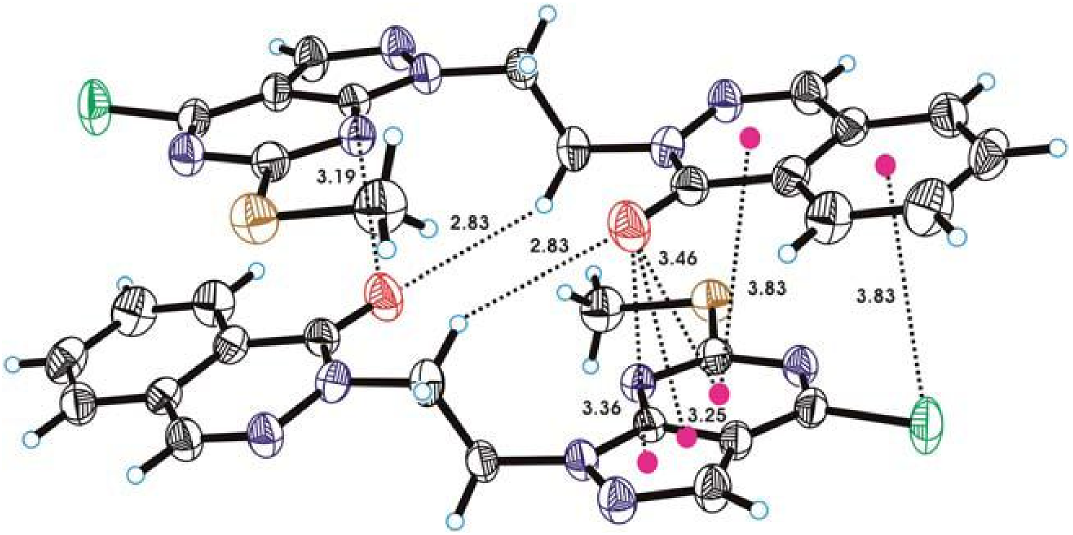

Figure 30. Crystal structure of compound **61** showing anti conformation with intermolecular C–H…O, O…arene, Cl…arene and π–π interactions [64b]

The crystal structure of **69** in which 4-SMe of compound **61** is replaced by electron donating dimethylamino group shows a *syn* conformation (**Fig. 31**). The torsion angle formed by NCCN atoms involving *ethylene* linker and two N atoms connecting it is 61.78º, confirming *syn* conformation. The distance between two N atoms linking two arene moieties is 2.96 Å which is less than sum of van der Waals radii of two N atoms (3.10 Å i.e. 2x1.55 Å for N). The distance between centroids of five member pyrazole ring of **PP** core and six member pyrimidone ring of phthalazinone system is 4.30 Å and distance between centroids of six member pyrimidine and six member heterocyclic ring of phthalazinone system is 4.35 Å (**Fig. 31**). The distance between centroids of nine member **PP** core and six membered pyrimidone ring of phthalazinone system is 4.19 Å. These distances and the torsional angle are very close to the distances and torsional angle observed in the crystal structure of compound **41** having SMe group at the 4-position which is slightly electron withdrawing in nature, in place of strongly electron donating NMe$_2$ group in **69**. The striking similarity of torsional angle (60.58^0 in **41** and 61.78^0 in **69**) and distance between the two N atoms connecting the linker (2.95 Å in **41** and 2.96 Å in **69**) along with other intramolecular distances is noteworthy**.** (**Table 3**)

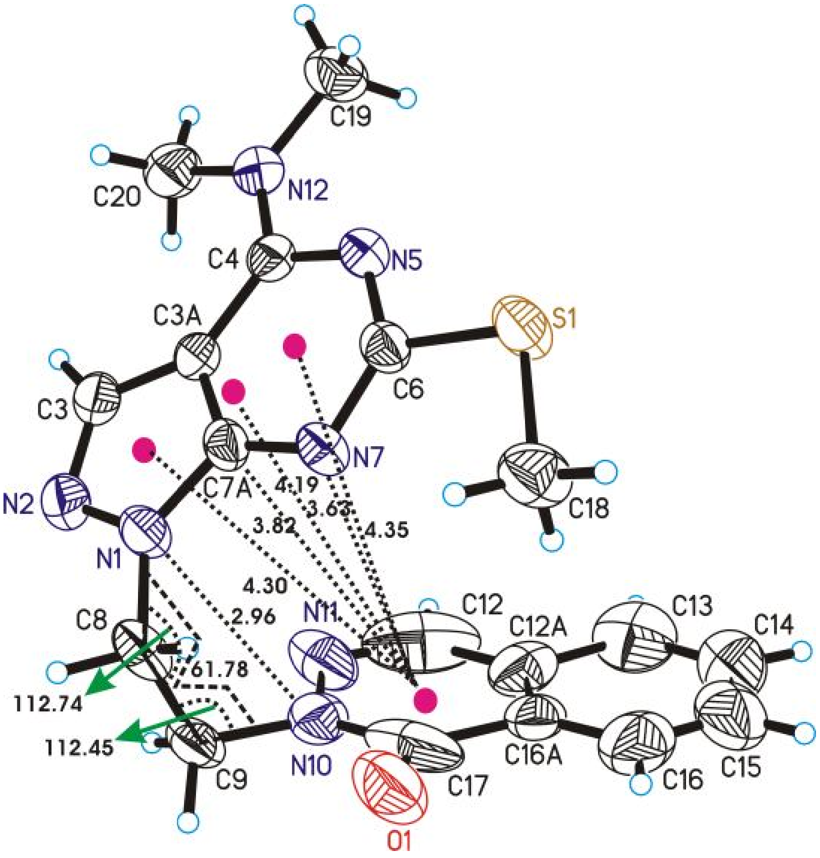

Figure 31. Crystal structure of **69** showing *syn* conformation with intramolecular π–π interactions

The crystal structure of **63** in which 6-SMe of compound **53** is replaced by 6-SO_2Me group shows a *syn* conformation[64b] (**Fig. 32**). The torsion angle formed by NCCN atoms involving *ethylene* linker and two N atoms connecting it is 62.52º, confirming *syn* conformation. The distance between two N atoms linking two arene moieties is 2.93 Å which is less than sum of van der Waals radii of two N atoms (3.10 Å i.e. 2x1.55 Å for N). The distance between centroids of five member pyrazole ring of PP core and six member pyrimidone ring of phthalazinone system is 4.18 Å and distance between centroids of six member pyrimidine and six member heterocyclic ring of phthalazinone system is 4.15 Å (**Fig. 32**). The distance between centroids of nine member PP core and six membered pyrimidone ring of phthalazinone system is 4.02 Å.

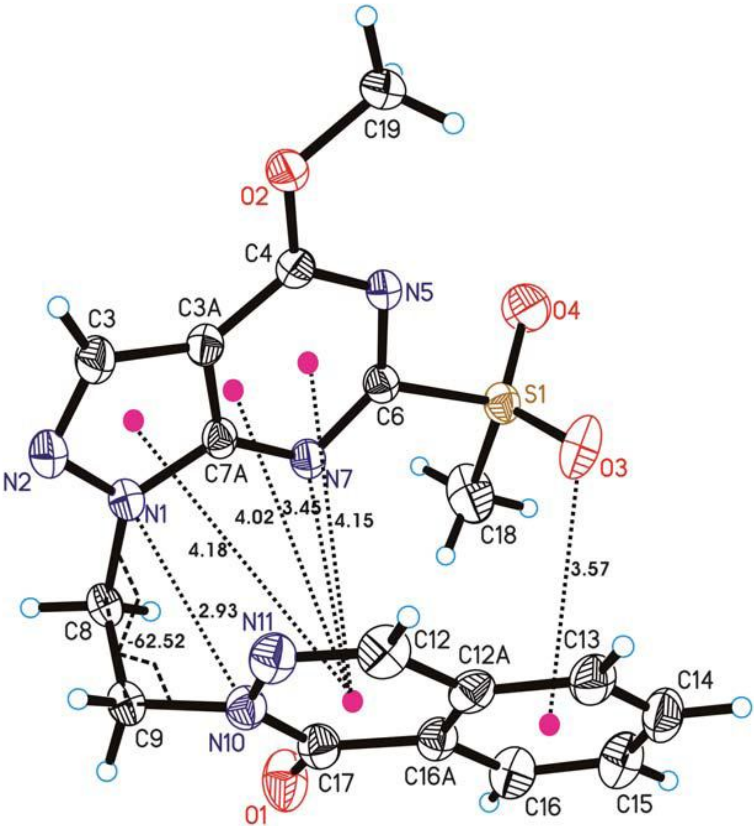

Figure 32. Crystal structure of compound **63** showing syn conformation with intramolecular π–π interactions and O…arene interactions [64b]

In addition to the intramolecular π–π interactions the structure is stabilized by intramolecular O…arene interaction with distance between oxygen atom and centroid of benzene ring being 3.57 Å.

The crystal structure of 2-(2-(4-chloro-6-(methylsulfonyl)-1*H*-pyrazolo[3,4-*d*]pyrimidin-1-yl)ethyl)phthalazin-1(2*H*)-one (**64**) in which 6-SMe group of compound **61** is replaced by 6-SO_2Me group shows an *anti* conformation[64b] (**Fig. 33**). The torsion angle formed by NCCN atoms involving *ethylene* linker and two N atoms connecting it is 173.81°, confirming *anti* conformation. The distance between two N atoms linking two arene moieties is 3.71 Å which is more than sum of van der Waals radii of two N atoms (3.10 Å i.e. 2x1.55 Å for N). Here again we observe strong intermolecular interactions. All the three oxygen atoms are involved in strong

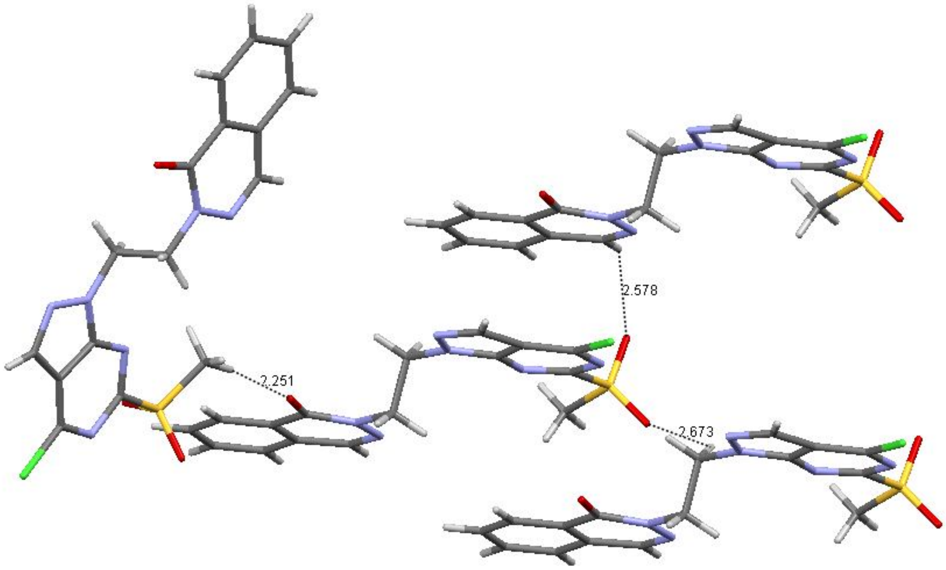

Figure 33. Crystal structure of compound **64** showing open conformation with intermolecular C-H…O interaction [64b]

intermolecular C-H...O interactions as represented by the sub van der waals distances and very favourable C-H...O angle as shown in the **Fig. 33** and listed below.

(i) 2.25 Å (C-H...O), 3.20 Å (H-C...O) and 171.77 (∠ C-H..O);

(ii) 2.58 Å (C-H...O), 3.25 Å (H-C...O) and 129.61 (∠ C-H..O) and

(iii) 2.67 Å (C-H...O), 3.30 Å (H-C...O) and 122.98 (∠ C-H..O).

In addition to the C-H…O interactions there is intermolecular π–π interactions, Cl…O[69] interaction and C-H…Cl interaction as shown in **Fig. 33**. The distance between centroids of five member pyrazole ring of PP core and six member benzene ring of phthalazinone system is 3.59 Å and distance between centroids of six member pyrimidine and six member heterocyclic ring of phthalazinone system is 3.59 Å (**Fig. 34**). The distance between centroids of nine member PP core and ten membered phthalazinone ring is 3.43 Å and is very close to the sum of the van der radii of two carbon atoms which is 3.4 Å. The distance of Cl...O interaction is 2.99 Å which is less than sum of van der waals radii of these atoms which is 3.25 Å (for Cl atom van der waals radii is 1.75 Å and for O atom it is 1.5 Å) and the C-H...Cl distance is 2.94 Å which is again less than sum of van der waals radii of these atoms which is 2.95 Å (for H atom van der waals radius is 1.2 Å). The H-C...Cl distance is 3.78 Å and ∠ C-H..Cl is 149.99°.

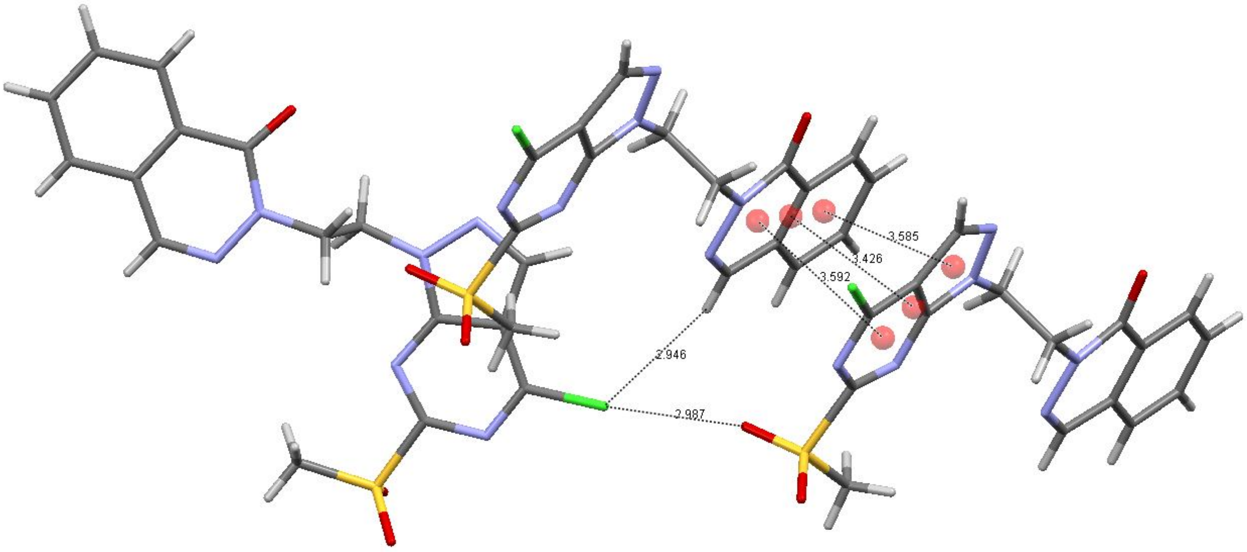

Figure 34. Crystal structure of **64** showing intermolecular π–π, Cl…O and C-H…Cl interaction[64b]

The crystal structure of 3-(2-(4-methoxy-6-(methylsulfonyl)-1*H*-pyrazolo[3,4-*d*]pyrimidin-1-yl)ethyl)quinazolin-4(3*H*)-one (**65**) shows a *syn* conformation.[64b] The torsion angle formed by NCCN atoms involving *ethylene* linker and two N atoms connecting it is 59.97º, confirming *syn* conformation. The distance between two N atoms linking two arene moieties is 2.93 Å which is less than sum of van der Waals radii of two N atoms (3.10 Å i.e. 2x1.55 Å for N). The distance between centroids of five member pyrazole ring of PP core and six member pyrimidone ring of quinazilinone system is 4.23 Å and distance between centroids of six member pyrimidine and six member heterocyclic ring of phthalazinone system is 4.06 Å (**Fig. 35**). The distance between centroids of nine member PP core and six membered pyrimidone ring of phthalazinone system is 3.99 Å.

In addition to the intramolecular π–π interaction a weak C-H... π interaction is also present in the molecule. The closest H contacts with the six membered phenyl ring of quinazolinone are 2.85 and 2.94 Å. These distances and the torosional angle are very close to the distances and torosional angle observed in the crystal structure of compound **63** which has phthalzinone nucleus in place of quinazolinone. This similarity in the two structures is noteworthy.

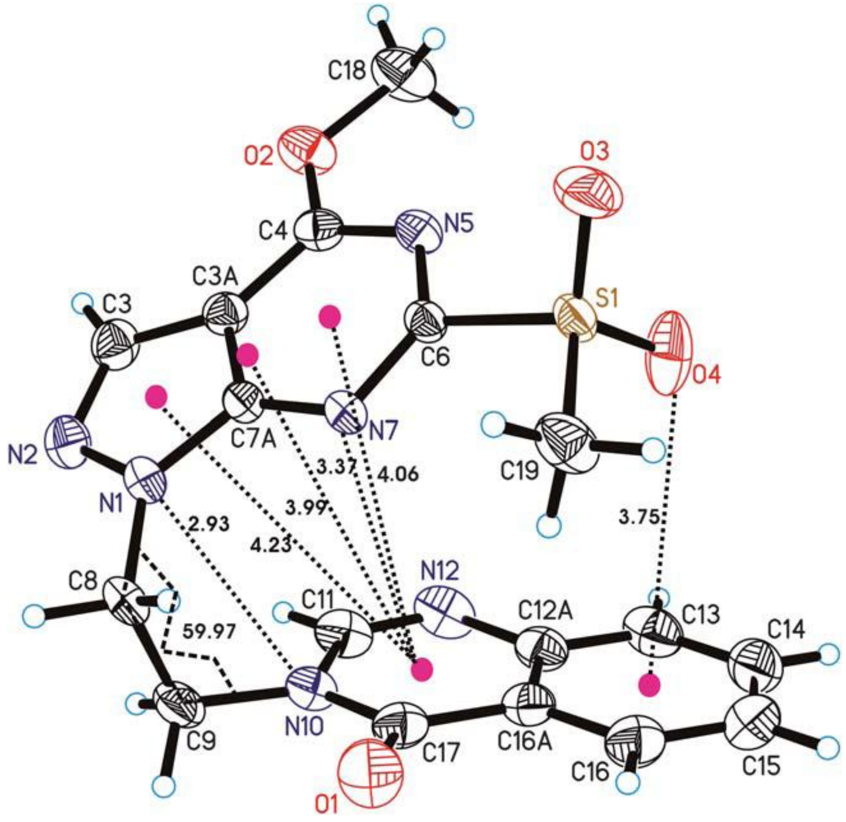

Figure 35. Crystal structure of compound **65** showing syn conformation with intramolecular π–π interactions [64b]

In the analysis of above crystal structures of compounds we observe that out of seven four compounds namely **41**, **69**, **63** and **65** are having syn conformation and rest three are having anti conformation. The folded compounds **41**, **69**, **63** and **65** have similar conformation as shown by the torsional angles and distances which is noteworthy. A summary of the important results obtained in the analysis of the above crystal structures is presented in the following **Table 3**.

Table 3: Important angle and distances obtained from the crystallographic study of compounds **41, 53, 61, 69, 63, 64** and **65.**

Comp. No.	Torsional angle (°)	Distance between two N atoms linking two arene moieties (Å)	Intramolecular Distance 1[*] (Å)	Intramolecular Distance 2[**] (Å)	Intramolecular Distance 3[***] (Å)
41	60.58	2.95	4.28	4.28	4.15
53	179.15	3.75			
61	172.38	3.72			
69	61.78	2.96	4.30	4.35	4.19
63	62.52	2.93	4.18	4.15	4.02
64	173.81	3.71			
65	59.97	2.93	4.23	4.06	3.99

[*] Distance between centroids of six membered heterocyclic ring of pht./ Q and five membered pyrazolo ring of **PP**.

[**] Distance between centroids of six membered heterocyclic ring of pht./ Q and six membered pyrimidine ring of **PP**.

[***] Distance between centroids of six membered heterocyclic ring of pht./ Q and nine membered **PP** ring

Important results obtained in this study are as under:

(i) In the ^{1}H NMR studies a significant upfield shift is seen in protons of compounds connected to the N^1-position of pyrazolo[3,4-*d*]pyrimidine nucleus indicating folded conformation while the compounds attached to the N^2-position of pyrazolo[3,4-*d*]-pyrimidine nucleus did not show any significant upfield shifts indicating open conformation. This shows the importance of position of attachment of linker to show intramolecular π–π interactions.

(ii) The change in the number of nitrogen or position of nitrogen in the ring in case of quinazolinone/phtalazinone/benzotriazinone nucleus does not have significant effect on the intramolecular π–π interactions as shown by the upfield shifts as compared to their respective monomeric compounds. This shows that these nucleus have similar stacking behavior with the pyrazolo[3,4-*d*]pyrimidine nucleus.

(iii) The change of substituent at the 4- or 6- position from electron withdrawing SMe/ Cl/ SO_2Me group to electron donating OMe/pyrrolidine/NMe_2 etc. did not have significant effect on intramolecular π–π interactions in solution state as determined by the ^{1}H NMR studies. However dramatic substituent effect was seen in solid state. Thus four compounds namely **41**, **63**, **69** and **65** show folded conformation due to intramolecular π–π interactions while three other compounds **53**, **61** and **64** showed open or anti conformation. This shows the subtle nature of these interactions and their sensitivity towards environmental conditions as a small change in the substituent or changes the conformation of the molecule from syn to anti (as in compound **41** and **53**) and again from anti to syn (as in compound **53** and **63**). In the solution state studies (^{1}H NMR) the concentration of compound (5-10 mg in 0.5ml of $CDCl_3$) in the solution is low and it can be safely assumed that the molecules are surrounded by solvent molecules only and no intermolecular interactions between the molecules is present. In case of solid state, however, the situation is different. Here the molecule is surrounded by similar molecules and the two arene moieties not only have to come close enough (<3 Å, as in **41**, **63**, **65** and **69**) at the point of contact (which is less than the sum of van der waal radii of two N atoms , thus causing severe steric hindrance), intramolecular π–π interactions have also to compete with other strong intermolecular interactions to show a syn conformation in 1,2-diarylethanes.

(iv) The folded compounds **41**, **69**, **63** and **65** show striking similarity in the solid state structure as shown by the torsional angles which has values in the range of 59-63^o and the distance between the two N atoms linking the two arene moieties which has values in the range of 2.93-2.96 Å. This close range of values in compounds having different substituents and different arene moieties suggest that the conformation control due to intramolecular π–π interactions observed in these molecules is robust from crystal engineering point of view.

3.5 Biological activity

Compounds **41, 42, 43, 45, 48, 51, 53, 63, 64, 67, 68, 70** and **71** were tested for antithrombotic activity in mice at 30 µM concentrations in collaboration with Dr. Madhu Dikshit, Pharmacology Division, CDRI, Lucknow. The results are shown below (**Table 4**).

Table 4: Biological activity

Compound	Dose	% Protection
41	30 μM/kg, po	20%
42	30 μM/kg, po	40%
45	30 μM/kg, po	40%
51	30 μM/kg, po	30%
53	30 μM/kg, po	0%
63	30 μM/kg, po	0%
64	30 μM/kg, po	45%
67	30 μM/kg, po	0%
68	30 μM/kg, po	40%
70	30 μM/kg, po	50%
71	30 μM/kg, po	0%

3.6 Conclusion

In conclusion, this study shows that the intramolecular stacking propensity of *ethylene* linker based dissymmetrical pyrazolo[3,4-*d*]pyrimidine compounds having quinazolinone/ phtalazinone/benzotriazinone nucleus at the other end have similar stacking propensity to the *ethylene* linker based symmetrical pyrazolo[3,4-*d*]pyrimidine compounds in solution state. More importantly, we have successfully demonstrated, for the first time, that conformation control due to arene interactions can be achieved in1,2-diaryl *ethylene* linker compounds in solid state. Apparently, two arene systems not only have to come close enough (<3 Ǻ, as in **41**, **63** and **65**) at the point of contact (which is much less than 3.4 Ǻ, for two benzenoid systems thus causing severe steric hindrance), intramolecular π–π interactions have also to compete with other strong intermolecular interactions to show a syn conformation in 1,2-diarylethanes.

This work together with our earlier work on *trimethylene*, *butylidene* linkers for 1,3-diaryl-propanes, opens a new window for conformation control in flexible 1,2-diaryethanes. In addition, the worthiness of the pyrazolo[3,4-*d*]pyrimidine core as a novel system for studying arene interactions, both in solution and solid state, is demonstrated once again.

3.7 Experimental Section

3.7.1 Synthesis of 3-(2-(6-(methylthio)-4-(pyrrolidin-1-yl)-1*H*-pyrazolo[3,4-*d*]pyrimidin-1-yl)ethyl)- benzo[*d*][1,2,3]triazin-4(3*H*)-one (48).

48: Yield: 93.5%; mp: 140-142 °C; MS (ESI) m/z 409 $[M+H]^+$; ^1H NMR (300 MHz, $CDCl_3$): δ (ppm): 1.91-1.96 (m, 2H, CH_2 pyrrolidino), 2.07-2.12 (m, 2H, CH_2 pyrrolidino), 2.20 (s, 3H, SCH_3), 3.65-3.73 (m, 4H, NCH_2 pyrrolidino), 4.86 (s, 4H, NCH_2), 7.74 (s, 1H, Ar-H), 7.73-7.78 (m, 1H, Ar); 7.86-7.91 (m, 1H, Ar); 8.00-8.03 (m, 1H, Ar); 8.30-8.33 (m, 1H, Ar); ^{13}C NMR (50 MHz, $CDCl_3$) δ (ppm): 13.70, 24.30, 25.85, 44.97, 47.34, 47.99, 49.63, 98.86, 119.65, 124.92, 128.20, 132.13, 133.52, 134.66, 144.08, 154.07, 155.06, 155.72, 169.00; Anal. Calcd. for $C_{19}H_{20}N_8OS$: C, 55.87; H, 4.94; N, 27.43; Found: C, 55.94; H, 5.04; N, 23.56.

3.7.2 Synthesis of 2-(2-(6-(methylthio)-4-(piperidin-1-yl)-1*H*-pyrazolo[3,4-*d*]pyrimidin-1-yl)ethyl)- phthalazin-1(2*H*)-one (49).

49: Yield: 92%; mp: 116-118 °C; MS (ESI) m/z 422 $[M+H]^+$; ^1H NMR (300 MHz, $CDCl_3$): δ (ppm): 1.64-1.72 (m, 6H, CH_2 piperidinyl), 2.21 (s, 3H, SCH_3), 3.82-3.87 (m, 4H, NCH_2 piperidinyl), 4.65-4.68 (m, 2H, NCH_2), 4.80 -4.84 (m, 2H, NCH_2), 7.59-7.63 (m, 1H, Ar), 7.71-7.80 (m, 2H, Ar), 7.81 (s, 1H, Ar-H), 7.87 (s, 1H, Ar-H), 8.38-8.41 (m, 1H, Ar). Anal. Calcd. for $C_{21}H_{23}N_7OS$: C, 59.84; H, 5.50; N, 23.26; Found: C, 59.94; H, 5.74; N, 23.56.

3.7.3 Synthesis of 2-(2-(6-(methylthio)-4-morpholino-1*H*-pyrazolo[3,4-*d*]pyrimidin-1-yl)ethyl)phthalazin-1(2*H*)-one (50).

50: Yield: 90%; mp: 110-112 °C; MS (ESI) m/z 424 $[M+H]^+$; ^1H NMR (300 MHz, $CDCl_3$): δ (ppm): 2.21 (s, 3H, SCH_3), 3.80-3.83 (m, 6H, NCH_2 morpholinyl), 3.88-3.91 (m, 4H, OCH_2 morpholinyl), 4.65-4.69 (m, 2H, NCH_2), 4.82 -4.86 (m, 2H, NCH_2), 7.60-7.63 (m, 1H, Ar), 7.71-7.79 (m, 2H, Ar), 7.80 (s, 1H, Ar-H), 7.87 (s, 1H, Ar-H), 8.37-8.40 (m, 1H, Ar); ^{13}C NMR (50 MHz, $CDCl_3$) δ (ppm): 13.68, 45.32, 50.88, 66.48, 98.04, 126.05, 126.58, 127.73, 129.67, 131.50, 132.79, 133.04, 137.48, 155.70, 156.07, 159.56, 168.58. Anal. Calcd. for $C_{19}H_{20}N_8OS$: C, 56.72; H, 5.00; N, 23.15; Found: C, 56.89; H, 5.04; N, 23.56.

3.7.4 Synthesis of 2-(2-(6-(methylthio)-4-oxo-4,5-dihydro-1*H*-pyrazolo[3,4-*d*]pyrimidin-1-yl)ethyl phthalazin-1(2*H*)-one (51).

51: Yield: 80%; mp: > 250 °C; MS (ESI) m/z 355 $[M+H]^+$; ^1H NMR (300 MHz, $CDCl_3$) δ (ppm): 2.26 (s, 3H, SMe), 4.66-4.69 (m, 2H, NCH_2), 4.80-4.83 (m, 2H, NCH_2), 7.61–7.64 (m, 1H, Ar-H), 7.74–7.84 (m, 2H, Ar-H), 7.87 (s, 1H, Ar-H), 7.99 (s, 1H, Ar-H), 8.39–8.42 (m. 1H, Ar-H) ^{13}C NMR (75 MHz, DMSO-d$_6$) δ (ppm): 13.19, 46.05, 51.69, 103.59, 126.53, 127.63, 127.76, 130.26, 132.87, 134.47, 135.68, 138.48, 153.34, 159.58. Anal. Calcd. for $C_{16}H_{14}N_6OS_2$: C, 54.23; H, 3.98; N, 23.71; Found: C, 54.21; H, 3.84; N, 23.75.

3.7.5 Synthesis of 3-(2-(6-(methylthio)-4-oxo-4,5-dihydro-1*H*-pyrazolo[3,4-*d*]pyrimidin-1-yl)ethyl) quinazolin-4(3*H*)-one (52).

52: Yield: 80%; mp: > 250 °C; MS (ESI) m/z 355 $[M+H]^+$; ^{1}H NMR (300 MHz, DMSO-*d$_6$*) δ (ppm): 2.16 (s, 3H, SMe), 4.32-4.41 (m, 2H, NCH_2), 4.61-4.71 (m, 2H, NCH_2), 7.46 –7.58 (m, 1H, Ar-H), 7.58 (s, 1H, Ar-H), 7.76 -7.84 (m, 2H, Ar-H), 8.00 (s, 1H, Ar-H), 8.11–8.15 (m. 1H, Ar-H). Anal. Calcd. for $C_{16}H_{14}N_6OS_2$: C, 54.23; H, 3.98; N, 23.71; Found: C, 54.25; H, 3.88; N, 23.79.

3.7.6 Synthesis of 2-(2-(4-methoxy-6-(methylthio)-1*H*-pyrazolo[3,4-*d*]pyrimidin-1-yl)ethyl)-phthalazin-1(2*H*)-one (53).

53: Yield: 88%; mp: 158–160 °C; MS (ESI) m/z 369 $[M+H]^+$; ^{1}H NMR (300 MHz, $CDCl_3$) δ (ppm): 2.25 (s, 3H, SMe), 4.06 (s, 3H, OMe), 4.66–4.70 (m, 2H, NCH_2), 4.84–4.89 (m, 2H, NCH_2), 7.59–7.61 (m, 1H, Ar-H), 7.71–7.81 (m, 2H, Ar-4H), 7.82 (s, 1H, Ar-H), 7.86 (s, 1H, Ar-H), 8.37–8.40 (m. 1H, Ar-H) ^{13}C NMR(75 MHz, $CDCl_3$) δ (ppm): 13.57, 45.32, 50.75, 53.84, 99.69, 125.80, 126.34, 127.47, 129.40, 131.31, 131.64, 132.87, 137.22, 155.88, 159.32, 162.45, 169.16. Anal. Calcd. for $C_{17}H_{16}N_6O_2S$: C, 55.42; H, 4.38; N, 22.81; Found: C, 55.30; H, 4.79; N, 22.95.

3.7.7 Synthesis of 3-(2-(4-Methoxy-6-(methylthio)-1*H*-pyrazolo[3,4-*d*]pyrimidin-1-yl)ethyl)-quinazolin-4(3*H*)-one (54).

54: Yield: 84%; mp: 156–158 °C; MS (ESI) m/z 369 $[M+H]^+$; ^{1}H NMR (300 MHz, $CDCl_3$) δ (ppm): 2.24 (s, 3H, SMe), 4.06 (s, 3H, OMe), 4.46–4.48 (m, 2H, NCH_2), 4.80–4.82 (m, 2H, NCH_2), 7.26 (s, 1H, Ar-H), 7.48–7.53 (m, 1H, Ar-H), 7.57–7.60 (m, 1H, Ar-H), 7.71–7.76 (m, 1H, Ar-H), 7.92 (s, 1H, Ar-H), 8.30–8.33 (m. 1H, Ar-H) ^{13}C NMR(75 MHz, $CDCl_3$) δ (ppm): 13.79, 45.20, 46.74, 54.20, 99.85, 121.75, 126.47, 127.23, 127.41, 132.68, 134.29, 145.66, 147.87, 156.27, 161.09, 162.67, 170.35. Anal. Calcd. for $C_{17}H_{16}N_6O_2S$: C, 55.42; H, 4.38; N, 22.81; Found: C, 55.28; H, 4.76; N, 22.99.

3.7.8 Synthesis of 2-(2-(4-methoxy-6-(methylthio)-2*H*-pyrazolo[3,4-*d*]pyrimidin-2-yl)ethyl)-phthalazin-1(2*H*)-one (55).

55: Yield: 84%; mp: 112–114 °C; MS (ESI) m/z 369 $[M+H]^+$; ^1H NMR (300 MHz, $CDCl_3$) δ (ppm): 2.59 (s, 3H, SMe), 4.02 (s, 3H, OMe), 4.80 (s, 4H, NCH_2), 7.63–7.66 (m, 1H, Ar-H),7.79 (s, 1H, Ar-H), 7.73 -7.79 (m, 2H, Ar-H), 8.02 (s, 1H, Ar-H), 8.37 -8.40 (m. 1H, Ar-H). Anal. Calcd. for $C_{17}H_{16}N_6O_2S$: C, 55.42; H, 4.38; N, 22.81; Found: C, 55.38; H, 4.66; N, 22.89.

3.7.9 Synthesis of 3-(2-bromoethyl)benzo[*d*][1,2,3]triazin-4(3*H*)-one (57).

57: Yield: 80%; mp: 90–92 °C; MS (ESI) m/z 252 $[M+H]^+$; ^1H NMR (300 MHz, $CDCl_3$) δ (ppm): 3.82 (t, *J* = 2.4 Hz, 2H, CH_2Br), 4.80 (t, *J* = 2.4 Hz, 2H, NCH_2), 7.80-7.86 (m, 1H, Ar-H), 7.95-8.00 (m, 1H, Ar-H), 8.18 (d, *J* = 8.1 Hz, 1H, Ar-H), 8.37 (d, *J* = 8.1 Hz, 1H, Ar-H).

3.7.10 Synthesis of 3-(2-(4-methoxy-6-(methylthio)-1*H*-pyrazolo[3,4-*d*]pyrimidin-1-yl)ethyl)benzo[*d*]- [1,2,3]triazin-4(3*H*)-one (59).

59: Yield: 58%; mp: 154–156 °C; MS (ESI) m/z 370 $[M+H]^+$; ^1H NMR (300 MHz, $CDCl_3$) δ (ppm): 2.26 (s, 3H, SMe), 4.04 (s, 3H, OMe), 4.91 (s, 4H, NCH_2), 7.75–7.80 (m, 1H, Ar-H), 7.84 (s, 1H, Ar-H), 7.89–7.94 (m, 1H, Ar-H), 8.04 (d, *J* = 6 Hz, 1H, Ar-H), 8.31 (s, *J* = 6 Hz, 1H, Ar-H). Anal. Calcd. for $C_{16}H_{15}N_7O_2S$: C, 52.02; H, 4.09; N, 26.54; Found: C, 52.38; H, 4.46; N, 26.89.

3.7.11. Synthesis of 3-(2-(4-methoxy-6-(methylthio)-2*H*-pyrazolo[3,4-*d*]pyrimidin-2-yl)ethyl)benzo[*d*] [1,2,3]triazin-4(3*H*)-one (60).

60: Yield: 88%; mp: 158–160 °C; MS (ESI) m/z 370 $[M+H]^+$; ^1H NMR (300 MHz, $CDCl_3$) δ (ppm): 2.61 (s, 3H, SMe), 4.05 (s, 3H, OMe), 4.85–4.89 (m, 2H, NCH_2), 5.04–5.08 (m, 2H, NCH_2), 7.80–7.84 (m, 1H, Ar-H), 7.83 (s, 1H, Ar-H), 7.94–7.99 (m, 1H, Ar-H), 8.12 (d, *J* = 6 Hz, 1H, Ar-H), 8.34 (s, *J* = 6 Hz, 1H, Ar-H). Anal. Calcd. for $C_{16}H_{15}N_7O_2S$: C, 52.02; H, 4.09; N, 26.54; Found C, 52.37; H, 4.42; N, 26.82.

3.7.12 Synthesis of 2-(2-(4-chloro-6-methylthio-1*H*-pyrazolo[3,4-*d*]pyrimidin-1-yl)ethyl)-phthalazin-1(2*H*)-one (61).

61: Yield: 85%; mp: 210–212 °C (Chloroform + Ethyl acetate); MS (ESI) m/z 373 $[M+H]^+$; ^1H NMR (300 MHz, $CDCl_3$) δ (ppm): 2.23 (s, 3H, SMe), 4.67–4.70 (m, 2H, NCH_2), 4.91–4.93 (m, 2H, NCH_2), 7.59–7.62 (m, 1H, Ar-H), 7.73–7.82 (m, 3H, Ar-4H), 7.98 (s, 1H, Ar-H), 8.36–8.39 (m. 1H, Ar-H) ^{13}C NMR(75 MHz, $CDCl_3$) δ (ppm): 13.84, 45.76, 50.67, 110.26, 126.01, 126.34, 127.40, 129.38, 131.59, 132.70, 133.15, 137.44, 153.57, 154.50, 159.37, 169.84. Anal. Calcd. for $C_{16}H_{13}ClN_6OS$: C, 51.54; H, 3.51; N, 22.54; Found: C, 51.65; H, 3.59; N, 22.65.

3.7.13 Synthesis of 3-(2-(4-chloro-6-(methylthio)-1*H*-pyrazolo[3,4-*d*]pyrimidin-1-yl)ethyl)quinazolin-4(3*H*)-one (62).

62: Yield: 86%; mp: 220–222 °C; MS (ESI) m/z 373 $[M+H]^+$; ^1H NMR (300 MHz, $CDCl_3$) δ (ppm): 2.25 (s, 3H, SMe), 4.46–4.50 (m, 2H, NCH_2), 4.82–4.86 (m, 2H, NCH_2), 7.31 (s, 1H, Ar-H), 7.46–7.57 (m, 2H, Ar-H), 7.69-7.74 (m, 1H, Ar-4H), 8.01 (s, 1H, Ar-H), 8.26 -8.29 (m. 1H, Ar-H). Anal. Calcd. for $C_{16}H_{13}ClN_6OS$: C, 51.54; H, 3.51; N, 22.54; Found: C, 51.68; H, 3.69; N, 22.64.

3.7.14 Synthesis of 2-(2-(4-methoxy-6-(methylsulfonyl)-1*H*-pyrazolo[3,4-*d*]pyrimidin-1-yl)ethyl) phthalazin-1(2*H*)-one (63).

63: Yield: 85%; mp: 198–200 °C; (Chloroform + Ethyl acetate); MS (ESI) m/z 401 $[M+H]^+$; ^1H NMR (300 MHz, $CDCl_3$) δ (ppm): 3.04 (s, 3H, SO_2Me), 4.23 (s, 3H, OMe), 4.70–4.73 (m, 2H, NCH_2), 4.98–5.02 (m, 2H, NCH_2), 7.63–7.66 (m, 1H, Ar-H), 7.73–7.86 (m, 2H, Ar-H), 7.87 (s, 1H, Ar-H), 8.09 (s, 1H, Ar-H), 8.33–8.36 (m. 1H, Ar-H) ^{13}C NMR(75 MHz, $CDCl_3$) δ (ppm): 38.52, 46.38, 50.72, 55.37, 103.44, 126.36, 127.39, 129.50, 131.80, 132.30, 133.34, 137.88, 154.05, 159.45, 161.89, 165.00. Anal. Calcd. for $C_{17}H_{16}N_6O_4S$: C, 50.99; H, 4.03; N, 20.99; Found: C, 51.25; H, 4.29; N, 20.95.

3.7.15 Synthesis of 2-(2-(4-chloro-6-(methylsulfonyl)-1*H*-pyrazolo[3,4-*d*]pyrimidin-1-yl)ethyl) phthalazin-1(2*H*)-one (64).

64: Yield: 87%; mp: 218-220 °C; (Chloroform + Ethyl acetate) MS (ESI) m/z 405 $[M+H]^+$; ^1H NMR (300 MHz, $CDCl_3$) δ (ppm): 3.11 (s, 3H, SO_2Me), 4.72–4.75 (m, 2H, NCH_2), 5.06–5.09 (m, 2H, NCH_2), 7.64–7.66 (m, 1H, Ar-H), 7.73–7.84 (m, 2H, Ar-H), 7.90 (s, 1H, Ar-H), 8.24 (s, 1H, Ar-H), 8.30–8.32 (m. 1H, Ar-H) ^{13}C NMR(75 MHz, $CDCl_3$) δ (ppm): 39.01, 47.01, 50.4, 114.72, 126.10, 126.51, 127.50, 129.40, 131.80, 133.20, 138.10, 152.40, 156.30, 159.30, 161.40. Anal. Calcd. for $C_{16}H_{13Cl}N_6O_3S$: C, 47.47; H, 3.24; N, 20.76; Found: C, 47.57; H, 3.29; N, 20.95

3.7.16 Synthesis of 3-(2-(4-methoxy-6-(methylsulfonyl)-1*H*-pyrazolo[3,4-*d*]pyrimidin-1-yl)ethyl) quinazolin-4(3*H*)-one (65).

65: Yield: 86%; mp: 208-210 °C; (Chloroform + Ethyl acetate) MS (ESI) m/z 401 $[M+H]^+$; ^1H NMR (300 MHz, $CDCl_3$) δ (ppm): 3.04 (s, 3H, SO_2Me), 4.24 (s, 3H, OMe), 4.52–4.55 (m, 2H, NCH_2), 4.94–4.97 (m, 2H, NCH_2), 7.35 (s, 1H, Ar-H), 7.49–7.60 (m, 2H, Ar-H), 7.72–7.77 (m, 1H, Ar-H), 8.15 (s, 1H, Ar-H), 8.29–8.31 (m. 1H, Ar-H) ^{13}C NMR(75 MHz, $CDCl_3$) δ (ppm): 38.63, 45.98, 46.83, 55.67, 103.56, 121.59, 126.56, 127.45, 127.71, 133.14, 134.71, 145.79, 147.46, 154.42, 160.94, 162.52, 165.28. Anal. Calcd. for $C_{17}H_{16}N_6O_4S$: C, 50.99; H, 4.03; N, 20.99; Found C, 51.05; H, 4.01; N, 21.10.

3.7.17 Synthesis of 3-(2-(4-methoxy-6-(methylsulfonyl)-1*H*-pyrazolo[3,4-*d*]pyrimidin-1-yl)ethyl) benzo[*d*][1,2,3] triazin-4(3*H*)-one (66).

66: Yield: 80%; mp: 230-232 °C; MS (ESI) m/z 401 $[M+H]^+$; ^1H NMR (300 MHz, $CDCl_3$) δ (ppm): 3.12 (s, 3H, SO_2Me), 4.22 (s, 3H, OMe), 4.93–4.96 (m, 2H, NCH_2), 5.04–5.07 (m, 2H, NCH_2), 7.77–7.84 (m, 1H, Ar-H), 7.91–7.97 (m, 1H, Ar-H), 8.06 (s, 1H, Ar-H), 8.04–8.08 (m, 1H, Ar-H), 8.28–8.33 (m. 1H, Ar-H). Anal. Calcd. for $C_{16}H_{15}N_7O_4S$: C, 47.88; H, 3.77; N, 24.43; Found C, 47.99; H, 3.87; N, 24.50.

3.7.18 Synthesis of 2-(2-(4-methoxy-6-(methylsulfonyl)-2*H*-pyrazolo[3,4-*d*]pyrimidin-2-yl)ethyl) phthalazin-1(2*H*)-one (67).

67: Yield: 86%; mp: 218-220 °C; MS (ESI) m/z 401 $[M+H]^+$; ^1H NMR (300 MHz, $CDCl_3$) δ (ppm): 3.43 (s, 3H, SO_2Me), 4.21 (s, 3H, OMe), 4.82–4.86 (m, 2H, NCH_2), 4.93–4.97 (m, 2H, NCH_2), 7.66–7.69 (m, 1H, Ar-H), 7.77–7.86 (m, 2H, Ar-H), 8.01 (s, 1H, Ar-H), 8.04 (s, 1H, Ar-H), 8.38–8.40 (m, 1H, Ar-H).

3.7.19 Synthesis of 2-(2-(4,6-dimethoxy-1*H*-pyrazolo[3,4-*d*]pyrimidin-1-yl)ethyl)phthalazin-1(2*H*)-one (68).

68: Yield: 82%; mp: 168-170 °C; MS (ESI) m/z 353 $[M+H]^+$; ^1H NMR (300 MHz, $CDCl_3$) δ (ppm): 3.60 (s, 3H, OMe), 4.05 (s, 3H, OMe), 4.66–4.70 (m, 2H, NCH_2), 4.81–4.84 (m, 2H, NCH_2), 7.57–7.60 (m, 1H, Ar-H), 7.71–7.79 (m, 2H, Ar-H), 7.83 (s, 1H, Ar-H), 7.85 (s, 1H, Ar-H), 8.37–8.39 (m, 1H, Ar-H).) ^{13}C NMR(75 MHz, $CDCl_3$) δ (ppm) 29.60, 45.34, 50.92, 54.07, 54.43, 99.01, 125.96, 126.49, 127.65, 129.54, 131.53, 131.96, 133.09, 137.36, 156.94, 159.48, 164.14, 165.04; Anal. Calcd. for $C_{17}H_{16}N_6O_3$: C, 57.95; H, 4.58; N, 23.85; Found: C, 58.05; H, 4.61; N, 24.10.

3.7.20 Synthesis of 2-(2-(4-(dimethylamino)-6-(methylthio)-1*H*-pyrazolo[3,4-*d*]pyrimidin-1-yl)ethyl) phthalazin -1(2*H*)-one (69).

69: Yield: 85%; mp: 118-120 °C; MS (ESI) m/z 382 $[M+H]^+$; ^1H NMR (300 MHz, $CDCl_3$) δ (ppm): 2.22 (s, 3H, SMe), 3.31 (s, 6H, NMe_2), 4.64 – 4.68 (m, 2H, NCH_2), 4.79 – 4.83 (m, 2H, NCH_2), 7.58 – 7.62 (m, 1H, Ar-H), 7.70 – 7.79 (m, 2H, Ar-H), 7.81b (s, 1H, Ar-H), 7.86 (s, 1H, Ar-H), 8.37 – 8.40 (m. 1H, Ar-H) ^{13}C NMR (75 MHz, $CDCl_3$) δ (ppm): 13.65, 38.58, 45.17, 50.90, 98.57, 125.99, 126.55, 127.71, 129.65, 131.41, 132.95, 133.62, 137.41, 155.37, 156.51, 159.55, 168.49.

3.7.21 Synthesis of 2-(2-(4,6-bis(methylthio)-1*H*-pyrazolo[3,4-*d*]pyrimidin-1-yl)ethyl)-phthalazine-1(2*H*)-thione (70).

70: Yield: 85%; mp: 136–138 °C (Ethyl acetate); MS (ESI) m/z 385 $[M+H]^+$; ^1H NMR (300 MHz, $CDCl_3$) δ (ppm): 2.24 (s, 3H, SCH_3), 2.64 (s, 3H, SCH_3), 5.04–5.07 (m, 2H, NCH_2), 5.26 - 5.29 (m, 2H, NCH_2), 7.59-7.62 (m, 1H, Ar-H), 7.79 -7.84 (m, 2H, Ar-H), 7.90 (s, 1H, Ar-H), 8.01 (s, 1H, Ar-H), 8.96 -8.99 (m, 1H, Ar-H).

3.7.22 Synthesis of 2-(2-(5-methyl-6-(methylthio)-4-oxo-4,5-dihydro-1*H*-pyrazolo[3,4-*d*]pyrimidin-1-yl)ethyl)phthalazin-1(2*H*)-one (71).

71: Yield: 85%; mp: 190-192 °C; MS (ESI) m/z 369 $[M+H]^+$; ^1H NMR (300 MHz, $CDCl_3$) δ (ppm): 2.33 (s, 3H, SMe), 3.42 (s, 6H, NMe), 4.64 – 4.68 (m, 2H, NCH_2), 4.76 -4.79 (m, 2H, NCH_2), 7.58–7.61 (m, 1H, Ar-H), 7.71 -7.80 (m, 2H, Ar-H), 7.86 (s, 1H, Ar-H), 7.95 (s, 1H, Ar-H), 8.36 -8.39 (m. 1H, Ar-H) ^{13}C NMR(75 MHz, $CDCl_3$) δ (ppm): 15.02, 29.54, 45.16, 50.99, 102.17, 125.97, 126.47, 127.60, 129.56, 131.58, 133.18, 135.48, 137.42, 151.22, 157.66, 159.46, 161.81.

3.7.23 Synthesis of 2-(2-(5-methyl-6-(methylsulfonyl)-4-oxo-4,5-dihydro-1*H*-pyrazolo[3,4-*d*]pyrimidin-1-yl)ethyl)phthalazin-1(2*H*)-one (72).

72: Yield: 85%; mp: 210-212 °C; MS (ESI) m/z 401 $[M+H]^+$; ^1H NMR (300 MHz, $CDCl_3$) δ (ppm): 3.22 (s, 3H, SO_2Me), 3.77 (s, 6H, NMe), 4.69–4.71 (m, 2H, NCH_2), 4.83 -4.87 (m, 2H, NCH_2), 7.63–7.66 (m, 1H, Ar-H), 7.79 -7.84 (m, 2H, Ar-H), 7.88 (s, 1H, Ar-H), 7.99 (s, 1H, Ar-H), 8.38 -8.41 (m. 1H, Ar-H).

3.7.24 Synthesis of 1-methyl-6-(methylthio)-4-(pyrrolidin-1-yl)-1*H*-pyrazolo[3,4-*d*]pyrimidine (74).

74: Yield: 85%; mp: 130-132 °C; MS (ESI) m/z 250 $[M+H]^+$; ^1H NMR (300 MHz, $CDCl_3$) δ (ppm): 1.96-2.00 (m, 2H, CH_2), 2.12-2.16 (m, 2H, CH_2), 2.58 (s, 3H, SMe), 3.77 (t, J = 6 Hz, 4H, NCH_2) 3.94 (m, 3H, NMe), 7.78 (s, 1H, Ar-H).

3.7.25 Synthesis of 1-methyl-6-(methylthio)-4-(piperidin-1-yl)-1*H*-pyrazolo[3,4-*d*]pyrimidine (75).

75: Yield: 85%; mp: 124-126°C; MS (ESI) m/z 264 $[M+H]^+$; ^1H NMR (300 MHz, $CDCl_3$) δ (ppm): 1.73 (brs, 6H, $3CH_2$), 2.58 (s, 3H, SMe), 3.90-3.95 (m, 4H, $2NCH_2$), 3.95 (s, 3H, NMe), 7.82 (s, 1H, Ar-H).

3.7.26 Synthesis of 1-methyl-6-(methylthio)-4-(morpholin-4-yl)-1*H*-pyrazolo[3,4-*d*]-pyrimidine (76).

76: Yield: 85%; mp: 128-130 °C; MS (ESI) m/z 264 $[M+H]^+$; ^1H NMR (300 MHz, $CDCl_3$) δ (ppm): 2.58 (s, 3H, SMe), 3.82-3.86 (m, 4H, NCH_2), 3.92-3.96 (m, 4H, OCH_2), 3.96 (s, 3H, NMe), 7.81 (s, 1H, Ar-H).

3.7.27 Synthesis of 4-chloro-1-methyl-6-(methylsulfonyl)-1*H*-pyrazolo[3,4-*d*]pyrimidine (80).

80: Yield: 75%: mp 168-170°C; MS (ESI) m/z 247 $[M+H]^+$; ^1H NMR (300 MHz, $CDCl_3$) δ (ppm): 3.45 (s, 3H, SO_2Me), 4.24 (s, 3H, NMe), 8.30 (s, 1H, Ar-H).

3.7.28 Synthesis of 2-methyl-4,6-bis(methylthio)-2*H*-pyrazolo[3,4-*d*]pyrimidine (86).

86: Yield: 75%; mp: 230-232°C; MS (ESI) m/z 227 $[M+H]^+$; ^1H NMR (300 MHz, $CDCl_3$) δ (ppm): 2.63 (s, 3H, SMe), 2.67 (s, 6H, SMe), 4.12 (m, 3H, NMe), 7.88 (s, 1H, Ar-H).

3.7.29 Synthesis of 4-methoxy-2-methyl-6-(methylthio)-2*H*-pyrazolo[3,4-*d*]pyrimidine (87).

87: Yield: 75%; mp: 110-112 °C; MS (ESI) m/z 212 $[M+H]^+$; ^1H NMR (300 MHz, $CDCl_3$) δ (ppm): 2.64 (s, 3H, SMe), 4.02 (s, 6H, SMe), 4.10 (m, 3H, NMe), 7.89 (s, 1H, Ar-H).

3.7.30 Synthesis of 4-methoxy-2-methyl-6-(methylsulfonyl)-2*H*-pyrazolo[3,4-*d*]pyrimidine (88).

88: Yield: 75%; mp: 150-152°C; MS (ESI) m/z 243 $[M+H]^+$; ^1H NMR (300 MHz, $CDCl_3$) δ (ppm): 3.45 (s, 3H, SO_2Me), 4.21 (s, 3H, OMe), 4.28 (m, 3H, NMe), 8.02 (s, 1H, Ar-H).

3.7.31 Synthesis of 2-methylphthalazin-1(2*H*)-one (89).

89: Yield: 75%; mp: 112-114 °C; MS (ESI) m/z 161 $[M+H]^+$; ^1H NMR (300 MHz, $CDCl_3$) δ (ppm): 3.86 (s, 3H, NMe), 7.67-7.70 (m, 1H, Ar-H), 7.71-7.81 (m, 2H, Ar-H), 8.14 (s, 1H, Ar-H), 8.42-8.45 (m, 1H, Ar-H).

3.7.32 Synthesis of 3-methylquinazolin-4(3*H*)-one (90).

90: Yield: 75%; mp: 104-106°C; MS (ESI) m/z 161 $[M+H]^+$; ^1H NMR (400 MHz, $CDCl_3$) δ (ppm): 3.62 (s, 3H, NMe), 7.52 (ddd, *J* = 8.2, 6.9, 1.6 Hz, 1H), 7.80–7.70 (m, 2H, Ar-H), 8.10 (s, 1H, Ar-H), 8.33 (dd, *J* = 8.0, 1.0 Hz, 1H, Ar-H).

3.7.33 Synthesis of 3-methylbenzo[*d*][1,2,3]triazin-4(3*H*)-one (91).

91: Yield: 75%; mp: 110-112 °C; MS (ESI) m/z 162 $[M+H]^+$; ^1H NMR (300 MHz, $CDCl_3$) δ (ppm): 4.06 (s, 3H, NMe), 7.77- 7.82 (m, 1H, Ar-H), 7.91- 7.96 (m, 1H, Ar-H), 8.17 (d, *J* = 6.0, 1H, Ar-H), 8.36 (d, *J* = 6.0, 1H, Ar-H).

3.8 References

1. Weinhold, F. *Nature* **2001**, *411*, 539.
2. Takahashi, O.; Kohno, Y.; Nishio, M. *Chem. Rev.* **2010**, *110*, 6049.
3. Carter, R. E.; Nilsson, B.; Olsson, K. *J. Am. Chem. Soc.* **1975**, *97*, 6155.
4. Lyttle, M. H.; Streitwieser, A., Jr.; Kluttz, R. Q. *J. Am. Chem. Soc.* **1981**, *103*, 3232.
5. Cram, D. J.; Elhafez, F. A. A. *J. Am. Chem. Soc.* **1952**, *74*, 5828.
6. Prelog, V. *Helv. Chim. Acta* **1953**, *36*, 308.
7. Barton, D. H. R. *Experientia* **1950**, *6*, 316.
8. Mo, Y.; Gao, J. *Acc. Chem. Res.* **2007**, *40*, 113.
9. Wolfe, S. *Acc. Chem. Res.* **1972**, *5*, 102.
10. Goodman, L.; Gu, H.; Pophristic, V. *J. Phys. Chem. A* **2005**, *109*, 1223.
11. O'Hagan, D.; Rzepa, H. S.; Schuler M.; Slawin A. M. Z. *Beilstein J. Org. Chem.* **2006**, *2*, 19.
12. Durig, J. R.; Liu, J.; Little, T. S.; Kalasinsky, V. F. *J. Phys. Chem.* **1992**, *96*, 8224.
13. Craig, N. C.; Chen, A.; Suh, K. H.; Klee, S.; Mellau, G. C.; Winnewisser, B. P.; Winnewisser, M. *J. Phys. Chem. A* **1997**, *101*, 9302.
14. Fernholt, L.; Kveseth, K. *Acta Chem. Scand. A: Phys. Inorg. Chem.* **1980**, *A34*, 163.
15. Takeo, H.; Matsumura, C.; Morino, Y. *J. Chem. Phys.* **1986**, *84*, 4205.
16. Goodwin, A. R. H.; Morrison, G. *J. Phys. Chem.* **1992**, *96*, 5521.
17. (a) Brunck, T. K.; Weinhold, F. *J. Am. Chem. Soc.* **1979**, *101*, 1700. (b) Radom, L.; Lathan, W. A.; Hehre, W. J.; Pople, J. A. *J. Am. Chem. Soc.* **1973**, *95*, 693. (c) Trindle, C.; Crum, P.; Douglass, K. *J. Phys. Chem. A* **2003**, *107*, 6236.
18. Werpetinski, K. S.; Cook, M. *J. Chem. Phys.* **1997**, *106*, 7124.
19. Wolfe, S.; Rauk, A.; Tel, L. M.; Csizmadia, I. G. *J. Chem. Soc. B: Phys. Org.* **1971**, *1*, 136.

20. Schuler, M.; O'Hagan D.; Slawin A. M. Z. *Chem. Commun.* **2005**, *34,* 4324.

21. O'Hagan, D.; Rzepa, H. S.; Schuler M.; Slawin, A. M. Z. *Beilstein J. Org. Chem.* **2006**, *2*, 19.

22. Morino, Y.; Kuchitsu, K. *J. Chem. Phys.* **1958**, *28*, 175.

23. Hirota, E. *J. Chem. Phys.* **1962**, *37*, 283.

24. Ohno, K.; Yoshida, H.; Watanabe, H.; Fujita, T.; Matsuura, H. *J. Phys. Chem.* **1994**, *98*, 6924.

25. (a) Yoshida, H.; Kaneko, I.; Matsuura, H.; Ogawa, Y.; Tasumi, M. *Chem. Phys. Lett.* **1992**, *196*, 601. (b) Yoshida, H.; Tanaka, T.; Matsuura, H. *Chem. Lett.* **1996**, 637.

26. Matsuura, H.; Yoshida, H.; Hieda, M.; Yamanaka, S.; Harada, T.; Shinya, K.; Ohno, K. *J. Am. Chem. Soc.* **2003**, *125*, 13910.

27. Bohn, R. K.; Padrdus, J. L.; August, J.; Brupbacger, T.; Jager, W. *J. Mol. Struct.* **1997**, *413*, 293.

28. (a) Atticks, K. A.; Bohn, R. K.; Michels, H. H. *Int. J. Quantum Chem.* **2001**, *85*, 514. (b) Atticks, K. A.; Bohn, R. K.; Michels, H. H. *Int. J. Quantum Chem.* **2002**, *90*, 1440.

29. (a) Hopkins, J. B.; Powers, D. E.; Smalley, R. E. *J. Chem. Phys.* **1980**, *72*, 5039. (b) Hopkins, J. B.; Powers, D. E.; Mukamel, S.; Smalley, R. E. *J. Chem. Phys.* **1980**, *72*, 5049.

30. Breen, P. J.; Warren, J. A.; Bernstein, E. R.; Seeman, J. I. *J. Am. Chem. Soc.* **1987**, *109*, 3453.

31. (a) Watt, M.; Hardebeck, L. K. E.; Kirkpatrick, C. C.; Lewis, M. *J. Am.Chem. Soc.* **2011**, *133*, 3854. (b) Wheeler, S. E. *J. Am. Chem. Soc.* **2011**, *133*, 10262. (c) Bravaya, K. B.; Kostko, O.; Ahmed, M.; Krylov, A. I. *Phys. Chem. Phys.* **2010**, *12*, 2292. (d) Grimme, S. *Angew. Chem. Int. Ed.* **2008**, *47*, 3430. (e) Janiak, C. *J. Chem. Soc. Dalton Trans.* **2000**, 3885. (f) Hunter, C. A.; Sanders, J. K. M. *J. Am. Chem. Soc.* **1990**, *112*, 5525.

32. (a) Burley, S. K.; Petsko, G. A. *Science* **1985**, *229*, 23. (b) Waters, M. L. *Biopolymers (Peptide Science)* **2004**, *76*, 435.

33. (a) Salonen, L. S.; Ellermann, M.; Diederich, F. *Angew. Chem. Int. Ed.* **2011**, *50*, 4808. (b) Bissantz, C.; Kuhn, B.; Stahl, M. *J. Med. Chem.* **2010**, *53*, 5061.

34. (a) Hunter, C. A. *Chem. Soc. Rev.* **1994**, *23*, 101. (b) Hunter, C. A.; Lawson, K. R.; Perkins, J. C.; Urch, J. *J. Chem. Soc. Perkin Trans. 2* **2001**, 651.

35. (a) Mishra B. K.; Sathyamurthy, N. *J. Phys. Chem. A* **2005**, *109*, 6. (b) Adams, H.; Harris, K.; Hembury, G.; Hunter, C. A.; Livingstone D.; McCabe, J. F. *Chem. Commun.* **1996**, 2531. (c) Rebek Jr, J. *Angew. Chem. Int. Ed. Engl.* **1990**, *29*, 245. (d) Cubberley, M. S.; Iverson, B. L. *J. Am. Chem. Soc.* **2001**, *123*, 7560.

36. (a) Gung, B. W.; Wekesa F.; Barnes, C. L. *J. Org. Chem.* **2008**, *73*, 1803. (b) Gung, B. W.; Xue X.; Zou, Y. *J. Org. Chem.* **2007**, *72*, 2469. (c) Gung, B. W.; Emenike, B. U.; Lewis, M.; Kirschbaum, K. *Chem. Eur. J.* **2010**, *16*, 12357. (d) Browne, D. T.; Eisinger J.; Leonard, N. J. *J. Am. Chem. Soc.* **1968**, *90*, 7302. (e) Leonard, N. J. *Acc. Chem. Res.* **1979**, *12*, 423. (f) Newcomb L. F.; Gellman, S. H. *J. Am. Chem. Soc.* **1994**, *116*, 4993. (g) Pang, Y.; Miller J.

L.; Kollman, P. A. *J. Am. Chem. Soc*. **1999**, *1717*, 121. (h) Itahara T. *J. Chem. Soc., Perkin Trans. 2* **1998,** 1455. (i) Itahara T.; Imamura, K. *Bull. Chem. Soc. Jpn.* **1994**, *67*, 203. (j) Itahara, T. *J. Chem. Soc. Perkin Trans. 2*, **1996**, 2695. (k) Nicholas, J. H.; Pablo, B.; Bernardo, H.; Aranzazudel C.; Jesus, J. *J. Am. Chem. Soc*. **1998**, *120*, 12371. (l) Paliwal, S.; Geib S.; Wilcox, C. S. *J. Am. Chem. Soc*. **1994**, *116*, 4497. (m) Wheeler S. E.; Houk, K. N. *J. Am. Chem. Soc.,* **2008**, *130*, 10854. (n) Cozzi, F.; Cinquini, M.; Annunziata, R.; Dwyer T.; Siegel, J. S. *J. Am. Chem. Soc.*, **1992**, *114*, 5729. (o) Cozzi, F.; Annunziata, R.; Benaglia, M.; Baldridge, K. K.; Aguirre, G.; Estrada, J.; Sritana-Anant Y.; Siegel, J. S. *Phys. Chem. Chem. Phys*. **2008**, *10*, 2686. (p) Grimme, S.; Muck-Lichtenfeld C.; Antony, J. *Phys. Chem. Chem. Phys*. **2008**, *10*, 3327. (q) Garcıa-Raso, A.; Fiol, J. J.; Badenas, F.; Solans X.; Font-Bardia, M. *Polyhedron* **1999**, *18*, 765.

37. (a) Biswas, G.; Chandra, T.; Avasthi K.; Maulik, P. R. *Acta Crystallogr.* **1995**, *C51*, 2453. (b) Avasthi, K.; Farooq, S. M.; Rawat, D. S.; Sharon A.; Maulik, P. R. *Acta Crystallogr.* **2003**, *C59*, o523. (c) Avasthi, K.; Aswal, S.; Kumar, R.; Yadav, U.; Rawat D. S.; Maulik, P. R. *J. Mol. Struct.* **2005**, *750*, 179. (d) Avasthi, K.; Farooq, S. M.; Aswal, S.; Raghunandan R. Maulik, P. R. *J. Mol. Struct.* **2007**, *827*, 88. (e) Avasthi, K.; Aswal, S.; Farooq, S. M.; Raghunandan R.; Maulik, P. R. *J. Mol. Struct.* **2008**, *888*, 327. (f) Avasthi, K.; Farooq, S. M.; Raghunandan R.; Maulik, P. R. *J. Mol. Struct.* **2009**, *927*, 27. (g) Avasthi, K.; Farooq, S. M.; Raghunandan R.; Maulik, P. R. *J. Mol. Struct.* **2006**, *785*, 106. (h) Avasthi, K.; Farooq, S. M.; Bal, C.; Kumar, R.; Tewari A. K.; Maulik, P. R. *J. Mol. Struct.* **2007**, *842*, 100. (i) Maulik, P. R.; Avasthi, K.; Biswas, G.; Biswas, S.; Rawat, D. S.; Sarkhel, S.; Chandra T.; Bhakuni, D. S. *Acta Crystallogr.* **1998**, *54*, 275. (j) Avasthi, K.; Aswal S.; Maulik, P. R. *Acta Crystallogr.* **2001**, *57*, 1324. (k) Avasthi, K.; Tewari, A.; Rawat, D. S.; Sharon A.; Maulik, P. R. *Acta Crystallogr.* **2002**, *58*, o494. (l) Avasthi, K.; Bhagat, D.; Bal, C.; Sharon, A.; Yadav U.; Maulik, P. R. *Acta Crystallogr.* **2003**, *59*, o409.
38. Some examples are: (a) Harada, J.; Ogawa K.; Tomoda S. *J. Am. Chem. Soc.* **1995**, *117*, 4476. (b) Kahr, B.; Mitchell, C. A.; Chance, J. F.; Clark, V.; Gantzel, P.; Baldridge K. K.; Siegel, J. S. *J. Am. Chem. Soc.* **1995**, *117*, 4479. (c) Shen, Q. *J. Mol. Struct*. **1998**, *471*, 57. (d) Harada J.; Ogawa, K. *Struct. Chem*. **2001**, *12*, 243. (e) Bhogala, B. R.; Vangala, V. R.; Smith, P. S.; Howard J. A. K.; Desiraju, G. R. *Cryst. Growth Des*. **2004**, *4*, 647. (f) Lia, B.; Zhoua, J.; Penga, Y.; Lia B.; Zhang, Y. *J. Mol. Struct*. **2004**, *707*, 187. (g) Liang Z. P.; Li, J. *Acta Crystallogr.* **2006**, *E62*, o5282. (h) Barbarin, C. R.; Najera B.; Elizondo, P. *Acta Crystallogr.* **2006**, *E62*, o5423.
39. (a) Avasthi, K.; Chandra, T.; Bhakuni, D. S. *Indian J. Chem.*, **1995**, *34B*, 944. (b) Avasthi, K.; Rawat, D. S.; Chandra T.; Bhakuni, D. S. *Indian J. Chem*. **1998**, *37B*, 754. (c) Avasthi, K.; Rawat, D. S.; Maulik, P. R.; Sarkhel, S.; Broder C. K.; Howard, J. A. K. *Tetrahedron Lett.* **2001**, *42*, 7115.
40. Dubey, R.; Tewari, A. K.; Ravikumar K.; Sridhar, B. *Bull. Korean Chem. Soc.* **2010**, *31*, 1326.
41. Ozdemir, G.; Isik, S. I.; Sancak, K.; Sasmaz S.; Okomusoglu, N. T. *Acta Crystallogr.* **2005**, *E61*, o2699.
42. Avasthi, K.; Ansari, A.; Kant, R.; Maulik, P. R.; Ravikumar, K.; Chattopadhyay P.; Adhikary, N. D. *CrystEngComm*. **2011**, *13*, 2039.

43. Vogtle, F. *Cyclophane Chemistry: Synthesis, Structures, and Reactions* J. Wiley: Chichester, New York, **1993**.

44. (a) Bolte, J.; Demuyunck, C.; Lhomme, J. *J. Med. Chem.* **1977**, *20*, 1607. (b) Bolte, J.; Demunck, C.; Lhomme, J. *J. Am. Chem. Soc.* **1976**, *98*, 613. (c) Bolte, C.; Demuynck, J.; Lhomme, J. *J. Med. Chem.* **1977**, *20*, 1607. (d) Bolte, J.; Demuynck, C. J.; Lhomme, J.; Fournie-Zaluski, M. C.; Roques, B. P. *Biochemistry* **1979**, *18*, 4928.

45. **Bro**wn D. J. *The Chemistry of Heterocyclic Compounds*, *The Pyrimidines* Taylor E. C., Ed.; vol. 23, J. Wiley & Sons: NY - Chichester - Brisbane - Toronto - Singapore, **1994**.

46. Koepfli, J. B.; Mead, J. F.; Brickman, J. A. *J. Am. Chem. Soc.* **1947**, *69*, 1837.

47. Kikuchi, H.; Taska, H.; Takaya, Y.; Iwabuchi, Y.; Ooi, H. *J. Med. Chem.* **2002**, *45*, 2563.

48. Joshi V.; Chaudhari, R. P. *Indian J. Chem.* **1987**, *26B*, 602.

49. Wright Jr.; W. B.; Tomcufcik, A. S. *Chem. Abstr.* **1987**, *107*, 198354.

50. Bartroli, J.; Turmo, E.; Alguero, M.; Boncompte, E.; Vericat, M. L.; Conte, L. *J. Med. Chem.* **1998**, *41*, 1869.

51. Saleh, M. A.; Adbel-Megged M. F.; Abdo M. A.; Abdel-Basset M. S. *Nucleosides, Nucleotides & Nucleic Acids* **2002**, *21*, 93.

52. Wolfe, J. F. *J. Med. Chem.* **1990**, *33*, 161.

53. Gupta, D. P.; Ahmad, S.; Kumar, A.; Shanker, K. *Indian J. Chem.* **1988**, *27B*, 1060.

54. Gupta, C. M.; Bhaduri, A. P.; Khanna, N. M. *J. Scient. Indian Res.* **1971**, *30*, 101.

55. Murray, K. J. *Drug News and Perspectives* **1993**, *6*, 150, and references cited therein.

56. Yamaguchi, M.; Kamei, K.; Koga, T.; Akima, M.; Kuroki, T.; Ohi, N. *J. Med. Chem.* **1993**, *36*, 4052.

57. Kleemann A.; Engel, J. *Pharmazeutische Wirkstoffe - Synthesen - Patente - Anwendungen* Vol. 5, Thieme, Stuttgart, **1982**.

58. Ueno, K.; Moroi, R.; Kitagawa, M.; Asano, K.; Miyazaki, S. *Chem. Pharm. Bull.* **1976**, *24*, 1068.

59. *Drugs of the Future* **1987**, *12*, 347 and references cited therein.

60. Scheffler, G.; Engel, J.; Kutscher, B.; Sheldrick, W. S.; Bell, P. *Arch. Pharm.* **1988**, *321*, 205.

61. *Drug Data Report*, **1991**, *13*, 495, and references cited therein.

62. Mueller R; Rachwal S.; Lee S.; Zhong S.; Li Y. X.; Haroldsen P.; Herbst T.; Tanimura S.; Varney M.; Johnson S.; Rogers G.; Street L. J. *Bioorg. Med. Chem. Lett.* **2011**, *21*, 6170.

63. Caliendo, G.; Fiorino, F.; Grieco, P.; Perissutti, E.; Santagada, V.; Meli, R.; Raso, G. M.; Zanesco A.; Nucci G. D. *Eur. J. Med. Chem.* **1999**, *34* ,1043.

64. (a) Aswal, S. Ph. D. Thesis; *Synthesis of flexible bicyclic nitrogenous heterocycles, their X-ray crystallographic studies and biological activities* **2006**, Jawaharlal Nehru University, New Delhi. (b) Avasthi, K.; Kumar, A.; Aswal, S.; Kant, R.; Raghunandan, R.; Maulik, P. R.; Khanna, R. S; Ravikumar, K. *CrystEngComm*. **2012**, *14*, 383.

65. Maulik, P.R.; Avasthi, K.; Sarkhel, S.; Chandra, T.; Rawat, D.S.; Logsdon, B.; Jacobson, R. A. *Acta Crystallogr*. **2000**, *C56*, 1361.

66. Nishio, M. *CrystEngComm*. **2004**, *6*, 130.

67. Desiraju, G. R.; Steiner T. *The Weak Hydrogen Bond*, Oxford University Press, Oxford, 1999.

68. (a) Egli, M.; Sarkhel, S. *Acc. Chem. Res.* **2007**, *40*, 197. (b) Jain, A.; Purohit, C. S.; Verma, S.; Sankararamakrishnan, R. *J. Phys. Chem. B* **2007**, *111*, 8680. (c) Wan, C. Q.; Chen, X. D.; Mak, T. C. W. *CrystEngComm*. **2008**, *10*, 475.

69. Rahman, A. N. M. M.; Bishop, R.; Craig D. C.; Scudder, M. L. *CrystEngComm*. **2002**, *4*, 510.

70. Voth, A. R.; Khuu, P.; Oishi K.; Shing Ho P. *Nature Chemistry* **2009**, *1*, 74.

CHAPTER-4

Synthesis, ^{1}H NMR and X-ray crystallographic studies of pyrazolo[3,4-*d*]pyrimidine and Phthalazinone/Quinazolinone/ Benzotriazinone based flexible dissymmetric polymethylene and butylidine linker compounds

4.1 Introduction

Heterocyclic chemistry is a key to the understanding of life processes and to our efforts to improve the quality of life for humankind.[1,2] Heterocycles play a major role in biochemical processes.[1] Most of the typical and essential constituents of living cells, DNA and RNA, are based on purine [adenine (**1**) and guanine (**2**)] and pyrimidine [cytosine (**3**), thymine (**4**) and uracil (**5**)] bases (**Fig. 1**), which are all aromatic heterocycles.

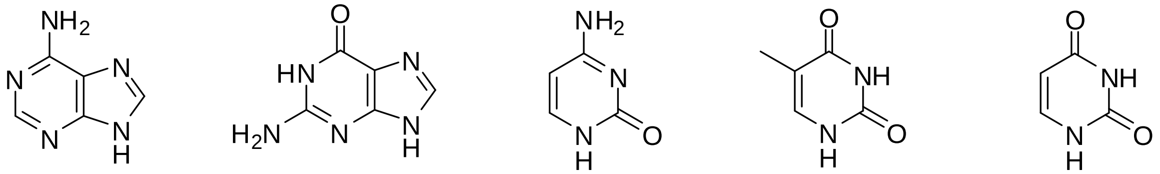

1 **2** **3** **4** **5**

Figure 1. Purine and pyrimidine bases

Two of the twenty amino acids namely tryptophan (**6**) and histidine (**7**) (**Fig. 2**) contain aromatic heterocycles. They participate along with other amino acids in protein constitution through amide linkages.

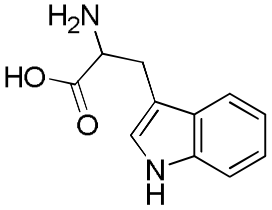

6

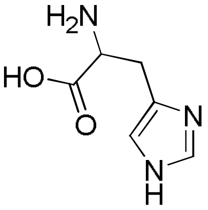

7

Figure 2. Heteroaromatic amino acids

Most of the coenzymes have aromatic heterocycles as major constituents. Coenzymes are essential for the biochemical redox reactions, e.g., nicotinamide adenine dinucleotide (NAD, **8**) and flavin adenine dinucleotide (FAD, **9**) (**Fig. 3**). Both are hydrogen transporters through their tautomeric forms that allow hydrogen uptake at the termini of the quinonoid chain. Thiamine pyrophosphate (**10**) is a coenzyme that assists the decarboxylation of pyruvic acid, a very important biological reaction.[2]

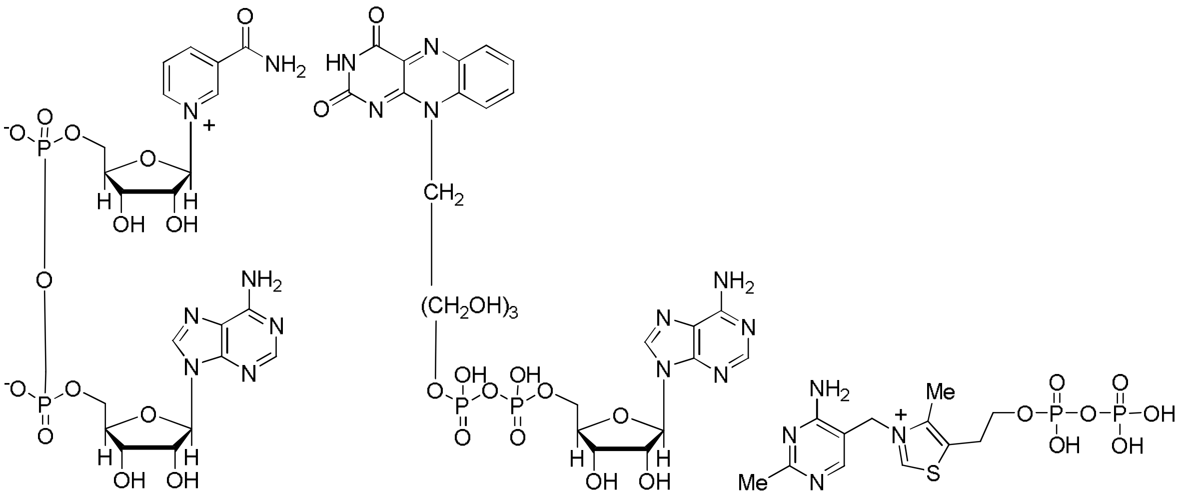

8 **9** **10**

Figure 3. Important coenzymes

Some important vitamins, **11-13**, are constructed on an aromatic heterocyclic scaffold (**Fig. 4**).

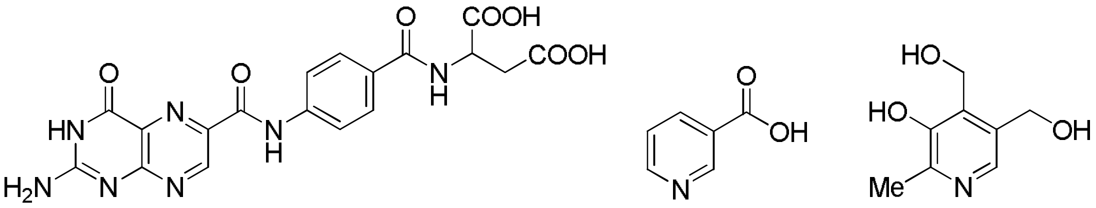

11 **12** **13**

Figure 4. A few heterocyclic vitamins

Porphyrin (**14**) is a heterocyclic macrocycle composed of four pyrrole subunits interconnected at their carbon atoms via methine bridges (**Fig. 5**). Porphyrin is present at the active site of hemoglobin (**15**), cytochrome (**16**), chlorophyll (**17**) etc. (**Fig. 5**) and thus plays a vital role in oxygen transport, biological electron transfer reactions and photosynthesis. Porphyrin derivatives are used in photodynamic therapy for dermatological diseases such as psoriasis, and for skin or subcutaneous cancer.[3-5]

A majority of drug molecules are heterocycles. Antibiotics such as penicillins and cephalosporins, alkaloids such as vinblastine, ellipticine, morphine, and reserpine, and cardiac glycosides such as the class of digitalis are heterocyclic compounds.[2] Given the huge importance of heterocycles in our lives it is of great importance to know how these heterocycles interact with each other and with their environment to produce a biological effect.

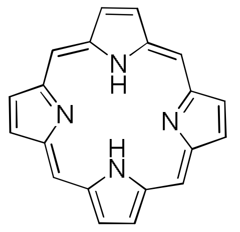

14

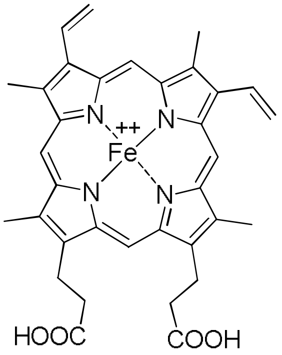

15

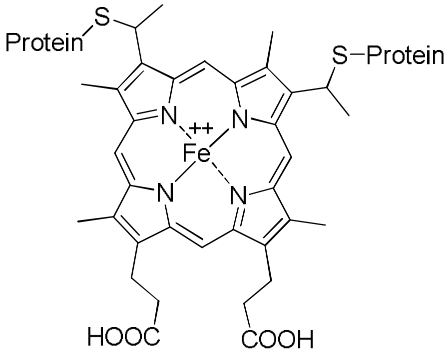

16

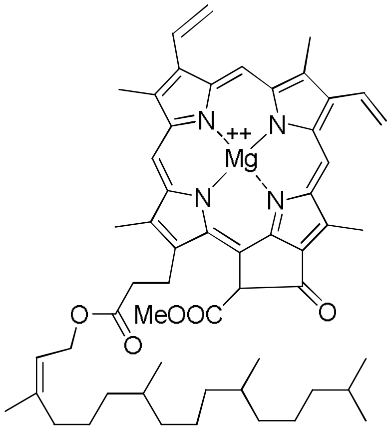

17

Figure 5. Porphyrin and porphyrin containing pigments

The biological activity of a chemical relies mostly on its capability to bind reversibly to an active site, such as a receptor, and this is usually determined by various non-covalent interactions.[6] Non-covalent interactions are considerably weaker than covalent interactions, which can range between ca. 150 kJ/mol to 450 kJ/mol. Non-covalent interactions range from 2 kJ/mol to 300 kJ/mol.[7] The term 'non-covalent interactions' includes a wide range of attractions and repulsions. These interactions include electrostatic interactions (e. g., ion-ion, ion-dipole, dipole-dipole), hydrogen bonding, metal-to-ligand bonding, π–π interactions, cation–π interactions, van der Waals forces, hydrophobic effects etc. A summary of energy range of important noncovalent interactions is presented in **Table 1**. A brief discussion on hydrogen bonding and lone pair- pi interactions is done in the following section of this chapter since these interactions play an important role in our studies. The other important weak noncovalent interaction, the π–π interaction in our study is already been reviewed in chapter one.

Table 1: Important non-covalent interactions[7]

Interaction	Strength (kJ/mol)	Example
Ion-ion	200-300	Tetrabutylammonium chloride
Ion-dipole	50-200	Potassium[18]crown-6
Dipole-dipole	5-50	Chloroform-Acetone
Hydrogen bonding	4-120	Water
Cation–π	5-80	K^+ in benzene
π–π	0-50	Benzene and graphite
Van der Waals	< 5 kJ/mol but variable depending on surface	Argon; packing in molecular crystals

4.1.1 Hydrogen Bonding [8-13]

Hydrogen bonding is one of the most important non-covalent interactions.[8-13] Fundamentally, H-bonding plays an important role in molecular association. In supramolecular chemistry, the hydrogen bond is able to control and direct the structures of molecular assemblies because it is sufficiently strong and sufficiently directional. Similarly, in biological systems it is of vital importance because it lies in an energy range intermediate between van der Waals interactions and covalent bonds. The energy range is one that permits hydrogen bonds to both associate and dissociate quickly at ambient temperatures. This twin ability renders the interaction well suited to achieving specificity of recognition within short time spans, a necessary condition for biological recognition that must take place around room temperature.

Hydrogen bonding phenomenon occurs when two chemical entities **X** and **Y** incorporates hydrogen atom **H** to form a pattern **X-H…Y** where the three dots denote the bond. X–H represents the hydrogen bond donor. The acceptor may be an atom or an anion Y, or a fragment or a molecule Y–Z, where Y is bonded to Z. In some cases, X and Y are the same. In more specific cases, X and Y are the same and X–H and Y–H distances are the same as well leading to symmetric hydrogen bonds. In any event, the acceptor is an electron rich region such as, but not limited to, a lone pair of Y or π-bonded pair of Y–Z.

It was Linus Pauling[9] who first drew the attention of people toward the hydrogen bond. According to him under certain conditions an atom of hydrogen is attracted by rather strong forces to two atoms instead of one, so that it may be considered to be acting as a bond between them and that they are purely electrostatic in nature. Steiner and Saenger[10] consider a hydrogen bond as any cohesive interaction X-H…Y where H carries a positive and Y a negative (partial or full) charge and the charge on X is more negative than on H. This definition, however, is incomplete as it suits only for the conventional hydrogen bonds (X and Y are strong electron withdrawing atoms such as O, N or F) wherein the forces are electrostatic in nature and is restrictive for the borderline cases as non-conventional hydrogen bonds or weak hydrogen bonds (WHB). The WHB, or non-conventional hydrogen bond, takes place when X or Y or both atoms are of moderate electronegativity and it has been a subject of thorough study in recent years. The book by Desiraju and Steiner is pioneering in this respect and presents a substantial body of evidence for the existence of weak hydrogen bonds such as the C–H…O and the C–H…N hydrogen bond.[11]

Hydrogen bond may be described in terms of the *d, D, θ* and *r* as shown below in the **Fig. 6**.

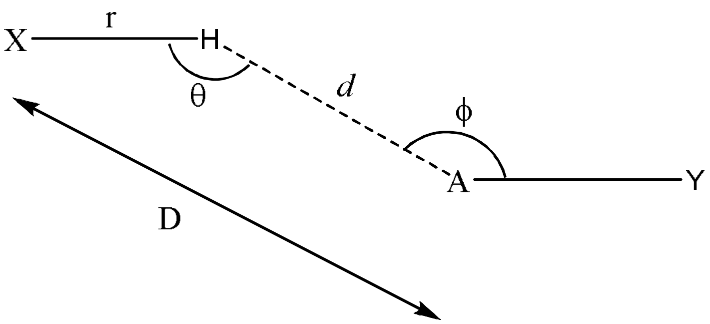

Figure 6. Definition of the geometrical parameters *d, D, r, θ* and *ϕ* for a hydrogen bond

If the hydrogen bond is extended on the acceptor side as X-H…A–Y, an acceptor angle *ϕ* may also be defined.

According to the latest IUPAC recommendations,[12] "Hydrogen bond is an attractive interaction between a hydrogen atom from a molecule or a molecular fragment X–H in which X is more electronegative than H, and an atom or a group of atoms in the same or a different molecule, in which there is evidence of bond formation."

Since hydrogen bonds are long-range interactions, a group X-H can be bonded to more than one acceptor A at the same time. For example, in case of bifurcated hydrogen bond the donor can bond with two acceptors X-H…(A_1, A_2). Similarly if three acceptors are involved a trifurcated hydrogen bond forms. Bifurcated hydrogen bonds can be either due to bifurcation of donors or acceptors (**Fig. 7**).

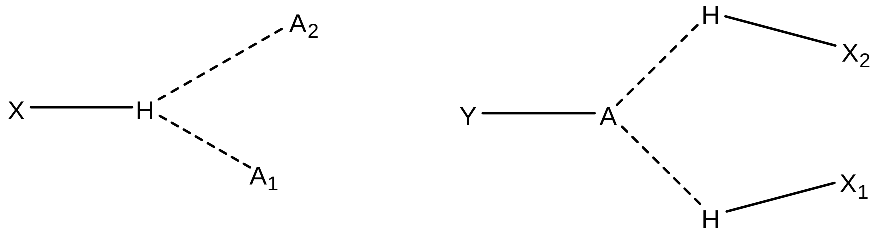

Bifurcated donor Bifurcated Acceptor

Figure 7. Bifurcated hydrogen bonds

The hydrogen bond covers a wide range of energies: from 2 kJ mol^{-1} to nearly 120 kJ mol^{-1} (**Table 1**). This means that the weakest hydrogen bonds are close in energy to van der Waals interactions and the strongest hydrogen bonds are stronger than some covalent bonds. Hydrogen bond can be classified as very strong, strong and weak on the basis of energetic and geometric properties and has been tabulated in the **Table 2**.

Table 2: Some properties of very strong, strong and weak hydrogen bonds[11]

	Very strong	**Strong**	**Weak**
Bond energy (-kcal/mol)	15-40	4-15	< 4
Examples	[F…H…F]$^-$ [N…H…N]$^+$ P—OH…O=P	O—H…O=C N—H…O=C O—H…O—H	C—H…O O—H…π Os—H…O
IR v_s relative shift	>25%	5-25%	< 5%
Bond lengths	H—A ~ X—H	H…A > X—H	H…A >> X—H
Lengthening of X—H (Å)	0.05-0.2	0.01-0.05	≤0.01
D (X…A) range (Å)	2.2-2.5	2.5-3.2	3.0-4.0
d(H…A) range (Å)	1.2-1.5	1.5-2.2	2.0-3.0
Bonds shorter than vdW	100%	Almost 100%	30-80%
Θ(X—H…A) range(˚)	175-180	130-180	90-180
Effect on crystal packing	Strong	Distinctive	Variable

4.1.1.1 The Weak Hydrogen bonds (**WHB**)[11-12]

Evidence has gradually accumulated in the previous five decades to show that weaker hydrogen bonds[11-12] are also ubiquitous, including X-H/π (X ~ O, N, halogen) and C-H/n interactions (n: lone pair electrons). Many examples of WHB can be found in supramolecular chemistry where these interactions can be exploited to design molecules in crystal structures or in solution to obtain the desired results and properties. WHB also govern the shape and the association of biological molecules and macromolecules. According to Desiraju and Steiner the weak hydrogen bond is characterized by energy less than 16 kJ/mol, a moderate electrostatic nature, a variable effect on crystal packing, a relative shift in the IR spectrum of less than 5% and a hydrogen bond length much greater than the molecular bond length. The criterion that can help distinguish between van der Waals and hydrogen bonded interactions, which is also recommended by the IUPAC task group, is directionality.[12] The three atoms involved in the hydrogen bond interaction tend toward linearity, although deviations up to 110^0 have been observed, and this is different from van der Waals interactions which do not show any directional preference. The directionality of the hydrogen bond is connected to the fact that it is due mainly to electrostatic forces and less to dispersion forces.

The C–H bond is the archetypical weak hydrogen bond donor.[11-12] The hydrogen donor propensity of the C–H bond is C(sp)–H > C(sp2)–H > C(sp3)–H and increases with the number of adjacent electron withdrawing groups. The C–H group in order to act as hydrogen bond donor must be bound to some electron withdrawing group; in other words the C–H hydrogen atom must be ‘‘activated’’. For example consider the case of dimethyl ether. The role of oxygen is double since it is an electron withdrawing group capable of activating aliphatic C–H bonds and a possible acceptor group for the WHB. The presence of the oxygen atom adjacent to the methylic group on the one hand increases the acidity of the methylenic hydrogen atoms and on the other hand the oxygen atom itself can accept WHB from the methylenic hydrogens of the second dimethylether moiety. In fact the two monomers are bound together by three CH…O linkages where one of the oxygen atoms acts as a bifurcated acceptor to two methylenic hydrogens of the other monomer the distances H…O being 2.53 and 2.65 A˚ with a angle of 143^0 (see **Fig. 8**).

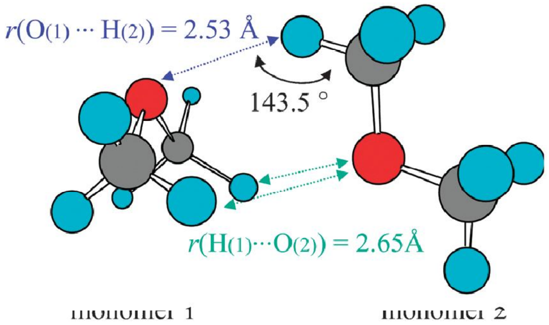

Figure 8. Structural parameter of the dimethylether dimer [12]

The earliest indication that an H atom attached to carbon can form hydrogen bonds is found in the paper of Kumler[15] who noted that the HCN behaves similarly to the other simple hydrogen bonded substances like HF, glycol, aliphatic carboxylic acids and their amides. It was specifically suggested that HCN molecules are associated with hydrogen bonds as H-C≡N…H-C≡N…H-C≡N, an arrangement that was found later in the crystal. Another evidence for the hydrogen bonded CH_3 group comes from the crystal study of dimethyl oxalate by Dougill and Jeffery[16] in 1953 wherein dense network of C-H…O contacts was actually demonstrated. Sutor[17] also demonstrated the existence of the C-H…O hydrogen bond in structures of theophylline, caffeine, uracil and few other compounds that contains $C(sp^2)$-H groups. Taylor and Kennard[18] properly revived these weak interactions in 1982 and it was after this paper the occurrence of these hydrogen bonding was accepted.

A wave of interest in weak hydrogen bonding has emerged in recent times in the different fields of structural chemistry and biology. It is now well documented that C-H…O and other types of weak hydrogen bonds are important as secondary interactions, and in many instances even play dominant role in crystal packing and molecular conformations, in molecular recognition processes, in stabilization of inclusion complexes and in stability and possibly even in the activity of biological macromolecules.[11-12,19]

Important electron withdrawing groups that “activate” the C-H bond are the halogen atoms, nitrogen and sulfur. The fluoroform molecule (CF_3H) has been investigated in many studies as a possible hydrogen bond donor with various partners.[20] The three fluorine atoms are able to activate the methylic hydrogen atom and the fluoroform molecule forms stable hydrogen bonded adducts. One of them is dioxane….trifluoromethane which is stabilized by one C–

H…O bond and two C–H…F bonds with similar bond distances and dissociation energies (rO…H, 2.315(85) A˚ , rF…H, 2.92(1) A˚ and E_D = 6.8 kJ/mol) and forming a cage like structure.[20] The hydrogen bond capabilities of the C–H bond towards the nitrogen atom have been assessed by a series of pioneering studies performed by Klemperer and coworkers on various molecular adducts of hydrocarbons with ammonia. Among their studies there are three cases where the coupling partners of ammonia are HCCH,[21] HCN[22] and CF_3H.[23]

While Oxygen, nitrogen, sulfur and the halogen atoms are the strong acceptors for the C-H bond donor, π systems such as aromatic rings are among the weak acceptors. The C-H…π is another more frequently occurring weak non-conventional hydrogen bond.[11, 24-25] Here the electron rich π- system acts as an acceptor. This π-system can be C=C double, C≡C triple bonds, C_6 and C_5 aromatic rings, heteroaromatics, convex surfaces of fullerenes or nanotubes. In context of the Pearson's HSAB concept, [26-27] these are hydrogen bonds between soft acid donors and hard base acceptors. Stabilization of the CH/π hydrogen bond comes mostly from the dispersion force. Contribution from the electrostatic energy is unimportant except for several special cases involving strong carbon acids such as chloroform or acetylenic C-H. [24]

The geometrical parameters required to describe C-H…π bond are the same as used for other conventional H-bondings.[24] However, in the present case it is the centre of the π-system (centroid in case of aromatic system and the centre of electron cloud in case of double or triple bond) from where the distances are measured (**Fig. 9**).

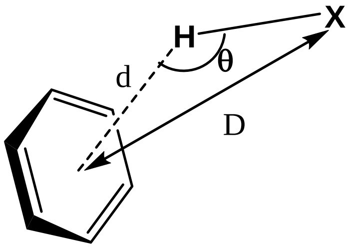

Figure 9. Definition of the geometrical parameters of the CH…π hydrogen bonds

The C-H…π interactions play an important role in conformation of molecules, in crystal packing, in host-guest complexes and in clatherates, which are well documented in literature.[28,29] Crystallographic database analyses provide firm evidence for the hydrogen bond nature of the C-H…π interaction. Braga[30] examined C-H…π interactions (π; C≡C, cyclopentadienyl and phenyl) in transition metal compounds. Umezawa *et al*.[31] reported statistical results on organic crystals. Combined database and MO studies were reported for C≡CH/π(C≡C) and CH/π (arene) interactions. Database surveys on transition metal complexes gave evidence of the CH/π hydrogen bond being an important factor in controlling the crystal packing and molecular structure of coordination and organometallic compounds. Such contact has also been observed in crystals of proteins and the importance of this interaction in molecular recognition has been realized. [28]

4.1.2 Lone pair – π interactions [32]

The interaction between a lone pair of electrons and the face of π systems is known as lone pair…π interactions.[32] The geometrical parameters required for a lone pair…π interaction is shown in the following (**Fig. 10**).

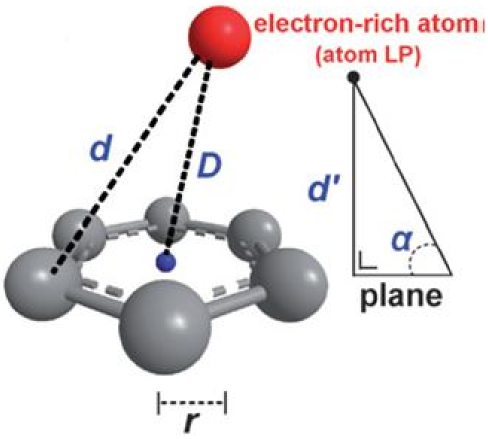

Figure 10. Schematic representation of the structural parameters used to characterize a lone pair…π contact [32]

These interactions were largely ignored by the scientific community for long and only in the past two decades interest in these types of interactions has considerably increased. This was because the arene moieties were considered electron rich and interaction between a lone pair of electrons and the π system of electrons were not thought to be feasible.

If we consider the case of interaction of water with benzene and hexafluorobenzene.[33] Benzene has a large, permanent quadrupole moment,[34] such that there is substantial negative electrostatic potential above and below the plane of the ring, and a belt of positive potential around the edge. Ionic and polar species interact with this moment as anticipated by purely electrostatic arguments. A prototype system is water…benzene. Water binds to benzene with a calculated 1.8 kcal/mol of binding energy in the geometry (**1**) expected from electrostatic arguments[35] (**Fig. 11**).

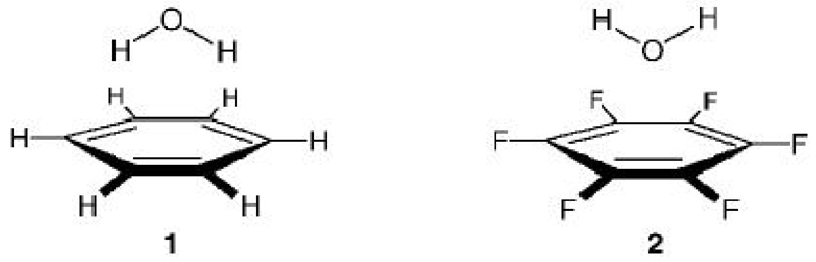

Figure 11. Interaction of water with (a) benzene and (b) hexafluorobenzene

Hexafluorobenzene has a quadrupole moment that is comparable in magnitude but opposite in sign to that of benzenes positive regions become negative and negative positive.[34] This leads, for example, to the very favorable stacking interaction between aryl and perfluoroaryl rings. Similar reasoning suggests that water should also bind to hexafluorobenzene but in the geometry of **2** with the water dipole moment reversed relative to the water…benzene interaction (**Fig. 11**). While quite reasonable from an electrostatic viewpoint, from another perspective this interaction is somewhat counterintuitive. It suggests that a π electron system should be attracted to a set of lone pair electrons. One might expect significant electron-electron repulsions that are not present for water…benzene.

Lone pair…π interactions appears to be of great importance for the stabilization of biological macromolecules,[32] as well as for the binding of inhibitors in the binding pocket of biochemical receptors. Egli and co-workers in 1995, reported an interesting case of lone-pair-π interactions observed in an biomacromolecule, i.e. Z-DNA.[36] It was shown that the stability of the left handed Z-DNA duplex (A-DNA and B-DNA are right-handed double stranded helices), despite poor base-pair stacking, is attributable to an unusual bonding interaction between the lone pair of an oxygen atom belonging to a cytidine 2’-deoxyribose unit and the guanidinium moiety of a guanosine (**Fig. 12**; interaction between O1 and the electron-deficient π-ring defined by the atoms C16 C17 N6 C18 N8 C19).

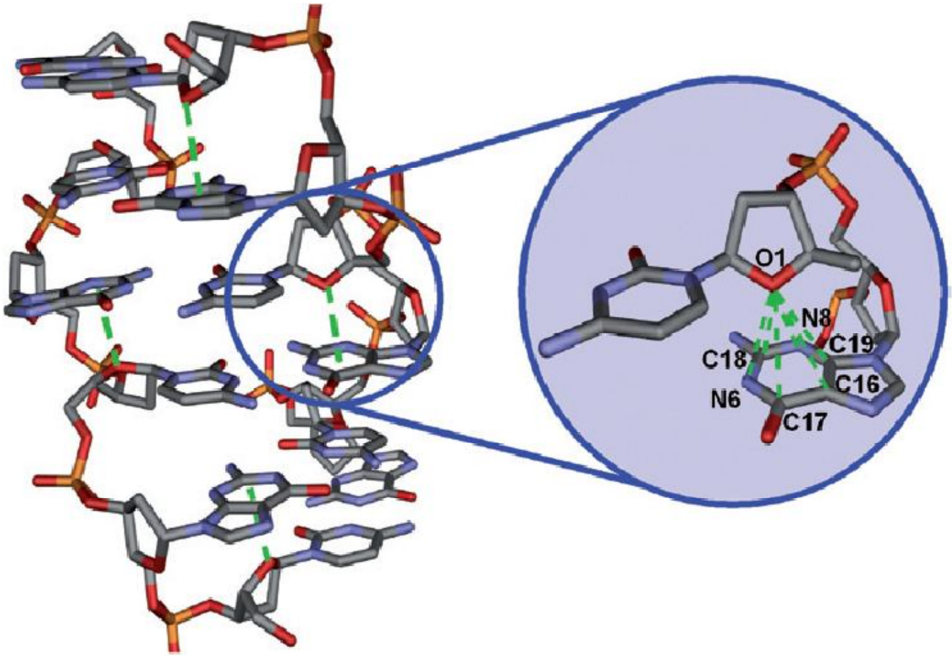

Figure 12. Lone pair…**π** interactions stabilizing the left-handed supramolecular structure of Z-DNA (Protein Data Bank refcode: 131D). Contact distances: 3.270 Ǻ (O1…N6), 2.975 Ǻ (O1…C18), 3.105 Ǻ (O1…N8), 3.353 Ǻ (O1…C19), 3.641 Ǻ (O1…C16), 3.611 Ǻ (O1…C17)[32]

Egli and co-workers in 2003 reported a remarkable example of H_2O---**π** interactions within a ribosomal frame-shifting RNA pseudoknot. Indeed, the crystal structure of this RNA pseudoknot has revealed lone pair nucleobase interactions characterized by a short contact distance of 2.93 Ǻ between a carbon atom of a cytosine moiety and the oxygen atom of a water molecule.[37]

An examination protein database by Sankararamakrishnan and co-workers was done for carbonyl (lp)–**π** interactions.[38] Over 250 protein structures from the databank were found where carbonyl oxygen atoms are within 3.5 Ǻ of the centroid of aromatic rings.

Recently, lone pair…**π** bonding contacts has been evidenced in small molecular host guest systems, [39-46] and a number of computational studies have demonstrated that such interactions between a lp donor and an aromatic acceptor can be energetically favourable.[47-49] In a recent study of Crystallographic Structural Database (CSD) the lone pair – π interactions appears to be directional.[50]

4.2 Objective

1) To study the effect of increasing the length of linker on intramolecular π–π interactions in comparison to seen in *ethylene* linker based dissymmetric pyrazolo[3,4-*d*]pyrimidine compounds (**Chapter 3**) having phthalazinone/quinazilinone and benzotriazinone moieties on the other side on intramolecular π–π interactions, both in solution and more importantly on solid state.
2) To study the effect of replacing *trimethylene* linker with *butylidine* linker in *trimethylene* linker based dissymmetric pyrazolo[3,4-*d*]pyrimidine compounds having phthalazinone/quinazilinone and benzotriazinone moieties on the other side on intramolecular π–π interactions, both in solution and solid state.

4.3 Synthesis and characterization

4.3.1 Synthesis and characterization of 2-(n-(4,6-bis(methylthio)-1*H*-pyrazolo[3,4-*d*]pyrimidin-1-yl)alkyl)phthalazin-1(2*H*)-one (25-28), 3-(3-(4,6-bis(methylthio)-1*H*-pyrazolo[3,4-*d*]pyrimidin-1-yl)propyl)quinazolin-4(3*H*)-one (29) and 3-(3-(4,6-bis(methylthio)-1*H*-pyrazolo[3,4-*d*]pyrimidin-1-yl)propyl)benzo[*d*][1,2,3]triazin-4(3*H*)-one (30).

Synthesis of compounds **25–30** was carried out following the procedures described in the thesis of Sangeeta Aswal[51] and is shown in **Scheme 1**. These compounds were characterized by NMR and mass spectrometric techniques and were compared with the values reported in the thesis.

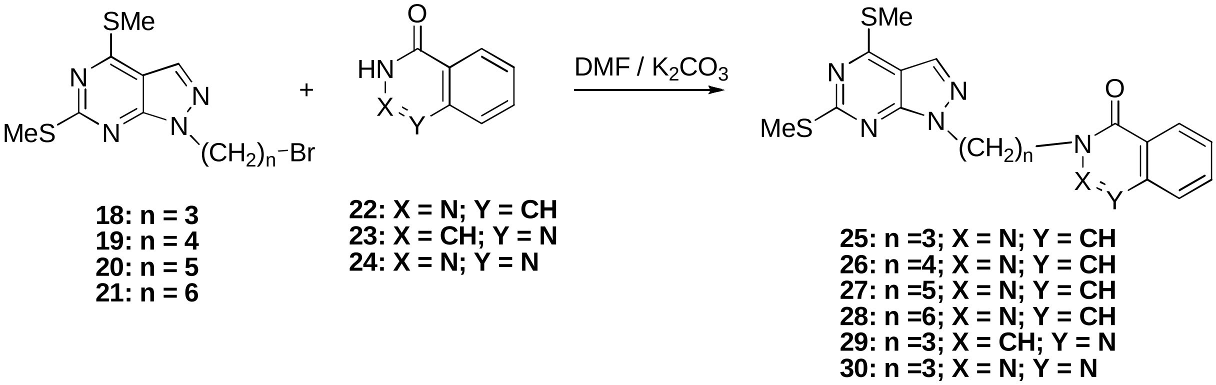

Scheme 1. Synthesis of compounds **25-30**

Proton NMR of compound **25** showed a multiplet between δ 2.46–2.58 for CH_2, two singlets at δ 2.52 and δ 2.66 for two SMe groups, two triplets at δ 4.31 and δ 4.50 for two NCH_2, two multiplets between δ 7.62–7.83 and between δ 8.37 -8.42, two singlets at δ 7.90 and δ 8.09 for six aromatic protons. Mass spectrum showed base peak corresponding to $[M+H]^+$ at *m/z* 399.

Proton NMR of compound **26** showed a multiplet between δ 1.81–2.04 for two CH_2, two singlets at δ 2.60 and δ 2.68 for two SMe groups, two triplets at δ 4.28 and δ 4.44 for two NCH_2, two multiplets between δ 7.65–7.83 and between δ 8.40-8.43, two singlets at δ 7.89 and at δ 8.13 for six aromatic protons. Mass spectrum showed base peak corresponding to $[M+H]^+$ at *m/z* 413.

Proton NMR of compound **27** showed multiplets between δ 1.35–1.44 and between δ 1.90–2.02, for three CH_2, two singlets at δ 2.61 and δ 2.68 for two SMe groups, two triplets at δ 4.28 and δ 4.38 for two NCH_2, two multiplets between δ 7.65–7.84 and between δ 8.40-8.43, two singlets at δ 7.88 and at δ 8.14 for six aromatic protons. Mass spectrum showed base peak corresponding to $[M+H]^+$ at *m/z* 427.

Proton NMR of compound **28** showed multiplets between δ 1.32–1.44 and between δ 1.88–2.00, for four CH_2, two singlets at δ 2.62 and δ 2.68 for two SMe groups, two triplets at δ 4.26 and δ 4.37 for two NCH_2, two multiplets between δ 7.65–7.84 and between δ 8.40- 8.43, two singlets at δ 7.86 and δ 8.13 for six aromatic protons. Mass spectrum showed base peak corresponding to $[M+H]^+$ at *m/z* 441.

Proton NMR of compound **29** showed a multiplet between δ 2.44–2.53 for CH_2, two singlets at δ 2.58 and δ 2.67 for two SMe groups, two triplets at δ 4.02 and δ 4.46 for two NCH_2, three multiplets between δ 7.46–7.52, between δ 7.67–7.77 and between δ 8.26-8.29, two singlets at δ 7.92 and δ 8.08 for six aromatic protons. Mass spectrum showed base peak corresponding to $[M+H]^+$ at *m/z* 399.

Proton NMR of compound **30** showed a multiplet between δ 2.55–2.64 for CH_2, two singlet at δ 2.52 and δ 2.66 for two SMe groups, a multiplet between δ 4.51–4.56 for two NCH_2, four multiplets between δ 7.76–7.81, between δ 7.88–7.96, between δ 8.11–8.14 and between δ

8.29-8.32, one singlet at δ 7.89 for five aromatic protons. Mass spectrum showed base peak corresponding to $[M+H]^+$ at *m/z* 400.

4.3.2 Regioselective nucleophilic substitution of 4-SMe group of different compounds.

4.3.2.1 Synthesis and characterization of 2-(3-(6-(methylthio)-4-(pyrrolidin-1-yl)-1*H*-pyrazolo[3,4-*d*]pyrimidin-1-yl)propyl)phthalazin-1(2*H*)-one (31), 2-(4-(6-(methylthio)-4-(pyrrolidin-1-yl)-1*H*-pyrazolo[3,4-*d*]pyrimidin-1-yl)butyl)phthalazin-1(2*H*)-one (32), 2-(6-(6-(methylthio)-4-(pyrrolidin-1-yl)-1*H*-pyrazolo[3,4-*d*]pyrimidin-1-yl)hexyl)phthalazin-1(2*H*)-one (33), 3-(3-(6-(methylthio)-4-(pyrrolidin-1-yl)-1*H*-pyrazolo[3,4-*d*]pyrimidin-1-yl)propyl)quinazolin-4(3*H*)-one (34), and 3-(3-(6-(methylthio)-4-(pyrrolidin-1-yl)-1*H*-pyrazolo[3,4-*d*]pyrimidin-1-yl)propyl)benzo[*d*][1,2,3] triazin-4(3*H*)-one (35).

Reaction of compounds **25, 26, 28, 29** and **30** with pyrrolidine under refluxing conditions gave compounds **31, 32**, **33**, **34**, and **35** respectively as shown in **Scheme 2**. These compounds were characterized by NMR and mass spectrometric techniques.

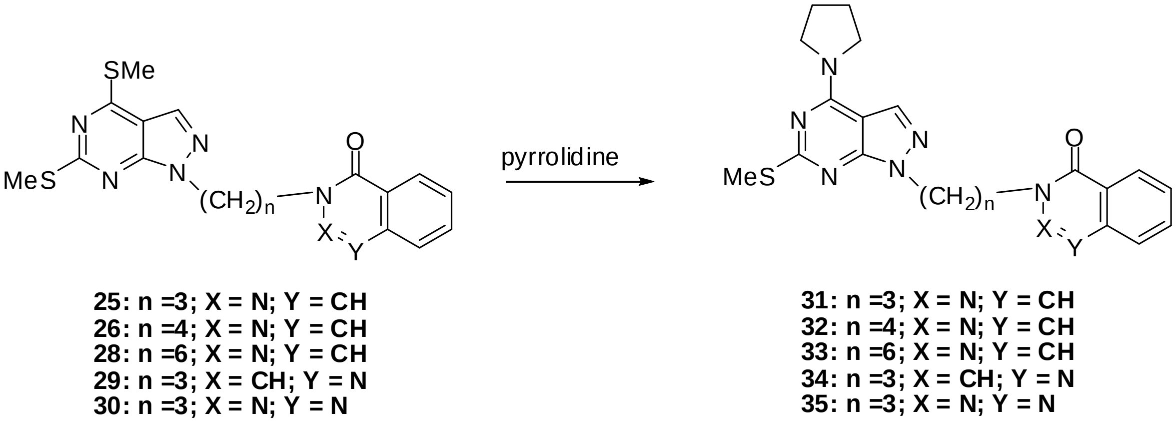

Scheme 2. Synthesis of compounds **31-35**

Proton NMR of compound **31** showed multiplets between δ 1.96–2.02, between δ 2.09–2.15, for two pyrrolidinyl CH_2 and between δ 2.44–2.54 for one linker CH_2, one singlet at δ 2.47 for SMe group, a triplet at δ 3.76 for two pyrrolidinyl NCH_2, two triplets at δ 4.30 and δ 4.45 for two NCH_2, two multiplets between δ 7.64–7.82 and between δ 8.38-8.42, two singlets at δ 7.81 and δ 8.11 for six aromatic protons. Mass spectrum showed base peak corresponding to $[M+H]^+$ at *m/z* 422.

Proton NMR of compound **32** showed a multiplet between δ 1.80–2.17 for two, for two pyrrolidinyl CH_2 and two linker CH_2, one singlet at δ 2.54 for one SMe, a triplet at δ 3.76 for two pyrrolidinyl NCH_2, two triplets at δ 4.28 and δ 4.39 for two NCH_2, two multiplets between δ 7.65–7.83 and between δ 8.37-8.42, two singlets at δ 7.78 and δ 8.14 for six aromatic protons.. Mass spectrum showed base peak corresponding to $[M+H]^+$ at *m/z* 436.

Proton NMR compound **33** showed multiplets between δ 1.22–1.42 and between δ 1.74–2.14, two pyrrolidinyl CH_2 and two linker CH_2, one singlet at δ 2.54 for one SMe a triplet at δ 3.73 for two pyrrolidinyl NCH_2, two triplets at δ 4.19 and δ 4.28 for two NCH_2, two multiplets between δ 7.64–7.78 and between δ 8.38-8.41, two singlets at δ 7.76 and δ 8.12 for six aromatic protons. Mass spectrum showed base peak corresponding to $[M+H]^+$ at *m/z* 464.

Proton NMR of compound **34** showed multiplets between δ 1.94–2.06 and between δ 2.08–2.20 for two pyrrolidinyl CH_2 and a quintet at δ 2.46 for one linker CH_2, one singlet at δ 2.55 for SMe group, a broad singlet at δ 3.77 for two pyrrolidinyl NCH_2, two triplets at δ 4.01 and δ 4.42 for two NCH_2, three multiplets between δ 7.49–7.54, between δ 7.68–7.76 and between δ 8.28-8.31, two singlets at δ 7.82 and δ 8.13 for six aromatic protons. Mass spectrum showed base peak corresponding to $[M+H]^+$ at *m/z* 422.

Proton NMR of compound **35** showed multiplets between δ 1.94–2.00 and between δ 2.08–2.16 for two pyrrolidinyl CH_2 and a quintet at δ 2.56 for one linker CH_2, one singlet at δ 2.45 for SMe group, a triplet at δ 3.75 for two pyrrolidinyl NCH_2, a multiplet between δ 4.46–4.56 for two NCH_2, four multiplets between δ 7.73–7.78, between δ 7.88–7.93, between δ 8.08–8.11 and between δ 8.28-8.31, one singlet at δ 7.79 for five aromatic protons. Mass spectrum showed base peak corresponding to $[M+H]^+$ at *m/z* 423.

4.3.2.2 Synthesis and characterization of 2-(3-(6-(methylthio)-4-oxo-4,5-dihydro-1*H*-pyrazolo[3,4-*d*]pyrimidin-1-yl)propyl)phthalazin-1(2*H*)-one (36) and 2-(4-(6-(methylthio)-4-oxo-4,5-dihydro-1*H*-pyrazolo[3,4-*d*]pyrimidin-1-yl)butyl)phthalazin-1(2*H*)-one (37).

Reaction of the compound (**25-26**) with NaOH(aq.) in MeOH under reflux for 5 h followed by acidification with glacial acetic acid under cold condition gave desired products **36** and **37** respectively (**Scheme 3**). These compounds were characterized by NMR and mass spectrometric techniques.

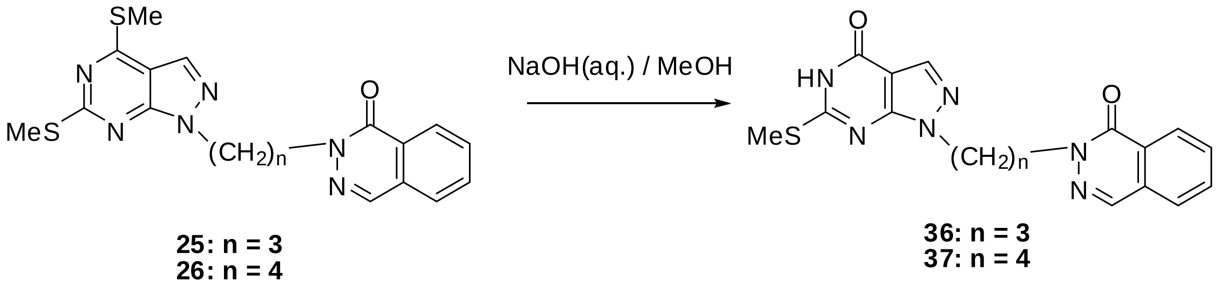

Scheme 3. Synthesis of compounds **36-37**

Proton NMR of compound **36** showed a quintet at δ 2.53 for CH_2, one singlet at δ 2.45 for one SMe, two triplets at δ 4.32 and δ 4.44 for two NCH_2, two multiplets between δ 7.75–7.93 and between δ 8.35-8.38, two singlets at δ 7.96 and δ 8.20 for six aromatic protons. Mass spectrum showed base peak corresponding to $[M+H]^+$ at *m/z* 369.

Proton NMR of compound **37** showed a multiplet between 1.86 - 2.06 for four CH_2, one singlet at δ 2.63 for one SMe, two triplets at δ 4.30 and δ 4.37 for two NCH_2, two multiplets between δ 7.66–7.82 for three aromatic proton and between δ 8.40-8.46 for one aromatic proton, two singlets at δ 8.00 and δ 8.14 for two aromatic protons. Mass spectrum showed base peak corresponding to $[M+H]^+$ at *m/z* 383.

4.3.2.3 Synthesis and characterization of 2-(3-(4-methoxy-6-(methylthio)-1*H*-pyrazolo[3,4-*d*]pyrimidin-1-yl)propyl)phthalazin-1(2*H*)-one (38), 2-(4-(4-methoxy-6-(methylthio)-1*H*-pyrazolo[3,4-*d*]pyrimidin-1-yl)butyl)phthalazin-1(2*H*)-one (39) and 3-(3-(4-methoxy-6-(methylthio)-1*H*-pyrazolo[3,4-*d*]pyrimidin-1-yl)propyl)quinazolin-4(3*H*)-one (40).

Reaction of the compound **25**, **26** and **29** with NaOMe in MeOH under reflux for 5 h followed by acidification with glacial acetic acid under cold condition gave desired products **38**, **39** and **40** respectively (**Scheme 4**). These compounds were characterized by NMR and mass spectrometric techniques.

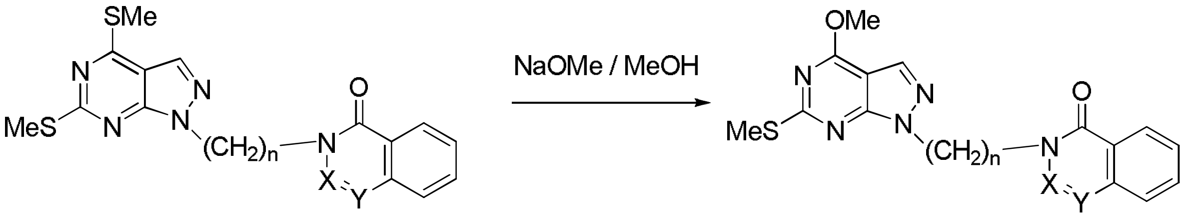

25: n =3; X = N; Y = CH
26: n =4; X = N; Y = CH
29: n =3; X = CH; Y = N

38: n =3; X = N; Y = CH
39: n =4; X = N; Y = CH
40: n =3; X = CH; Y = N

Scheme 4. Synthesis of compounds **38-40**

Proton NMR of compound **38** showed a multiplet between δ 2.48–2.57 for CH_2, a singlet at δ 2.48 for one SMe, a singlet at δ 4.09 for one OMe, two triplets at δ 4.31 and δ 4.50 for two NCH_2, two multiplets between δ 7.64–7.83 and between δ 8.38-8.41, two singlets at δ 7.89 and δ 8.10 for six aromatic protons. Mass spectrum showed base peak corresponding to $[M+H]^+$ at *m/z* 383.

Proton NMR compound **39** showed a multiplet between δ 1.82–2.04 for two CH_2, one singlet at δ 2.59 for one SMe, a singlet at δ 4.10 for one OMe, two triplets at δ 4.29 and δ 4.45 for two NCH_2, two multiplets between δ 7.66–7.82 and between δ 8.40-8.42, two singlets at δ 7.88 and δ 8.13 for six aromatic protons. Mass spectrum showed base peak corresponding to $[M+H]^+$ at *m/z* 397.

Proton NMR of compound **40** showed a multiplet between δ 2.45–2.53 for CH_2, one singlet at δ 2.58 for one SMe, a singlet at δ 4.12 for one OMe, two triplets at δ 4.03 and δ 4.47 for two NCH_2, three multiplets between δ 7.48–7.53, between δ 7.68–7.78, and between δ 8.28-8.31, two singlets at δ 7.92 and δ 8.08 for six aromatic protons. Mass spectrum showed base peak corresponding to $[M+H]^+$ at *m/z* 383.

4.3.3 Synthesis of chloro analogs of compounds 25-26.

4.3.3.1 Synthesis and characterization of 2-(3-(4-chloro-6-(methylthio)-1*H*-pyrazolo[3,4-*d*]pyrimidin-1-yl)propyl)phthalazin-1(2*H*)-one (41) and 2-(4-(4-chloro-6-(methylthio)-1*H*-pyrazolo[3,4-*d*]pyrimidin-1-yl)butyl)phthalazin-1(2*H*)-one (42).

Reaction of the compound **36** and **37** with $POCl_3$ under reflux for 5 h gave desired products **41** and **42** respectively (**Scheme 5**). These compounds were characterized by NMR and mass spectrometric techniques.

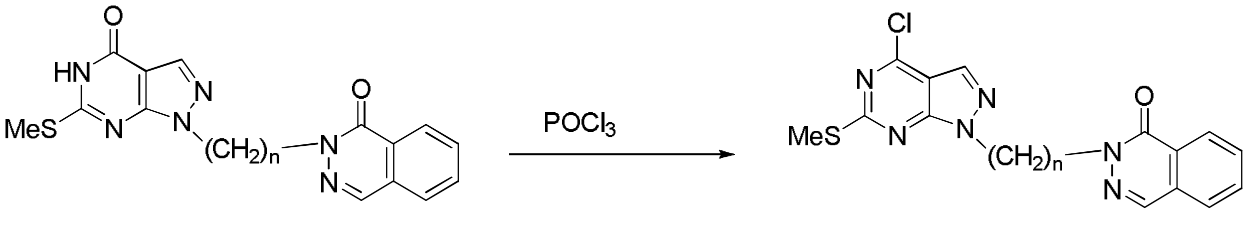

36: n =3
37: n =4

41: n =3
42: n =4

Scheme 5. Synthesis of compounds **41-42**

Proton NMR of compound **41** showed a quintet at δ 2.57 for CH_2, one singlet at δ 2.48 for one SMe, two triplets at δ 4.31 and δ 4.52 for two NCH_2, two multiplets between δ 7.66–7.84 and between δ 8.36-8.39, two singlets at δ 7.98 and δ 8.08 for six aromatic protons. Mass spectrum showed base peak corresponding to $[M+H]^+$ at *m/z* 387.

Proton NMR compound **42** showed a multiplet between δ 1.81–2.08 for two CH_2, one singlet at δ 2.60 for one SMe, two triplets at δ 4.11 and δ 4.49 for two NCH_2, two multiplets between δ 7.68–7.84 and between δ 8.40-8.43, two singlets at δ 7.98 and δ 8.13 for six aromatic protons. Mass spectrum showed base peak corresponding to $[M+H]^+$ at *m/z* 401.

4.3.4 Methylation of compound 36

4.3.4.1 Synthesis and characterization of 2-(3-(5-methyl-6-(methylthio)-4-oxo-4,5-dihydro-1*H*-pyrazolo[3,4-*d*]pyrimidin-1-yl)propyl)phthalazin-1(2*H*)-one (43).

Reaction of compound **36** with methyl iodide in DMF using K_2CO_3 at room temperature gave **43** (**Scheme 6**). This compound was characterized by NMR and mass spectrometric techniques.

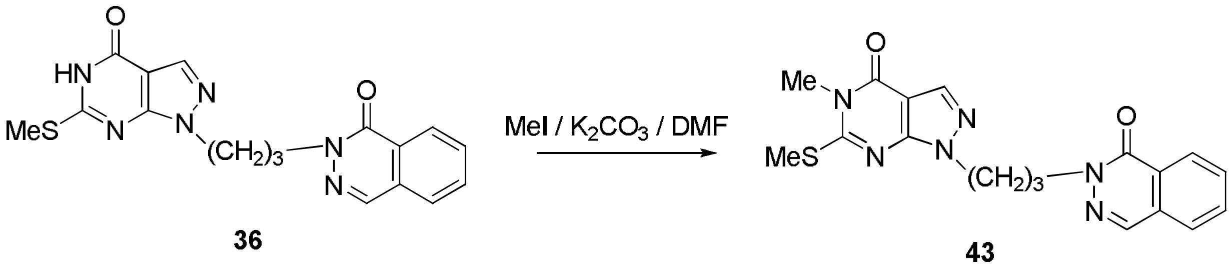

36

43

Scheme 6. Synthesis of compounds **43**

Proton NMR of compound **43** showed a multiplet at δ 2.46-2.56 for CH_2, a singlet at δ 2.48 for one SMe, a singlet at 4.09 for one NMe, two triplets at δ 4.30 and δ 4.49 for two NCH_2, two multiplets between δ 7.66–7.84 and between δ 8.38-8.42, two singlets at δ 7.89 and δ 8.10 for six aromatic protons. Mass spectrum showed base peak corresponding to $[M+H]^+$ at *m/z* 383.

4.3.5 Oxidation of 6- SMe group of compounds 38, 39 and 41 to SO_2Me group.

4.3.5.1 Synthesis and characterization of 2-(3-(4-methoxy-6-(methylsulfonyl)-1*H*-pyrazolo[3,4-*d*]pyrimidin-1-yl)propyl)phthalazin-1(2*H*)-one (44), 2-(4-(4-methoxy-6-(methylsulfonyl)-1*H*-pyrazolo[3,4-*d*]pyrimidin-1-yl)butyl)phthalazin-1(2*H*)-one (45) and2-(3-(4-chloro-6-(methylsulfonyl)-1*H*-pyrazolo[3,4-*d*]pyrimidin-1-yl)propyl)phthalazin-1(2*H*)-one (46).

Reaction of the compound **38, 39** and **41** with oxone in acetone at 0°C for 6 h gave desired products **44**, **45** and **46** respectively (**Scheme 7**). These compounds were characterized by NMR and mass spectrometric techniques.

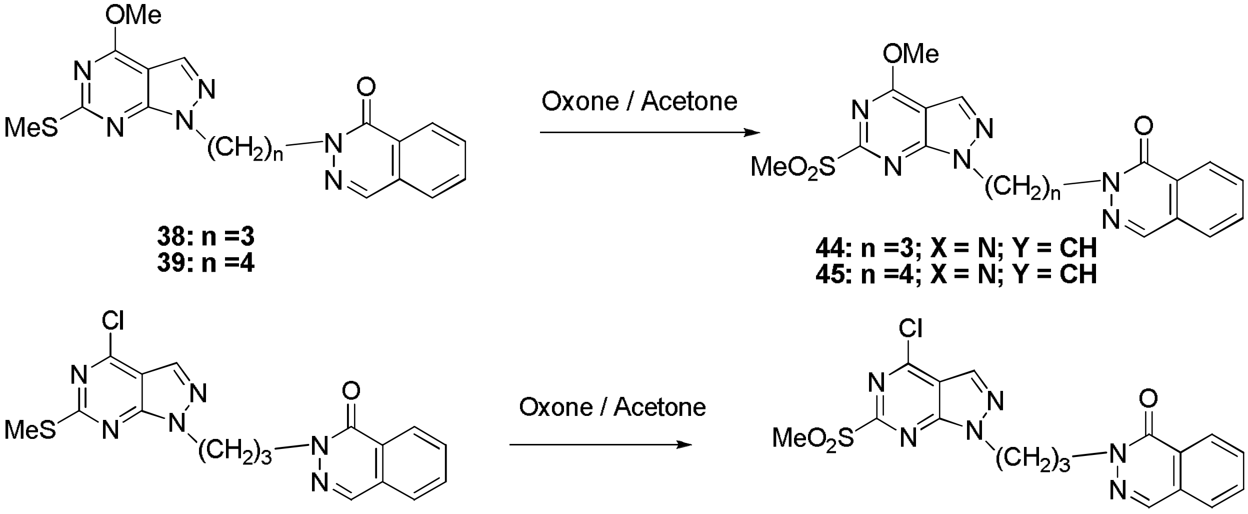

38: n =3
39: n =4

44: n =3; X = N; Y = CH
45: n =4; X = N; Y = CH

41

46

Scheme 7. Synthesis of compounds **46**

Proton NMR of compound **44** showed a quintet at δ 2.59 for CH_2, one singlet at δ 3.33 for one SO_2Me, one singlet at δ 4.25 for one OMe, two triplets at δ 4.31 and δ 4.61 for two NCH_2, two multiplets between δ 7.68–7.89 and between δ 8.37-8.39, one singlet at δ 8.12 (two protons) for six aromatic protons. Mass spectrum showed base peak corresponding to $[M+H]^+$ at *m/z* 415.

Proton NMR of compound **45** showed a multiplet between δ 1.81–2.11 for two CH_2, one singlet at δ 3.40 for one SO_2Me, one singlet at δ 4.26 for one OMe, two triplets at δ 4.29 and δ 4.57 for two NCH_2, two multiplets between δ 7.68–7.83 and between δ 8.38-8.41, two singlets at δ 8.11 and δ 8.15 for six aromatic protons. Mass spectrum showed base peak corresponding to $[M+H]^+$ at *m/z* 429.

Proton NMR of compound **46** showed a quintet at δ 2.64 for CH_2, one singlet at δ 3.38 for one SO_2Me, two triplets at δ 4.31 and δ 4.68 for two NCH_2, two multiplets between δ 7.68–7.85 and between δ 8.33-8.36, two singlets at δ 8.12 and δ 8.27 for six aromatic protons. Mass spectrum showed base peak corresponding to $[M+H]^+$ at *m/z* 419.

4.3.6 Synthesis and characterization of 2-(3-(4,6-bis(methylthio)-2*H*-pyrazolo[3,4-*d*]pyrimidin-2-yl)propyl)phthalazin-1(2*H*)-one (48).

Reaction of **22** in DMF using K_2CO_3 at room temperature gave **48**. This compound was characterized by NMR and mass spectrometric techniques.

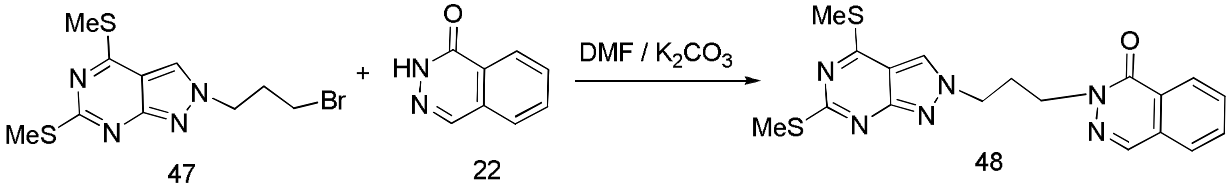

Scheme 8. Synthesis of compounds **48**

Proton NMR of compound **48** showed two singlets at δ 2.61 and δ 2.65 for two SMe groups (the signals for linker CH_2 protons are in between these two singlets as shown by the integration values of the protons which is for 8 protons), two triplets at δ 4.31 and δ 4.42 for two NCH_2, two multiplets between δ 7.68–7.82 and between δ 8.40-8.42, two singlets at δ 8.07 and δ 8.16 for six aromatic protons. Mass spectrum showed base peak corresponding to $[M+H]^+$ at *m/z* 399.

4.3.7 Synthesis and characterization of 2-(3-(4,6-bis(methylthio)-1*H*-pyrazolo[3,4-*d*]pyrimidin-1-yl)propyl)phthalazine-1(2*H*)-thione (49).

Reaction of compound **25** with P_2S_5 in β-picoline under refluxing conditions gave **49** (**Scheme 9**). This compound was characterized by NMR and Mass spectrometric techniques.

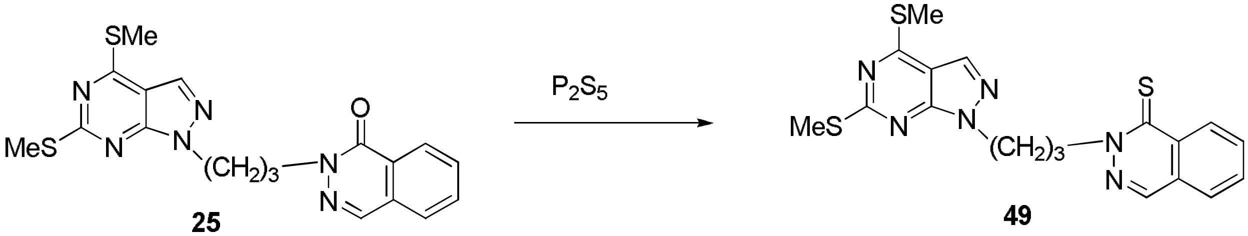

Scheme 9. Synthesis of compounds **49**

Proton NMR of compound **49** showed a multiplet between δ 2.61–2.71 for CH_2, two singlets at δ 2.55 and δ 2.71 for two SMe groups, two triplets at δ 4.53 and δ 4.88 for two NCH_2, three multiplets between δ 7.66–7.70, between δ 7.78–7.84 and between δ 8.94-8.97, two singlets at δ 7.92 and δ 8.34 for six aromatic protons. Mass spectrum showed base peak corresponding to $[M+H]^+$ at *m/z* 415.

4.3.8 Synthesis and characterization of 1-(2-(chloromethyl)allyl)-4,6-bis(methylthio)-1*H*-pyrazolo[3,4-*d*]pyrimidine (52) and 2-(2-(chloromethyl)allyl)-4,6-bis(methylthio)-2*H*-pyrazolo[3,4-*d*]pyrimidine (53).

Reaction of **50** with **51** in DMF using K_2CO_3 at room temperature gave **52** and **53** (**Scheme 10**). These compounds were characterized by NMR and mass spectrometric techniques.

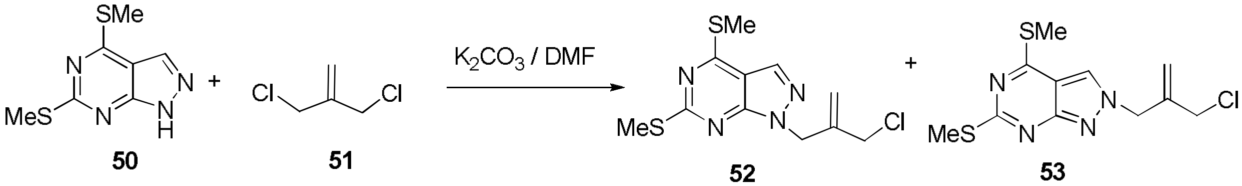

Scheme 10. Synthesis of compounds **52-53**

Proton NMR of compound **52** showed two singlets at δ 2.63 and δ 2.69 for two SMe groups, one singlet at δ 4.01 for CH_2Cl protons, one singlet at δ 5.12 for NCH_2 groups, two singlets at δ 5.14 and 5.36 for exomethylene CH and one singlet at δ 7.96 for one aromatic proton. Mass spectrum showed base peak corresponding to $[M+H]^+$ at *m/z* 301.

Proton NMR of compound **53** showed two singlets at δ 2.61 and δ 2.68 for two SMe groups, one singlet at δ 3.98 for CH_2Cl protons, one singlet at δ 5.06 for NCH_2 protons, two singlets at δ 5.27 and 5.44 for exomethylene CH and one singlet at δ 7.99 for one aromatic proton. Mass spectrum showed base peak corresponding to $[M+H]^+$ at *m/z* 301.

4.3.9 Synthesis and characterization of 2-(2-((4,6-bis(methylthio)-1*H*-pyrazolo[3,4-*d*]pyrimidin-1-yl)methyl)allyl)phthalazin-1(2*H*)-one (54), 3-(2-((4,6-bis(methylthio)-1*H*-pyrazolo[3,4-*d*]pyrimidin-1-yl)methyl)allyl)quinazolin-4(3*H*)-one (55) and 3-(2-((4,6-bis(methylthio)-1*H*-pyrazolo[3,4-*d*]pyrimidin-1-yl)methyl)allyl)benzo[*d*][1,2,3]triazin-4(3*H*)-one (56).

Reaction of compound **52** with **22** in DMF using K_2CO_3 at room temperature gave **54**. Reaction of compound **52** with **23** gave **55** and reaction of compound **52** with **24** gave **56** (**Scheme 11**). These compounds were characterized by NMR and mass spectrometric techniques.

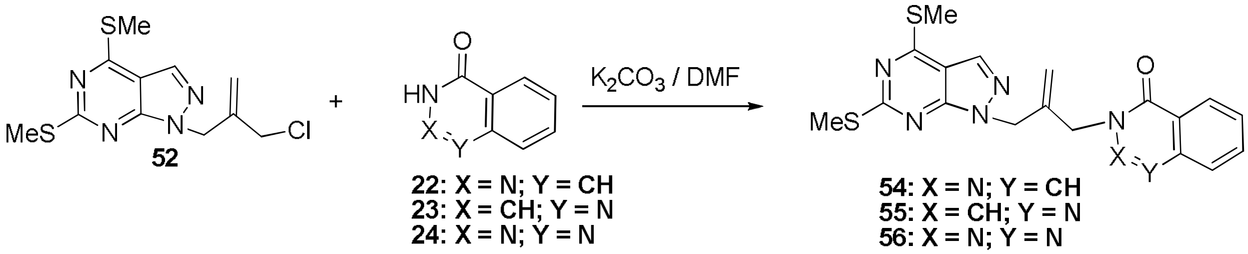

52

22: X = N; Y = CH
23: X = CH; Y = N
24: X = N; Y = N

54: X = N; Y = CH
55: X = CH; Y = N
56: X = N; Y = N

Scheme 11. Synthesis of compounds **54-56**

Proton NMR of compound **54** showed two singlets at *δ* 2.38 and *δ* 2.65 for two SMe groups, two singlets at *δ* 4.84 and 5.04 for NCH_2 groups, two singlets at *δ* 5.17 and 5.23 for exomethylene CH, three multiplets between δ 7.65–7.67, between δ 7.75–7.80 and between δ 8.34-8.37, two singlets at δ 7.92 and δ 8.05 for six aromatic protons. Mass spectrum showed base peak corresponding to $[M+H]^+$ at *m/z* 411.

Proton NMR of compound **55** showed two singlets at *δ* 2.48 and *δ* 2.67 for two SMe groups, two singlets at *δ* 4.61 and 5.03 for NCH_2 groups, two singlets at *δ* 5.23 and 5.32 for exomethylene CH, three multiplets between δ 7.48–7.52, between δ 7.67–7.78 and between δ 8.24-8.27, two singlets at δ 7.91 and δ 7.94 for six aromatic protons. Mass spectrum showed base peak corresponding to $[M+H]^+$ at *m/z* 411.

Proton NMR of compound **56** showed two singlets at *δ* 2.42 and *δ* 2.66 for two SMe groups, two singlets at *δ* 5.05 and 5.08 for NCH_2 groups, two singlets at *δ* 5.24 and 5.28 for exomethylene CH, four multiplets between δ 7.78–7.82, between δ 7.91–7.97 between δ 8.12-8.15 and between δ 8.27-8.30, one singlet at δ 7.91 for five aromatic protons. Mass spectrum showed base peak corresponding to $[M+H]^+$ at *m/z* 412.

4.3.10 Synthesis and characterization of 2-(2-((4,6-bis(methylthio)-2*H*-pyrazolo[3,4-*d*]pyrimidin-2-yl)methyl)allyl)phthalazin-1(2*H*)-one (57).

Reaction of compound **53** with **22** in DMF using K_2CO_3 at room temperature gave **57** (**Scheme 12**).

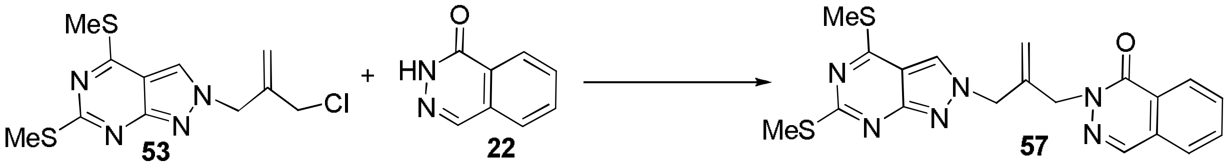

Scheme 12. Synthesis of compounds **57**

Proton NMR of compound **57** showed two singlets at δ 2.59 and δ 2.65 for two SMe groups, two singlets at δ 4.84 and 5.01 for NCH_2 groups, two singlets at δ 5.31 and 5.41 for exomethylene CH, three multiplets between δ 7.65–7.68, between δ 7.74–7.83 and between δ 8.37-8.40, two singlets at δ 8.06 and δ 8.13 for six aromatic protons. Mass spectrum showed base peak corresponding to $[M+H]^+$ at *m/z* 411.

4.3.11 Regioselective nucleophilic substitution of 4-SMe group of compounds 54 and 57.

4.3.11.1 Synthesis and characterization of 2-(2-((6-(methylthio)-4-(pyrrolidin-1-yl)-1*H*-pyrazolo[3,4-*d*]pyrimidin-1-yl)methyl)allyl)phthalazin-1(2*H*)-one (58) and 2-(2-((6-(methylthio)-4-(pyrrolidin-1-yl)-2*H*-pyrazolo[3,4-*d*]pyrimidin-2-yl)methyl)allyl)-phthalazin-1(2*H*)-one (59).

Reaction of compounds **54** and **57** with pyrrolidine under refluxing conditions gave compounds **58** and **59** respectively as shown in **Scheme 13**. These compounds were characterized by NMR and mass spectrometric techniques.

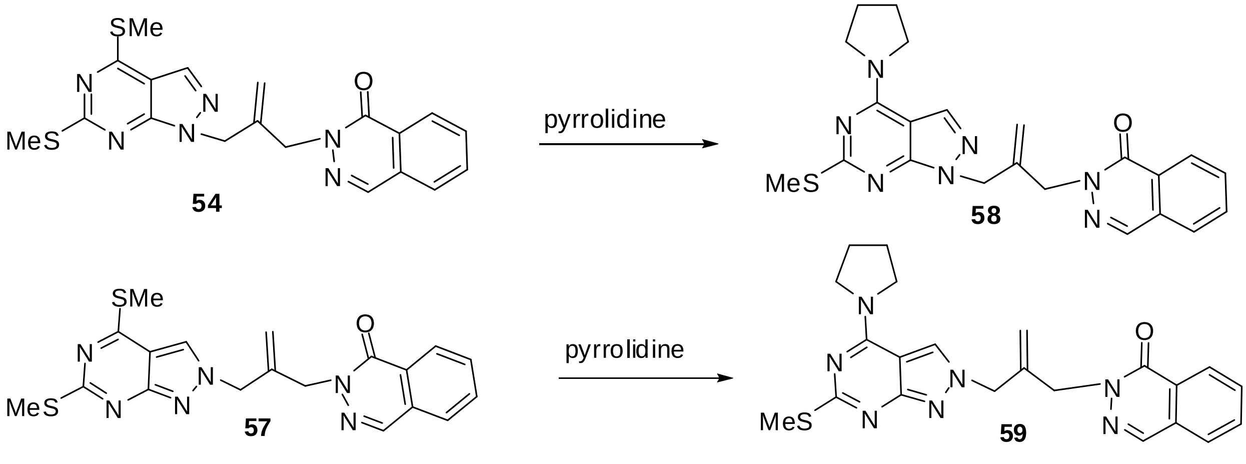

Scheme 13. Synthesis of compounds **58-59**

Proton NMR of compound **58** showed multiplets between δ 1.97–2.01 and between δ 2.10–2.14 for two pyrrolidinyl CH_2, one singlet at δ 2.33 for SMe group, a triplet at δ 3.75 for two pyrrolidinyl NCH_2, two singlets at δ 4.30 and δ 4.45 for two NCH_2, two singlets at *δ* 5.13 and 5.17 for exomethylene CH, two multiplets between δ 7.66–7.80 and between δ 8.35-8.38, two singlets at δ 7.82 and δ 8.09 for six aromatic protons. Mass spectrum showed base peak corresponding to $[M+H]^+$ at *m/z* 434.

Proton NMR of compound **59** showed multiplet between δ 1.97–2.13 for two pyrrolidinyl CH_2, one singlet at δ 2.55 for SMe group, a multiplet between δ 3.68–3.72 for two pyrrolidinyl NCH_2, two singlets at δ 4.83 and δ 4.95 for two NCH_2, two singlets at *δ* 5.31 and 5.34 for exomethylene CH, two multiplets between δ 7.66–7.82 and between δ 8.34-8.37, two singlets at δ 7.95 and δ 8.13 for six aromatic protons. Mass spectrum showed base peak corresponding to $[M+H]^+$ at *m/z* 434.

4.3.11.2 Synthesis and characterization of 2-(2-((4-methoxy-6-(methylthio)-1*H*-pyrazolo[3,4-*d*]pyrimidin-1-yl)methyl)allyl)phthalazin-1(2*H*)-one (60).

Reaction of the compound **54** with NaOMe in MeOH under reflux for 5 h followed by acidification with glacial acetic acid under cold condition gave **60** (**Scheme 14**). This compound was characterized by NMR and mass spectrometric techniques.

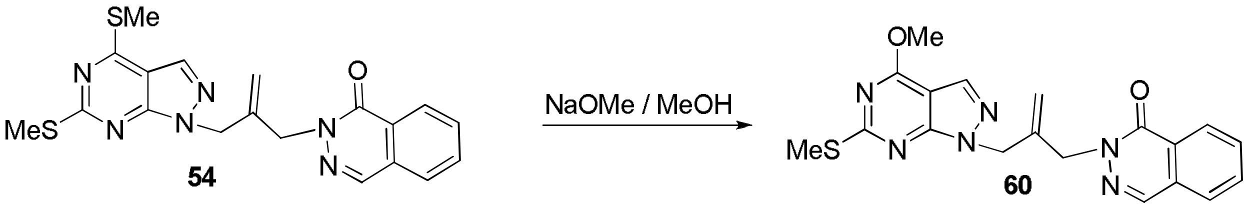

Scheme 14. Synthesis of compounds **60**

Proton NMR of compound **60** showed two singlets at *δ* 2.35 for SMe protons and *δ* 4.08 for OMe protons, two singlets at *δ* 4.84 and 5.04 for NCH_2 groups, two singlets at *δ* 5.17 and 5.23 for exomethylene CH, two multiplets between δ 7.66–7.83 and between δ 8.34-8.37, two singlets at δ 7.92 and δ 8.07 for six aromatic protons. Mass spectrum showed base peak corresponding to $[M+H]^+$ at *m/z* 395.

4.3.11.3 Synthesis and characterization of 2-(2-((6-(methylthio)-4-oxo-4,5-dihydro-1*H*-pyrazolo[3,4-*d*]pyrimidin-1-yl)methyl)allyl)phthalazin-1(2*H*)-one (61).

Reaction of the compound **54** with NaOH(aq.) in MeOH under reflux for 5 h followed by acidification with glacial acetic acid under cold condition gave **61** (**Scheme 15**). This compound was characterized by NMR and mass spectrometric techniques.

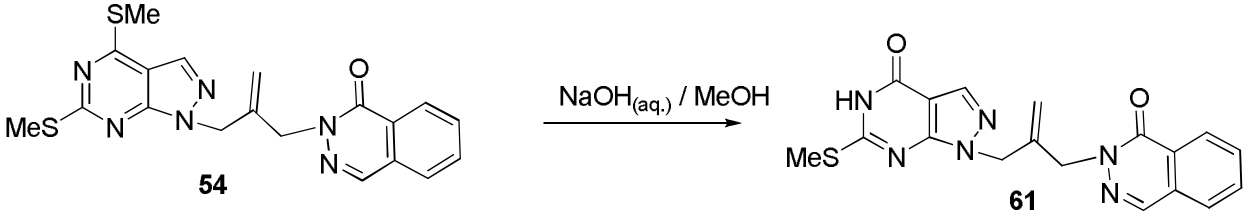

Scheme 15. Synthesis of compounds **61**

Proton NMR of compound **61** showed one singlet at δ 2.39 for one SMe, two singlets at *δ* 4.88 and 4.99 for NCH_2 groups, two singlets at *δ* 5.20 and 5.28 for exomethylene CH, two multiplets between δ 7.66–7.81 and between δ 8.38-8.41, two singlets at δ 8.01 and δ 8.06 for six aromatic protons and a broad singlet at δ 9.54 for one NH proton. Mass spectrum showed base peak corresponding to $[M+H]^+$ at *m/z* 381.

4.3.12 Synthesis of chloro analog of compounds 54.

4.3.12.1 Synthesis and characterization of 2-(2-((4-chloro-6-(methylthio)-1*H*-pyrazolo[3,4-*d*]pyrimidin-1-yl)methyl)allyl)phthalazin-1(2*H*)-one (62).

Reaction of the compound **61** with $POCl_3$ under reflux for 5 h gave **62** (**Scheme 16**). This compound was characterized by NMR and mass spectrometric techniques.

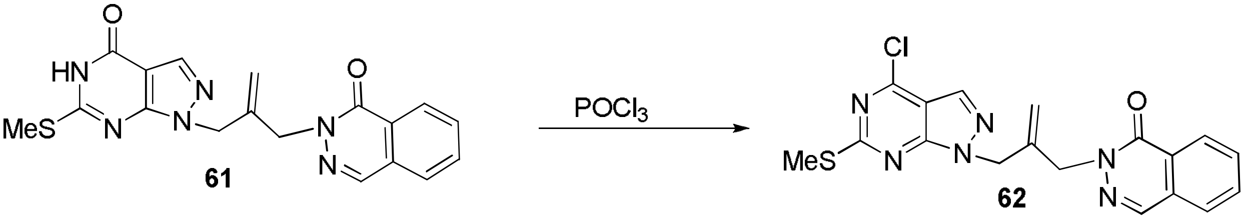

Scheme 16. Synthesis of compounds **62**

Proton NMR of compound **62** showed one singlet at δ 2.31 for one SMe, two singlets at *δ* 4.84 and 5.07 for NCH_2 groups, two singlets at *δ* 5.26 and 5.33 for exomethylene CH, two multiplets between δ 7.66–7.85 and between δ 8.31-8.33, two singlets at δ 8.02 and δ 8.04 for six aromatic protons. Mass spectrum showed base peak corresponding to $[M+H]^+$ at *m/z* 399.

4.3.13 Synthesis and characterization of 2-(2-((4-methoxy-6-(methylsulfonyl)-1*H*-pyrazolo[3,4-*d*]pyrimidin-1-yl)methyl)allyl)phthalazin-1(2*H*)-one (63).

Reaction of the compound **60** with oxone in acetone at 0°C for 6 h gave **63** (**Scheme 17**). These compounds were characterized by NMR and mass spectrometric techniques.

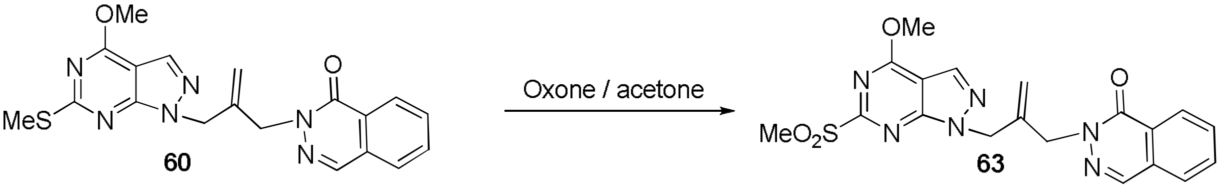

Scheme 17. Synthesis of compounds **63**

Proton NMR of compound **63** showed two singlets at δ 3.24 for one SO_2Me and *δ* 4.25 for OMe protons, two singlets at *δ* 4.83 and 5.16 for NCH_2 groups, two singlets at *δ* 5.20 and 5.33 for exomethylene CH, two multiplets between δ 7.70–7.85 and between δ 8.33-8.36, two singlets at δ 8.12 and δ 8.15 for six aromatic protons. Mass spectrum showed base peak corresponding to $[M+H]^+$ at *m/z* 427.

4.3.14 Synthesis and characterization of reference compounds.

Synthesis and characterization of reference compounds **64-75** (**Fig. 13**) has been discussed in **Chapter 3**.

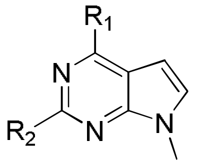

64: R_1 = SMe; R_2 = SMe
65: R_1 = Pyrrolidine; R_2 = SMe
66: R_1 = OMe; R_2 = SMe
67: R_1 = OH; R_2 = SMe
68: R_1 = Cl; R_2 = SMe
69: R_1 = OMe; R_2 = SO_2Me
70: R_1 = Cl; R_2 = SO_2Me

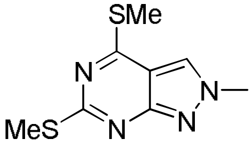

71

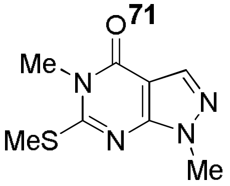

72

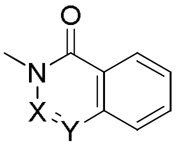

73: X = N; Y = CH
74: X = CH; Y = N
75: X = N; Y = N

Figure 13. Reference compounds

4.4 Result and discussion

The present study was undertaken to study the effect of increasing the length of linker on intramolecular π–π interactions seen in comparison to *ethylene* linker based dissymmetric pyrazolo[3,4-*d*]pyrimidine compounds (**Chapter 3**) having phthalazinone/quinazilinone and benzotriazinone moieties on the other side both in solution and more importantly on solid state. The effect of replacing *butylidine* linker in place of *trimethylene* linker on intramolecular π–π interactions was also studied. The selection of *butylidine* linker is based on following observations:

(i) This new linker is quite similar to *trimethylene* linker as far as carbon atom in the linker is concerned but has an extra methylene carbon attached to central C of earlier *trimethylene* linker through a double bond. Net result of this additional methylene moiety at central C of *trimethylene* linker is a theoretical increase in earlier angle of 109º (tetrahedral) to 120º (planar).

(ii) Both 1,3-dibromo propane for *trimethylene* linker and methallyl dichloride for *butylidene* linker, are commercially available.

4.4.1 Proton NMR studies:

Important ^{1}H NMR shifts of monomeric reference compounds and dimeric compounds synthesized for the present study is shown in the following **Table 3**.

Important results obtained from this ^{1}H NMR studies are as follows:

(i) In contrast to the large upfield shifts seen in case of *ethylene* linker homologs connected to the N^1 position of pyrazolopyrimidine nucleus (**Chapter 3**), in case of *trimethylene* linker compounds we see a small upfield shift, in protons of groups substituted at 6-position of pyrazolopyrimidine nucleus. The corresponding shifts in phthalazinone 4-H and quinazolinone 2-H are also very small (**Table 3**). When compared to the magnitude of upfield shifts of *trimethylene* linker based symmetrical pyrazolo[3,4-*d*]pyrimidine compounds (**Table 4**), we find that the magnitude of upfield shifts are smaller. This indicates that there is some intramolecular interaction between the two arene moieties but these are much weaker as compared to the corresponding *ethylene* linker compounds and also weaker as compared to the similar substituted *trimethylene* linker based symmetrical pyrazolo[3,4-*d*]pyrimidine compounds. The exact nature of intramolecular interaction (e.g. C-H…π or π–π etc.) in these compounds based on the ^{1}H NMR shifts is difficult to predict. In an earlier study on 4,6-bis(methylsulfanyl)-1-phthalimido-propyl-1-*H*-pyrazolo[3,4-*d*]pyrimidine upfield shifts in 6-SMe protons in the ^{1}H NMR spectra were observed but X-ray crystallography revealed that the compound was folded due to intramolecular C-H…π interaction and not due to intramolecular π–π interaction.[52] Also based on these ^{1}H NMR shift values and on comparing with our results obtained in the study of *trimethylene* linker based symmetrical and dissymmetrical pyrazolo[3,4-*d*]pyrimidine compounds done previously in our lab, the conformation of the molecule cannot be assigned as folded or open and it is more likely that the molecule either exists in a conformation that is somewhere in between these two conformations or is in rapid equilibrium between these two conformation.

(ii) This drastic effect on intramolecular arene interactions between the two arene moieties on increasing one methylene unit in the linker was a bit surprising since in case of *ethylene* linker compound corresponding to compound **25** arene interactions were strong enough to overcome the repulsive steric forces and crystal lattice forces to show folded conformation in the solution as well as in solid state. This is also in contrast to the results seen in case of *ethylene* and *trimethylene* linker based

Table 3: Important ^{1}H NMR shifts of compounds used in the present study.

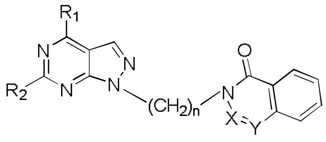
25-28,31-34, 38, 39,41, 42, 44-46 : X =N; Y = CH;
29, 34, 40: X =CH; Y = N;
30, 35: X =N; Y = N

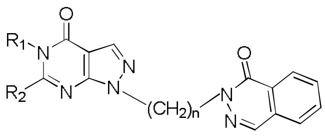
36, 37, 43

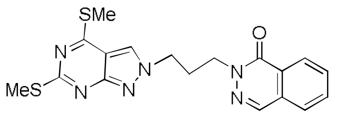
48

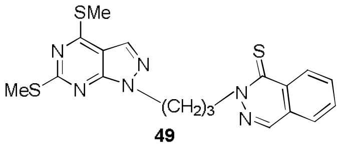
49

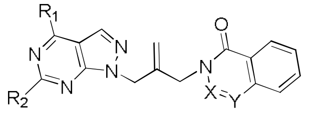
54, 58, 60-63: X=N; Y = CH;
55: X =CH; Y = N
56: X =N; Y = N

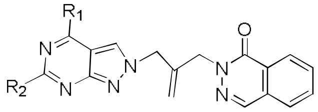
57, 60

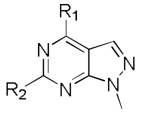
64-66, 68-70

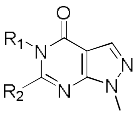
67, 72

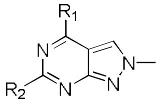
71

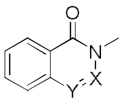
73,74

Comp. No.	**n**	**R_1**	**R_2**	**δ 6-SMe/ SO_2Me/ OMe (PP)**	**δ 2-H/4-H (Q/Pht.)**	**Δδ = 6-SMe/ SO_2Me/ OMe (PP, mono)- 6-SMe/ SO_2Me/ OMe (PP, dimer)**	**Δδ = 2-H/4-H(Q/Pht., monomer) - 2-H/4-H (Q/Pht., dimer)**
64	-	SMe	SMe	2.68	-	-	-
71	-	SMe	SMe	2.67	-	-	-
65	-	pyrrolidine	SMe	2.58	-	-	-
66	-	OMe	SMe	2.63			
68	-	Cl	SMe	2.64			
69	-	OMe	SO_2Me	3.42			
70	-	Cl	SO_2Me	3.45			
71	-	H	SMe	2.54*			
72	-	Me	SMe	2.64			
73	-	-	-	-	8.14		
74	-	-	-	-	8.10		
25	3	SMe	SMe	2.52	8.09	0.16	0.05
26	4	SMe	SMe	2.60	8.13	0.08	0.01
27	5	SMe	SMe	2.61	8.14	0.07	0.00
28	6	SMe	SMe	2.62	8.13	0.06	0.01
29	3	SMe	SMe	2.58	8.08	0.10	0.02
30	3	SMe	SMe	2.52	-	0.16	-
31	3	pyrrolidine	SMe	2.47	8.11	0.11	0.03
32	4	pyrrolidine	SMe	2.54	8.14	0.04	0.00
33	6	pyrrolidine	SMe	2.54	8.12	0.04	0.02

34	3	pyrrolidine	SMe	2.55	8.13	0.03	-0.03
35	3	pyrrolidine	SMe	2.45	-	0.13	-
36	3	H	SMe	2.53	8.20	-	-0.06
37	4	H	SMe	2.63	8.14	-	0.00
38	3	OMe	SMe	2.48	8.10	0.15	0.04
39	4	OMe	SMe	2.59	8.13	0.04	0.01
40	3	OMe	SMe	2.58	8.08	0.05	0.02
41	3	Cl	SMe	2.48	8.08	0.16	0.06
42	4	Cl	SMe	2.60	8.13	0.04	0.01
43	3	Me	SMe	2.48	8.10	0.16	0.04
44	3	OMe	SO_2Me	3.33	8.12	0.11	0.02
45	4	OMe	SO_2Me	3.40	8.15	0.02	-0.01
46	3	Cl	SO_2Me	3.38	8.12	0.07	0.02
48	3	SMe	SMe	2.61	8.16	0.06	-0.02
49	3	SMe	SMe	2.55	8.34	0.13	-
54	-	SMe	SMe	2.38	8.05	0.30	0.09
55	-	SMe	SMe	2.48	7.94	0.20	0.16
56	-	SMe	SMe	2.42	-	0.26	-
57	-	SMe	SMe	2.59	8.13	0.08	0.01
58	-	pyrrolidine	SMe	2.33	8.09	0.25	0.05
59	-	pyrrolidine	SMe	2.55	8.13	0.03	0.01
60	-	OMe	SMe	2.35	8.07	0.28	0.07
61	-	H	SMe	2.39	8.06	-	0.08
62	-	Cl	SMe	2.31	8.04	0.33	0.10
63	-	OMe	SO_2Me	3.24	8.12	0.18	0.02

* data collected in DMSO-d_6

symmetric pyrazolo[3,4-*d*]pyrimidine compounds where in both cases similar shifts were observed. This once again demonstrates the subtle nature of these interactions.

(iii) In case of higher linker homologs the shifts are still smaller and in these cases it can be safely assumed that the two arene moieties do not have any intramolecular arene interactions and the compounds have open conformation.

(iv) In case of *trimethylene* linker compounds connected to the N^2-position of pyrazolo pyrimidine nucleus no significant upfield shifts are observed in either protons of groups substituted at 6-position of pyrazolo pyrimidine nucleus or phthalazinone 4-H. This is similar to the results observed in case of corresponding *ethylene* linker compounds and also to the *trimethylene* linker based symmetrical pyrazolo pyrimidine compounds. This indicates absence of intramolecular π–π interaction between the two arene moieties and suggests open conformation for this compound.

(v) In case of *butylidine* linker compounds connected to the N^1-position of pyrazolopyrimidine nucleus we observe a significant upfield shifts in the protons of groups substituted at 6-position of pyrazolopyrimidine nucleus which is greater than the upfield shifts of corresponding *trimethylene* linker compounds but smaller than the corresponding *ethylene* linker compounds. The upfield shifts in the phthalazinone 4-H and quinazolinone 2-H are also greater than the corresponding *trimethylene* linker compounds. When compared to the upfield shifts of *trimethylene* linker based symmetrical pyrazolo[3,4-*d*]pyrimidine compounds (**Table 3**), we find that the upfield shifts are significantly greater. This indicates that there is significant intramolecular π–π interactions between the two arene moieties and the compounds have folded conformation as seen in case of *trimethylene* linker based symmetrical pyrazolo[3,4-*d*]pyrimidine compounds.

(vi) As in earlier cases of *ethylene* or *trimethylene* linker, in case of *butylidine* linker compounds connected to the N^2-position of pyrazolopyrimidine nucleus there is no significant upfield shift in protons and suggest open conformation for the molecule.

Table 4: ^{1}H NMR shifts in some *trimethylene* linker symmetrical pyrazolo[3,4-*d*]pyrimidine compounds.

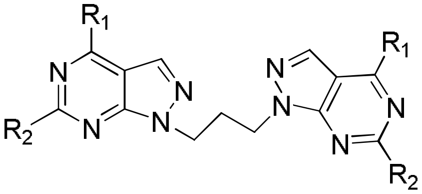

Comp. No.	**R$_1$**	**R$_2$**	**δ 6-SMe/ SO$_2$Me (PP)**	**Δδ = 6-SMe/ SO$_2$Me/ OMe (PP, mono)- 6-SMe/ SO$_2$Me/ OMe (PP, dimer)**	**Reference**
76	SMe	SMe	2.42	0.26	53a
77	OMe	SMe	2.42	0.21	53b
78	Cl	SMe	2.47	0.17	53c
79	OMe	SO$_2$Me	3.30	0.12	53b

4.4.2 X-Ray crystallographic study

In this present study we were able to prepare and study crystals of 2-(3-(4,6-bis(methylthio)-1*H*-pyrazolo[3,4-*d*]pyrimidin-1-yl)propyl)phthalazin-1(2*H*)-one (**25**), 2-(3-(6-(methylthio)-4-oxo-4,5-dihydro-1*H*-pyrazolo[3,4-*d*]pyrimidin-1-yl)propyl)phthalazin-1(2*H*)-one (**36**), 3-(3-(4,6-bis(methylthio)-1*H*-pyrazolo[3,4-*d*]pyrimidin-1-yl)propyl)quinazolin-4(3*H*)-one (**29**), 3-(3-(6-(methylthio)-4-(pyrrolidin-1-yl)-1*H*-pyrazolo[3,4-*d*]pyrimidin-1-yl)propyl)benzo[*d*][1,2,3]triazin-4(3*H*)-one (**35**) and 2-(2-((4-chloro-6-(methylthio)-1*H*-pyrazolo[3,4-*d*]pyrimidin-1-yl)methyl)allyl)phthalazin-1(2*H*)-one (**62**).

The crystal structure of compound **25** shows open conformation (**Fig. 14**). There is no intramolecular π–π interaction between the rings as shown in the figure. Although the structure is open but is not fully stretched. The distance between the two N atoms (N6 and N3) connecting the linker is 4.33 Ǻ. On careful analysis of the crystal structure we observe that the structure is stabilized by intramolecular C-H…N and C-H…O interactions (**Table 5**) as shown in the **Fig. 14**.

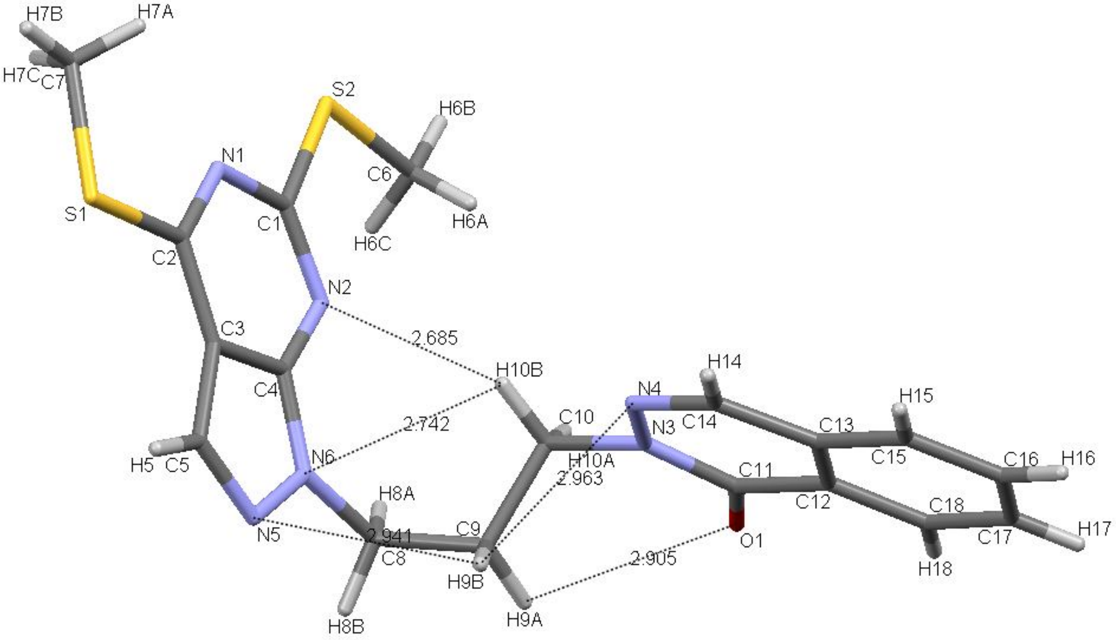

Figure 14: Crystal structure of compound **25** showing open conformation

Table 5: Important characteristic features of hydrogen bonds present in compound **25**

Intramolecular hydrogen bond	d (Å)	D (Å)	θ (^{0})
C10-H10B…N2	2.69	3.42	132.40
C10-H10B…N6	2.74	3.10	102.68
C9-H9A…O1	2.90	3.33	107.70
C9-H9B…N5	2.94	3.22	98.06
C9-H9B…N4	2.96	3.22	96.22

The crystal structure of compound **36** also shows open conformation (**Fig. 15**). There is also no intramolecular π–π interaction between the rings as shown in the **Fig. 15**. The distance between the two N atoms (N5 and N2) connecting the linker is 4.39 Ǻ which is very close to the distance (4.33 Ǻ) seen in the crystal structure of compound **25**. On careful analysis of the crystal structure we observe that the structure is stabilized by intramolecular C-H…N interactions (**Table 6**) as shown in the **Fig. 15**.

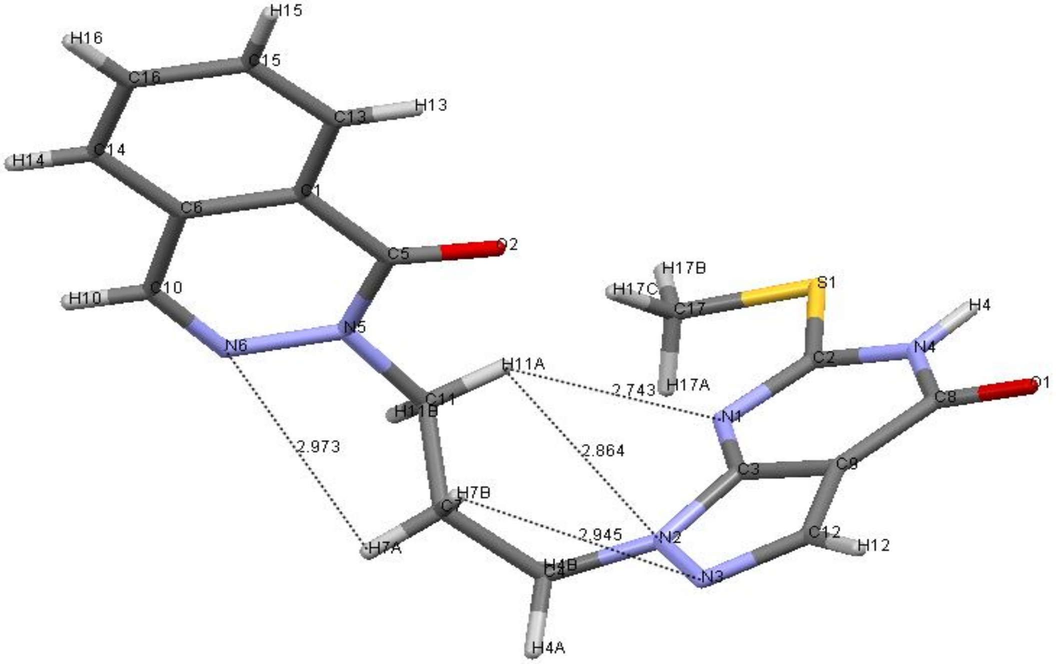

Figure 15: Crystal structure of compound **36** showing open conformation

Table 6: Important characteristic features of hydrogen bonds present in compound **36**.

Intramolecular hydrogen bond	d (Å)	D (Å)	θ (^{0})
C11-H11A…N1	2.74	3.51	136.41
C11-H11A…N2	2.86	3.19	100.98
C7-H7B…N3	2.95	3.25	99.18
C7-H7A…N6	2.97	3.14	91.01

The crystal structure of compound **29** shows open conformation (**Fig. 16).** There is no intramolecular π–π interaction between the rings as shown in **Fig 16**. The distance between the two N atoms (N3 and N1) connecting the linker is 3.94 Ǻ On careful analysis of the crystal structure we observe that the structure is stabilized by intramolecular C-H…N and C-H…O interactions (**Table 7**) as shown in the **Fig. 16**.

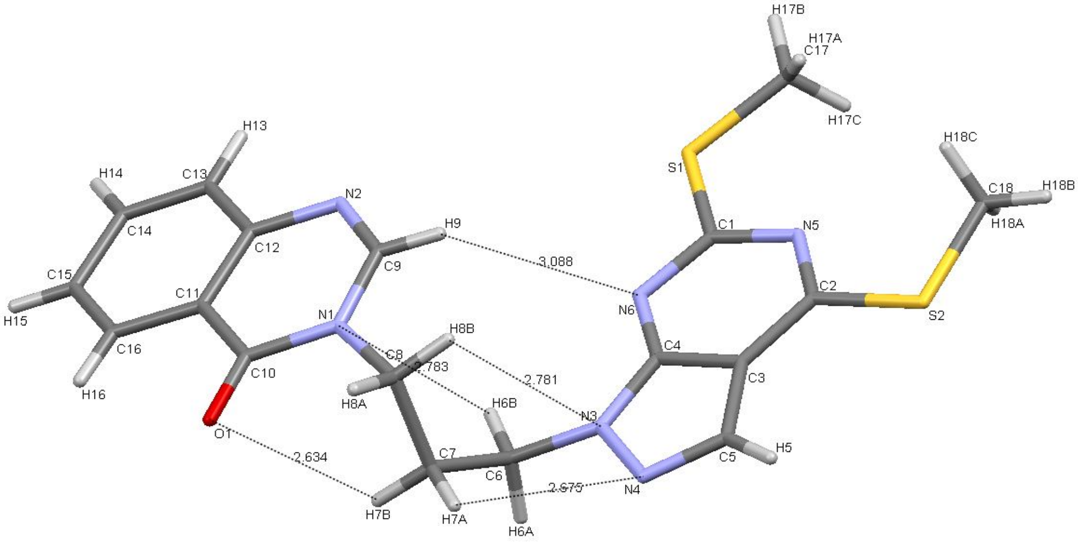

Figure 16: Crystal structure of compound **29** showing open conformation

Table 7: Important characteristic features of hydrogen bonds present in compound **29**.

Intramolecular hydrogen bond	d (Å)	D (Å)	θ (^{0})
C7-H7B…O1	2.63	3.17	115.04
C7-H7A…N4	2.68	3.02	101.37
C8-H8B…N3	2.78	3.13	101.71
C6-H6B…N1	2.78	3.12	101.43
C9-H9…N6	3.09	3.76	130.72

The crystal structure of compound **35** shows open conformation (**Fig. 17).** There is no intramolecular π–π interaction between the rings as shown from the **Fig**. **17**. The distance between the two N atoms (N3 and N8) connecting the linker is 4.45 Å. On careful analysis of the crystal structure we observe that the structure is stabilized by intramolecular C-H…N and C-H…O interactions (**Table 8**) as shown in the **Fig. 17**.

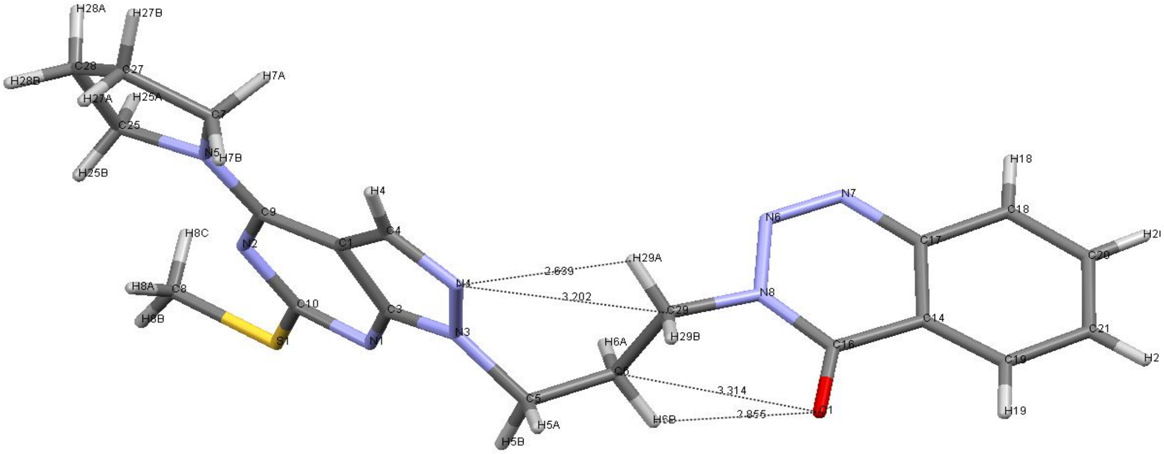

Figure 17: Crystal structure of 3compound **35** showing open conformation

Table 8: Important characteristic features of hydrogen bonds present in compound **35**

Intramolecular hydrogen bond	d (Å)	D (Å)	θ (^{0})
C29-H29A…N6	2.70	3.20	112.72
C6-H6B…O1	2.86	3.31	109.95

The crystal structure of compound **62** shows folded conformation (**Fig**. **18**). The distance between the two N atoms (N1 and N3) connecting the linker is 3.35Å. This distance is similar to the distances (3.09-3.54 Å) observed in case of *trimethylene* linker based symmetrical pyrazolo[3,4-*d*]pyrimidine compounds (**Table 1**, **Chapter 3**) which are folded due to intramolecular π–π interactions. However in the present case the structure is folded due to intramolecular O…arene interactions as shown in the **Fig**. **18** and not due to intramolecular π–π interactions. The closest distance between the centroids of two rings is 4.63 Å as shown in the **Fig**. **18,** which is much larger than the earlier observed intramolecular π–π interactions distances (3.69-4.23 Ǻ) observed in *trimethylene* linker based symmetrical pyrazolo[3,4-*d*]pyrimidine compounds (**Table 1**, **Chapter 3**). On the other hand the distance between oxygen atom and the centroid of nine member pyrazolo[3,4-*d*]pyrimidine ring is 3.13 Ǻ which is smaller than the sum of van der Waals radii of oxygen and carbon (1.5 Ǻ+ 1.7 Ǻ = 3.2 Ǻ). The distance between oxygen atom and centroid of five member pyrazolo ring is 3.23 Ǻ and that of six member pyrimidine ring is 3.35 Ǻ. These distances indicate towards presence of strong O…arene interactions in the molecule.

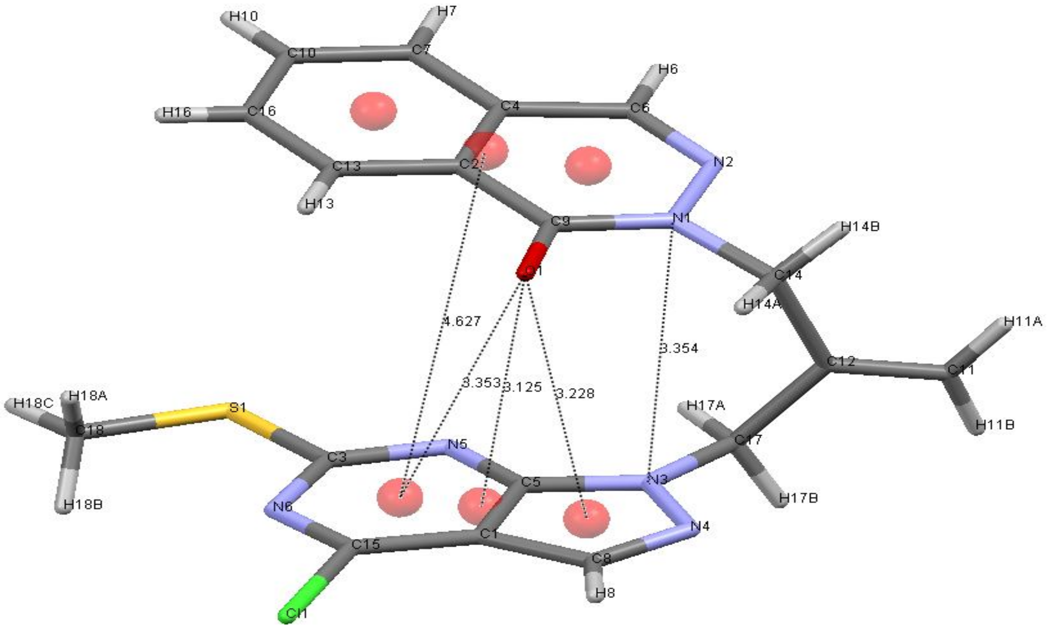

Figure 18: Crystal structure of compound **62** showing folded conformation due to intramolecular O…arene interactions

4.5 Biological activity

Compounds **27, 28, 30, 31, 36, 37, 39, 41, 42, 44 and 45** were tested for antithrombotic activity in mice at 30 µM concentrations in collaboration with Dr. Madhu Dikshit, Pharmacology Division, CDRI, Lucknow. The results are shown in table given below.

Table 9: Biological activity

Compound	Dose	% Protection
27	30 µM/kg, po	0%
28	30 µM/kg, po	40%
30	30 µM/kg, po	50%
31	30 µM/kg, po	40%
36	30 µM/kg, po	40%
37	30 µM/kg, po	0%
39	30 µM/kg, po	40%
41	30 µM/kg, po	30%
42	30 µM/kg, po	0%
44	30 µM/kg, po	40%
45	30 µM/kg, po	40%

4.6 Conclusion

In conclusion this study shows the subtle and competitive nature of weak noncovalent forces such as arene interactions and weak hydrogen bonding in controlling the conformation of the molecule where a small change in the structure of the molecule or in the environment of the molecule can change the overall conformation of the molecule. Thus in case of *ethylene* linker based dissymmetrical pyrazolo[3,4-*d*]pyrimidine compounds having quinazolinone/ phtalazinone/ benzotriazinone nucleus at the other end the conformation of structure is folded and is controlled mainly by intramolecular arene interactions (**Chapter 3**). When the linker is changed from *ethylene* to *propylene* the conformation is now open and is controlled mainly by intramolecular weak hydrogen bonding and finally when the linker is changed from *propylene* to *butylidine* the conformation of the molecule is again folded and controlled by intramolecular arene interactions.

This work together with our earlier work on *trimethylene, butylidene* linkers for 1,3-diaryl-propanes, opens a new window for studying factors responsible for conformation control in flexible molecules. These models may also provide an important experimental basis for further development of computational/theoretical models for a better understanding of arene interactions in flexible compounds both at the molecular and supramolecular level.

4.7 Experimental section

4.7.1 Synthesis of 2-(3-(4,6-bis(methylthio)-1*H*-pyrazolo[3,4-*d*]pyrimidin-1-yl)propyl)-phthalazin-1(2*H*)-one (25).

25: Yield: 75%; mp: 94–96 °C; MS (ESI) *m/z* 399 $[M+H]^+$; ^{1}H NMR (300 MHz, $CDCl_3$) δ (ppm): 2.52 (s, 3H, SCH_3), 2.46-2.58 (m, 2H, CH_2), 2.66 (s, 3H, SCH_3), 4.31 (t, 2H, J = 6.8 Hz, NCH_2), 4.50 (t, 2H, J = 6.8 Hz, NCH_2), 7.62–7.83 (m, 3H, Ar), 7.90 (s, 1H, pyrazolo[3,4-*d*]-pyrimidinyl), 8.09 (s, 1H, phthalazinyl) 8.37–8.42 (m, 1H, Ar); ^{13}C NMR (50 MHz, $CDCl_3$): 11.71, 14.10, 28.05, 44.52, 48.51, 109.31, 125.82, 126.59, 127.74, 129.44, 131.52, 132.91, 137.62, 151.72, 159.20, 164.655, 168.44; Anal. Calcd. for $C_{18}H_{20}N_8S_4$: C, 45.36; H, 4.23; N, 23.51; Found: C, 45.09; H, 4.52; N, 23.72.

4.7.2 Synthesis of 2-(4-(4,6-bis(methylthio)-1*H*-pyrazolo[3,4-*d*]pyrimidin-1-yl)butyl)-phthalazin-1(2*H*)-one (26).

26: Yield: 82%; mp: 126–128 °C; MS (ESI) *m/z* 413 $[M+H]^+$; ^{1}H NMR (300 MHz, $CDCl_3$) 1.81-2.04 (m, 4H, CH_2), δ (ppm): 2.60 (s, 3H, SCH_3), 2.68 (s, 3H, SCH_3), 4.28 (t, 2H, J = 6.8 Hz, NCH_2), 4.38 (t, 2H, J = 6.8 Hz, NCH_2), 7.65–7.83 (m, 3H, Ar), 7.89 (s, 1H, pyrazolo[3,4-*d*]-pyrimidinyl), 8.13 (s, 1H, phthalazinyl) 8.40–8.43 (m, 1H, Ar); ^{13}C NMR (50 MHz, $CDCl_3$): 11.82, 13.34, 13.77, 45.75, 50.85, 108.61, 126.98, 126.51, 127.64, 129.57, 131.47, 131.98, 133.02, 137.39, 152.44, 159.47, 164.62, 168.58;); Anal. Calcd. for $C_{19}H_{20}N_6OS_2$: C, 55.32; H, 4.89; N, 20.37; Found: C, 55.40; H, 4.92; N, 20.39.

4.7.3 Synthesis of 2-(5-(4,6-dimethylsulfanyl-1*H*-pyrazolo[3,4-*d*]pyrimidin-1-yl)-pentyl)-2*H*-phthalazin-1-one (27).

27: Yield: 84%; mp: 104–106 °C; MS (ESI) *m/z* 427 $[M+H]^+$; ^{1}H NMR (300 MHz, $CDCl_3$) 1.35-1.44 (m, 2H, CH_2), 1.90-2.02 (m, 4H, CH_2), δ (ppm): 2.61 (s, 3H, SCH_3), 2.68 (s, 3H, SCH_3), 4.28 (t, 2H, J = 6.8 Hz, NCH_2), 4.38 (t, 2H, J = 6.8 Hz, NCH_2), 7.65–7.84 (m, 3H, Ar), 7.88 (s, 1H, pyrazolo[3,4-*d*]pyrimidinyl), 8.14 (s, 1H, phthalazinyl) 8.40–8.43 (m, 1H, Ar); Anal. Calcd. for $C_{20}H_{22}N_6OS_2$: C, 56.32; H, 4.19; N, 21.86; Found: C, 56.34; H, 4.24; N, 21.88.

4.7.4 Synthesis of 2-(6-(4,6-bis(methylthio)-1*H*-pyrazolo[3,4-*d*]pyrimidin-1-yl)hexyl)-phthalazin-1(2*H*)-one (28).

28: Yield: 80%; mp: 102–104 °C; MS (ESI) *m/z* 441 $[M+H]^+$; ^1H NMR (300 MHz, $CDCl_3$) 1.32-1.44 (m, 4H, CH_2), 1.88-2.00 (m, 4H, CH_2), δ (ppm): 2.62 (s, 3H, SCH_3), 2.68 (s, 3H, SCH_3), 4.26 (t, 2H, *J* = 6.8 Hz, NCH_2), 4.37 (t, 2H, *J* = 6.8 Hz, NCH_2), 7.65–7.84 (m, 3H, Ar), 7.86 (s, 1H, pyrazolo[3,4-*d*]pyrimidinyl), 8.13 (s, 1H, phthalazinyl) 8.40–8.43 (m, 1H, Ar).

4.7.5 Synthesis of 3-(3-(4,6-bis(methylthio)-1*H*-pyrazolo[3,4-*d*]pyrimidin-1-yl)propyl)-quinazolin-4(3*H*)-one (29).

29: Yield: 80%; mp: 136–138 °C; MS (ESI) *m/z* 399 $[M+H]^+$; ^1H NMR (300 MHz, $CDCl_3$) 2.44-2.53 (m, 2H, CH_2), δ (ppm): 2.58 (s, 3H, SCH_3), 2.67 (s, 3H, SCH_3), 4.02 (t, 2H, *J* = 6.8 Hz, NCH_2), 4.46 (t, 2H, *J* = 6.8 Hz, NCH_2), 7.46–7.52 (m, 1H, Ar), 7.67–7.77 (m, 2H, Ar), 7.92 (s, 1H, pyrazolo[3,4-*d*]pyrimidinyl), 8.08 (s, 1H, quinazolinyl) 8.26–8.29 (m, 1H, Ar). ^{13}C NMR (50 MHz, $CDCl_3$): 11.74, 14.20, 28.37, 43.76, 44.52, 109.33, 121.06, 126.47, 127.12, 127.37, 131.86, 134.06, 146.61, 148.02, 151.88, 160.97, 165.08, 168.96; Anal. Calcd. for $C_{18}H_{18}N_6OS_2$: C, 54.25; H, 4.55; N, 21.08; Found: C, 53.85; H, 4.40; N, 20.85.

4.7.6 Synthesis of 3-(3-(4,6-bis(methylthio)-1*H*-pyrazolo[3,4-*d*]pyrimidin-1-yl)propyl)-benzo[*d*][1,2,3]triazin-4(3*H*)-one (30).

30: Yield: 84%; mp: 108–110 °C; MS (ESI) *m/z* 400 $[M+H]^+$; ^1H NMR (300 MHz, $CDCl_3$) 2.55-2.64 (m, 2H, CH_2), δ (ppm): 2.52 (s, 3H, SCH_3), 2.66 (s, 3H, SCH_3), 4.51-4.56 (m, 4H, NCH_2), 7.76–7.81 (m, 1H, Ar), 7.88–7.96 (m, 1H, Ar), 7.89 (s, 1H, pyrazolo[3,4-*d*]pyrimidinyl) 8.11–8.14 (m, 1H, Ar). 8.29–8.32 (m, 1H, Ar). ^{13}C NMR (50 MHz, $CDCl_3$): 11.76, 14.16, 28.24, 44.35, 47.34, 109.34, 119.62, 124.97, 128.18, 131.77, 132.28, 134.69, 144.08, 151.81, 155.35, 164.83, 168.67; Anal. Calcd. for $C_{17}H_{17}N_7OS_2$: C, 51.11; H, 4.29; N, 24.54; Found: C, 51.05; H, 4.30; N, 24.85.

4.7.7 Synthesis of 2-(3-(6-(methylthio)-4-(pyrrolidin-1-yl)-1*H*-pyrazolo[3,4-*d*]pyrimidin-1-yl)propyl)- phthalazin-1(2*H*)-one (31).

31: Yield: 92%; mp: 96-98 °C; MS (ESI) *m/z* 422 $[M+H]^+$; ^1H NMR (300 MHz, $CDCl_3$): δ (ppm): 1.96-2.02 (m, 2H, CH_2 pyrrolidino), 2.09-2.15 (m, 2H, CH_2 pyrrolidino), 2.44-2.54 (m, 2H, CH_2), 2.47 (s, 3H, SCH_3), 3.76 (t, 4H, *J* = 5.05, 2 x NCH_2pyrrolidino), 4.30 (t, 2H, *J* = 7.0 Hz, NCH_2), 4.45 (t, 2H, *J* = 6.9 Hz, NCH_2), 7.64–7.82 (m, 3H, Ar), 7.81 (s, 1H, pyrazolo[3,4-*d*]pyrimidinyl), 8.11 (s, 1H, phthalazinyl) 8.38–8.42 (m, 1H, Ar). ^{13}C NMR (50 MHz, $CDCl_3$): 13.96, 24.32, 25.87, 44.22, 47.33, 47.96, 48.67, 98.95, 125.80, 126.59, 127.83, 129.52, 131.42, 132.76, 132.84, 137.56, 154.20, 154.37, 159.17, 168.66; Anal. Calcd. for $C_{21}H_{23}N_7OS$: C, 59.84; H, 5.50; N, 23.26; Found C, 59.86; H, 5.48; N, 23.20.

4.7.8 Synthesis of 2-(4-(6-(methylthio)-4-(pyrrolidin-1-yl)-1*H*-pyrazolo[3,4-*d*]pyrimidin-1-yl)butyl)- phthalazin-1(2*H*)-one (32).

32: Yield: 92%; mp: 96-98 °C; MS (ESI) *m/z* 436 $[M+H]^+$; ^1H NMR (300 MHz, $CDCl_3$): δ (ppm): 1.80-2.17 (m, 8H, CH_2 pyrrolidino and CH_2 linker), 2.54 (s, 3H, SCH_3), 3.76 (t, 4H, *J* = 6.6 Hz, 2 x NCH_2pyrrolidino), 4.28 (t, 2H, *J* = 6.6 Hz, NCH_2), 4.39 (t, 2H, *J* = 6.6 Hz, NCH_2), 7.65–7.83 (m, 3H, Ar), 7.78 (s, 1H, pyrazolo[3,4-*d*]pyrimidinyl), 8.14 (s, 1H, phthalazinyl) 8.37–8.42 (m, 1H, Ar). ^{13}C NMR (50 MHz, $CDCl_3$): 14.57, 24.81, 26.07, 27.03, 46.63, 47.84, 48.49, 50.85, 99.39, 126.32, 127.08, 128.33, 130.02, 131.91, 133.09, 133.34, 138.06, 154.73, 159.74, 169.16; Anal. Calcd. for $C_{22}H_{25}N_7OS$: C, 60.67; H, 5.79; N, 22.51; Found C, 60.58; H, 5.70; N, 22.46.

4.7.9 Synthesis of 2-(6-(6-(methylthio)-4-(pyrrolidin-1-yl)-1*H*-pyrazolo[3,4-*d*]pyrimidin-1-yl)hexyl)- phthalazin-1(2*H*)-one (33).

33: Yield: 92%; mp: 90-92 °C; MS (ESI) *m/z* 464 $[M+H]^+$; ^1H NMR (300 MHz, $CDCl_3$): δ (ppm): 1.22-1.42 (m, 4H, CH_2 linker), 1.74-2.14 (m, 8H, CH_2 pyrrolidino and CH_2 linker), 2.54 (s, 3H, SCH_3), 3.73 (t, 4H, *J* = 7.5 Hz, NCH_2 pyrrolidino), 4.19 (t, 2H, *J* = 7.5 Hz, NCH_2), 4.28 (t, 2H, *J* = 7.5 Hz, NCH_2), 7.64–7.78 (m, 3H, Ar), 7.76 (s, 1H, pyrazolo[3,4-*d*]pyrimidinyl), 8.12 (s, 1H, phthalazinyl) 8.38–8.41 (m, 1H, Ar).

4.7.10 Synthesis of 3-(3-(6-(methylthio)-4-(pyrrolidin-1-yl)-1*H*-pyrazolo[3,4-*d*]pyrimidin-1-yl)propyl)-quinazolin-4(3*H*)-one (34).

34: Yield: 92%; mp 140-142 °C; MS (ESI) *m/z* 422 $[M+H]^+$; δ (ppm): 1.94-2.06 (m, 2H, CH_2 pyrrolidino), 2.08-2.20 (m, 2H, CH_2 pyrrolidino), 2.46 (quint, 2H, *J* = 6.0 Hz, CH_2), 2.55 (s, 3H, SCH_3), 3.77 (brs, 4H, NCH_2pyrrolidino), 4.01 (t, 2H, *J* = 6.7 Hz, NCH_2), 4.42 (t, 2H, *J* = 6.0 Hz, NCH_2), 7.49-7.54 (m, 1H, Ar), 7.68-7.76 (m, 2H, Ar), 7.82 (s, 1H, Ar, pyrazolo[3,4-*d*]pyrimidinyl), 8.13 (s, 1H, H-3 quinazolinyl), 8.28-8.31 (m, 1H, Ar); ^{13}C NMR (50 MHz, $CDCl_3$): 13.96, 24.32, 25.87, 44.22, 47.33, 47.96, 48.67, 98.95, 125.80, 126.59, 127.83, 129.52, 131.42, 132.76, 132.84, 137.56, 154.20, 154.37, 159.17, 168.66; Anal. Calcd. for $C_{21}H_{23}N_7OS$: C, 59.84; H, 5.50; N, 23.26; Found C, 59.86; H, 5.53; N, 23.23.

4.7.11 Synthesis of 3-(3-(6-(methylthio)-4-(pyrrolidin-1-yl)-1*H*-pyrazolo[3,4-*d*]pyrimidin-1-yl)propyl)benzo[d][1,2,3]triazin-4(3*H*)-one (35).

35: Yield: 90%; mp 128-130 °C; MS (ESI) *m/z* 423 $[M+H]^+$; δ (ppm): 1.94-2.00 (m, 2H, CH_2 pyrrolidino), 2.08-2.16 (m, 2H, CH_2 pyrrolidino), 2.56 (quint, 2H, *J* = 6.6 Hz, CH_2), 2.45 (s, 3H, SCH_3), 3.75 (t, 4H, NCH_2 pyrrolidino), 4.46-4.56 (m, 4H, NCH_2), 7.73-7.78 (m, 1H, Ar), 7.82 (s, 1H, Ar, pyrazolo[3,4-*d*]pyrimidinyl), 7.88-7.93 (m, 1H, Ar), 8.08-8.11 (m, 1H, Ar), 8.28-8.31 (m, 1H, Ar); ^{13}C NMR (50 MHz, $CDCl_3$): 14.08, 24.41, 25.98, 28.43, 44.11, 47.44, 47.53, 48.09, 99.01, 119.79, 125.04, 128.18, 132.24, 133.04, 134.66, 144.18, 154.22, 154.48, 155.38, 168.92; Anal. Calcd. for $C_{20}H_{22}N_8OS$: C, 56.85; H, 5.25; N, 26.52; Found C, 57.05; H, 5.30; N, 26.82.

4.7.12 Synthesis of 2-(3-(6-(methylthio)-4-oxo-4,5-dihydro-1*H*-pyrazolo[3,4-*d*]pyrimidin-1-yl)propyl)phthalazin-1(2*H*)-one (36).

36: Yield: 90%; mp 220-222 °C; MS (ESI) *m/z* 369 $[M+H]^+$; δ (ppm): 2.53 (quint, 2H, *J* = 6.6 Hz, CH_2), 2.45 (s, 3H, SCH_3), 4.32 (t, 2H, *J* = 6.6 Hz, NCH_2), 4.39 (t, 2H, *J* = 6.6 Hz, NCH_2), 7.75–7.93 (m, 3H, Ar), 7.96 (s, 1H, pyrazolo[3,4-*d*]pyrimidinyl), 8.20 (s, 1H, phthalazinyl) 8.35–8.38 (m, 1H, Ar); ^{13}C NMR (50 MHz, $CDCl_3$+ DMSO-d_6): 14.59, 29.64, 46.44, 104.65, 127.94, 129.14, 133.70, 135.18, 136.59, 140.18, 154.03, 160.80, 161.48, 162.27; Anal. calcd. for $C_{17}H_{16}N_6O_2S$: calcd. C, 55.42; H, 4.38; N, 22.81; found C, 55.65; H, 4.40; N, 23.02.

4.7.13 Synthesis of 2-(4-(6-(methylthio)-4-oxo-4,5-dihydro-1*H*-pyrazolo[3,4-*d*]pyrimidin-1-yl)butyl)phthalazin-1(2*H*)-one (37).

37: Yield: 90%; mp 190-192 °C; MS (ESI) *m/z* 383 $[M+H]^+$; δ (ppm): 1.86-2.06 (m, 4H, CH_2), 2.63 (s, 3H, SCH_3), 4.30 (t, 2H, *J* = 6 Hz, NCH_2), 4.37 (t, 2H, *J* = 6 Hz, NCH_2), 7.66–7.82 (m, 3H, Ar), 8.00 (s, 1H, pyrazolo[3,4-*d*]pyrimidinyl), 8.14 (s, 1H, phthalazinyl) 8.40–8.46 (m, 1H, Ar); Anal. Calcd. for $C_{18}H_{18}N_6 O_2S$: C, 56.53; H, 4.74; N, 21.97; Found: C, 56.63; H, 4.80; N, 22.05.

4.7.14 Synthesis of 2-(3-(4-methoxy-6-(methylthio)-1*H*-pyrazolo[3,4-*d*]pyrimidin-1-yl)propyl)phthalazin-1(2*H*)-one (38).

38: Yield: 75%; mp 124–126 °C; MS (ESI) *m/z* 399 $[M+H]^+$; ^1H NMR (300 MHz, $CDCl_3$) δ (ppm): 2.48 (s, 3H, SCH_3), 2.48-2.57 (m, 2H, CH_2), 4.09 (s, 3H, OCH_3), 4.31 (t, 2H, *J* = 6.8 Hz, NCH_2), 4.50 (t, 2H, *J* = 6.8 Hz, NCH_2), 7.64–7.83 (m, 3H, Ar), 7.89 (s, 1H, pyrazolo[3,4-

d]pyrimidinyl), 8.10 (s, 1H, phthalazinyl) 8.38–8.41 (m, 1H, Ar); Anal. Calcd. for $C_{18}H_{18}N_6O_2S$: C, 56.53; H, 4.74; N, 21.97; Found: C, 56.66; H, 4.81; N, 22.03.

4.7.15 Synthesis of 2-(4-(4-methoxy-6-(methylthio)-1*H*-pyrazolo[3,4-*d*]pyrimidin-1-yl)butyl)phthalazin-1(2*H*)-one (39).

39: Yield: 82%; mp: 116–118 ^{o}C; MS (ESI) *m/z* 397 $[M+H]^+$; ^{1}H NMR (300 MHz, $CDCl_3$) δ (ppm): 1.82-2.04 (m, 4H, CH_2), 2.59 (s, 3H, SCH_3), 4.10 (s, 3H, OCH_3), 4.29 (t, 2H, J = 6.9 Hz, NCH_2), 4.45 (t, 2H, J = 6.9 Hz, NCH_2), 7.66–7.82 (m, 3H, Ar), 7.88 (s, 1H, pyrazolo[3,4-*d*]pyrimidinyl), 8.13 (s, 1H, phthalazinyl) 8.40–8.42 (m, 1H, Ar); Anal. calcd. for $C_{19}H_{20}N_6O_2S$: C, 57.56; H, 5.08; N, 21.20; found: C, 57.64; H, 5.12; N, 21.29.

4.7.16 Synthesis of 3-(3-(4-methoxy-6-(methylthio)-1*H*-pyrazolo[3,4-*d*]pyrimidin-1-yl)propyl)quinazolin-4(3*H*)-one (40).

40: Yield: 92%; mp: 130-132°C; MS (ESI) *m/z* 383 $[M+H]^+$; ^{1}H NMR (300 MHz, $CDCl_3$) δ (ppm): 2.45-2.53 (m, 2H, CH_2), 2.58 (s, 3H, SCH_3), 4.12 (s, 3H, OCH_3), 4.03 (t, 2H, J = 6.8 Hz, NCH_2), 4.47 (t, 2H, J = 6.8 Hz, NCH_2), 7.48–7.53 (m, 1H, Ar), 7.68–7.78 (m, 2H, Ar), 7.92 (s, 1H, pyrazolo[3,4-*d*]pyrimidinyl), 8.08 (s, 1H, quinazolinyl) 8.28–8.31 (m, 1H, Ar). ^{13}C NMR (50 MHz, $CDCl_3$): 14.26, 28.48, 43.92, 44.60, 54.20, 100.04, 122.07, 126.58, 127.22, 127.47, 131.82, 134.17, 146.73, 148.13, 155.62, 161.10, 162.82; Anal. calcd. for $C_{18}H_{18}N_6O_2S$: C, 56.53; H, 4.74; N, 21.97; Found: C, 56.25; H, 4.90; N, 22.05.

4.7.17 Synthesis of 2-(3-(4-chloro-6-(methylthio)-1*H*-pyrazolo[3,4-*d*]pyrimidin-1-yl)propyl)phthalazin-1(2*H*)-one (41).

41: Yield: 80%; mp: 140-142°C; MS (ESI) *m/z* 387 $[M+H]^+$; ^{1}H NMR (300 MHz, $CDCl_3$) δ (ppm): 2.48 (s, 3H, SCH_3), 2.57 (quint, J = 6.9 Hz, 2H, CH_2), 4.31 (t, 2H, J = 6.9 Hz, NCH_2), 4.52 (t, 2H, J = 6.9 Hz, NCH_2), 7.66–7.84 (m, 3H, Ar), 7.98 (s, 1H, pyrazolo[3,4-*d*]pyrimidinyl), 8.08 (s, 1H, phthalazinyl) 8.36–8.39 (m, 1H, Ar); ^{13}C NMR (50 MHz, $CDCl_3$): 14.27, 27.86, 29.65, 44.95, 48.34, 110.43, 125.92, 126.66, 127.75, 129.45, 131.73, 132.42, 133.14, 137.79, 153.80, 153.90, 159.30, 169.88;. Anal. calcd. for $C_{17}H_{15}ClN_6OS$: C, 52.78; H, 3.91; N, 21.72; Found: C, 52.90; H, 3.92; N, 21.95.

4.7.18 Synthesis of 2-(4-(4-chloro-6-(methylthio)-1*H*-pyrazolo[3,4-*d*]pyrimidin-1-yl)butyl)phthalazin-1(2*H*)-one (42).

42: Yield: 80%; mp: 126–128 ^{o}C; MS (ESI) *m/z* 401 $[M+H]^+$; ^{1}H NMR (300 MHz, $CDCl_3$) δ (ppm): 1.81-2.08 (m, 4H, CH_2), 2.60 (s, 3H, SCH_3), 4.11 (t, 2H, *J* = 6.9 Hz, NCH_2), 4.49 (t, 2H, *J* = 6.9 Hz, NCH_2), 7.68–7.84 (m, 3H, Ar), 7.98 (s, 1H, pyrazolo[3,4-*d*]pyrimidinyl), 8.13 (s, 1H, phthalazinyl) 8.40–8.43 (m, 1H, Ar); Anal. calcd. for $C_{18}H_{17}ClN_6OS$: C, 53.93; H, 4.27; N, 8.84; Found: C, 54.05; H, 4.29; N, 8.90.

4.7.19 Synthesis of 2-(3-(5-methyl-6-(methylthio)-4-oxo-4,5-dihydro-1*H*-pyrazolo[3,4-*d*]-pyrimidin-1-yl)propyl)phthalazin-1(2*H*)-one (43).

43: Yield: 85%; mp: 160-162°C; MS (ESI) *m/z* 383 $[M+H]^+$; ^{1}H NMR (300 MHz, $CDCl_3$) δ (ppm): 2.48 (s, 3H, SCH_3), 2.48-2.57 (m, 2H, CH_2), 4.09 (s, 3H, NCH_3), 4.31 (t, 2H, *J* = 6.8 Hz, NCH_2), 4.50 (t, 2H, *J* = 6.8 Hz, NCH_2), 7.64–7.83 (m, 3H, Ar), 7.89 (s, 1H, pyrazolo[3,4-*d*]pyrimidinyl), 8.10 (s, 1H, phthalazinyl) 8.38–8.41 (m, 1H, Ar); ^{13}C NMR (50 MHz, $CDCl_3$): 14.17, 28.22, 44.70, 48.58, 54.13, 99.97, 125.93, 126.73, 129.57, 131.51, 133.05, 137.77, 155.46, 159.34, 162.78, 169.33 Anal. Calcd. for $C_{18}H_{18}N_6\,O_2S$: C, 56.53; H, 4.74; N, 21.97; Found: C, 56.73; H, 4.82; N, 22.02.

4.7.20 Synthesis of 2-(3-(4-methoxy-6-(methylsulfonyl)-1*H*-pyrazolo[3,4-*d*]pyrimidin-1-yl)propyl)phthalazin-1(2*H*)-one (44).

44: Yield: 85%; mp: 148-150°C; MS (ESI) *m/z* 415 $[M+H]^+$; ^{1}H NMR (300 MHz, $CDCl_3$) δ (ppm): 2.57 (quint, *J* = 6.9 Hz, 2H, CH_2), 3.33 (s, 3H, SO_2CH_3), 4.25 (s, 3H, OCH_3), 4.31 (t, 2H, *J* = 6.9 Hz, NCH_2), 4.61 (t, 2H, *J* = 6.9 Hz, NCH_2), 7.68–7.89 (m, 3H, Ar), 8.12 (s, 2H, pyrazolo[3,4-*d*]pyrimidinyl and phthalazinyl) 8.37–8.39 (m, 1H, Ar); Anal. calcd. for $C_{18}H_{18}N_6O_4S$: C, 52.17; H, 4.38; N, 20.28; Found: C, 52.27; H, 4.42; N, 20.32.

4.7.21 Synthesis of 2-(4-(4-methoxy-6-(methylsulfonyl)-1*H*-pyrazolo[3,4-*d*]pyrimidin-1-yl)butyl)phthalazin-1(2*H*)-one (45).

45: Yield: 85%; mp: 136-138°C; MS (ESI) *m/z* 429 $[M+H]^+$; ^{1}H NMR (300 MHz, $CDCl_3$) δ (ppm): 1.81-2.11 (m, 4H, CH_2), 3.40 (s, 3H, SO_2CH_3), 4.26 (s, 3H, OCH_3), 4.29 (t, 2H, *J* = 6.9 Hz, NCH_2), 4.57 (t, 2H, *J* = 6.9 Hz, NCH_2), 7.68–7.83 (m, 3H, Ar), 8.11 (s, 1H, pyrazolo[3,4-*d*]pyrimidinyl), 8.15 (s, 1H, phthalazinyl) 8.38–8.41 (m, 1H, Ar); Anal. calcd. for $C_{19}H_{20}N_6OS_2$: C, 53.26; H, 4.70; N, 19.61; Found: C, 53.36; H, 4.80; N, 19.71.

4.7.22 Synthesis of 2-(3-(4-chloro-6-(methylsulfonyl)-1*H*-pyrazolo[3,4-*d*]pyrimidin-1-yl)propyl)phthalazin-1(2*H*)-one (46).

46: Yield: 85%; mp: 140-142 °C; MS (ESI) *m/z* 419 $[M+H]^+$; ^1H NMR (300 MHz, $CDCl_3$) δ (ppm): 2.64 (quint, *J* = 6.9 Hz, 2H, CH_2), 3.38 (s, 3H, SO_2CH_3), 4.25 (s, 3H, OCH_3), 4.31 (t, 2H, *J* = 6.9 Hz, NCH_2), 4.68 (t, 2H, *J* = 6.9 Hz, NCH_2), 7.68–7.85 (m, 3H, Ar), 8.12 (s, 1H, pyrazolo[3,4-*d*]pyrimidinyl) 8.27 (s, 2H, phthalazinyl) 8.33–8.36 (m, 1H, Ar); ^{13}C NMR (50 MHz, $CDCl_3$): 27.64, 39.41, 45.64, 48.01, 95.39, 114.66, 126.10, 126.47, 127.53, 129.40, 131.80, 132.94, 133.22, 138.12, 152.35, 156.31, 159.24, 161.38.. Anal. calcd. for $C_{17}H_{15}ClN_6O_3S$: C, 48.75; H, 3.61; N, 20.06; Found: C, 48.90; H, 3.72; N, 20.35.

4.7.23 Synthesis of 2-(3-(4,6-bis(methylthio)-2*H*-pyrazolo[3,4-*d*]pyrimidin-2-yl)propyl)-phthalazin-1(2*H*)-one (48).

48: Yield: 75%; mp: 100–102 °C; MS (ESI) *m/z* 399 $[M+H]^+$; ^1H NMR (300 MHz, $CDCl_3$) δ (ppm): 2.61 (s, 3H, SCH_3), 2.61-2.65 (m, 2H, CH_2), 2.65 (s, 3H, SCH_3), 4.31 (t, 2H, *J* = 6.0 Hz, NCH_2), 4.42 (t, 2H, *J* = 6.0 Hz, NCH_2), 7.67–7.82 (m, 3H, Ar), 8.07 (s, 1H, pyrazolo[3,4-*d*]pyrimidinyl), 8.16 (s, 1H, phthalazinyl) 8.40–8.42 (m, 1H, Ar); Anal. Calcd. for $C_{18}H_{20}N_8S_4$: C, 45.36; H, 4.23; N, 23.51; Found: C, 45.29; H, 4.42; N, 23.78.

4.7.24 Synthesis of 2-(3-(4,6-bis(methylthio)-1*H*-pyrazolo[3,4-*d*]pyrimidin-1-yl)propyl)phthalazine-1(2*H*)-thione (49).

49: Yield: 75%; mp: 112–114 °C; MS (ESI) *m/z* 415$[M+H]^+$; ^1H NMR (300 MHz, $CDCl_3$) δ (ppm): 2.55 (s, 3H, SCH_3), 2.61-2.71 (m, 2H, CH_2), 2.71 (s, 3H, SCH_3), 4.53 (t, 2H, *J* = 6.9 Hz, NCH_2), 4.88 (t, 2H, *J* = 6.9 Hz, NCH_2), 7.66–7.70 (m, 1H, Ar), 7.78–7.84 (m, 2H, Ar), 7.92 (s, 1H, pyrazolo[3,4-*d*]pyrimidinyl), 8.34 (s, 1H, phthalazinyl) 8.94–8.97 (m, 1H, Ar); Anal. Calcd. for $C_{18}H_{18}N_6S_3$: C, 52.15; H, 4.38; N, 20.27; Found: C, 51.95; H, 4.20; N, 20.78.

4.7.25 Synthesis of 1-(2-(chloromethyl)allyl)-4,6-bis(methylthio)-1*H*-pyrazolo[3,4-*d*]-pyrimidine (52):

52: Yield: 60%; mp: oily; MS (ESI) *m/z* 301$[M+H]^+$; ^1H NMR (300 MHz, $CDCl_3$) δ (ppm): 2.63 (s, 3H, SCH_3), 2.69 (s, 3H, SCH_3), 4.01 (s, 2H, CH_2Cl), 5.12 (s, 2H, NCH_2), 5.14 (s, 1H, exomethylene CH), 5.36 (s, 2H, exomethylene CH), 7.96 (s, 1H, Ar).

4.7.26 Synthesis of 2-(2-(chloromethyl)allyl)-4,6-bis(methylthio)-2*H*-pyrazolo[3,4-*d*]-pyrimidine (53).

53: Yield: 20%; oily; MS (ESI) *m/z* 301[M+H]$^+$; ^{1}H NMR (300 MHz, $CDCl_3$) δ (ppm): 2.61 (s, 3H, SCH_3), 2.68 (s, 3H, SCH_3), 3.98 (s, 2H, CH_2Cl), 5.06 (s, 2H, NCH_2), 5.27 (s, 1H, exomethylene CH), 5.44 (s, 2H, exomethylene CH), 7.99 (s, 1H, Ar).

4.7.27 Synthesis of 2-(2-(4,6-bis(methylthio)-1*H*-pyrazolo[3,4-*d*]pyrimidin-1-yl)methyl)allyl)phthalazin-1(2*H*)-one (54).

54: Yield: 80%; mp: 106-108 °C; MS (ESI) *m/z* 411[M+H]$^+$; ^{1}H NMR (300 MHz, $CDCl_3$) δ (ppm): 2.38 (s, 3H, SCH_3), 2.65 (s, 3H, SCH_3), 4.84 (s, 2H, NCH_2), 5.04 (s, 2H, NCH_2), 5.17 (s, 1H, exomethylene CH), 5.23 (s, 2H, exomethylene CH), 7.65–7.67 (m, 1H, Ar), 7.75–7.80 (m, 2H, Ar), 7.92 (s, 1H, pyrazolo[3,4-*d*]pyrimidinyl), 8.05 (s, 1H, phthalazinyl) 8.34–8.37 (m, 1H, Ar); ^{13}C NMR (50 MHz, $CDCl_3$): 11.76, 13.97, 49.54, 53.31, 109.27, 117.20, 125.93, 126.75, 127.78, 129.45, 131.66, 132.10, 133.05, 137.90, 139.25, 143.42, 151.98, 159.18, 164.73, 168.69; Anal. Calcd. for $C_{19}H_{18}N_6OS_2$: C, 55.59; H, 4.42; N, 20.47; Found: C, 55.95; H, 4.45; N, 20.78.

4.7.28 Synthesis of 3-(2-(4,6-bis(methylthio)-1*H*-pyrazolo[3,4-*d*]pyrimidin-1-l)methyl)allyl)-quinazolin-4(3*H*)-one (55).

55: Yield: 85%; mp: 116-118 °C; MS (ESI) *m/z* 411[M+H]$^+$; ^{1}H NMR (300 MHz, $CDCl_3$) δ (ppm): 2.48 (s, 3H, SCH_3), 2.67 (s, 3H, SCH_3), 4.61 (s, 2H, NCH_2), 5.03 (s, 2H, NCH_2), 5.23 (s, 1H, exomethylene CH), 5.32 (s, 2H, exomethylene CH), 7.48–7.52 (m, 1H, Ar), 7.67–7.78 (m, 2H, Ar), 7.91 (s, 1H, pyrazolo[3,4-*d*]pyrimidinyl), 7.94 (s, 1H, quinazolinyl) 8.24–8.27 (m, 1H, Ar); ^{13}C NMR (50 MHz, $CDCl_3$): 11.83, 14.13, 48.08, 49.38, 109.26, 118.43, 121.89, 126.76, 127.33, 127.45, 132.47, 134.23, 138.42, 146.03, 147.81, 152.02, 160.71, 165.06, 169.25; Anal. Calcd. for $C_{19}H_{18}N_6OS_2$: C, 55.59; H, 4.42; N, 20.47; Found: C, 55.85; H, 4.49; N, 20.88.

4.7.29 Synthesis of 3-(2-(4,6-bis(methylthio)-1*H*-pyrazolo[3,4-*d*]pyrimidin-1-yl)methyl)allyl)benzo[*d*][1,2,3]triazin-4(3*H*)-one (56).

56: Yield: 82%; mp: 118-120 °C MS (ESI) *m/z* 412[M+H]$^+$; ^{1}H NMR (300 MHz, $CDCl_3$) δ (ppm): 2.42 (s, 3H, SCH_3), 2.66 (s, 3H, SCH_3), 5.05 (s, 2H, NCH_2), 5.08 (s, 2H, NCH_2), 5.24

(s, 1H, exomethylene CH), 5.28 (s, 2H, exomethylene CH), 7.78–7.82 (m, 1H, Ar), 7.91–7.97 (m, 1H, Ar), 7.91 (s, 1H, pyrazolo[3,4-*d*]pyrimidinyl), 8.12–8.15 (m, 1H, Ar), 8.27–8.30 (m, 1H, Ar); Anal. Calcd. for $C_{18}H_{17}N_7OS_2$: C, 52.54; H, 4.16; N, 23.83; Found: C, 52.64; H, 4.19; N, 23.88.

4.7. 30Synthesisof2-(2-(4,6-bis(methylthio)-2*H*-pyrazolo[3,4-*d*]pyrimidin-2-l)methyl)allyl)-phthalazin-1(2*H*)-one (57).

57: Yield: 80%; mp: 112-114 °C; MS (ESI) *m/z* 411[M+H]$^+$; ^{1}H NMR (300 MHz, $CDCl_3$) δ (ppm): 2.59 (s, 3H, SCH_3), 2.65 (s, 3H, SCH_3), 4.84 (s, 2H, NCH_2), 5.01 (s, 2H, NCH_2), 5.31 (s, 1H, exomethylene CH), 5.41 (s, 2H, exomethylene CH), 7.65–7.68 (m, 1H, Ar), 7.74–7.83 (m, 2H, Ar), 8.06 (s, 1H, pyrazolo[3,4-*d*]pyrimidinyl), 8.13 (s, 1H, phthalazinyl) 8.37–8.40 (m, 1H, Ar); ^{13}C NMR (50 MHz, $CDCl_3$): 11.81, 14.15, 53.27, 57.12, 109.05, 120.13, 124.25, 126.01, 126.59, 127.57, 129.47, 131.74, 133.20, 138.01, 138.25, 158.52, 159.27, 166.20, 168.35; Anal. Calcd. for $C_{19}H_{18}N_6OS_2$: C, 55.59; H, 4.42; N, 20.47; Found: C, 55.85; H, 4.48; N, 20.86.

4.7.31 Synthesis of 2-(2-(6-(methylthio)-4-(pyrrolidin-1-yl)-1*H*-pyrazolo[3,4-*d*]pyrimidin-1-yl)methyl)allyl)-phthalazin-1(2*H*)-one (58).

58: Yield: 84%; mp: 130-132 °C; MS (ESI) *m/z* 434 [M+H]$^+$; ^{1}H NMR (300 MHz, $CDCl_3$) δ (ppm): 1.97–2.01 (m, 2H, pyrrolidinyl CH_2) 2.10–2.14 (m, 1H, pyrrolidinyl CH_2) 2.33 (s, 3H, SCH_3), 3.75 (t, *J* = 6.9 Hz, 1H, pyrrolidinyl NCH_2), 4.30 (s, 2H, NCH_2), 4.45 (s, 2H, NCH_2), 5.13 (s, 1H, exomethylene CH), 5.17 (s, 2H, exomethylene CH), 7.66–7.80 (m, 3H, Ar), 7.82 (s, 1H, pyrazolo[3,4-*d*]pyrimidinyl), 8.09 (s, 1H, phthalazinyl) 8.35–8.38 (m, 1H, Ar); ^{13}C NMR (50 MHz, $CDCl_3$): 13.83, 24.37, 25.94, 47.42, 48.07, 49.28, 53.34, 98.92, 116.38, 125.95, 126.79, 127.92, 129.59, 131.58, 132.99, 133.41, 137.92, 139.79, 154.25, 154.70, 159.21, 168.93; Anal. Calcd. for $C_{22}H_{23}N_7OS$: C, 60.95; H, 5.35; N, 22.62; Found: C, 61.05; H, 5.48; N, 22.86.

4.7.32 Synthesis of 2-(2-(6-(methylthio)-4-(pyrrolidin-1-yl)-2*H*-pyrazolo[3,4-*d*]pyrimidin-2-yl)methyl)allyl)-phthalazin-1(2*H*)-one (59).

59: Yield: 84%; mp: 126-128 °C; MS (ESI) *m/z* 434 [M+H]$^+$; ^{1}H NMR (300 MHz, $CDCl_3$) δ (ppm): 1.97–2.13 (m, 4H, pyrrolidinyl CH_2), 2.55 (s, 3H, SCH_3), 3.68–3.72 (m, 4H, pyrrolidinyl NCH_2), 4.83 (s, 2H, NCH_2), 4.95 (s, 2H, NCH_2), 5.31 (s, 1H, exomethylene CH), 5.34 (s, 2H, exomethylene CH), 7.66–7.82 (m, 3H, Ar), 7.95 (s, 1H, pyrazolo[3,4-*d*]pyrimidinyl), 8.13 (s, 1H, phthalazinyl) 8.34–8.37 (m, 1H, Ar); Anal. Calcd. for $C_{22}H_{23}N_7OS$: C, 60.95; H, 5.35; N, 22.62; Found: C, 61.05; H, 5.40; N, 22.86.

4.7.33 Synthesis of 2-(2-((4-methoxy-6-(methylthio)-1*H*-pyrazolo[3,4-*d*]pyrimidin-1-yl)methyl)allyl) phthalazin-1(2*H*)-one (60).

60: Yield: 84%; mp: 120-122 °C; MS (ESI) *m/z* 395 $[M+H]^+$; ^1H NMR (300 MHz, $CDCl_3$) δ (ppm): 2.35 (s, 3H, SCH_3), 4.08 (s, 3H, OCH_3), 4.84 (s, 2H, NCH_2), 5.04 (s, 2H, NCH_2), 5.17 (s, 1H, exomethylene CH), 5.23 (s, 2H, exomethylene CH), 7.66–7.83 (m, 3H, Ar), 7.92 (s, 1H, pyrazolo[3,4-*d*]pyrimidinyl), 8.07 (s, 1H, phthalazinyl) 8.34–8.37 (m, 1H, Ar); Anal. Calcd. for $C_{19}H_{18}N_6O_2S$: C, 57.85; H, 4.60; N, 21.31; Found: C, 57.95; H, 4.65; N, 21.66.

4.7.34 Synthesis of 2-(2-((6-(methylthio)-4-oxo-4,5-dihydro-1*H*-pyrazolo[3,4-*d*]pyrimidin-1-yl)methyl)allyl)- phthalazin-1(2*H*)-one (61).

61: Yield: 84%; mp: 216-220 °C; MS (ESI) *m/z* 381 $[M+H]^+$; ^1H NMR (300 MHz, $CDCl_3$) δ (ppm): 2.39 (s, 3H, SCH_3), 4.88 (s, 2H, NCH_2), 4.99 (s, 2H, NCH_2), 5.20 (s, 1H, exomethylene CH), 5.28 (s, 2H, exomethylene CH), 7.66–7.81 (m, 3H, Ar), 8.01 (s, 1H, pyrazolo[3,4-*d*]pyrimidinyl), 8.06 (s, 1H, phthalazinyl) 8.38–8.41 (m, 1H, Ar), 9.54 (bs, 1H, NH); Anal. Calcd. for $C_{19}H_{18}N_6O_2S$: C, 56.83; H, 4.24; N, 22.09; Found: C, 56.95; H, 4.35; N, 22.26.

4.7.35 Synthesis of 2-(2-((4-chloro-6-(methylthio)-1*H*-pyrazolo[3,4-*d*]pyrimidin-1-yl)methyl)allyl)phthalazin-1(2*H*)-one (62).

62: Yield: 84%; mp: 138-140 °C; MS (ESI) *m/z* 399 $[M+H]^+$; ^1H NMR (300 MHz, $CDCl_3$) δ (ppm): 2.39 (s, 3H, SCH_3), 4.88 (s, 2H, NCH_2), 4.99 (s, 2H, NCH_2), 5.20 (s, 1H, exomethylene CH), 5.28 (s, 2H, exomethylene CH), 7.66–7.81 (m, 3H, Ar), 8.01 (s, 1H, pyrazolo[3,4-*d*]pyrimidinyl), 8.06 (s, 1H, phthalazinyl) 8.38–8.41 (m, 1H, Ar), 9.54 (bs, 1H, NH); ^{13}C NMR (50 MHz, $CDCl_3$): 14.05, 49.92, 53.13, 110.35, 117.99, 125.95, 126.69, 127.68, 129.35, 131.81, 132.84, 133.20, 137.94, 138.84, 153.73, 154.04, 159.11, 170.00; Anal. Calcd. for $C_{18}H_{15}ClN_6OS$: C, 54.20; H, 3.79; N, 21.07; Found: C, 54.35; H, 3.95; N, 21.26.

4.7.36 Synthesis of 2-(2-(4-methoxy-6-(methylsulfonyl)-1*H*-pyrazolo[3,4-*d*]pyrimidin-1-yl)methyl)allyl)- phthalazin-1(2*H*)-one (63).

63: Yield: 82%; mp: 120-122 ^{o}C; MS (ESI) *m/z* 427 $[M+H]^+$; ^{1}H NMR (300 MHz, $CDCl_3$) δ (ppm): 2.39 (s, 3H, SCH_3), 4.88 (s, 2H, NCH_2), 4.99 (s, 2H, NCH_2), 5.20 (s, 1H, exomethylene CH), 5.28 (s, 2H, exomethylene CH), 7.66–7.81 (m, 3H, Ar), 8.01 (s, 1H, pyrazolo[3,4-*d*]pyrimidinyl), 8.06 (s, 1H, phthalazinyl) 8.38–8.41 (m, 1H, Ar), 9.54 (bs, 1H, NH); Anal. Calcd. for $C_{19}H_{18}N_6O_4S$: C, 53.51; H, 4.25; N, 19.71; Found: C, 53.61; H, 4.35; N, 19.80.

4.7.37 Synthesis of 2-methylphthalazin-1(2*H*)-one (73).

73: Yield: 92%; MS (ESI) *m/z* 161 $[M+H]^+$; ^{1}H NMR (300 MHz, $CDCl_3$) δ (ppm): 3.85 (s, 3H, NCH_3), 7.66–7.80 (m, 3H, Ar), 8.14 (s, 1H, Ar) 8.41–8.44 (m, 1H, Ar).

4.7.38 Synthesis of 3-methylquinazolin-4(3*H*)-one (74).

74: Yield: 92%; MS (ESI) *m/z* 161 $[M+H]^+$; ^{1}H NMR (300 MHz, $CDCl_3$) δ (ppm): 3.62 (s, 3H, NCH_3), 7.52 (ddd, *J* = 8.2, 6.9, 1.6 Hz, 1H), 7.70–7.80 (m, 2H, Ar), 8.10 (s, 1H, Ar), 8.33 (dd, *J* = 8.0, 1.0 Hz, 1H, Ar).

4.7.39 Synthesis of 3-methylbenzo[*d*][1,2,3]triazin-4(3*H*)-one (75).

75: Yield: 92%; MS (ESI) *m/z* 162 $[M+H]^+$; ^{1}H NMR (300 MHz, $CDCl_3$) δ (ppm): 4.06 (s, 3H, NCH_3), 7.77–7.82 (m, 1H, Ar), 7.91–7.96 (m, 1H, Ar), 8.15 (d, *J* = 6 Hz, 1H, Ar) 8.36 (d, *J* = 6 Hz, 1H, Ar).

4.8 References

1. Pozharskii, A. F.; Soldatenkov, A. T.; Katritzky, A. R. *Heterocycles in Life and Society*; John Wiley & Sons: New York, **1997**.
2. Balaban, A. T.; Oniciu, D. C.; Katritzky, A. R. *Chem. Rev.* **2004**, *104*, 2777.
3. (a) Gomer, C. J.; Ed. *Future Directions and Applications in Photodynamic Therapy*; Proc. SPIE, Int. Soc. Opt. Eng. IS6; SPIE: Bellingham, WA, **1990**. (b) Gray, H. B.; Lever, A. B. P.; Eds. *Iron Porphyrins*; Wiley: New York, **1989**.
4. Kessel, D.; Ed. *Methods in Porphyrin Photosensitization*; Plenum Press: New York, **1986**.
5. Smith, K.M.; Lee, S. J.; Shiau, F. Y.; Pandey, R.K.; Jagerovic, N. In *Photodynamic Therapy and Biomedical Lasers*; Spinelli, P., Dal Fante, M., Marchesini, R., Eds.; Elsevier: Amsterdam, **1992**, 769.

6. Cerny, J.; Hobza, P. *Phys. Chem. Chem. Phys.* **2007**, *9*, 5291.

7. Steed, J. W.; Atwood, J. L.; *Supramolecular Chemistry*, John Wiley & Sons: Chichester, England, **2000**.

8. Desiraju, G. R. *Angew. Chem., Int. Ed.* **2011**, *50*, 52.

9. Pauling, L. *The nature of the chemical bond*; Cornell University Press, Ithaca, New York, **1939**.

10. Steiner, T.; Saenger, W. *J. Am. Chem. Soc.* **1993**, *115*, 4540.

11. Desiraju, G. R.; Steiner, T. *The Weak Hydrogen Bond in Structural Chemistry and Biology*; Oxford University Press: Oxford, **1999**.

12. Melandri, S. *Phys. Chem. Chem. Phys.* **2011**, *13*, 13901.

13. Pimentel, G. C.; McClellan, A. L. *The hydrogen bond*, W.H. Freeman and Co., San Francisco, **1960**.

14. Goswami, M.; Arunan, E. *Phys. Chem. Chem. Phys.* **2009**, *11*, 8974.

15. Kumler, W. D. *J. Am. Chem. Soc.* **1935**, *57*, 600.

16. Dougill, M. W.; Jeffrey, G. A. *Acta Crystallographia* **1953**, *6*, 831.

17. Sutor, D. J. *Nature* **1962**, *195*, 68.

18. Taylor, R.; Kennard, O. *J. Am. Chem. Soc.* **1982**, *104*, 5063.

19. Desiraju, G. R. *Accounts of Chemical Research* **1996**, *29*, 441.

20. Favero, L. B.; Giuliano, B. M.; Melandri, S.; Maris, A.; Ottaviani, P.; Velino B.; Caminati, W. *J. Phys. Chem.* A **2005**, *109*, 7402.

21. Fraser, G. T.; Leopold, K. R.; Kemplerer, W. *J. Chem. Phys.* **1984**, *80*, 1423.

22. Fraser, G. T.; Leopold, K. R.; Nelson, D. D.; Tung A.; Klemperer, W. *J. Chem. Phys.* **1984**, *80*, 3073.

23. Fraser, G. T.; Lovas, F. J.; Suenram, R. D.; Nelson D. D.; Klemperer, W. *J. Chem. Phys.* **1986**, *84*, 5983.

24. Nishio, M.; Hirota, M.; Umezawa, Y. *The CH/π Interaction. Evidence, Nature, and Consequences*; Wiley-VCH: New York, **1998**.

25. Nishio, M. *CrystEngComm.* **2004**, *6*, 130.

26. Pearson, R. G. *J. Am. Chem. Soc.* **1963**, *85*, 3533.

27. Pearson, R. G. *J. Chem. Education* **1968**, *45*, 643.

28. Takahashi, O.; Kohno, Y.; Nishio, M. *Chem. Rev.* **2010**, *110*, 6073.

29. Takahashi, O.; Kohno, Y.; Saito, K.; Nishio, M. *Chem. Eur. J.* **2003**, *9*, 756.

30. Braga, D.; Grepioni, F.; Desiraju, G. R. *Chem. Rev.* **1998**, *98*, 1375.

31. Umezawa, Y.; Tsuboyama, S.; Honda, K.; Uzawa, J.; Nishio, M. *Bull. Chem. Soc. Jpn.* **1998**, *71*, 1207.

32. Mooibroek, T. J.; Gamez, P.; Reedijk, J. *CrystEngComm.* **2008**, *10*, 1501.

33. Gallivan, J. P.; Dougherty, D. A. *Org. Lett.* **1999**, *1*, 103.

34. Williams, J. H. *Acc. Chem. Res.* **1993**, *26*, 593.

35. Suzuki, S.; Green, P. G.; Bumgarner, R. E.; Dasgupta, S.; Goddard, W. A., III; Blake, G. A. *Science* **1992**, *257*, 942.

36. Egli, M.; Gessner, R. V. *Proc. Natl. Acad. Sci. U. S. A.* **1995**, *92*, 180.

37. Sarkhel, S.; Rich, A.; Egli, M. *J. Am. Chem. Soc.* **2003**, *125*, 8998.

38. Jain, A.; Purohit, C. S.; Verma, S.; Sankararamakrishnan, R. *J. Phys. Chem. B* **2007**, *111*, 8680.

39. Wan, C. Q.; Chen, X. D.; Mak, T. C. W. *CrystEngComm.* **2008**, *10*, 475.

40. Kitson, P. J.; Song, Y. F.; Gamez, P.; Hoog, P. de; Long, D. L.; Parenty, A. D. C.; Reedijk, J.; Cronin, L. *Inorg. Chem.* **2008**, *47*, 1883.

41. Lu, Z. L.; Gamez, P.; Mutikainen, I.; Turpeinen, U.; Reedijk, J. *Cryst. Growth Des.* **2007**, *7*, 1669.

42. Mooibroek, T. J.; Teat, S. J.; Massera, C.; Gamez, P.; Reedijk, J. *Cryst. Growth Des.* **2006**, *6*, 1569.

43. Gautrot, J. E.; Hodge, P.; Cupertino, D.; Helliwell, M. *New J. Chem.* **2006**, *30*, 1801.

44. Rahman, A.; Bishop, R.; Craig, D. C.; Scudder, M. L. *CrystEngComm*. **2003**, *5*, 422.

45. Rahman, A.; Bishop, R.; Craig, D. C.; Scudder, M. L. *CrystEngComm*. **2002**, 510.

46. Bishop, R.; Scudder, M. L.; Craig, D. C.; Rahman, A.; Alshahateet, S. F. *Mol. Cryst. Liq. Cryst.* **2005**, *440*, 173.

47. Gung, B. W.; Zou, Y.; Xu, Z. G.; Amicangelo, J. C.; Irwin, D. G.; Ma S. Q.; Zhou, H. C. *J. Org. Chem.* **2008**, *73,* 689.

48. Amicangelo, J. C.; Gung, B. W.; Irwin, D. G.; Romano, N. C. *Phys. Chem. Chem. Phys.* **2008**, *10*, 2695.

49. Gung, B. W.; Xue, X. W.; Reich, H. J. *J. Org. Chem.* **2005**, *70*, 7232.

50. Mooibroek T. J.; Gamez, P. *CrystEngComm*. **2012**, *14*, 1027.

51. Aswal, S. Ph. D. Thesis; *Synthesis of flexible bicyclic nitrogenous heterocycles, their X-ray crystallographic studies and biological activities* **2006**, Jawaharlal Nehru University, New Delhi.

52. Avasthi, K.; Bhagat, D.; Bal, C.; Sharon, A.; Yadav, U.; Maulik, P. R. *Acta Cryst.* **2003**, *C59,* o409.

53. (a) Avasthi, K.; Chandra, T.; Bhakuni, D.S. *Indian J. Chem.* **1995**, *34B*, 944. (b) Avasthi, K.; Farooq, S.M.; Aswal, S.; Raghunandan, R.; Maulik, P.R. *J. Mol. Struct.* **2007**, *827*, 88. (c) Avasthi, K.; Farooq, S. M.; Raghunandan, R.; Maulik, P.R. *J. Mol. Struct.* **2009**, *927*, 27.

List of Publications

1. Avasthi, K.; Kumar, Amar; Aswal, S.; Kant, R.; Raghunandan, R.; Maulik, P. R.; Khanna, R. S.; Ravikumar, K. Role of arene interactions and substituent effects in conformational (syn/anti) control of 1,2-diarylethanes, *CrystEngComm* **2012**, *14*, 383–388.
2. Avasthi, K.; Kumar, Amar An overview of arene–arene interactions and application of uni-molecular models for their understanding, *Chemistry & Biology Interface* **2012** *(In Press).*

CrystEngComm

Cite this: *CrystEngComm*, 2012, **14**, 383

www.rsc.org/crystengcomm

COMMUNICATION

Role of arene interactions and substituent effects in conformational (*syn*/*anti*) control of 1,2-diarylethanes†‡

Kamlakar Avasthi,*[a] Amar Kumar,[a] Sangeeta Aswal,[a] Ruchir Kant,[b] Resmi Raghunandan,[b] Prakas R. Maulik,[b] Ranjana S. Khanna[c] and Krishnan Ravikumar[d]

Received 4th August 2011, Accepted 18th November 2011
DOI: 10.1039/c1ce06001e

Conformational analysis of nine designed flexible 1,2-diarylethanes with different substituents show *syn* conformation due to π–π interactions by ^{1}H NMR in solution, this carries over to the solid state for three compounds while two show *anti* conformation in the solid state by X-ray crystallography and the remaining compounds do not give diffraction quality crystals.

A knowledge of weak noncovalent forces that control conformation in flexible compounds is of fundamental importance since these are the most important factors controlling the shape and the dynamics of complex polymeric molecules like DNA and proteins. However, these forces are still not well understood and remain a challenge to the chemical community, mainly due to the fact that many of these forces are present simultaneously in drug–receptor complexes. Arene interactions constitute one of these forces and in spite of its established importance in chemistry,[1] biology[2] and drug development,[3] its application as a tool in molecular recognition or crystal engineering remains a problem. For example, to answer which molecule having an arene residue at the termini of polymethylene (*e.g.* ethylene, propylene *etc.*) linker will show intramolecular folding due to arene (especially offset face-to-face mode) interaction in solution, is not easy even today. Furthermore, when present in solution, determining in which case it is strong enough to survive in the solid state is even more difficult.

In the literature, various models based on different scaffolds to facilitate arene interactions have been proposed for their understanding.[4] These studies can be divided into two main types, first intermolecular[5] which is important from drug–receptor, protein–DNA, protein–protein interaction *etc.* and second intramolecular[6] which is important especially from DNA/RNA structures, where in single strand it is intramolecular while in double it is both inter- and intramolecular. Intramolecular arene interaction is also important at the molecular level for developing models for a better understanding of arene interactions in general and exploration of the newly emerging concept of conformational control in flexible compounds having at least two arene moieties connected by polymethylene linker (*e.g.* propylene,[6d–6g, 6q, 7] and ethylene[6d,6h–6j]) Electronic effects of the substituents are also widely believed to have a significant effect on arene interaction,[1,4–6] however, currently there is a lot of debate going on over this and new developments are emerging while older concepts are being challenged.[1b]

1,2-Diarylethanes are the simplest unbiased flexible model to understand how two arene moieties (similar/different) interact with each other intramolecularly for controlling observed folded conformation of the molecule both in solution and more importantly in the crystal state. Interestingly, 1,2-diphenylethane, 1,3-di-phenylpropane and 1,4-diphenylbutane are open in the solid state indicating that the phenyl moiety is not a good system for studying intramolecular arene interactions in such unbiased flexible models. In the absence of arene interactions, conformations of such 1,2-diphenylethanes due to the steric effect of the bulky arene residues, are normally expected to be *anti* and this is supported by the crystal structures of many 1,2-diphenylethanes having a wide variety of electron donating and withdrawing substituents in the literature.[8] Even when the *ethylene* linker is between two N atoms the conformation remains *anti*, clearly indicating that a smaller van der Waals radii of the N atom in comparison to the C atom alone is not enough reason to show *syn* conformation in crystals.[8f–8h]

On the other hand, a few studies have shown that such structures are capable of existing in *folded* conformation in solution. A study, as early as 1968, by Leonard *et al.* on nucleic acid bases connected by *ethylene* and *propylene* linkers clearly showed, that intramolecular interactions between arene residues were responsible for observed folding in solution.[6d] Later by Itahara on adenine (by ^{1}H NMR)[6h–6j] and by us on pyrazolo[3,4-*d*]pyrimidine (PP) core based *ethylene* linker compounds (by ^{1}H NMR) showed that 1,2-diarylethanes are capable of existing in *syn* conformation in solution.[9] Recently, Dubey *et al.* described that *ethylene* linker compounds with PP cores at their termini show folded conformation in solution both by circular dichroism (CD) and variable temperature ^{1}H NMR studies, however,

---

[a] *Medicinal and Process Chemistry Division, CSIR-Central Drug Research Institute, Lucknow, 226001, India. E-mail: kavasthi@rediffmail.com*
[b] *Molecular and Structural Biology Division, CSIR-Central Drug Research Institute, Lucknow, 226001, India*
[c] *Department of Chemistry, Banaras Hindu University, Varanasi, 221005, India*
[d] *X-Ray Crystallography Division, CSIR-Indian Institute of Chemical Technology, Hyderabad, 500007, India*

† Electronic supplementary information (ESI) available: Synthesis, experimental set-up, additional figures, tables and characterization details. CCDC reference numbers 816595 (**5b**), 816596 (**5d**), 833097 (**5f**), 837594 (**5i**) and 837595 (**5g**). For ESI and crystallographic data in CIF or other electronic format see DOI: 10.1039/c1ce06001e

‡ CDRI Communication No. 8163.

no solid state evidence for *syn* conformation due to arene interactions was provided.[10] One case, 1,2-bis[5-oxo-3-(*n*-propyl)-4,5-dihydro-3*H*-1,2,4-triazol-4-yl]ethane is known to have a *syn* conformation in the solid state[11] but it is not mentioned whether the extensive hydrogen bonding due to the water present in the molecule or the arene/O··· arene interactions is actually responsible for the observed *syn* conformation.

Since 1995, our work on PP core based flexible *propylene*/*Leonard* linker compounds has shown that intramolecular folding is possible due to arene interactions both in solution and more importantly in the solid state, from a crystal engineering angle, as shown by more than a dozen truly flexible symmetrical (**1a**, **1b**, **1e–1g** and **2a–2c**, Fig. 1 and Fig. S1, ESI†) and two related dissymmetrical compounds (Fig. S1, ESI†).[7,9] The main difference between **1** and **2** is that the pyrimidine of **1** is replaced by pyrimidone system in **2**. Very recently, the scope of the PP core for studying arene interaction in flexible symmetrical and dissymmetrical compounds has been considerably increased by replacing a truly flexible *propylene*/*Leonard* linker with a less mobile *butylidene* linker (**1o**, Fig. S1, ESI†).[12] Interestingly, Vogtle refers to singly linked molecules that adopt π-stacked conformations as "protophanes".[13]

These results have prompted us to apply PP core to common 1,2-diarylethanes. Our initial efforts in getting *syn* conformation in the solid state due to intramolecular π–π interactions in the *ethylene* linker symmetrical compound based on PP core were not successful.[9c] A careful analysis of the crystal structures (**1**; $n = 3$, **2a–2c**, Fig. 1 and Fig. S3, ESI†) revealed that except for **1b** (Fig. 1 and Fig. S3, ESI†) having bulky groups at both 4- and 6-positions, five membered pyrazolo moieties are at a maximum distance from each other (*e.g.* 4.48 and 4.62 Å between centroids in **1a** and **2a** respectively) while six membered pyrimidine/pyrimidone residues are partially overlapped (*e.g.* 3.71 and 3.77 Å between centroids in **1a** and **2a** respectively). Since for the *ethylene* linker homolog **1c** (Fig. 1) of the symmetrical *propylene* linker compound **1a** (Fig. 1) both PP moieties have to come close to each other in order to achieve a *syn* conformation and this situation may not be sterically/electronically favourable especially in the solid state where competing intermolecular interactions are present to give a more favourable *anti* conformation. Therefore, it was decided to replace the pyrazolo residue by the pyrimidone type of moiety, as it was well tolerated in compounds of the series **2** and is also present in nucleic acid bases. Thus, a commercially available quinazolinone containing pyrimidone residue was selected for the study. The reaction product from the reaction of 1-(2-bromoethyl)-4,6- dimethylsulfany-l*H*-pyrazolo[3,4-*d*]pyrimidine, (**3a**)[9a] with quinazolinone (**4a**) gives **5a** (Fig. 2) which by ^{1}H NMR (CDCl$_3$) analysis shows intramolecular folding when compared to the reference compounds (**3b** and **4b**, Fig. 2 and Table S4, ESI†). However, all attempts to get single crystals of **5a** for X-ray crystallography failed forcing us not to pursue this study for the time being. Next, phthalazinone (**4c**) which is isomeric with quinazolinone and also commercially available was selected to replace one PP core of **1a** (Fig. 1 and ESI†). Thus, reaction of phthalazinone (**4c**) with **3a** in DMF in the presence of anhydrous potassium carbonate gave the desired *ethylene* product **5b** in good yield (ESI†). To our satisfaction the new *ethylene* linker compound **5b** also shows significant up-field shift in ^{1}H NMR (CDCl$_3$) as compared to the reference compounds, **3b** and **4d** (Fig. 2 and Table S4, ESI†) thus, indicating a folded conformation. More importantly, **5b** gives good crystals and the solid state structure of **5b** shows a *syn* conformation (Fig. 3). The torsion angle formed by NCCN atoms involving the *ethylene* linker and two N atoms connecting it is 60.58°, confirming *syn* conformation. The

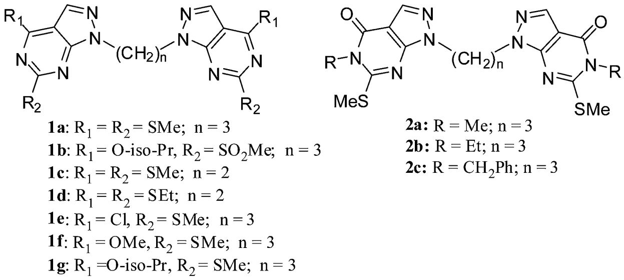
1a: $R_1 = R_2 = SMe$; $n = 3$
1b: $R_1 = O\text{-iso-Pr}$, $R_2 = SO_2Me$; $n = 3$
1c: $R_1 = R_2 = SMe$; $n = 2$
1d: $R_1 = R_2 = SEt$; $n = 2$
1e: $R_1 = Cl$, $R_2 = SMe$; $n = 3$
1f: $R_1 = OMe$, $R_2 = SMe$; $n = 3$
1g: $R_1 = O\text{-iso-Pr}$, $R_2 = SMe$; $n = 3$
2a: $R = Me$; $n = 3$
2b: $R = Et$; $n = 3$
2c: $R = CH_2Ph$; $n = 3$

Fig. 1 Pyrazolo[3,4-*d*]pyrimidine core based *propylene* and *ethylene linker* compounds.

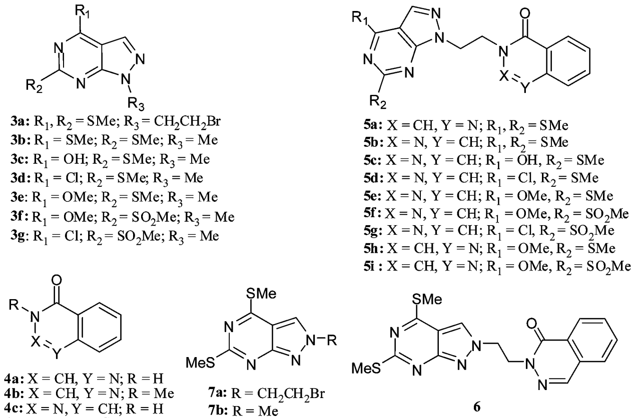
3a: $R_1, R_2 = SMe$; $R_3 = CH_2CH_2Br$
3b: $R_1 = SMe$; $R_2 = SMe$; $R_3 = Me$
3c: $R_1 = OH$; $R_2 = SMe$; $R_3 = Me$
3d: $R_1 = Cl$; $R_2 = SMe$; $R_3 = Me$
3e: $R_1 = OMe$; $R_2 = SMe$; $R_3 = Me$
3f: $R_1 = OMe$; $R_2 = SO_2Me$; $R_3 = Me$
3g: $R_1 = Cl$; $R_2 = SO_2Me$; $R_3 = Me$
5a: $X = CH$, $Y = N$; $R_1, R_2 = SMe$
5b: $X = N$, $Y = CH$; $R_1, R_2 = SMe$
5c: $X = N$, $Y = CH$; $R_1 = OH$, $R_2 = SMe$
5d: $X = N$, $Y = CH$; $R_1 = Cl$, $R_2 = SMe$
5e: $X = N$, $Y = CH$; $R_1 = OMe$, $R_2 = SMe$
5f: $X = N$, $Y = CH$; $R_1 = OMe$, $R_2 = SO_2Me$
5g: $X = N$, $Y = CH$; $R_1 = Cl$, $R_2 = SO_2Me$
5h: $X = CH$, $Y = N$; $R_1 = OMe$, $R_2 = SMe$
5i : $X = CH$, $Y = N$; $R_1 = OMe$, $R_2 = SO_2Me$
4a: $X = CH$, $Y = N$; $R = H$
4b: $X = CH$, $Y = N$; $R = Me$
4c: $X = N$, $Y = CH$; $R = H$
4d: $X = N$, $Y = CH$; $R = Me$
7a: $R = CH_2CH_2Br$
7b: $R = Me$
6

Fig. 2 *Ethylene* linker compounds (**5**) derived from PP core (**3**) and quinazolinone/phthalazinone (**4**) and reference compounds.

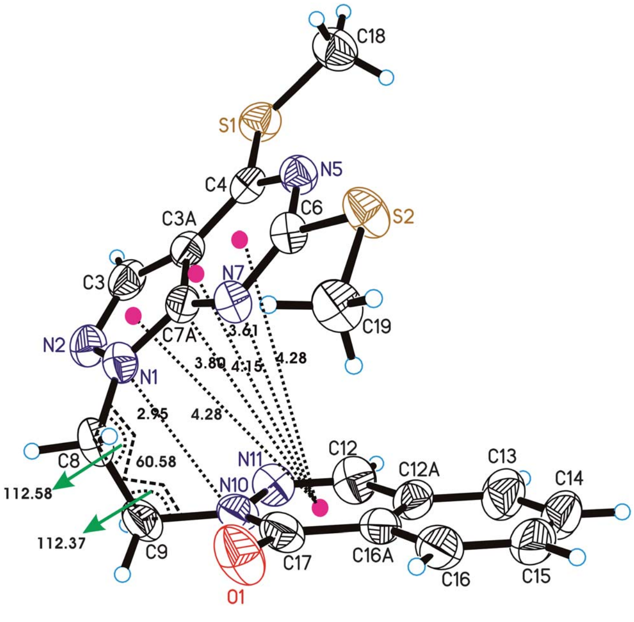

Fig. 3 ORTEP diagram of **5b** (at 30% probability level) showing *syn* conformation with intramolecular π–π interactions.

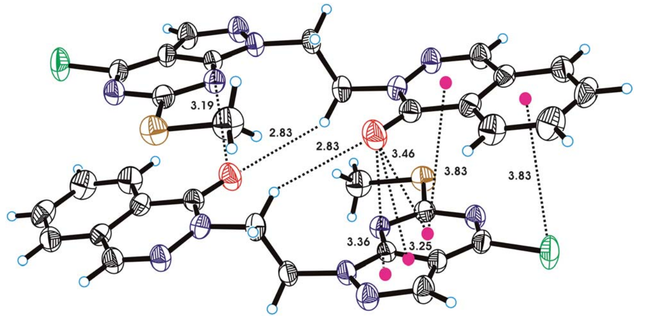

Fig. 4 Crystal structure of **5d** showing open conformation with intermolecular C–H···O, O···arene, Cl–arene and π–π interactions.

distance between two N atoms linking two arene moieties is 2.95 Å which is less than the sum of van der Waals radii of two N atoms (3.10 Å *i.e.* 2 × 1.55 Å for N) and less than 3.09 seen in **1b** with extra C in its linker. The distance between centroids of the five membered pyrazole ring of the PP core and six membered pyrimidone ring of the phthalazinone system is 4.28 Å which is similar to the distance of 4.28 Å between centroids of the six membered pyrimidine and six membered heterocyclic ring of the phthalazinone system (Fig. 3). It is important to mention that 4.23 Å is the maximum distance seen in folded compounds (**1a**, **1b**, **1e–1g** and **2a–2c**, Fig. 1 and Table S2, ESI†) that shows such a distance in the range of 3.69–4.23 Å. The distance between centroids of nine membered PP core and six membered pyrimidone ring of the phthalazinone system is 4.15 Å. Some close distances between two six membered pyrimidine and pyrimidone rings of phthalazinone are C7A···N11 = 3.42, N7···N10 = 3.42 and N7···C17 = 3.50 Å confirming intramolecular stacking. Finally, there is no intramolecular S···arene (4.96 and 5.07 Å)[3a] or significant CH–π interactions[14] confirming that the *syn* conformation is due to intramolecular π–π interactions. The variable temperature (−50 to 50 °C) ^{1}H NMR study on **5b** shows an increase in the magnitude of up-field shift (difference of two SMe protons) with decrease in temperature indicating that the molecule exists in folded and unfolded states at room temperature in $CDCl_3$. Surprisingly, the N^2- isomer (**6**, ESI†) of **5b** prepared similarly from 2-(2-bromoethyl)-4,6-dimethylsulfany-l*H*-pyrazolo[3,4-*d*]pyrimidine (**7a**)[9a] and phthalazinone does not show much up-field shift in its ^{1}H NMR (Table S4, ESI†) indicating the absence of intramolecular folding due to different positions of linker. It is important to mention here that such a drastic change in the conformation due to different positions of linker in two isomeric compounds was also observed in the *propylene* linker compound **1a** and its N^2-isomer.[15] The variable temperature (−50 to 50 °C) ^{1}H NMR study on the N^2-isomer, **6** does not show a comparable change in the chemical shift (difference of two SMe protons) in its ^{1}H NMR further confirming the presence of only the open form (Table S3, ESI†). To test the robustness of the *syn* conformation in **5b** formed due to intramolecular arene interaction, substituents effects, were studied. The compound **5c** prepared from **5b** (ESI†) also shows up-field shift for the methylsulfanyl group in ^{1}H NMR indicating a folded conformation, however, crystals of **5c** suitable for crystallography could not be prepared, presumably due to the presence of ionisable H (from lactam) capable of forming stronger H-bonding. Replacement of the 4-SMe group in **5b** by a common electron withdrawing Cl group *via* **5c** gives **5d** (ESI†) which also shows significant up-field shifts in its ^{1}H NMR in comparison to **4d** and **3d** (Fig. 2, **3a** and **3b**, Table S4, ESI†) indicating folded conformation in solution. The solid state structure of **5d**, however, shows an *anti* conformation (torsion angle = 172.38°, Fig. 4) with a distance between two N atoms linking two arene moieties of 3.72 Å.

Furthermore, a comparable distance of 3.70 Å was also shown by our earlier symmetrical *ethylene* compound **1d** (Fig. 1) with *anti* conformation.[9c] A careful analysis of the crystal structure of **5d** shows strong O···arene dimerization (3.25 Å) with the closest distance between O···C of 3.19 Å which is less than the van der Waals radii of O and C atoms and intermolecular O···Ar interactions are of current interest.[16] Additional C–H···O (2.83, 3.61 Å and 138.1°)[17] Cl···arene (3.83 Å)[18] and π–π interactions (3.83 Å) are also present in this dimer. It is interesting to mention here that symmetrical **1e** with the Cl group at a similar 4-position is also devoid of intramolecular π–π interactions.[7f]

Next, the electron withdrawing Cl group is replaced by the common electron donating methoxy group. The new compound **5e** obtained by the reaction of **5b** with sodium methoxide (ESI†) again shows an up-field shift in its ^{1}H NMR like compounds **5b–5d**, (Table S4, ESI†) indicating intramolecular folding, however, crystals of **5e** suitable for crystallography could not be prepared.

Following this, the 6-SMe group of **5e**, which defied our attempts to give diffraction quality crystals, is replaced by the strong electron withdrawing SO_2Me group by oxidation to give a new compound **5f**. Once again **5f** shows an up-field shift in its ^{1}H NMR like compounds **5b–5e**, (Table S4, ESI†) indicating folded conformation. The solid state structure of **5f** shows a *syn* conformation (torsion angle = 62.52°, Fig. 5). The distance between two N atoms linking two arene moieties is 2.93 Å which is very comparable to 2.95 as seen in **5b**. It is important to mention here that symmetrical **1j** (Fig. S1, ESI†) with an

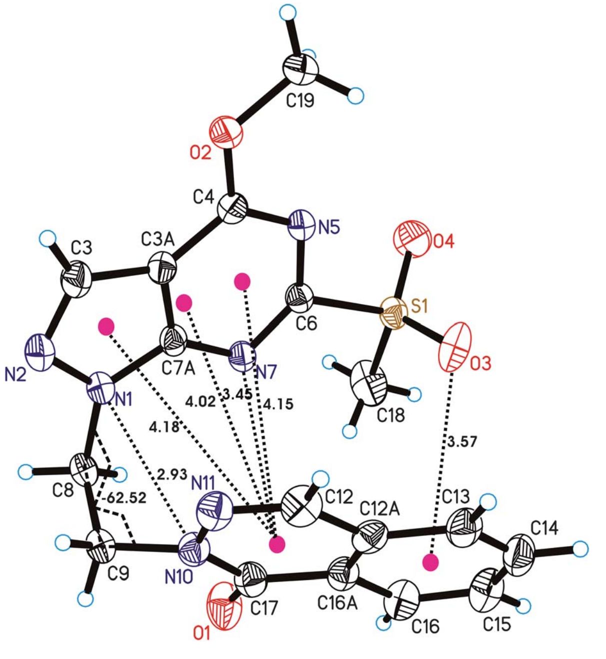

Fig. 5 ORTEP diagram of **5f** (at 30% probability level) showing *syn* conformation with intramolecular π–π interactions and O···arene interactions.

OMe group at a similar 4-position and an SO$_2$Me group at the 6-position is also folded due to intramolecular π–π interactions.[7d]

Encouraged by this result on **5f** it was decided to convert **5d** in to sulfone (**5g**) and see its effect on conformation. New sulfone **5g** shows an up-field shift in its ^{1}H NMR like compounds **5b–5e**, (Table S4, ESI†) indicating folded conformation. The solid state structure of **5g**, however, shows *anti* conformation (torsion angle = 173.81°, N1···N10 = 3.71 Å, Fig. 6). This result is quite interesting in showing that the strong electron withdrawing SO$_2$Me group alone is not responsible for the *syn* conformation seen earlier in **5f**. Presumably, the involvement of the Cl group at the 4-position in many intermolecular noncovalent interactions in both compounds (**5d** and **5f**) is a possible reason for the existence of the open conformation.

Finally, the third sulfone **5i** was prepared from **5h** following a similar method as described for **5f** and **5g**. The sulfone **5i** shows an up-field shift in its ^{1}H NMR like compounds **5b–5e**, (Table S4, ESI†) indicating a folded conformation in solution. The solid state structure of **5i** shows *syn* conformation (torsion angle = 59.97°, Fig. 7). This result is very comparable to that of **5f** (and **5b**) except for the fact that **5i** has the smallest value of torsion angle out of the three folded structures (**5b**, **5f** and **5i**). Furthermore, other intermolecular distances in **5i**, in general, are also smaller in comparison to the other two folded compounds (**5b** and **5f**). A careful analysis of compound **5i** revealed the presence of a much weaker CH···π interaction. The closest H contacts with the six membered phenyl ring of quinazolinone are 2.85 and 2.95 Å. Earlier, we reported an unusual folded conformation of a dissymmetrical propylene linker compound (**8a**, Fig. S1, ESI†) with a PP core and a phthalimido moiety solely due to CH···π interaction (Table 1).[7l] Similar comparison of two other compounds (**5b** and **5f**) showed much less acceptable distances for the presence of CH···π interaction (Table 1). It is important to mention that while all four different compounds (Table 1) with one PP moiety show unusual intramolecular folding they have different reasons for folding. The first three compounds belong to the ethylene series while the last one is a propylene linker compound. In **5b** intramolecular folding is almost solely due to arene interaction while in **8a** it is solely due to CH···π interaction. Though compound **5i** shows two very good distances (2.85 and 2.95 Å) for CH···π interaction of which the first is sub-van der Waal, the distance of 4.20 Å between C(19) and involved centroid is beyond 4.0 Å, generally considered the upper limit. This may be explained by the fact that the main conformation controlling factor in **5i** is intramolecular π···π interaction and not CH···π interaction. In view of this explanation a contribution from CH···π interaction seems much less for **5f** and **5b** (Table 1). Finally, another compound (**8b**, Fig. S1, ESI†) in which the 4-SMe group of **8a** was replaced by a pyrrolidino moiety, intramolecular folding due to CH···π interaction disappeared resulting in a normal extended/open structure. Out of three sulfones, two with 4-OMe groups are folded and one with the 4-Cl in place of OMe is open. Two folded isomeric sulfones differ in having either phthalazinone or quinazolinone residues. Striking, similarity of the three solid state *syn* conformations of **5b**, **5f** and **5i** having different substituents and different arenes (phthalazinone or quinazolinone) is noteworthy and shows that the folded motif mainly due to intramolecular π–π interactions is robust from a crystal engineering point of view.

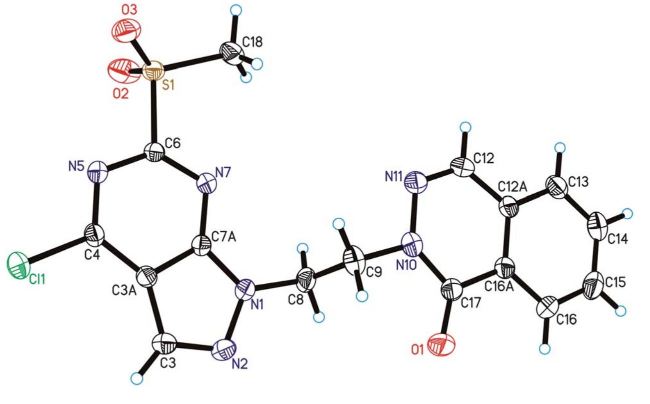

Fig. 6 ORTEP diagram of **5g** (at 30% probability level) showing *syn* conformation with intramolecular π–π interactions and O···arene interactions.

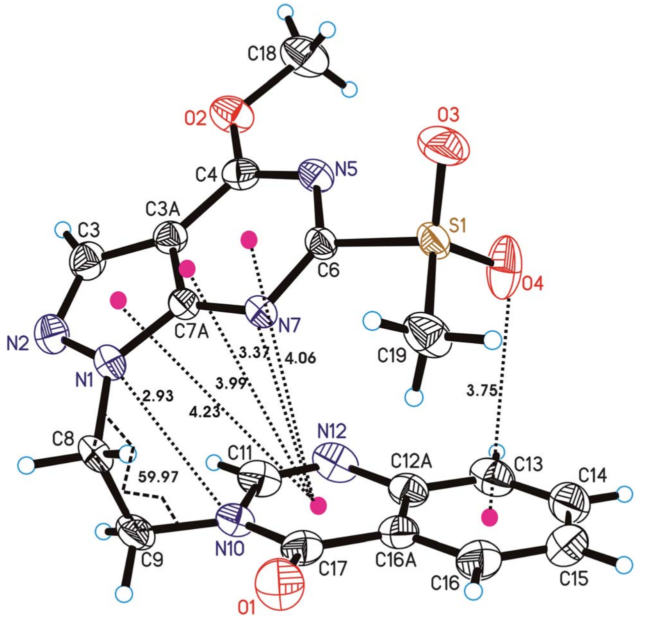

Fig. 7 ORTEP diagram of **5i** (at 30% probability level) showing *syn* conformation with intramolecular π–π interactions and O···arene interactions.

In conclusion, all nine compounds (**5a–5i**) are folded due to intramolecular π–π interaction in solution as shown by their ^{1}H NMR data. This PP core based dissymmetric ethylene model shows very good tolerance for various substituents (SMe, OMe, OH, Cl and SO$_2$Me) in solution. A similar trend was followed by our *propylene/Leonard* compounds in solution. For the three compounds (**5b**, **5f** and **5i**) with limited variation in substituents (SMe, OMe and SO$_2$Me) these interactions are strong enough for the *syn* conformation to carry over to the solid state, while for the two chloro compounds (**5d** and **5g**) it changes to an *anti* conformation in the solid state due to strong intermolecular interactions. Apparently, two arene systems not only have to come close enough (<3 Å, as in **5b**, **5f** and **5i**) at the point of contact (which is much less than 3.4 Å for two benzenoid systems thus causing severe steric hindrance), intramolecular π–π interactions have also to compete with other strong intermolecular interactions to show a *syn* conformation in 1,2-diarylethanes. A careful consideration of these factors may help in designing new 1,2-diarylethanes capable of existing in the *syn* conformation in the solid state. In our view, this study is the first in

Table 1 Important CH···π interaction data obtained from X-ray crystallographic studies on **5b**,**5f**, **5i** and **8a**

Compound no.	Distance between C(19) & C16A/Å	Distance between C(19)H & C16A (C(18)H & C16A in **5f**)/Å	Distance between C(19) and C16 (C(18)H & C16 in **5f**)/Å	Distance between C(19)H & C16 (C(18)H & C16 in **5f**/Å	Distance between centroids of phenyl ring of phthalazinone/quinazolinone/ phthalimide & C(19) (C(18) in **5f**)/Å
5b	4.106	3.168	3.992	3.049	4.563
5f	4.240	3.379	4.073	3.248	4.387
5i	3.720	2.852	3.64	2.945	4.201
8a	3.579	2.985	3.611	3.274	3.602

the literature where a systematic study for the ability of arene interactions to control the conformation both in solution and solid state together with the dramatic substituents effect on the solid state conformation has been demonstrated. Interestingly, 4-SMe, 4-OMe and 6-SO_2Me groups were also tolerated in symmetrical *propylene/Leonard* compounds for showing folded conformation in the solid state. This work together with our earlier work on *propylene/Leonard* and *butylidene* linkers for 1,3-diaryl-propanes, opens a new window for conformation control in flexible 1,2-diaryethanes. In addition, the worthiness of the PP core as a novel system for studying arene interactions, both in solution and solid state, is demonstrated once again. Above all the conformational control due to different common substituents of organic/medicinal chemistry, in the solid state is demonstrated which is very important from molecular recognition and crystal engineering angles. These models may provide an important experimental basis for further development of computational/theoretical models for a better understanding of arene interactions in flexible compounds both at the molecular and supramolecular level.

Acknowledgements

KA is grateful to DST, New Delhi, India for financial support (grant nos. SP/S1/G-44/99 and SR/S1/OC-14/2010). AK, SA and RR are thankful to CSIR, New Delhi, India for SRF. PRM is thankful to CSIR, New Delhi, India for Emeritus Scientist Scheme [No. 21 (0766)/09/EMR-II]

Notes and references

1 (*a*) M. Watt, L. K. E. Hardebeck, C. C. Kirkpatrick and M. Lewis, *J. Am. Chem. Soc.*, 2011, **133**, 3854; (*b*) S. E. Wheeler, *J. Am. Chem. Soc.*, 2011, **133**, 10262; (*c*) K. B. Bravaya, O. Kostko, M. Ahmed and A. I.Krylov, *Phys. Chem. Chem. Phys.*, 2010, **12**, 2292; (*d*) S. Grimme, *Angew. Chem.*, 2008, **120**, 3478; *Angew. Chem. Int. Ed.*, 2008, 47, 3430; (*e*) C. Janiak, *J. Chem. Soc., Dalton Trans.*, 2000, 3885; (*f*) C. A. Hunter and J. K. M. Sanders, *J. Am. Chem. Soc.*, 1990, **112**, 5525.

2 (*a*) S. K. Burley and G. A. Petsko, *Science*, 1985, **229**, 23; (*b*) M. L. Waters, *Biopolymers*, 2004, **76**, 435.

3 (*a*) L. S. Salonen, M. Ellermann and F. Diederich, *Angew. Chem.*, 2011, **123**, 4908; *Angew. Chem. Int. Ed.*, 2011, 50, 4808; (*b*) C. Bissantz, B. Kuhn and M. Stahl, *J. Med. Chem.*, 2010, **53**, 5061.

4 (*a*) C. A. Hunter, *Chem. Soc. Rev.*, 1994, **23**, 101; (*b*) C. A. Hunter, K. R. Lawson, J. Perkins and C. J. Urch, *J. Chem. Soc. Perkin Trans*, 2001, 651.

5 (*a*) B. K. Mishra and N. Sathyamurthy, *J. Phys. Chem. A*, 2005, **109**, 6; (*b*) H. Adams, K. Harris, G. Hembury, C. A. Hunter, D. Livingstone and J. F. McCabe, *Chem. Commun.*, 1996, 2531; (*c*) J. Rebek Jr, *Angew. Chem., Int. Ed. Engl.*, 1990, **29**, 245; (*d*) M. S. Cubberley and B. L. Iverson, *J. Am. Chem. Soc.*, 2001, **123**, 7560.

6 (*a*) B. W. Gung, F. Wekesa and C. L. Barnes, *J. Org. Chem.*, 2008, **73**, 1803; (*b*) B. W. Gung, X. Xue and Y. Zou, *J. Org. Chem.*, 2007, **72**, 2469; (*c*) B. W. Gung, B. U. Emenike, M. Lewis and K. Kirschbaum, *Chem.–Eur. J.*, 2010, **16**, 12357; (*d*) D. T. Browne, J. Eisinger and N. J. Leonard, *J. Am. Chem. Soc.*, 1968, **90**, 7302; (*e*) N. J. Leonard, *Acc. Chem. Res.*, 1979, **12**, 423; (*f*) L. F. Newcomb and S. H. Gellman, *J. Am. Chem. Soc.*, 1994, **116**, 4993; (*g*) Y. Pang, J. L. Miller and P. A. Kollman, *J. Am. Chem. Soc.1999*, 1717, **121**; (*h*) T. Itahara, *J. Chem. Soc., Perkin Trans. 2*, 1998, 1455; (*i*) T. Itahara and K. Imamura, *Bull. Chem. Soc. Jpn.*, 1994, **67**, 203; (*j*) T. Itahara, *J. Chem. Soc., Perkin Trans. 2*, 1996, 2695; (*k*) J. H. Nicholas, B. Pablo, H. Bernardo, C. Aranzazudel and J. Jesus, *J. Am. Chem. Soc.*, 1998, **120**, 12371; (*l*) S. Paliwal, S. Geib and C. S. Wilcox, *J. Am. Chem. Soc.*, 1994, **116**, 4497; (*m*) S. E. Wheeler and K. N. Houk, *J. Am. Chem. Soc.*, 2008, **130**, 10854; (*n*) F. Cozzi, M. Cinquini, R. Annunziata, T. Dwyer and J. S. Siegel, *J. Am. Chem. Soc.*, 1992, **114**, 5729; (*o*) F. Cozzi, R. Annunziata, M. Benaglia, K. K. Baldridge, G. Aguirre, J. Estrada, Y. Sritana-Anant and J. S. Siegel, *Phys. Chem. Chem. Phys.*, 2008, **10**, 2686; (*p*) S. Grimme, C. Muck-Lichtenfeld and J. Antony, *Phys. Chem. Chem. Phys.*, 2008, **10**, 3327; (*q*) A. Garcıa-Raso, J. J. Fiol, F. Badenas, X. Solans and M. Font-Bardia, *Polyhedron*, 1999, **18**, 765.

7 (*a*) G. Biswas, T. Chandra, K. Avasthi and P. R. Maulik, *Acta Crystallogr., Sect. C: Cryst. Struct. Commun.*, 1995, **51**, 2453; (*b*) K. Avasthi, S. M. Farooq, D. S. Rawat, A. Sharon and P. R. Maulik, *Acta Crystallogr., Sect. C: Cryst. Struct. Commun.*, 2003, **59**, o523; (*c*) K. Avasthi, S. Aswal, R. Kumar, U. Yadav, D. S. Rawat and P. R. Maulik, *J. Mol. Struct.*, 2005, **750**, 179; (*d*) K. Avasthi, S. M. Farooq, S. Aswal, R. Raghunandan and P. R. Maulik, *J. Mol. Struct.*, 2007, **827**, 88; (*e*) K. Avasthi, S. Aswal, S. M. Farooq, R. Raghunandan and P. R. Maulik, *J. Mol. Struct.*, 2008, **888**, 327; (*f*) K. Avasthi, S. M. Farooq, R. Raghunandan and P. R. Maulik, *J. Mol. Struct.*, 2009, **927**, 27; (*g*) K. Avasthi, S. M. Farooq, R. Raghunandan and P. R. Maulik, *J. Mol. Struct.*, 2006, **785**, 106; (*h*) K. Avasthi, S. M. Farooq, C. Bal, R. Kumar, A. K. Tewari and P. R. Maulik, *J. Mol. Struct.*, 2007, **842**, 100; (*i*) P. R. Maulik, K. Avasthi, G. Biswas, S. Biswas, D. S. Rawat, S. Sarkhel, T. Chandra and D. S. Bhakuni, *Acta Crystallogr., Sect. C: Cryst. Struct. Commun.*, 1998, **54**, 275; (*j*) K. Avasthi, S. Aswal and P. R. Maulik, *Acta Crystallogr., Sect. C: Cryst. Struct. Commun.*, 2001, **57**, 1324; (*k*) K. Avasthi, A. Tewari, D. S. Rawat, A. Sharon and P. R. Maulik, *Acta Crystallogr., Sect. C: Cryst. Struct. Commun.*, 2002, **58**, o494; (*l*) K. Avasthi, D. Bhagat, C. Bal, A. Sharon, U. Yadav and P. R. Maulik, *Acta Crystallogr., Sect. C: Cryst. Struct. Commun.*, 2003, **59**, o409.

8 Some examples are: (*a*) J. Harada, K. Ogawa and S. Tomoda, *J. Am. Chem. Soc.*, 1995, **117**, 4476; (*b*) B. Kahr, C. A. Mitchell, J. F. Chance, R. V. Clark, P. Gantzel, K. K. Baldridge and J. S. Siegel, *J. Am. Chem. Soc.*, 1995, **117**, 4479; (*c*) Q. Shen, *J. Mol. Struct.*, 1998, **471**, 57; (*d*) J. Harada and K. Ogawa, *Struct. Chem.*, 2001, **12**, 243; (*e*) B. R. Bhogala, V. R. Vangala, P. S. Smith, J. A. K. Howard and G. R. Desiraju, *Cryst. Growth Des.*, 2004, **4**, 647; (*f*) B. Lia, J. Zhoua, Y. Penga, B. Lia and Y. Zhang, *J. Mol. Struct.*, 2004, **707**, 187; (*g*) Z. P. Liang and J. Li, *Acta Crystallogr., Sect. E: Struct. Rep. Online*, 2006, **62**, o5282; (*h*) C. R. Barbarin, B. Najera and P. Elizondo, *Acta Crystallogr., Sect. E: Struct. Rep. Online*, 2006, **62**, o5423.

9 (*a*) K. Avasthi, T. Chandra and D. S. Bhakuni, *Indian J. Chem.*, 1995, **34B**, 944; (*b*) K. Avasthi, D. S. Rawat, T. Chandra and D. S. Bhakuni, *Indian J. Chem.*, 1998, **37B**, 754; (*c*) K. Avasthi, D. S. Rawat,

P. R. Maulik, S. Sarkhel, C. K. Broder and J. A. K. Howard, *Tetrahedron Lett.*, 2001, **42**, 7115.

10 R. Dubey, A. K. Tewari, K. Ravikumar and B. Sridhar, *Bull. Korean Chem. Soc.*, 2010, **31**, 1326.

11 G. Ozdemir, S. I. Isik, K. Sancak, S. Sasmaz and N. T. Okomusoglu, *Acta Crystallogr., Sect. E: Struct. Rep. Online*, 2005, **61**, o2699.

12 K. Avasthi, A. Ansari, R. Kant, P. R. Maulik, K. Ravikumar, P. Chattopadhyay and N. D. Adhikary, *CrystEngComm*, 2011, **13**, 2039.

13 F. Vogtle *Cyclophane Chemistry: Synthesis, Structures, and Reactions*; J. Wiley: Chichester, New York, 1993.

14 M. Nishio, *CrystEngComm*, 2004, **6**, 130.

15 P. R. Maulik, K. Avasthi, S. Sharkel, T. Chandra, D. S. Rawat, B. Logsdon and R. A. Jacobson, *Acta Crystallogr., Sect. C: Cryst. Struct. Commun.*, 2000, **56**, 1361.

16 (*a*) M. Egli and S. Sharkhel, *Acc. Chem. Res.*, 2007, **40**, 197; (*b*) A. Jain, C. S. Purohit, S. Verma and R. Sankararamakrishnan, *J. Phys. Chem. B*, 2007, **111**, 8680; (*c*) C.-Q. Wan, X.-D. Chen and T. C. W. Mak, *CrystEngComm*, 2008, **10**, 475.

17 G. R. Desiraju, T. Steiner *The Weak Hydrogen Bond*, Oxford University Press, Oxford, 1999.

18 A. N. M. M Rahman, R. Bishop, D. C. Craig and M. L. Scudder, *CrystEngComm*, 2002, **4**, 510.

From: Editor <editor@cbijournal.com>
Sent: Mon, 03 Sep 2012 10:53:00
To: <kavasthi@rediffmail.com>
Subject: CBI-1506-2012-162-Acceptance letter

CBI-1506-2012-162

Dear Dr. **Kamlakar Avasthi**

I am pleased to confirm that your paper entitled “**An overview of arene–aren interactions and application of uni-molecular models for their understanding**” has been accepted for publication in to Chemistry& Biology Interface.

Thanking you

ISSN: 2249 –4820

Chemistry & Biology Interface, 2012, xx, xx, xxx-xxx

Chemistry & Biology Interface

An official Journal of ISCB, Journal homepage; www.cbijournal.com

Review Paper

An overview of arene–arene interactions and application of uni-molecular models for their understanding[†]

Kamlakar Avasthi* and Amar Kumar

Medicinal and Process Chemistry Division, CSIR-Central Drug Research Institute, Lucknow, 226001, India

Keywords: Arene interactions, intramolecular π–π interactions, flexible molecular models, propylene linker, molecular recognition and supramolecular chemistry

Abstract: Interactions involving arene moieties are ubiquitous in nature and play an important role in variety of processes such as molecular recognition, crystal engineering, drug-receptor interactions, drug development etc. Understanding the nature of this weak but important noncovalent interaction will not only help us to get an insight of working of bio-macromolecules like DNA and proteins, but also help us to understand functioning of drug molecules inside the body since a majority of drug molecules contain one or another arene moiety. In addition to these it will also help in the development of new technologies such as organic semiconducting materials. One major problem in the understanding of these weak interactions is that these are easily overwhelmed by the presence of other much stronger interactions such as classical hydrogen bonding (involving two hetero atoms) etc. which makes it very difficult to decipher their exact contribution. Therefore, to overcome this problem several molecular models have been developed in the literature where these interactions can be studied in simpler and more controlled environment usually in the absence of stronger noncovalent interactions. The purpose of this review is to present the reader an overview of arene interactions and to focus on the different strategies used to develop new models for studying arene interactions especially the uni-molecular flexible models. Proper understanding of these interaction should be of immense value to chemist, medicinal chemist, biologist and supramolecular chemist and to all those interested in interface areas of chemistry and biology.

1. Introduction

Atoms and molecules can interact together leading to the formation of another molecule, by covalent interactions, or a molecular cluster, by noncovalent interactions. A covalent bond is formed when partially occupied orbitals of the interacting atoms overlap and a pair of electrons are shared by these atoms. Covalent bonds are shorter than 2 Å. In case of noncovalent interactions no such sharing of electrons takes place and these interactions act at distances of several angstroms. Noncovalent interactions were first recognized by J. D. van der Waals in the nineteenth century (1). Since then it has now been recognized that noncovalent interactions are involved in a vast number of

---

Corresponding Authors* E-mail: kavasthi@rediffmail.com

[†] CDRI communication no. 8312

phenomena related to the whole realm of molecular and macromolecular science such as molecular recognition, drug receptor interactions, solvent effect in reactions and the ability of geckos to climb rapidly up smooth vertical surfaces, even flat glass (2). Weak noncovalent interactions like stacking interactions (arene/ arene-arene/ π–π interactions) unlike their conventional counterparts (e.g. classical hydrogen bonding which are well characterized) or other un-conventional counterparts where H is attached to C atom instead of N/O or S atoms, are not well understood. Due to their weak nature they are usually difficult to observe in presence of stronger forces such as classical hydrogen bonding (involving two hetero atoms like O/N/S) and thus they are difficult to study both theoretically and experimentally (2,3). These forces often work together and their collective effect brings a profound change in molecular structure (conformation) as well as in supramolecular structure. In nature, where functions of bio-macromolecules like proteins, enzymes, DNA, etc., which are directly related to their structure, these weak forces play a very important role since easy formation as well as easy decomposition of molecular structures are required. These forces are sensitive to the environmental conditions and a slight change of conditions like temperature, pH etc., can bring about a significant change in conformation and hence function.

Interactions involving two or more aromatic residues are known as π–π interactions. These are among the most important but least understood of the noncovalent interactions. These interactions, though modest in energy, play a crucial role in such diverse areas as protein folding, base-to-base stacking in DNA/RNA, host-guest binding in supramolecular assemblies, crystal engineering, drug-receptor interactions and other molecular recognition processes. Since the seminal paper of Hunter on π–π interactions in 1990 (4) this area has seen increased activity and several reviews and books have appeared in the literature (5) which have highlighted different aspects of arene interactions. Recent studies have provided new insight into the driving forces, stability and selectivity of these interactions (6). The purpose of this review is to present a general overview of π–π interactions, its importance in biological and non-biological processes and to focus on the different strategies used to develop new models for studying arene interactions. The main emphasis is, however, on the uni-molecular (molecular) systems especially, where solid state structures are also known by X-ray crystallography, since bimolecular systems have been generally well covered in earlier reviews by Hunter (5h) and others (5d, 5f). C–H…π interactions involving at least one arene system will also be not discussed here as excellent reviews are available on this relatively well developed theme (5k, 5l). Main advantages of uni-molecular (molecular) systems are convenient synthesis, ^{1}H NMR and crystallographic studies. Another important advantage is that these models can be studied both at molecular and supramolecular level with ease. For example if linker between two arenes is positioned at proper place resulting system may be studied at molecular level by ^{1}H NMR spectroscopy. If a good crystal is available same study could easily be extended to supramolecular level. Intramolecular folding indicated by ^{1}H NMR spectroscopy, if strong, may show up in solid state by X-ray crystallography. Such two studies together on any system give formidable information about arene interactions compared to any other methodology. Once a good model is developed it can be easily applied to variety of other arene residues and substituents effect. Intramolecular arene interactions are especially important for understanding of DNA/RNA structures and protein folding. Once they are understood in depth it should be possible to apply them for drug development where they are essentially intermolecular.

2. The nature and geometry of arene–arene interaction.

The attraction between two aromatic residues present in the same or different molecules is known as arene–arene interaction or π–π interaction. The π–π interactions are weak in strength with the energy ranging from 0-50 kJ/mol (7). There are four types of π–π interaction geometries, face-to-face, edge-to-face, parallel displaced and Y-shaped (**Figure 1**) (4, 5b, 5c). Typical centroid to centroid distance for two interacting arenes in intermolecular mode is more than 3.6 Å (5h, and 5i). Another criterion of minimum distance for parallel offset arene interaction is that it is 0.4 Å longer than the sum of van der Waals radii of involved atoms (5f). Edge-to-face and parallel-displaced geometries are the most common geometries found in structural chemistry (8). Computational studies on benzene dimer showed that the edge-to-face and parallel-displaced geometries are nearly iso-energetic with binding energy of about 2 kcal/mol (9a, 9b). Face-to-face stacked geometry is commonly observed with donor–acceptor pairs. The benzene-perfluorobenzene interaction is an excellent example of this type of aromatic interaction and has been calculated to provide -15.5 kJ/mol stability (9c). In addition, there are also continuums of intermediate geometries (10a-c). Different computational techniques used for studying non-covalent interactions, including π–π interactions have been reviewed recently (9d).

There are four basic packing types for aromatic compounds reported in literature (**Figure 2**) (11). In simple herringbone structure, the nearest neighbours are non parallel. In sandwich-herringbone packing, the herringbone motif is made up of sandwich-like diads. In the third type, called β, the main interactions are between parallel translated molecules. The fourth type, called γ is characterised by 'graphitic' planes.

The nature of arene–arene interaction is still not well understood (5g, 8). Arene interactions have been proposed to consist of van der Waals, hydrophobic and electrostatic forces, however, contribution and magnitude of each of these components may vary from case to case and is a matter of many investigations. Hunter and Sanders (1990) proposed an electrostatic model to explain the strong geometrical requirements for interactions between aromatic molecules (4). They considered the σ-framework and the π-electrons separately and demonstrated that net favorable π–π interactions are actually the result of σ–π attractions that overcome π–repulsions. By using an idealized π–system, some general rules for predicting the geometry of favorable π–π interactions were derived. The electrostatic component has been proposed to arise from the interactions of the quadrupole moments of the aromatic rings. Though, benzene has no net dipole, it has an unequal distribution of charge, with greater electron-density on above and below the faces of the ring and reduced electron-density on the edge, which gives rise to the quadrupole moment. The edge-to-face and parallel-displaced geometries are stabilized due to electrostatic σ–π attraction while the face-to-face geometry is destabilized due to π–π repulsion (**Figure 3**). Generally, electron withdrawing groups in aromatic rings reinforce while electron donating groups weaken π–π interactions. Presence of heteroatom in aromatic ring also reinforces the π–π interactions.

For example, highly accurate quantum chemical computations revealed that benzene–pyridine and pyridine dimer bind more strongly than the benzene dimer in several configurations, and in contrast to the benzene dimer, parallel-displaced configurations can be significantly preferred over T-shaped configurations (12).

Recently, it has been found from the survey of crystallographic data stored in Cambridge Crystallographic Database that the stacking interactions in crystals of simple aromatic hydrocarbons become important only for molecules with more than three rings (13). Whereas for crystals of nitrogen substituted heterocyclic aromatic molecule, the stacking interactions become important for doubly substituted single ring molecules itself. Generally speaking, the stacking is reinforced with the increasing number of nitrogen in the ring (13a, 13b). Substitution of the hydrogen atom of an aromatic hydrocarbon by an electron withdrawing atom like F, Cl etc. or an electron withdrawing group like NO_2 reinforces the stacking interactions (13a). In a recent article (2011) however, such view of substituents effect on stacking interactions has been challenged by Wheeler (6). According to him the substituents effect can be better described as arising from local, direct interactions of the substituent with the proximal vertex of the other ring. Thus substituent effects in stacking interactions are additive, regardless of whether the substituents are on the same or opposite rings. Moreover, according to him, substituents effect are also insensitive to the introduction of heteroatom on distant parts of either stacked ring. Apparently all this refers to intermolecular interactions.

3. Importance of arene–arene interactions

3.1 Arene–arene interactions in biological systems

Arene–arene interactions are ubiquitous in nature. They are believed to provide stability to duplex DNA (14), they have been proposed to contribute to the unique properties of thermophilic proteins (15), they may play a role in aggregation of amyloid β in Alzheimer's disease (16), and they are common motifs in bio-molecular recognition.

3.1.1 Stabilization of DNA structure

DNA is a polynucleotide. The nucleotides of DNA are made from purine or pyrimidine rings (aromatic nitrogenous bases). Within the DNA molecule, the aromatic rings are lying nearly perpendicular to the length of the DNA strand (**Figure 4**). The faces of these rings are arranged parallel to each other with the distance of 3.4 Å (B-DNA), allowing the two adjacent bases to participate in π–π interaction. Though a π–π interaction is much weaker than a covalent bond, the sum of all π–π interactions within the double-stranded DNA molecule creates a large net stabilizing energy (17).

3.1.2 Protein folding

Protein folding is a process by which a polypeptide folds into its characteristic and functional 3D-structure to from a random coil. The π–π interactions, in addition to hydrogen bond play important role in protein folding. Burley and Petsko through a X-ray crystallographic study involving 34 high-resolution protein structures, analyzed the frequency of aromatic pairs and their interaction geometry (distance and dihedral angle) and concluded that around 60 % of aromatic side chains of phenylalanine, tyrosine, and tryptophan were involved in arene interactions (18). Aromatic rings separated by distances ranging from 4.5 to 7 Å and dihedral angles near 90° were found to be the most common. Pair-wise non bonded potential energy calculations indicated that 54 % of the aromatic interactions are attractive by 1-2 kcal/ mol. McGaughey, *et al.* extended the analysis to a larger sample of proteins and suggested that the parallel-displaced geometry was a preferred orientation (19). Remarkably, none of these two studies described the face-to-face geometry.

In another study of a larger database of 52 proteins, Hunter, *et al.* examined the orientational preferences of phenylalanine side chains in proteins using crystallographically derived atomic coordinates (20). They observed that these interacting pairs are found in a wide range of T-shaped (edge-to-face) and parallel-displaced (offset-stacked) arrangements, but they are scattered over a wide variety of conformational space with no strongly preferred single orientation.

Aromatic-aromatic interactions between phenylalanine side chains in peptides have been probed by the structure determination in crystals of three peptides: Boc-Val-Ala-Phe-Aib- Val-Ala-Phe-Aib-OMe, (I); Boc-Val-Ala-Phe-Aib-Val-Ala-Phe-Aib-Val-Ala-Phe-Aib-OMe, (II); Boc-Aib-Ala-Phe-Aib-Phe-Ala-Val-Aib-OMe, (III) (21). X-ray diffraction studies reveal that all three peptides adopt helical conformations in the solid state with the Phe side chains projecting outward. Inter-helix association in the crystals is promoted by Phe-Phe interactions. A total of 15 unique aromatic pairs have been characterized in the three independent crystal structures. The distances between the centroids of aromatic pair ranges from 5.11 to 6.86 Å, while the distance of closest approach of ring carbon atoms ranges from 3.27 to 4.59 Å. T-shaped and parallel-displaced arrangements of aromatic pairs were observed, in addition to several examples of inclined arrangements.

Aromatic π–π interactions not only determine biological structures but also modulate the physical properties of residues at enzyme active sites. In CuII-containing redox metalloproteins, the stacking of a CuII-coordinated His imidazole with a Phe side chain in the second coordination sphere affects the properties of the imidazole ring, such as its pKa value, the reduction potential E_m of the metal center, and the electron-transfer (ET) properties of the protein (22). Intramolecular stacking between a phenyl ring and the pyridine ring of a nicotinamide derivative increases the basicity of the pyridine N atom by about 0.5 pKa units (23).

Amyloids are extracellular or intracellular proteinaceous deposits exhibiting cross β-sheet structure. The amyloid formation leads to several neurodegenerative diseases like Alzheimer’s disease, Parkinson’s disease etc. The mechanism of amyloid formation is not fully understood. Analyses of a variety of short functional fragments from unrelated amyloid-forming proteins, a remarkable occurrence of aromatic residues was observed. The finding of aromatic residues in a diverse fragment raised the possibility that π–π interactions might play a significant role in the molecular recognition and self-assembly processes that lead to amyloid formation (16).

The X-ray structure of a 12-mer peptide having polypeptide sequence KFFEAAAKKFFE revealed that the polypeptides formed anti-parallel β-sheets in a cross-β arrangement. The anti-parallel β-sheets were zipped together by means of π–π interactions between adjacent phenylalanine rings and salt-bridges between charge pairs (glutamic acid–lysine), thus controlling and stabilizing the structure (**Figure 5**). These interactions are likely to be important in the formation and stability of other amyloid fibrils (24a). Bradford *et al.* in 2008 reported amyloid-like behavior of amphiphilic foldamers in aqueous solution (24b). These amphiphilic foldamers exhibited spectral characteristics consistent with folding in the pleated, stacked geometry characteristic of foldamers.

3.2 Arene-arene interactions in structure based drug design

The drug design based on knowledge of the three dimensional structure of the biological target (receptor) obtained through methods such as X-ray crystallography or NMR spectroscopy is known as structure-based drug design (or direct drug design). Most of the drugs produce their effect only after binding with its receptor. Most of the receptors are proteins but sometimes it may be a nucleic acid (particularly DNA). A drug generally, binds to its receptor through non-covalent interactions. The π–π interaction, in addition to H-bonding, is one of the most important non-covalent interactions involved in binding of drug with receptor as majority of the drugs are aromatic and the concentration of aromatic amino acid residue is particularly high in the cavity of receptor. Thus, proper understanding of π–π interaction is needed for structure based drug design (5a, 5g). Aricept (E2020, **1**) is a drug developed to treat symptoms of Alzheimer's disease. The X-ray crystallographic analysis of the complex of Aricept (E2020) with the enzyme acetyl cholinesterase revealed π–π, OH…π, and cation–π interactions as major forces that stabilize the association (**Figure 6**) (25).

DNA is a target for drug design to prevent cell replication. The π–π interaction plays a pivotal role in intercalation of drugs into DNA. The intercalation prevents DNA replication by inhibiting topoisomerase enzyme. The DNA intercalators contain aromatic residue which intercalate between DNA base pairs and the intercalator-DNA complex is stabilized by π–π interaction between aromatic residue of intercalator and nitrogenous bases of DNA. For example, daunomycin (**2**, **Figure 7**) is a chemotherapeutic of anthracycline family which has been used since 40 years for the treatment of specific type of leukemia (acute myeloid leukemia and acute lymphocytic leukemia). Structural study showed that it bound to the DNA preferentially via intercalation between GC base pairs in triplet sequences composed of two adjacent GC and CG followed by AT base pairs (**Figure 7**) (26a). DFT calculation showed that the complex gained 2/3 of its overall stability from π–π stacking interactions (26b).

The anti cancer drug 1843U89 (**3**) binds the active site of thymidylatesynthase and inhibits the transformation of dUMP to dTMP which is essential for the production of DNA. X-Ray structure of ternary complex revealed that the drug interacted with active site and dUMP through π–π interactions (**Figure 8**) (27).

3.3 Arene–arene interactions in organic synthesis

Arene interactions can play a significant role in organic synthesis (28). These interactions have been proposed to influence the yield and/or selectivity of different reaction types: intra- and intermolecular photochemical reactions (29), allylic oxidations (30), ruthenium-catalyzed transfer hydrogenations

(31), titanium-catalyzed oxidations of sulfides (32) and others (33).

Asymmetric di-hydroxylation of styrene (**4**) with optically active diamine (**5**) gave corresponding *R* diol (**6**) in 83% yield and 96% ee (**Figure 9**) (34). The reason for enantioselectivity was favorable π–π interaction between the substrate and naphthyl group; exposing the *si* face to hydroxylation and shielding the *re* face for the attack.

McIntosh *et al.* found that the benzylation of naphthyl cyclohexane (**8**) gave corresponding benzylated (**9**) product with >98% de. The de was attributed to the π–π interactions which in turn established an anti-gauche orientation for the enolate dianion (**Figure 10**) (35).

Metal free Friedel-Crafts alkylation of substituted pyrrole (**10**) with cinnamaldehyde (**11**) in the presence of imidazolidinone catalyst (**12**) gave alkylated product **13 (Figure 11**) in 97% ee. It was suggested that π–shielding of the cinnamaldehyde derived iminium ion (**14**) contributed to facial selectivity (36).

The *exo*/*endo* ratio in epoxidation of compound **15** (**Figure 12**) was significantly affected by the nature of the substituent present in phenyl ring. The proportion of *endo* product (**17**) increased with the increasing electron withdrawing tendency of the substituent. This result was rationalized by considering that the transition state (**18**) for *endo* product was stabilized by π–π interaction between phenyl ring of m-CPBA and substrate, and the stability of the transition state (**18**) was further enhanced by increasing electron withdrawing substituents (37).

In asymmetric allylation of aromatic and heteroaromatic aldehydes (**19**) reaction rates were enhanced and enantioselectivity were observed for electron-deficient benzaldehydes, in comparison to phenyl or electron-donor-substituted aldehydes, when performing the reaction with a methoxynaphthalene bearing isoquinoline N-oxide catalyst, **21** (38). This suggests for a role of arene–arene interactions between the reacting aldehyde and the catalyst. Additionally, the loss of selectivity when exchanging the solvent from dichloromethane to acetonitrile supports the role of aromatic interactions in the transformation. Enantioselectivity was further enhanced using an electron-rich trimethoxyphenyl N-oxide catalyst (**Figure 13a**).

Arene–arene interactions have also been proposed to influence the stereo chemical outcome in the synthesis of aromatic propargylamines (**27**, **Figure 13b**) (39). A chiral CuI complex with a pyridine bis(oxazoline) ligand (**26**) was found to catalyze the reaction of aromatic aldehydes (**23**) with amines (**24**) and alkynes (**25**) to give propargylamines with high yield and enantio-selectivity. In the postulated transition state, the ligand complexes the substrate in a manner which enables two edge-to-face and one aromatic stacking interaction, thus blocking one face from the attack of the copper acetylide.

4. Models used for studying arene–arene interactions.

Due to the weak nature of aromatic interactions it is very difficult to study these types of interactions both experimentally and theoretically. In biological systems where other stronger interactions like classical hydrogen bonding coexists with these weak interactions it is not possible to study the role played by these interactions. Thus, small molecule model systems have been developed to study arene–arene interactions in simpler and more controlled environments. This has been documented in several reviews (5a, 40). The model systems are classified as either bi-molecular or uni-molecular systems, where the arene interactions are inter- or intramolecular.

4.1 Bimolecular model systems.

In these models, in order to study interactions involving two aromatic rings, a variety of structures have been designed such as cyclophanes (40, 41), molecular clefts (42), molecular tweezers (43-47), molecular clips (48) etc. which acts as hosts to different aromatic guests. In addition to these structures simple spacers have also been used connecting two aromatic residues to act as molecular tweezers for complexing aromatic chromophores. For example bisfunctional derivatives **28** (**Figure 14**) with an acetylenic linker based on caffeine (or 7-methyl theophylline) showed an increase in association constant relative to simple caffeine derivatives when complexed with planar aromatic guests such as 2,6-dihydroxy-benzoate and 1,3-dihydroxy-2-naphthoate (43).

These model systems have proven to be useful method of investigating the nature and significance of aromatic interactions as molecular recognition elements in biological and non-biological systems. As stated earlier such models (bimolecular) are well covered in Hunter’s (5d) and other reviews (5e, 5h) and will not be discussed further. It is mentioned here due to its historical importance and features like flexibility in linker and a bicyclic arene core which is related to purine/theophylline or caffeine molecules of significant biological importance and many uni-molecular models which are discussed in next section are based on such arenes.

4.2 Uni-molecular/molecular model systems.

These models have both the interacting arene residues in the same molecule. These systems can, in principle, provide better control over the arene–arene geometry and can be studied in a wide range of solvent environment. Survey of the literature shows that various type of molecular models with varying degree of flexibility have been developed for the study of intramolecular π–π interactions. In this review we have tried to classify them on the basis of number of atoms between the arene moieties.

4.2.1 Models in which the two arene moieties are separated by three atom *propylene* linker.

The *trimethylene* linker and other linkers related to it in which the two arene moieties are separated by three atoms are perhaps the most common linkers used in the study of arene interactions. Here in this section and its subsection we try to present some examples from the literature where this linker is used as such or modified to suit the study of intramolecular π–π interactions. We have not strictly restricted ourselves to *trimethylene* linkers only as in some of these studies other linkers (e.g. *ethylene*, *butylene* etc.) are also used for the sake of completeness of the studies.

4.2.1.1 Fully flexible models in which the two arene moieties are separated by three atoms.

4.2.1.1.1 Leonard/propylene linker models.

One of the earliest attempts to study intramolecular arene-arene interactions in a systematic way was reported by Browne *et al.* in 1968. Browne *et al.* pioneered the use of *polymethylene* linker, especially a *trimethylene* linker for studying stacking interactions among nucleic acid bases. (**29**, **Figure 15**) (49a). One of the major advantages of using flexible models based on *polymethylene* linker is that flexible systems can relax into the optimum geometry for aromatic π–π interaction and therefore provide a better opportunity to characterize the geometrical preferences caused by these interactions.

Nucleic acid bases containing purines and pyrimidines are stacked one above the other in nucleic acids with a distance of about 3.4 Å between adjacent bases. The use of *trimethylene* linker is based on the fact that it gives a desired distance of around 3.4 Å if two aromatic systems are stacked when connected by it. This linker at the same time does not dictate stacking, as in the absence of stacking interactions the molecule may remain open. They synthesized a series of twelve di-nucleotide analogs in which the bases are connected by a *trimethylene* chain, B-$(CH_2)_3$-B′, where B and B′ are 9-substituted adenine or guanine or 1-substituted cytosine, thymine or uracil residues (**Figure 16**). These compounds were studied optically at concentrations low enough to preclude formation of intermolecular complexes so that the perturbations associated with the 1:1 interaction of a pair of bases could be characterized, namely by UV spectra in aqueous solution at room temperature and by emission spectra in 1:1 ethylene-glycol-water glass in the vicinity of 77° K. In the series of B-$(CH_2)_3$-B′ the order of interaction in neutral aqueous solution is purine-purine > purine-pyrimidine > pyrimidine-pyrimidine as judged by hypochromism (decrease in integrated UV absorption intensity of B-C_n-B′ compared with equimolar B-$(CH_2)_2$-CH_3 and B′-$(CH_2)_2$-CH_3). The length of *polymethylene* chain was also changed to C_2 and C_6. In a series of 9,9′-polymethylene-bis(adenines) the order of interaction deduced from hypochromism and emission studies was n = 3 > 2 & 6. Reduced interaction at n = 2 reflected the impossibility of this molecule assuming folded, parallel-plane conformation which would allow maximal interaction as in Ad-C_3-Ad. An entropy effect was probably responsible for decreased interaction in the n = 6 compound relative to n = 3 (49a). The orientation effect studies were done by Leonard and Ito by synthesizing six different trimethylene-bis(adenine) isomers having different positions of attachment to the terminal adenines and therefore having differently oriented ring- axis permissible in their stacked conformations, in order to determine stacking interactions between two parallel adenine rings oriented at different axis angles toward each other (**Figure 17**) (49b). The percent hypochromism ‘*H*’ for the long wavelength UV absorption band for each of these compounds has been determined by comparison of the UV spectrum of trimethylene-bis-adenine in aqueous solution with the composite spectrum of the two half molecules, the appropriate propyl-adenines. The ‘*% H*’ follows a dependence upon the folded conformations available to the individual trimethylene-bis(adenines). Later on, Leonard (1979) reviewed such work on *trimethylene* bridged flexible diaryl compounds showing stacking interactions in solution, however, no X-ray structure of any compound with one *trimethylene* linker was mentioned (49c).

4.2.1.1.2 Miscellaneous *trimethylene* linker models.

Bis(theophyllin-8-yl)propane (**33**, **Figure 18**) is normally considered as the first *trimethylene* linker compound to show intramolecular folding in solid state though with extensive hydrogen bonding (50). Here it is important to mention that this compound belongs to biologically important xanthine class which is well known for face-to-face intermolecular interaction in solid by X-ray crystallography (51). It is important to mention that arene residue of this compound is similar to one mentioned in bimolecular model **28**.

Bis-thymine (**34**, **Figure 18**) is another compound which shows intramolecular folding in solid by X-ray structure though again with extensive H-bonding (52). Compound **35** (**Figure 18**) shows intramolecular interactions by UV studies (53), however, **35** (**Figure 18**) and its methyl iodide salt failed to show any intramolecular folding when studied by X-ray crystallography (54, 55). Avasthi *et al.* reported X-ray crystal structure of 1,3-bis(8-chlorotheophyllin-7-yl)propane (**36**) which is closely related to **33**, as far as arene core and linker are concerned, but does not have ionizable protons, without any intramolecular folding (**Figure 19**) (56). Moreover, **36** has no disorder in the *propylene* linker unlike **33** which has disorder in its linker. It is important to mention that in compounds **32**, **34** and **36** the *propylene* linker is between two N atoms while in **33** it is positioned between two C atoms and in **35** it is between one N and one C atom.

It is interesting to mention that finally, after about 30 years of Browne's study, compound **32** (**Figure 20**) was shown to have a folded conformation in solid state by X-ray crystallography (57).

4.2.1.1.3 *Propylene/Leonard* linker models based on pyrazolo[3,4-*d*]pyrimidine core.

Since 1995, research group at CDRI, Lucknow has been working on pyrazolo[3,4-*d*]pyrimidine (**PP**) core based poly-methylene, especially *trimethylene* linker compounds, in a systematic way, for investigating the conformation directing role of arene–arene interactions. **PP** system (**37**), which is isomeric with biologically important purine system (**38**) of DNA, the best known example of stacking interaction, was selected due to our experience in its chemistry and ease of handling (different activity of two methanesulfanyl groups, solubility, crystallization, isolation and characterization of isomeric products etc.) (58a-d). The first question we asked if **PP** core based *trimethylene* linker compound (**39**) can show intramolecular folding due to intramolecular π–π interaction in solution by ^{1}H NMR and second if yes, is it strong enough to survive in solid state? Thus, in 1995 we reported, for the first time, the use of **PP** ring system (**37**) which is isomeric with biologically significant purine (**38**) system for studying aromatic π–π interaction. All the three expected isomeric dimers (**39-41**, **Figure 21**) were easily isolated by column chromatography and characterized (59a). Formation of three isomeric compounds raised another important question of the effect of position of linker on intramolecular π–π interaction. Interestingly, only one compound (**39**) formed in about 50 % showed unusual up-field shift for 6-methanesulfanyl protons in its ^{1}H NMR indicating intramolecular *folding* (59a). The most important feature of these new fully flexible models is that they do not have any strong ionizing groups such as OH, NH, NH_2, SH etc., capable of forming classical H-bonding. This strategy was devised so that contribution of weaker arene–arene interactions towards conformation control, if any, could be determined without interference of stronger conventional H-bonding.

This unusual *folding* was indeed due to intramolecular π–π interaction was easily confirmed by X-ray crystallographic studies (59b). The X-ray crystal structure revealed that **39** was *folded* at the centre of the *trimethylene* bridge to form an unusual *U-motif* and the two **PP** rings were nearly planar with an angle between the least-squares planes of 13.2° (ORTEP diagram shown in **Figure 22**) (59b). The centroids of two partially overlapping six member pyrimidine rings are represented as X1A and X1B and the distance between two centroids X1A and X1B is 3.71 Å which confirms that the two aromatic moieties are stacked due to intramolecular π–π interaction. The distance between two N atoms bearing linker is 3.28 Å which is much less than 4.9 Å seen in fully extended theophylline *trimethylene* linker compound (**36**). Vogtle refers to singly linked molecules that adopt π–stacked conformations as ''*protophanes*'' (59c).

Robustness of the unusual *U-motif* formed due to intramolecular stacking in **39** was further confirmed in over a dozen compounds having various substituents at 4 and 6 positions (60). For instance, intramolecular stacking between the two pyrazolo[3,4-*d*]pyrimidine moieties remain intact when 4-methylsulfanyl groups are replaced by bulky isopropxy groups (**42**, **Fig 23**), thus showing tolerance for bulkiness of the substituents (60c).

Surprisingly, the symmetrical cyano compound (**43**) is devoid of intramolecular π–π interactions and shows open conformation (**Figure 24**) (60f). This is surprising because literature studies indicate that electron withdrawing substituents increase the propensity of intramolecular stacking interactions, however, more work is needed before any conclusion can be drawn.

Surprisingly, positional isomer **40** isolated as co-product with **39**, did not show intramolecular stacking either by ^{1}H NMR data analysis in solution (59), or by X-ray crystallography (**Figure 25**) in solid (61). Thus, indicating that proper positioning of the *trimethylene* linker to achieve proper orientation of two involved arenes was crucial and mere presence of a *trimethylene* linker between two arene systems is not enough to show intramolecular stacking. Careful examination of structure of **40** revealed presence of weak intramolecular CH…N interaction (61).

Avasthi *et al.* later on reported synthesis (62) and X-ray structures of **45** (63) derived from **39** via intermediate **44** (**Figure 26**). Proton NMR data analysis of this compound like earlier compound **39** indicated intramolecular stacking (62). Formation of the unusual *U-motif* due to intramolecular stacking was also confirmed by X-ray crystallography.

Significance of *trimethylene* linker for facilitating intramolecular stacking, from crystal engineering point of view was further highlighted by the fact that **46**, a higher homolog of **45**, did not show any intramolecular stacking by ^{1}H NMR data analysis (64) and in fact an *extended* conformation was observed by X-ray crystallography (**Figure 27**).

To probe the generality of **PP** core to study arene interactions, studies were undertaken on dissymmetric **PP** core based polymethylene linker compounds. Thus, compound **47** showed *folded* conformation in solution as well as in solid state due to π–π interaction while its positional isomer **48** was open in solution (65).

Since use of the *propylene* linker for studying intramolecular stacking interactions between nucleic acid bases was pioneered by Leonard in 1968 and our success in utilizing it successfully in many compounds with **PP** system has prompted us to propose the name *Leonard* linker for *propylene* linker in 2005 (60c). Importance of the *propylene* linker compounds containing 4 bonds between two N atoms of bases can be easily appreciated by realizing that two adjacent bases in DNA with a noncovalent separation of about 3.4 Å involves 11 bonds of covalent linker (involving sugar and phosphate).

Recently, ^{1}H NMR, CD and X-ray crystallographic study on related **PP** core based *polymethylene* compounds (**49-50**, **Figure 29**) has been reported by another research group. These compounds were folded in solution by ^{1}H NMR and CD studies, however, X-ray crystallography of one *propylene* linker compound, **49a** showed an *open* conformation (**Figure 41**) (66). Interestingly, reasons for the absence of intramolecular stacking in **49a** were not discussed. It is important to mention that compound **49a** does not have two methanesulfanyl groups at 6-position present in our **PP** based compound **39** (**Figure 21**).

Key data of some important compounds in *folded*/*open* conformation are shown in **Table 1**. This also gives an idea as how conformation changes in response to different substituents. The first compound **36** is based on purine system, which is isomeric with **PP** system, and is used as reference compound as it is in open conformation and shows maximum distance between two N atoms bearing *propylene* linker. The **Table 1** has three *propylene* linker compounds based on **PP** core of which two are symmetrical and one is dissymmetrical. Important thing about these three compounds is the fact that distance between two N atoms connecting linker is < 4 Å which is much less than 4.91 Å of reference compound **36**.

Perusal of data in **Table 1** reveals interesting findings which are listed below.

1. Intramolecular distance between two centroids of six member pyrimidine rings of folded compounds (**39**, **42**, **45** and **47**) varies in the range of 3.69-4.10 Å.
2. The distance between two N atoms bearing *propylene* linker in *folded* compounds (**39**, **42**, **45** and **47**) varies in narrow range of 3.24-3.50 Å as compared to 4.91 Å in fully *extended*/*open* compound **36**.
3. The angle between the least square planes of arenes in *folded* compounds (**39**, **42**, **45** and **47**) is fairly constant (11.62-14.99).
4. The angle at central C of *propylene* linker also remains fairly constant in both *folded* and *open* compounds indicating absence of any strain due to π–π interaction.
5. The dramatic effect of the position of linker is demonstrated by unique pair of two isomeric compounds (**39** and **40**), symmetrical **39** is *folded* while dissymmetrical **40** is *open*.
6. Dramatic effect due to displacement of two methanesulfanyl groups at 4-position in *folded* **39** by cyano groups results in the formation of new compound **43** which is *open* due to absence of intramolecular arene interaction. Interestingly, both compounds (**39** and **43**) are *folded* in solution by ^{1}H NMR analysis.
7. Finally, all *folded* compounds show similar conformation in other words unusual *U-motif* described earlier is quite robust.

4.2.1.1.4 *Butylidene* linker model with *three* atoms in linker.

In this section, now for the sake of continuity with our **PP** core based *propylene* linker work, we will describe our work on *butylidene* linker. Main similarity between these two linkers is that both have three atoms in linker. This linker also like *propylene* linker does not dictate intramolecular folding/stacking, thus in absence of intramolecular arene interaction molecule may remain in extended conformation. During the course of our earlier work it was realized that in many cases *propylene* linker compounds with different arene systems (e.g. purine) showing intramolecular folding by ^{1}H NMR in solution failed to give X-ray diffraction quality crystals. This forced us to look for another linker closely related to *propylene* linker and *butylidene* linker appeared to be a reasonable choice. Enforcing rigidity by putting one extra methylene unit at the central carbon of *propylene* linker reduces overall flexibility of *butylidene* linker. This decrease in total number of conformations (as compared to the fully flexible *propylene* linker) will hopefully facilitate the crystallization process. Thus, the first compound synthesized with *butylidene* linker was *butylidene* linker analog (**51**, **Figure 30**) of the first *propylene* linker dimer (**39**) of **PP**. The solid state conformation of the new *butylidene* linker compound **50** shows that important features such as orientation and distances between the two rings are quite comparable with that of compound **39** (67). Most significant feature of this linker is the demonstration of folded conformation for isomeric purine *butylidene* linker compound (**52**). Our earlier efforts in isolating corresponding purine compound with *propylene* linker were not successful (68).

In conclusion, the scope of **PP** core for studying arene interactions in flexible linker compounds has been considerably increased by providing an alternative for truly flexible *propylene* linker with less mobile *butylidene* linker.

4.2.1.1.5 Itahara model.

Similar *polymethylene* linkers have been utilized by Itahara to investigate stacking interactions between various purine, pyrimidine and xanthine bases in solution by ^{1}H NMR. Some of the systems (**53-57**, **Figure 31**) studied by Itahara are shown below (69, 70, 71). The N^6-methylation was found to increase the population of intermolecular aggregates in the buffer solution at pD 7.0 and had an additive effect on aggregation which was interpreted due to hydrophobic effect of the N^6-methyl groups. The aggregation of **53a** and **53b (Figure 31**) was found to depend on the length of the *polymethylene* chains (71). A relationship between the chemical shifts of adenine and xanthine ring protons of 7-[-(6-aminopurin-9-yl)alkyl]-1,3-dimethylxanthines (**56**) and the number of carbons (n = 2-10) in their *polymethylene* chains has been compared with that of 1-[-(6-aminopurin-9-yl)alkyl]-3,7-dimethylxanthines (**57**) in the buffer solutions at pD 7.0, 1.0 and 13.0 and in organic solvents. The relationship of **56** is clearly distinct from that of **57**. The concentration dependence and the effects of temperature on the chemical shifts of **56** and **57** have also been investigated. While the upfield shifts of the ring protons of **56** and **57** in the buffer solutions at pD 7.0 and 13.0 are explained in terms of stacking interactions between adenine and xanthine rings.

4.2.1.1.6 Gellman model.

Hydrophobic effect has a significant influence on aromatic interactions since water molecules prefer to interact among themselves rather than with aromatic surfaces. Newcomb and Gellman carried out a series of experiments to investigate this effect for two covalently tethered aromatic groups. A comparison of the stacking tendencies of phenyl, naphthyl and heterocyclic (adenine) rings in aqueous solution was carried out using ^{1}H NMR spectroscopy to study the conformational properties of carboxylate derivatives **58-65** (**Figure 32**) (72). The results are most consistent with the alignment of partial positive and negative charges on neighboring groups as the main force influencing the stacking interactions.

Naphthyl units connected by a flexible linker were prepared to further probe hydrophobic collapse. The three atom linker previously used forced a near parallel arrangement, but the four atom linker in **64** allowed different approaches of the aromatic moieties. An X-ray crystal structure of **64** showed an edge-to-face arrangement of the naphthyl rings and ^{1}H NMR experiments showed that the naphthyl rings are in close proximity in aqueous solution. The chemical shift differences between **64** and **65** in benzene were very similar to those in water, which suggests that the hydrophobic effect have little influence on the folding of this molecule. An excellent review has appeared recently, where along with this some other models are discussed in detail (72c).

4.2.1.1.7 Kollman model.

To understand the driving forces of aromatic stacking interactions in water, Pang *et al.* (1999) performed conformational searches, molecular dynamics simulations, potential of mean force (PMF) and free energy perturbation (FEP) calculations, syntheses and ^{1}H NMR studies on sodium 2,2-bis(indol-1-yl-methyl)acetate (**66**) (73). The conformational searches on **66** revealed that the *isobutyric acid* linker allowed the molecule to adopt the tilted T-shaped stacked, off-center stacked, face-to-face stacked, and non-stacked conformations in a vacuum (**Figure 33**). The PMF and FEP calculations suggested that the most thermodynamically stable conformers in water were the tilted T-shaped stacked and non-stacked conformers. The ^{1}H NMR result of **65** in D_2O and DMSO-d_6 at 22 °C revealed that both the tilted T-shaped stacked and nonstacked conformers were populated in D_2O and DMSO-d_6. Furthermore, population of the tilted T-shaped stacked conformation was greater in D_2O than in DMSO-d_6. These results, therefore, suggested that the hydrophobic effect played an important role in the stacking interaction of **66** in water. In this study it was concluded that indole was not a good system for studying intramolecular arene interaction.

4.2.1.2 Semi-rigid models in which the two arene moieties are separated by *three* atoms.

In addition to these flexible three carbon (C3) linkers other models having semi rigid scaffolds have been developed to study interactions involving aromatic rings in which the flexibility of linker has been curtailed which significantly decreases the total number of conformational structures thereby facilitating the two aromatic units to stay close to each other for a longer period of time. In this context, two models have been discussed i.e., the cyclohexane model and the *butylidene* model. The cyclohexane model developed by Williams *et al.*, has the *trimethylene* linker unit as a part of the cyclohexane ring.

4.2.1.2.1 Williams model based on cyclohexyl scaffold.

Williams *et al.* undertook a computational study of the substituted *cis*-1,3-diphenylcyclohexanes (**67a-c**) (**Figure 34**) to suggest novel experimental models for the investigation of arene–arene interactions

(74). Energy minima were located for diaxial conformers (a) in which aryl rings are coplanar and π–stacked and (b) in which aryl rings adopt an edge-to-face or intermediate conformation. The average distance (centre to centre) of 4.4 Å, outside the van der Waals contact distance of 3.4 Å and the minimum inter-ring distance of 3.5 Å was obtained for all diaxial conformers considered in this study. In all cases the results (a) showed good agreement with literature data on related experiments and (b) demonstrated the dominance of arene-arene electrostatic contributions to conformational energy over the negligible orbital mixing and charge transfer interactions.

4.2.1.3 Rigid models in which the two arene moieties are separated by *three* atoms of naphthyl scaffold.

In addition to these flexible and semi rigid scaffolds, some rigid scaffolds have also been developed to study interactions involving aromatic rings in which the trimethylene linker is a part of a rigid structure such as an aromatic ring. The following two model illustrates this point.

4.2.1.3.1 Cozzi model with mono cyclic arenes.

Cozzi *et al.* in 1992 developed 1,8-diaryl naphthalene based model **68** (**Figure 35a**) for studying the nature of arene–arene interaction (75a). Semi-empirical calculation showed that the phenyl rings were perpendicular to naphthalene. At room temperature all the compounds showed distinct signals in ^{1}H NMR for o/o′, m/m′ which was consistent with the restricted rotation of the phenyl groups. From the line shape analysis using different temperature NMR technique the barrier to rotation for the phenyl ring was determined. Barrier to rotation was found to increase with the increasing electron withdrawing tendency of the substituents. From this study they concluded that the nature of arene–arene interaction between two phenyl rings was electrostatic type and not charge-transfer type. The main drawback of this model was that the distance between point of attachment of two phenyl rings to naphthalene system was quite small (2.8 Å) that due to steric effect they have no option but to adopt a stacked conformation. To overcome this draw back the same group after 16 years synthesized 1,8-diaryl biphenylenes (**69** and **70**) in which the distance between two aryl rings was in the range of the distance required for arene interaction (**Figure 35b**). Barrier to rotation was found to increase with the increasing electron withdrawing tendency of the substituents in **69** while opposite result was found in **70** (75b).

4.2.1.3.2 Tumambac model bi- and tricyclic arenes.

Tumambac and Wolf have reported the preparation of highly congested 1,8-diacridylnaphthalene **71** for metal-ion-selective and enantioselective sensing using fluorescence spectroscopy (76). As a consequence of the bulkiness of the co-facial acridyl moieties, no sign of rotation about the chiral acridylnaphthalene axis of **71**, i.e., *syn*/*anti*-interconversion, has been observed even at very high temperature. Incorporation of significantly smaller substituents such as pyridyl or quinolyl rings into the peri-positions of naphthalene affords diheteroarylnaphthalenes **72** exhibiting a wide range of conformational stability.

4.2.2 Models in which the two arene moieties are separated by flexible linker of *four* atoms.

Chloroquine is a well known drug for treatment of malaria and its mode of action involves binding to the nucleic acids. It is believed that arene interaction between the aromatic system of chloroquine and the nucleotide bases plays an important role in this process. Several models involving quinoline nucleus for studying stacking interactions between the aminoquinoline ring of the antimalarial chloroquine and the purine bases have been synthesized by Bolte *et al*. (77) in which the quinoline linked to the purine base (adenine and guanine) by a trimethylene chain (**Fig 37**, **73-77**). It is reported in these studies that adenine and guanine exhibit equal affinity for the quinoline nucleus as reflected by very close hypochromism values observed for the two models at all temperatures studied. In another study Bolte *et al.* showed that when chloro is removed (**74**) or is substituted by bromo (**75**) the stacking propensity with the purine base decreases (77d). This indicates towards the special role of chloro substituent. Nucleic acid base thymine linked by a *trimethylene* chain have been shown to interact with proflavine face-to-face in dilute aqueous solution (**Fig. 37**, **78**) (78). PUVA therapy, a photochemotherapy employing psoralen and UVA, has been used for a long time in the treatment of a number of skin disorders, such as psoriases, vitiligo, mycosis fungoides, chronic leukemia, and so on. In this, formation of an intercalated complex between psoralens and DNA is an important step, which markedly affects the successive covalent photobinding to the macromolecule. In order to investigate these processes, some of synthetic models related to DNA-intercalating molecules were prepared. Decout *et al.* prepared a series of psoralen-O-$(CH_2)_3$-adenine (**79**, **Figure 38**) and 8-methoxy-psoralenadenine (**80**, **Figure 38**) and showed that *polymethylene* bridges allow intramolecular ring-ring stacking between the two aromatic units (79). The model **75** showed the highest value of hypochromism indicating most efficient ring-ring stacking between the two aromatic units linked by four atoms. Compound **80b** showed much stronger fluorescence than all other compounds **80a**, **80c-d** indicating that the complexes adopt different preferred geometries according to chain length. No X-ray crystallographic studies were reported on these compounds.

4.2.3 Models in which the two arene moieties are separated by semi rigid linker having *six*/*seven* atoms.

4.2.3.1 Model based on triptycene.

Gung *et al.* prepared a series of triptycene-derived compounds for studying arene–arene interactions in the parallel-displaced orientation (**Figure 39a** and **39b**) (80a). Here the two interacting arene moieties are essentially separated by six atoms of which three atoms are part of a special tetracyclic scaffold (triptycene) which brings the interacting arene moieties close to each other facilitating the arene interaction. The extent of arene–arene interaction was determined by measuring *syn*/*anti* ratio using low temperature ^{1}H NMR study. This study revealed that the interactions between the arenes bearing electron–donating groups (EDG) **81** (**Figure 39a**) were either negligible or slightly repulsive, while the interactions between arenes bearing electron-withdrawing groups (EWG) were attractive. Intermediate free energy values were obtained for those compounds bearing arenes with one EDG and one EWG. For studying the stacking interactions between a benzene ring and a heterocyclic ring (pyridine or pyrimidine) Gung *et al.* used a series of similar triptycene-derived scaffolds **82** (**Figure 39b**) (80b).

Compared to the corresponding control compounds where a benzene ring was in the position of the heterocycle, higher attractive interactions were observed as indicated by the higher *syn/anti* ratios. The greatest attractive interactions were observed between a pyrimidine ring and *N,N*-dimethylamino-benzene, consistent with a predominant donor–acceptor interaction.

4.2.3.2 Molecular balance model.

Carroll *et al.* developed molecular balance **83-85** (**Figure 40**) to study the face-to-face arene–arene interactions (81). In this model the two arene moieties are effectively separated by *seven* atoms. These *seven* atoms are part of a special scaffold which allows limited flexibility to the interacting arene moieties and thus allowing them to interact more favorably. Thus arene interactions could be observed for benzenoid compounds which normally are known to exist in open conformation in fully flexible polymethylene linkers (82). The balance adopted distinct *folded* and *unfolded* conformations due to restricted rotation about a C_{aryl}-N_{imide} bond. Molecular modeling studies predicted that the benzene ring of the phenyl ether arm was perfectly positioned in the *folded*-conformer to form an effective offset face-to-face interaction with the arene shelf and the phenyl ether arm could not adopt an edge-to-face geometry in the *folded*-conformer because it was held too closely. The strength of the face-to-face π–π interaction was assessed by measuring the ratio of *folded* to *unfolded* conformers by ^{1}H NMR. The measured *folded*/*unfolded* ratios of balances **83-85** in $CDCl_3$ showed a strong correlation between the size of the arene shelf, which is consistent with the presence of an arene–arene interaction. Balances **83** and **84** with the arene of larger surface area displayed higher degrees of folding with *folded/unfolded* ratios of 0.56 and 0.42 respectively. The smaller benzene shelf of balance **85** is too small to form π–π interactions with the phenyl arm and thus had a significantly lower *folded/unfolded* ratio of 0.11.

4.2.3.3 Model based on pyrene with flexible linkers of more than *seven* atoms.

Zachariasse *et al.* reported synthesis of a large series of α,ω-bis(2-pyrenyl-carboxy)alkanes (**86a-p**, **Figure 41**) (83). Here, the two interacting arene moieties are separated by *seven* or more atoms. These atoms form a part of a flexible chain. Evidence for intramolecular pyrene dimers was obtained by ^{1}H NMR spectra showing shielding of all the aromatic protons with respect to model; 2-substituted pyrene. The dimers (**86g-p**, **Figure 41**) showed a symmetrical sandwich structure, whereas, the dimers (**86a-f**, **Figure 41**) attributed geometry in which the pyrenyl moieties were shifted along their long axis. Intramolecular aromatic π–π stacking was also reported in closely related compound, **87 (Figure 41)** (84).

4.2.3.4 Model based on electron donor–acceptor concept with flexible linker of *seven* atoms

Herrandon *et al.* investigated intramolecular interactions between different aromatic groups in a series of di-esters consisting of two aromatic groups linked by a *2-methyl-1,3-propanedioxy* spacer by ^{1}H NMR study (**Figure 42**) (85). This spacer permitted *U-shaped* conformations which placed the two terminal aromatic groups close together, parallel in a face-to-face arrangement. For the symmetrical di-esters **88** and **89** neither the chemical shifts of the aromatic group protons nor the vicinal coupling constants measured in the spacer provided any evidence for a high fraction of *U-shaped* conformers. In both the cases, the conformational distribution of the spacer was similar to that found for **93**, indicating that the planar aromatic groups in **88** and **89** experienced no significant mutual attractive interactions.

In contrast, substantial up-field shifts were observed in the resonance frequencies of all aromatic protons in the anthracenyl and 3,5-dinitrophenyl groups of the unsymmetrical di-ester **90** relative to those for the aromatic protons of the respective monoesters **91**, **92** and symmetrical di-esters **88** and **89**. Analysis of the temperature dependence of the vicinal coupling constants indicated highly populated *gauche* states of the two central C-C bonds of the spacer chain, consistent with a total fraction of U-shaped conformers of about 80% at ambient temperature. From the analysis of NOE experiments dinitrophenyl ring in **90** was found to be centered almost directly above the central ring of the anthracenyl group with a distance of 3.1 Å between the central point of the dinitrophenyl ring and the anthracenyl plane, and an angle of about 20° between the para axes of the two aromatic groups. The stabilization of the *U-shaped* conformers in **90** was rationalized in terms of quadrupole interactions between the two aromatic groups. The quadrupole moments associated with the two aromatic groups in **90** had opposite sign, resulting in a significant attractive interaction when the groups were oriented face-to-face. For the symmetrical di-esters (**88** and **89**) the interacting aromatic groups had identical quadrupole moments and the interaction was repulsive in the face-to-face arrangement.

4.2.3.5 Chong model.

Recently, Chong *et al*. developed a molecular balance for studying face-to-face arene–arene interactions in solution and solid state (**Figure 43**) (86). The balance had a large central 1,4,5,8-naphthalene diimide surface that formed intramolecular arene–arene interactions with two pendent arms. The molecular balance could exist in *syn* and *anti* forms. In *syn* form only one arm was involved in stacking with one surface of 1,4,5,8-naphthalene diimide while in *anti* form both the arms were involved. *Syn* and *anti* forms were not readily inter-convertible in solution and their concentration can be determined by ^{1}H NMR. Thus, *anti/syn* ratio was taken as a criterion for measuring the strength of arene–arene interactions. *Anti/syn* ratio was found to increase with the increasing surface area of Ar-group, indicating that the strength of arene–arene interactions increased with the increasing surface area of the interacting aromatic groups.

4.2.4 *Ethylene* linker models.

After demonstrating the potential of **PP** core in *propylene* and *butylidene* linker models we decided to apply **PP** system to *ethylene* linker and to check if system is good enough to show *syn* conformation in *ethylene* linker models. In very recent communication, we showed that weak arene interactions are capable of controlling conformation even in dissymmetrical 1,2-diarylethanes in which one arene residue is based on **PP** core, both in solution and in the solid state. Thus, first *ethylene* linker compound (**98**) was prepared by the reaction of 1-bromoethyl-4,6-dimethylsulfanyl-pyrazolo[3,4-*d*]pyrimidine with commercial phthalazinone. The compound, **98** was isolated as only product and no O-alkylated product was obtained. ^{1}H NMR of the compound, **98** showed intramolecular *folding* which was also confirmed by X-ray crystallography (**Figure 44**) (87). It is important to mention that except presence of intramolecular π–π interaction there is no other intramolecular interaction like CH…π or S…arene interaction. The distance between centroids of two six member rings is 4.28 Å which is slightly more than uppermost value of the range (3.71-4.10 Å, **Table 1**) seen in *propylene* linker models. Furthermore, the distance between two N atoms bearing linker is 2.95 Å which is less than sum of the van der Waals radii of two involved N atoms.

5. Conclusion and future developments:

Present review gives an account of what has been done in the area of development of molecular models for better understanding of arene interaction during last two decades, highlighting again that nature of the arene interaction is indeed quite complex. The major problem is that of transferability i.e. understanding gained from one model cannot be easily applied to new model. While solution studies on different conformations (e.g. *folded*/*open*) by spectroscopic techniques give lot of information from molecular recognition point of view, solid state studies on different conformations (e.g. *folded*/*open*) give precise geometry and is important not only from molecular recognition point of view but must for crystal engineering point of view. Even though large amount of research has been done on arene interaction in last two decades our ability to use them effectively in a predictable way in a new situation remains unsatisfactory. Predictable use of arene interactions is highly desirable for molecular recognition, crystal engineering, drug-development and protein folding studies. Current limitations in understanding of arene interactions clearly shows that much more research needs to be done in future for their fruitful utilization in times to come. Development of more unbiased molecular models looks to be one promising area for future research. Size and electronic effects of different substituents on intramolecular interactions has both expected and un-expected outcome. When a substituent is not involved in strong intermolecular interaction its effect on intramolecular conformation is easy to predict, however, in other situations when substituent can get involved in strong intermolecular interactions, its effect on intramolecular conformation due to arene interaction becomes unpredictable. Since 1,2-diphenylethane, 1,3-diphenylpropane and 1,4-diphenylbutane are open in the solid state, in our opinion, the phenyl moiety is not a good system for studying intramolecular arene interactions in such unbiased flexible models (87). Similarly, models based on semi-rigid and rigid scaffolds may give somewhat biased information as compared to fully flexible *propylene* linker models. Comparison of the results on same arene core with *propylene*, *butylidene* and *ethylene* linker models, as exemplified in this review with **PP** core, may give valuable insights for better understanding of subtle effects of different substituents on the arene interactions. Our work with unbiased linkers also opens new avenue for conformational control due to arene interactions in flexible compounds having two heterocycles (same/different).

Acknowledgement:

KA is grateful to DST, New Delhi, India for financial support (grant nos. SP/S1/G-44/99 and SR/S1/OC-14/2010). AK is thankful to CSIR, New Delhi, India for SRF. KA is also thankful to P. R. Maulik, Molecular and Structural Biology Division, CSIR-Central Drug Research Institute, Lucknow, 226001, India [Emeritus Scientist, Scheme No. 21(0766)/09/EMR-II].

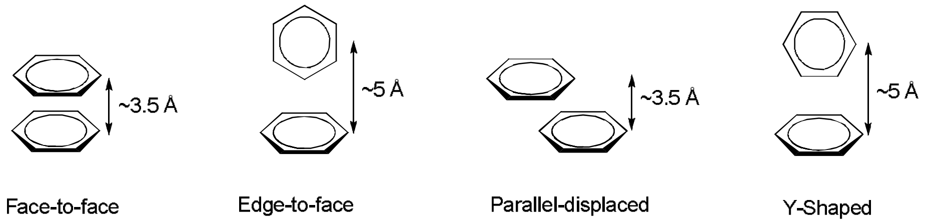

Figure 1. Four types of π–π interaction geometries (4, 5b, 5c)

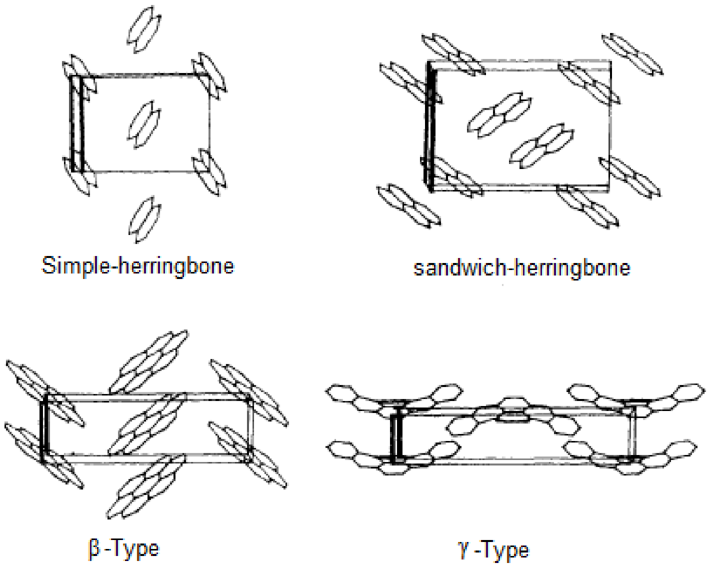

Figure 2. Four basic packing types for aromatic compounds (11)

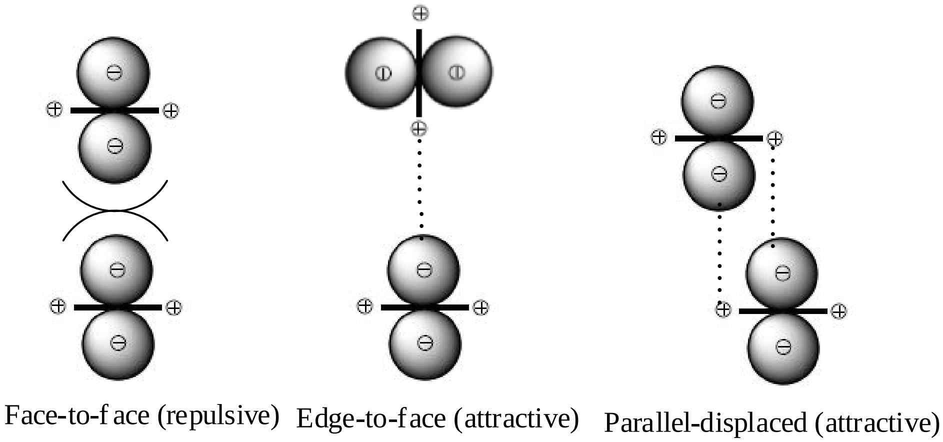

Figure 3. Electrostatic interaction between σ and π-systems of aromatic molecules (4)

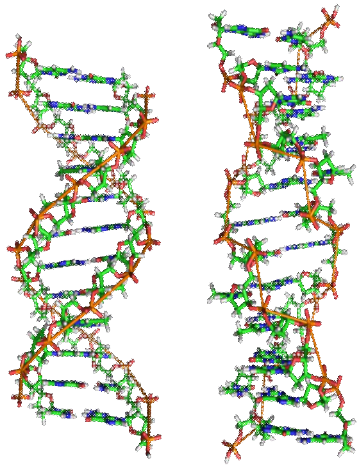

B-DNA Z-DNA

Figure 4. Base pair stacking in B and Z forms of DNA

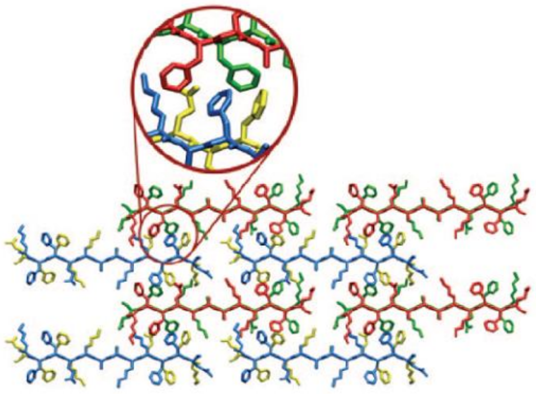

Figure 5. Crystal packing of 12-mer amyloid showing importance of π–π staking in stabilizing crystal structure (24a)

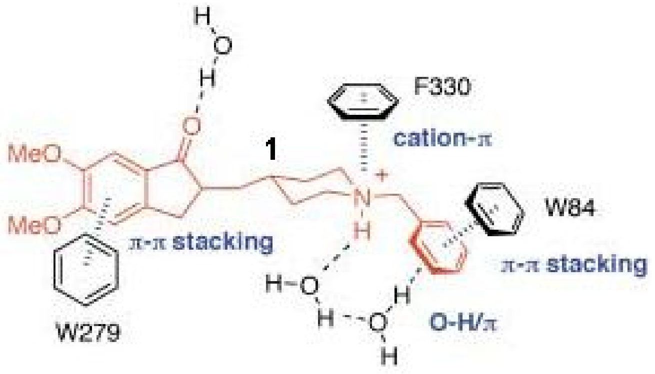

Figure 6. Binding mode of the anti-Alzheimer drug E2020 within the active site of acetyl cholinesterase from Torpedo californica (25)

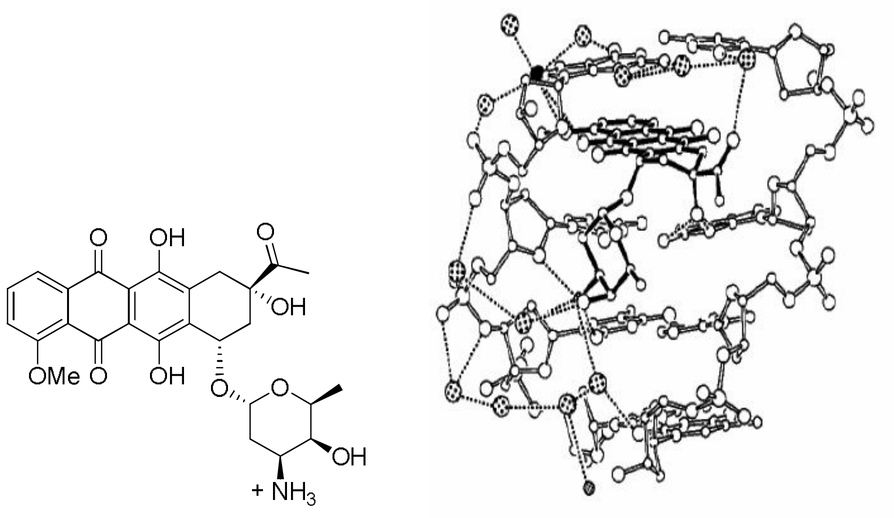

Figure 7. Daunomycin (**2**) and Daunomycin-DNA complex d (CGATGC) (26a)

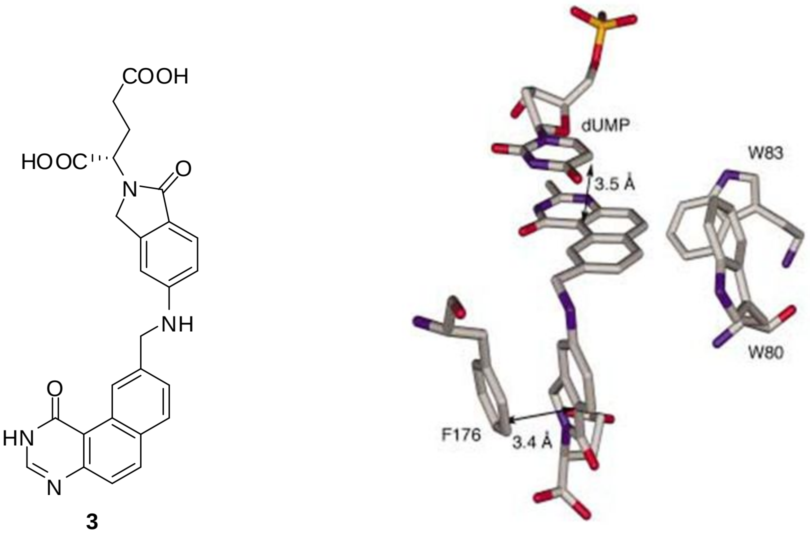

Figure 8. Arene–arene Interaction between dUMP and the anticancer drug 1843U89 bound at the active site of thymidylate Synthase (27)

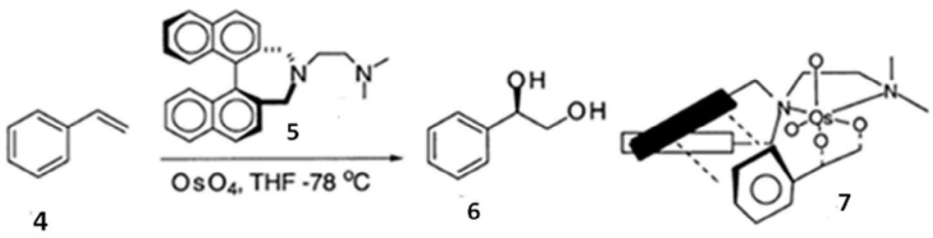

Figure 9. Enatioselective dihydroxylation of styrene (34)

Figure 10. Diestereoselective benzylation (35)

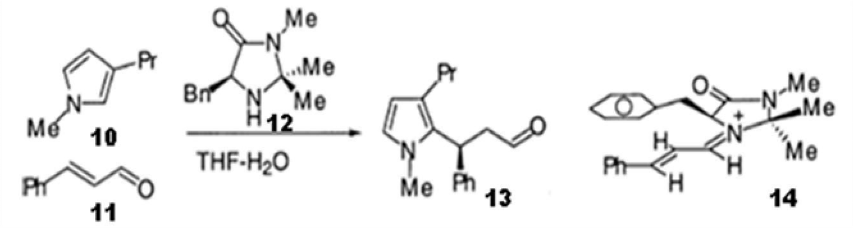

Figure 11. Enantioselective metal free Friedel-Crafts alkylation of substituted pyrrole (36)

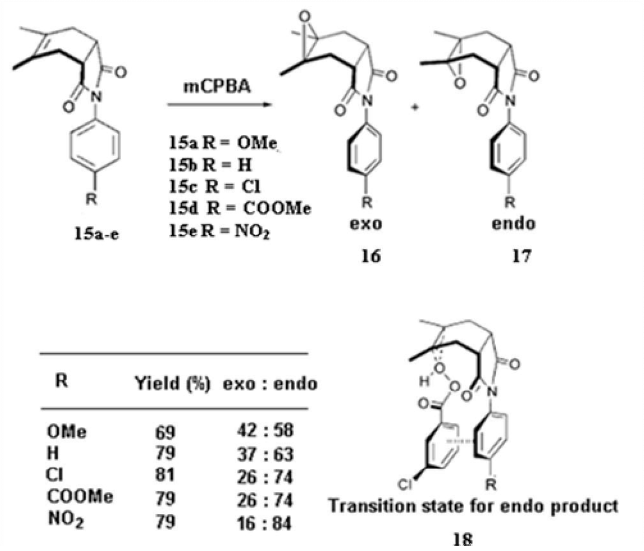

R	Yield (%)	exo : endo
OMe	69	42 : 58
H	79	37 : 63
Cl	81	26 : 74
COOMe	79	26 : 74
NO_2	79	16 : 84

Figure 12. Stereoselective epoxidation (37)

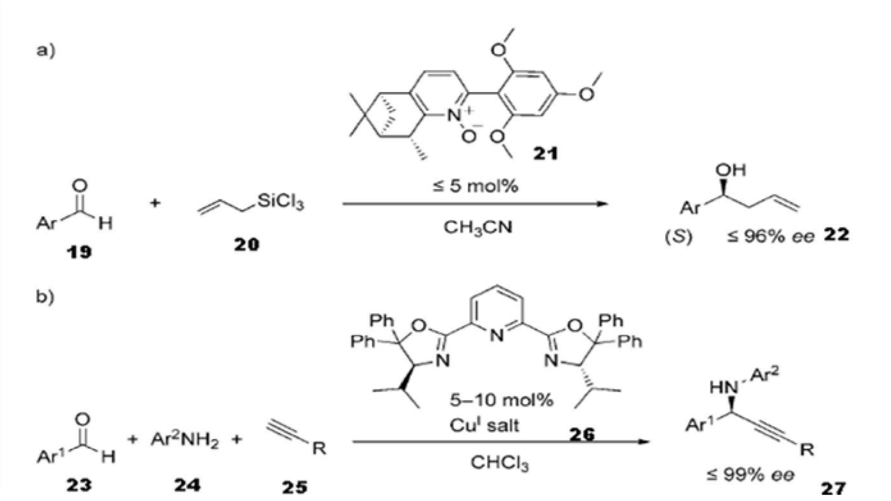

Figure 13. (a) allylation of aromatic aldehydes with chiral pyridine- type N-oxides (38) (b) for the three-component synthesis of propargylamines (39)

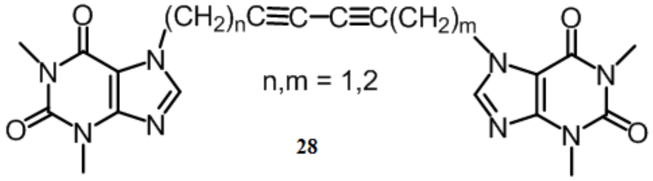

Figure 14. Whitlock’s molecular tweezers (43)

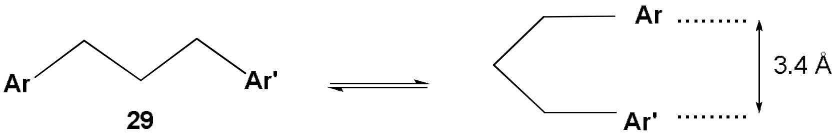

Open conformation Closed conformation

Where Ar and Ar′ are 9-substituted adenine or guanine or 1-substituted cytosine, thymine or uracil residues

Figure 15. Browne *et al.* model

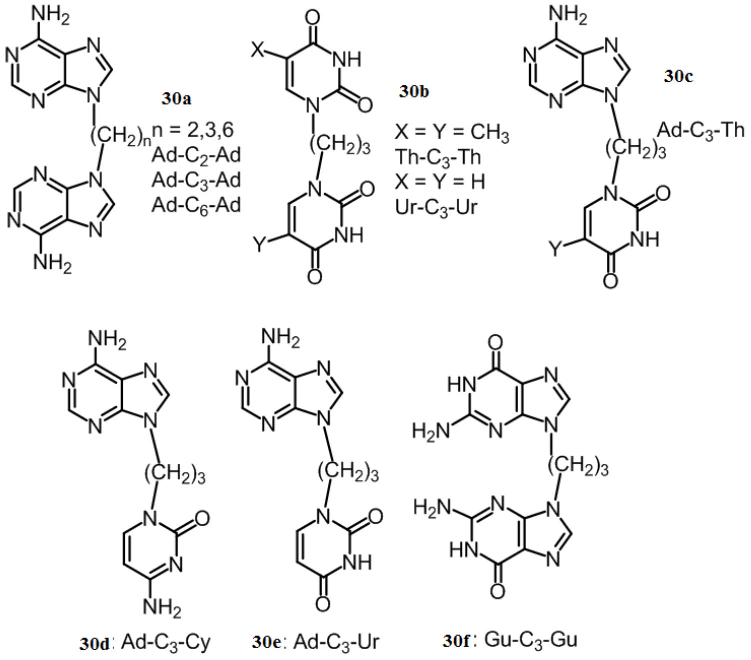

Figure 16. Dinucleotide analogs connected by *polymethylen*e/*trimethylene* linker

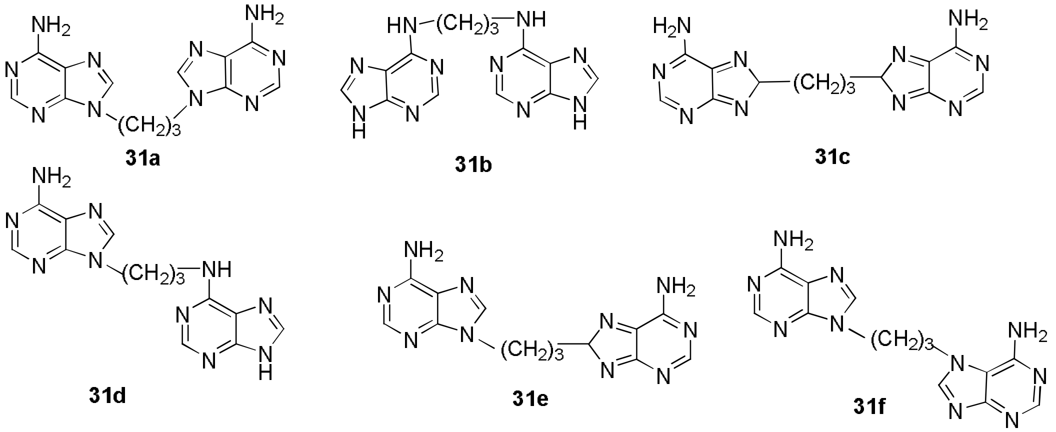

Figure 17. Dimers of adenine linked through different positions to study orientation effect on stacking.

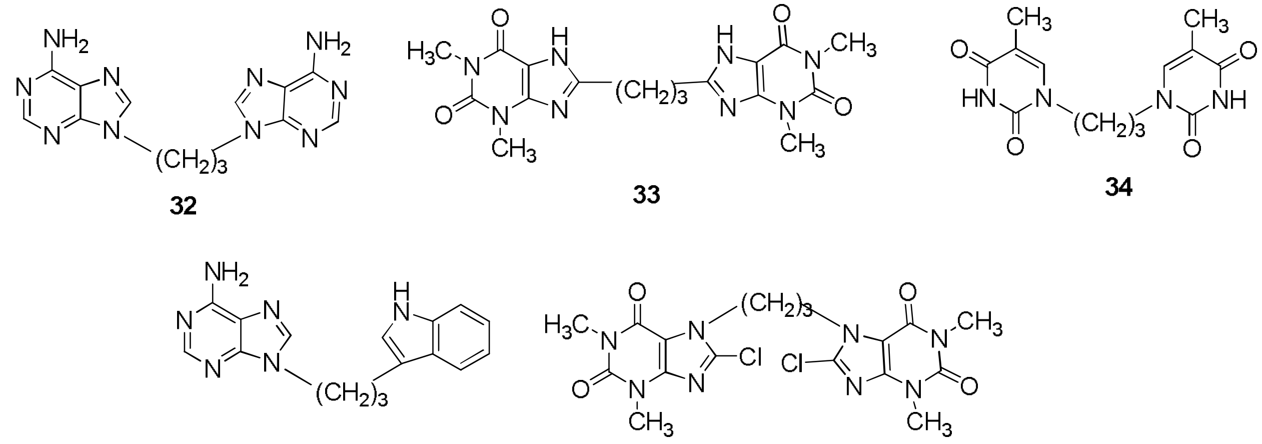
32 **33** **34**

35 **36**

Figure 18. Different *trimethylene* linker compounds in the literature.

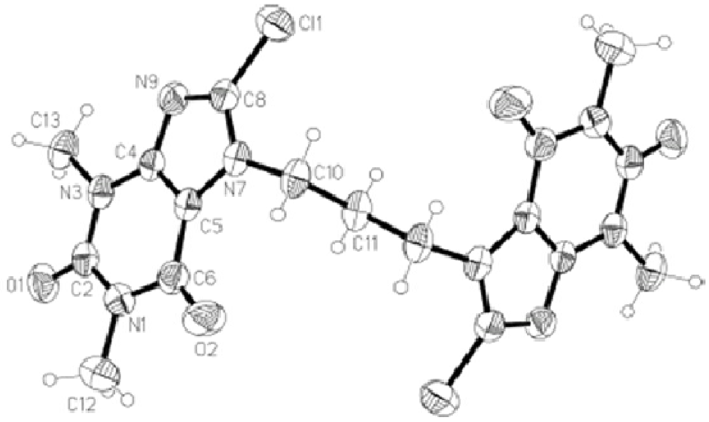

Figure 19. ORTEP diagram of **36** showing open conformation (56)

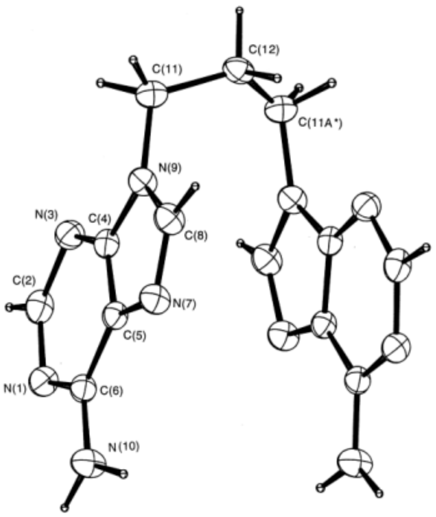

Figure 20. ORTEP diagram of **32** (57)

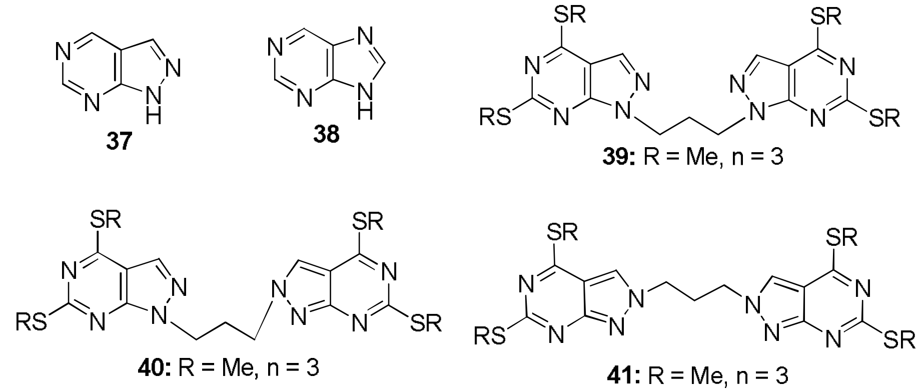

37

38

39: R = Me, n = 3

40: R = Me, n = 3

41: R = Me, n = 3

Figure 21. Pyrazolo[3,4-*d*]pyrimidine based *trimethylene* linker compounds

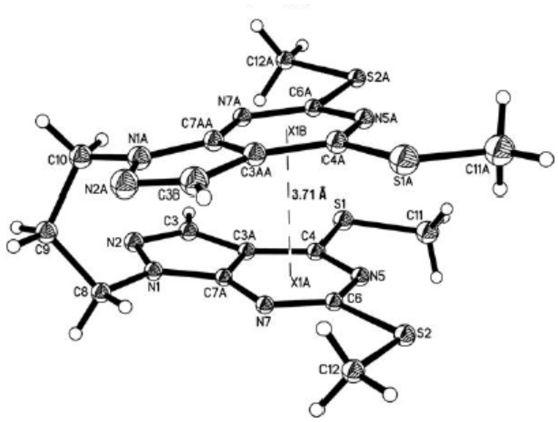

Figure 22. ORTEP diagram of **39** with atomic numbering scheme (59b)

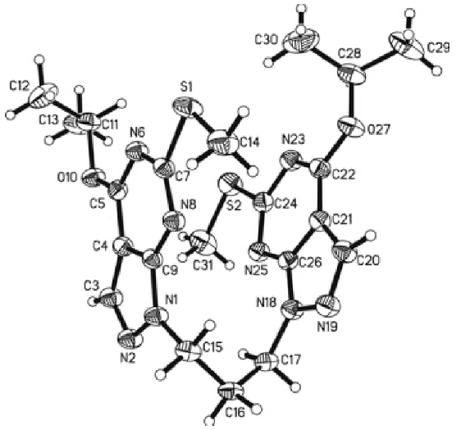

Figure 23. ORTEP diagram of **42** (at 30% probability level) with atomic labeling scheme (60c)

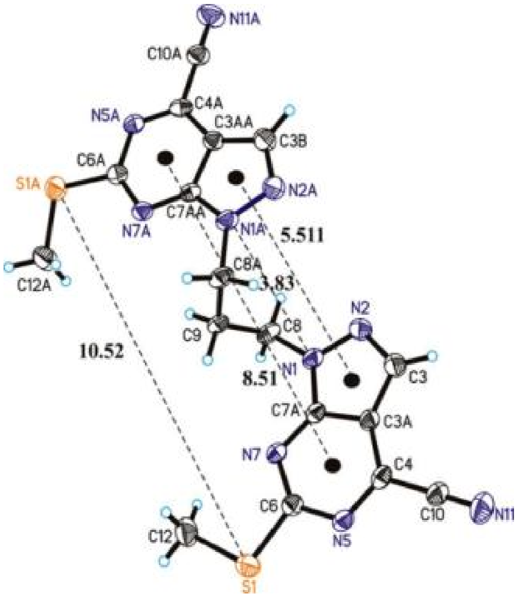

Figure 24: ORTEP diagram of **43** with atomic numbering scheme (60f).

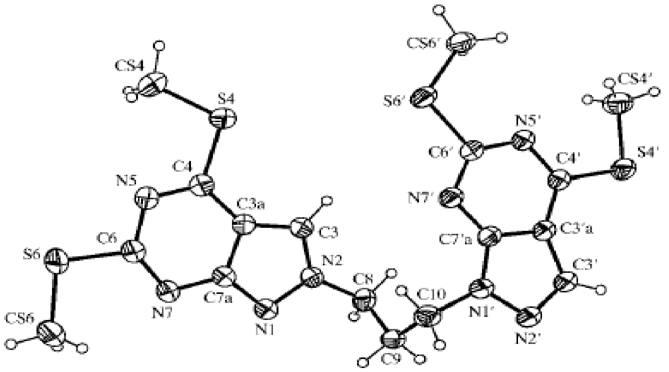

Figure 25. ORTEP diagram of **40** showing open conformation (61)

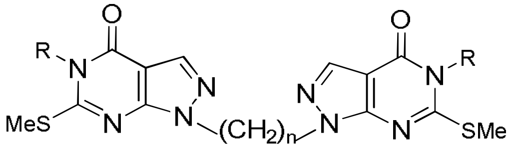

44: R = H, n = 3
45: R = Me, n = 3
46: R = Me, n = 4

Figure 26. Pyrazolo[3,4-*d*]pyrimidone compounds derived from **39**

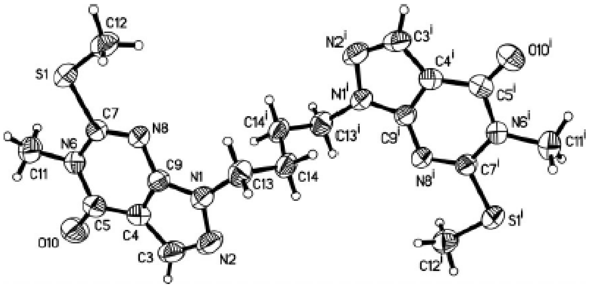

Figure 27. Displacement ellipsoid plot (50% probability), showing the molecular structure of **46** with the atomic labeling scheme (64)

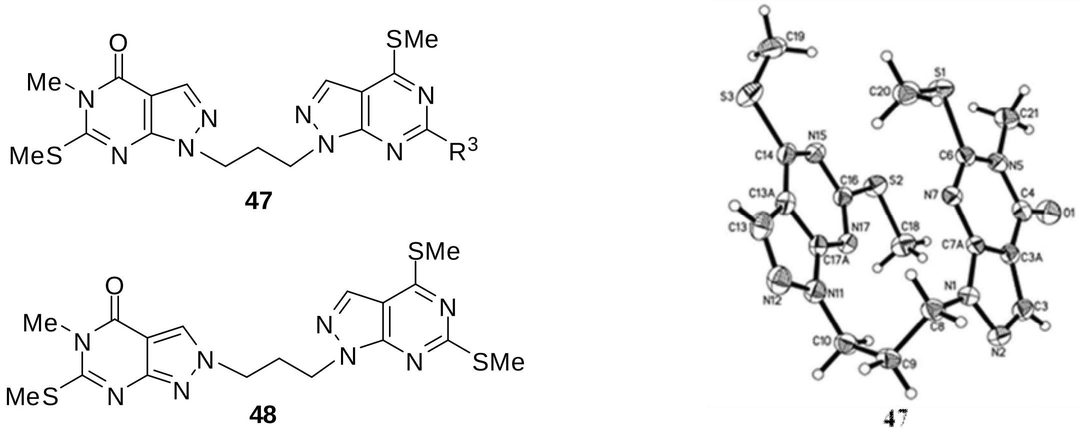

47

48

47

Figure 28. ORTEP Diagram of 47 (at 30% probability level) with atomic labeling scheme (65).

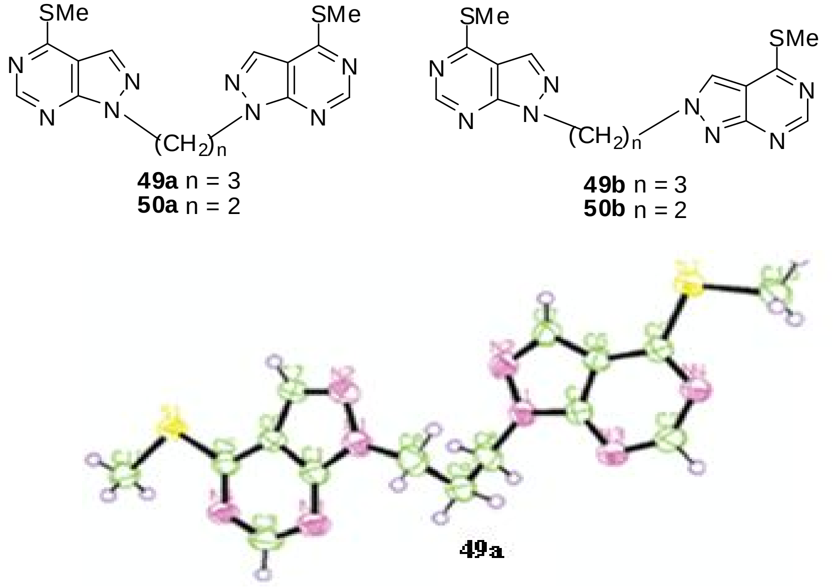

49a n = 3
50a n = 2

49b n = 3
50b n = 2

49a

Figure 29. 4-Methylsulfany-lpyrazolo[3,4-*d*]pyrimidine based *ethylene* and *propylene* linker compounds (66).

Table 1. Important geometrical data obtained from X-ray crystallographic studies of *propylene* linker compounds based on pyrazolo[3,4-*d*]pyrimidine and isomeric purine systems.

Compound No.	**Distance between two N atoms connecting linker (Å)**	**Intramolecular *π-π* stacking distance between two centroids of pyrimidine ring (Å)**	**Angle between the least square planes (°)**	**Angle at central C of *propylene* linker (°)**	**Folded or open**	**Reference**
36	4.91	8.60	78.51	112.3	Open	56
39	**3.28**	3.71	13.2	114.11	**Folded**	59
40	3.96	7.29	9.3	114.87	Open	61
42	**3.24**	3.69	14.99	114.43	**Folded**	60c
43	3.88	8.51	0.36	115.02	Open	60f
45	**3.35**	3.77	12.48	115.16	**Folded**	63
47	**3.50**	4.10	11.62	114.87	**Folded**	65
49a	3.69	8.32	3.78	115.60	Open	66

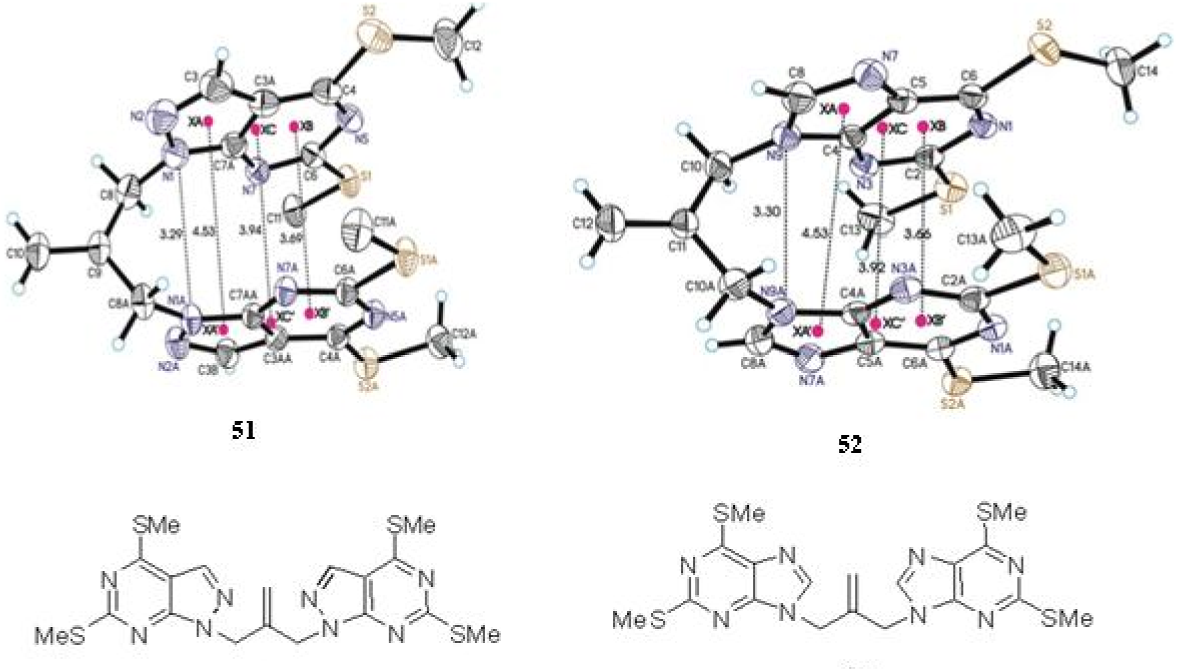

51

52

(a)

(b)

Figure 30. (a) Pyrazolo[3,4-*d*]pyrimidine based *butylidene* linker compound, **51**; (b) Purine based *butylidene* linker compound **52** (67)

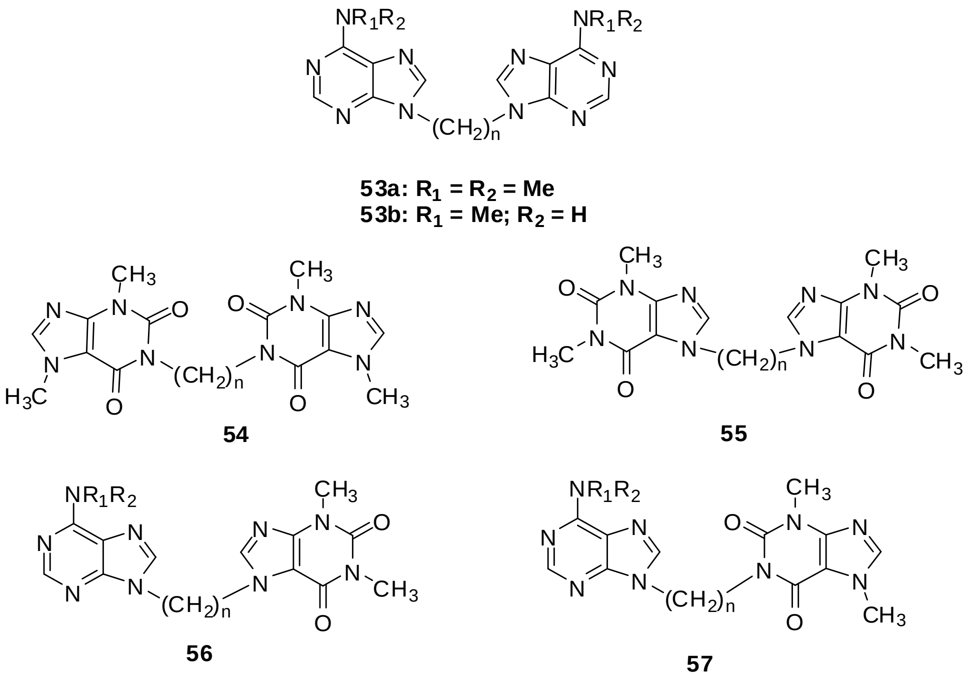

Figure 31. *Polymethylene* linker compounds of purine and xanthine bases used by Itahara

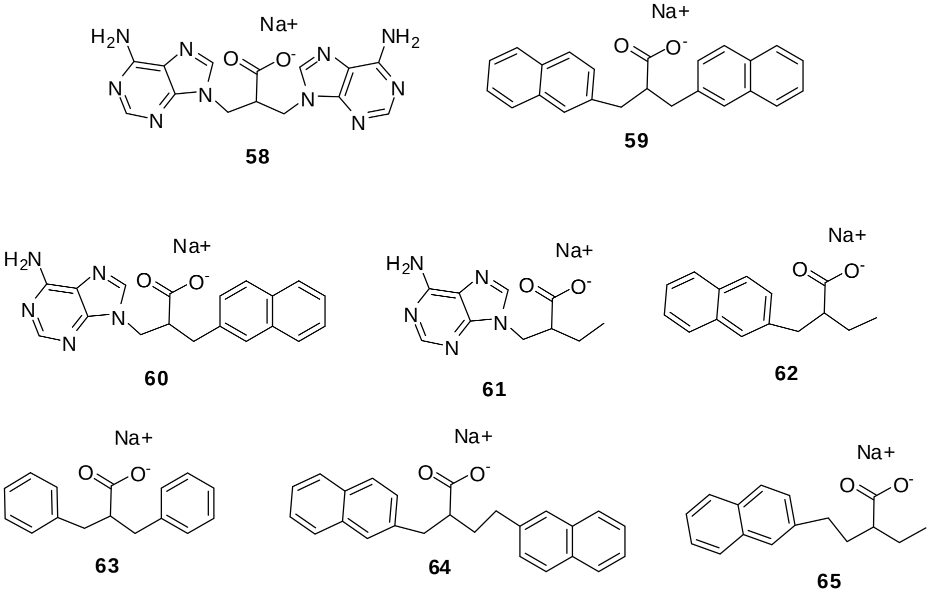

Figure 32. Compounds used to probe intramolecular aromatic interactions in water (72)

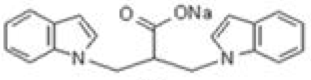

66

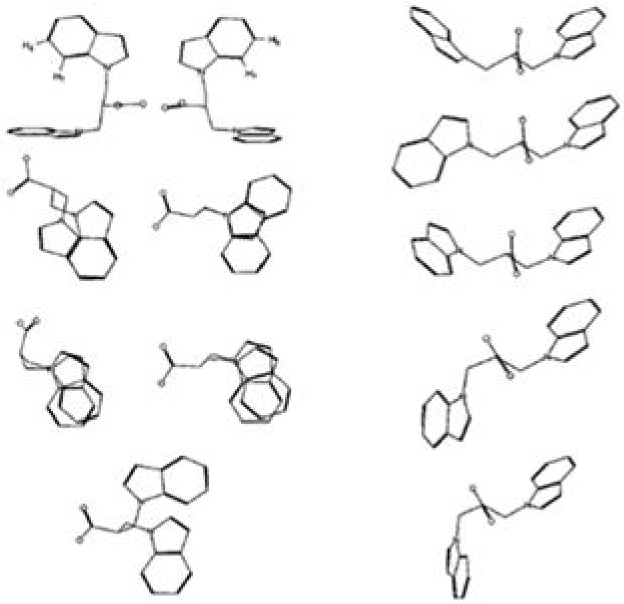

Figure 33. Conformations of **66** identified from the conformational search (73)

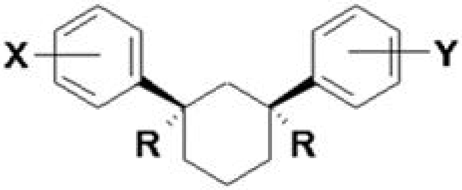

67a: R = H; X,Y = p-(H, NO_2, NH_2, etc.)
67b: R = H; X,Y = m- (H, NO_2, NH_2, etc.)
67c: R = Me; X,Y = p-(H, NO_2, NH_2, etc.)

Figure 34. Cyclohexyl based models

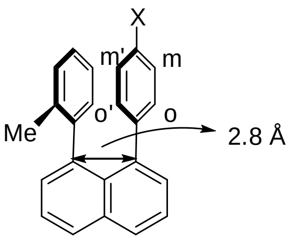

68

X = H, Me, OMe, Cl, NO_2, COOMe

Figure 35a. Substituted 1,8-diarylnaphthalenes (75a)

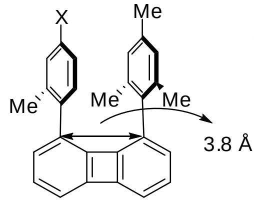

69

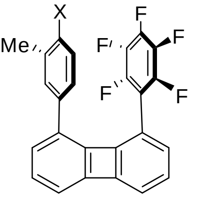

70

X = Cl, H, OMe

Figure. 35b. Substituted 1,8-diarylbiphenylene (75b)

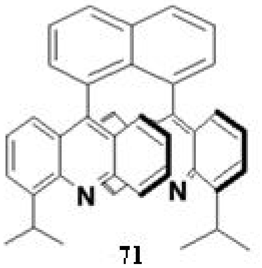

71

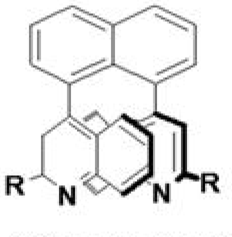

72: R = Me, *i*-Pr, Ph

Figure 36. Naphthyl based model having bi- and tricyclic arenes (76)

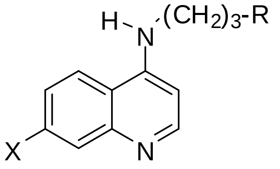

	X	R
73:	Cl	9- Adenine
74:	H	9- Adenine
75:	Br	9- Adenine
76:	Cl	9- Guanine
77:	H	9- Guanine

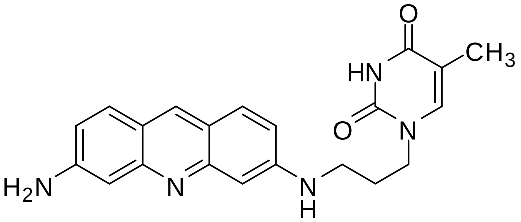

78

Figure 37. (a) *Polymethylene* linked quinoline compound (77) (b) *polymethylene* linked proflavine compounds (78)

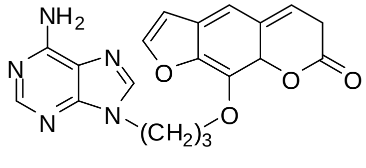

79

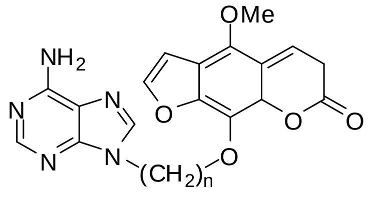

80a-d: n = 2,3,5,6

Figure 38. *Polymethylene* linked psoralen compounds (79)

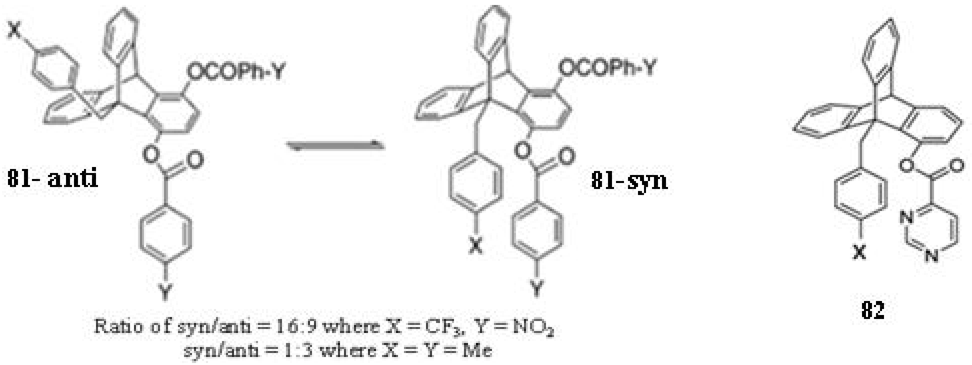

81- anti

81-syn

82

Ratio of syn/anti = 16:9 where X = CF_3, Y = NO_2
syn/anti = 1:3 where X = Y = Me

Figure 39a. Triptycene based models for studying arene interaction between (a) benzenoid systems, **81** (80a); (**b**) between benezenoid and heterocycles **82** (80b)

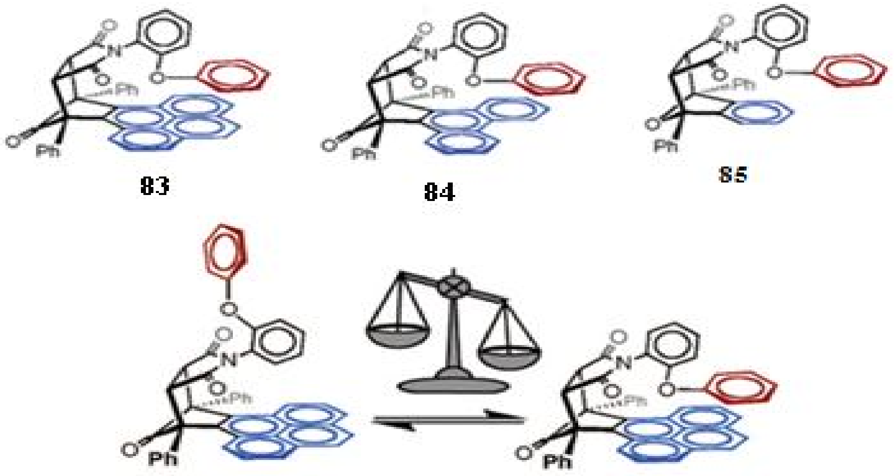

83

84

85

Figure 40. Carroll *et al.* model (81)

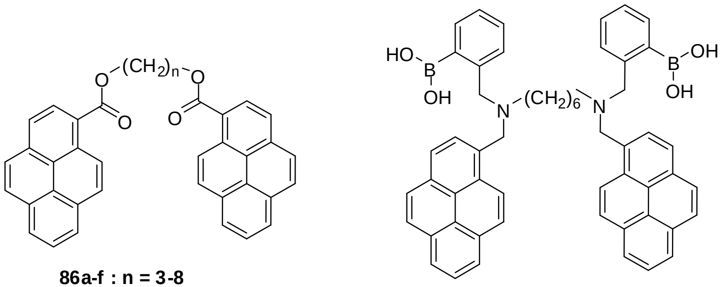

86a-f : n = 3-8
86g-p: n = 9-16, 22, 32

87

Figure 41. *Polymethylene* linked pyrenyl compounds (83, 84)

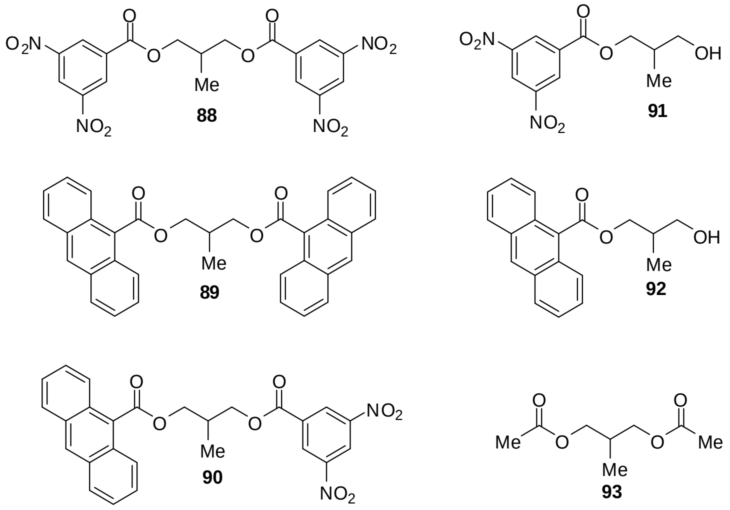

Figure 42. *2-Methyl-1,3-propanedioxy* spacer based diesters and monoesters (85)

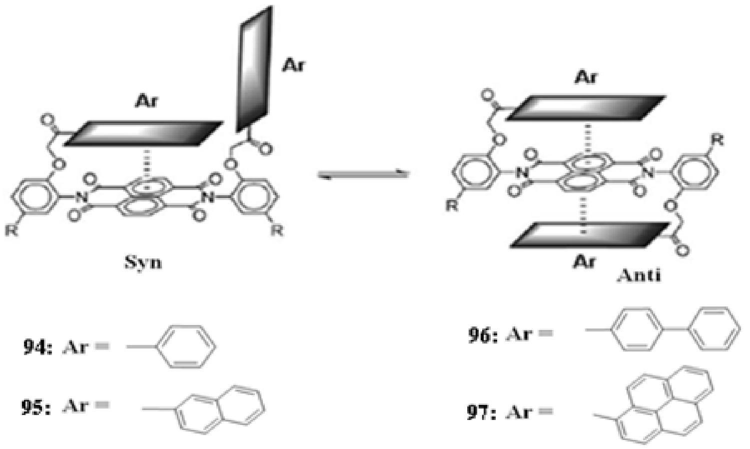

Figure 43. Chong *et al.* molecular balance for studying face-to-face arene–arene interactions (86)

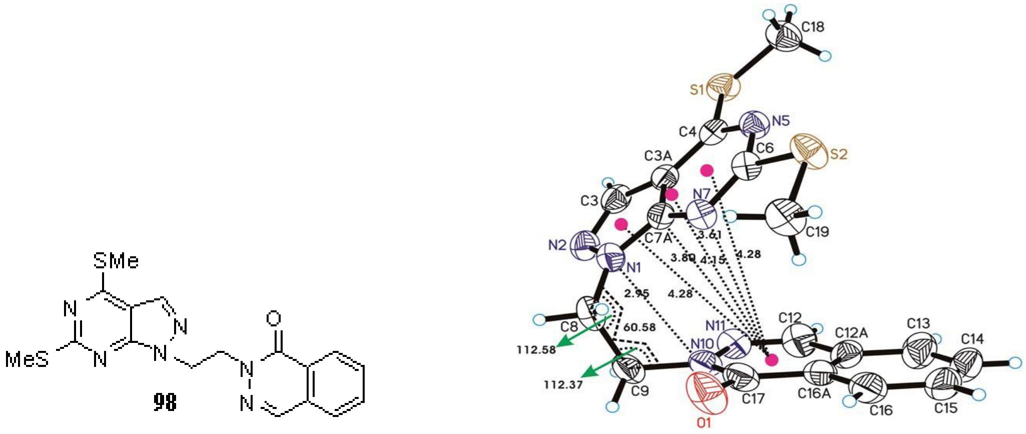

Figure 44. Pyrazolo[3,4-*d*]pyrimidine based dissymmetric *ethylene* linker compound **98** (87)

6. References

[1] K. Muller-Dethlefs, P. Hobza, Chem. Rev. 2000, 100, 143-168.

[2] P. Hobza, R. Zahradník, K. Muller-Dethlefs, Collect. Czech. Chem. Commun. 2006, 71, 443-531.

[3] P. Hobza, K. Muller-Dethlefs, Non-Covalent Interactions: Theory and Experiment, RSC Publishing, 2009.

[4] C. A. Hunter, J. K. M. Sanders, J. Am. Chem. Soc. 1990, 112, 5525-5534.

[5] (a) L. S. Salonen, M. Ellermann, F. Diederich, Angew. Chem. Int. Ed. 2011, 50, 4808-4842. (b) S. E. Wheeler, A. J. McNeil, P. Muller, T. M. Swager, K. N. Houk, J. Am. Chem. Soc. 2010, 132, 3304-3311. (c) T. F. Headen, C.A. Howard, N. T. Skipper, M. A. Wilkinson, D. T. Bowron, A. K Soper, J. Am. Chem. Soc. 2010, 132, 5735-5742. (d) A. K. Tewari, R. Dubey, Bioorg. Med. Chem. 2008, 16, 126-143. (e) E. A. Meyer, R. K. Castellano, F. Diederich, Angew. Chem. Int. Ed., 2003, 42, 1210-1250. (f) I. Dance, CrystEngComm. 2003, 5, 208-221. (g) M. L. Waters, Curr. Opin. Chem. Biol. 2002, 6, 736-741. (h) C. A. Hunter, K. R. Lawson, J. Perkins, C. J. Urch, J. Chem. Soc. Perkin Trans 2, 2001, 651-669. (i) C. A. Hunter, Chem. Soc. Rev. 1994, 23, 101-109. (j) C. A. Hunter, Angew. Chem. Int. Ed., 1993, 32, 1584-1586. (k) M. Nishio, M. Hirota, Y. Umezawa, The CH/π Interaction. Evidence, Nature, and Consequences; Wiley-VCH: New York, 1998. (l) M. Nishio, CrystEngComm. 2004, 6, 130-158. (m) W. B. Jennings, B. M. Farrell, J. F. Malone, Acc. Chem. Res. 2001, 34, 885-894. (n) G. R. Desiraju, J. J. Vittal, A. Ramanan, Crystal Engineering: A Textbook; World Scientific Publishing Co. Pt. Ltd.: Singapore, 2011. (o) E. R. T. Tiekink, J. Zukerman-Schpector, The Importance of Pi-Interactions in Crystal Engineering: Frontiers in crystal engineering; John Wiley & Sons: West Sussex, 2012.

[6] S. E. Wheeler, J. Am. Chem. Soc. 2011, 133, 10262-10274.

[7] J. W. Steed, J. L. Atwood, Supramolecular Chemistry; Wiley: Chichester, 2000.

[8] S. Grimme, Angew. Chem., Int. Ed., 2008, 47, 3430-3434.

[9] (a) P. Hobza, H. L. Selzle, E. W. Schlag, J. Phys. Chem. 1996, 100, 18790-18794. (b) S. Tsuzuki, T. Uchimaru, K. Matsumura, M. Mikami, K. Tanabe, Chem. Phys. Lett. 2000, 319, 547-554. (c) J. West, S. Mecozzi, D. A. Dougherty, J. Phys. Org. Chem. 1997, 10, 347-350. (d) K. E. Riley, M. Pitonak, P. Jurecka, P. Hobza, Chem. Rev. 2010, 110, 5023-5063.

[10] (a) T. Blundell, J. Singh, J. Thornton, S.K. Burley, G. A. Petsko, Science 1986, 234, 1005. (b) S. Tsuzuki, K. Honda, T. Uchimaru, M. Mikami, K. Tanabe, J. Am. Chem. Soc. 2002, 124, 104-112.

[11] (a) G. R. Desiraju, A. Gavezzotti, J. Chem. Soc. Chem. Commun. 1989, 621-623. (b) G. R. Desiraju, Chem. Commun. 1997, 1475-1482.

[12] E. G. Hohenstein, C.D. Sherrill, J. Phys. Chem. A 2009, 113, 878- 886.

[13] (a) R. R. Choudhury, R. Chitra, CrystEngComm. 2010, 12, 2113-2121. (b) T. Itahara, K. Imaizumi, J. Phys. Chem. B 2007, 111, 2025-2032.

[14] (a) E. T. Kool, Annu. Rev. Biophys. Biomol. Struct. 2001, 30, 1-22. (b) J. Sponer, K. E. Riley, P. Hobza, Phys. Chem. Chem. Phys. 2008, 10, 2595-2610.

[15] N. Kannan, S. Vishveshwara, Protein Eng. 2000, 13, 753-761.

[16] E. Gazit, FASEB J. 2002, 16, 77-83.

[17] (a) P. Hobza, Sponer, J. Chem. Rev. 1999, 99, 3247-3276. (b) C. A. Hunter, J. Mol. Biol. 1993, 230, 1025-1054. (c) E. T. Kool, J.C. Morales, K. M. Guckian, Angew. Chem. Int. Ed. Engl. 2000, 39, 990–1009.

[18] S. K. Burley, G. A. Petsko, Science 1985, 229, 23-28.

[19] G. B. McGaughey, M. Gagnu, A. K. Rappe, J. Biol. Chem. 1998, 273, 15458-15463.

[20] C. A. Hunter, J. Singh, J. M. Thornton, J. Mol. Biol. 1991, 218, 837-846.

[21] S. Aravinda, N. Shamala, C. Das, A. Sriranjini, I. L. Karle, P. Balaram, J. Am. Chem. Soc. 2003, 125, 5308-5315.

[22] S. Yanagisawa, P. B. Crowley, S. J. Firbank, A. T. Lawler, D. M. Hunter, W. McFarlane, C. Li, T. Kohzuma, M. J. Banfield, C. Dennison, J. Am. Chem. Soc. 2008, 130, 15420-15428.

[23] P. Acharya, Chattopadhyaya, J. Pure Appl. Chem. 2005, 77, 291-311.

[24] (a) O. S. Makin, E. Atkins, P. Sikorski, J. Johansson, L. C. Serpell, Proc. Natl. Acad. Sci. 2005, 102, 315-320. (b) V. J. Bradford, B.L. Iverson, J. Am. Chem. Soc. 2008, 130, 1517-1524.

[25] G. Kryger, I. Silman, J. L. Sussman, J. Physiol. 1998, 92, 191-194.

[26] (a) C. A. Frederick, L. D. Williams, G. Ughetto, G. A. van der Marel, J. H. van Boom, A. Rich, A. H. J. Wang, Biochemistry 1990, 29, 2538-2549. (b) G. Barone, C. F. Guerra, A.; Noemi, S. A. Lauria, A. M. Almerico, F. M. Bickelhaupt, J. Biomol. Struct. Dyn. 2008, 26, 115-129.

[27] A. Weichsel, W. R. Montfort, Nat. Struct. Biol. 1995, 2, 1095-1101.

[28] (a) G. B. Jones, B. J. Chapman, Synthesis 1995, 475-497. (b) G. B. Jones, Tetrahedron 2001, 57, 7999-8016. (c) M. Nishio, Tetrahedron 2005, 61, 6923-6950.

[29] (a) I. Skoric, N. Basaric, Z. Marinic, A. Visnjevac, B. Kojic-Prodic, M. Sindler-Kulyk, Chem. Eur. J. 2005, 11, 543-551. (b) S. Grimme, C. Diedrich, M. Korth, Angew. Chem. Int. Ed. 2006, 45, 625-629. (c) S. Karthikeyan, V. Ramamurthy, J. Org. Chem. 2006, 71, 6409-6413. (d) S. Karthikeyan, V. Ramamurthy, J. Org. Chem. 2007, 72, 452-458. (e) I. Skoric, M. Smehil, Z. Marinic, K. Molcanov, B. Kojic-Prodic, Sindler-Kulyk, M. J. Photochem. Photobiol. A 2009, 207, 190-196.

[30] (a) S. K. Ginotra, V. K. Singh, Org. Biomol. Chem. 2006, 4, 4370-4374. (b) S. K. Ginotra, V. K. Singh, Tetrahedron 2006, 62, 3573-3581.

[31] P. Brandt, P. Roth, P. G. Andersson, J. Org. Chem. 2004, 69, 4885-4890.

[32] (a) F. Naso, M. A. M. Capozzi, A. Bottoni, M. Calvaresi, V. Bertolasi, F. Capitelli, C. Cardellicchio,

Chem. Eur. J. 2009, 15, 13417-13426. (b) G. Santoni, M. Mba, M. Bonchio, W. A. Nugent, C. Zonta, G. Licini, Chem. Eur. J. 2010, 16, 645-654.
[33] (a) J. J. Carb, A. Lleds, D. Vogt, C. Bo, Chem. Eur. J. 2006, 12, 1457-1467. (b) J. A. G. Bodkin, B. Bacskay, M. D. McLeod, Org. Biomol. Chem. 2008, 6, 2544-2553. (c) K. Katagiri, T. Tohaya, H. Masu, M. Tominaga, I. Azumaya, J. Org. Chem. 2009, 74, 2804-2810.
[34] C. Rosini, R. Tanturli, P. Pertici, P. Salvadori, Tetrahedron: Asymmetry 1996, 7, 2971-2982.
[35] J. M. McIntosh, E. J. Kiser, Z. Tian, Can. J. Chem. 1998, 76, 147-151.
[36] N. A. Paras, D.W.C. McMillan, J. Am. Chem. Soc. 2001, 123, 4370-4371.
[37] K. Kishikawa, M. Naruse, S. Kohmoto, M. Yamamoto, K. Yamaguchi, J. Chem. Soc., Perkin Trans.1, 2001, 462-468.
[38] (a) A. V. Malkov, L. Dufkov, L. Farrugia, P. Kocovsky, Angew. Chem. 2003, 115, 3802-3805. (b) A. V. Malkov, M. Bell, F. Castelluzzo, P. Kocovsky, Org. Lett. 2005, 7, 3219-3222.
[39] A. Bisai, V. K. Singh, Org. Lett. 2006, 8, 2405-2408.
[40] S. B.; Ferguson, F. Diederich, Angew. Chem. Int. Ed. Engl. 1986, 25, 1127-1129.
[41] D. B. Smithrud, Diederich, F. J. Am. Chem. Soc. 1990, 112, 339-343.
[42] A. W. Schwabacher, S. Zhang, W. Davy, J. Am. Chem. Soc. 1993, 115, 6995-6996.
[43] C. W. Chen, H. W. Whitlock, J. Am. Chem. Soc. 1978, 100, 4921-4922.
[44] S. C. Zimmerman, C. M. Vanzyl, J. Am. Chem. Soc. 1987, 109, 7894-7896.
[45] S. C. Zimmerman, C. M. Vanzyl, G. S. Hamilton, J. Am. Chem. Soc. 1989, 111, 1373-1381.
[46] S. C. Zimmerman, K. W. Saionz, Z. J. Zeng, Proc. Natl. Acad. Sci. 1993, 90, 1190-1193.
[47] S. C.; Zimmerman, K. W. Saionz, J. Am. Chem. Soc. 1995, 117, 1175-1176.
[48] R. P. Sijbesma, A. P. M. Kentgens, R. J. M., Nolte, J. Org. Chem. 1991, 56, 3199-3201.
[49] (a) D. T. Browne, J. Eisinger, N.J. Leonard, J. Am. Chem. Soc. 1968, 90, 7302-7323. (b) N. J. Leonard, K. Ito, J. Am. Chem. Soc. 1973, 95, 4010-4016. (c) N. J. Leonard, Acc. Chem. Res.1979, 12, 423-429.
[50] L. S. Rosen, A. Hybl, Acta Crystallogr. 1971, B27, 952-960.
[51] M. Falk, W. Chew, J. A. Walter, W. Kwiatkowski, K. D. Barclay, G. A. Klassen, Can. J. Chem. 1998, 76, 48-56.
[52] J. K. Frank, I. C. Paul, J. Am. Chem. Soc., 1973, 95, 2324-2332.
[53] K. Mutai, B. A. Gruber, N. J. Leonard, J. Am. Chem. Soc. 1975, 97, 4095-4104.
[54] G. Bunick, D. Voet, Acta Crystallogr. 1982, B38, 575-580.
[55] T. Ishida, M. Shibata, K. Fujii, M. Inove, Biochemistry 1983, 22, 3571-3581.
[56] P. R. Maulik, K. Avasthi, S. Sarkhel, A. Sharon, D. S. Rawat, C. Bal, Acta Crystallogr. 2001, E57, o1163-1165.
[57] A. Garcia-Raso, J. J. Fiol, F. Badenas, X. Solans, M. Font-Bardia, Polyhedron 1999, 18, 765-772.
[58] (a) K. Avasthi, D. S. Bhakuni, Synthesis 1989, 876-878. (b) S. Misra, S. Jain, K. Avasthi, D. S. Bhakuni, Nucleosides & Nucleotides 1990, 9, 837-846. (c) K. Avasthi, K. Deo, N. Garg, D. S. Bhakuni, Bioorg. Med. Chem. Lett. 1991, 1, 249-252. (d) K. Avasthi, N. Garg, T. Chandra, D. S. Bhakuni, P. P. Gupta, R. C. Srimal, Eur. J. Med. Chem. 1993, 28, 585-591.
[59] (a) K. Avasthi, T. Chandra, D. S. Bhakuni, Indian J. Chem. 1995, 34B, 944-949. (b) G. Biswas, T. Chandra, K. Avasthi, P. R. Maulik, Acta Crystallogr. 1995, C51, 2453-2455. (c) F. Vogtle, Cyclophane Chemistry: Synthesis, Structures and Reactions, J. Wiley, Chichester, New York, 1993.
[60] (a) K. Avasthi, D. S. Rawat, P. R. Maulik, S. Sarkhel, C. K. Broder, J. A. K. Howard, Tetrahedron Lett. 2001, 42, 7115-7117. (b) K. Avasthi, S. M. Farooq, D. S. Rawat, A. Sharon, P. R. Maulik, Acta Crystallogr. 2003, C59, o523-524. (c) K. Avasthi, S. Aswal, R. Kumar, U. Yadav, D. S. Rawat, P. R. Maulik, J. Mol. Struct. 2005, 750, 179-185. (d) K. Avasthi, S. M. Farooq, S. Aswal, R. Raghunandan, P. R. Maulik, J. Mol. Struct. 2007, 827, 88-94. (e) K. Avasthi, S. Aswal, S. M. Farooq, R. Raghunandan, P. R. Maulik, J. Mol. Struct. 2008, 888, 327-336. (f) K. Avasthi, S. M. Farooq, R. Raghunandan, P. R. Maulik, J. Mol. Struct. 2009, 927, 27-36.
[61] P. R. Maulik, K. Avasthi, S. Sarkhel, T. Chandra, D. S. Rawat, B. Logsdon, R. A. Jacobson, Acta Crystallogr. 2000, C56, 1361-1363.
[62] K. Avasthi, D. S. Rawat, T. Chandra, D. S. Bhakuni, Indian J. Chem. 1998, 37B, 754-759.
[63] P. R. Maulik, K. Avasthi, G. Biswas, D.S. Rawat, S. Sarkhel, T. Chandra, D. S. Bhakuni, Acta Crystallogr. 1998, C54, 275-277.
[64] K. Avasthi, S. M. Farooq, A. Sharon, P. R. Maulik, Acta Crystallogr. 2002, E58, o940-941.
[65] K. Avasthi, S. M. Farooq, R. Raghunandan, P. R. Maulik, J. Mol. Struct. 2006, 785, 106-113.
[66] R. Dubey, A. K. Tewari, K. Ravikumar, B. Sridhar, Bull. Korean Chem. Soc. 2010, 31, 1326-1330.
[67] K. Avasthi, A. Ansari, R. Kant, P. R. Maulik, K. Ravikumar, P. Chattopadhyay N. D. Adhikary, CrystEngComm. 2011, 13, 2039-2046.
[68] K. Avasthi et al. (unpublished results).
[69] T. Itahara, K. Imamura, Bull. Chem. Soc. Jpn. 1994, 67, 203-209.
[70] T. Itahara, J. Chem. Soc. Perkin Trans. 2, 1998, 1455-1462.
[71] T. Itahara, Bull. Chem. Soc. Jpn. 2000, 73, 1621-1631.
[72] (a) L. F. Newcomb, T. S. Haque, S. H. Gellman, J. Am. Chem. Soc. 1995, 117, 6509-6519. (b) L. F. Newcomb, S. H. Gellman, J. Am. Chem. Soc. 1994, 116, 4993-4994. (c) I. K. Mati, S. L. Cockroft, Chem. Soc. Rev. 2010, 1648-1650.
[73] Y. Pang, J. L. Miller, P. A. Kollman, J. Am. Chem. Soc. 1999, 121, 1717-1725.
[74] V. E. Williams, R. P. Lemieux, G. R. J. Thatcher, J. Org. Chem. 1996, 61, 1927-1933.
[75] (a) F. Cozzi, M. Cinquini, R. Annunziata, T. Dwyer, J. S. Siegel, J. Am. Chem. Soc. 1992, 114, 5729-5733.

(b) F. Cozzi, R. Annunziata, M. Benaglia, K. K. Baldridge, G. Aguirre, J. Estrada, Y. Sritana-Anant, J. S. Siegel, Phys. Chem. Chem. Phys. 2008, 10, 2686-2694.

[76] G. E. Tumambac, C. Wolf, J. Org. Chem. 2005, 70, 2930-2938.

[77] (a) J. Bolte, C. Demunck, J. Lhomme, J. Am. Chem. Soc. 1976, 98, 613-615. (b) C. Demunck, J. Bolte, J. Lhomme, J. Med. Chem. 1977, 20, 106-113. (c) J. Bolte, C. Demuynck, J. Lhomme, J. Med. Chem. 1977, 20, 1607-1611. (d) J. Bolte, C. Demuynck, J. Lhomme M. C. Fournie-Zaluski, B. P. Roques, Biochemistry 1979, 18, 4928-4935.

[78] J. F. Constant, J. Fahy, J. Lhomme, Tetrahedron Lett. 1987, 28, 1777-1780.

[79] J. L. Decout, J. Lhomme, Photochem. Photobiol. 1983, 37, 155-161.

[80] (a) B. W. Gung, X. Xue, H. Reich, J. Org. Chem. 2005, 70, 3641-3644. (b) B. W. Gung, F. Wekesa, C. L. Barnes, J. Org. Chem. 2008, 73, 1803-1808.

[81] W. R. Carroll, P. Pellechia, K.D. Shimizu, Org. Lett. 2008, 10, 3547-3550.

[82] (a) M. Arslan, E. Asker, J. Masnovic, R. J. Baker, Acta Cryst. 2007, E63, o1800-o1801. (b) J. Harada, K. Ogawa and S. Tomoda, J. Am. Chem. Soc., 1995, 117, 4476-4478. (c) M. Fleck, M. Walter Acta Cryst. 2005, E61, o4099-o4100. (d) M. Arslan, E. Asker, J. Masnovic, R. J. Baker, Acta Cryst. 2007, E63, o2400-o2402.

[83] P. Reynders, W. Kuhnle, K. A. Zachariasse, J. Am. Chem. Soc. 1990, 112, 3929-3939.

[84] S. Arimori, M. L. Bell, C. S. Oh, K. A. Frimat, T. D. James, J. Chem. Soc. Perkin Trans. 1, 2002, 803-808.

[85] N. J. Heaton, P. Bello, B. Herrandon, A. del Campo, J. Jimenez-Barbero, J. Am. Chem. Soc. 1998, 120, 12371-12384.

[86] Y. S. Chong, W. R. Carroll, W. G. Burns, M. D. Smith, K. D. Shimizu, Chem. Eur. J. 2009, 15, 9117–9126.

[87] K. Avasthi, A. Kumar, S. Aswal, R. Kant, R. Raghunandan, P. R. Maulik, R. S. Khanna, K. Ravikumar, CrystEngComm. 2012, 14, 383-388.

CURRICULUM VITAE

1. PERSONAL INFORMATION

Name	Amar Kumar
Father's name	Shri Umesh Nandan Prasad Singh
Date of birth	10/07/1980
Nationality	Indian
Language known	Hindi, English and Urdu
Gender	Male
Marital status	Married
Permanent address	Haripara, Hirapur, Dhanbad, Jharkhand: 826001
Email	amarleo123@gmail.com
Mobile no.	+919891111589

2. EDUCATIONAL QUALIFICATIONS

S. No.	**Degree**	**Board/University**	**Subject(s)**	Year	Division
1	High School	CBSE	Hindi, English, Math, Science and Social Science	1995	I
2	Intermediate	CBSE	Hindi, English, Math, Physics and Chemistry	1997	I
3	B. Sc.(H) Chemistry	University of Delhi	Chemistry, Math, and Physics	2002	I
4	M. Sc.	University of Delhi	Organic Chemistry	2004	I
5	Ph. D.	CDRI, Lucknow (Enrolled at B. H. U.)	Organic Chemistry	Joined on 17/02/2006	

3. ACADEMIC ACHIEVEMENTS

1. **Qualified National Eligibility Test for CSIR-JRF**
2. **Qualified** in GATE-2005.

4. PUBLICATIONS

1. Avasthi, K.; Kumar, Amar; Aswal, S.; Kant, R.; Raghunandan, R.; Maulik, P. R.; Khanna, R. S.; Ravikumar, K., Role of arene interactions and substituent effects in conformational (syn/anti) control of 1,2-diarylethanes, *CrystEngComm* **2012**, *14*, 383–388.
2. Avasthi, K.; Kumar, Amar An overview of arene–arene interactions and application of uni-molecular models for their understanding, *Chemistry & Biology Interface* **2012** *(In Press).*

AMAR KUMAR